Improved Measurements of Solar Irradiance by Means of Detailed Pyranometer Characterisation

A Report of Task 9: Solar Radiation and Pyranometry

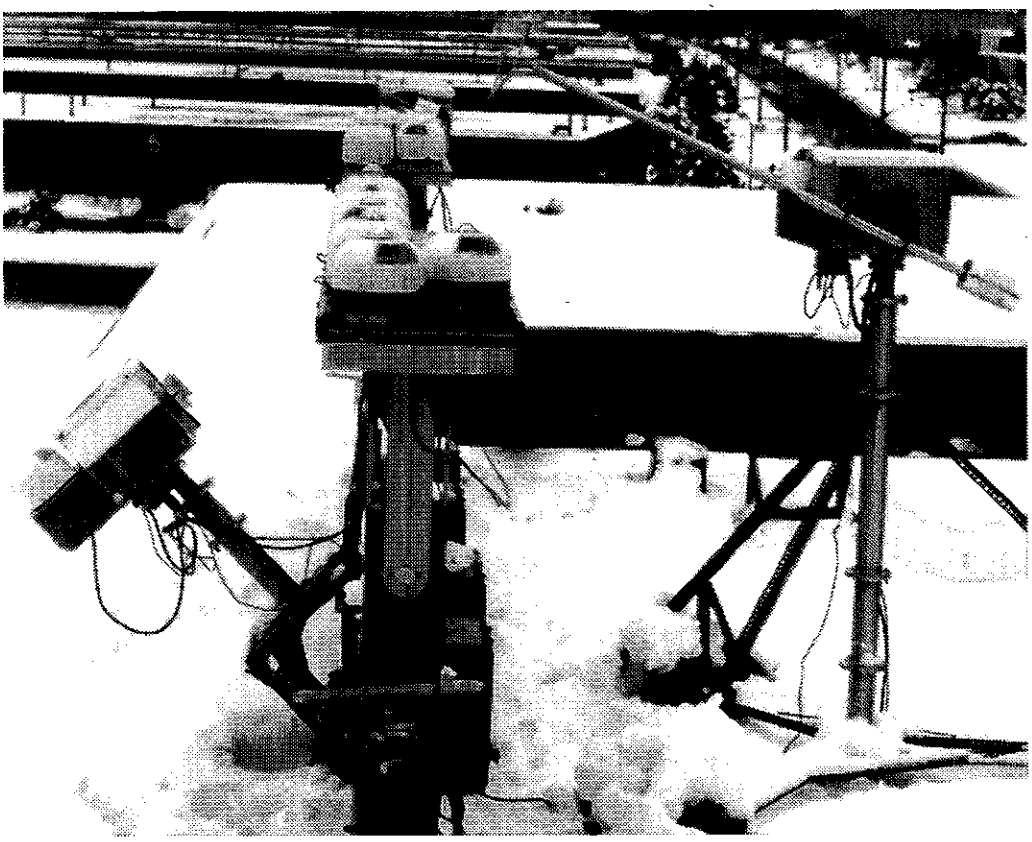

April 1996

INTERNATIONAL ENERGY AGENCY
Solar Heating & Cooling Programme

GENERAL INFORMATION ABOUT THE IEA

INTERNATIONAL ENERGY AGENCY

The International Energy Agency, founded in November 1974, is an autonomous body within the framework of the Organization for Economic Cooperation and Development (OECD) which aims to coordinate the energy policies of its members. The twenty-three member countries seek to create the conditions in which the energy sectors of their economies can make the fullest possible contribution to sustainable economic development and to the well-being of their people and the environment. The European Commission also participates in the work of the Agency.

The policy goals of the IEA include diversity, efficiency and flexibility within the energy sector, the ability to respond promptly and flexibly to energy emergencies, the environmentally sustainable provision and use of energy, more environmentally-acceptable energy sources, improved energy efficiency, research, development and market deployment of new and improved energy technologies, and cooperation among all energy market participants.

These goals are addressed in part through a program of collaboration in the research, development and demonstration of new energy technologies consisting of about 40 Implementing Agreements. The IEA's R&D activities are headed by the Committee on Energy Research and Technology (CERT) which is supported by a small Secretariat staff in Paris. In addition, four Working Parties (in Conservation, Fossil Fuels, Renewable Energy and Fusion) are charged with monitoring the various collaborative agreements, identifying new areas for cooperation and advising the CERT on policy matters.

IEA SOLAR HEATING AND COOLING PROGRAM

The Solar Heating and Cooling Program was one of the first collaborative R&D agreements to be established within the IEA, and, since 1977, its Participants have been conducting a variety of joint projects in active solar, passive solar and photovoltaic technologies, primarily for building applications. The twenty members are:

Australia	France	Spain
Austria	Germany	Sweden
Belgium	Italy	Switzerland
Canada	Japan	Turkey
Denmark	Netherlands	United Kingdom
European Commission	New Zealand	United States
Finland	Norway	

A total of twenty projects or "Tasks" have been undertaken since the beginning of the Solar Heating and Cooling Program. The overall program is monitored by an Executive Committee consisting of one representative from each of the member countries. The leadership and management of the individual Tasks are the responsibility of Operating Agents. These Tasks and their respective Operating Agents are:

*Task 1: Investigation of the Performance of Solar Heating and Cooling Systems - Denmark
*Task 2: Coordination of Research and Development on Solar Heating and Cooling - Japan
*Task 3: Performance Testing of Solar Collectors - Germany/United Kingdom
*Task 4: Development of an Insulation Handbook and Instrument Package - United States
*Task 5: Use of Existing Meteorological Information for Solar Energy Application - Sweden
*Task 6: Solar Systems Using Evacuated Collectors - United States
*Task 7: Central Solar Heating Plants with Seasonal Storage - Sweden
*Task 8: Passive and Hybrid Solar Low Energy Buildings - United States
*Task 9: Solar Radiation and Pyranometry Studies - Canada/Germany
*Task 10: Material Research and Testing - Japan
*Task 11: Passive and Hybrid Solar Commercial Buildings - Switzerland
Task 12: Building Energy Analysis and Design Tools for Solar Applications - United States
Task 13: Advanced Solar Low Energy Buildings - Norway
Task 14: Advanced Active Solar Systems - Canada
Task 15: Not initiated
Task 16: Photovoltaics in Buildings - Germany
Task 17: Measuring and Modelling Spectral Radiation - Germany
Task 18: Advanced Glazing Materials - United Kingdom
Task 19: Solar Air Systems - Switzerland
Task 20: Solar Energy in Building Renovation - Sweden
Task 21: Daylighting in Buildings - Denmark
*Completed

Improved Measurement of Solar Irradiance by Means of Detailed Pyranometer Characterisation

D.I. Wardle
Atmospheric Environment Service
4905 Dufferin Street, Downsview, Ontario, M3H 5T4, Canada

L. Dahlgren
Swedish Meteorological and Hydrological Institute,
S-60176, Norrköping, Sweden

K. Dehne
Deutscher Wetterdienst, Meteorologisches Observatorium Potsdam
P.O. Box 600552, 14405 Potsdam, Germany, *formerly DWD, Hamburg*

L. Liedquist
Swedish National Testing and Research Institute
Box 857, S-50115, Borås, Sweden, *formerly Swedish National Testing Institute*

L.J.B. McArthur
National Atmospheric Radiation Centre, Atmospheric Environment Service
4905 Dufferin Street, Downsview, Ontario, M3H 5T4, Canada

Y. Miyake
Eko Instruments Trading Co., Ltd.
Sasazuka Center Bldg. 1-6, Sasazuka 2-chome, Shibuya-ku, Tokyo 151 Japan

O. Motschka
Zentralanstalt für Meteorologie und Geodynamik
Hohe Warte 38, A-1190, Wien, Austria

C.A. Velds
Royal Netherlands Meteorological Institute
P.O. Box 201, 3730 AE De Bilt, Netherlands

C.V. Wells
National Renewable Energy Laboratory, *formerly Solar Energy Research Institute*
1617 Cole Boulevard, Golden, Colorado 80401, USA

Solar Heating and Cooling Programme Task 9
Report IEA-SHCP-9C-2
INTERNATIONAL ENERGY AGENCY
APRIL 1996

Front cover: The NARC field calibration facility on the roof of the Atmospheric Environment Service building in Downsview.

Back cover: A pyranometer, inclined at 45°, in a ventilated housing, measuring the diffuse irradiance. The outline of the shadow of the tracking disc can be seen around the pyranometer dome.

Copies of this report, IEA-SHCP-9C-2,
are available at $65 from the

National Atmospheric Radiation Centre
Atmospheric Environment Service
4905 Dufferin Street
Downsview ON. M3H 5T4
Canada

ABSTRACT

The work of Subtask 9C-*Pyranometry* of Task 9-*Solar Radiation and Pyranometry Studies* of the IEA Solar Heating and Cooling Program is the subject of this report. Discrepancies in pyranometer calibration and characterization had been found by the participants in Task 3-*Performance Testing of Solar Collectors* and the resulting level of uncertainty in radiation measurement limited the achievement of their task. Subtask 9C was constituted to resolve these discrepancies and to demonstrate improved measurement of radiation.

The focus of the work is on determining the effects of factors other than irradiance on the signals from pyranometers, which is the meaning of characterisation in the context of pyranometry. If the charcterisation is accurate and if the interfering factors are known, then the pyranometer signal can, in principle, be corrected to give a more accurate measurement of irradiance. The report addresses non-linearity in response and the influences of the direction and spectrum of the radiation, the instrument temperature and its rate of change, the tilt of the instrument, the thermal radiation environment and the ventilation of the instrument. The physical basis and a suitable formulation of these unwanted influences are given as is a new expression of the directional response that is now adopted in the International Standards Organization document ISO 9060. Also three sets of conditions for Benchmark calibrations are defined in order to facilitate comparison of calibration techniques. Methods of characterisation that are used by the participating laboratories are examined with the purpose of assessing the accuracy of their respective results. As well, the results from different laboratories of several types of characterization on identical instruments are compared. Altogether, results from eleven laboratories on nearly thirty pyranometers of seven types have been examined.

The characterisation results and many types of comparison are presented. In some cases the agreement between laboratories is satisfactory in the sense that it is explicable in terms of the assessed accuracy of techniques used at the laboratories; in other cases the discrepancies are larger than expected. A significant conclusion is that 10-minute average measurements with an rms uncertainty of less than 20Wm^{-2} at 1000Wm^{-2} are possible but often not achieved even by the best efforts of leading radiation laboratories. This is based in part on comparisons of Benchmark calibrations on identical instruments by different laboratories. New findings from this work on offset or zero signals can significantly improve measurements of low intensity solar radiation by some of the types of pyranometer. The report includes a chapter which lists different procedures for measuring solar radiation and estimates of the associated uncertainties.

Executive Summary

This report is the outcome of Subtask C of Task 9 of the IEA Solar Heating and Cooling Program (SHCP). IEA-SHCP Task 9 -*Solar Radiation and Pyranometry Studies* was initiated in 1982 to address the continuing need for better data on solar radiation and meteorology in the assessment of the solar energy resource and for better measurements in the testing of solar converters. There were initiatially three subtasks, each coordinated by a lead country:

9A Small-Scale Time and Space Variability of Solar Radiation (Austria).
9B Validation of Solar Irradiance Simulation Models (Canada)
9C Pyranometry (Canada)

Three more subtasks were added in 1987:

9D Techniques for Supplementing Network Data for Solar Energy Applications (Switzerland)
9E Representative Design Years for Solar Energy Applications (Denmark)
9F Irradiance Measurements for Solar Collector Testing (Canada)

The origin of Subtask 9C is in IEA-SHCP Task 3 -*Performance Testing of Solar Collectors.* The particants in Task 3 found that uncertainties in radiation measurments were limiting the accuracy with which the conversion efficiency of collectors could be determined. Their investigation into the characterisation of pyranometers then revealed surprisingly large discrepancies between results from different laboratories. The goal of Subtask 9C was to resolve these discrepancies and to demonstrate the extent to which characterisation could be used to reduce the uncertainities in radiation measurement. The participating countries were Austria, Canada, Germany, Japan, the Netherlands, Sweden and the United States. Experiments were conducted on nearly all aspects of characterisation. These experiments and much of the analysis were completed prior to 1990. The conclusions are currenlty valid, not superceded by any other analysis. The recently developed Kipp and Zonen CM21 pyranometer might have been included in the study had the experiments been performed later. Due to the wide range of the work, the report is written as a general account of pyranometer characterisation. It is intended for researchers involved in radiation measurement or in solar conversion technology.

The concept of an ideal pyranometer and the departures of real pyranometers from this ideal model provide the basis for formulating the work and analysing the results. An ideal pyranometer is one that would generate an output voltage or signal V exactly

proportional to the irradiance E , with the constant of proportionality being the responsivity, R_C. Thus:

$$V = R_C \cdot E \qquad [i]$$

The behaviour of even the best available (thermoelectric) pyranometers could depart sufficiently from this ideal to generate differences of up to 10% between simultaneous measurements made with colocated pyranometers calibrated for different applications by different established meteorological institutes as reported, for example, by Task 3 in "Results of a Pyranometer Comparison", 1980.

Because the pyranometer output signal is influenced by the specific conditions under which the measurements are made (for example, ambient temperature and direction of the radiation) errors may be introduced by the simple and generally used assumption that the responsivity is the same in the application as during the calibration.

The rationale for this work, and for the earlier Task 3 project "Results of an Outdoor and Indoor Pyranometer Comparison," 1984, is that these errors can be corrected if the behaviour of the pyranometer under different conditions can be determined and if the conditions at the time of the measurement are known. For example, if it is known that the responsivity of a particular pyranometer decreases by 1% for every 6°C rise in temperature, the measurements with that pyranometer can be corrected provided the instrument temperature at the time of measurement is known.

Characterisation in this report means the determination of how the output signal depends on the conditions to which the instrument is subjected. The discrepancies in the extensive characterization data obtained from this work (as well as from the Task 3 1984 project) caused the main emphasis to be on techniques for characterisation and their accuracies rather than the demonstration of improved measurements. Parts of the original work plan of Subtask 9C were therefore postponed, being transferred into Subtask 9F. These include IEA-SHCP-9F-1 -*Using Pyranometers in Tests of Solar Energy Converters , step-by-step instructions* completed in 1995 and IEA-SHCP-9F-5 -*Improvement of Pyranometer Data by Cosine Error Corrections* completed in 1993.

The work reported here is based on a multi-laboratory approach in which results obtained at many different institutes from many different instruments are compared. In addition

to the nine authors representing eight separate organisations, workers from six other organisations, including two manufacturers, have participated. Pyranometers were lent to the co-ordinating laboratory (the National Atmospheric Radiation Laboratory(NARC) of Canada) by four manufacturers and by three of the institutions which had participated in Task 3. Nearly thirty pyranometers have been tested by more than one laboratory; seventeen have been tested by at least four laboratories. This has enabled discrepancies to be evaluated and estimates to be made of the accuracy of different characterisation techniques. Characterisation assessments have been made on the same group of pyranometers by different organisations whenever possible and the expert participants have used their own methods of choice with no attempt being made to force them to adopt the same protocols.

The pyranometer response function (defined as the expression of the output signal of a pyranometer subjected to various conditions as a function of variables that describe those conditions) is fundamental in this study. Characterisation of a pyranometer provides the data from which its response function can be specified. The response function of a real pyranometer is inevitably more complex than Equation i, on page ii, which is the response function of an ideal pyranometer.

This study has considered the influence of the following variables on pyranometer output:

$\underline{s}$ direction of the incident radiation

T temperature of the pyranometer

β tilt of the pyranometer from the horizontal

E level of irradiance (this allows non-linearity to be specified),

λ wavelength of the radiation

P net thermal radiation (i.e., the difference between the downward long-wave radiation and black-body radiation at the temperature of the instrument

$\dot{T}$ rate of change of temperature

Ventilation — the air flow regime around the pyranometer.

The following response function has been used to accommodate these variables:

$$V = R_0 \cdot F_S \cdot F_T \cdot F_{\not\!E} \cdot F_\lambda \cdot (E + Z) \qquad \text{[ii]}$$

in which the symbols represent:

R_0 responsivity in some specified (possibly benchmark) conditions.

F correction factors which are each functions of the subscript variables. They are equal to unity in the conditions for which R_0 is specified and would be equal to unity in all conditions if the pyranometer were ideal.

Z an offset equivalent irradiance - the error that would be caused by assuming that a pyranometer gives a zero signal when the irradiance is zero (the dependence of this offset on long-wave irradiance and rate of change of ambient temperature has been studied together with the influence of ventilation on the dependence).

The rigorous definitions in this response function, and a brief physical explanation of why the variables can be separated in this way, are given. The characterisation measurements in this work can be accommodated by this formulation down to the noise level which is usually in the range 1-2 Wm^{-2}.

The independent variables are not all of the same type, for example:

Instrument Tilt

Instrument Tilt is well-understood and usually chosen specifically by the experimenter so that, if the correction factor for pyranometer tilt has been accurately measured, the correction to the measurement is immediately available.

Irradiance Level

Irradiance Level (E) is similar to instrument tilt, being a variable that is always known to an accuracy that permits a correction for non-linearity to be made.

Temperature

Temperature differs from instrument tilt because there may be significant uncertainty in its value, either because of inaccurate measurement or because no measurements are taken. Correction to the irradiance measurement for the effect of temperature has two components of uncertainty: that deriving from the uncertainty in method of characterisation and that which results from uncertainty in the actual temperature. This is not a trivial consideration. For example, a type of pyranometer which (from most viewpoints) performs extremely well in normal temperatures has a very high coefficient of responsivity change with temperature at low temperatures so that an uncertainty of 5°C in the instrument temperature at -30°C overrides all other sources of error.

Direction of the Incident Radiation

Direction of the Incident Radiation differs in nature from the preceding types of variable. Under laboratory conditions, an illuminating beam of radiation may be established from only one direction but, in the field, radiation comes from all directions. This multi-directionality is handled properly in the formal definitions given in this report and, if the radiance distribution at the time of measurement is known precisely, the appropriate correction can be derived from the directional characterisation. It is important to note that under field conditions the operator does not usually know much about the radiance distribution. The accuracy of a particular irradiance measurement, therefore, depends on both the accuracy in directional characterisation and the extent to which the radiance distribution (which may be expressed statistically) is known. It is important to note that a pyranometer which has a good directional response will generate smaller irradiance measurement errors than an instrument which does not have uniform directional response, no matter how well characterised the latter may be.

Spectral Distribution of the Radiation

Spectral Distribution of the Radiation, like radiance distribution, cannot usually be described by a single variable but does not lead to significant uncertainties in measurements by thermoelectric pyranometers. This is due to the combination of the relatively mild spectral non-uniformity in response and the small variability in spectra of natural short-wave radiation.

Concerning the response equation (Equation ii), the subtask work can be summarised in relation to each term as follows:

R_0 Benchmark conditions have been defined in the report to represent a "standard" solar testing configuration and a "standard" meteorological configuration and one other configuration. Extensive comparisons on the determination of responsivity (R_0) for these conditions on identical instruments have been made between different institutions. The results generally show standard deviations of ~1.0% indicating that the inter-laboratory discrepancies do not originate solely because calibrations were undertaken under different environmental conditions. However, the large discrepancies noted during the early 1980s can be ascribed to differences, for different types of pyranometer, between these two "standard" benchmarks.

In addition to comparing benchmark calibrations, the report contains an extensive matrix of calibration results undertaken by about twelve institutes, sometimes using several methods, on identical instruments. The matrix identifies systematic differences between calibrations by different institutions.

Fs Directionality is usually the main source of measurement errors. A new specification of directional errors has been formulated called the "1000 Wm^{-2} absolute directionality error" which has several advantages over the traditional *cosine error*. For example, it directly expresses the maximum irradiance measurement error that could occur in outdoor conditions if directionality were ignored. Some of the authors would like to see the *cosine error* expression replaced but there is not a consensus on this.

Laboratory characterisation techniques have been documented and results compared showing that, particularly with the better pyranometers, discrepancies

between results from three or four laboratories amounted to only 3-4 Wm^{-2} in the 1000 Wm^{-2} directionality error.

Field measurements of directionality usually apply to global radiation and have to be converted, using assumptions about the sky radiance distribution, to enable comparison with laboratory measurements. The field measurements were principally made at two institutes and the results show more variability than those from laboratories. The agreement between field and laboratory characterisation is satisfactory in many cases. There are however some clear differences which may be caused by non-linearity and other effects but these cases have not been analysed in detail.

F_T Large, unanticipated discrepancies of 2-3% were found between some laboratories although in the limited temperature range of 0-30°C these were smaller. The mandate for Subtask 9F includes provisions for improving the techniques for temperature characterisation.

$F_{\beta,E}$ Laboratory measurements of both non-linearity and tilt are generally satisfactory with a discrepancy of less than 3 Wm^{-2}.

F_λ Laboratory tests were made on responsivity as a function of lamp spectrum. Definitive results were obtained which are attributed to the known spectral properties of the glass and of the black or black and white surfaces in the pyranometers. The spectral non-uniformity of thermoelectric pyranometers used in natural radiation is not a significant source of error.

Z The offset signal in pyranometers exposed to the night sky was studied statistically and related to long-wave radiation and ambient temperature change. Specific field experiments were also undertaken to examine the effect of changing the long-wave radiation, and both the long-wave radiation and temperature change (thermal shock) were studied in the laboratory.

P Results on long-wave radiation obtained using different techniques and from different laboratories agree quite well. The agreement is best, and the influence least, when pyranometers are enclosed in ventilated housings where the effect is about the same for most double-dome pyranometers (i.e., *circa* 2.0-2.5% of the net thermal radiation). The offset signal recorded under natural observing conditions will then vary between zero and 4 Wm^{-2}, depending on the infrared condition of the sky.

$\dot{T}$ Results for temperature change and thermal shock are rather variable which may reflect the difficulties of establishing identical thermal conditions in different laboratories and/or in the field. Some types of pyranometer are significantly worse than others with respect to this characteristic. Generally, a change of 10°C during one hour induces an offset signal of less than 4 Wm^{-2}.

Ventilation It is strongly recommended that pyranometers be enclosed in a ventilated housing which reduces variability in the offset signals caused by long-wave radiation and changes in temperature.

Although the complete treatment of measurement errors arising from directionality and sky radiance distributions has been left to Subtask 9F, some approximate estimates suggest that overall uncertainties in the range 20-40 Wm^{-2} (2σ) can be achieved with several of the better pyranometers. (These values refer to ten-minute averages when the irradiance is high. e.g. 10-20 Wm^{-2}rms at 1000 Wm^{-2}.)

The potential levels of accuracy attainable using instruments of different levels of quality and complexity are estimated. These estimates should be useful for determining strategies and instrumental requirements needed to achieve a given level of performance.

The findings of the report do not contradict the conventional and established wisdom that the most accurate method of measuring global irradiance requires two instruments: a cavity radiometer (measuring direct irradiance) and a good pyranometer equipped with a tracking, shading disc (measuring diffuse irradiance). The global irradiance can then be derived from the sum of the direct and diffuse components.

Some have expressed concern that pyranometer ageing (the change in responsivity with time) is a serious problem introducing errors that may reach ~4% annually. The authors believe that this assessment is not realistic and that changes in responsivity greater than one percent per year are unusual. However, it is probable that some small instabilities in responsivity will have occurred during the work and contributed to the inter-laboratory discrepancies.

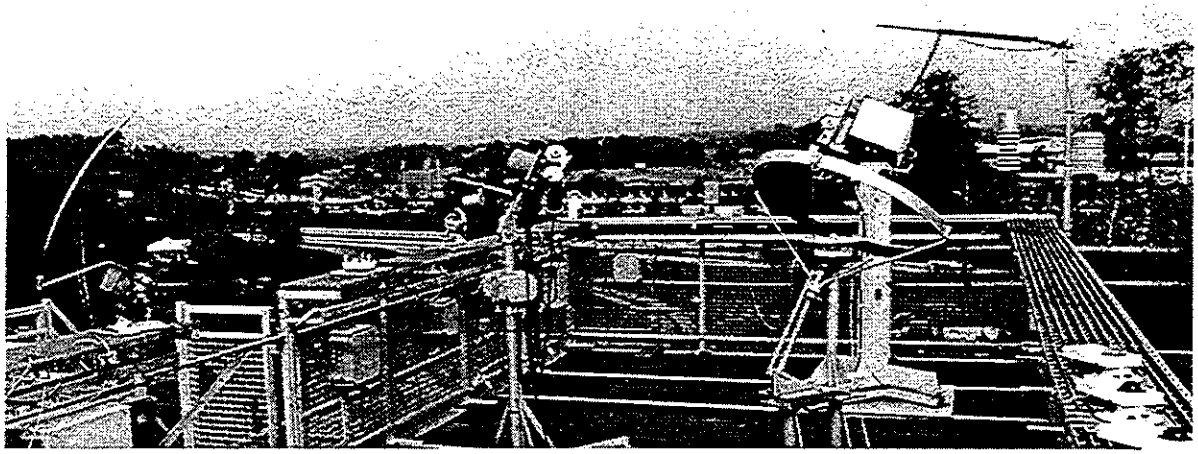

Roof of the Swedish Meterological and Hydrological Institute, Norrköping, Sweden.

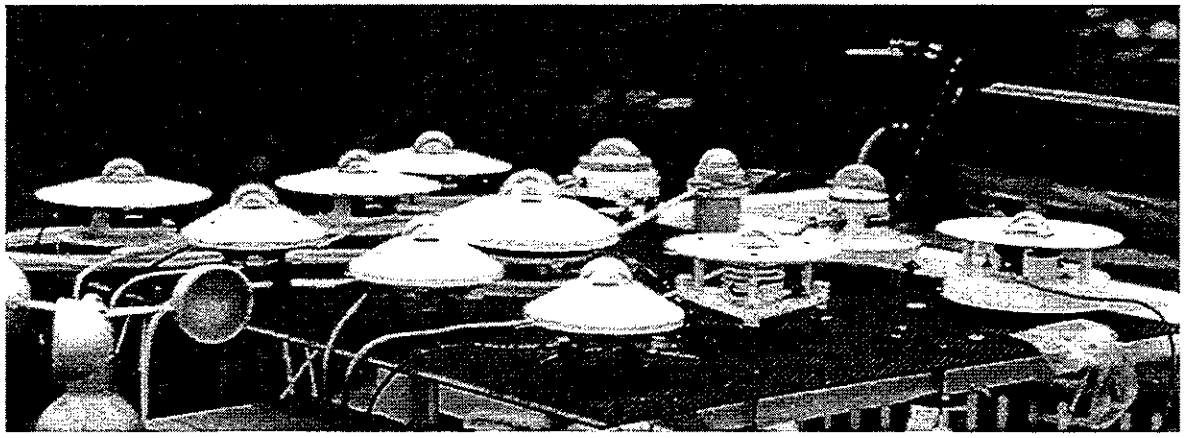

Pyranometers at the National Technology Institute (TNO), Delft, Netherlands.

Table of Contents

Abbreviations of Institutes, Instruments and Others

Abbreviation	Institute, Laboratory, Centre etc.
AES	Atmospheric Environment Service, Government of Canada
"Austria"	see ZFMG
"Boras"; "BO"	see SP
"Davos"; "DA"	see WRC
DFVLR	*Deutsche Forschungs- und Versuchsanstalt für Luft- und Raumfahrt.*, Stuttgart, Germany
DWD	*Deutsch Wetterdienst*: German Weather Office, see MOH
"Delft"	Kipp & Zonen
DSET	Desert Sands Environmental Testing Laboratory, New River,Arizona, USA
"Eppley"	The Eppley Radiation Laboratories, Rhode Island, USA. (included here because it participated as a testing laboratory)
"Hamburg"; HA"	MOH
"Kipp"; "KI"; K&Z	Kipp & Zonen, Delft, Netherlands. (included here because it participated as a testing laboratory)
KNMI	*Koninklijk Nederlands Meteorologisch Instituut*, see RNMI
MOH	*Meteorologisches Observatorium Hamburg*; DWD (Meteorogical Observatory at Hamburg, now located in Potsdam)
NARC	National Atmospheric Radiation Centre of AES
"Norrk"	see SMHI
NREL	National Renewable Energy Laboratory, Golden, Colorado, USA
RNMI	Royal Netherlands Meteorological Institute, de Bilt. (KNMI)
SERI	Solar Energy Research Institute, now NREL
SP	*Statens Provningsanstalt*, Borås, Sweden. (National Testing Institute)
SRF	Solar Research Facility, National Oceanic and Atmospheric Agency, Boulder, Colorado, USA
SMHI	Swedish Meteorological and Hydrological Institute, Norrköping
TPD/TNO	Technical Physics Office of the National Technology Institute, Delft, Netherlands.
"Toronto"; "TO"	see NARC
"Vienna"; "VI"	see ZFMG
WRC	World Radiation Centre, Davos, Switzerland
ZFMG	*Zentralanstalt für Meteorology und Geodynamik*, Vienna, Austria

Abbreviation	Pyranometer
CM5	Kipp & Zonen CM 5, black two-dome instrument, identical to CM 6 except for sun-shield for body
CM10	Kipp & Zonen CM 10, black two-dome instrument, identical to CM 11 except for sun-shield for body
CSIRO	see PT
Eko	see MS-42
"Eppley"	see PSP
EP07	Middleton EP 07, black two-dome instrument.
"Kipp"	see CM5, CM10
"Middleton"	see EP07
MS-42	Eko black and White instrument (single dome)
MS-801	Eko, Prototype pyranometer, not generally tested in this study
NIP	Normal Incidence Pyrheliometer
PSP	Eppley "Precision spectral pyranometer", black two-dome instrument.
PT	Proctor- Trickett developmental black pyranometer lent by Dr David Proctor of CSIRO, Australia.
"Schenk"	see Star
Star	Schenk Star black and white one-dome pyranometer
SS-25	Swissteco SS-25
"Swissteco"	see SS-25

Abbreviation	Miscellaneous
ASM	Alternating shade method of pyranometer calibration
CSM	Component summation method of calibration
SDGM	Simultaneous diffuse and global method of calibration
rms	Root mean square
WRR	World Radiometric Reference (maintained at Davos by WRC)

Symbols, definitions, units, sections, equations

Symbol	Definition	Unit	Section	Equ'n
A	coefficient in regression of Z	Wm^{-2}	1.5	1.5
B	coefficient in regression of Z	-	1.5	1.5
C	coefficient in regression of Z	$Whm^{-2}K^{-1}$	1.5	1.5
a	coefficient in expression of heat balance	$Wm^{-2}K^{-1}$	2.3	2.6
b	coefficient in expression of heat balance	$Wm^{-2}K^{-2}$	2.3	2.6
c	coefficient in expression of heat balance	$Wm^{-2}K^{-2}$	2.3	2.6
C	Calibration factor– reciprocal of responsivity	$Wm^{-2}\cdot mV^{-1}$	4.2.1	
C_{35} , C_D	Calibration factors for global radiation at solar elevation 35° and for diffuse radiation.	$Wm^{-2}\cdot mV^{-1}$	4.2.1	4.11
D	Diffuse irradiance	Wm^{-2}	4.2.1	4.11
$D_{\max}(\theta,\phi)$	range of variation of cosine error with azimuth	%	4.1.1	4.7
E	Irradiance	Wm^{-2}	1.2	1.1
E_l	Downward long-wave irradiance	Wm^{-2}	6.1	
$E_\lambda(\lambda)$	Spectral irradiance	$Wm^{-2}nm^{-1}$	7.2	7.8
F	Corrections to standard responsivity R_0 for :	-	1.5	
$F_{\underline{s}}(\underline{s})$	—for the direction of incident radiation	-	1.5	1.3
$F_T(T)$	—for the temperature of the pyranometer	-	1.5	1.3
$F_{\beta E}(\beta,E)$	—for instrument tilt and non-linearity	-	1.5	1.3
$F_\lambda(\lambda)$	—for wavelength of incident light	-	1.5	1.3
G	Global radiation	Wm^{-2}	4.2.2	4.14
H	absorbed power per unit area of receiver surface	Wm^{-2}	2.3	2.5
h	solar elevation	-	4.2.1	4.11
I	Direct beam normal incidence irradiance	Wm^{-2}	4.2.1	4.11
K	A heat conductivity factor in a pyranometer	$Wm^{-2}K^{-1}$	2.3	2.4
$L(\theta,\phi)$	Distribution of radiance	$Wm^{-2}sr^{-1}$	7.2	7.9
$M(\theta,\phi)$	Signal during a laboratory test of directionality	μV	4.1.1	4.3

continued..

..continued

Symbol	Definition	Unit	Section	Equ'n
P	long-wave effective irradiance	Wm^{-2}	1.5, 6.1	1.4
$Q_x(x)$	*error term* $=1-F_x(x)$, where x is any of the standard input variables	-	7.3	7.11
p	coefficient of thermoelectric potential	μVK^{-1}	2.4	2.9
q	coefficient of thermoelectric potential	μVK^{-2}	2.4	2.9
R	Responsivity of a pyranometer	$\mu VW^{-1}m^2$	1.4	1.2
R_0	Responsivity at defined conditions	$\mu VW^{-1}m^2$	1.5	1.3
R_C	Responsivity, a single (constant value).	$\mu VW^{-1}m^2$	1.2	1.1
$R(\theta,\phi)$	Responsivity for beam radiation from a specified direction	$\mu VW^{-1}m^2$	4.1	4.1
R_D , R_G	Responsivity of a pyranometer measuring diffuse radiation and.global radiation	$\mu VW^{-1}m^2$	4.2.2	4.13
R_N	Responsivity of a pyrheliometer	$\mu VW^{-1}m^2$	4.2.2	4.13
$\underline{s}$	Direction of radiation	-	1.5	1.3
$\underline{s}^*$	Symbol for a radiance distribution	-	7.2	7.9
t , δt	time, small increment in time	s	6.1	-
T	Temperature	K	1.5	1.3
T_0	A standard temperature	K	2.3	2.1
T_a , T_i	Ambient temperature, instrument temperature	K	6.1	
T_{pyg}	Pyrgeometer temperature	K	6.1	
$\dot{T}$	Rate of change of temperature	Kh^{-1}	1.5	1.3
ΔT	Temperature above a standard temperature	K	2.3	2.1
δT	Temperature across a thermopile	K	2.3	2.1
V	Output voltage (from a pyranometer)	μV	1.2	1.1
V_{out}	Percentage of total signal change achieved t seconds after an irradiance change	%	5.2	5.1
V_D , V_G	Output voltage from a pyranometer measuring diffuse radiation, global radiation	μV	4.2.2	4.13
V_N	Output voltage from a pyrheliometer	μV	4.2.2	4.13
V_Z	Output voltage with no irradiance	μV	1.4	1.2
Z	Zero-offset irradiance $Z=V_Z/R$	Wm^{-2}	1.4	1.2

continued..

..continued

Symbol	Definition	Units	Section	Equ'n
β	Tilt of a pyranometer, normal horizontal is $\beta = 0$	-	1.5	1.3
$\beta(\theta)$	Equivalent out-of-level angle from variation of responsivity with azimuth	-	4.1.1	4.8
Δ	difference between results from two laboratories		4.1.3	4.9
$\Delta_{max}(\theta)$	maximum difference between results from two laboratories of the *1000 watt absolute error.*	Wm^{-2}	4.1.3	4.10
$\delta(\theta,\phi)$	directional error, *cosine error*	%	4.1.1	4.1
$\bar{\delta}(\theta)$	azimuth averaged cosine error	%	4.1.1	4.6
$\delta_E(\theta,\phi)$	absolute directional error with irradiance E	Wm^{-2}	4.1.1	4.4
$\delta_t(\theta,\phi)$	*1000 watt absolute directioal error*	Wm^{-2}	4.1.1	4.5
$\bar{\delta}_t(\theta)$	azimuth-averaged $\delta_t(\theta,\phi)$	Wm^{-2}	4.1.1	4.6
$\Delta\bar{\delta}_t(\theta)$	difference between values from two laboratories of the azimuth-averaged 1000 watt absolute error	Wm^{-2}	4.1.3.1	4.9c
$\ddot{\delta}_G$	*cosine response* for global radiation. (responsivity compared with responsivity at solar altitude, h=35, for global radiation.)	-	4.2.1	4.11
$\ddot{\delta}_I$	as above for direct beam radiation	-	4.2.1	4.12
Φ	Thermoelectric potential	μV	2.4	2.8
ϕ	azimuth of radiation on a pyranometer	-	1.5	1.3
λ	wavelength	nm	1.5	1.3
λ^*	indicating a spectrum	-	7.2	7.8
θ	incidence angle of radiation on a pyranometer	-	1.5	1.3
θ	solar zenith distance (same as above if the pyranometer is in the usual horizontal orientation).	-	7.3.2	7.16
σ	Stefan's constant ($5.6697\ 10^{-8}$)	$Wm^{-2}K^{-4}$	2.3	
σ	Standard deviation	-	1.1	
Ψ	fractional linear temperature coefficient of responsivity	K^{-1}	5.8	5.3

concluded

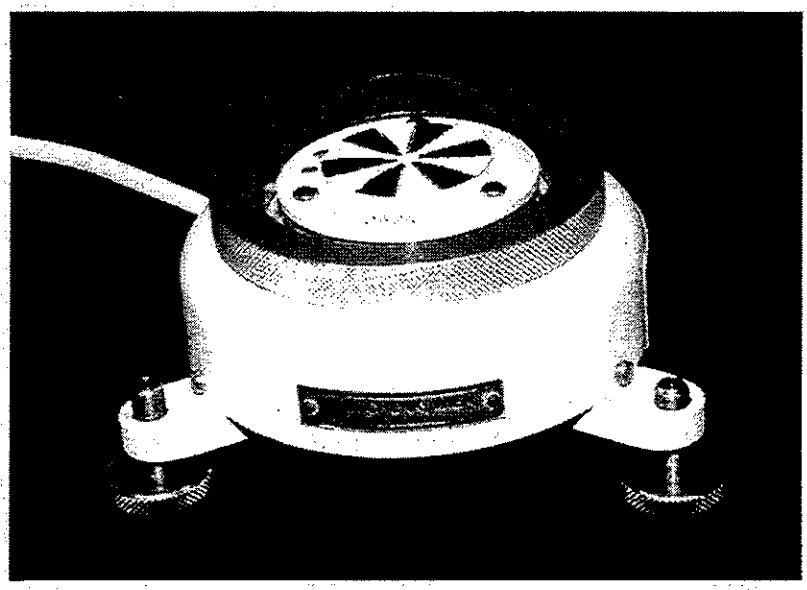

Schenk Star

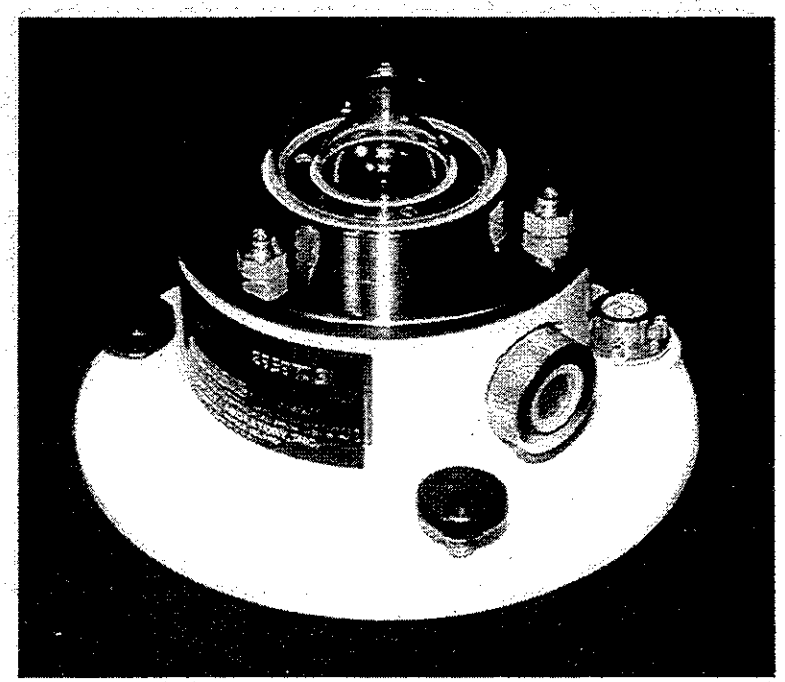

Eppley PSP

Foreword: Subtask 9C and this report

IEA SHCP Subtask 9C -*Pyranometry* was initiated because work in IEA SHCP Task3 -*Performance Testing of Solar Collectors* had shown that the quality of radiation measurements was generally inadequate for testing solar collectors.

The plan for Subtask 9C was to demonstrate the use of characterisation to improve measurements made with pyranometers. The central problem is the unwanted response of pyranometers to factors other than irradiance. In the context of this report, therefore, the word characterise means to determine the quantitative effect of these factors on the output voltage from the pyranometer.

The methodology of Subtask 9C relies heavily on comparing calibrations and measurements of characteristics made on the same group of pyranometers by many radiation laboratories, including those of five national radiation centres. Discrepancies between instruments and laboratories are analysed to indicate the nature of uncertainties in the measurement of radiation. A similar approach had been used in the earlier Task 3 project "Results of an Outdoor and Indoor Pyranometer Comparison," reported in 1984.

Chapter 1 describes the background to the work and also introduces the transfer function, which assimilates the results of characterisation measurements. The physical origins of the unwanted pyranometer responses are examined in Chapter 2, which completes the introductory material. The activities of the main participants are described in Chapter 3.

Characterisation methods and their accuracy are addressed in Chapters 4, 5 & 6. These comprise more than half of the main report. Additional information, particularly on the influence of the direction of the radiation, is given in four appendices.

The transfer function is revisited in Chapter 7, which includes a formal derivation and a simple example of using the transfer function to evaluate measurement uncertainty.

Calibration results are compared and analysed in Chapter 8. These include 150 comparisons of results from established calibration routines and 33 comparisons of benchmark calibrations that were specifically designed for this study.

Different ways of measuring irradiance with pyranometers are listed in Chapter 9, together with potential accuracies. This may be useful to those who have to make the best choice of equipment subject to limited resources.

Chapter 10 identifies what has, and has not, been achieved with regard to characterisation, calibration and the original objective

The Bibliography at the end of the report lists several IEA SHCP documents from Task 3 and Task 9 that are related to this study.

Chapter 1. Introduction

1.1 Background, thermoelectric pyranometers

Pyranometers are instruments designed to measure solar radiation in the atmosphere. Their most common application is to measure the downward solar irradiance (global radiation) for which they are mounted in the standard horizontal orientation. Pyranometers are often inverted so as to measure the upward horizontal irradiance which is the solar radiation reflected by the ground. Solar energy applications of pyranometry include these as well as measurements that require the instrument to be tilted so as to study the efficiency of tilted flat plate collectors. Another application in solar energy is the measurement of radiation from solar simulators. These applications are all limited, in some aspects, by the uncertainty of pyranometer measurements.

Thermoelectric pyranometers are generally more accurate than the other main class which is photoelectric and are the subject of this report. In thermoelectric pyranometers the measurement is based on the rise in temperature of a some black-painted surface that is exposed to the radiation. The output signal is a voltage generated by a thermopile from the temperature difference between this black surface and some other part of the instrument that is either not exposed to the sun or is a similar surface painted white so as not to absorb radiation from the sun. The latter arrangement results in a *black-and-white* pyranometer; the surfaces are usually divided into several segments and interspersed. The others are called *black* pyranometers. Both types are equipped with at least one transparent dome so as to isolate the black surface from the effects of the local environment, especially the wind. This report focuses on two *black-and-white* and five *black* pyranometer models.

1.2 Response function, characterisation and measurement uncertainty

The title *The Improved Measurement of Solar Irradiance by Detailed Characterisation of Pyranometers* implies that the simple function

$$V = R_C \cdot E \qquad [1.1]$$

output [μV] = responsivity [μV·W^{-1}m^2] · irradiance [Wm^{-2}]

with a constant value (R_C) for the responsivity, does not describe the response of pyranometers to the required accuracy. An accuracy of 20 Wm^{-2} (2σ), equivalent to being

95% confident that a measured value is within ±20 Wm^{-2} of the true value, is widely considered to be adequate for testing collectors and exceeds that which has been generally achievable to date. This task group therefore adopted a value of 20 Wm^{-2} (2σ) as its target and shows that this is achievable in some limited circumstances.

A response function of a pyranometer is an expression of its output signal in terms of the radiation to which it is exposed and of any other factors that affect the signal.

Clearly Equation 1.1 is a response function. It is very simple and it states that the signal is proportional to the irradiance which is what a pyranometer is intended to measure. It also implies, by the absence of any other variables, that the signal depends on the irradiance alone. Equation 1.1 therefore represents the behaviour of an ideal pyranometer. In order to compute the irradiance from the signal of such an instrument, one would merely divide the signal by the responsivity.

Irradiance measurements are almost invariably computed by dividing pyranometer signals by constant responsivities. This can generate significant errors because Equation 1.1 does not, as already stated, accurately represent the signals from real pyranometers. With some pyranometers now in use these errors can be as large as 50 Wm^{-2}, or 5% of the maximum irradiance.

The essential work of Subtask 9C has been to investigate the development of response functions which more accurately represent pyranometer signals and the extent to which measurement uncertainty can be quantified and, more importantly, reduced by using these.

A response function characterises a pyranometer in the sense that it describes the behaviour of the instrument. However, in the context of this report, characterisation more often means the investigation and measurement of the effects different factors have on the output signal. In this sense, the response function is built on the results of characterisation experiments.

It is important to note at this early stage that even a complete characterisation and a corresponding absolutely accurate response function will not eliminate error unless the conditions under which the measurements are taken are completely specified. In practice, when the best available response function is used, the remaining overall uncertainty includes contributions from both the uncertainty in the response function and also the input variables to the function. These components will be called the "Characterisation

Uncertainty" which comes from not knowing the properties of the instrument and the "Specification Uncertainty" which comes from not knowing the conditions in which the instrument is used. The latter is often the dominant component.

1.3 Work plan

The work was based on a multi-laboratory study of the response function and its inversion to derive irradiance from the pyranometer signal. It depended upon the ability to measure key influences on the response of pyranometers (i.e., in order of importance: directionality; temperature; tilt; linearity; colour, etc.) and on inter-laboratory comparisons of Benchmark Calibrations made under field and laboratory conditions.

As work progressed a number of considerations necessitated departures from the original plan.

- Preliminary results showed that there were greater discrepancies in the response functions than had been expected (not only between those obtained under field and laboratory conditions, but also within each category) and, as a consequence of this, the group assigned priority to evaluating the errors in pyranometer characterisation.
- Although the errors that derive from the inversion of the response function did not receive the attention that they deserve, the modelling exercises, reported in 7.3, form a sound basis for further work. IEA-SHCP-9F-5 -*Improvement of Pyranometer Data by Cosine Error Corrections (1994)* is a good example.
- The exchange of pyranometers between institutes was limited by logistic considerations so that whilst adequate it was less than optimal and the inter-laboratory comparison was not therefore as comprehensive as intended.
- Although the report shows that there has been a substantial improvement in calibration uniformity since the late 1970s, the intention was to have a clearer demonstration of the standards now achievable by having leading research groups test the methods developed here. This is scheduled in further task studies and is beyond the current scope.
- The problem of instrumental ageing was not subject to a dedicated experiment as planned and is also scheduled for future programs.

1.4 The form of the response function

Derivations with more detail are given later. In particular, Chapter 7 covers the general definition, Chapter 6 deals with the offset more thoroughly and details of the description are given in Chapter 4. Equation 1.1 does not accommodate the following aspects of the behaviour of real pyranometers:

1. There is an offset between the zero of the signal and the zero of the irradiance such that in the absence of radiation there is a signal output (V_z) which is known as the *dark signal.* A definite radiation input ($-Z$) is therefore needed to generate a zero output signal.

2. The output is influenced by the pyranometer's environment (i.e., temperature, long-wave radiation, wind, etc.) and by the nature of the radiation (i.e., direction, wavelength, etc.).

3. Even when all other factors are held constant, the relationship between the output signal and the input irradiance is not usually linear as indicated by Equation 1.1.

The zero offset is accommodated by writing either:

$$V = R \cdot E + V_z \qquad [1.2a]$$

or:

$$V = R \cdot (E + Z) \qquad [1.2b]$$

which are equivalent and in which

$$V_z = R \cdot Z \qquad [1.2c]$$

The dependence on other variables (2) and the non-linearity (3) are also accommodated by Equation 1.2 if the responsivity R is regarded as a function of those variables and of the irradiance. In effect, the equation defines both the responsivity and the zero offset and both are functions of several variables.

In this work there are about eight variables which have been identified as influencing R or Z. Fortunately their effects are largely independent and this allows R to be expressed as a product of a number of simple functions and Z as the sum of a few terms. The separation will be given in the next paragraph after listing the variables.

1.5 The independent (input) variables

The following influences on the responsivity have been identified in this work:

$\underline{s}$ or θ and ϕ	which describe the direction of the radiation
T	temperature of the instrument
β	tilt of the instrument
E	irradiance (which allows non-linearity to be specified)
λ	wavelength of the radiation.

In addition, effects on the offset by the following have been measured:

P	net thermal radiation (defined in Chapter 6)
$\dot{T}$	rate of change in ambient temperature
also the	ventilation imposed on the pyranometer (i.e., whether or not the instrument is mounted in a ventilated housing)

The following separation has been found to be sufficiently accurate:

$$R(\underline{s},T,\beta,E,\lambda) = R_0 \cdot F_{\underline{s}}(\underline{s}) \cdot F_T(T) \cdot F_{\beta E}(\beta,E) \cdot F_\lambda(\lambda) \qquad [1.3]$$

where R_0 is the responsivity under a specific standard set of conditions, and the remaining terms in the product are correction factors expressing the requisite modification to R_0 because the specific conditions differ from standard. The correction factors equal unity when the variables represent standard conditions and approximate unity (i.e. between 0.9 and 1.1) in most other cases. Substitution of Equation 1.3 into Equation 1.2 gives

$$V = R_0 \cdot F_{\underline{s}}(\underline{s}) \cdot F_T(T) \cdot F_{\beta E}(\beta,E) \cdot F_\lambda(\lambda) \cdot [E + Z(P,\dot{T},\text{ventilation})] \qquad [1.4]$$

which is the general form of the response functions used in this report. Further, the offset has been parameterised by:

$$Z(P,\dot{T},vent) = A + B \cdot P + C \cdot \dot{T} \qquad [1.5]$$

where A, B and C are constants for given ventilation.

1.6 Uncertainties of characterisation and specification

Figure 1.6 shows a hypothetical characterisation of responsivity versus temperature — the two curves being $R(T) \pm \Delta R$ where ΔR is the uncertainty in the measured responsivity $R(T)$. The temperature range of the characterisation and potential use of the pyranometer is $T_{low} < T < T_{high}$. When the instrument is in use, the irradiance E is derived from the signal V according to $V - V_z = R \cdot E$ and clearly the signal, the dark signal V_z and the responsivity all have uncertainties that affect irradiance measurements. However, in most circumstances the error in the signal measurement (voltage) is negligible and, in what follows in this section, the uncertainty in the dark signal will be disregarded.

The uncertainty in responsivity has two components: ΔR caused by imperfect characterisation and $\Delta T \cdot \mathrm{d}R/\mathrm{d}T$ which may arise because the temperature is known only with a range $\pm\Delta T$. These two components can be called *uncertainty of characterisation* and *uncertainty of specification*. There is no *a priori* reason for one to be larger or smaller than the other. They are most likely independent and the equation in Figure 1.6 shows their combined effect on the measurement uncertainty in this case.

Figure 1.6 also shows the uncertainty if the temperature were known only to the extent of being within the operating range $T_{low} < T < T_{high}$. It is represented by the full range of plotted responsivity values. This would also be the range or error that would be in effect without characterisation. Thus the figure shows the overall improvement from using temperature characterisation.

Similar considerations apply for the other input variables, although the specification uncertainties for instrument tilt and linearity are negligible. For temperature it is advisable to use the instrument temperature rather than the air temperature. In the special case of the CM 10 at temperatures lower than -30°C, it is important to measure the instrument temperature with an accuracy better than 1°C because the responsivity is very sensitive to temperature.

Describing the directional properties of the incident radiation is itself a problem, one which is addressed, and formally solved, in Chapter 7 by defining the variable $\underline{s}^*$. However, the information implicit in the definition is most unlikely to be available. In the absence of that information, it is often assumed that diffuse radiation is isotropic. The radiance distribution from the sky is then specified as just two scalar variables, the direct beam

radiation and the diffuse (isotropic) radiation. In any event, it is clear the uncertainty of specification of directionality can be, and often is, a significant source of error.

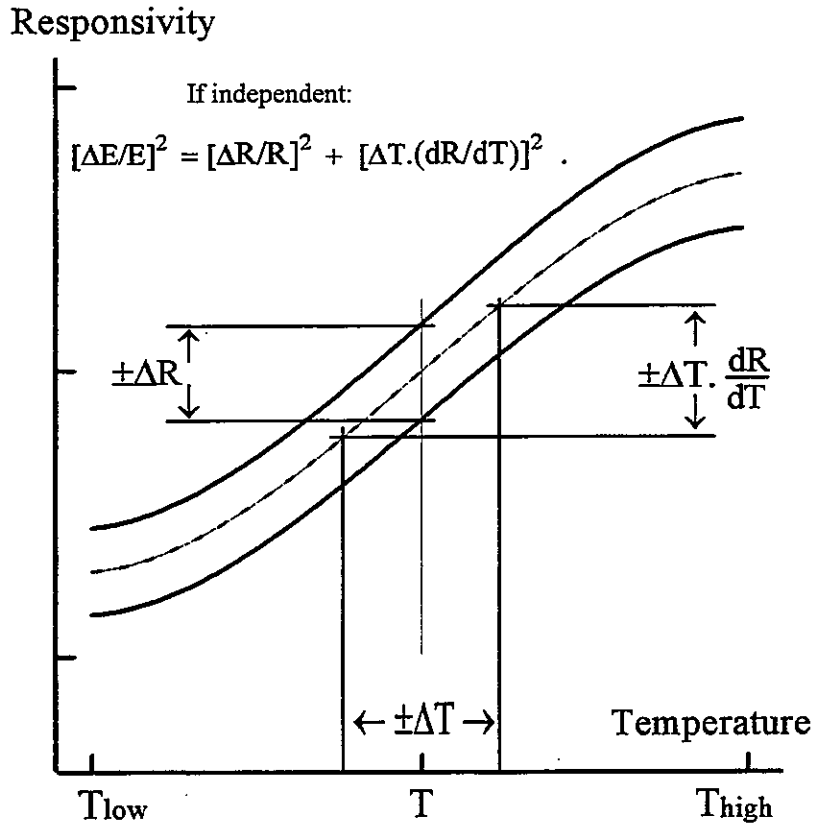

Figure 1.6: Illustrating Uncertainties of Specification and Characterization.

Chapter 2. The Physical Origins Of Non-Ideal Behaviour in Pyranometers

2.1 Introduction

Characterising the extraneous dependencies of the pyranometer output signal - which should be a linear function of incident irradiance alone - and correcting measurements for their effect, is the central subject of this report. If the causes of these unwanted dependencies, or aberrations, can be understood it will facilitate the development of characterisation techniques. The two together - understanding, and good characterisation - are both essential if improved pyranometers are to be developed.

This section addresses the causes of the aberrations in terms of four processes which occur in the pyranometer and which comprise a staged development of the output signal generated from the incident radiation. There are gaps in our knowledge of pyranometer behaviour and this account is of necessity incomplete but, to the writers' belief, there is no other which offers a treatment of this wide range of aberrations. Those under consideration are essentially as introduced in Chapter 1, namely:

$\underline{s}$	directionality
T	temperature dependence
β	tilt dependence
E	non-linearity
λ	spectral dependence
zero-offset signal	and its dependence on both long-wave radiation E_λ and temperature change T
signal delay	i.e., the time lag between a change in irradiance and the corresponding change in output voltage

where the symbols refer to the appropriate independent variables. The four processes occurring on the pyranometer are:

I. transmission of the radiation through the dome(s)

II. absorption of the radiation (usually by black paint)

III. generation of the temperature difference between the hot and cold junctions of the thermopile

IV. generation of the output voltage by the thermopile.

These operate in a cause-and-effect progression in the sense that the input for each process is the output from the preceding one. Thus, the output voltage occurs because of a temperature difference across the thermopile which is caused by absorption of radiation which has passed through the glass domes of the pyranometer. Also, the input to the first process is the incident irradiance which is to be measured. Each process can contribute to various aberrations and it is unlikely that those arising in one process will be cancelled by opposite effects in another process.

The potential contributions of each process to the aberrations are indicated in Table 2.1. From this it is evident that directional and spectral aberrations can be attributed uniquely to processes I and II; Process III may contribute to all other listed aberrations; and Process IV may contribute only to the temperature aberration and non-linearity. The nature of these effects will be considered in the following sections where it is demonstrated that special linkages exist between non-linearity and both temperature and tilt dependence.

Table 2.1

Process Short Name / Aberration Dependence On	I. Radiation Transmission	II. Radiation Absorption	III. Temperature Divergence	IV. Electrical Conversion
Direction	**yes**	**yes**	no	no
Temperature	no	no	**yes**	**yes**
Tilt	no	no	**yes**	no
Non-Linearity	no	no	**yes**	**yes**
Spectral	**yes**	**yes**	no	no
Offset	no	no	**yes**	no
Signal Delay	no	no	**yes**	no

2.2 Processes I and II: the transmission of radiation through pyranometer domes and its absorption by the receiver surface

The glass and paint used in pyranometers are essentially linear and instantaneous in their responses Over the temperature range in which pyranometers operate, the glass transmittance and paint absorbance do not change significantly. Therefore the first two processes contribute to none of the listed aberrations except directionality and spectral sensitivity.

Domes contribute to directionality because of their finite thickness which allows multiple reflections to concentrate radiation in small, discrete areas for particular directions of the incident beam. These concentrations are called caustics. They may fall on parts of the receiver which are particularly sensitive and, for example, cause the slightly enhanced response of the Eppley PSP near 70° incidence. Domes with surface blemishes, or those which are non-spherical, also cause directional aberrations.

Spectral aberrations arise principally because of the lack of transmission of some domes in the near infrared and in the UV-B and because of reduced absorption by some black paints in the near infrared.

The incorrect orientation of the receiver surface can contribute seriously to directionality. However, orientation in most pyranometers is carefully controlled in the manufacture, and part of the routine characterisation should be to locate the radiometric axis of the pyranometer and to mount the pyranometer according to this axis.

Similarly, directional aberration will arise if the surface is not planar. The black paint may be less absorptive at high (near grazing) incidence than for normal incidence and this effect is a departure from Lambertian absorption. It is unusual for the departure from the ideal to be in the opposite direction (i.e., an increase in absorption). For example, the enhanced responsivity of the Kipp and Zonen CM 11, at incidence angle greater than 80° is caused by the optics of the domes rather than by the paint.

It is important to note that when a pyranometer is subject to very high temperature, or to high internal humidity for prolonged periods, the properties of the black paint can change. It may then look either dark grey or very dark green and there may be noticeable reflection from the receiver at high incidence. The spectral and directional characteristics are then changed as well as the responsivity.

2.3 Process III: the generation of the temperature difference across the thermopile

The temperature across the thermopile is determined by the energy balance of the black surface. Energy is gained by the absorption of short-wave radiation and lost by emission of thermal radiation, conduction of heat through the air within the domes, convection through the air and by conduction through solid materials to the body of the pyranometer. In terms of power per unit area H the balance can be expressed as:

absorbed power	=	exchange of thermal radiation	(i)
(H in Wm^{-2})		+ conduction through the air	(ii)
		+ convection through the air	(iii)
		+ conduction through solid material	(iv)

The terms in this equation are addressed using a simple model which allows a rough estimation of their contributions to non-linearity and to the dependencies of responsivity on tilt and temperature. There are only two temperatures describing the pyranometer in the model: the hot junctions of the thermopile and the receiver surface are at $(T_0 + \Delta T + \delta T)$ while every other part of the instrument is at $(T_0 + \Delta T)$. $T_0 = 300$ K is a standard temperature so that the ambient temperature is therefore $(T_0 + \Delta T)$ and the temperature difference across the thermopile is δT.

i) The net loss of energy by thermal radiation per unit area is

$$\sigma\left((T_0 + \Delta T + \delta T)^4 - (T_0 + \Delta T)^4\right)$$

where σ is the Stefan-Boltzmann constant. Expanding this up to second order terms in δT and ΔT and using $T_0 = 300$ K , as well as $4\sigma T_0^3 = 6.1$, gives:

$$\text{loss by thermal radiation} = \delta T \cdot 6.1 \cdot \left(1 + \frac{\Delta T}{100} + \frac{\delta T}{200}\right) \quad Wm^{-2} \qquad [2.1]$$

ii) Conduction through the air to the domes has been estimated for the Eppley PSP by Berdahl and Frohm (1982) as 12 $Wm^{-2}K^{-1}$. This value is used here to approximate air conduction in all similar thermal pyranometers. Air conductivity is proportional to the square root of absolute temperature. Including this temperature dependence gives:

$$\text{loss by air conduction} = \delta T \cdot 12 \cdot \left(1 + \frac{\Delta T}{600} + \frac{\delta T}{1200}\right) \quad \text{Wm}^{-2} \qquad [2.2]$$

iii) A square-law dependence of the convective heat transfer on temperature difference is proposed. It should be noted that M.C. Anderson (1972) determined a $\delta T^{1.32}$ dependence of the total heat transfer (conduction plus convection) from her measurements on an MG pyranometer which is very similar to the CM-5. However her formula gives large non-linearities which are not consistent with the CM-5 measurements in this work. Also there is no indication in pyranometer non-linearity measurements of any sharp onset of convection at a critical Reynolds number such as occurs with a large horizontal surface in free air. While the measurements do not rule out a threshold at very low irradiance, they are consistent with the proposed square-law dependence which is therefore adopted as a simple approximation suitable for the consideration of pyranometer non-linearity. The square law is physically reasonable, given laminar flow, in that it follows from the heat transfer being proportional to the product of the temperature difference and the air velocity and from the air velocity being proportional to the temperature difference. The following form is suggested:

$$\text{loss by convective transfer} = 0.06 \cdot (\delta T)^2 \quad \text{Wm}^{-2} \qquad [2.3]$$

The proportionality constant 0.06 has been chosen to fit the observed behaviour of the CM-5 pyranometer in the usual horizontal orientation. Whether convection is enhanced or decreased with increasing temperature is not known.

Convection is the only process which is dependent on gravity and which can account for changes in responsivity with the tilt of the instrument. When the pyranometer is horizontal the air moves up in the centre above the receiver and down near the domes but when the instrument is tilted at ninety degrees, the air flows up in contact with the hot receiver and down near the cool domes. This convective pattern involves more flow over the hot surface and must be more effective at transporting the heat. As the pyranometer is tilted, the convective transfer is therefore enhanced progressively and we suggest that convective transfer is doubled at 90 degrees of tilt.

iv) Conduction of heat through solid material is linear with temperature gradient. The temperature dependence of the conductivity is disregarded because values for metals

and semi-conductors are usually much smaller than 0.1% K^{-1}. The following expression can therefore be used:

$$\text{loss by solid conduction} = K \cdot \delta T \quad \text{Wm}^{-2} \qquad [2.4]$$

The conduction factor K depends on the construction of the pyranometer . In what follows, two values K=32 (Case C) and K=182 (Case P) are considered. These values roughly simulate the Kipp and Zonen CM-5 and Eppley PSP pyranometers to the extent that the temperature difference across the thermopile is approximately 5K or 20K, respectively, when the irradiance is 1000 Wm^{-2}.

Expressing the above heat balance algebraically:

$$\text{H} = \delta T \cdot 6.1 \cdot \left(1+\frac{\Delta T}{100}+\frac{\delta T}{200}\right) + \delta T \cdot 12 \cdot \left(1+\frac{\Delta T}{600}+\frac{\delta T}{1200}\right) + 0.06(\delta T)^2 + K \cdot \delta T \quad \text{Wm}^{-2} \qquad [2.5]$$

Rearranging this yields:

$$\text{H} = (a + b\Delta T) \cdot \delta T + c \cdot (\delta T)^2 \quad \text{Wm}^{-2} \qquad [2.6]$$

where

$a = K + 6.1 + 12 \quad (= K + 18)$

$b = 0.061 + 0.020 = 0.081$

$c = 0.03 + 0.01 + 0.06 = 0.10$

Equation 2.6 can be written as $\delta T = \left(1+\frac{b}{a}\Delta T+\frac{c}{a}\delta T\right)^{-1}\frac{\text{H}}{a}$ Since the second and third terms in the bracket are much smaller than unity it follows that $\delta T = \text{H}/a$ is an approximate solution for δT and further that:

$$\delta T = \left(\frac{\text{H}}{a}\right)\left(1 - \frac{\Delta T \cdot b}{a} - \frac{c \cdot \text{H}}{a^2}\right) \qquad [2.7]$$

is accurate to the first order in $b\Delta T/a$ and $c\text{H}/a^2$. This expression identifies that, given the assumptions described above, the temperature difference caused by the absorption of radiation is not exactly linear and depends on the temperature of the instrument. The contribution of the heat balance to the temperature coefficient of responsivity is $-b/a$. Defining the non-linearity as the fractional difference between responsivity at 1000 Wm^{-2}

and at zero incident radiation gives $-1000 \cdot c / a^2$ for the non-linearity. Table 2.3 shows these expressions evaluated specifically for the two cases.

It is well known that convection is the source of the tilt effect. The assumption made here, that convection is pure quadratic in δT, leads to the conclusion that the tilt effect is proportional to irradiance and therefore small when irradiance is low and is confirmed by measurement. By making the assumption (see above) that convection is twice as effective when the pyranometer is mounted on a vertical surface as that which occurs with the conventional horizontal orientation, the tilt effect can be estimated by changing the factor 0.06 to 0.12 in Equations 2.3 and 2.5 and deriving the right-hand column in Table 2.3.

Comment on these examples is made in Section 2.5 and the definitions of non-linearity and tilt used in this chapter are shown in Figure 2.3

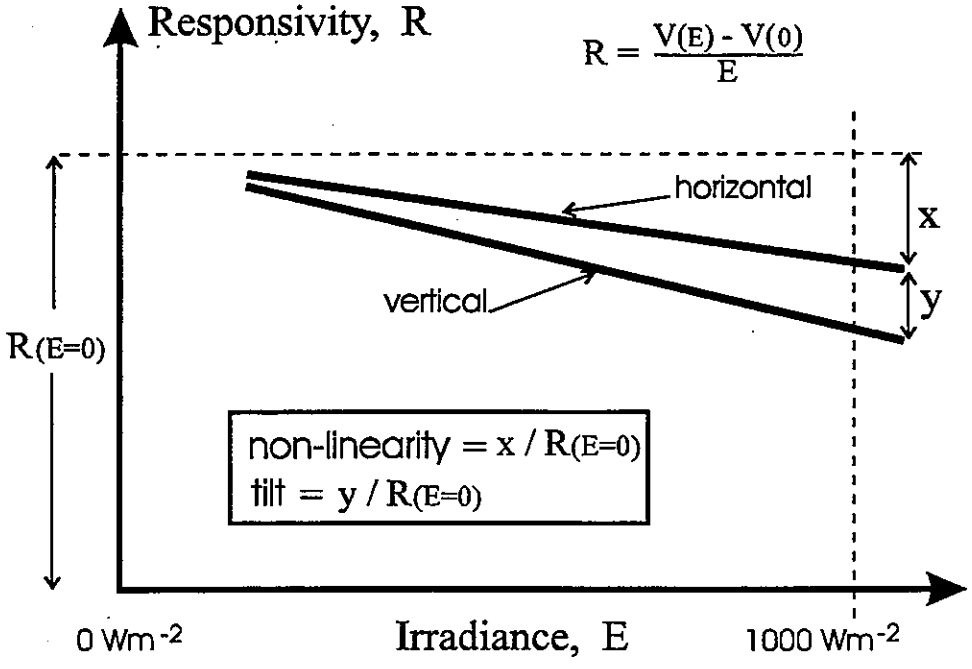

Figure 2.3 Showing the definitions of non-linearity and tilt as well as the linear dependence of responsivity on irradiance predicted in the simple analysis used here.

Table 2.3

THERMAL BALANCE EFFECTS	Temperature Rise at 1000 Wm^{-2}	Temperature Coefficient of Responsivity	Non-linearity 1000 $W.m^{-2}$ vs Zero	Tilt at 1000 Wm^{-2} Vertical vs Horizontal
Case P	~5 K	-0.04% K^{-1}	-0.25%	-0.15%
Case C	~20 K	-0.16% K^{-1}	-4.0%	-2.4%

Before leaving Process III it should be identified as the source both of zero-offsets and of signal delay. Up to this point, the temperature difference across the thermopile has been explained as the result of an energy balance. How quickly the balance is attained depends primarily on the thermal mass of the receiver surface and to some extent on the thermal mass and conductivities of the cold junctions of the thermopile. The latter usually have a larger time constant. Chapter 5 includes specification of the signal delay. The zero-offset is due to a temperature difference occurring across the thermopile when there is no incident short-wave radiation. Chapter 6 shows that the main causes of zero-offset are changes in ambient temperature and long-wave radiation.

2.4 Process IV: generation of the output voltage by the thermopile

The output from the thermopile is the final stage in the generation of the output signal from the pyranometer. The behaviour of thermocouples has been well understood for more than a century, their output being temperature dependent and not perfectly linear. Their output is the difference in thermoelectric potential Φ at the two temperatures between the two metals i.e.,

$$V = \Phi\left(T_0 + \Delta T + \delta T\right) - \Phi\left(T_0 + \Delta T\right) \qquad [2.8]$$

and, to the accuracy required here, Φ can be expressed as a quadratic in $T - T_0$ with coefficients p, q in the second and third terms. Then:

$$V = p\cdot\left(\Delta T + \delta T\right) + q\cdot\left(\Delta T + \delta T\right)^2 - p\cdot\Delta T - q\cdot\left(\Delta T\right)^2 \qquad [2.9]$$

$$V = p\cdot\delta T\left(1 + \frac{\Delta T\cdot 2q}{p} + \frac{\delta T\cdot q}{p}\right) \qquad [2.10]$$

in which the two expressions in parentheses show the contribution of the thermocouple to temperature dependence and non-linearity. Specifically, the temperature coefficient of responsivity is $2q/p$ and the non-linearity is $(1000/a)q/p$ where a is defined in the previous section (i.e., 200 $Wm^{-2}K^{-1}$ for P, 50 $Wm^{-2}K^{-1}$ for C).

The thermoelectric constants both for copper-constantan and manganin-constantan, the materials often used for pyranometer thermopiles, are approximately 40 $\mu V.K^{-1}$ for p, and 0.045 $\mu V.K^{-2}$ for q. Using these values gives the following contributions (Table 2.4):

Table 2.4

Thermopile Effects	Temperature Coefficient of Responsivity	Non-linearity 1000 $W.m^{-2}$ vs zero	Tilt
Case P	+0.225% K^{-1}	+0.56%	zero
Case C	+0.225% K^{-1}	+2.25%	zero

2.5 Discussion of the effects of processes III and IV

Table 2.5 shows the combined contributions from the thermopile and the thermal transfer effects to the pyranometer aberrations. It's elements are formed by adding the corresponding ones in Tables 2.3&2.4.

Table 2.5

Combined model (theoretical) effects of thermal balance and thermocouple temperature				
Case	Temp. Rise	Temperature Coefficient of Responsivity	Non-Linearity 1000 Wm^{-2} vs zero	Tilt at 1000 Wm^{-2}
P	~5K	+0.18% K^{-1}	+0.31%	-0.15%
C	~20K	+0.06%K^{-1}	-1.75%	-2.4%

Case P was chosen to represent an Eppley PSP which has a 50-junction copper-constantan thermopile and the relatively low temperature rise of 5K at 1000W m^{-2}. The predicted overall non-linearity is +0.31% is very small and this is confirmed by measurements. The same situation applies to the tilt effect, predicted at -0.15%. The predicted temperature effect +0.18% K^{-1} is unfortunately not easily validated because the PSP has an internal temperature compensation thermistor.

Case C represents the Kipp CM-5 instrument with a 14-junction manganin-constantan thermopile and a temperature rise of about 20K at 1000 Wm^{-2} (Later model CM-5s have been fitted with different thermopiles). The predicted values for non-linearity -1.75% and tilt effect -2.4% are realistic. Measured values for the CM-5 are -2.0% for non-linearity and -2.1% for tilt (see Chapter 5, MOH, Hamburg). Also the linear change of responsivity with irradiance level, which is indicated from all the processes considered here, is generally consistent with measurements of non-linearity on the CM-5 and other instruments.

Case C does not give the right value for the overall temperature coefficient. The predicted value is +0.06% K^{-1} while the measured value is about -0.12% K^{-1}. Perhaps the air-conductivity term should be increased due to air conduction happening at the back of the thermopile through a thinner layer of air to the instrument body. If the term were indeed three times larger, the predicted temperature coefficient would be negative and the tilt and non-linearity corrections would not be greatly changed. However, there are other possibilities, for example a temperature dependence in the solid conductivity which, *a priori*, are equally possible.

The two cases illustrate that, when the pyranometer design provides enough thermal conductivity between the hot and cold junctions to limit the temperature rise to less than about 5K, the tilt effect and the non-linearity can be negligible.

Non-linearity and tilt dependence can be easily corrected through characterisation because the signal level and tilt are inevitably known but it is much easier if there are no aberrations. In at least one laboratory (NARC), the directional response of pyranometers was for many years measured with the instruments mounted vertically and at significant power. It was not realised that the results for some instruments, like the CM-5, should be corrected for vertical rather than horizontal non-linearity. Once this requirement is understood, it is still possible that the correction might be made improperly because it is complicated. Obviously, it is preferable not to have to make such corrections.

The CM-10 is interesting in that it has no tilt dependence but it does have a small and positive temperature coefficient of responsivity. One can therefore see that the temperature rise is not large but large enough to produce non-linearity in the special thermopile of the CM-10. It is also sensitive to temperature but there is a compensating circuit that masks the nature of the temperature dependence.

2.6 Conclusions

(i) The aberrations predicted from this simple examination of the physical processes are similar to those commonly observed in pyranometers.

(ii) The thermoelectric effects are of opposite sign to those of air conduction, convection and thermal radiation.

(iii) Most of the observed dependence of responsivity on tilt and level of irradiance (see §5.6) is well simulated by a simple approximation in which the heat transfer by convection has square-law dependence on temperature difference.

(iv) If there is significant dependence on tilt, non-linearity will likely be present and will itself also be dependent on tilt. This requires correction for tilt and non-linearity to be expressed as $F_{\beta E}(\beta, E)$ rather than separately as $F_{\beta}(\beta) \cdot F_{E}(E)$, as in Chapter 1.

(v) Pyranometers designed to have small temperature gradients across the thermopile can show negligible non-linearity and negligible susceptibility to tilt.

Chapter 3. Inventory of Participants' Work and of Assistance From Various Agencies

3.1 Introduction

Seven countries participated in Subtask 9C and in several of the countries more than one agency was involved. This chapter attempts to list where different elements of the work were undertaken and identify the contributions made by non-participating institutions, including the loan of many pyranometers by the manufacturers.

3.2 Contributions From Participating Countries

3.2.1 Austria

The *Zentralanstalt für Meteorlogie und Geodynamik* was the Task participant undertaking a large number of characterisation experiments both in the laboratory and in the field. Laboratory experiments included measurement of the directionality and non-linearity and important experiments on the effects of changing ambient temperature on pyranometers. Field calibrations were done on the main group of pyranometers. The Schenk company of Vienna generously loaned three instruments for three years to the IEA for this Sub-Task.

3.2.2 Canada

The National Atmospheric Radiation Centre (NARC) at the Atmospheric Environment Service (AES) of Canada provided the Sub-Task leadership, including arranging for the movement of pyranometers between laboratories. Field calibrations on the main group of instruments were done on the roof of the AES building in Toronto. In addition, all the pyranometers were calibrated at the beginning and at the end of the experiments (1984-1987) in the NARC sphere. The three Benchmark Calibrations were also done on the main group and data on temperature and directionality were supplied for the relevant chapters. Chapter 6, on offset signal, was contributed by NARC. The writing of this report was co-ordinated and edited by the AES.

3.2.3 Germany

The *Deutscher Wetterdienst* (DWD) of Hamburg was the German participating agency. Very thorough characterisation of directionality, linearity and tilt susceptibility were made on the main group of pyranometers at the Hamburg laboratory. In addition, some key experiments, including that which demonstrated that linearity was absent for very low irradiances, were done by the DWD. Chapter 4 on directionality was written by the DWD participant.

3.2.4 Japan

The Eko Trading Company was the participating agency. The company also supplied five pyranometers for the task and a variety of test results. The participant contributed extensively to the organisation of the work and made an evaluation of measurement errors resulting from pyranometer aberrations. To do this a radiation model was developed to simulate the angular distribution of radiance in a variety of circumstances.

3.2.5 Netherlands

The Royal Netherlands Meteorological Institute (KNMI) was the leading participating agency. A large amount of meticulous indoor characterisation, including directional response, linearity, tilt, experiments on wavelength sensitivity and thermal shock as well as some outdoor calibration was done by the *Technische Physische Dienst* of Delft (TNO-TP). The Kipp and Zonen company loaned several pyranometers of two types, performed laboratory measurements of directionality, made the results available to the Subtask and participated in some of the meetings. As well as co-ordinating this multi-agency contribution, the KNMI, wrote the important Chapter 8 on the comparison of benchmark responsivities.

3.2.6 Sweden

Two Swedish agencies participated in the Task: the *Statens Provningsanstalt* (SP) at Borås and the Swedish Meteorological and Hydrological Institute (SMHI) at Norrrköping. The SP primarily contributed to laboratory work, including an investigation of spectral sensitivity. Field characterisation and determination of Benchmark calibration factors and the writing of part of the chapter on directionality was done at SMHI. The extensive results on directionality, linearity and temperature response generated by the SP for Task 3 were made available for Task 9.

3.2.7 USA

The Solar Energy Research Institute (SERI) at Golden, Colorado was the lead US agency and co-ordinated the extensive contributions from three other institutions: the NOAA Solar Radiation Facility, Boulder Colorado, the Eppley Laboratory, Newport, Rhode Island and the Desert Sand Environmental Testing Laboratories (DSET), New River, Arizona. Eppley provided three pyranometers for characterisation both in Task 3 and Task 9. All four US agencies performed outdoor calibration in tilted and horizontal orientation and Benchmark calibration factors were derived from this work and used in Chapter 7. Experiments on the transient response of pyranometers to radiation were performed at two laboratories (DSET and Eppley). The temperature coefficient of responsivity and the effects of changing temperature were studied at three laboratories (SERI, NOAA, Eppley). Chapter 5 was

written by the participant from SERI and the US contribution is summarised in the report SERI/TR-215-2925.

3.3 Assistance and Informal Participation

An earlier project, Task 3 of the Solar Heating and Cooling Program, was led by the German *Kernforschungsanlage* at Jülich. The leader and several of the participants of this Task participated informally and constructively in a significant fraction of the work and the discussions leading from it. In addition, all results from Task 3 were made available for Task 9.

The World Radiation Centre at Davos in Switzerland, which was a major participant in Task 3 but not formally in Task 9, made a similarly valuable contribution to this Task.

Two helpful contributions were made from Australia, although Australia was not a participant either in Task 3 or in Task 9. The Middleton Company loaned two production pyranometers and Dr. David Proctor loaned a novel developmental pyranometer. All three of these instruments were part of the main group, tested at several laboratories. Their inclusion increased the number of types from five to seven allowing generic pyranometer behaviour to be more easily identified.

Chapter 4. The Dependence of Pyranometer Responsivities on the Direction of the Incident Radiation

Directional response can be measured both in the laboratory and in the field.

Laboratory measurements are usually made by changing the orientation of a pyranometer relative to a steady, unidirectional beam of radiation from a lamp. These measurements generally have the advantage of reproducibility because the environment is controlled and they can also be made at irradiance levels that are sufficiently low to exclude the effects of non-linearity and tilt.

Field measurements are always the basis for the absolute calibration of pyranometers. The methods involve measuring the direct beam radiation with a reference pyrheliometer while exposing the pyranometer to the global radiation and may also involve shading the pyranometer intermittently from the direct beam. These calibrations can constitute a directional characterisation of the instrument if done at different solar elevations. Results from field measurements are inevitably affected by changing atmospheric conditions and the resulting variability may make assigning a calibration, or determining a directionally factor, more difficult. It is usually necessary to take measurements over a wide range of conditions and to make suitable averages. However, the variability over the ensemble is an indicator of the accuracy of the measurement in realistic (outdoor) conditions.

Comparing field and laboratory results is necessary but problematic. Only one of the field methods, the alternating shade method (ASM), can evaluate the directional response immediately but it is extremely time consuming and cannot be done on many instruments. The other field techniques expose the pyranometer to global radiation (diffuse and direct beam) continuously. Some pyranometers exhibit tilt and non-linearity errors when exposed to normal solar irradiance levels, which complicates the analysis.

Chapter 4 examines the laboratory techniques from several institutes and compares their results. Two field experiments are also described and their results examined for implications regarding measurement uncertainty. Data from both field experiments are analysed to yield responsivities to unidirectional radiation and are therefore suitable for comparison with laboratory results.

4.1 Laboratory measurements

Section 4.1 examines the techniques for laboratory determination of directionality used by six institutes. The results from characterising identical pyranometers at different laboratories are analysed in detail.

4.1.1 Definitions and general remarks

a) The function $R(\theta, \phi)$ describes the responsivity of a pyranometer when it is illuminated by radiation from a single direction. The incidence angle θ is the angle between the radiation direction and the pyranometer axis. The azimuth angle ϕ, in this report, is referenced to the cable. Thus $\theta = 0$ specifies normal incidence while $\theta = 90, \phi = 0$ specifies the direction of the cable. The ideal pyranometer would have a responsivity independent of direction. The non-ideal directional behaviour is traditionally described by the percentage departure $\delta(\theta, \phi)$ of the responsivity from its value at normal incidence. Thus

$$\delta(\theta,\phi) = \left[\frac{R(\theta,\phi)}{R(\theta=0°)} - 1\right] \cdot 100 \qquad [4.1]$$

It is related to the direction correcting factor, $F_{\underline{s}}(\underline{s})$, provided the standard condition for $F_{\underline{s}}(\underline{s})$ is normal incidence, by

$$\delta(\theta,\phi) = \left(F_{\underline{s}}(\underline{s}) - 1\right) \cdot 100 \qquad [4.2]$$

Because laboratory measurements of directionality are usually made by recording the pyranometer signal $M(\theta, \phi)$ different incidence directions using a beam of constant intensity, an alternative expression is

$$\delta(\theta,\phi) = \left[\frac{M(\theta,\phi)}{M(\theta=0)\cdot\cos\theta} - 1\right] \cdot 100 \qquad [4.3]$$

This shows that $\delta(\theta,\phi)$ is the relative deviation of $M(\theta,\phi) / M(\theta = 0°)$ from the ideal $\cos\theta$, which is the rationale for it being called the *cosine error*. It is usually expressed as a percentage, which is done here, although it is given per mil (0.1%) in the Tables 4.1.3.1b-n in Appendix AA.

It can be useful to express directionality as the absolute error that would occur if responsivity variation were ignored and the normal incidence responsivity were used in place of the correct value for the actual direction. This absolute error, δ_E in Wm^{-2}, when measuring a beam of defined normal incidence intensity, E, is related to the *cosine error*, in percent, by

$$\delta_E(\theta,\phi) = 0.01 \cdot E(\theta = 0°) \cdot \delta(\theta,\phi) \cdot \cos\theta \qquad [4.4]$$

Generally, $\delta_E(\theta,\phi)$ has the advantage that it varies much less rapidly with direction than does $\delta(\theta,\phi)$. Setting $E(0°) = 1000 Wm^{-2}$ is appropriate for solar energy applications and this $1000 Wm^{-2}$ *absolute directionality error*, $\delta_t(\theta,\phi)$, as described in ISO9060, is related to the *cosine error* by

$$\delta_t(\theta,\phi) = 10 \cdot \delta(\theta,\phi) \cdot \cos\theta \qquad [4.5]$$

Azimuth averaged versions $\overline{\delta}(\theta)$ and $\overline{\delta_t}(\theta)$ of $\delta(\theta,\phi)$ and $\delta_t(\theta,\phi)$ are convenient and are used in the following analysis. These averages are usually based on measurement at 12 azimuths (30° increments). They are related similarly to [4.5] above by

$$\overline{\delta_t}(\theta) = 10 \cdot \overline{\delta}(\theta) \cdot \cos\theta \qquad [4.6]$$

The percentage range of variation of responsivity at various azimuth angles and at a given incidence angle is represented in what follows by

$$D_{\max}(\theta) = \delta(\theta,\phi_1) - \delta(\theta,\phi_2) \qquad [4.7]$$

where ϕ_1 and ϕ_2 are the azimuth angles at which maximum and minimum values of responsivity occur at constant incidence angle θ. Finally, an equivalent angle of tilt $\beta(\theta)$ is defined such that an ideal pyranometer misaligned by β would give the same $D_{\max}$ as is actually observed. These quantities are related by

$$\beta(\theta) = 0.285 \cdot \operatorname{cotan}\theta \cdot D_{\max}(\theta) \qquad [4.8]$$

where β is in degrees and $D_{\max}$ is in percent.

b) Pyranometers that show small cosine error in the laboratory usually have relatively small errors under field conditions. However, laboratory studies usually enable the physical behaviour of the instruments to be determined more precisely than is possible in the field because the influence of a number of unknown factors and variables present under field conditions is avoided.

c) Each participating IEA institute and their facilities (indicated in parentheses) are used to identify their results and data in later sections of the report.

The Statens Provningsanstalt (National Testing Institute) of Sweden, Borås, Sweden (BORÅS or BO). The institute installed a computer-controlled testing system (goniometric turntables) primarily for work closely related to IEA Task 3.

Kipp & Zonen, Delft, Netherlands (DELFT or KI). The optical laboratory was established for the development and control of CM11 pyranometers.

Zentralanstalt für Meteorologie und Geodynamik (Central Institution for Meteorology and Geodynamics), Vienna, Austria (VIENNA or VI). The test laboratory of this institution was established to control the production of Schenk Star pyranometers.

Meteorologisches Observatorium Hamburg (Meteorological Observatory Hamburg) of Deutscher Wetterdienst (German Weather Service), Hamburg, FRG (HAMBURG or HA). The test laboratory was established to control the quality of pyranometers used in climatological networks and was improved for the IEA test activities.

The Physical Meteorological Observatory Davos, Davos, Switzerland (DAVOS or DA). The observatory is the WMO World Radiation Centre. A laboratory test device with a computer controlled goniometer was installed for co-operative workin the IEA Task 3 pyranometer testing programme. This observatory did not participate in IEA Task 9 activities.

The National Atmospheric Radiation Centre (NARC), Canadian Atmospheric Environment Service, Downsview, Canada (TORONTO or TO). The apparatus used for this work was constructed in the early 1970s by J.R. Latimer for the evaluation of instruments (Eppley model 2, PSP, Kipp CM2, CM6) being installed in the Canadian network. The measurement sequence adopted for these IEA measurements (Table 4.1.2a) was slightly different from the Latimer sequence and provides for better checks against stray light and zero signal drifts. The NARC technique retains a number of other limitations, for example, the homogeneity and divergence of the beam are not adequately controlled.

d) The following subchapters compile and compare results obtained in an inter-laboratory test comparison in which selected pyranometers were circulated between sites. The deviations are discussed with regard to specific differences in the protocol and are

compiled in tabular form; conclusions are drawn concerning the status of the laboratory test techniques; and improved protocols are recommended.

4.1.2 Survey of the applied test procedures and apparatus

The principal methods used for indoor testing by the six laboratories are compiled in Table 4.1.2a and may be helpful for explaining potential discrepancies. One laboratory uses a polar orbiting lamp to adjust the angle of incidence, the remainder are equipped with goniometric tables to turn the pyranometer in the stationary beam of a fixed lamp. Five of the laboratories measure the azimuthal response directly by variation of the azimuth angle at fixed incidence angles.

One laboratory measures the zero-offset by shading for each angle. The others take fewer zero readings. The reading time varies between 30 seconds and 2 minutes and, in one case, it is defined in real time by a criterion based on the rate of change of the measurements.

Experimental design factors that may influence accuracy are specified for the six laboratories in Table 4.1.2b. The lamps and filters that are used have three types of spectral distributions:

1. typical tungsten lamp spectrum limited by a filter to approximately the visible wavelengths
2. total tungsten or xenon spectrum with a condenser lens
3. tungsten lamp used without an optical condenser with the pyranometer deployed in the horizontal (not vertical) position.

Normal incident irradiances are relatively low, in the range 50-250 Wm^{-2} , with the exception of two laboratories which have tested with normal incident irradiances of 500 Wm^{-2} or more. The high radiant fluxes are obtained with the pyranometer as close as 25 cm from the condenser of the lamp, while in the other cases the distance is 1 m or more. Low values are preferred to avoid interferences or confusion with non-linearity effects. Beam divergences are in the range 0.5-3.0°. The inhomogeneities of the beam irradiance are specified for receiver surfaces of different diameters (one laboratory has an extremely high value of 10% within a circle of 70 mm diameter).

The white sun screen of the pyranometer is replaced by a black screen to avoid disturbing reflections at one laboratory. The pyranometers are ventilated in two cases to minimise potential thermal offsets.

Many procedures are used to find the correct position of $\theta = 0°$. In one case the final adjustment is obtained by the mathematical treatment of the data assuming an ideal symmetry for the values at incidence angles of ±70°.

The number of axes for the goniometric movement of the pyranometers varies between 1 (for azimuth angles) and 3 (inclusive tilt variation) and the accuracy of angle readings is generally ±0.1° (<1° in the case of the polar orbiting lamp).

The resolution of the data acquisition systems used at different laboratories varies between 10 nV and 1.0 μV.

Table 4.1.2a Compilation of important items of the test methods of participating laboratories

Item	Borås	Delft	Vienna	Hamburg	Davos	Toronto
Adjustment of the Angles of Incidence and Azimuth	goniometric rotation of pyranometer, 2 turntables	as for Borås	rotation of lamp in polar orbit; rotation of pyranometer in azimuthal orbit	as for Borås	as for Borås but with 3 turntables	single goniometric rotation of the pyranometer about a vertical axis
Measured Azimuthal Response	as variation of cosine error in 6 azimuthal planes (comb. measurements)	directly, at fixed angles of incidence	as for Delft	as for Delft	as for Delft but combined with tilt angle variations	as for Borås but only in 3 azimuthal planes
Zero Offset Measurement Protocol	zero reading after shading at each angle for calculation of measure-ment values	as for Borås but before and after an azimuth run: use of the mean zero value for mV calculation	only DVM — zero automatic	as for Borås for cosine response	with a sequence of 154 readings: 9 additional zero readings for calculation of mV	1 zero reading after lamp shading within the 20 readings for 1 azimuth plane
Reading Time	30-60 s dependent on type of pyranometer	1 min (incidence angle): 30 s (azimuth variation)	at least 30 s and after the 10μV digit is stable	2 min (angle of incidence) 30 s (azimuth variation)	given by a criterion of stabilised signal: the first and last readings of the 5 samples within 1 s must be within 4% of the mean signal	2 minutes

Table 4.1.2b Compilation of important items of the test equipment of participating laboratories

	Item	Borås	Delft	Vienna	Hamburg	Davos	Toronto
Source	spectral type	tungsten-halogen +IR filter ≤800 nm	xenon-high pressure	tungsten	xenon-high pressure	xenon-high pressure	quartz-halogen
	optics	condenser	condenser, flat & concave mirrors	—	quartz condenser	condenser, beam splitter, neutral filter	no
	movement angle (error)	no —	no —	zenith to horizon <1°	no —	no —	no —
Beam *at receiver surface*	normal incident irradiance (instability)	50 Wm^{-2} (± 0.1%)	250 Wm^{-2} (± 0.2%)	85 Wm^{-2} (<0.5%)	180 Wm^{-2} (± 0.2%)	500-1000 Wm^{-2} (<1%)	700 Wm^{-2} (<0.2%)
	divergence	1.9°	0.5°	~3°	0.7°		»2.6°
	inhomogeneity	0.1% within 30 mm ϕ	2% within 40 mm ϕ	1% within 70 mm ϕ	0.5% within 25mm ϕ	10% within 70 mm ϕ	not measured
	polarisation	≤5%	<1%?				
	stray light elimination	3 diaphragms (zero meas.)	black walls (zero)	3 diaphragms	3 diaphragms , black walls (zero reading)		3 diaphragms
Pyranometer Mount	distance to source condenser	0.9 m	2 m	1 m	5 m	0.25 m	0.6 m
	pyran. tilt	90° (vertical)	90° (vertical)	0° (horizontal)	90° (vertical)	90° (or other tilts)	90° (vertical)
	pyran. sun screen	used	used black screen	used	used		not used
	pyran. vent	–	–	–	from top	from top	–
	adjustment to θ = 0° (normal incidence)	reflected beam & mathematical treatment at ±70°	photometric at θ = 0°	spirit level	reflector cap over receiver		spirit level + 90° machine block
	goniometric table: axis of turntables	1. vertical diameter of RS 2. normal to centre of RS	as for Borås	1. normal to centre of RS (for azimuth adjustments)	1. vertical diameter of RS 2. normal to centre of RS	as in Borås and 3. horizontal diameter of RS (tilt adjust.)	1. vertical diameter of RS
	angle (error)	±0.1°	±0.1°	<1°	±0.1°		<0.2°
DVM	resolution	10 nV	1000 nV	1000 nV	100 nV		1000 nV

Abbreviations: *RS = receiver surface; Cond. = condenser; Pyran. = pyranometer; Vent. = ventilation*

Table 4.1.3.1a Round robin pyranometers for which indoor directional response was tested by different laboratories (indicated by site)

Pyranometers			Sites						Ref. Tables & Figures 4.1.3.1.[*]			
Make	Type	Serial No.	Borås	Delft	Vienna	Hamburg	Davos	Toronto	Tbls	Figures		
EPP	PSP	20523	X			X	X		b	c	h	l
EPP	PSP	20524	X	X			X		c	c	h	l
EPP	PSP	18135	X									
EPP	PSP	17750	X		X	X	X	X	m	c	h	l
K&Z	CM5	773992	X		X	X	X	X	k	b	g	k
K&Z	CM5	785047	X			X	X	X	h	b	g	k
K&Z	CM5	774120	X				X	X				
K&Z	CM5	773656	X	X			X	X	d	b	g	k
K&Z	CM10	810120	X	X		X	X		l	a	f	j
K&Z	CM10	810122	X				X					
K&Z	CM10	810119	X	X	X	X	X		n	a	f	j
K&Z	CM10	810121	X	X			X		b	a	f	j
SCH	Star	1626	X				X	X				
SCH	Star	2186	X				X					
SCH	Star	2209	X	X			X		e	e	i	m
SCH	Star	2217	X				X					
EKO	MS42	81901	X				X	X				
EKO	MS42	81907	X				X					
EKO	MS42	81908	X	X			X		f	d	i	m
EKO	MS42	81909	X				X					
SWT	SS-25	113	X				X					
SWT	SS-25	114	X	X			X		g	d	i	m
MID	EP07	123			X	X			j	e	i	m
MID	EP07	124										
CSR	PT	115		X								

4.1.3 Comparison of test results on directional response of pyranometers

Results on thirteen pyranometers each tested by three or more laboratories have been intercompared. Table 4.1.3.1a indicates where each pyranometer was tested, which of the Tables 4.1.3.1b-n, in Appendix AA that contains the comprehensive data from the tests made on it and the figures at the end of §4.1.4 in which its characteristics are plotted.

4.1.3.1 Presentation of test results

The basic data are indoor measurements of $\delta(\theta,\phi)$ defined by Equation 4.1. The data were excerpted from the individual laboratories' final reports or from the IEA Task 3 Report *Results of an Outdoor and Indoor Pyranometer Comparison* (1984) and the IEA Task 9 Symposium Proceedings *Recent Advances in Pyranometry* (Norrköping, January 1984).. The Davos' values in the tables are interpolated relative to the angle of incidence and represent only a small part of the data. The Toronto values are taken from an internal NARC report.

1. The values for $\delta(\theta,\phi)$ are presented in Tables 4.1.3.1b-n, in Appendix AA, where each table contains the results for one pyranometer. The azimuth is in 30° increments; the principal θ– values are 20°, 40°, 60°, 70° and 80°. Azimuth-averaged results $\overline{\delta}(\theta)$ and $\overline{\delta}_t(\theta)$ are given for each incidence angle as are values for the maximum azimuthal variation $D_{max}(\theta)$ and the corresponding inclination angle $\beta(\theta)$ (Equations 4.7&8). The prefix Δ is used to indicate inter-laboratory differences in results. The differences $\Delta\delta$ between the corresponding δ—values of laboratory XY and a reference laboratory (usually Borås)

$$\Delta\delta(\theta,\phi) = \delta(\theta,\phi,XY) - \delta(\theta,\phi,REF) \quad \text{or} \quad \Delta\delta = \delta(XY) - \delta(REF) \qquad [4.9a]$$

$$\Delta\overline{\delta}(\theta) = \overline{\delta}(\theta,XY) - \overline{\delta}(\theta,REF) \quad \text{or} \quad \Delta\overline{\delta} = \overline{\delta}(XY) - \overline{\delta}(REF) \qquad [4.9b]$$

$$\Delta\overline{\delta}_t(\theta) = \overline{\delta}_t(\theta,XY) - \overline{\delta}_t(\theta,REF) \quad \text{or} \quad \Delta\overline{\delta}_t = \overline{\delta}_t(XY) - \overline{\delta}_t(REF) \qquad [4.9c]$$

are also listed in the tables. Another quantity indicative of reproducibility between laboratories is the maximum Δ_{max} difference in $\delta_t(\theta,\phi)$ to be found at a given incidence angle, defined by

$$\Delta_{max}(\theta) = \Delta\delta_t(\theta,\phi_m) \geq \Delta\delta_t(\theta,\phi) \quad \textit{for all } \phi \qquad [4.10]$$

The main intention here is to investigate the inter-laboratory differences to determine the most reliable test methods. The comparison is based mainly on the following three quantities

1. the azimuth averaged 1000 Wm^{-2} absolute error $\overline{\delta}_t(\theta)$

2. $\Delta_{max}(\theta)$ according to Equation 4.10, mostly for $\theta \geq 60°$, and

3. β the out-of-level angle corresponding to the azimuth variation, according to Equations 4.7&8.

The agreement of the directional test results for two laboratories is considered *good* if their differences $\Delta\overline{\delta}(\theta)$ are within the range that can be calculated from the essential limits of experimental accuracy — an irradiance instability in the lamp of ±0.2% and an incidence angle inaccuracy of ±0.1° — given in Table 4.1.3.2a.

Table 4.1.3.2a

θ	30°	40°	50°	60°	70°	80°
$\Delta\overline{\delta}(\theta)$ ±%	0.3	0.35	0.4	0.5	0.7	1.2
$\Delta\overline{\delta}_t(\theta)$ ±Wm^{-2}	2.6	2.9	2.6	2.5	2.3	2.1

The corresponding absolute error $\Delta\overline{\delta}_t(\theta)$ approximates to ±2.5 Wm^{-2} for all incidence angles and is therefore a practical measure of consistency. Two laboratories subject to the same essential limits should produce results that agree within this range. Based on this and in order to simplify the comparison, three classes of agreement between laboratories have been defined

good agreement (absolute deviations $|\Delta\overline{\delta}_t(\theta)| < 2.5$ Wm^{-2} for all θ),
moderately good agreement (when, for all θ , $|\Delta\overline{\delta}_t| < 5$ Wm^{-2}) and,
moderate agreement (when, for all θ , $|\Delta\overline{\delta}_t| < 10$ Wm^{-2}).

Because the largest number of Task 9 pyranometers were tested in the BORÅS series, these results are generally used as the reference for $\Delta\overline{\delta}$ and $\Delta\overline{\delta}_t$ The results available from

DAVOS and TORONTO have poorer azimuth resolution than the others which limits the scope of the comparison..

Appendix AA contains summary paragraphs on the results from each of the thirteen pyranometers and similar summaries for each of the seven types of pyranometer. The detailed results of the comparison can be read in these paragraphs.

The results are presented graphically as follows

Figures 4.1.3.1a-e; values of $\overline{\delta}_t(\theta)$ for groups of pyranometers
Figures 4.1.3.1f-i; the differences $\Delta\overline{\delta}_t(\theta)$ between laboratories
Figures 4.1.3.1j-m; $\Delta_{max}(\theta)$ between laboratories as defined by Equation 4.10

It will be noted that, while good agreement is evident in several cases, nearly all the plots require a range of 40 Wm^{-2} or more which indicates poor procedures in other cases.

Table 4.1.3.2 shows the largest inter-laboratory (BO-XY) differences $\Delta_{max}(\theta)$ in measurements of the *1000 Wm^{-2} absolute directionality error* $\delta_t(\theta,\phi)$ on the thirteen pyranometers that were tested. In a few cases Hamburg data were the reference. The extent of the agreement to the reference values is indicated by the three defined classes.

Table 4.1.3.2 Results of the comparison of $|\Delta\bar{\delta}_t(\theta)|$ values of the Delft, Hamburg, Vienna, Toronto and Davos laboratories with reference values from Borås

Pyranometer	Laboratory				
Type & No.	Delft	Hamburg	Vienna	Toronto	Davos
CM10 #810121 CM10 #810120 CM10 #810119	good agreement good agreement good agreement	— good agreement good agreement	— — 26.0 Wm^{-2} (20.0)	— — —	— 1.0 Wm^{-2} (11.0) —
CM5 #773656 CM5 #785047 CM5 #773942	good agreement — —	— 13.0 Wm^{-2} (9.5) 8.5 Wm^{-2} (0.5) moder. agreement	— — 17.0 Wm^{-2} (13.0)	17.0 Wm^{-2} (17.0) 18.0 Wm^{-2} (18.0) 16.0 Wm^{-2} (15.0)	— 7.0 Wm^{-2} (15.0) 6.9 Wm^{-2} (1.0.0) moder. agreement
PSP #20524F3	3.4 Wm^{-2} (3.0) moderately good agreement	—	—	—	—
PSP #20523F3	—	6.8 Wm^{-2} (6.0) moder. agreement	—	—	—
PSP #17750F3	—	20.0 Wm^{-2} (17.0)	23.0 Wm^{-2} (21.0)*	good agreement*	—
Schenk Star #2209	3.2 Wm^{-2} (2.0) moderately good agreement	—	—	—	—
Eko MS42 #81908	8.2 Wm^{-2} (8.0) moder.. agreement	—	—	—	—
Swt. SS25 #114	18.0 Wm^{-2} (10.0)	—	—	—	—
Mid. EP07 #123	—	—	7.4 Wm^{-2} (0.0)* moder.. agreement	—	—

The degree of consistency between laboratories is indicated by "good agreement", "moderately good agreement" and "moderate agreement" if the absolute deviations $|\Delta\delta_t(\theta)|$ are within 2.5, 5.0 and 10.0 Wm^{-2} respectively. The figures outside and inside the parentheses indicate the maximum $|\Delta\bar{\delta}_t|$ and $|\Delta\delta_t(60°)|$ respectively. Figures marked by an asterisk indicate reference values from the Hamburg dataset.

4.1.3.2 Comparison of the results by laboratory

SP Borås

A low irradiance is used to give good beam homogeneity and also to minimise the effects of tilt on non-linear effects. A 10 nV digital voltmeter is used to measure the small signal and the offset is determined for each measurement value. The pyranometers are not ventilated, but the infra-red component of the beam is removed by a threshold filter. The mathematical levelling at θ = 70° should produce small values for β. The reading time is very short. Because the Borås data are taken as reference for the comparative tests, it should be noted that:

- the values for δ_t from BO are generally higher than those of the other laboratories
- the values for β at 70° or 60° are generally the lowest compared with those of the other laboratories and
- in the case of PSP #17750 (see Table 4.1.3.1m or Figure 4.1.3.1c) the values for δ_t are exceptionally high, which suggests the reference values may be doubted; the discrepancy could be related to the spectral properties of this instrument; the $\delta_t\left(20°,\ \phi\right)$ values for CM5 #773992 (Figure 4.1.3.1b) are exceptionally low.

Kipp & Zonen, Delft

The beam irradiance of 250 Wm^{-2} is at the border of the low irradiance test-level. The homogeneity of the beam is only specified for 40 mm diameter, but for most of the receivers the homogeneity within 25 mm is essential. The levelling is established photometrically at 60°. The reading time is short. The pyranometer is not ventilated. The zero offset is only measured twice during each azimuth run. The δ_t-comparison with the reference data yields:

- *good agreement* for CM10 and CM5
- *moderately good agreement* for the Schenk Star #2209
- *moderate agreement* for Eko MS42 #81908

In general the KI-values are relatively lower than BO & HA. The value of β varies with θ much less in the KI-result than in the reference result, but the means are similar in magnitude.

MOH, Hamburg

The beam configuration has no critical specification, but does not allow pyranometers with receiver diameters larger than 50 mm to be tested. The 100 nV resolution of the digital voltmeter is helpful in making accurate measurements at large values of θ. because of the low normal incidence irradiance of 180 Wm^{-2}. The pyranometer ventilation improves the stability during the cosine error tests. The 2-minute cycle of reading represents the longest reading time (as for Toronto) and corresponds to that used in the outdoor calibration routine at MOH. The simple levelling procedure supposes that the receiver plane is parallel to the top surface of the casing. The δ_t comparison with the reference data yields:

- *good agreement* for the two CM10 pyranometers tested
- *moderately good agreement* for one of the two PSP pyranometers tested
- *moderate agreement* for one of the two CM5 pyranometers tested (*good agreement* if $\theta \geq 40°$)

Large deviations occur for the PSP #17750 but, in this case, the reference data of Borås are of doubtful quality. In general, the δ_t values follow: BO > HA > KI > VI. For β, the HA values usually exceed the reference values but no significant difference has been found in testing CM10 pyranometers.

ZFMG, Vienna

The test technique is important because of the horizontal positioning of the pyranometers and because the routine control requirements for Schenk Star pyranometers allow large receivers to be tested. The beam configuration gives a relatively high homogeneity over a diameter of 70 mm but there is a low irradiance value (85 Wm^{-2})and relatively high divergence. The low signal strength necessitates frequent measurement of the offset. The limited resolution of the digital voltmeter inevitably contributes to a loss of precision in testing at larger angles of incidence, especially if the pyranometer signal is small (e.g., for the CM10).

In the case of the EP07 pyranometer, the δ_t values deviate from those of the HA by less than 7.5 Wm^{-2} (*moderate agreement*). The results for the other three tested pyranometers are

$\Delta\delta_t$ > 10 Wm^{-2} for CM5 pyranometers, using BO values as reference

$\Delta\delta_t$ > 12 Wm^{-2} for CM10 pyranometers, using BO values as reference

$\Delta\delta_t$ > 16 Wm^{-2} for PSP #17750, using HA values as reference.

The β values are higher than the corresponding BO values and lower than the HA values.

NARC, Toronto

The applied test irradiance of 700 Wm^{-2} approaches typical outdoor conditions but does not yield an ideal cosine response because at high irradiances, the signal is influenced to some extent by the effects of non-linearity and tilt (see § 2.4). The lack of homogeneity (which is not quantified but probably significant at high irradiances) probably also contributes to the uncertainty.

The results are only given for two or three azimuthal planes so values of δ_t have been evaluated as a mean of only four or six single values. The values of $\bar{\delta}(\theta)$ for the three CM5 pyranometers deviate greatly from the reference (TO<<BO); the maximum values of $\Delta\delta_t$ (approximately 17 Wm^{-2}) are nearly identical with the $\Delta\delta_t(60°)$. The similar dependence on θ of $\Delta\delta_t(\theta)$ for all CM5 instruments (see Figure 4.1.3.1g) is remarkable and suggests the existence of systematic errors. The Davos test results for instrument CM5 #785047 are within the same order of magnitude. In the case of the δ_t results for PSP #17750 F3, the differences from the Hamburg values are quite small when $\theta > 40°$ meeting the *good agreement* criterion(see Figure 4.1.3.1h).

The values for β are taken from the NARC table of data and are mostly higher than those calculated by other laboratories. The small number of azimuth angles precludes a detailed comparison.

WRC, Davos

High irradiance values which are greater than 500 Wm^{-2} (see remarks on NARC, Toronto, above) are obtained by putting the pyranometers close to the xenon lamp. The pyranometers are ventilated to minimise warming. The inhomogeneity of the beam is only specified for a diameter of 70 mm. The effect for pyranometers with much smaller receiver surfaces cannot be estimated. Another source of uncertainty may be the algorithm that determines the reading time from the stability of five samples within a period of only one second (the resulting times are relatively short, see Table4.1.2a).

According to the sets of single values for δ given in the IEA Task 3 report, the mean values of $\delta(\theta)$ are only calculated from the data obtained from the "north" and "east" azimuthal directions which limits the accuracy of the mean values.

In the case of two CM5 instruments, the deviations from the reference are, for one pyranometer, comparable to those of the TO results. For the other instrument, the $\Delta\delta_t(\theta)$ are lower than 7 Wm^{-2} (see Figure 4.1.3.1g) and fulfil the *moderate agreement* conditions. In the case of one CM10 pyranometer, the deviations are about 10 Wm^{-2} .

4.1.4 Conclusions

a) Generally, the percentage mean *cosine errors* δ of the different test laboratories deviate absolutely from each other by less than 1.0% for incidence angles θ up to 40°.

b) With regard to the agreement achieved in the values of the *1000 Wm^{-2} absolute directionality error* δ_t compared with the results of BORÅS):

- For all CM10 pyranometers tested, two laboratories (KI and HA) with low irradiance test conditions, achieved δ_t results of *good agreement.* Consequently, the differences in the test procedures of BO, KI, and HA (beam quality and spectrum; reading time; ventilation; etc.) are not critical in the case of CM10 pyranometers, or possibly are not revealed because of compensation effects. In the case of CM10 instruments, the cosine error is relatively small (see Figure 4.1.3.1a).

- The KI Laboratory also achieves *good agreement* for the CM5 and Schenk Star pyranometers and a *moderate agreement* for the PSP and the Eko MS42 instruments. Larger deviations have been observed in the results for the Swissteco pyranometer. Apart from the latter, the δ_t results of the KI and BO test method are in good general agreement.

- The HA laboratory achieved *moderate agreement* for only one of the two CM5 pyranometers and *moderately good agreement* for one of the PSP instruments. A comparison with the KI results is not possible because only one CM10 pyranometer has been tested by both laboratories.

- *Good agreement* does not imply that the data are necessarily correct.

c) The maximum deviations Δ_{max} between single values of $\delta_t(\theta,\phi)$ obtained from different laboratories (determined at the same azimuth ϕ and incidence θ) are less than 5 Wm^{-2} for the CM10 instruments. In the other cases of *good agreement,* Δ_{max} can

be as much as 10 Wm^{-2}. The value Δ_{max} may be interpreted as the maximum of the procedural and operational uncertainty if single values of cosine errors are considered.

d) The inter-laboratory differences in the measurement of the out-of-level angle β are in the order of 0.1°. For CM10 pyranometers, the smallest values are in the mathematically -levelled BO data. The values of $\beta(\theta)$ generally vary up to 0.5°, and are sometimes higher but not less stable.

e) The number of instruments calibrated indoors is too small to draw reliable statistical conclusions from the indoor tests.

f) The following investigations should be undertaken to identify the causes of the discrepancies in the directionality measurements:

- comparison of the laboratory results (especially the reference values) with the corresponding outdoor test results from Norrköping and Toronto,
- further cosine error tests of PSP and CM5 pyranometers to complete the content of Table 4.1.4 and re-testing of PSP #17750 F3 from Borås
- laboratory investigation of how the measurement of directionality is influenced by: polarisation, homogeneity and the spectrum of the beam; sampling procedures and the ventilation of the pyranometer
- cosine error tests under the *best* conditions (e.g., with ventilated pyranometer and longer reading time in Borås; by use of better digital voltmeter and zero reading after each angle adjustment, or by improvement of lamp stability, in other laboratories. It may be noted that later tests done at Borås indicated that the voltage resolution rather than reading time or ventilation was the limiting factor in the earlier Borås measurements).

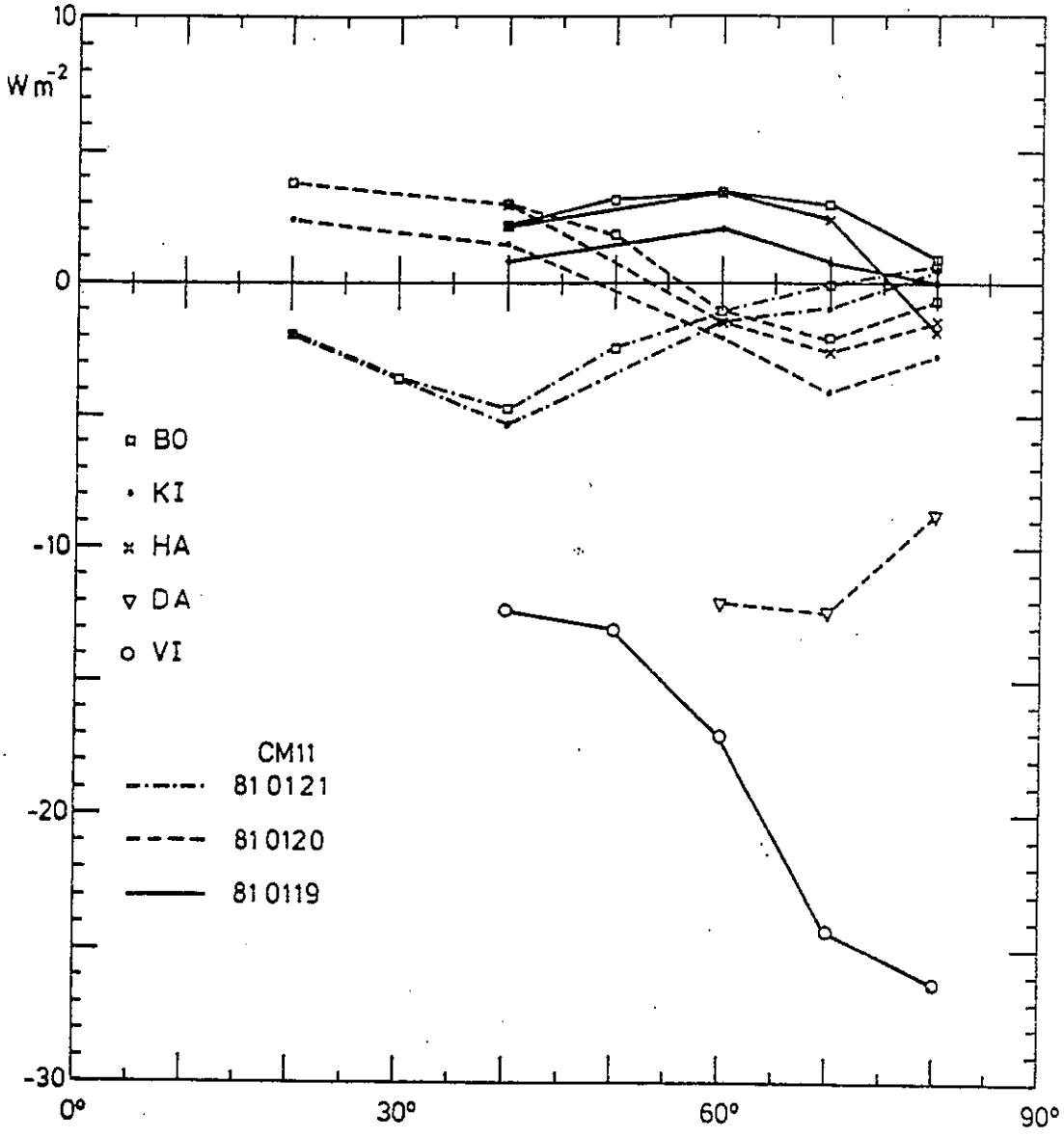

Fig. 4.1.3.1a : Dependence on the incidence angle θ of the absolute effective cosine errors $\bar{\delta}_t(\theta)$ for pyranometers of type CM11

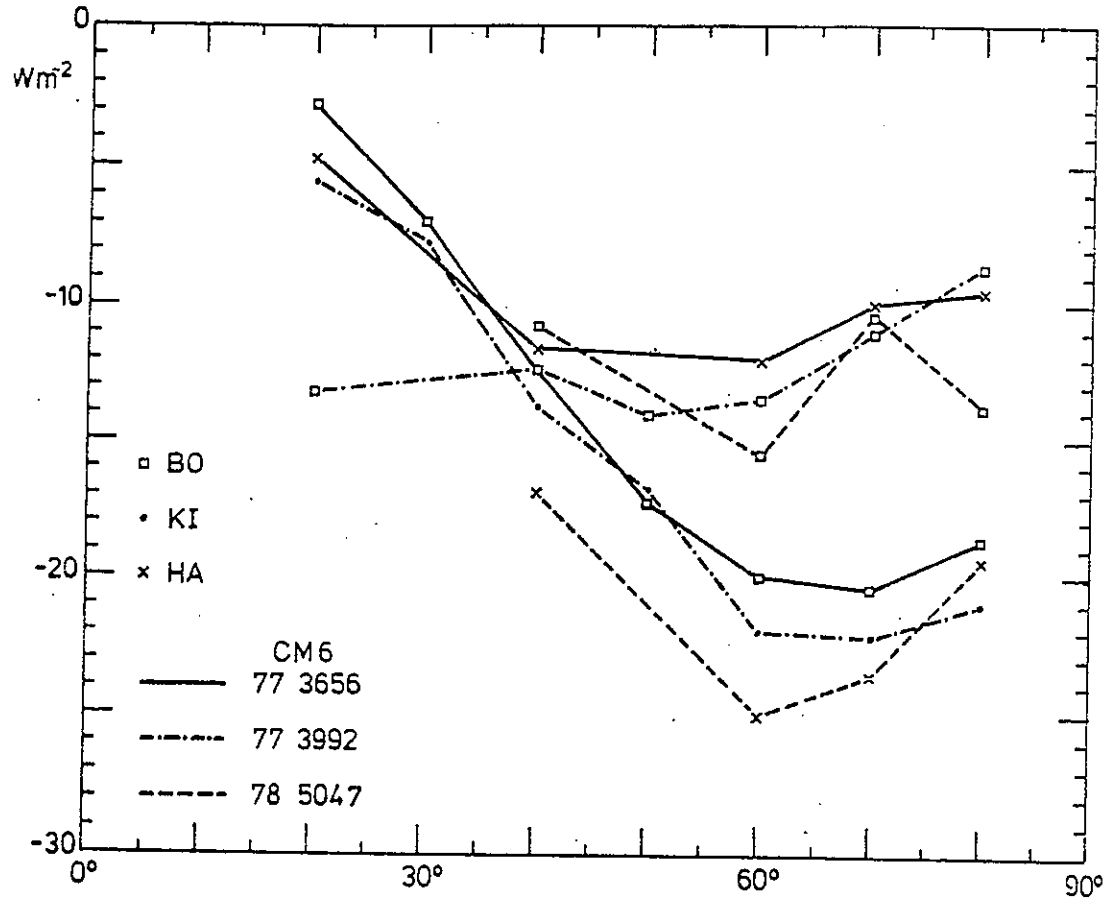

Fig. 4.1.3.1b : Dependence on the incidence angle θ of the absolute effective cosine errors $\bar{\delta}_t(\theta)$ for pyranometers of type CM6

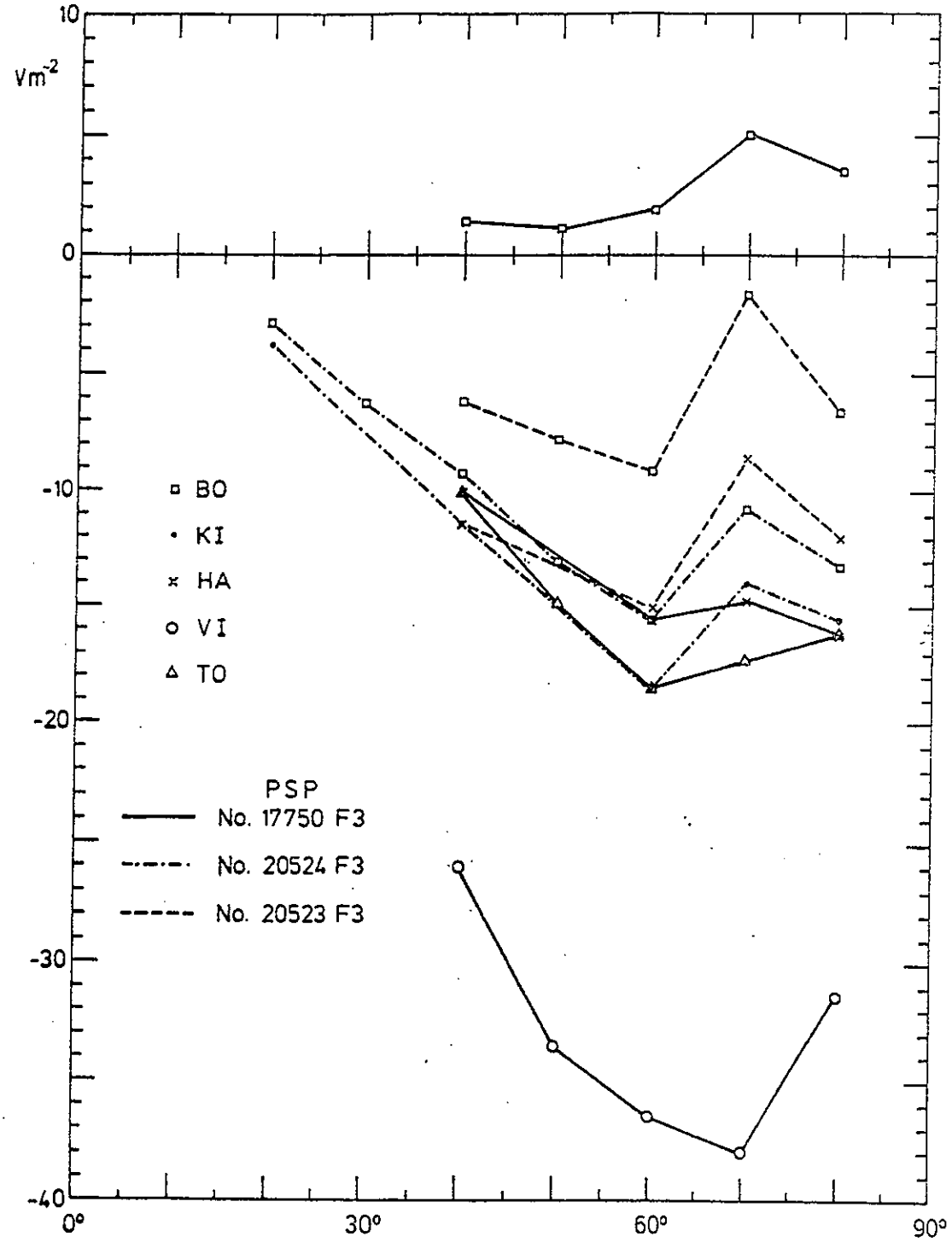

Fig. 4.1.3.1c : Dependence on the incidence angle θ of the absolute effective cosine errors $\bar{\delta}_t(\theta)$ for pyranometers of type PSP

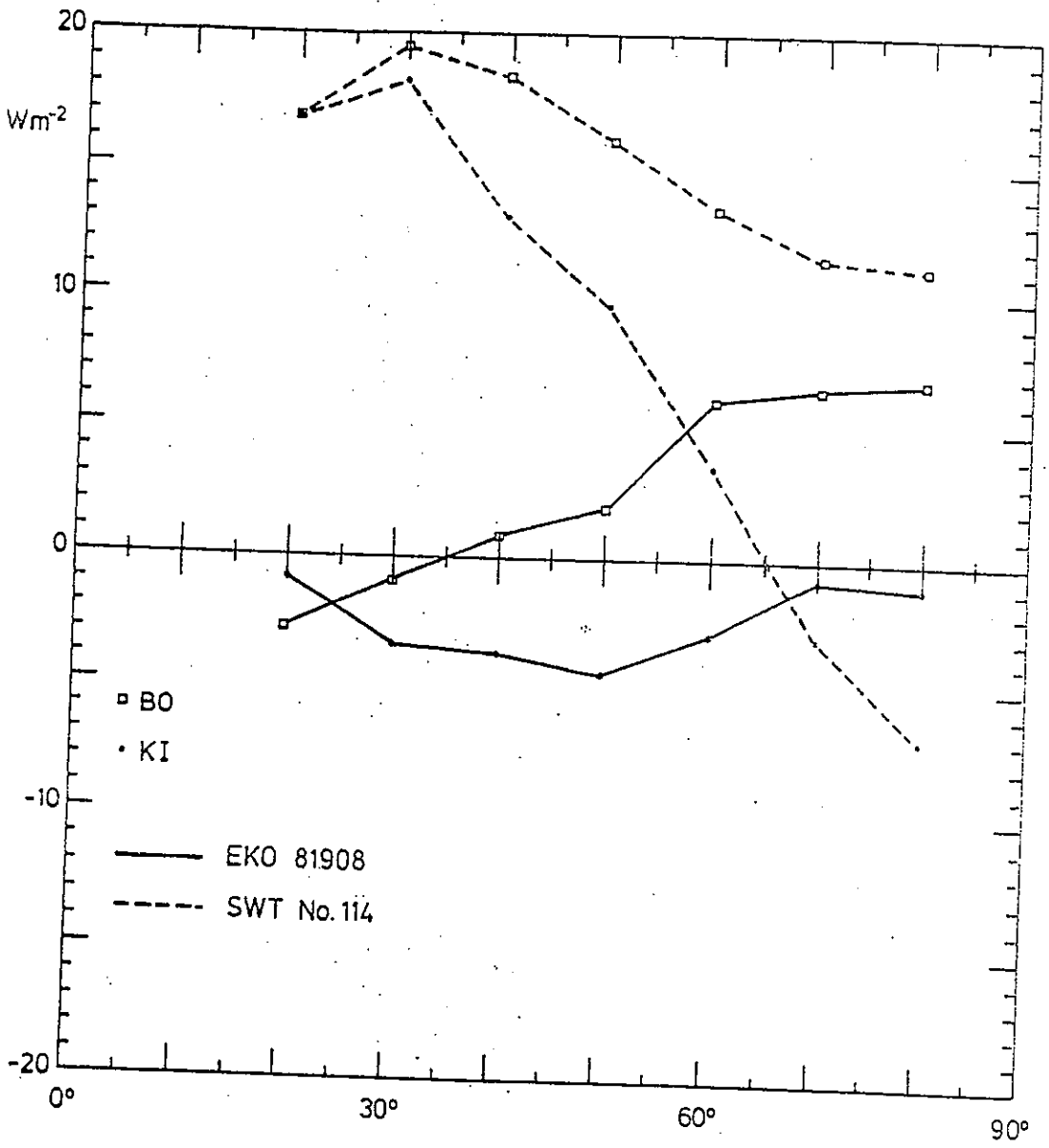

Fig. 4.1.3.1d : Dependence on the incidence angle θ of the absolute effective cosine errors $\bar{\delta}_t(\theta)$ for one pyranometer of type Eko MS-42 and one pyranometer of type SWT

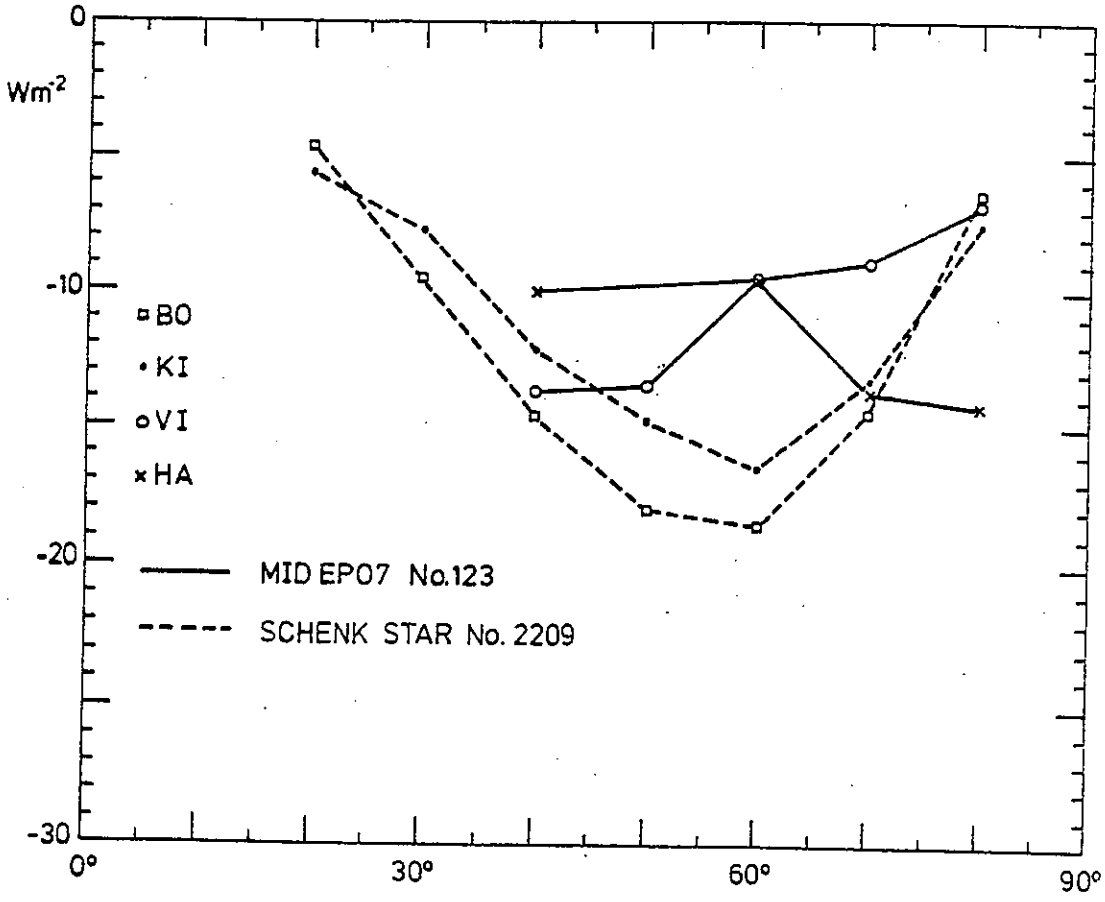

Fig. 4.1.3.1e : Dependence on the incidence angle θ of the absolute effective cosine errors $\bar{\delta}_t(\theta)$ for one pyranometer of type Schenk Star and one pyranometer of type MID EP07

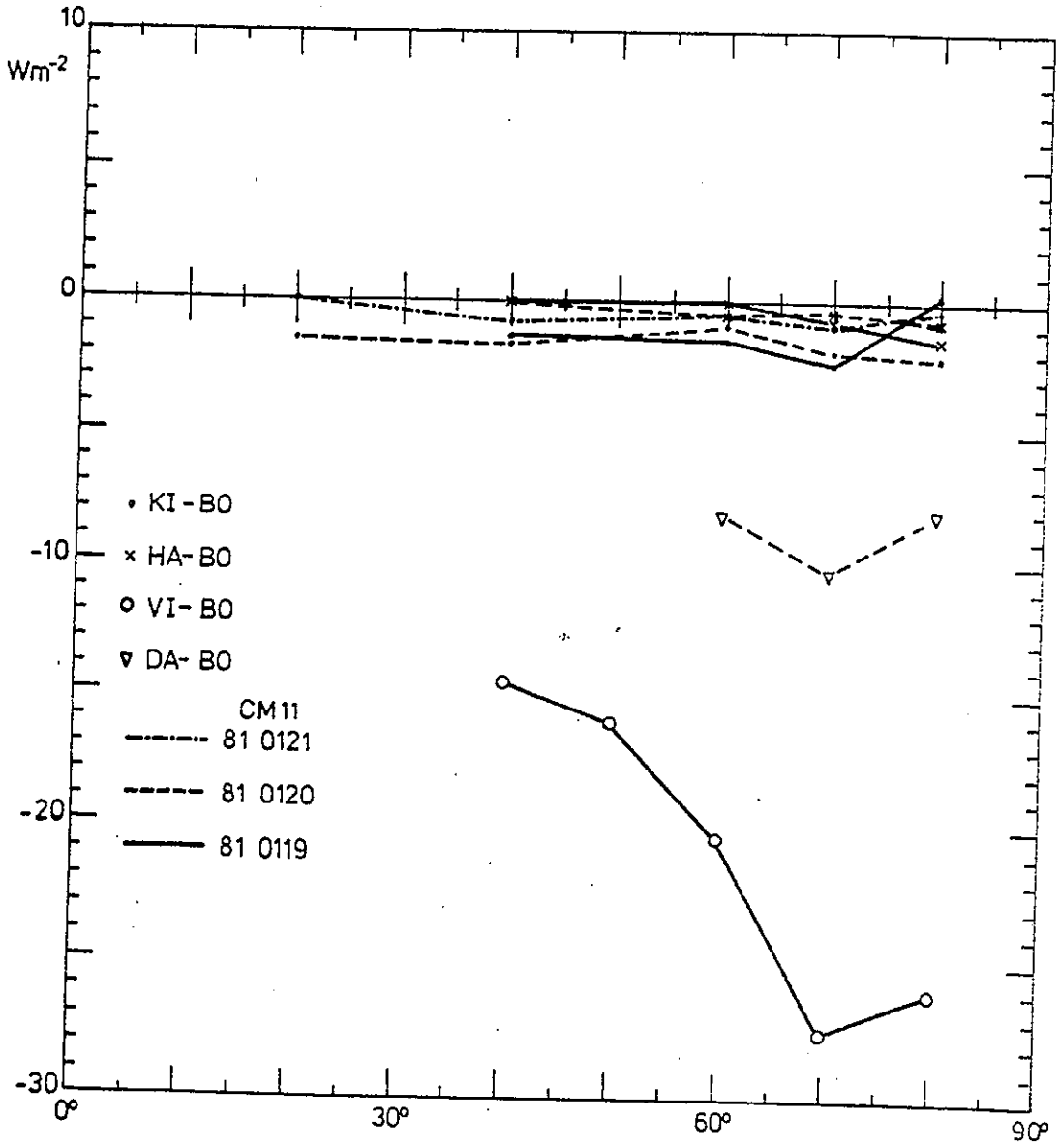

Fig. 4.1.3.1f : Dependence on the incidence angle θ of the difference $\Delta\delta_t(\theta)$ between the $\bar{\delta}_t$ - results of the indicated laboratories for pyranometers of type CM11

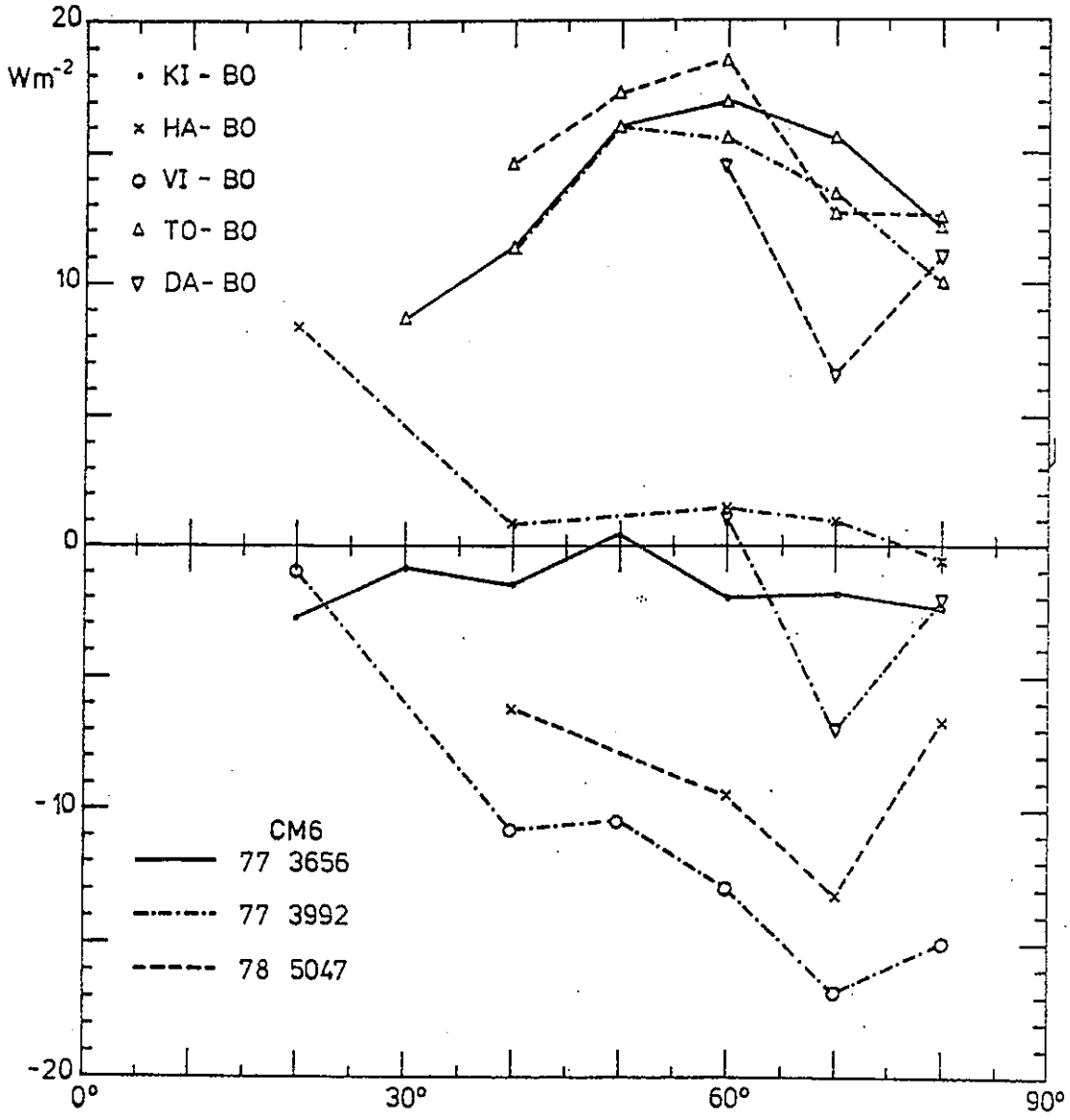

Fig. 4.1.3.1g : Dependence on the incidence angle θ of the difference $\Delta\delta_t(\theta)$ between the $\bar{\delta}_t$- results of the indicated laboratories for pyranometers of type CM6

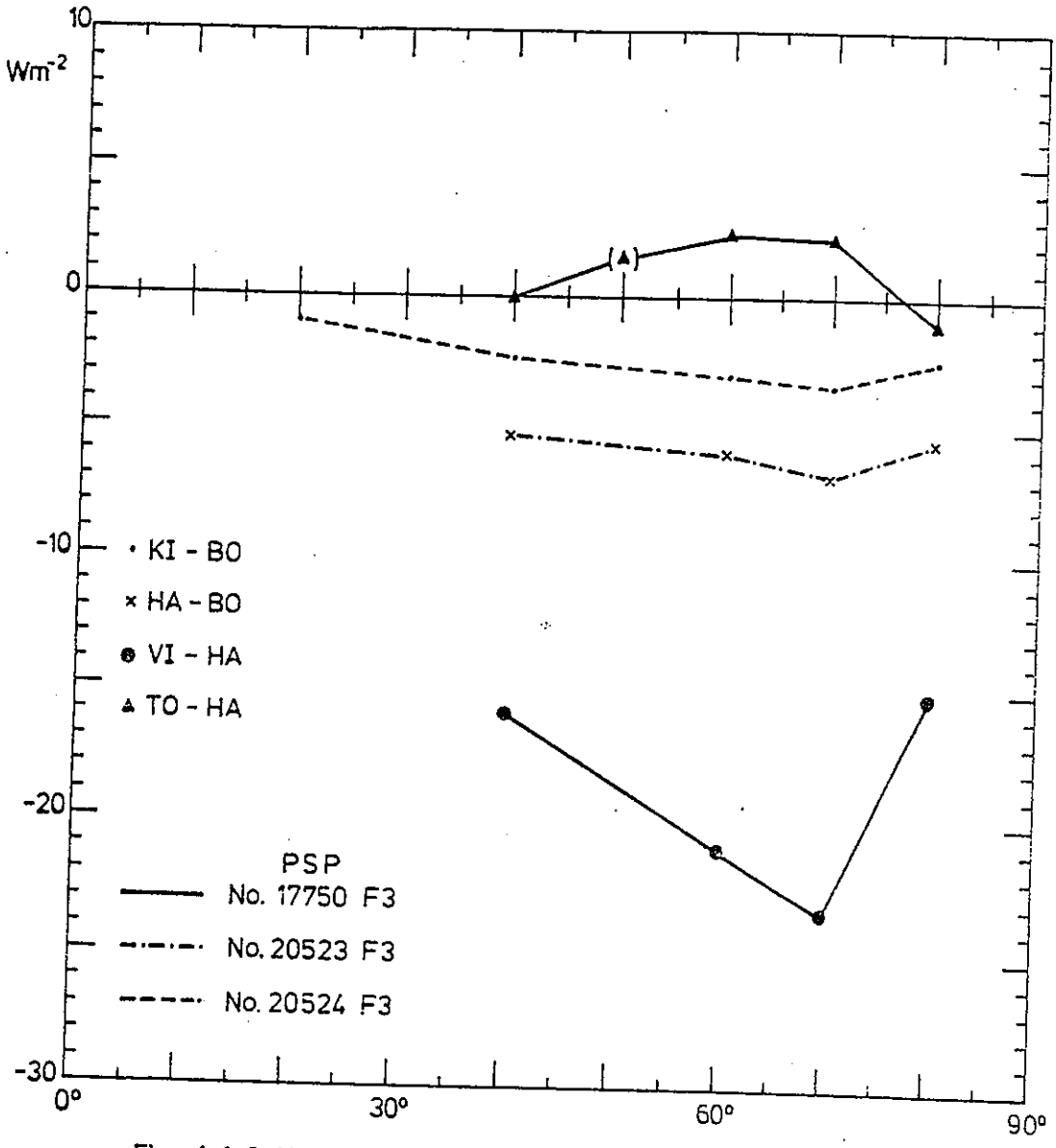

Fig. 4.1.3.1h : Dependence on the incidence angle θ of the difference $\Delta\delta_t(\theta)$ between the $\bar{\delta}_t$ - results of the indicated laboratories for pyranometers of type PSP

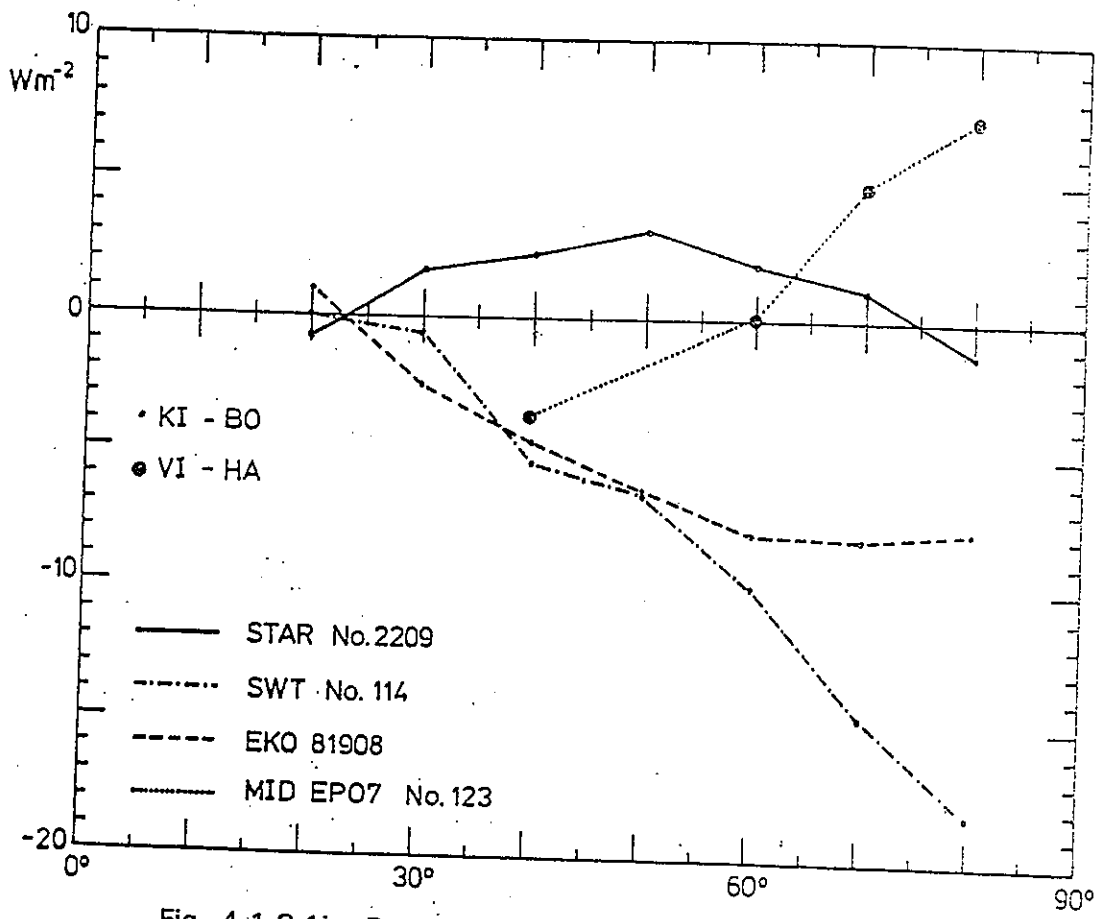

Fig. 4.1.3.1i : Dependence on the incidence angle θ of the difference $\Delta\delta_t(\theta)$ between the $\bar{\delta}_t$ - results of the indicated laboratories for 4 pyranometers of different type (Schenk Star, SWT, Eko MS-42 and MID EP07)

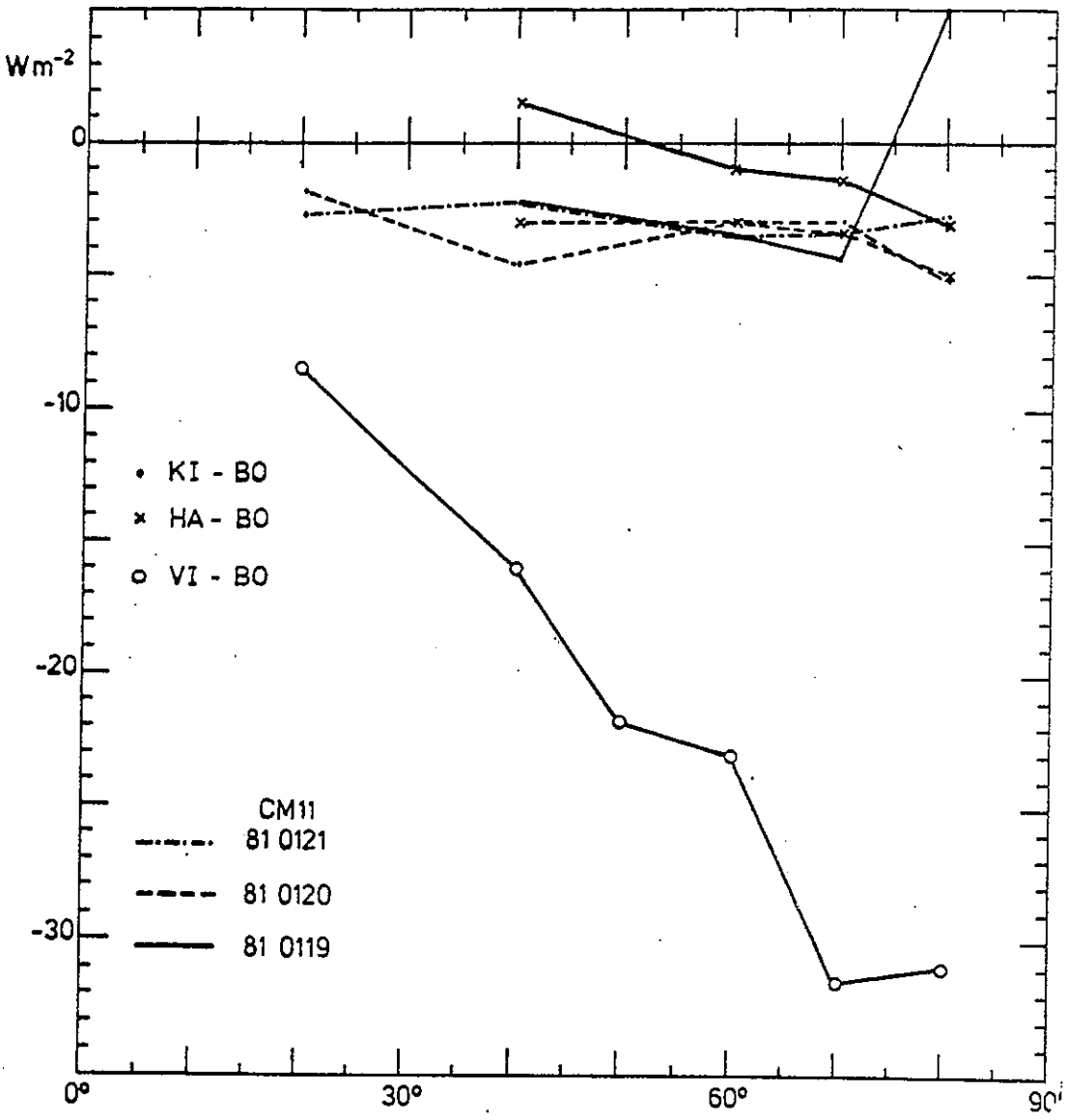

Fig. 4.1.3.1j : Dependence on the incidence angle θ of the maximum difference $\Delta_{max}(\theta)$ between the $\delta_t(\theta,\phi)$ - results of the indicated laboratories for pyranometers of type CM11

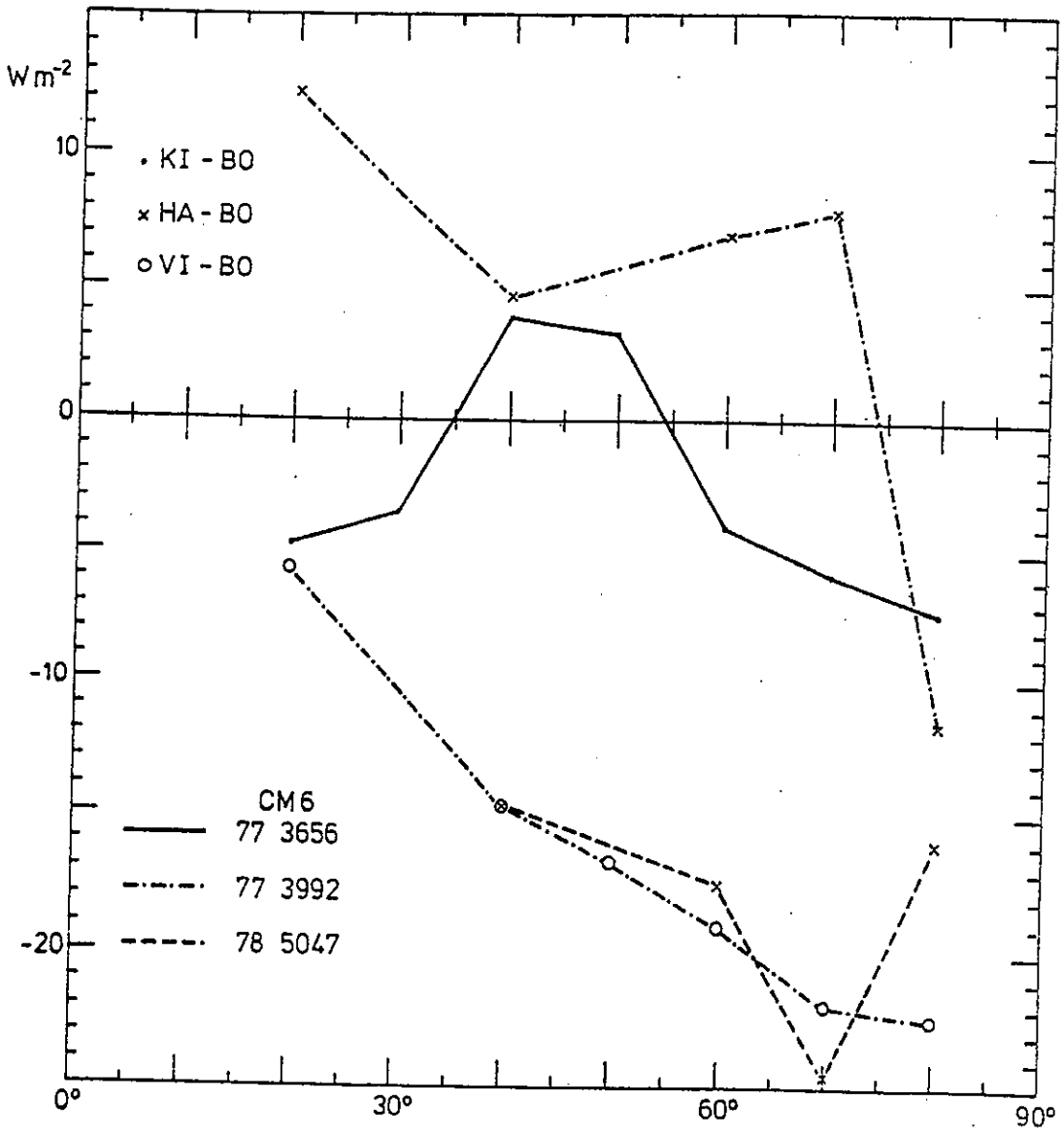

Fig. 4.1.3.1k : Dependence on the incidence angle θ of the maximum difference $\Delta_{max}(\theta)$ between the $\delta_t(\theta,\phi)$ - results of the indicated laboratories for pyranometers of type CM6

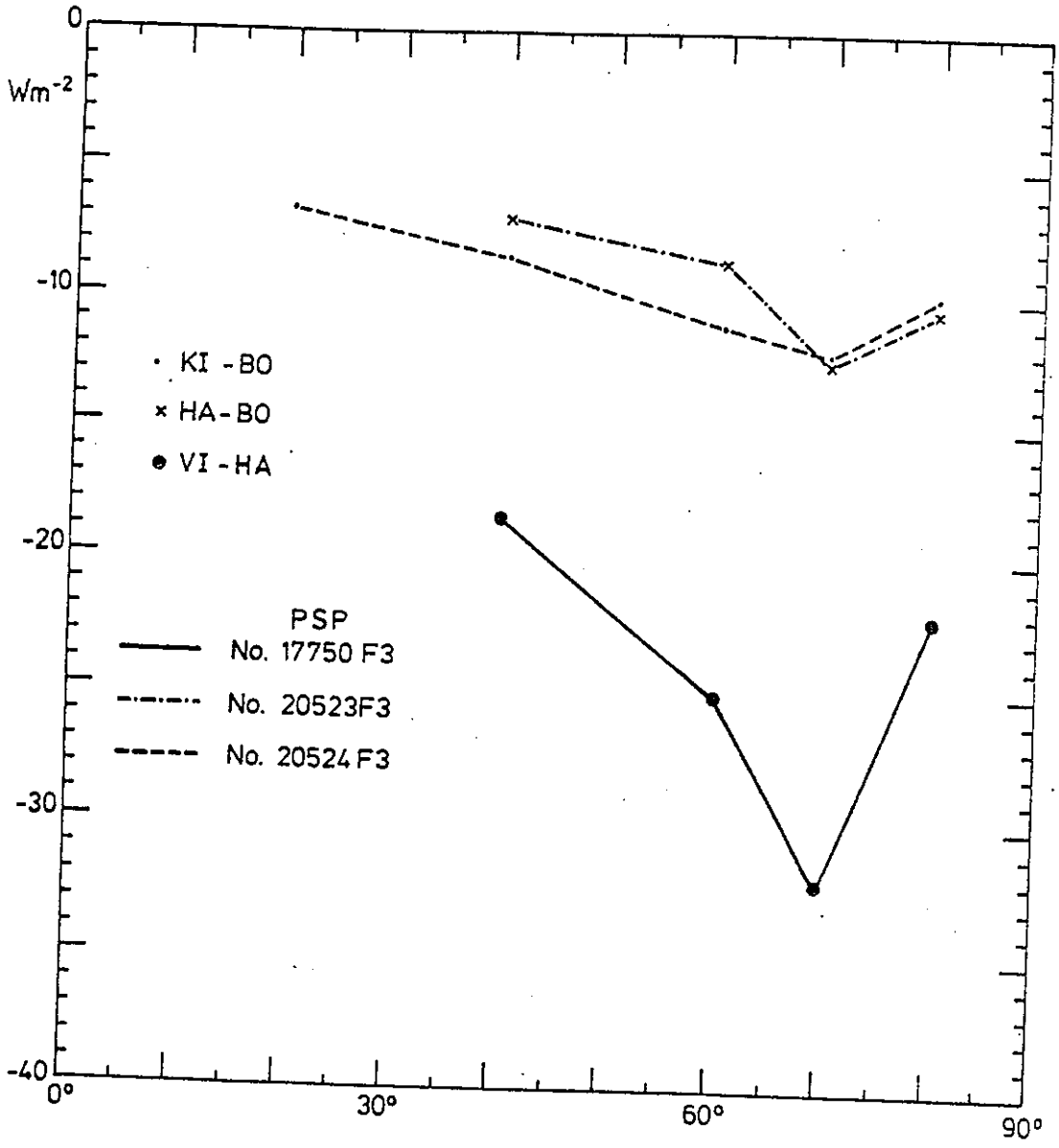

Fig. 4.1.3.11 : Dependence on the incidence angle θ of the maximum difference $\Delta_{max}(\theta)$ between the $\delta_t(\theta,\phi)$ - results of the indicated laboratories for pyranometers of type PSP

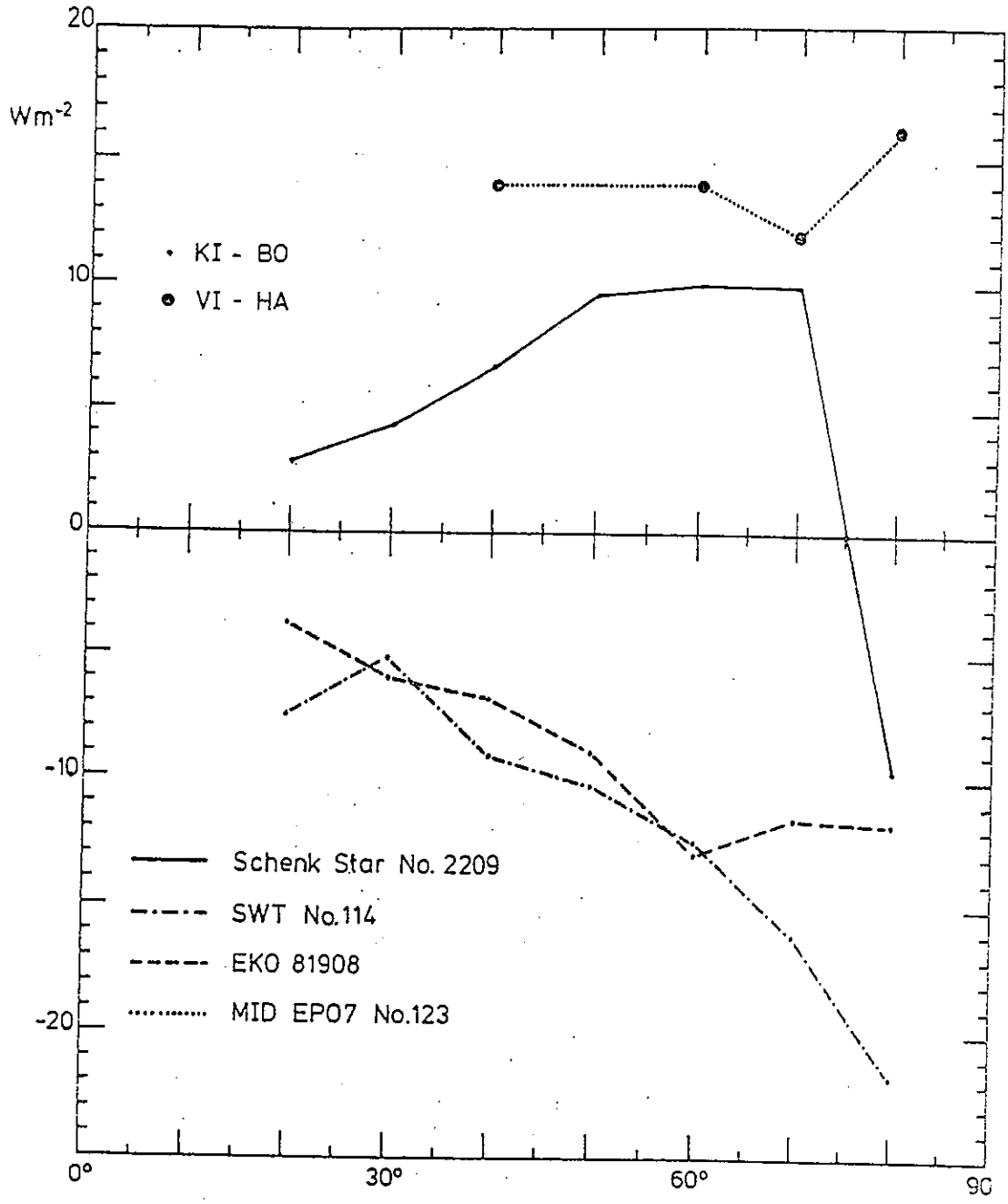

Fig. 4.1.3.1m : Dependence on the incidence angle θ of the maximum difference $\Delta_{max}(\theta)$ between the $\delta_t(\theta,\phi)$ - results of the indicated laboratories for 4 pyranometers of different type (Schenk Star, SWT, Eko MS-42 and MID EP07).

4.2 Field Measurements

Several field investigations were performed by Subtask 9C or in association with it. Their calibration results are contained in §8 where discrepancies between different institutions are examined. Two field experiments are described in detail here and results are given either in the main text or appendices.

4.2.1 Norrköping experiment - directional response determined by field measurement

The field experiment at Norrköpping (58.6°N, 16.1°E) to measure directional response began in April 1984 and continued until the end of 1985. Pyranometers were tested in the horizontal and 45° tilted orientation. The six IEA instruments were:

Swissteco SS25 #113A,
Schenk-1626,
Kipp and Zonen CM10 #810120,
Kipp and Zonen CM5 #785047,
Eppley PSP #20523,
Eko MS42 #A81901.

4.2.1.1 Instrumentation

As reference for horizontal measurements, the sum of the direct and diffuse components was used $I \cdot \sin h + D$ measured with the Eppley NIP #17007 and Kipp and Zonen CM10 #810132, respectively. The latter instrument was shaded with a sun-following disc. To check the reliability of the reference system, the standard pyranometer CM10 #800080, belonging to SMHI and characterised by frequent calibrations against Ångström pyrheliometer #171, was included in the group to be investigated. Instrument CM10 #800080 has also been used as an ultimate reference when determining the responsivities of pyranometers at the solar elevation 35°, the angle of incidence 55° and at normal incidence.

Measurements were made with the pyranometers at an inclination of 45° between August and November 1985. The diffuse radiation was measured with a tilted pyranometer shaded with a sun-following disc. First the pyranometers were oriented towards the south (azimuth 180°), but in mid-September the orientation was changed to south-west (azimuth 230.5°).

During the period when the pyranometers faced south, the reference consisted of Eppley NIP #20918 and Kipp and Zonen CM10 #820133. During the last period NIP #17007 was again used.

The test pyranometers were not radiometrically levelled. The resolution of the HP3455A digital voltmeter of the data acquisition system is 1.0 μV.

4.2.1.2 The Reference Instruments

The calibration factor, which is the reciprocal of responsivity, of NIP #17007 was determined as 122.28 Wm^{-2} mV^{-1} based on 124 calibrations against Å 171. The pyrheliometer, NIP #20918, which was used temporarily during the first half of the tilt measurement, was calibrated against Å 171 with a calibration factor determined as 119.49 Wm^{-2} mV^{-1}.

Measurements of diffuse radiation were all referenced to CM10 800080, the standard pyranometer at SMHI. A calibration factor for CM10 #800080, valid for diffuse radiation, was calculated as the weighted mean of all calibrations done against Å 171 with solar elevations above 20°, the weights being derived from the assumption that diffuse radiation is isotropic. The value so obtained for diffuse radiation, 164.12 Wm^{-2} mV^{-1} deviates very little from that in regular use, 164.35 Wm^{-2} mV^{-1}.

The pyranometer used for measuring diffuse radiation on a horizontal surface, CM10 #810132, was compared with the reference instrument, CM10 #800080, for 803 hours with completely overcast sky. Correction was made for the offset signals, the diffuse calibration for the reference was used and it was assumed that the influence of the shading disc was negligible. The comparison resulted in the calibration factor 218.58 Wm^{-2} mV^{-1} for CM10 #810132.

The reference pyranometer for measuring diffuse radiation on tilted surfaces, CM10 #820133, was calibrated by comparison with CM10 #800080 using hourly mean values with solar elevation approximately 35° during a 35-day period in April and May, 1985. The result for CM10 #820133 was determined as 211.37 Wm^{-2} mV^{-1}.

4.2.1.3 Evaluation

Raw data from instruments tested in the horizontal position were evaluated using offset corrections and preliminary calibrations for the IEA pyranometers at a solar elevation of 35°.

The latter were derived from the early results of the comparison and are listed in Table 4.2.1.4e. No temperature corrections were made.

The evaluation has been extended to give the cosine response for the direct component so as to be more easily compared with results from laboratory investigations and outdoor calibrations with the alternating shade method. For this purpose, the calibration factors valid for diffuse radiation were determined by comparison with the standard pyranometer, CM10 #800080, for 507 hours under overcast conditions in the period from March to November, 1984. The mean temperature during the comparison was 10.3 C. The responsivities are listed in Table 4.2.1.4e.

The *cosine response* $\ddot{\delta}$ which is defined here as the responsivity at a given solar elevation divided by the value at 35°, is computed from:

$$\ddot{\delta}_G = \frac{V \cdot C_{35°}}{I \cdot \sin h + D} \qquad \text{for the global radiation} \qquad [4.11]$$

$$\ddot{\delta}_I = \frac{(V - D/C_D) \cdot C_{35°}}{I \cdot \sin h} \qquad \text{for the direct component} \qquad [4.12]$$

where

V	=	signal from the pyranometer in millivolts,
D	=	diffuse radiation measured with the reference pyranometer
h	=	solar elevation
C_D	=	calibration constant for diffuse radiation,
$C_{35°}$	=	calibration constant for global radiation at $h = 35°$,
$I \cdot \sin h$	=	vertical component of direct radiation measured by the reference pyrheliometer.

Several approximations and simplifications have been made when trying to separate the cosine response from the direct component. No temperature corrections have been applied which may lead to large errors in the difference $V - D/C_D$ at low solar elevations when the diffuse radiation constitutes the major part of the global radiation. The assumption of isotropy may have the same effect. The offset corrections have been determined from the offset values found during night hours using the assumption that the cooling of the glass domes of the pyranometers by radiation loss to the clear sky is the same as during the daytime and can be added or subtracted from the output of the instruments (see §6.7).

Also, the normalisation in equation 4.12 should be against the responsivity at $h = 35°$ for direct not global radiation.

4.2.1.4 Presentation of results

Tables 4.2.1.4a&b show the cosine response of pyranometers in the horizontal position for global and direct radiation, respectively.

Table 4.2.1.4c shows the cosine response of pyranometers inclined at 45°. Cases with increasing and decreasing angle of incidence are separated. The mean temperatures at angle of incidence 55° and for all incidence angles are given in Table 4.2.1.4d.

Benchmark responsivities for horizontal measurements at h = 35°, BMHO, for tilted measurements at i = 55° BMTO, and at near normal incidence, BMTN, have been calculated from Tables 4.2.1.4a-d. The BMHO values are in Table 4.2.1.4e and BMTO and BMTN values in Table 4.2.1.4f. A correction of 0.2%, which arises from the normalisation of the cosine response of the reference instrument CM10 #800080, is included in these values.

Figures 4.2.1.4a-g show the cosine response for individual instruments which are summarised below.

4.2.1.5 Review of results for each instrument.

SS25 #113A

Responsivity decreases strongly with decreasing solar elevation and increasing incidence angle with the pyranometer in horizontal and tilted position respectively. The reason for the difference between forenoon and afternoon values is not clear (Figure 4.2.1.4a].

CM5 #785047

Responsivity is approximately independent of solar elevation and incidence angle in the interval h = 10°-50° and i = 5°-80° respectively. At lower solar elevations and larger incidence angles the responsivity increases strongly (Figure 4.2.1.4b).

Table 4.2.1.4a Cosine response: global radiation on horizontal surface.

Pyranometer			Solar Elevation — Degrees 2.5	5	10	15	20	25	30	35	40	45	50
SS25 #113A	*am*	*m*	0.892	0.897	0.929	0.945	0.958	0.971	0.980	0.988	0.994	1.003	0.999
		s	0.072	0.045	0.024	0.018	0.015	0.011	0.009	0.009	0.011	0.008	0.006
		n	7	10	20	21	19	18	17	14	14	12	3
	pm	*m*	0.984	0.943	0.967	0.986	0.995	1.003	1.010	1.013	1.017	1.018	1.013
		s	0.065	0.048	0.023	0.015	0.013	0.012	0.010	0.009	0.008	0.007	0.010
		n	9	10	20	20	20	18	17	17	16	15	4
CM5 #785047	*am*	*m*	1.066	1.035	1.013	1.007	1.008	1.007	1.004	1.003	1.001	1.003	1.000
		s	0.047	0.041	0.018	0.016	0.012	0.007	0.006	0.006	0.007	0.003	0.004
		n	7	10	19	21	19	18	17	14	14	11	3
	pm	*m*	1.065	1.047	1.017	1.017	1.009	1.008	1.005	1.004	1.005	1.004	1.003
		s	0.035	0.042	0.022	0.014	0.012	0.009	0.008	0.007	0.006	0.005	0.007
		n	6	6	19	20	20	18	17	17	16	15	4
EKO #A81901	*am*	*m*	1.057	0.988	0.982	0.982	0.983	0.986	0.989	0.996	1.001	1.008	1.016
		s	0.093	0.045	0.022	0.023	0.020	0.017	0.016	0.015	0.014	0.012	0.004
		n	7	11	20	21	19	18	17	14	14	12	2
	pm	*m*	0.972	0.990	1.009	1.017	1.015	1.012	1.011	1.011	1.015	1.015	1.019
		s	0.041	0.031	0.012	0.010	0.012	0.011	0.012	0.011	0.012	0.011	0.010
		n	10	11	20	20	20	18	17	17	16	15	4
CM10 #810120	*am*	*m*	1.034	1.013	0.996	0.995	0.994	0.998	1.00	1.003	1.006	1.009	1.005
		s	0.044	0.031	0.015	0.013	0.011	0.008	0.007	0.007	0.008	0.006	0.007
		n	7	10	20	21	19	18	17	14	14	11	3
	pm	*m*	0.999	0.989	0.987	0.995	0.998	1.002	1.005	1.009	1.013	1.015	1.013
		s	0.050	0.051	0.017	0.012	0.011	0.008	0.008	0.007	0.007	0.007	0.007
		n	6	7	20	20	20	18	17	17	16	15	4
CM10 #800080	*am*	*m*	1.036	1.020	0.998	0.979	0.981	0.986	0.991	0.994	0.998	1.001	1.000
		s	0.063	0.034	0.013	0.010	0.010	0.008	0.006	0.006	0.006	0.006	0.010
		n	7	10	20	21	19	18	16	13	14	12	2
	pm	*m*	1.019	1.008	0.998	0.985	0.987	0.993	0.997	1.001	1.004	1.004	1.005
		s	0.037	0.018	0.014	0.008	0.006	0.006	0.006	0.005	0.005	0.008	0.006
		n	7	9	20	20	20	18	17	17	14	15	4
SCH #1626	*am*	*m*	1.038	1.009	1.010	1.006	1.000	1.001	0.998	0.996	0.996	0.994	0.986
		s	0.055	0.047	0.019	0.013	0.009	0.008	0.006	0.006	0.008	0.004	0.003
		n	7	10	20	21	19	18	17	14	14	11	3
	pm	*m*	0.994	0.981	1.006	1.011	1.009	1.009	1.006	1.000	0.996	0.992	0.987
		s	0.025	0.043	0.021	0.012	0.009	0.006	0.005	0.005	0.004	0.004	0.003
		n	6	9	20	20	20	18	17	17	15	15	4
PSP #20523	*am*	*m*	0.997	0.970	0.983	0.987	1.006	1.001	1.001	1.006	1.011	1.016	1.019
		s	0.055	0.036	0.018	0.015	0.014	0.010	0.008	0.007	0.007	0.006	0.005
		n	7	13	20	21	19	18	17	14	14	12	3
	pm	*m*	0.931	0.916	0.951	0.973	0.997	0.997	0.998	1.005	1.011	1.016	1.018
		s	0.023	0.054	0.021	0.014	0.010	0.009	0.008	0.007	0.006	0.005	0.008
		n	4	8	20	20	20	18	17	17	16	15	4
Temp. C	*am*		+9.4	+7.8	+7.7	+8.5	+9.6	+11.0	+12.0	+13.2	+14.2	+14.8	+19.1
	pm		+13.9	+13.7	+15.6	+16.2	+16.6	+17.2	+17.5	+17.6	+17.4	+17.4	+20.2

Table 4.2.1.4b Cosine response: direct component on horizontal surface.

Pyranometer			Solar Elevation — Degrees										
			2.5	5	10	15	20	25	30	35	40	45	50
SS25 #113A	*am*	*m*	0.661	0.729	0.841	0.895	0.923	0.947	0.962	0.974	0.984	0.995	0.990
		s	0.225	0.094	0.048	0.038	0.027	0.019	0.018	0.012	0.014	0.010	0.002
		n	7	10	20	21	18	18	17	14	14	12	2
	pm	*m*	0.595	0.681	0.886	0.949	0.973	0.987	1.000	1.006	1.012	1.013	1.008
		s	0.283	0.164	0.057	0.028	0.021	0.018	0.014	0.012	0.010	0.009	0.010
		n	7	9	20	20	20	18	17	17	16	15	4
CM5 #785047	*am*	*m*	1.176	1.022	0.995	0.991	0.995	0.994	0.994	0.995	0.992	0.995	0.994
		s	0.205	0.094	0.031	0.023	0.018	0.015	0.010	0.006	0.008	0.006	0.004
		n	6	9	19	21	19	19	17	14	14	12	3
	pm	*m*	1.241	1.049	0.999	1.005	0.997	0.997	0.994	0.995	0.997	0.996	0.996
		s	0.201	0.128	0.045	0.023	0.015	0.012	0.010	0.008	0.007	0.006	0.006
		n	6	7	19	20	20	18	17	17	16	15	4
EKO #A81901	*am*	*m*	1.164	0.906	0.918	0.944	0.952	0.961	0.970	0.981	0.987	0.998	1.012
		s	0.384	0.121	0.064	0.039	0.033	0.028	0.024	0.020	0.018	0.016	0.003
		n	7	11	20	21	19	18	17	14	14	12	3
	pm	*m*	0.546	0.829	0.962	0.994	0.997	0.996	0.998	1.001	1.005	1.006	1.012
		s	0.271	0.153	0.040	0.018	0.016	0.013	0.014	0.013	0.015	0.012	0.010
		n	10	11	20	20	20	18	17	17	16	15	4
CM10 #810120	*am*	*m*	1.081	1.002	0.977	0.982	0.984	0.995	0.995	0.999	1.003	1.008	1.003
		s	0.119	0.073	0.029	0.022	0.016	0.010	0.010	0.008	0.010	0.006	0.008
		n	7	10	20	20	19	17	17	14	14	12	3
	pm	*m*	0.932	0.927	0.954	0.980	0.990	0.996	1.002	1.007	1.012	1.015	1.013
		s	0.305	0.181	0.042	0.021	0.016	0.011	0.010	0.008	0.008	0.008	0.008
		n	5	6	20	20	20	18	17	17	16	15	4
CM10 #800080	*am*	*m*	1.106	1.034	0.975	0.967	0.971	0.981	0.987	0.992	0.997	1.001	1.000
		s	0.163	0.066	0.023	0.017	0.014	0.012	0.008	0.007	0.008	0.007	0.001
		n	7	11	20	21	19	18	16	13	14	12	2
	pm	*m*	1.091	1.031	0.973	0.974	0.980	0.989	0.995	1.000	1.005	1.005	1.006
		s	0.329	0.073	0.033	0.014	0.009	0.008	0.008	0.007	0.006	0.010	0.007
		n	7	9	20	20	20	18	17	17	14	15	4
SCH #1626	*am*	*m*	1.117	0.989	0.995	0.996	0.989	0.992	0.989	0.989	0.988	0.986	0.980
		s	0.311	0.125	0.033	0.020	0.013	0.010	0.009	0.007	0.009	0.004	0.003
		n	7	10	20	21	19	18	17	14	14	12	3
	pm	*m*	0.811	0.866	0.984	1.001	1.001	1.002	0.999	0.993	0.989	0.984	0.978
		s	0.218	0.140	0.042	0.021	0.015	0.010	0.008	0.007	0.006	0.005	0.003
		n	7	9	20	20	20	18	17	17	16	15	4
PSP #20523	*am*	*m*	0.937	0.907	0.940	0.960	0.994	0.989	0.991	0.999	1.005	1.012	1.017
		s	0.147	0.079	0.037	0.029	0.022	0.015	0.013	0.010	0.009	0.008	0.005
		n	7	11	20	21	19	18	17	14	14	12	3
	pm	*m*	0.465	0.584	0.860	0.931	0.979	0.982	0.987	0.997	1.006	1.012	1.015
		s	0.188	0.272	0.057	0.027	0.018	0.013	0.011	0.009	0.007	0.006	0.008
		n	4	8	20	20	20	18	17	17	16	15	4
Temp. C	*am*		+9.4	+7.8	+7.7	+8.5	+9.6	+11.0	+12.0	+13.2	+14.2	+14.8	+19.1
	pm		+13.9	+13.7	+15.6	+16.2	+16.6	+17.2	+17.5	+17.6	+17.4	+17.4	+20.2

Table 4.2.1.4c Cosine response: global radiation on 45° sloping surface oriented in azimuths 180° and 230.5°.

Pyranometer	Conditions			Angle of Incidence																
				87.5	85	80	75	70	65	60	55	50	45	40	35	30	25	20	15	10	5
SS25-113A	Azimuth 180°	Decr	*m*	---	0.971	0.963	0.977	0.986	0.985	0.996	1.001	1.005	1.007	1.008	1.009	1.010	1.011	1.012	1.012	1.002	0.996
			s		0.030	0.023	0.002	0.006	0.010	0.012	0.008	0.010	0.007	0.009	0.009	0.008	0.007	0.008	0.008	0.004	---
			n		3	3	3	2	2	2	66	6	6	6	4	4	4	4	4	2	1
		Incr	*m*	0.945	0.911	0.941	0.953	0.958	0.969	0.974	0.981	0.988	0.991	1.003	0.998	1.000	1.003	1.007	1.008	1.003	0.997
			s	0.078	0.040	0.023	0.16	0.008	0.009	0	0.003	0.001	0	0.008	0.001	0	0.001	0.001	0.002	0.004	---
			n	4	4	4	4	3	3	2	2	2	2	3	3	3	3	3	3	2	1
	Azimuth 230.5°	Decr	*m*			0.942	0.960	0.974	0.983	0.992	0.997	1.002	1.005	1.009	1.013	1.009	1.017				
			s			0.012	0.007	0.007	0.006	0.004	0.005	0.005	0.006	0.006	0.005	0.004	0.016				
			n			5	11	12	12	12	10	9	10	10	9	2	2				
		Incr	*m*									1.019	1.025	1.022	1.021	1.020					
			s									---	0.010	0.004	0.003	---					
			n									1	5	6	6	1					
CM5-785047	Azimuth 180°	Decr	*m*		1.170	1.058	1.017	1.016	1.010	1.009	1.007	1.004	1.001	0.999	0.997	0.996	0.996	0.996	0.995	0.990	0.991
			s		0.056	0.023	0.001	0.006	0.006	0.013	0.006	0.006	0.005	0.006	0.006	0.006	0.006	0.006	0.006	0.003	---
			n		3	3	3	2	2	2	6	6	6	6	4	4	4	4	4	2	1
		Incr	*m*	1.095	1.068	1.023	1.018	1.011	1.005	0.998	0.999	0.999	0.999	1.002	0.995	0.995	0.995	0.997	0.997	0.994	0.991
			s	0.022	0.037	0.019	0.010	0.009	0.011	0.001	0.001	0.001	0.001	0.008	0.001	0.001	0.001	0.001	0.002	0	---
			n	4	4	4	4	3	3	2	2	2	2	3	3	3	3	3	3	2	1
	Azimuth 230.5°	Decr	*m*			1.026	1.018	1.017	1.013	1.009	1.007	1.004	1.001	1.002	1.003	0.998	1.005				
			s			0.006	0.006	0.003	0.003	0.004	0.004	0.003	0.003	0.003	0.004	0.002	0.015				
			n			2	8	9	9	9	9	8	9	9	9	2	2				
		Incr	*m*									1.019	1.021	1.014	1.010	1.004					
			s									---	0.012	0.004	0.003	---					
			n									1	5	6	6	1					

Continued ...

Table 4.2.1.4c *Continued*

Pyranometer	Conditions			Angle of Incidence																
				87.5	85	80	75	70	65	60	55	50	45	40	35	30	25	20	15	10	5
EKO-A61901	Azimuth 180°	*Decr*	*m*		1.176	1.017	0.995	0.982	0.978	0.978	0.975	0.974	0.976	0.981	0.984	0.987	0.990	0.993	0.996	0.997	1.000
			s		0.146	0.048	0.013	0	0.013	0.019	0.009	0.006	0.006	0.006	0.003	0.002	0.002	0.003	0.002	0.001	---
			n		3	3	3	2	2	2	6	6	6	6	4	4	4	4	4	2	1
		Incr	*m*	1.095	1.050	0.990	0.985	0.976	0.976	0.976	0.979	0.979	0.977	0.988	0.984	0.987	0.990	0.994	0.996	0.996	0.998
			s	0.070	0.025	0.018	0.014	0.009	0.012	0.014	0.012	0.011	0.010	0.006	0.007	0.007	0.005	0.004	0.007	0.001	---
			n	4	4	4	4	3	3	2	2	2	2	3	3	3	3	3	3	2	1
	Azimuth 230.5°	*Decr*	*m*				0.995	0.991	0.988	0.986	0.988	0.990	0.989	0.990	0.991	0.992	1.00				
			s				---	0	0.002	0.003	0.007	0.005	0.004	0.004	0.005	0.003	0.015				
			n				1	2	2	2	2	2	2	2	2	2	2				
		Incr	*m*																		
			s																		
			n																		
CM10-810120	Azimuth 180°	*Decr*	*m*		1.019	0.979	0.960	0.971	0.975	0.980	0.985	0.989	0.993	0.996	0.999	1.001	1.005	1.007	1.009	1.006	1.002
			s		0.075	0.034	0.004	0.011	0.009	0.010	0.006	0.007	0.007	0.010	0.008	0.007	0.005	0.006	0.006	0.005	---
			n		3	3	3	2	3	3	6	6	6	6	4	4	4	4	4	2	1
		Incr	*m*	1.104	1.101	1.052	1.044	1.043	1.037	1.030	1.029	1.028	1.026	1.030	1.023	1.020	1.020	1.018	1.017	1.011	1.017
			s	0.023	0.046	0.012	0.010	0.010	0.009	0	0	0.001	0.001	0.007	0.001	0.002	0.001	0.002	0.004	0.001	---
			n	4	4	4	4	3	3	2	2	2	2	3	3	3	3	3	3	2	1
	Azimuth 230.5°	*Decr.*	*m*			1.016	1.008	1.005	1.004	1.006	1.009	1.010	1.010	1.011	1.013	1.016	1.024				
			s			0.005	0.009	0.008	0.006	0.004	0.003	0.004	0.005	0.003	0.002	0.003	0.013				
			n			5	11	12	12	12	10	9	9	10	9	2	2				
		Incr	*m*									1.006	1.005	1.006	1.010	1.012					
			s									---	0.004	0.003	0.002	---					
			n									1	4	6	6	1					

Continued...

Table 4.2.1.4c *Continued*

Pyranometer	Conditions			Angle of Incidence																
				87.5	85	80	75	70	65	60	55	50	45	40	35	30	25	20	15	10	5
CM10-800080	Azimuth 180°	*Decr*	*m*		1.109	1.032	0.980	0.981	0.982	0.987	0.994	0.996	0.997	0.997	0.997	0.998	1.000	1.002	1.003	0.999	0.999
			s		0.077	0.054	0.005	0.006	0.010	0.008	0.009	0.007	0.007	0.009	0.007	0.007	0.006	0.007	0.006	0.004	---
			n		3	3	3	2	2	4	6	6	6	6	4	4	4	4	4	2	1
		Incr	*m*	1.042	1.043	0.994	0.992	0.994	0.996	0.996	0.998	1.001	1.002	1.010	1.002	1.002	1.003	1.004	1.004	1.001	0.999
			s	0.010	0.020	0.013	0.009	0.006	0.009	0.004	0.006	0.003	0.004	0.006	0.003	0.003	0.003	0.002	0.004	0.001	---
			n	4	4	4	4	3	3	2	2	2	2	3	3	3	3	3	3	2	1
	Azimuth 230.5°	*Decr*	*m*			1.005	0.993	0.993	0.995	0.999	1.003	1.004	1.005	1.006	1.008	1.008	1.013				
			s			0.010	0.005	0.005	0.003	0.002	0.004	0.004	0.005	0.004	0.003	0.004	0.013				
			n			5	11	12	12	12	10	9	10	10	9	2	2				
		Incr	*m*									0.996	0.996	1.000	1.004	1.005					
			s									---	0.007	0.004	0.003	---					
			n									1	5	6	6	1					
SCH-1626	Azimuth 180°	*Decr*	*m*		0.942	0.990	0.990	0.982	0.975	0.975	0.971	0.967	0.963	0.960	0.958	0.956	0.954	0.953	0.951	0.947	0.951
			s		0.067	0.010	0.003	0.010	0.008	0.009	0.006	0.007	0.004	0.005	0.006	0.006	0.006	0.006	0.006	0.004	---
			n		3	3	3	2	2	3	6	6	6	6	4	4	4	4	4	2	1
		Incr	*m*	1.014	1.054	1.049	1.032	1.022	1.007	0.989	0.980	0.973	0.965	0.967	0.962	0.955	0.954	0.952	0.952	0.950	0.949
			s	0.043	0.074	0.026	0.016	0.016	0.012	0.006	0.004	0.004	0.001	0.006	0.006	0.002	0.002	0.001	0.003	0	---
			n	4	4	4	4	3	3	2	2	2	2	3	3	3	3	3	3	2	1
	Azimuth 230.5°	*Decr*	*m*			1.003	0.996	0.989	0.981	0.978	0.974	0.970	0.968	0.968	0.967	0.963	0.970				
			s			0.004	0.006	0.005	0.003	0.005	0.004	0.003	0.004	0.005	0.004	0.004	0.020				
			n			5	11	12	12	12	10	9	10	9	2	2					
		Incr	*m*									0.999	1.001	0.983	0.973	0.962					
			s									---	0.012	0.006	0.002	---					
			n									1	5	6	5	1					

Continued...

Table 4.2.1.4c *Concluded*

Pyranometer	Conditions			Angle of Incidence															
				87.5	85	80	75	70	65	60	55	50	45	40	35	30	25	20	15	10	5
PSP-20523	Azimuth 180°	*Decr*	*m*		1.023	1.006	0.959	0.989	0.985	0.981	0.985	0.992	0.995	1.00	1.003	1.000	1.010	1.014	1.018	1.019	1.022
			s		0.107	0.066	0.003	0.006	0.011	0.011	0.007	0.007	0.004	0.006	0.005	0.004	0.006	0.006	0.003	0.001	---
			n		3	3	3	2	2	3	5	6	6	6	4	4	4	4	4	2	1
		Incr	*m*	0.986	.0980	0.996	1.006	1.019	1.011	1.007	1.012	1.014	1.016	1.024	1.020	1.021	1.023	1.024	1.026	1.023	1.021
			s	0.034	0.019	0.011	0.010	0.005	0.009	0.007	0.006	0.005	0.004	0.006	0.003	0.003	0.002	0.003	0.005	0.005	---
			n	4	4	4	4	3	3	2	2	2	2	2	3	3	3	3	3	2	1
	Azimuth 230.5°	*Decr*	*m*			0.979	0.987	1.006	0.998	0.996	0.995	1.003	1.005	1.008	1.010	1.017	1.021				
			s			0.009	0.011	0.009	0.005	0.005	0.016	0.005	0.005	0.005	0.006	0.003	0.010				
			n			5	11	12	121	12	10	9	10	10	9	2	2				
		Incr	*m*									0.980	0.975	0.993	1.002	1.009					
			s									---	0.013	0.007	0.004	---					
			n									1	5	6	6	1					

Table 4.2.1.4d Mean temperature during the inclined test.

		Mean temperature at all angles of incidence	Mean temperature at 55° incidence
Azimuth 180°	Decr	+10.2 C	+9.6 C
Azimuth 180°	Incr	+16.6 C	+16.7 C
Azimuth 230.5°	Decr	+8.7 C	+9.3 C
Azimuth 230.5°	Decr	+9.4 C	

Table 4.2.1.4.e Horizontal surface. Responsivities ($\mu V \cdot W^{-1}\ m^2$) referred to CM10-800080 at solar elevation 35° and for diffuse radiation.

Pyranometer Make & No	Responsivity Diffuse	Preliminary Responsivity Global	Responsivity Direct	Responsivity Global BMHO
SS25 #113A	15.85	15.27	15.17	15.33
CM5 #785047	12.19	11.77	11.74	11.84
Eko #A81901	8.35	7.95	7.90	8.00
CM10 #810120	4.58	4.51	4.36	4.55
CM10 # 800080	6.09	6.08	6.07	6.08
SCH # 1626	15.00	14.63	14.53	14.63
PSP #20523	10.05	9.73	9.73	9.81

Table 4.2.1.4f Inclination 45°. Responsivities ($\mu V \cdot W^{-1}\ m^2$) at 55° incidence angle and at normal incidence.

Pyranometer *Make & No*	Responsivity i = 55°, Direct BMTO	Responsivity i = 55°, Global	Responsivity Normal incidence BMTN
SS25 #113A	15.25	15.13	15.41
CM5 #785047	11.87	11.80	11.73
Eko #A81901	7.79	7.70	7.93
CM10 #810120	4.54	4.52	4.57
CM10 #800080	6.09	6.09	6.11
SCH #1626	14.27	14.14	13.94
PSP #20523	9.68	9.68	9.95

Eko #A81901

There is a large difference between forenoon and afternoon values of the responsivity for the pyranometer in the horizontal position while the difference between the corresponding values for the tilted pyranometer is negligible. The responsivity of the horizontal pyranometer decreases with decreasing solar elevation to about 10°. At lower elevations the values are uncertain. For the tilted pyranometer, the responsivity decreases with increasing incidence angle to about 70° and increases at greater angles (Figure 4.2.1.4c).

CM10 #800080

Responsivity decreases with decreasing solar elevation and increasing incidence angle for the horizontal and tilted pyranometers, respectively. A minimum is reached at h = 15°-20° and i = 75°-80°. At lower solar elevations and larger incidence angles, the responsivity increases markedly (Figure 4.2.1.4d).

Schenk #1626

This is the only instrument in the test that shows increasing responsivity with decreasing solar elevation and increasing incidence angle, respectively. At solar elevations less than 5-10°, and incidence angles greater than 80-85°, the uncertainty of the values does not allow any conclusions concerning the reasons for this anomalous response (Figure 4.2.1.4e).

PSP #20523

A pronounced decrease in the responsivity with decreasing solar elevation and increasing incidence angle is evident. The difference between responsivities associated with decreasing and increasing incidence angles may be caused by an error in the orientation of the tilted pyranometer (Figure 4.2.1.4f).

CM10 #810120

Responsivity of the horizontal pyranometer decreases slightly with decreasing solar elevation for global radiation. The decrease for direct radiation is more pronounced and has a minimum at 15°-20° (disregarding the afternoon values for low solar elevations). The large difference between decreasing and increasing incidence angle for the tilted pyranometer may be due to an error in the orientation (Figure 4.2.1.4g).

4.2.1.6 Estimation Of Errors

Errors from the offset signals, from misalignment of the pyranometers and from incorrect responsivities in the reference instruments contribute to the uncertainty of field directionality measurements. The effects of a 1.0 Wm^{-2} offset error, misalignments of 0.2°, 0.5° and 1.0°, and 1.0% and 2.0% errors in the reference measurements have been calculated and are shown in Tables 4.2.1.5a,b&c. These calculations used mean values of the global, diffuse and direct radiation from the duration of the experiment.

Table 4.2.1.5a percentage errors from a 1.0 Wm^{-2} error in offset correction

		Global on Horizontal		Direct on Horizontal		Global on Tilted		Direct on Tilted	
		am %	*pm* %	*am* %	*pm* %	*am* %	*pm* %	*am* %	*pm* %
h = 2.5°	i = 87.5°	3.3	5.6	9.1	33.3		1.4		4.2
h = 5.0°	i = 85.0°	1.6	2.3	3.1	6.7	1.5	1.2	2.7	2.9
h = 10.0°	i = 80.0°	0.7	0.9	1.3	1.8	0.7	0.8	1.0	1.4
h = 35.0°	i = 55.0°	0.2	0.2	0.2	0.2	0.2	0.2	0.2	0.2

Table 4.2.1.5b percentage errors from misaligning the tested pyranometers

		Error 0.2°		Error 0.5°		Error 1.0°	
		Global %	*Direct* %	*Global* %	*Direct* %	*Global* %	*Direct* %
h = 2.5°	i = 87.5°	1.4-2.2	8.0	3.4-5.7	20.0	6.9-11.5	40.0
h = 5.0°	i = 85.0°	1.5-2.3	4.0	3.6-5.8	10.0	7.3-11.6	20.0
h = 10.0°	i = 80.0°	1.1-1.4	2.0	2.6-3.4	4.9	5.3-6.9	9.9
h = 35.0°	i = 55.0°	0.4	0.5	1.0-1.1	1.2	1.9-2.2	2.5

Table 4.2.1.5c percentage errors from incorrect calibration of the reference instruments

		2% Error in D		1% Error in I	
		Global %	*Direct* %	*Global* %	*Direct* %
h = 2.5°	θ = 87.5°	1.3-1.7	3.5-10.7	0.2-0.4	1
h = 5.0°	θ = 85°	0.9-1.3	1.9-3.9	0.3-0.5	1
h = 10.0°	θ = 80°	0.6-1.0	0.8-1.9	0.5-0.7	1
h = 35.0°	θ = 55°	0.3-0.4	0.3-0.7	0.8-0.9	1

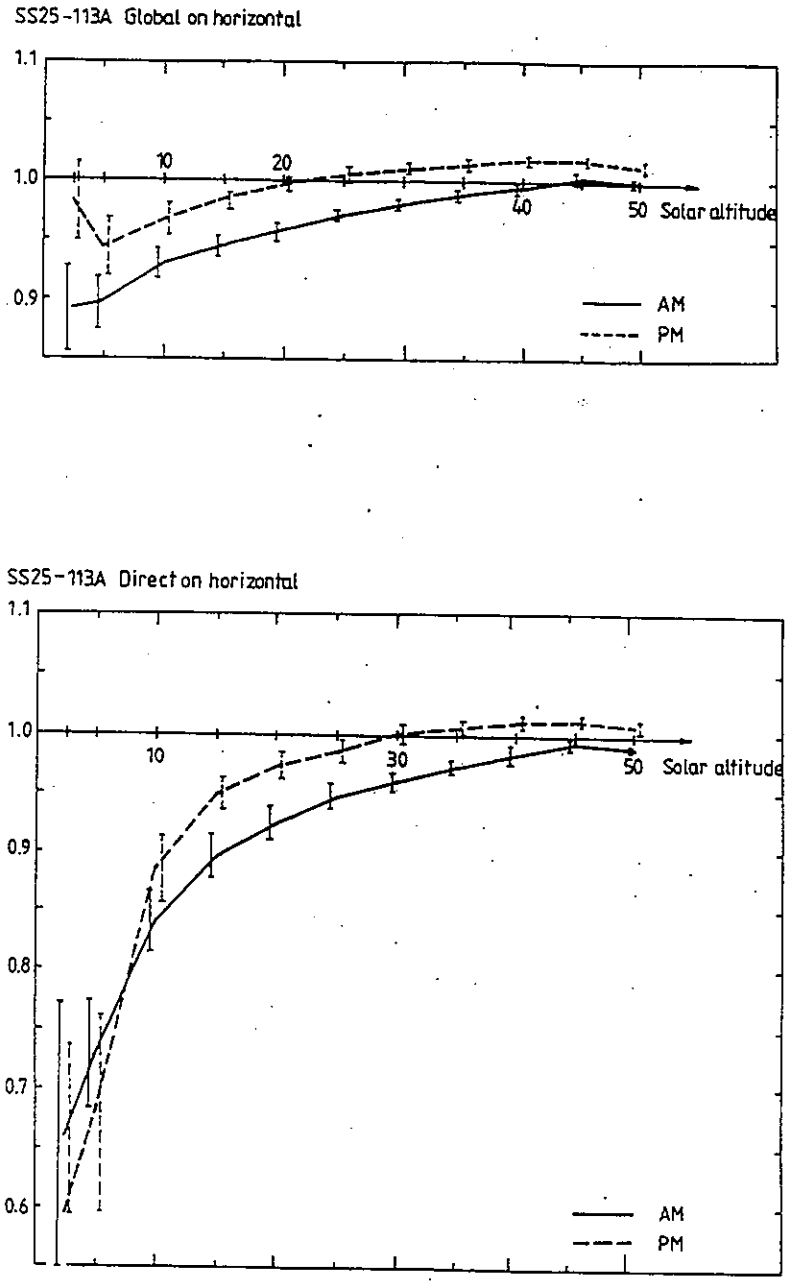

Figure 4.2.1.4a: Cosine response. The vertical bars are standard deviations

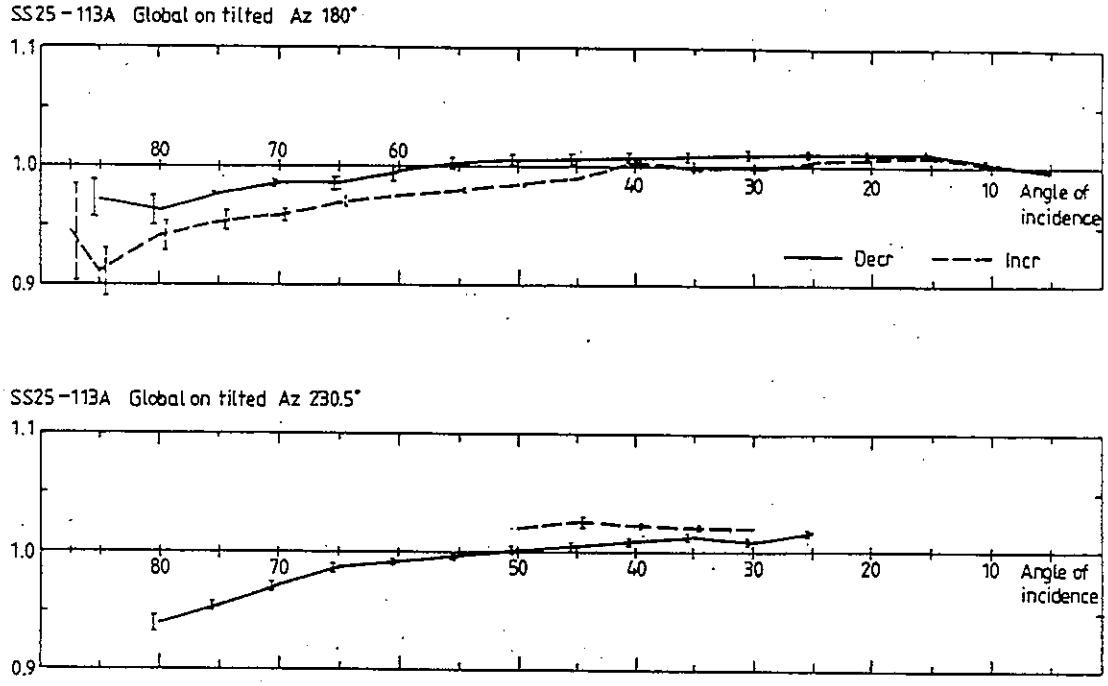

Figure 4.2.1.4a: Cosine response. The vertical bars are standard deviations

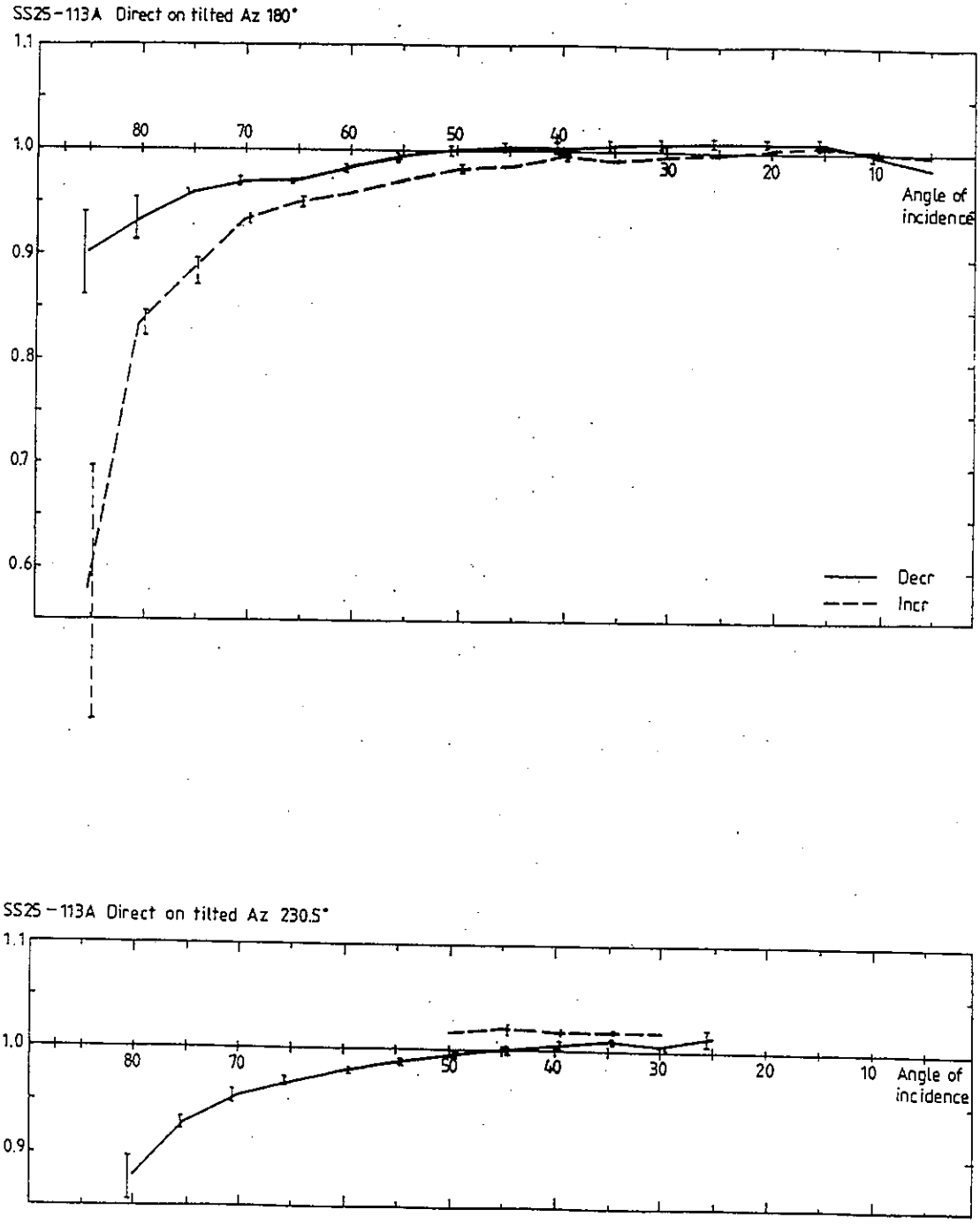

Figure 4.2.1.4a: Cosine response. The vertical bars are standard deviations

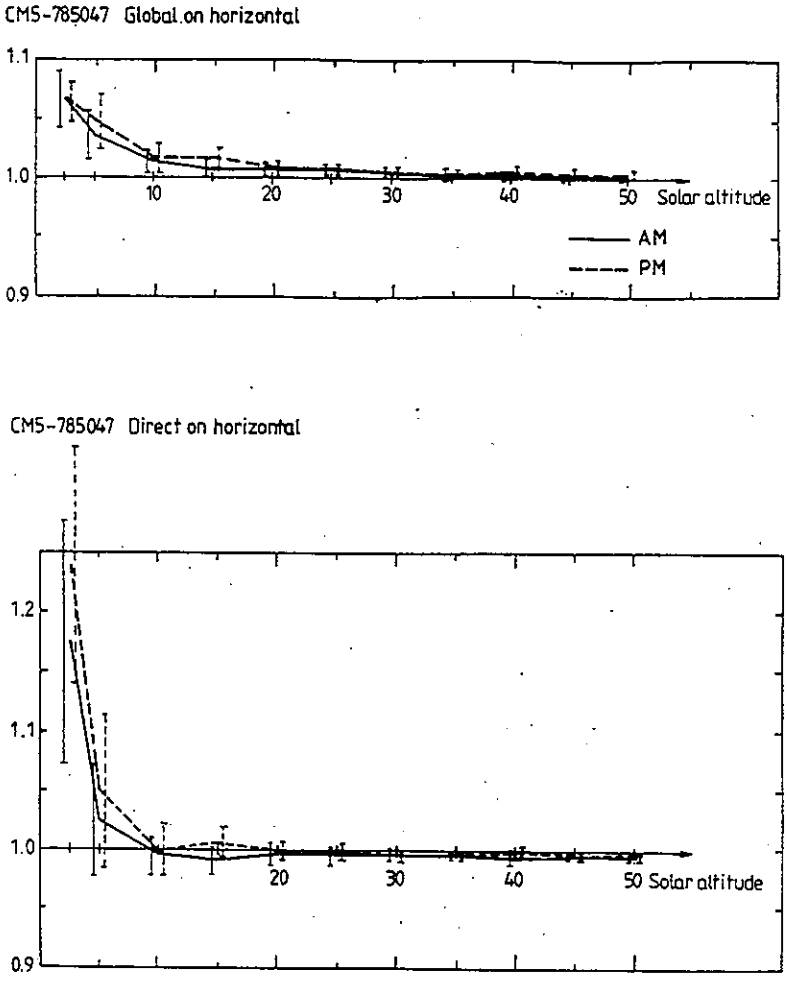

Figure 4.2.1.4b: Cosine response. The vertical bars are standard deviations.

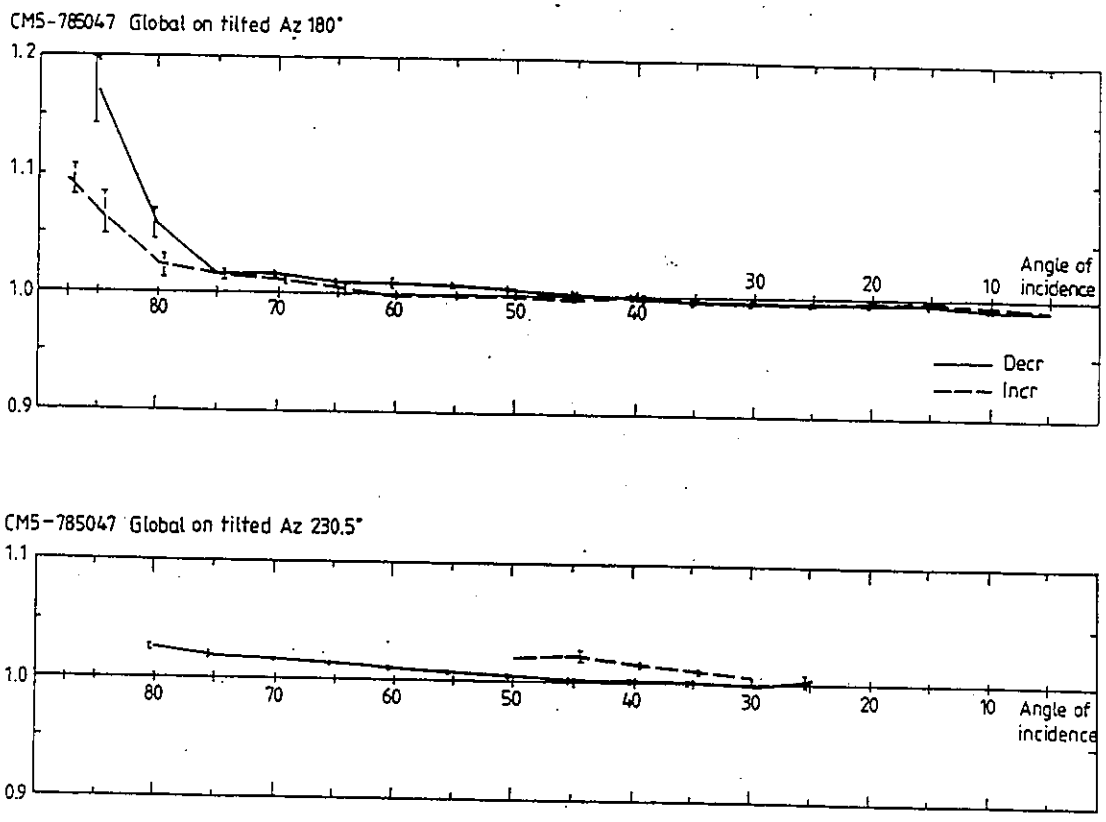

Figure 4.2.1.4b: Cosine response. The vertical bars are standard deviations

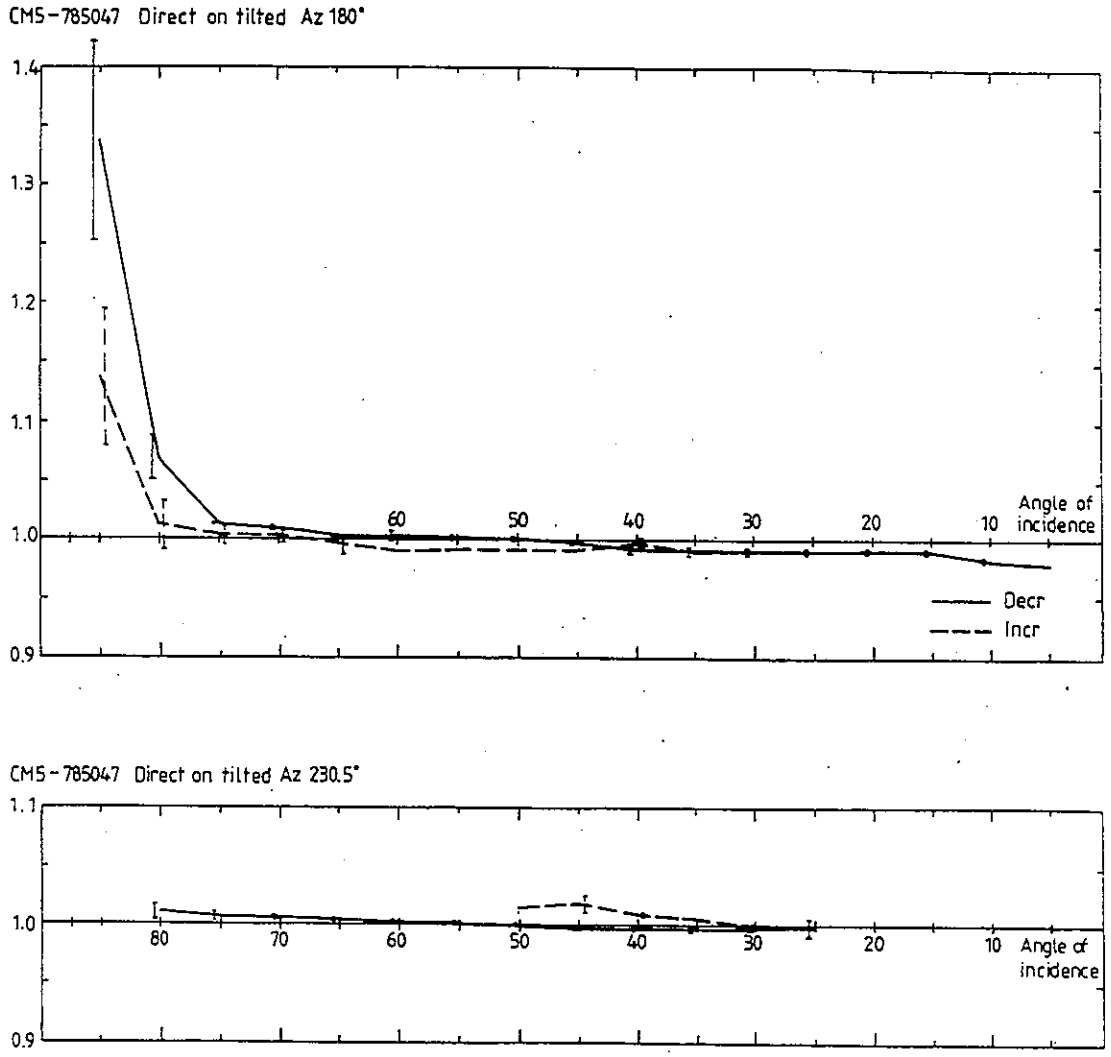

Figure 4.2.1.4b: Cosine response. The vertical bars are standard deviations

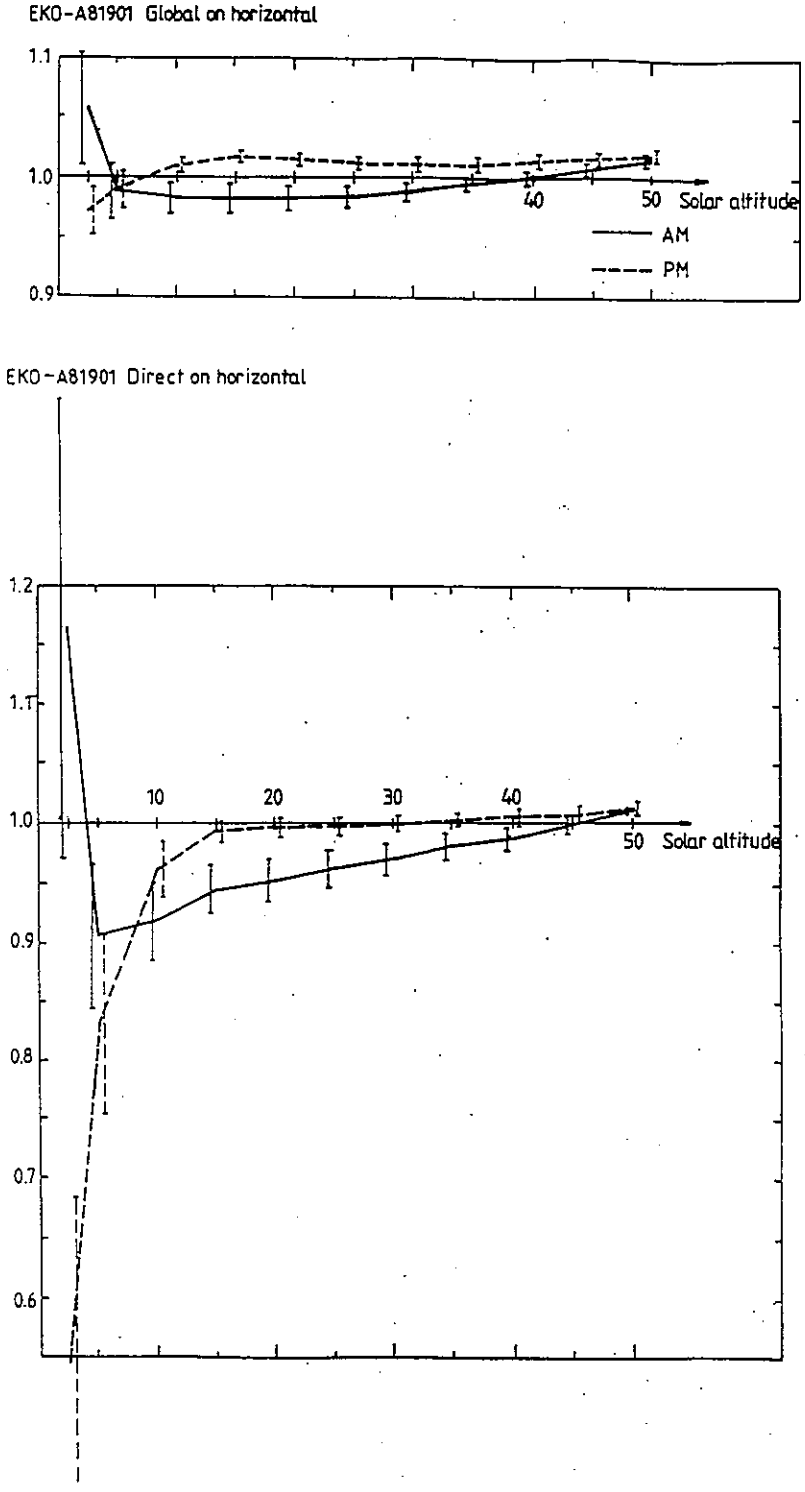

Figure 4.2.1.4c: Cosine response. The vertical bars are standard deviations

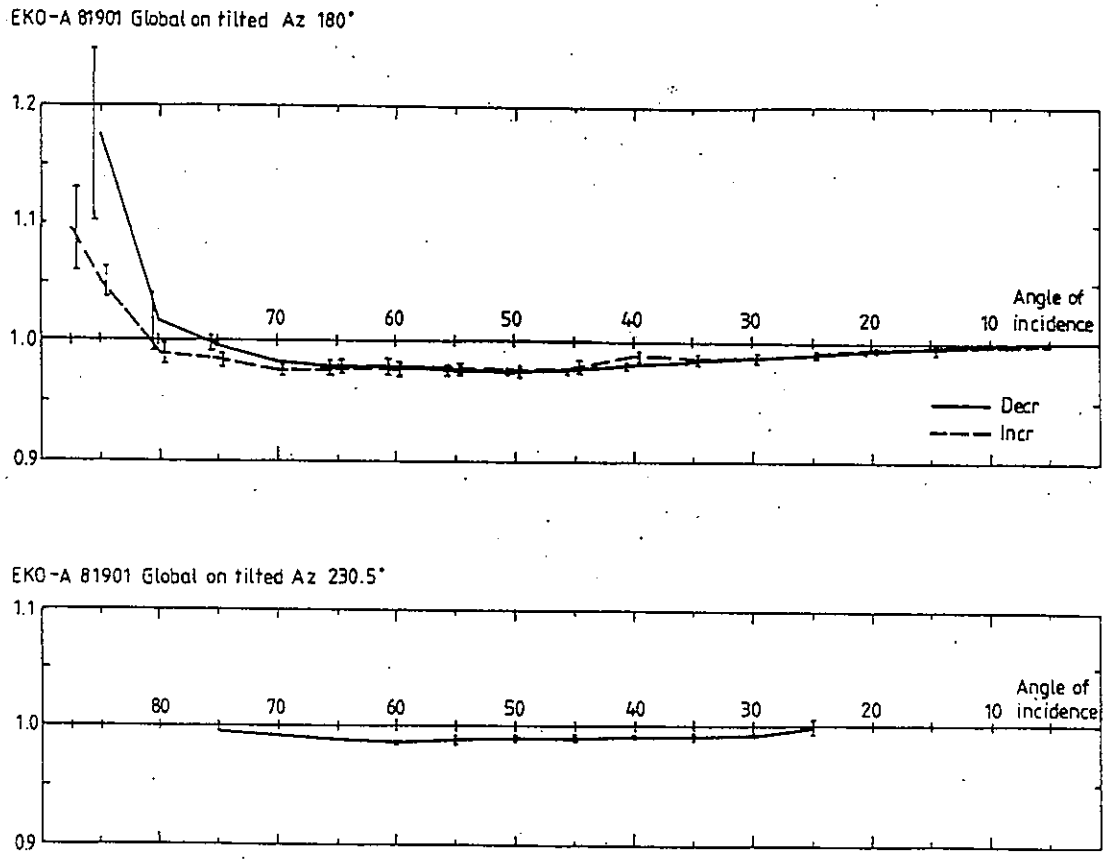

Figure 4.2.1.4c: Cosine response. The vertical bars are standard deviations

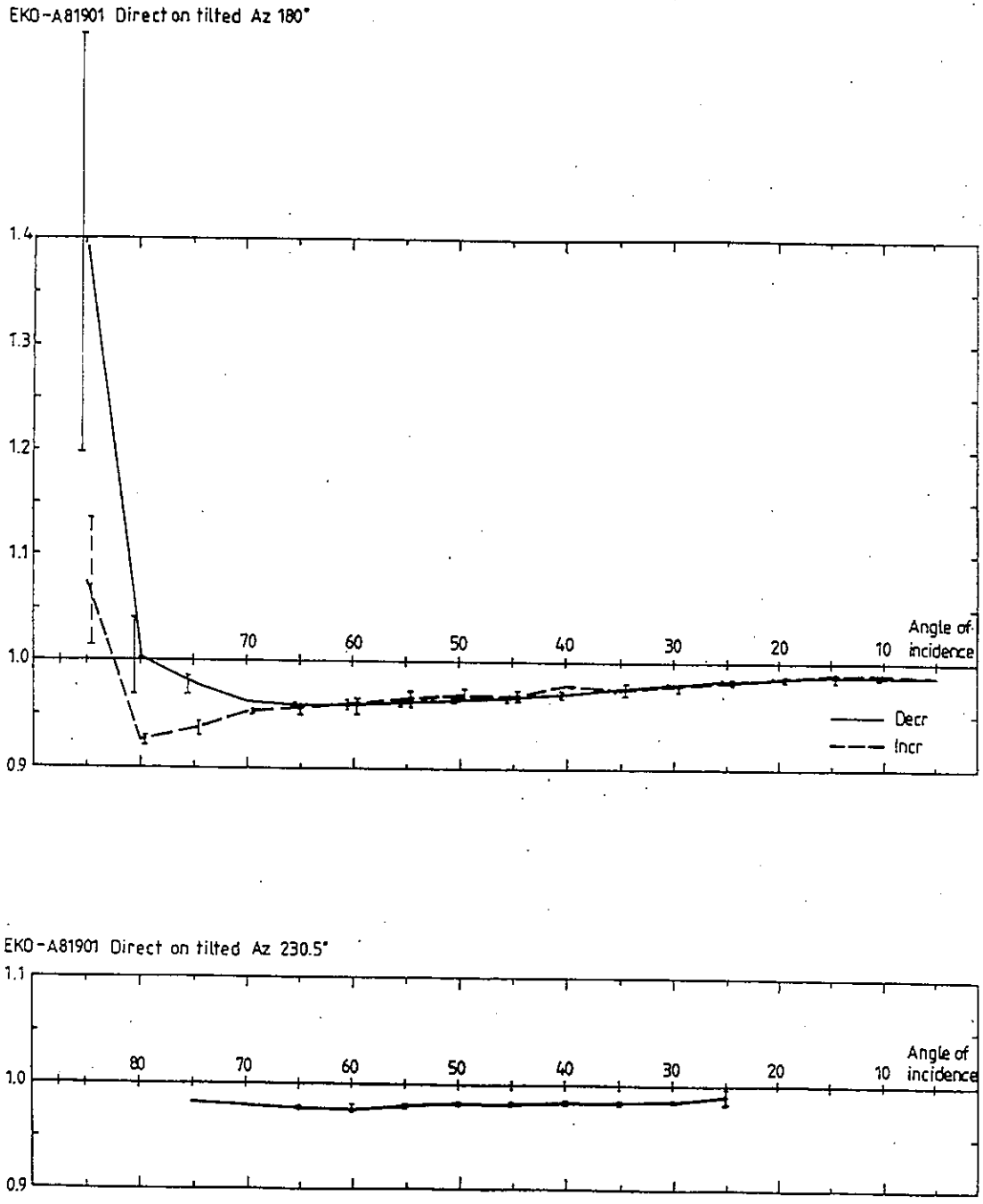

Figure 4.2.1.4c: Cosine response. The vertical bars are standard deviations

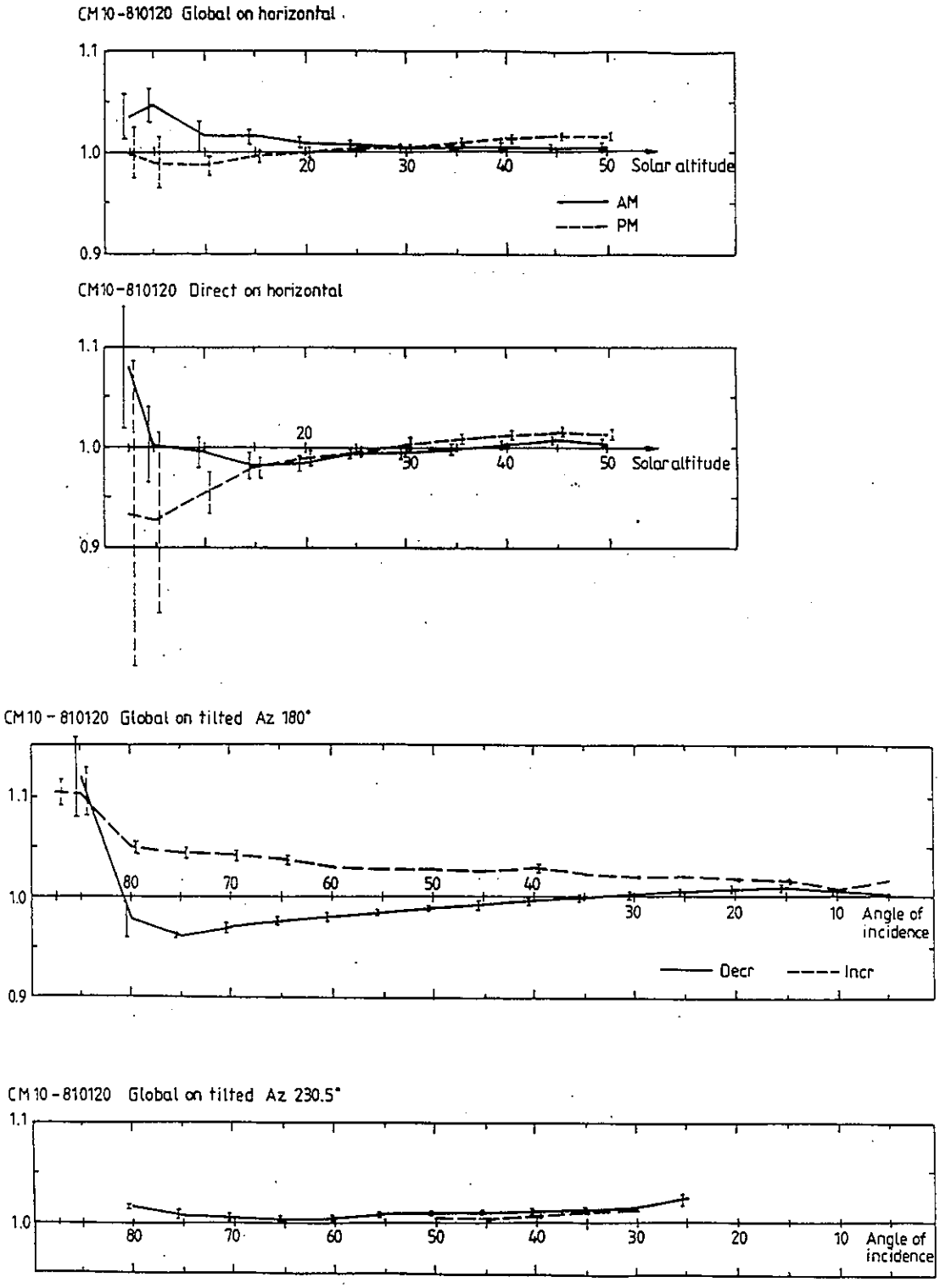

Figure 4.2.1.4d: Cosine response. The vertical bars are standard deviations.

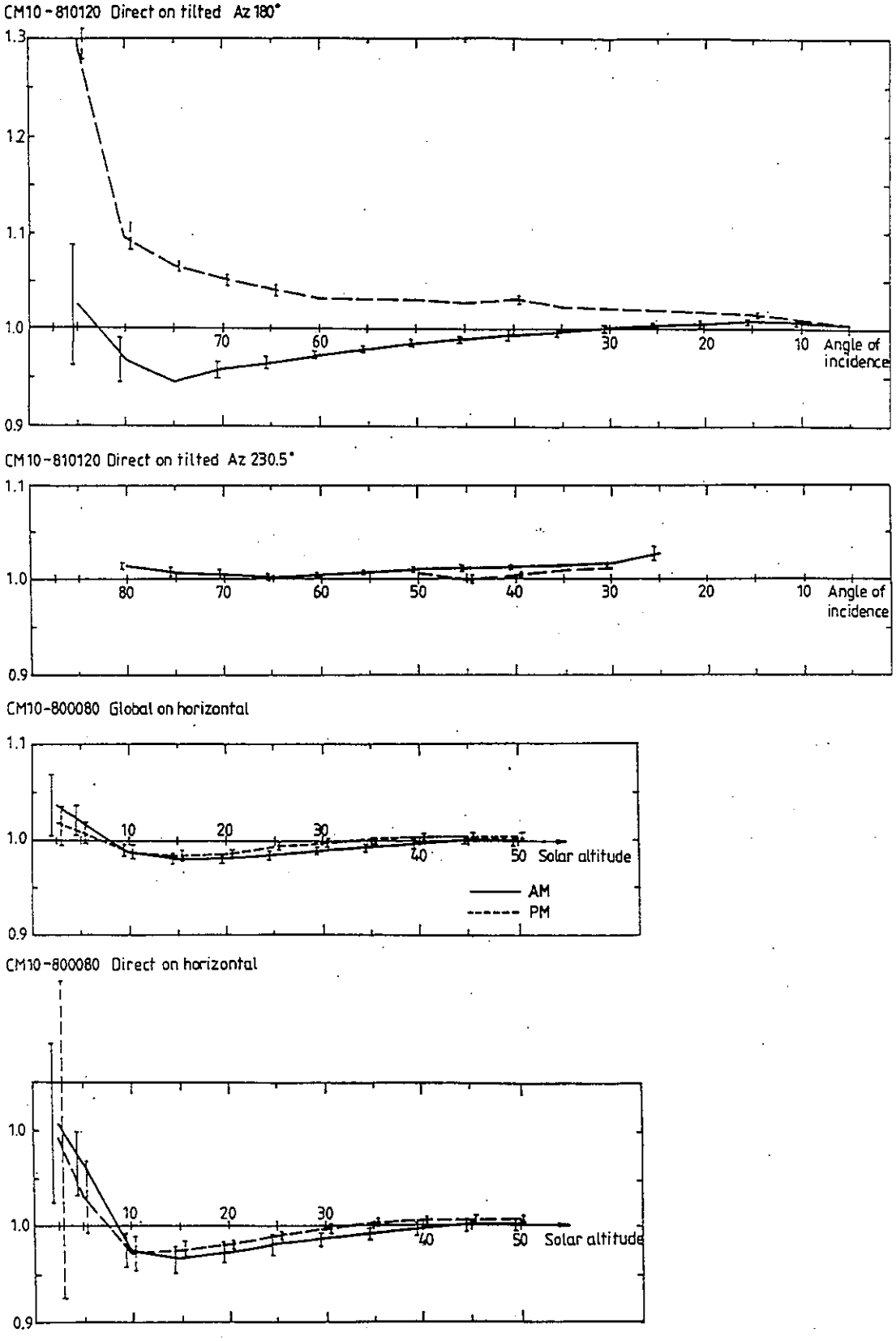

Figure 4.2.1.4d+g Cosine response. The vertical bars are standard deviations.

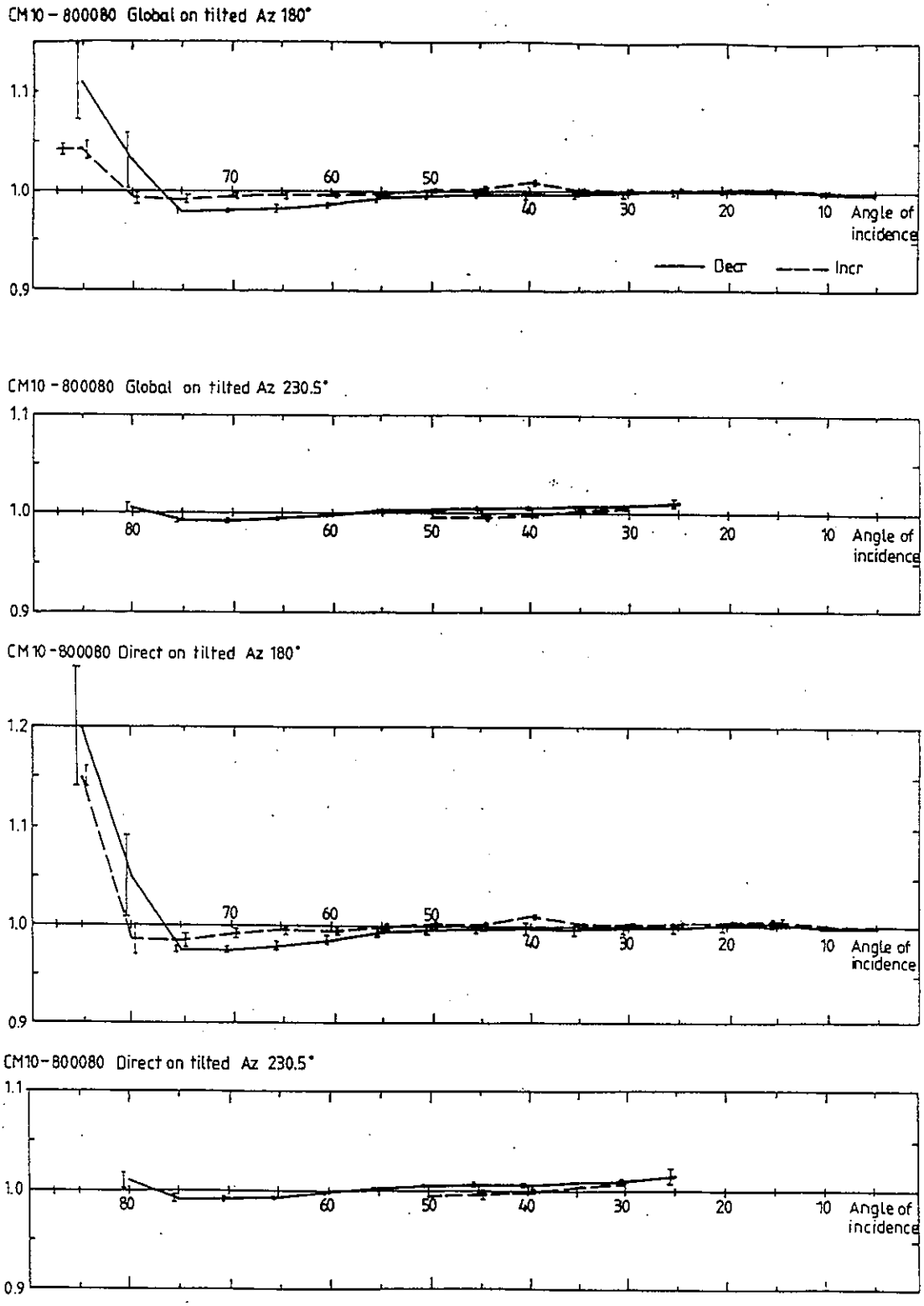

Figure 4.2.1.4g: Cosine response. The vertical bars are standard deviations.

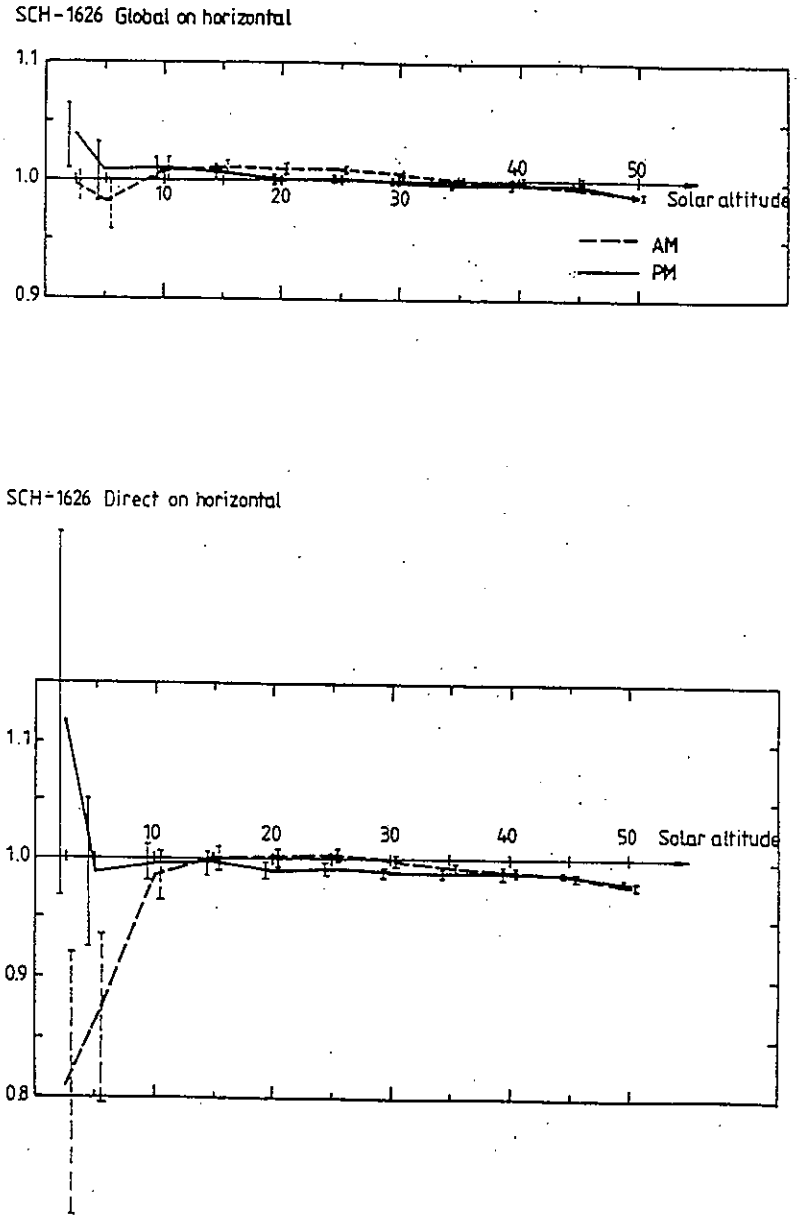

Figure 4.2.1.4e: Cosine response. The vertical bars are standard deviations.

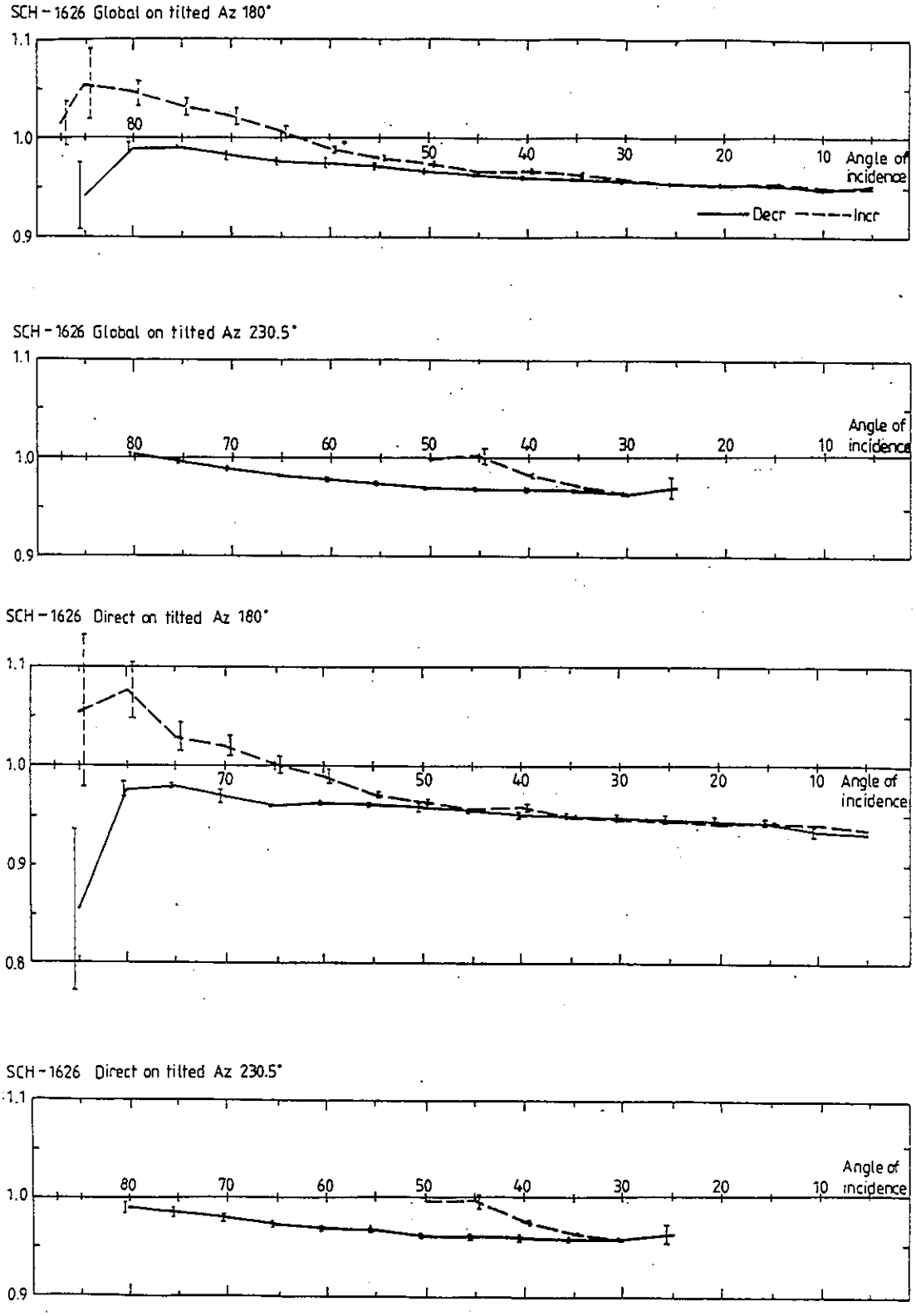

Figure 4.2.1.4e: Cosine response. The vertical bars are standard deviations.

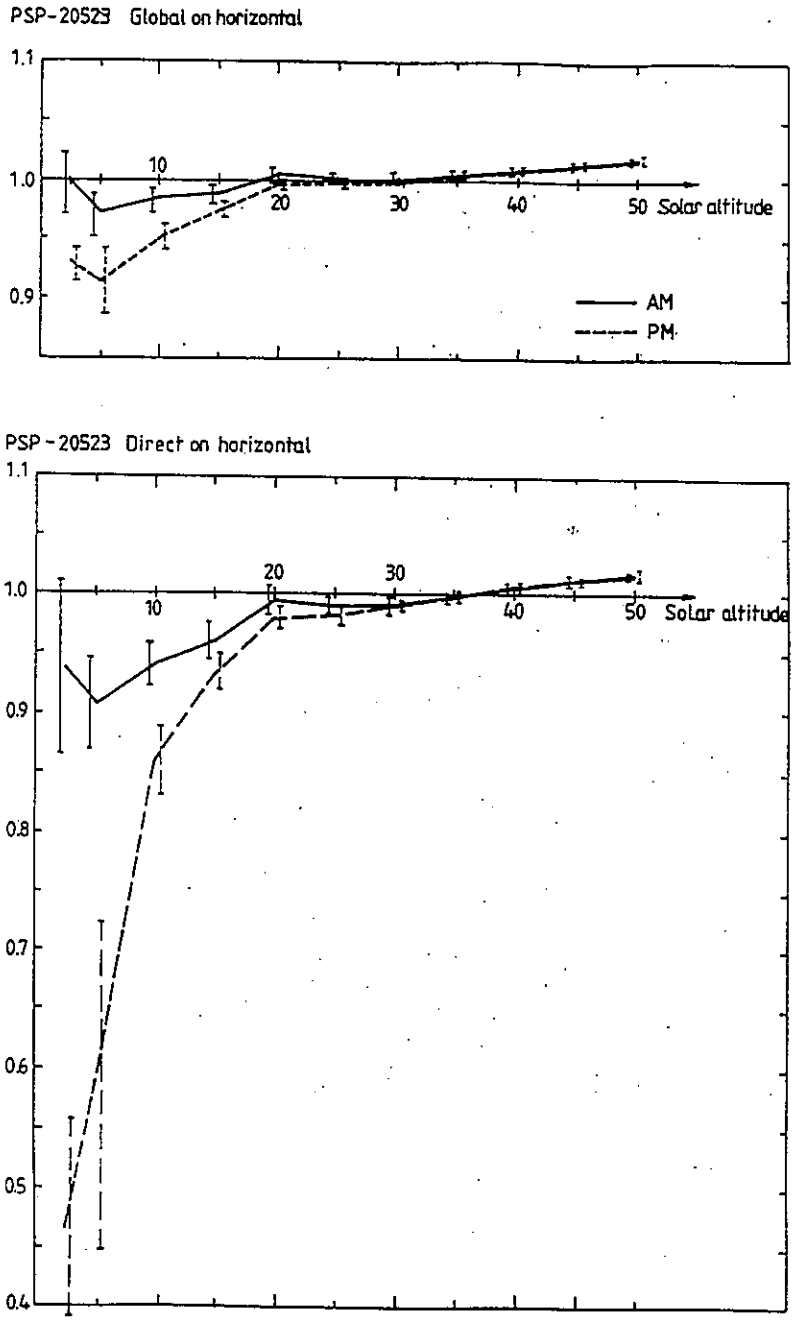

Figure 4.2.1.4f: Cosine response. The vertical bars are standard deviations.

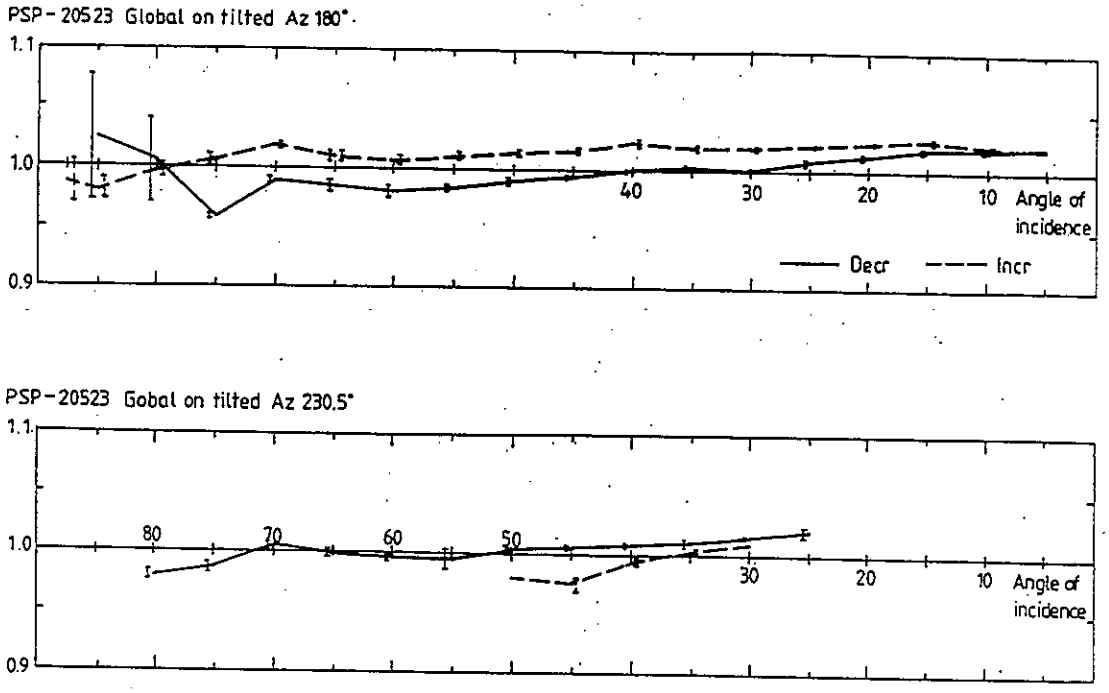

Figure 4.2.1.4f: Cosine response. The vertical bars are standard deviations.

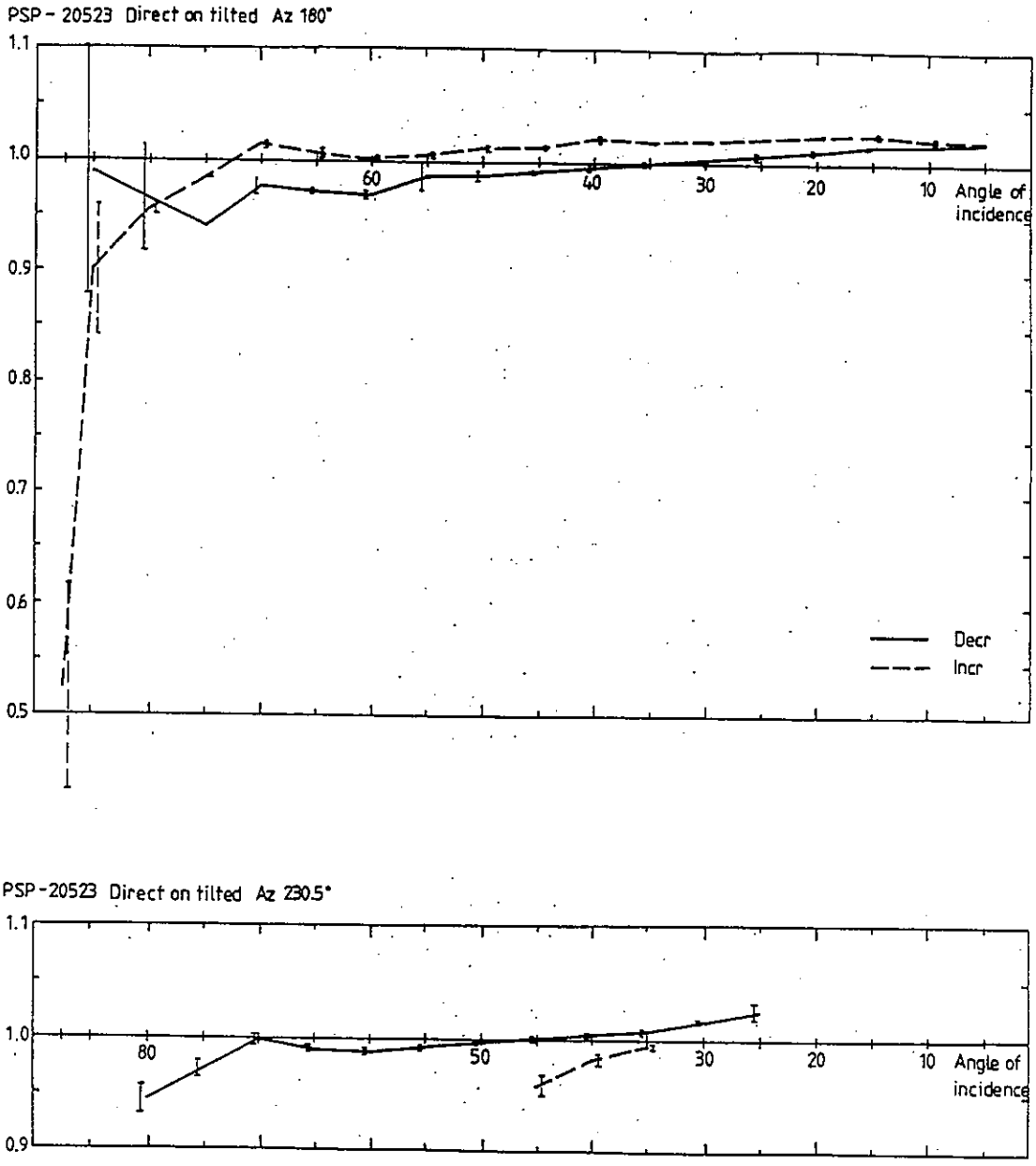

Figure 4.2.1.4f: Cosine response. The vertical bars are standard deviations.

4.2.2 Toronto experiment: directional response determined by field measurement

Twenty six of the IEA pyranometers were subjected to field tests in Toronto. These pyranometers with some others belonging to NARC and some pyrgeometers were exposed on the AES facility during period of about twenty months in 1983-84, not all of them for the whole duration. All the field calibrations are based on the Canadian reference Hickey-Frieden cavity radiometer HF#18747. The data from all the pyranometers have been analysed to provide a variety of calibrations and characterisations. These include benchmark calibrations, which are examined in Chapter 8. The main subject of this section is the determination of the directional response of pyranometers both in the horizontal and 45°-tilted orientations. In addition, the data obtained at night have been used to study the behaviour of the offset signals as reported in Chapter 6.

4.2.2.1 Deployment of radiometers.

Four computer controlled solar trackers were operated at the AES roof during the IEA test. Three of these were mounted in the usual manner with the main axis vertical. The first tracker was used for Normal Incidence Pyrheliometers(NIPs) and for the cavity radiometer. The NIPs were present at all times; the cavity radiometer was deployed only on days when rain was not anticipated. The second tracker carried a CM10 pyranometer and an Eppley PIR pyrgeometer each with an 11 cm shading disc at a distance of approximately 1.1 m. The discs shaded the pyranometer and pyrgeometer from the sun for most of the experiment; on a few days they were operated in a 10-minute on, 10-minute off alternating shade sequence. The third tracker carried up to three pyranometers so that they were permanently normal to the solar beam. One of these was usually shaded by a disc which was sometimes operated in the alternating on/off manner. The fourth tracker was installed tilted 45° in a direction 22° east of south. A CM10 pyranometer was mounted on this tracker with a similar shading disc so that it measured the diffuse component of the 45°-slope irradiance. Like the horizontally mounted shaded pyranometer and the shaded normal incidence one, this pyranometer was also subjected to the intermittent shading sequence for several short periods each lasting for a few days.

Most of the pyranometers were mounted on two tables at the southern edge of the roof. These tables were constructed so that they could be tilted by precisely 45°. When, the tables were tilted, which was for about 40% of the experiment, their field of view comprised only the sky and part of the ground that was at least 50 m away and fairly uniform. The furthest pyranometers were about 5 m apart and it is believed that the incident radiation was identical for all of them.

The pyranometer mounted on the tilted tracker was between the two tables and had the same field of view.

Most of the pyranometers and the pyrgeometers were enclosed in the NARC ventilated housing which is described in Chapter 6.

4.2.2.2 Data acquisition and control

The data acquisition system comprised a 60-channel reed-relay multiplexer and a 6½ digit voltmeter. These were controlled by a desktop computer. The sampling rate was once per 12 seconds; 1-minute averages were computed and stored on 9-track tape. Each tape contained about two months of data. Forty five of the sixty channels were used for voltage measurements; the remaining fifteen were used for measuring the resistance of various thermisters, including one which measured air temperature. The cavity radiometer was controlled by the same computer. It was self-calibrated and zeroed during a seven-minute period every 30 minutes.

4.2.2.3 Preparatory Analysis

A number of procedures were done prior to the investigation of directionality.

The first task was to calibrate the pyrheliometers against the cavity radiometer and to examine their stability. This work is described in the report of the Norrköping Symposium. It was established that the root mean square difference between NIP and cavity radiometer values was 3-5Wm^{-2}. This was considered good enough to use the NIPs for the reference for the pyranometer calibrations. However, in some cases it was decided as well to use the cavity radiometer directly; unfortunately, the amount of data available with the cavity radiometer is much less because of its limited deployment.

The three CM10 pyranometers that measured horizontal diffuse, tilted diffuse and the diffuse centred in the solar direction were first calibrated. This was done both by the Alternating Shade Method(ASM), which is described in detail in Appendix BB, and by the Simultaneous Diffuse and Global Method (SDGM). On the basis of the results of these methods, a responsivity for diffuse radiation was chosen for each of these three pyranometers.

Figure 4.2.2.3a illustrates results from the ASM obtained during a two-month period on the tilted diffuse pyranometer. There are 280 points each obtained from one 20-minute cycle. Three outlying points may be the result of tracking malfunction. Nearly all the other points (259) are within a two percent range. Because of the 45°-tilt, there is some data quite close to normal incidence, and in the whole range $\theta < 80^{\circ}$, there is little evidence of directional error on this CM10.

Figure 4.2.2.3b illustrates a calibration by the SDGM. These data are ten-minute averages accumulated over a two-month period. Three instruments are involved, the reference NIP measuring the normal incidence radiation (I), the shaded pyranometer measuring the diffuse radiation (D) and another pyranometer measuring the global radiation (G). Defining the pyrheliometer and pyranometer responsivities as R_N, R_D and R_G respectively and the signals from the three as V_N, V_D and V_G, the ordinate of the plot is V_D / V_G and the abscissa is $V_N \cdot \cos\theta / V_G$. On the assumption the three instruments are perfect in the sense that $V_G = R_G \cdot G$ etc., and because $G = D + I \cdot \cos\theta$, it follows that there is a linear relation between the two variables and that its gradient is $-R_D / R_N$; also that the two intercepts are R_D / R_G and R_N / R_G.

$$\frac{V_D}{V_G} = \frac{R_D}{R_G} + \frac{R_D}{R_N} \cdot \frac{V_N \cdot \cos\theta}{V_G} \qquad [4.13]$$

The SDGM was used only to derive the responsivity of the diffuse instruments from the NIP via the gradient. The responsivity of the global pyranometer is better evaluated from the same data by the more obvious Component Summation Method, described later, which was the basic method used in the Norrköping experiment (§4.2.1).

The tightness of the plot and the straightness of the line in Figure 4.2.2.3b give at least a qualitative justification of the assumptions for these two pyranometers and the SDGM. The points which are far away from the line arise from tracking errors either of the NIP or the shading disc, and have to be rejected in the analysis. The eight values obtained for this and seven other two-month periods over the 20-month duration have an estimated standard deviation of about 0.8% and agree with the values obtained by the ASM. The method therefore, for these instruments at least, is a valid alternative to the ASM. It is particularly useful since, unlike the ASM, it does not interrupt the measurements and does not require the extra mechanism of alternating shading. It probably does not work so well with pyranometers that have larger directionality errors than these CM10s.

With the calibrations for the NIPs and the diffuse instruments established, an accurate reference measurement of global radiation becomes available throughout most of the dataset. Using such a reference measurement to evaluate the responsivity of another pyranometer to global radiation is often called the Component Summation Method (CSM). In principle this could have been used to evaluate the responsivities for global radiation for all the other instruments; in practice it was done only for three, two of which were chosen because they appeared to have very little directionality error. These were two CM10s, one mounted on each of the tiltable tables. Figures 4.2.2.3c shows the calibration data for one of these when it was in the horizontal orientation. Figure 4.2.2.3d shows the calibration of the same pyranometer in the tilted orientation. The ordinate is the responsivity evaluated as the output voltage divided by the global radiation measured as the sum of the direct and diffuse components. These pyranometers were designated as reference instruments for both global and tilted global radiation.

The responsivities for global radiation for the remaining pyranometers were calculated from their output voltages divided by the voltage from one of the reference global instruments. Benchmark responsivities were calculated by restricting the data to conditions that approximated the defined benchmark conditions, and extrapolating as required (Chapter 8). A condensed description of the derivation of these results and the results themselves are in Appendix BB.

4.2.2.4 Directionality analysis

A large amount of data on the directionality of response to global radiation could be presented but it would be of little value because global radiation can be anything from isotropic to 90% direct beam radiation. Such data would not be comparable with laboratory measurements of $\delta(\theta,\phi)$ which refer to unidirectional incident radiation.

Therefore an analysis was devised, similar to that used on the Norrköping data, to calculate the response to direct beam radiation. It is described here and has been used for most of the pyranometers.

The method is based on the assumption that the responsivity of the tested pyranometer to diffuse radiation R_D, is constant. Also it requires measurements of both global and diffuse radiation from other instruments. With this assumption, the signal from the tested pyranometer can be written as:

$$V = R_D \cdot D + R(\theta) \cdot (G - D) \qquad [4.14]$$

so that directional response of the tested pyranometer is

$$R(\theta) = \frac{V - R_D \cdot D}{G - D} \qquad [4.15]$$

The data for D and G come from one of the diffuse shaded pyranometers and one of the reference global instruments. They are assumed to have negligible directional error.

The result of using this algorithm depends on the value chosen for R_D which should itself be a weighted mean $R(\theta)$ over the hemisphere. In this application, the data is not available over the whole range of 0<θ<90° so an exact solution cannot be found. However, about half of the diffuse radiation originates in the range 30°<θ<60° over which data is usually available. With this in mind, R_D values were chosen, by successive approximations, so that they were the mean of the computed $R(\theta)$ in the 30-60° range. It is important to note that a change in R_D produces a much smaller change in $R(\theta)$ than in the difference between R_D and the mean of $R(\theta)$ which is the quantity by which R_D is chosen. The ratio of these changes is D/G. The data are selected for high direct to global ratios according to the criterion shown in Figure 4.2.2.4a. This results in the D/G ratio always being less than 0.5 within 30°<θ<60°. Consequently, the selection of R_D is not a major source of error in $R(\theta)$.

Results of this analysis for two pyranometers are shown in the top panels of Figures 4.2.2.4a,b. As shown in the legends, corrections to the two pyranometer voltages have been made for the dark (offset) signals. The ordinate is chosen to show the fractional departure of the responsivity from some arbitrary value, which can be deduced from the term "-ln(1.480)" in the ordinate legend of Figure 4.2.2.4a. The centre line represents 1.48 times the responsivity of the reference (CM10 #810166, R=4.68). The graph is comparable to the usual plot of direction errors (cosine plots), but it is not normalised. Results like Figure 4.2.2.4 from most of the other pyranometers are in Appendix CC.

4.2.2.5 1000 Wm^{-2} directional errors

The 1000 Wm^{-2} absolute directional error has been introduced in section 4.1.1, as $\overline{\delta}_t(\theta)$, defined by equation 4.5. The verbal definition is: *the error, when measuring a 1000 Wm^{-2} irradiance from a single direction, caused by using the normal incidence responsivity instead of the responsivity specific to that direction.*

Because the direct solar beam is never much more than 1000 Wm^{-2}, the range of δ_t values gives an approximate upper limit to the error that might occur in outdoor usage owing to the directionality of the pyranometer response. For this reason, and others, it may be preferred to the traditional percentage or fractional variation of responsivity $\delta(\theta,\phi)$ used in the previous section. The full mathematical definition, following ISO 9060 (1990E), is:

$$\delta_t(\theta,\phi) \quad = \quad 1000 \cdot \cos(\theta) \cdot \frac{R(\theta,\phi) - R(\theta=0)}{R(\theta=0)} \qquad [4.16]$$

Since azimuth variation is ignored in the NARC field analysis, the definition that will be used here is:

$$\overline{\delta}_t(\theta) \quad = \quad 1000 \cdot \cos(\theta) \cdot \frac{R(\theta) - R(\theta=0)}{R(\theta=0)}. \qquad [4.17]$$

A value for $R(\theta=0)$ is required to calculate δ_t. This presents no problem for laboratory data, but here there are no data near normal incidence in the horizontal orientation and not many for the tilted orientation. The values used for this analysis are estimates based on the $R(\theta)$ data available for the lowest θ. This is essentially filling in the gap in the 4.2.2.4 Figures. The results are shown in the lower panels of the Figures and in Appendix CC. In the legend on each plot the $R(\theta=0)$ value that has been used is specified by the "normal incidence adjustment". It means, in the case of Figure 4.2.2.4b, that:

$$R(\theta=0) \quad = \quad R_{\#810166} \cdot 1.480 \cdot \exp(n.i.adj) \qquad [4.18]$$

These adjustments range from -2.0% to + 3.5%.

4.2.2.6. Discussion of results

The potential accuracy of these field results is the first subject that needs to be addressed. It is well-known that two good pyranometers of the same type, mounted side-by-side and using the same data acquisition system can give impressive agreement. When the NARC field measurements are compared against each other in this manner the rms scatter for the ten-minute averages is often as low as 3 Wm^{-2} for several thousand observations over a two-month period. This 3 Wm^{-2} value can be regarded as noise in the basic signal. The measurement uncertainty cannot be less than this.

Of greater relevance to measurement uncertainty are the determinations of Benchmark Responsivities in the NARC experiment. These were done over a total two-year period in several two-month intervals (described in Appendix AA with the results listed in the first four tables of Appendix BB).

The temporal stability of a Benchmark calibration is an important statistic. For example, the calibration from the first two months could be used to calculate the irradiance during the remaining months and the measurements assessed to determine how closely they fit the reference. The reference used for the NARC Benchmarks were the measurements made with the NIP and the shaded pyranometers and the first calibration was done on an Eppley PSP. Eight responsivities for BMHO were obtained in this manner, called the "direct method" (also CSM). About 1000 data points throughout the two-year period were used, corresponding to conditions similar to BMHO (i.e. solar elevation around 35 degrees and irradiance around 600 Wm^{-2}). The spread was 1.1% in the sample of eight with a standard deviation of 0.4%, equivalent to 2.4 Wm^{-2}. The typical scatter of the individual ten-minute readings in each two-month period was, as above, about 3 Wm^{-2}. Disregarding the contribution from the reference, the single pyranometer measurements therefore appear to have an rms uncertainty of about 5 Wm^{-2}. All the other pyranometers were assigned Benchmarks by using the calibrated PSP as the reference in place of the direct and diffuse combination. The results of this method are called "Relative Benchmarks" in Appendix AA. The reproducibility for some of the tested instruments was as good as those given by the direct method.

In summary, the internal reproducibility of the measurements in the NARC experiments appears to be below the 10 Wm^{-2} rms level for the ten-minute averages throughout the two-year period. In view of this, the level of discrepancy between institutes' Benchmarks, analysed in Chapter 8, is surprisingly large in most cases.

The results for the directionality in general show the same features as those of laboratory measurements. A good example can be seen for the Eppley PSP on page 3, Appendix CC. The scatter of the points in these curves is generally less for the instruments with lower directional errors. Some of the curves show evidence of misalignment.

The NARC field results on three CM5s, like the Norrköping field data on CM5 #775047, are different from the laboratory data on the same instruments. The field data do not generally show the decline in responsivity from $\theta = 30^\circ$ to $\theta = 60^\circ$ that is shown in most of the laboratory data (Figure 4.1.3.1b versus pp15-21 &58-61 in Appendix CC and Figure 4.2.1.4b). The difference may be caused by the non-linearity and azimuth dependence of the CM5 fortuitously compensating for the effects of the mean directional error $\overline{\delta}(\theta)$. However, this interpretation has not been tested by detailed analysis.

The 1000 Wm^{-2} directional error plots indicate that several of the CM10s are within the 10 Wm^{-2} ISO 9060 criterion for a secondary standard reference pyranometer. In general, the PSPs are at 15 Wm^{-2}, as are some CM5s. There are very few measurements with the error exceeding 40 Wm^{-2}.

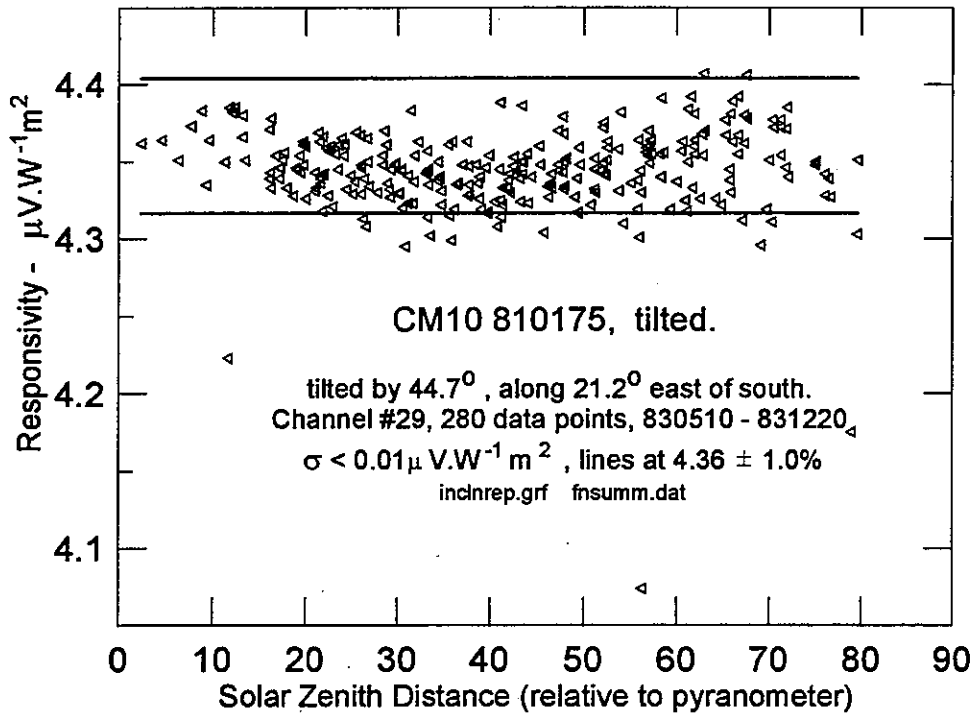

Figure 4.2.2.3a. Automated alternating sun-shade calibration of a tilted pyranometer at AES, Toronto.

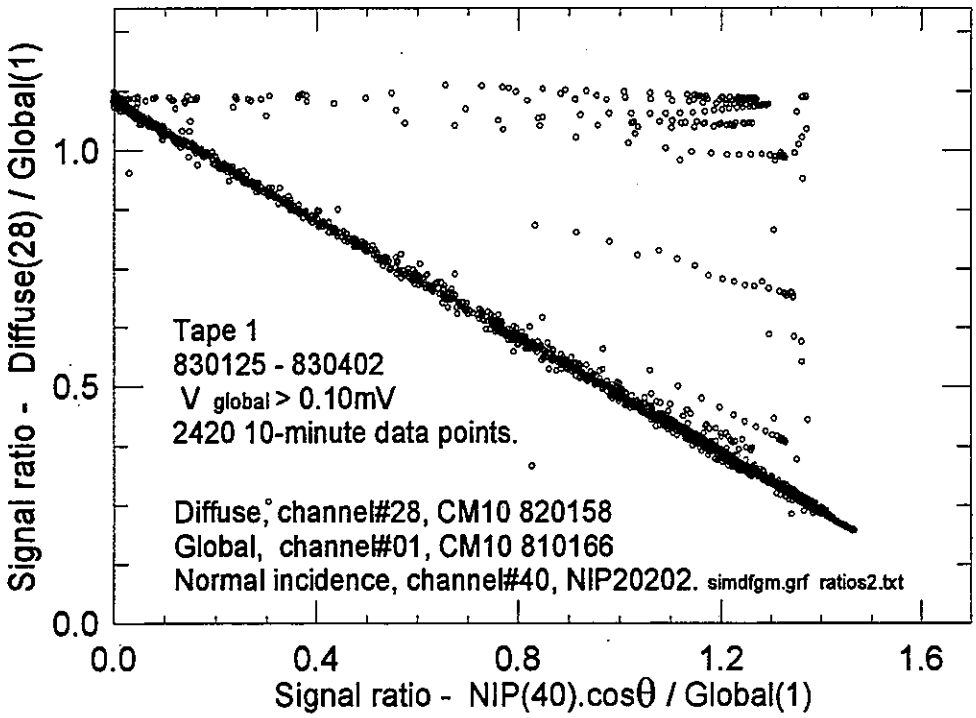

Figure 4.2.2.3b. Simultaneous calibration of pyrnaometers measuring horizontal diffuse and global radiation.

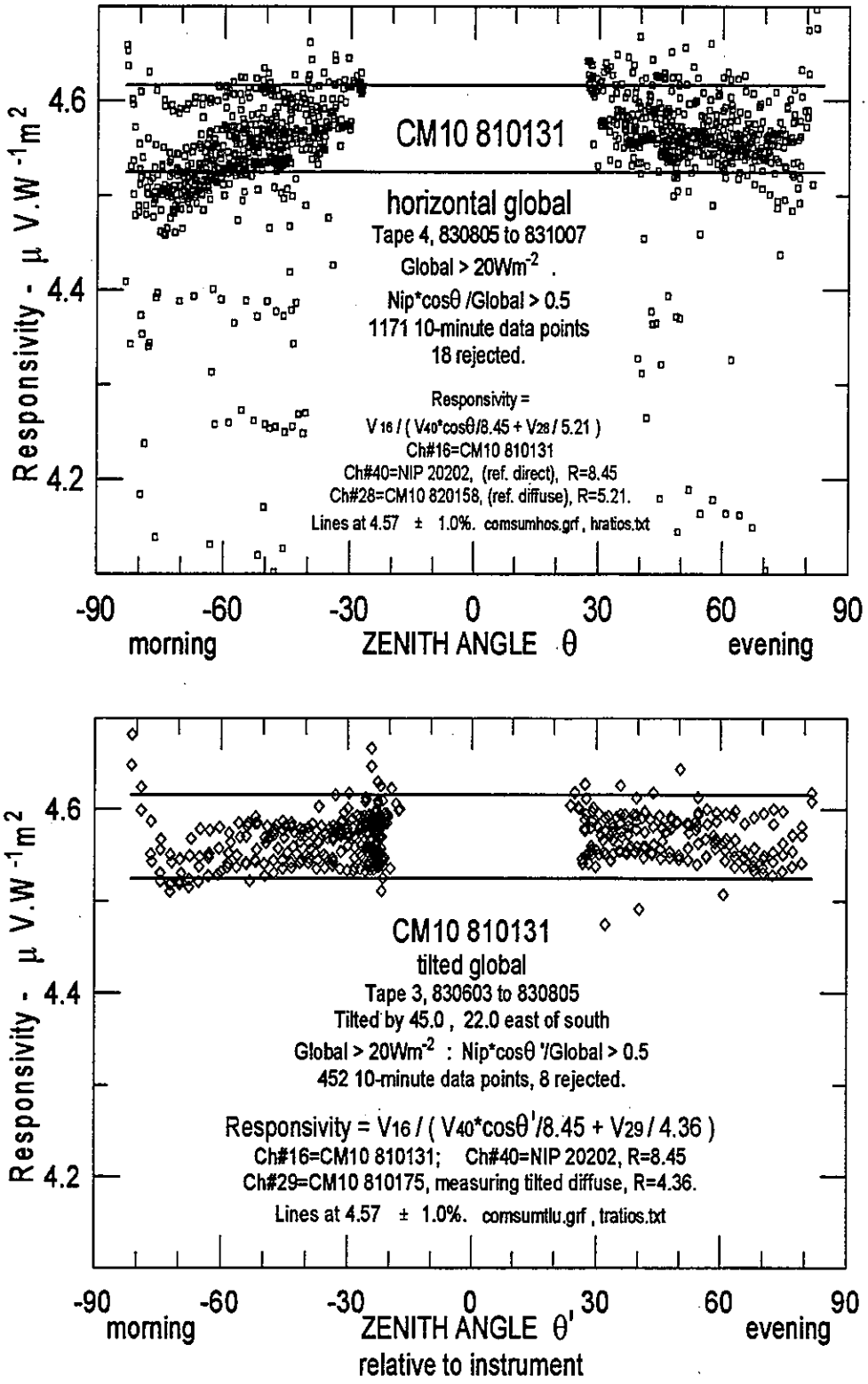

Figure 4.2.2.3c,d. Component summation calibrations of a pyranometer in the horizontal and tilted orientations.

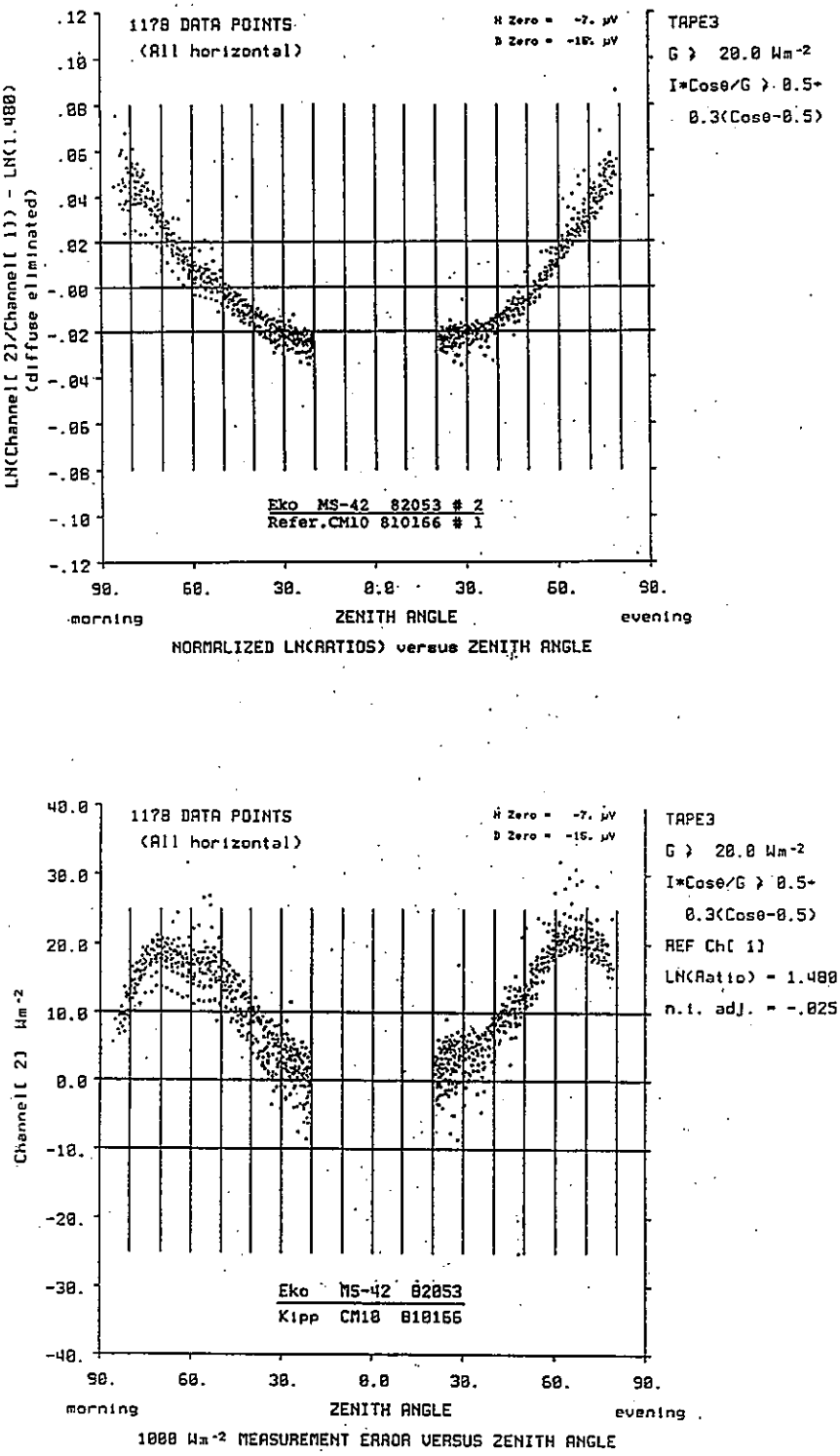

Figure 4.2.2.4a

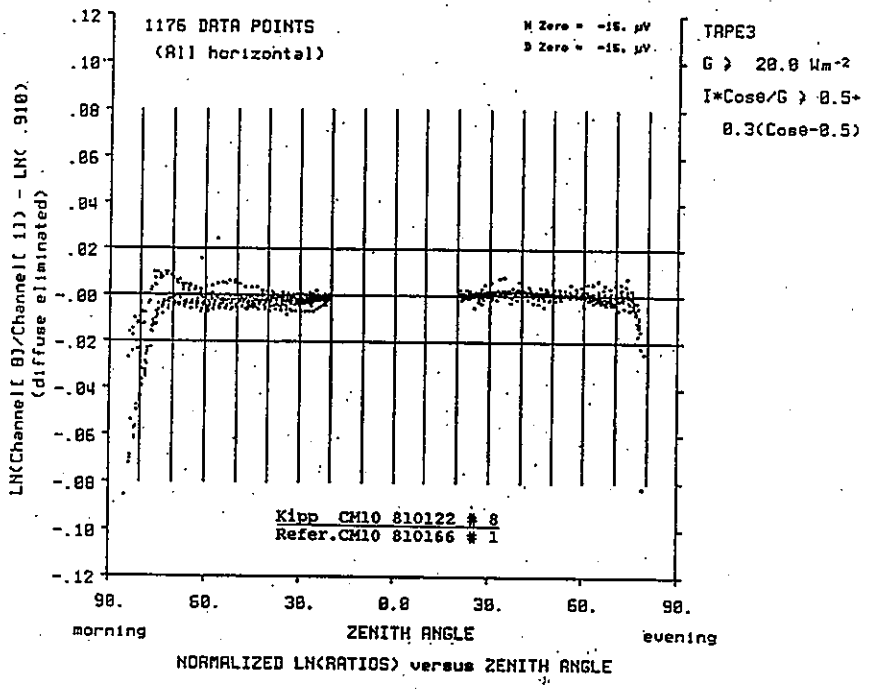

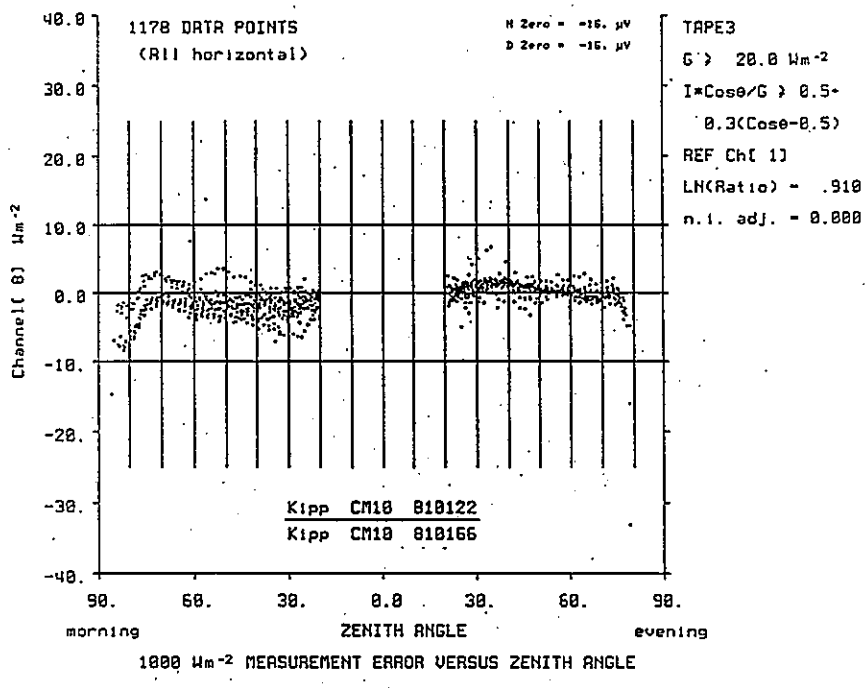

Figure 4.2.2.4b

Chapter 5. Signal Delay, Temperature, Non-Linearity, Instrument Tilt and Spectral Effects

5.1 Introduction

Pyranometers are simple instruments. Nevertheless, in actual use, they respond to many facets of their environment in ways, not necessarily simple, that modify the output signals. These changes are not readily distinguished from the desired output from solar irradiance alone.

This chapter addresses the speed with which pyranometers respond to radiation and their responses to a number of influences, specifically: temperature and its rate of change, non-linearity, tilt, spectral response and other interfering phenomena. The effects of temperature, non-linearity and spectral response are described as changes in responsivity. Subjecting a pyranometer to continually increasing or continually decreasing ambient temperature induces an offset signal. This effect is described in section 5.4 and offsets are examined more generally in chapter 6. The delay between a change in the incident irradiance and the corresponding signal is addressed first.

5.2 Signal delay

An adequate knowledge of the signal delay of the instrument is necessary both for characterising the pyranometer and for a correct interpretation of a measurement.

Signal delays are normally expressed in terms of time constants which are defined as the time required to come to within 36.8% (1/e) of the final, steady-state or equilibrium signal in response to a step change in irradiance input. The output from an instrument with a single time constant would approach the steady-state signal according to a single exponential decline. Thermoelectric pyranometers do not correspond to this model. Their signals clearly exhibit two components with distinct magnitudes and time constants. There may even be a third component of longer duration but smaller magnitude.

The first and major component of signal delay is the quite fast response of the black thermal sensing surface with its attached thermopile. Seven of the eight pyranometer models tested had principal time constants in the range 1-7 seconds. This component accounts for from 96% to 99.7% percent of the pyranometer output and is not significantly affected by ventilating the instrument. A system with data sampling faster than once per

second is required to get a reasonably accurate measurement of the time constant but that may not be required, as discussed later. The time constant may be different, depending on whether the irradiance is increasing or decreasing, but the experimental evidence for this is inconclusive.

The second component is believed to be due to the heating of the domes and re-radiation to the thermal sensor; its time constant was measured on four models giving results in the range 80-240 seconds. It can be different depending on whether the irradiance is increased or decreased and it is strongly dependent on ventilation.. The effect of this long time constant source must be evaluated, because it may contribute as much as about 4% of the total output signal in sunlight (and possibly more under artificial light illumination). This time constant must be taken into consideration when establishing the timing cycle for in the alternating sun/shade method (ASSM) of calibration for different models of pyranometers.

The time to reach a point within 0.1% of the final steady-state signal becomes important if a 1% accuracy in establishing the responsivity of a pyranometer is being attempted. Obviously, this requires careful measurements and a good knowledge of the time constants for the specific pyranometer. For example, if the second component contributes 2% of the total output of the pyranometer, it must be given time to decay to 1/20th of its output, which requires three time constants or 9 minutes for an instrument with a second time constant of 180 seconds. This can be significantly reduced by ventilation and the result would be valid in an application provided the pyranometer were ventilated in the same manner.

A third component may be associated with the heating or cooling of the body of the instrument (this structure serves as the heat sink and reference point for the cold junctions of "black" pyranometers). No effective measure of this component was apparent in results available from the IEA tests. Ventilated housings, such as the NARC model, protect the pyranometer body from direct sunlight and therefore greatly reduce the change in body temperature from changes in incident irradiance. Radiation shields supplied with most of the IEA pyranometers provide the same protection when instruments are not in ventilated housings. Given either of these mounting configurations, one may conclude that the third component is negligible.

A variety of techniques and measurement apparatus was used by the different laboratories to measure the time constants of pyranometers. Although the final results do not

necessarily agree closely, sufficient information has been obtained to generate some useful conclusions. The most important conclusion is that the second time constant influences the pyranometer calibration more than is usually stated, and must be taken into account in the alternating sun/shade method.

Table 5.2a contains the values of the time constants as measured by the various laboratories using a variety of techniques. They are plotted in Figure 5.1. The values from columns 2 and 3 were scaled from strip-chart recordings made at Kipp and Zonen, Delft, Holland. Columns 4 and 5 were scaled at the 90% points on graphs determined from strip-chart recordings made at the Zentralanstalt fur Meteorologie und Geodynamik, Vienna. Columns 6 and 7 are taken from notes on the ZFMG charts.

The Eppley Laboratory (column 8) used a special system originally designed to determine the time constants of detectors used in the ERB satellite experiment. This system used a computer-controlled digital voltmeter which rapidly measured the pyranometer output while intermittently shading and unshading the pyranometer from direct sunlight. The $1/e$ time constant was calculated by optimising the fit of an exponential to all the data.

DSET (column 9) determined the time constants using their data logger which took measurements every 2 seconds. Time constants were determined for each instrument by the average between two experiments — one comprising shading and the other unshading. The time constant was taken as the average time(s) to reach 63.2% of the full scale change in readings (taking into account any zero offsets).

The values determined by Kipp and Zonen in 1984 and published in the TPD report are given in column 10. Data from Table 1.2 in that report are plotted in Figure 5.2 where the "100% recovered" point (taken at 180 s by definition, if not arrived at sooner) is arbitrarily plotted on the 0.01% line of the semi-log plot.

MOH, Hamburg used a shuttered artificial light source (a stabilised xenon arc lamp). The pyranometer output was measured with a strip chart recorder to get the initial response (column 11) and a digital voltmeter to obtain measurements of the second time constant. Tests were performed without and with ventilation of the pyranometer (columns 12 and 13).

These measurements can be compared with those of Nast (1985) who undertook outdoor shading and unshading experiments using the difference between the irradiances

determined by two PSPs, where one was to be shaded (or unshaded) and the second was used to compensate for the changing final value of the diffuse or total global irradiance. These outdoor results are given in columns 14 through 17 of Table 5.2a. Data were taken from his linear plots given on pp. 331 and 332 in the Norrköping proceedings, and plotted in semi-log form. Three-term exponential equations were fitted to these data. Figures 5.3 & 5.4 show the results of the curve fit on both the full time span measured (540 s) and on the first 60 s of the shading experiment. The experiment was repeated twice, and the data were handled as one set for these plots and analyses. No recognisable third time constant was found.

The third term obtained through the curve-fitting is a constant which Nast ascribed to the small final differences in irradiance values as calculated from the two pyranometers in the test, using their own, presumably slightly mismatched, calibration factors. If this constant portion is removed, the equation becomes:

$$V_{out} = 98.42e^{-t/2.75} + 1.58e^{-t/126.8} \qquad [5.1]$$

where V_{out} is the percentage of the full scale reading t seconds after shading the pyranometer.

Equation 5.1 shows that, initially, 1.58% of the output is due to a component with a time constant of 126.8 s and the major (initial) response has a time constant of 2.75 seconds.

Table 5.2a Comparison of time constants (1/*e* in seconds) : pyranometer response as measured at various laboratories.

1 Model & Serial No.	2 K&Z (Incr)	3 K&Z (Decr)	4 Austria Plots (Incr)	5 Austria Plots (Decr)	6 Austria Notes (Incr)	7 Austria Notes (Decr)	8 Eppley Outdoor (Ave)	9 DSET Outdoor (Ave)	10 Kipp Indoor (Decr)	11 Hamburg Indoor (Decr)	12 Hamburg Unvent. (Decr)	13 Hamburg Vent. (Decr)	14 DFVLR Outdoor (Incr)	15 DFVLR Outdoor (Incr)	16 DFVLR Outdoor (Decr)	17 DFVLR Outdoor (Decr)	18 DFVLR Indoor (Decr)
CM10 800090																	136.0
CM10 810119	3.6	3.3	0.8	2.2	0.9	2.1	3.6	5.0		3.2	85.0	83.0					
CM10 810120	3.6	3.6															
CM10 810121	3.6	3.6							4.0								
CM10 810122	3.9	3.9					3.1	5.0									
CM10 830092								5.0									
CM10 830093							3.8										
CM5 763141																	232.0
CM5 773656									3.0								
CM5 773992			1.5	1.1	4.7					2.0	185.0	150.0					
CM5 774120							2.5	3.0									
CSIRO 115									22.0								
Eko 81907							3.5	4.0									
Eko 81908									4.0								
MID 123			2.8	3.2	3.5					4.9	150.0	90.0					
PSP 17750f3			0.4	0.5	0.4					0.9	170.0	130.0					
PSP 17863f3							1.1	2.0									
PSP 17880f3							1.1	2.0									
PSP 18376													1.9	174.4	2.7	126.8	176.0
PSP 20524f3									1.0								
PSP 21017							1.1										
PSP 24191f3							1.1	2.0									
SWISS 114									4.0								
Schenk 1285			2.6	2.7	2.7												
Schenk 2186							5.5	6.0									
Schenk 2209									6.5								
Schenk 2251			3.2	3.5	3.5												

The two unshading experiments by Nast were analysed similarly and are plotted in Figures 5.5 & 5.6. The "3 Term Fit" curves present the results of determining the amplitudes and time constants for three terms . As above, the third term is a constant due to the offset between the two pyranometers. The "2 Term Fit" was made by fixing the first time constant at 1.1 s (Eppley's value) and its amplitude at 98.1% , and then analysing the residual for two terms. This was done to see how well the 1.1 s time constant-based curve would fit the first recorded data points at 10 seconds. Figure 5.6 shows that the "3 Term Fit" is preferable. Disregarding the constant term it becomes:

$$V_{out} = 100 - 98.26e^{-t/1.9} + 1.71e^{-t/174.4} \qquad [5.2]$$

The second component has a magnitude of 1.71% and a time constant of 174 s.

The time required to get within 0.1% of the full signal value is 8.25 minutes, according to equation 2. At 5 minutes, the signal is 0.3% away from its final value and at 30 seconds it is 1.4% away. Therefore, using 30-second shade/unshade cycles in the ASSM calibration would result in responsivities that were 1.4% to low.

Ventilation, as Nast and Dehne have demonstrated, has a significant impact on the second time constant. These outdoor tests may have been influenced by sufficiently different wind conditions to have caused the observed difference between the shading and unshading second time constants (126 s and 174 s respectively).

The second time constant for a CM10 of 136 s was measured by Nast by an indoor experiment and the corresponding magnitude was 0.5%. These figures dictate a 220 s period for the shade/unshade calibrations of CM10s again using the rather stringent 0.1% criterion. The results of his indoor determinations for the CM10, CM5, and PSP are given in column 18 of Table 5.2a.

It appears that the first (major) time constant of the pyranometer is often not the time constant which will determine when the signal has completed 99% or more of its total change. It is therefore not the important factor setting the timing of the shade/unshade cycles and may not have to be measured very accurately depending on the application.

The first time constant is relevant in studies of rapid changes of irradiance. It expresses the limit to the pyranometer's ability to detect fast changes and the maximum useful sampling frequency, which is $2.2 / t_1$ Hz. Taking data faster than this rate increases the data volume without providing any additional information on the irradiance.

The ASM calibration could be operated slightly faster than determined by the 0.1% approach criterion but there would have to be a correction that was well measured and known to be stable. Ventilation is obviously extremely advantageous in that it reduces the time constant and makes it much less dependent on ambient winds thus permitting faster and more accurate calibration.

From the information presented, more investigation appears necessary. Particular attention should be given to confirming the sources of the multiple time constants (including a possible third one) and the methods used to measure them adequately. The calibration procedures, especially the timing presently used for shade/unshade calibrations should be re-examined and corrected as necessary.

5.3 Temperature

Unfortunately, all thermocouple materials in present use are slightly non-linear and temperature dependent. For this reason and others mentioned in chapter 2, the ouput from the thermopile of a pyranometer inevitably has a temperature dependence.

Several models of pyranometers incorporate internal temperature compensation. This is usually accomplished by adding a temperature-dependent attenuater circuit between the thermopile output and the pyranometer output connections. Typically, a thermistor is used as the temperature-sensitive element in this attenuating network. The variation of the thermistor's resistance with temperature is used in the attenuator to compensate for the variation in output of the thermopile with temperature. However, this compensation is not perfect and varies from instrument to instrument of the same model. Therefore, if measurements of high quality are required, it is important to know the temperature characteristics of the individual pyranometer that is being used rather than statistics that apply to its type.

Tests were performed at several laboratories to measure the change in responsivity as a function of temperature, also called the *temperature coefficient of responsivity.* Different

techniques and apparatus were employed in the measurement of temperature coefficient, including the methods for determining and correcting for zero drift and in regard to what temperature was measured (test chamber or ambient air temperature versus pyranometer body temperature).

The data displayed here have been normalised to +25 C, causing the curves to be tightly grouped in that region. The method used to perform the normalisation was to fit a polynomial to the data for the curve, solve for the value of the equation at 25 C, then divide all the ordinate-values of the data points by that value, and then plot the curve from normalised data.

Two pyranometers incorporating temperature compensation networks are the Eppley PSP and the Kipp and Zonen CM10. The next two figures give some idea of how well laboratories have done in duplicating results over the long- and short term. Figure 5.7 displays the results from four determinations of the temperature coefficient of one instrument (PSP #12617) performed in one laboratory (the Solar Radiation Facility of the National Oceanic and Atmospheric Administration) during a 22 month interval. These data were obtained from NOAA, courtesy of Mr. E. Flowers, to determine the repeatability of their measurement process. There is no apparent drift evidenced, in that the November 1983 and the March 1984 determinations were the closest together in time and the farthest apart in results. The largest spread in Figure 5.7 is a 1.5% range near -30 C. A third order curve fit was made to these data, which is plotted in Figure 5.8, along with the residuals from the curve-fitting process. The residuals range from about +0.8% to -0.4% over a nearly 100 C temperature range.

Figure 5.9 shows data taken over a range of about 60 C on CM10 #810122 by Kipp and Zonen at the time of manufacture. The curve fit shows residuals not exceeding about ±0.3%. Pyranometers are often used outside this temperature range (for which the compensation of #810122 was designed). Figure 5.10 displays the results of five determinations of the temperature coefficient of the same instrument by four laboratories over three and a half years. The solid black circles plot the data taken in 1982 at the Statensprovningsanstalt (SP), Borås, Sweden with zero offset corrections that SP determined when they re-ran another CM10 using a new zero correction scheme. Figures 5.10 & 5.11 show the steep slope of the temperature coefficient at low temperature, which appears to be typical of CM10s.

This difference in slope of the responsivity versus temperature becomes quite apparent when the derivatives of the curves are taken (Figure 5.12). The implication is that in determining and applying the temperature coefficients, the temperature must be determined quite accurately for CM10s at low temperatures. For example an error of 1 C in measuring the temperature at -30 C can result in an error of 0.43% for the CM10 and an error of 0.08% for the PSP. Of course, these factors are characteristics for these individual instruments, and should be evaluated for a specific instrument at a specific temperature when assessing the errors in irradiance measurement due to errors in temperature measurement. The best strategy is to use the body temperature of the instrument both when measuring the temperature coefficient and when using the instrument. For best results, this approach should be used for all instruments.

The effect of zero offset correction schemes applied to temperature coefficient determinations was demonstrated by SP, Borås when their technique was improved in 1985. Several pyranometers that had been tested in 1982 were re-tested in 1985 using the improved zero offset subtraction method. Two new model Eko units were also tested with and without the improved zero correction. The differences are large (Figure 5.13) and cause changes in temperature coefficients from -1.5% to +2.8% depending upon the model and the temperature.

The results of tests on two Kipp & Zonen CM5 instruments were analysed to show not only the influence of temperature on responsivity, but also to show the differences in the results between the various laboratories and between repeated measurements in the same laboratory. These are shown in Figure 5.14.

For CM5 #773656, there is a maximum difference in the measured response of just over 2% between NARC and NOAA (at about -25 C). The 1% difference between the 1982 and 1985 tests performed at SP contains both the repeatability factor and the change in the offset correction method at that laboratory.

For CM5 #774120, there is a larger spread in temperature response data, amounting to about 4.5% at the -25 C region. Eppley made two determinations of temperature coefficient, with a difference of just over 2% near -20 C.

Differences between test results of greater than 4% at about -20 C and 2.5% at temperatures as high as -5 C are shown for the Eppley PSP #17880 in Figure 5.15

Plots of the families of curves for the various models are shown in Figure 5.11 & Figure 5.17 through Figure 5.21

Calibration of pyranometers for the season of the year in which they are to be used can also reduce the errors caused by difficulties in obtaining and applying adequate temperature coefficient data. It seems proper that the technique for measuring the pyranometer temperature during field use should be similar to the technique used for making that measurement during the characterisation of the pyranometer's temperature coefficient. Measuring the instrument body temperature in both cases is expected to yield the best results, although this is rarely done by any laboratory.

It can be seen that to achieve irradiance measurements with accuracies approaching ±1% over a useful range of temperature (the goal for collector testing and engineering measurements), the methods of determining the temperature coefficient of responsivity require further investigation, refinement, and continued inter-laboratory comparisons to confirm the improvements. From this should come the ability to design better pyranometers.

5.4 Rate of change of temperature

If the construction of the pyranometer is such that forcing a temperature change on the instrument from an external source (such as a change in ambient air temperature) causes a change in the difference in temperature between the hot and the cold junctions in the thermopile, then there will be a spurious voltage developed as long as that difference in temperature exists. Kipp and Zonen conducted a test in which a nearly constant rate of change of temperature was forced upon six models of pyranometers in a dark test chamber. According to the plot shown in the report, the first 40 minutes gave a rise at a rate of 10 K h^{-1}, followed by an additional 50 minute period at a rate of 6 K h^{-1} (Figure 5.22). The chamber ventilator created a wind speed of about 1 ms^{-1}. The error signals from the pyranometers peaked at about the 40-minute mark. Figure 5.23 reproduces the curves from the Kipp and Zonen work published in the TPD report.

The Schenk acts as an ideal black and white instrument with nearly perfect balance, having an error signal equivalent to about 0.1 Wm^{-2}. The Eppley PSP generated the largest error signal, equivalent to +5.5 Wm^{-2}. The CM10 generated a signal equivalent to approximately

+3.0 Wm^{-2} · The Eko, the Swissteco and the CM5 generated signals equivalent to about +1.9 Wm^{-2} , +0.9 Wm^{-2} and -0.9 Wm^{-2}, respectively. Dividing the error signals by the rate of change of temperature gives approximately +0.65 Whm^{-2} K^{-1} for the PSP and about +0.33 Whm^{-2} K^{-1} for the CM10. These estimates are examined in more detail in section 6.5.

The negative result for the CM5 is interesting. It indicates that the hot junctions of the thermopile which are in thermal contact with the receiver surface are, in this instrument, more closely connected thermally to the main body than are the cold junctions.

Thermal shock tests were also performed at Kipp and Zonen, by subjecting the pyranometers to an abrupt -5 C temperature change when moved from a well-ventilated temperature chamber at 25 C to a dark room at 20 C with a fan blowing directly across the pyranometers to establish a similar ventilation. Figure 5.24 portrays the result of this test, as copied directly from the Norrköping report. The PSP and the CM10 results were reproducible to 10%. These results may not be sufficiently well-quantified to determine factors for transfer functions but they are a good beginning in determining the order of magnitude of the corrections and a possible technique for determining them.

A thermal test was also performed at ZFMG in Vienna. The temperature in a darkened chamber was changed from 30 C to 39 C in about 30 min, and then back to 30 C again after a delay. During the transition, the temperature changed at the rate of approximately 27.6 K h^{-1} for about 10 min. The results indicate similar trends.

Qualitatively, the results from the thermal shock tests and the constant rate of change of temperature agree. Two notable exceptions occurred during the shock tests that were not apparent during the tests with continuous increase or decrease of temperature. These were the very large and abrupt outputs from the Eko and the CSIRO instruments and the Swissteco's small negative output followed by a larger and longer positive swing when subjected to the negative thermal shock.

Correcting for these errors during outdoor testing using the rate of change in ambient temperature or the difference between the ambient and instrument temperature is examined in Chapter 6.

It should be recognised that stray thermal voltages generated in the connectors, temperature compensation circuits, and in wiring (both internal and external to the instruments) may cause additional error signals which add to those generated by the thermopiles under conditions of changing temperature. Placing insulation around the connector may be the most effective preventative technique to be applied. Ventilation also improves the performance of pyranometers under conditions of changing ambient temperature.

5.5 Non-linearity

Participating laboratories made linearity tests at least up to the level of 1,000 Wm^{-2} and in some cases up to 1,250 Wm^{-2}. Irradiances encountered in practice sometimes exceed even this value.

Figure 5-25

Figure 5-25 shows the results of testing three different models of pyranometers at Kipp and Zonen, with the data normalised to 500 Wm^{-2}. The Kipp apparatus measured non-linearity with the pyranometer horizontal. The CM5 was measured in two different azimuthal orientations, as indicated by the cable "up" and the cable to the "side", when the instrument was later to be tilted for the tilt error measurements made in the same apparatus. These two results show a spread of about 0.4% at the 250 and 1,000 Wm^{-2} levels giving an indication of repeatability for one instrument in one laboratory.

Figure 5-26

Figure 5-26 displays the results from MOH, Hamburg running four different models referenced to both 500 and 1,000 Wm^{-2}.

Figures 5-27

Figure 5-27 shows a family of PSP linearity curves based on data from SP, Borås and MOH, Hamburg. These show the non-linearity of the six PSPs within +0.1% to -0.2% over irradiances up to 1,000 Wm^{-2}.

Figure 5-28

Figure 5-28 presents a family of CM10 linearity curves, based on data for five instruments as measured at SP and MOH. Normalisation to both 500 and 1,000 Wm^{-2} was used by the laboratories. Non-linearity errors from 0.9% to 1.8% occurred over the irradiance range of 30 to 1,000 Wm^{-2}.

Figure 5-29

Figure 5-29 shows the results from linearity tests performed at three laboratories on five different CM5s, normalised to both 500 Wm^{-2} and 1,000 Wm^{-2} and non-linearities approaching 1.9%.

Figures 5-30 and 5-31

Figures 5-30 and 5-31 show wide spreads in linearity results from testing five different Schenk Star pyranometers at SP, and for six Eko Model MS42 pyranometers, tested at both SP and TPD. The results are normalised to 500 Wm^{-2} and the spreads are 2.4% for the Schenk Star and 2.5% for the Eko MS42.

Figure 5-32

Figure 5-32 shows that the new Eko Model MS801 is remarkably linear, according to test results from SP, Borås.

These results from testing of linearity appear to have an interesting relationship to tilt behaviour, as is discussed in the following section.

5.6 Tilt

Tilt error is used to describe the fact that the output voltage from a pyranometer (with a fixed irradiance input) varies with orientation of the pyranometer from horizontal (tilt angle $\beta = 0$) to vertical ($\beta = 90^{\circ}$). Three laboratories made tests on tilting at irradiances up to 1,250 Wm^{-2}.

Figures 5-33 through 5-37

Figures 5-33 through 5-37 plot the data measured by SP, Borås for several instruments of the same type. The PSP, CM10, CM5, Schenk, and Eko MS42 measured at an irradiance level of 1 KWm^{-2} are shown, with tilt errors as large as -3% for some instruments. These results show the combined effects of variability between instruments and repeatability within one laboratory. Second order curves were fitted to the data to provide some indication of the general behaviour for the CM5, Schenk, and Eko MS42 families of instruments. No data were available showing the repeatability of measuring the tilt effect at any of the laboratories.

Figures 5-38 through 5-40

Figures 5-41 through 5-40 show the relative response of a PSP, CM10, and CM5 measured at three different laboratories at different irradiance values.

Figures 5-41 through 5-46

Figures 5-41 and 5-42 show graphs of tilt error plotted against tilt angle at four irradiance levels and plotted against irradiance at tilt angles from 0° to 90° for CM5 #785047, measured at Borås. Similar plots are shown for the Schenk Star #2221 in Figures 5.43 and 5.44, and for the Eko #81909 in Figures 5.45 and 5.46. the relative response of a PSP, CM10, and CM5 measured at three different laboratories at different irradiance values.

In summary, the tilt error is very small (less than 0.2%) for some models which also have low non-linearity. For most instruments with a large non-linearity, tilt error is a function of both tilt angle and irradiance. In nearly all cases, tilt error increases with irradiance. In the CM5, tilt error depends significantly on the azimuth of the tilting axis. Linearity and tilt on the Eko instruments and linearity on the Schenk instruments are shown to be quite variable from instrument to instrument.

Most of the data from instruments with significant tilt effects are consistent with the model behaviour in Figure 2.3. However, some Schenk and Eko instruments tested at Boras show an increase in responsivity as irradiance is increased from zero to 500 Wm^{-2} which is not consistent with the model.

5.7 Spectral response

Spectral response was investigated at Borås in September 1985 with the intention of measuring the responsivity for irradiance (calibration factor) of pyranometers at several equally spaced wavelengths in the range 300-2500 nm. This was not possible in practice because pyranometers are not very sensitive detectors and radiant flux from monochromators is small, even with the largest bandwidth settings. It is also desirable to have a very uniform irradiance distribution over the detector surface which adds to the difficulties of using monochromators for this task

As an alternative, glass filters were used to select different wavelength distributions (Liedquist, 1990). The set up for the measurement was very simple. A 24V, 250W tungsten

halogen lamp was used with a condensing mirror and lenses within a Kodak Carousel slide projector (Table 5.7a). A removable infrared (IR) cut-off filter was placed between the lenses. Different spectral filters were placed in the slide carrier. Long-wave IR radiation was blocked by a filter comprising 8 mm thick plexiglass and 2 mm thick ordinary glass elements in combination, with the plexiglass facing the source. The cut-off wavelength of this filter is 2000 nm. The filter was cooled to ambient temperature by a fan in order to reduce long wave IR radiation emission from the filter itself.

A diaphragm tube reduced the influence from stray radiation and from changes in the long wave IR radiation level from the surroundings.

Each pyranometer was vertically positioned (with a cable connection upwards) about one meter from the condenser. At this distance the irradiance is very uniform. The variation is less than 0.2% over a surface corresponding to that of the Kipp & Zonen CM10 detector surface and less than 0.5% over the detector surface of the Schenk Star pyranometer.

A Laser Precision RS 3940 was used as a reference absolute radiometer, having a pyroelectric detector with a gold coated black surface and an area of 0.5 cm^2. The pyranometer and the reference detector (including its chopper) were placed on a rotating stage that could be positioned into the optical path quickly and conveniently to an accuracy of 1.0 mm or better in distance and translational position. The reference detector had no window and was therefore very sensitive to long wave IR radiation. The temperature of the surroundings seen by the detector must be kept constant during the measurement.

Eight different spectra (Table 5.7a) were used, of which one serves as a reference for the measurements with the others. There were two basic spectra: one with 24V on the lamp and with the IR cut-off filter in position; the other with 8V on the lamp and with the IR cut-off filter removed. The first of these was the reference. From this spectrum four other spectra were selected using the following Schott filters: BG 28 (1 mm), BG 38 (2 mm), VG 9 (1 mm) and RG 665 (1 mm). The other basic spectrum was also used, directly and also filtered by a Schott filter RG 1000 (2 mm). The eighth spectrum was formed with 24V on the lamp without the IR cut-off filter and with an interference filter having 1500 nm centre wavelength and 60 nm half power bandwidth. This filter is placed outside the projector but in front (nearer the source) of the long wave IR blocking filter. The effective wavelengths, i.e. half integrated irradiance below and half above, are for the spectra in the mentioned order 595, 491, 548, 549, 699, 1210, 1317 and 1501 nm.

This experiment was performed on nine pyranometers. Seven of these were IEA Task 9 pyranometers. The other two were Eko MS801 double dome type pyranometers owned by Eko. Table 5.7a shows the result of the measurements. Most striking is that both the Kipp & Zonen pyranometers have a flat response for all spectra while all the others have decreasing responsivity for IR radiation. All pyranometers have a flat response in the visible wavelength range except for the Schenk Star in the blue and the CSIRO in the red region.

The reproducibility of the measurements was typically 0.5% in the visible range; 1% for the broadband IR spectra and 2% for the narrow band IR spectrum (1500 nm). The irradiance levels on the pyranometers range from 1.5-22.0 Wm^{-2} for the different spectra (Table 5.7a). At these low levels it was necessary to use a symmetrical procedure for the measurements at each specific spectrum as there was, in spite of precautions, a remaining change in the radiance of the surrounds seen by the reference detector. The pyranometer output voltage also changed somewhat during the measurement. Each pyranometer was left for stabilisation for at least a few hours after handling them for measurement. The procedure was: RD, RDZ, RD, P, PZ, P, RD, RDZ, RD, where:

RD = reference detector reading,
RDZ = reference detector zero reading,
P = pyranometer reading,
PZ = pyranometer zero reading.

Table 5.7a Result of the measurements: relative responsivity of pyranometers for irradiance in different wavelength bands

Pyranometer	Ref. Spectrum *24V no IR*	BG28 *24V no IR*	BG38 *24V no IR*	VG9 *24V no IR*	RG665 *24V no IR*	WG9 *8V IR*	RG1000 *8V IR*	IF1500 *24V IR*	Respons. $\mu VW^{-1}m^2$
K&Z CM5 #773656	1.00	0.99	1.00	1.00	1.01	1.02	1.02	1.02	11.70
K&Z CM10 #810121	1.00	0.99	1.00	1.00	1.00	1.01	1.01	1.01	4.59
Eppley PSP #20524	1.00	0.99	1.00	1.00	1.00	0.93	0.92	0.90	10.20
Schenk Star #2209	1.00	0.97	1.00	1.00	1.02	0.94	0.93	0.94	15.40
EKO MS42 #81908	1.00	1.00	1.00	1.00	0.99	0.86	0.83	0.80	10.10
EKO MS801 #85022	1.00	0.99	1.00	1.00	1.00	0.92	0.89	0.85	6.83
EKO MS801 #85023	1.00	0.99	1.00	1.00	1.00	0.92	0.89	0.84	6.63
Swisteco #114	1.00	0.99	1.00	1.00	1.00	0.95	0.94	0.90	15.90
CSIRO PT #115	1.00	1.01	1.01	1.00	0.97	0.82	0.79	0.74	4.24
Irradiance Wm^{-2}	21.5	4.0	11.2	5.4	4.4	16.6	11.4	1.5	
EffectiveWavelength nm	595	491	548	549	699	1210	1317	1501	

A 10 nV resolution Keithley 180 voltmeter was used to measure the pyranometer output. The waiting time for the pyranometer readings was 1-2 minutes, depending on the pyranometer type.

The result of the measurements concerning the PSP and CM10 relation in the IR response confirmed similar measurements at Kipp & Zonen in a preliminary report by van Wely in April 1985. He also repeated the measurements 1) putting CM10 domes on the PSP and also 2) without the domes and got the same low response in the IR for the PSP. He concluded that the mean absorptivity of the PSP black paint must be considerably lower in the 1100-2700 nm range than between 300-1100 nm.

5.8 Variation of response with temperature under field conditions

The following results were calculated from the benchmark responsivities derived from the NARC (1983-1984) field experiment. The data set is divided into ten (approximately) two-month intervals identified by the number used to label the 9-track tape on which the sub-set is recorded (e.g., Tape #1, Tape #2 etc.). Absolute benchmark calibrations for each two-month period were first calculated for the instrument on channel 0 (an Eppley PSP) by the method described elsewhere in §8.3.3. Benchmark calibrations for the other instruments were determined relative to the performance of this instrument. Benchmark ratios relative to channel 0 were used to compute the fractional linear temperature coefficients Ψ of responsivity R defined by:

$$F_T = 1+\Psi\cdot(T-T_0) \qquad [5.3]$$

$$R(T) = R(T_0)\cdot\left[1+\Psi\cdot(T-T_0)\right] \qquad [5.4]$$

Values of Ψ for each instrument were computed from pairs of consecutive benchmark ratios of the same type where the mean temperature was different by 10 C or more. There was one result (case) for each instrument when the difference in the mean temperature between two consecutive data tapes was greater than 10 C.

Data from the same instrument types were combined except in the case of the two Middleton EP07 pyranometers which appear to be significantly different. The means and standard errors of the means were calculated except for the Middleton #123 and

Swissteco #113 where the errors were estimated because of the very small sample size. No results are given for Swissteco #114 because of the poor data quality.

The results from this analysis of the benchmark ratios are relative to channel 0. The absolute linear temperature coefficient for channel 0 was estimated from a similar analysis of absolute benchmarks, so that the results for other channels could be transformed into absolute results. The channel 0 result was 0.0±0.0002 making the transformation fortuitously simple — there being no change, except in the error estimate. These data cover the temperature range -8 C to +27 C and the results are given in Table 5.8a.

Table 5.8a

Instrument Type	Number of Instruments	Number of Cases	Temperature Coefficient	Standard Error	Standard Error Relative to Ch. 0
PSP Ch 0	1	10	+0.0000	±0.0002	(------)
PSP Ch 17	1	7	+0.0001	±0.0002	(0.0001)
Schenk	3	12	-0.0008	±0.0003	(0.0002)
Kipp CM5	3	3	-0.0013	±0.0004	(0.0003)
Kipp CM10	4	6	-0.0002	±0.0003	(0.0002)
Eko MS42	4	10	-0.0001	±0.0003	(0.0002)
Middleton Ch 10	1	4	+0.0010	±0.0005	(0.0005)
Middleton Ch 9	1	2	-0.0000	±0.0005	
Swissteco Ch12	1	1	-0.0008	±0.0005	

It should be noted that the typical error of determination is about ±0.0003 or 1% in the range of 30 C. Field results are obviously limited in precision, being influenced by variables other than changes in temperature. In particular, the azimuth range on any of the benchmarks changes significantly from tape to tape. Nevertheless, uncertainties in these field results on temperature coefficient are comparable to those obtained under laboratory conditions.

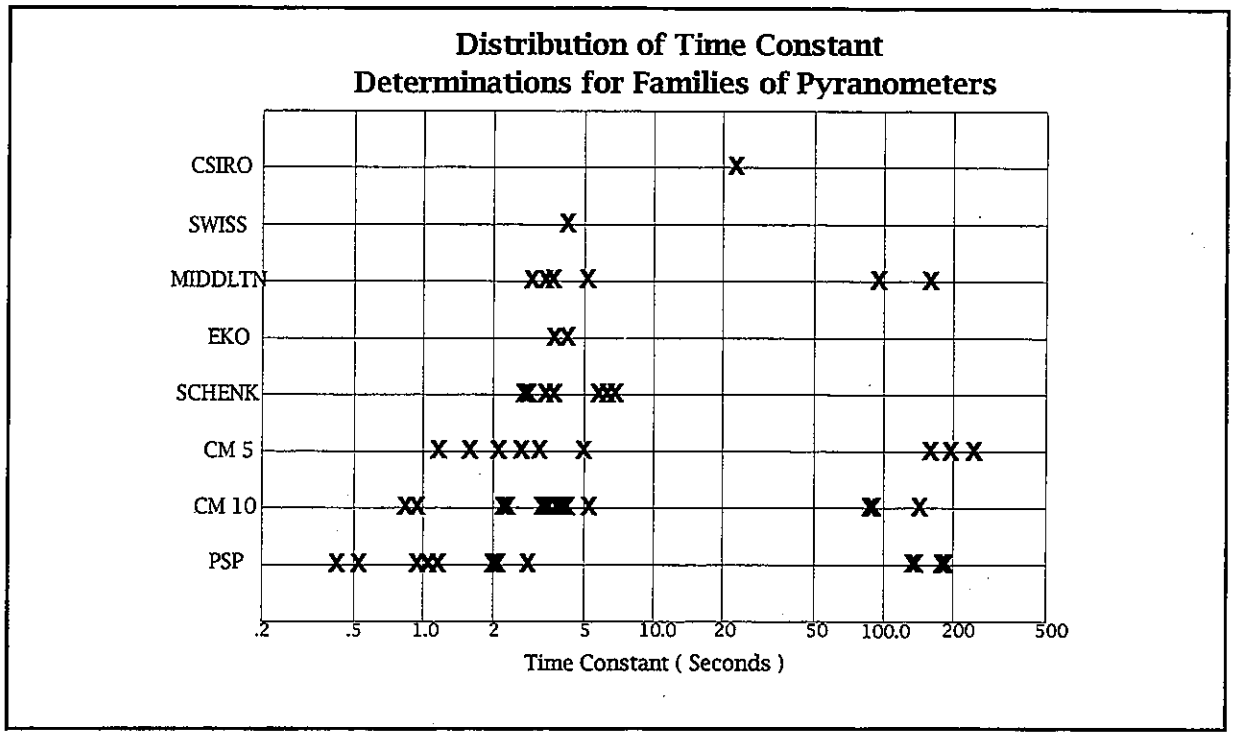

Figure 5.1

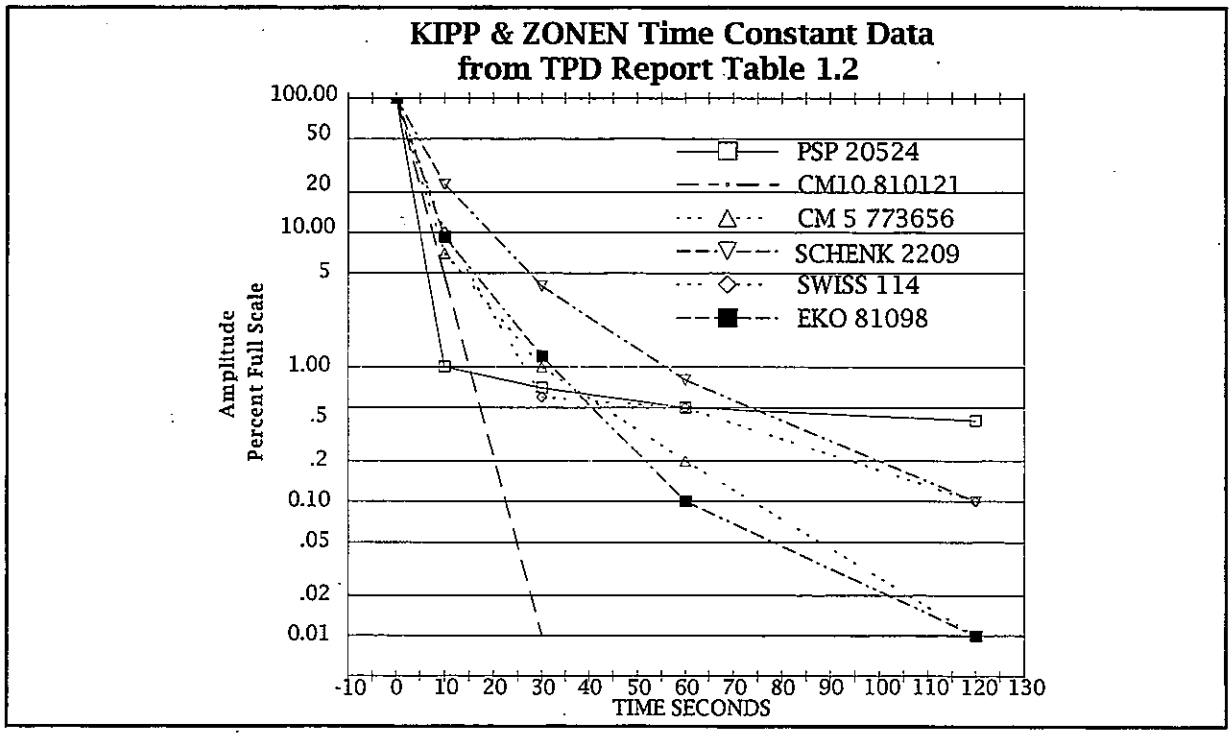

Figure 5.2

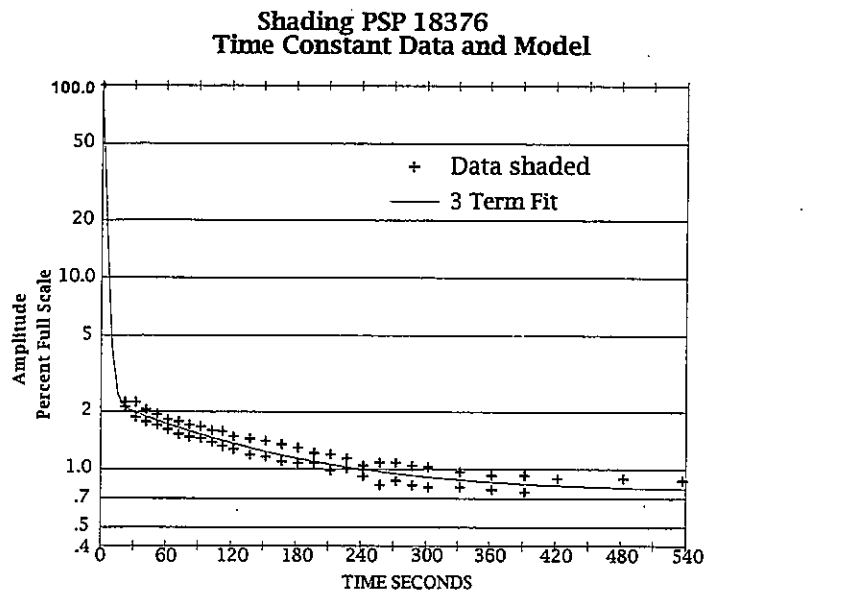

Figure 5.3

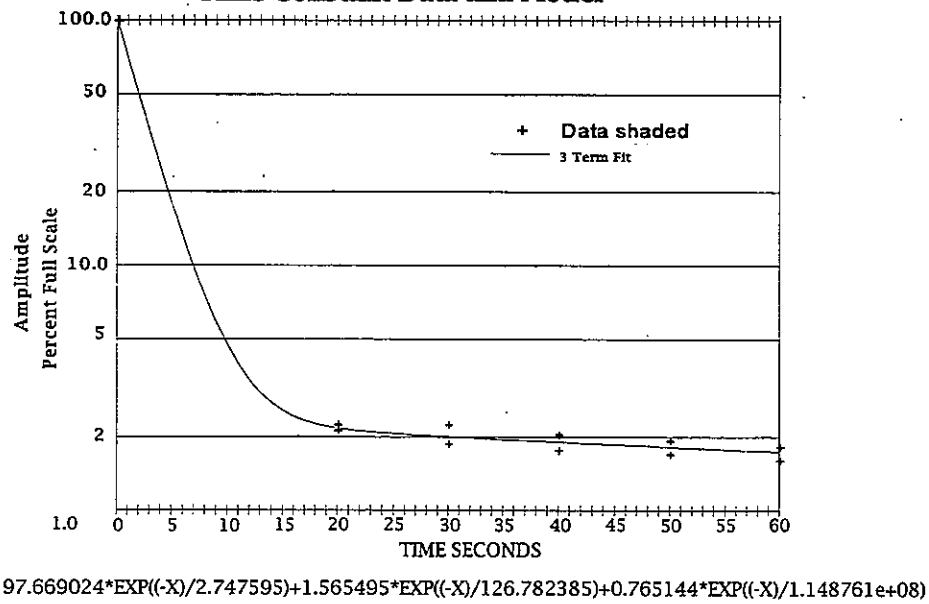

Figure 5.4

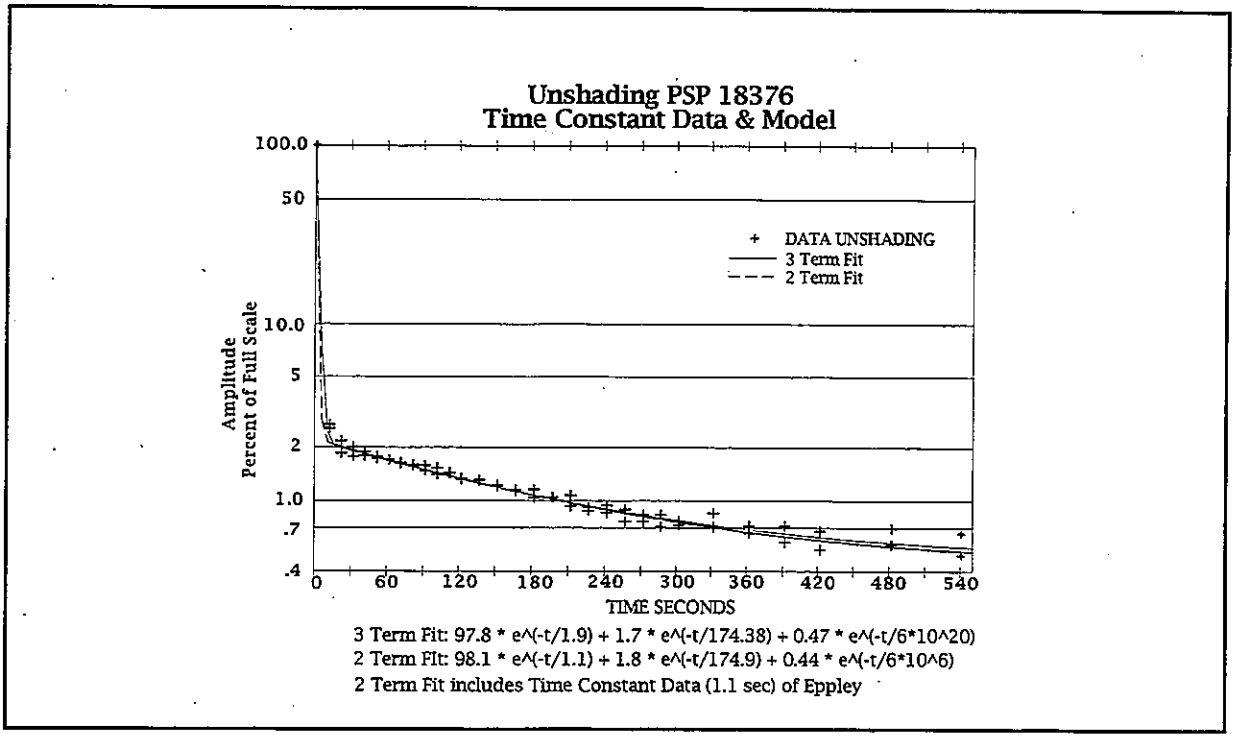

Figure 5.5

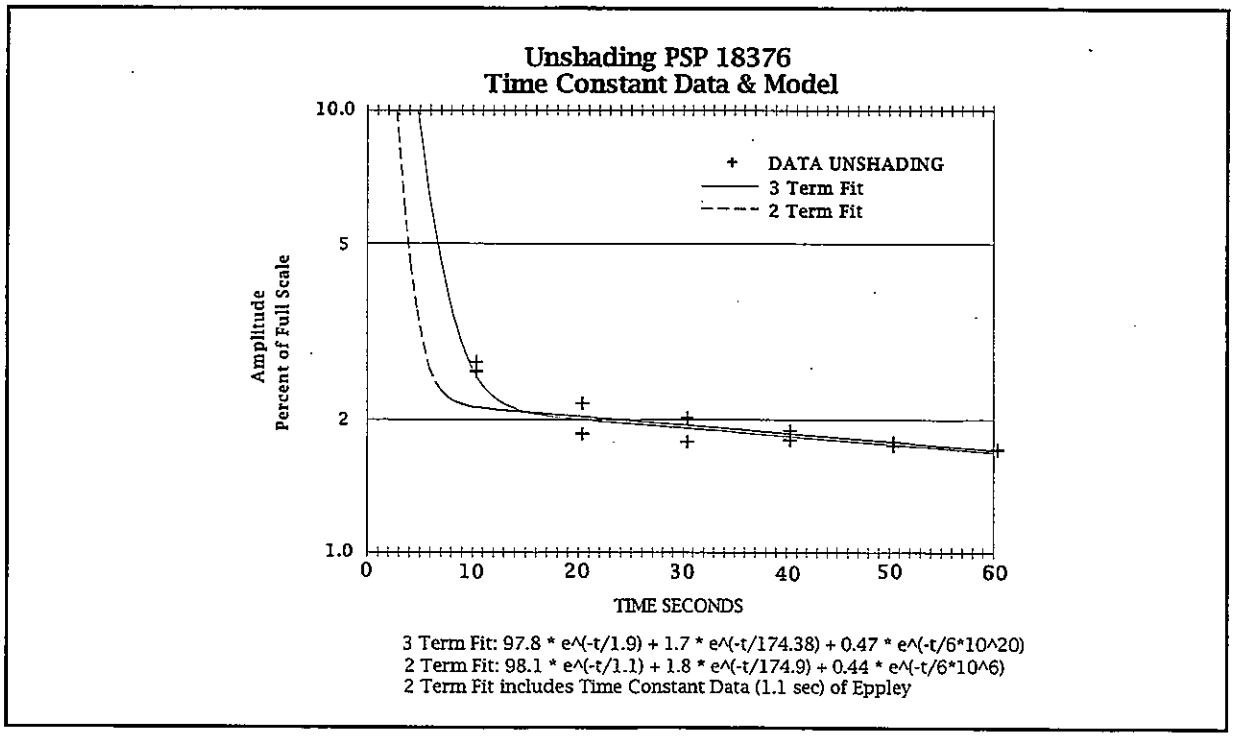

Figure 5.6

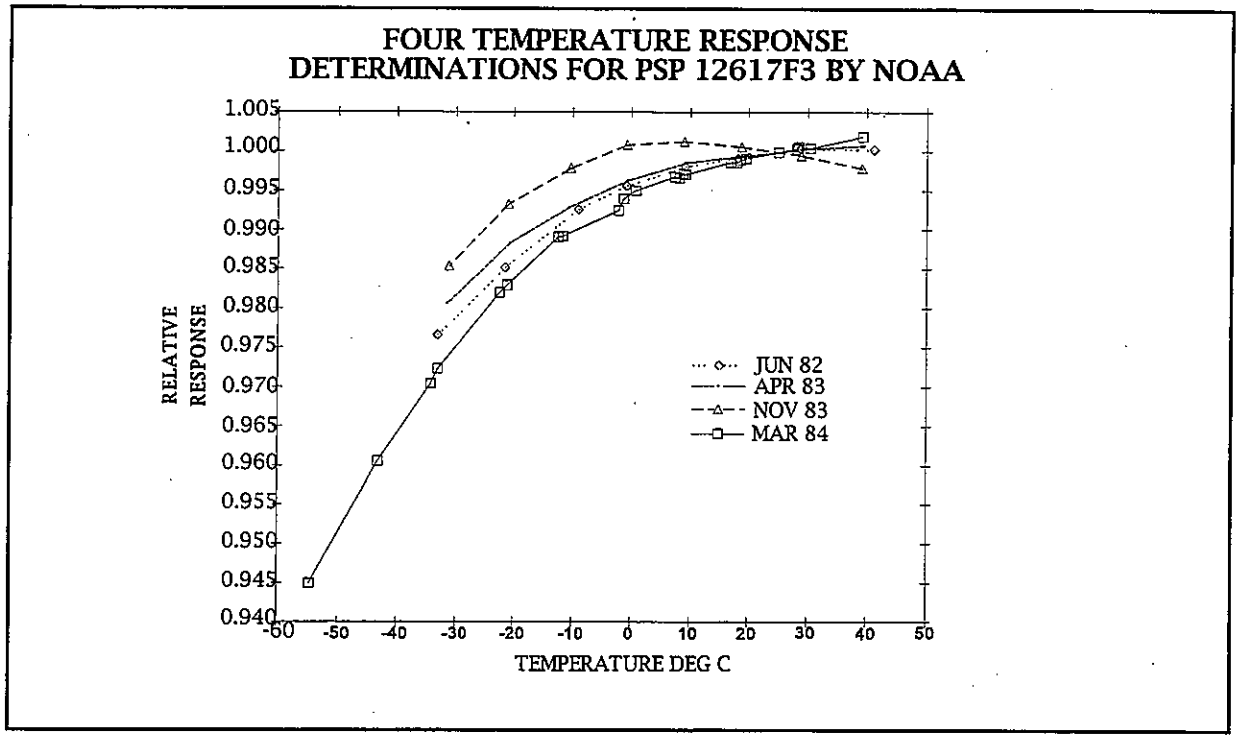

Figure 5.7

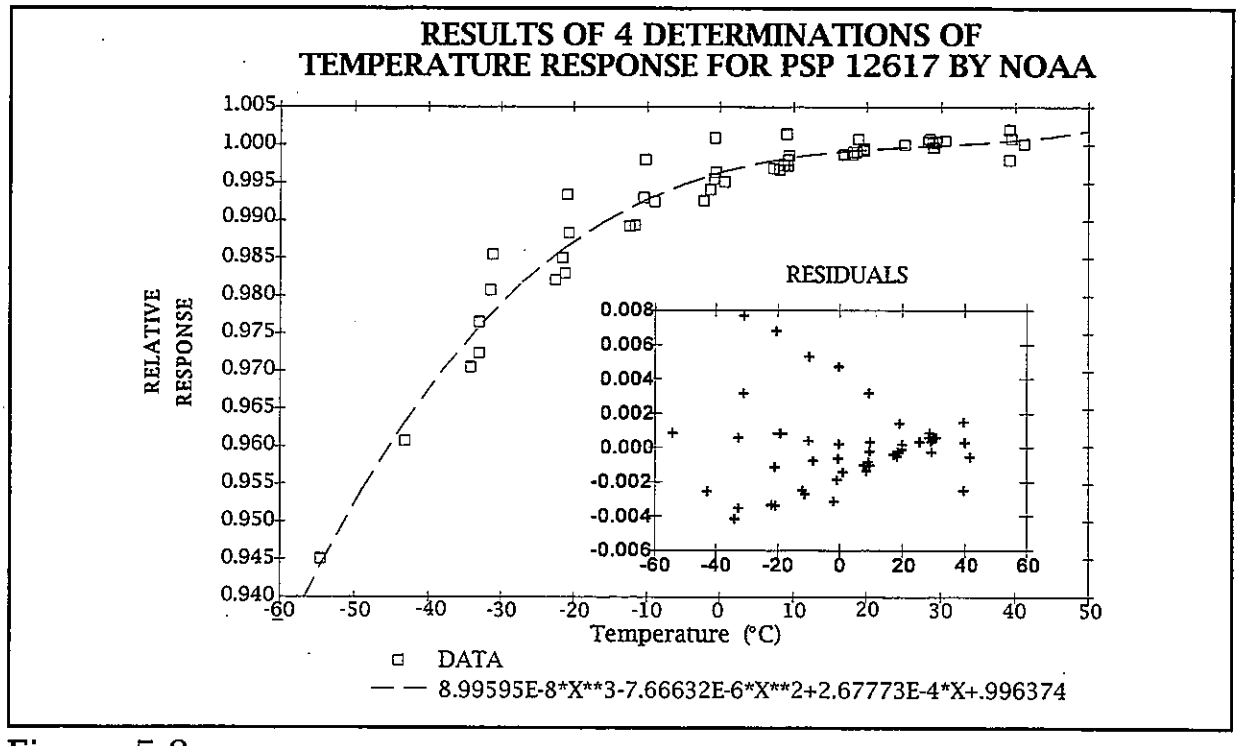

Figure 5.8

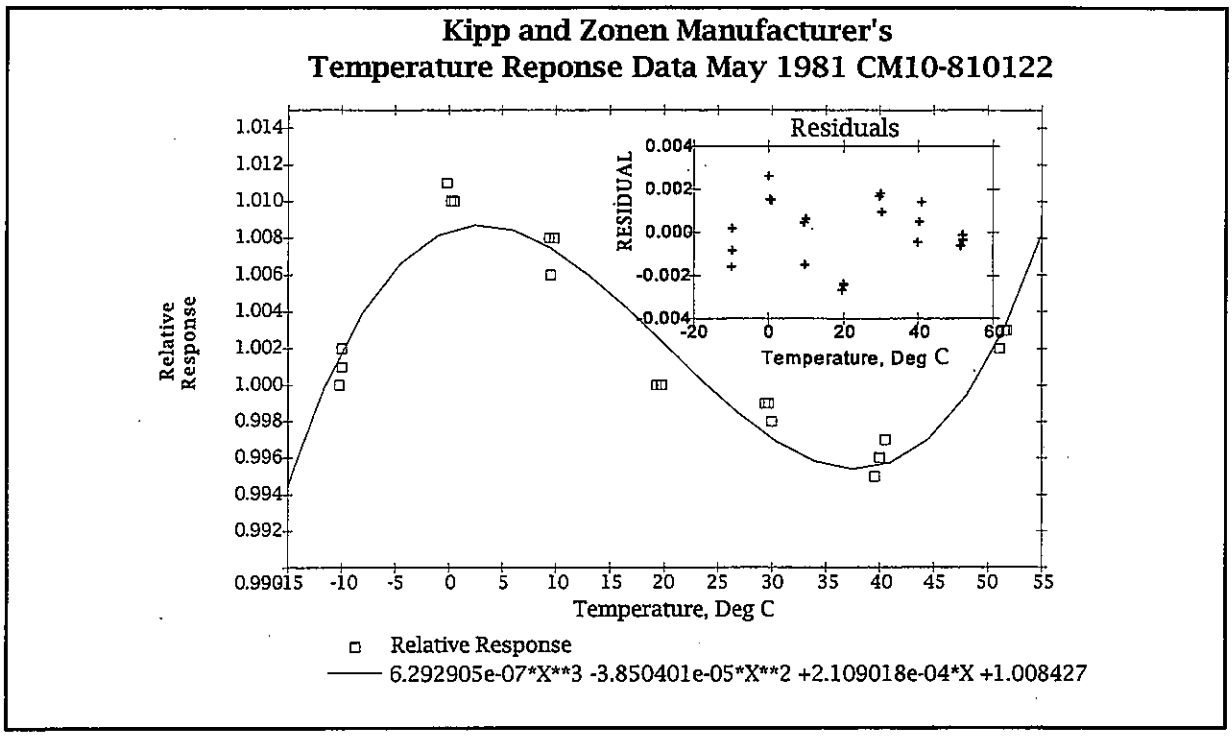

Figure 5.9

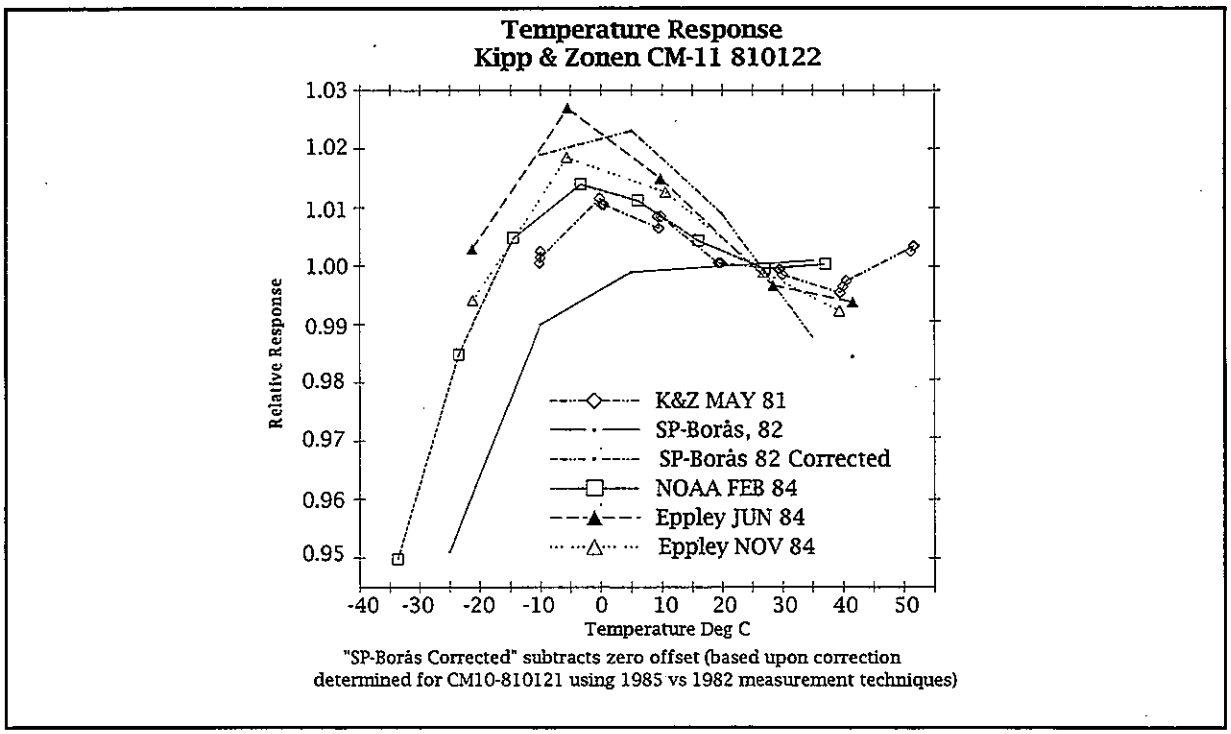

Figure 5.10

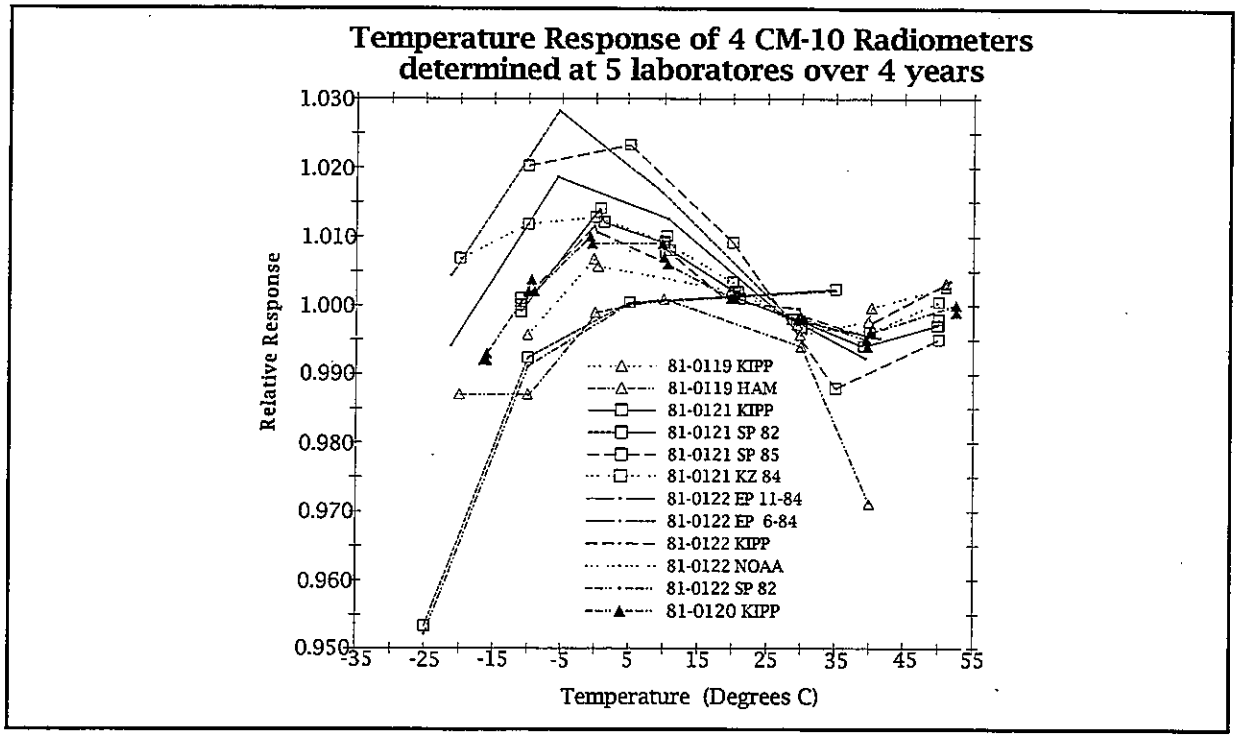

Figure 5.11

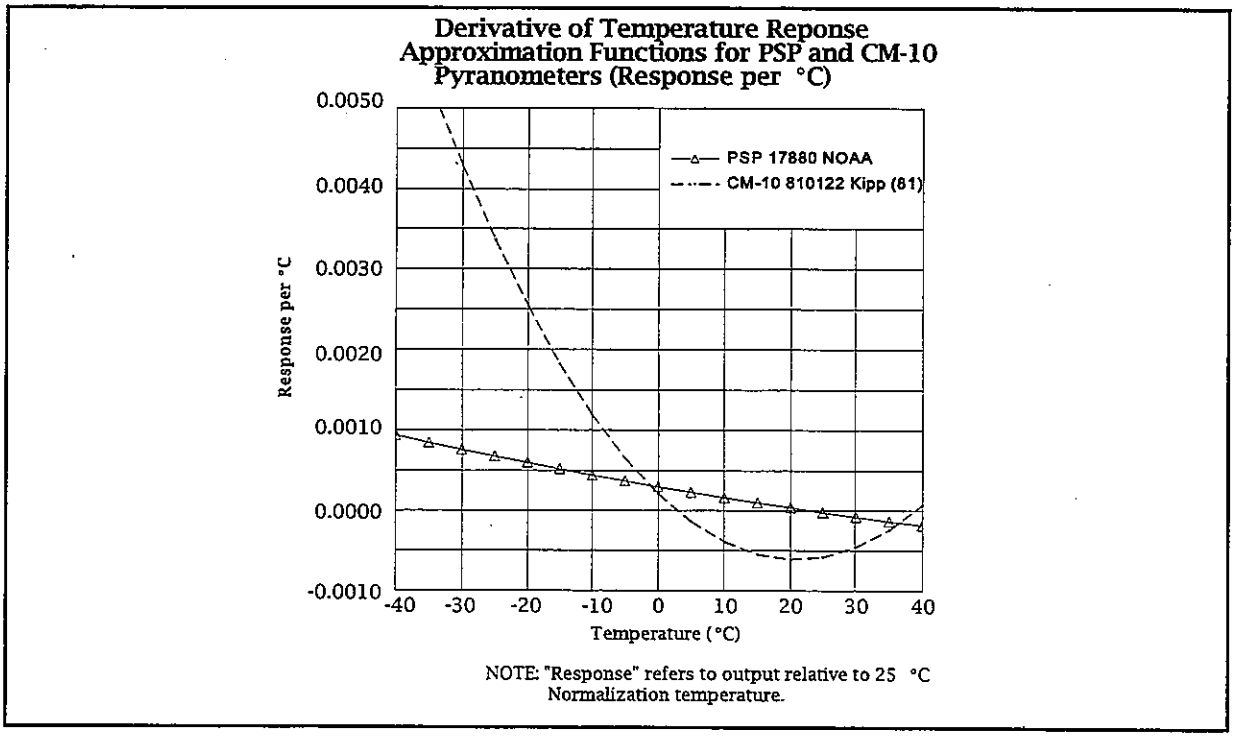

Figure 5.12

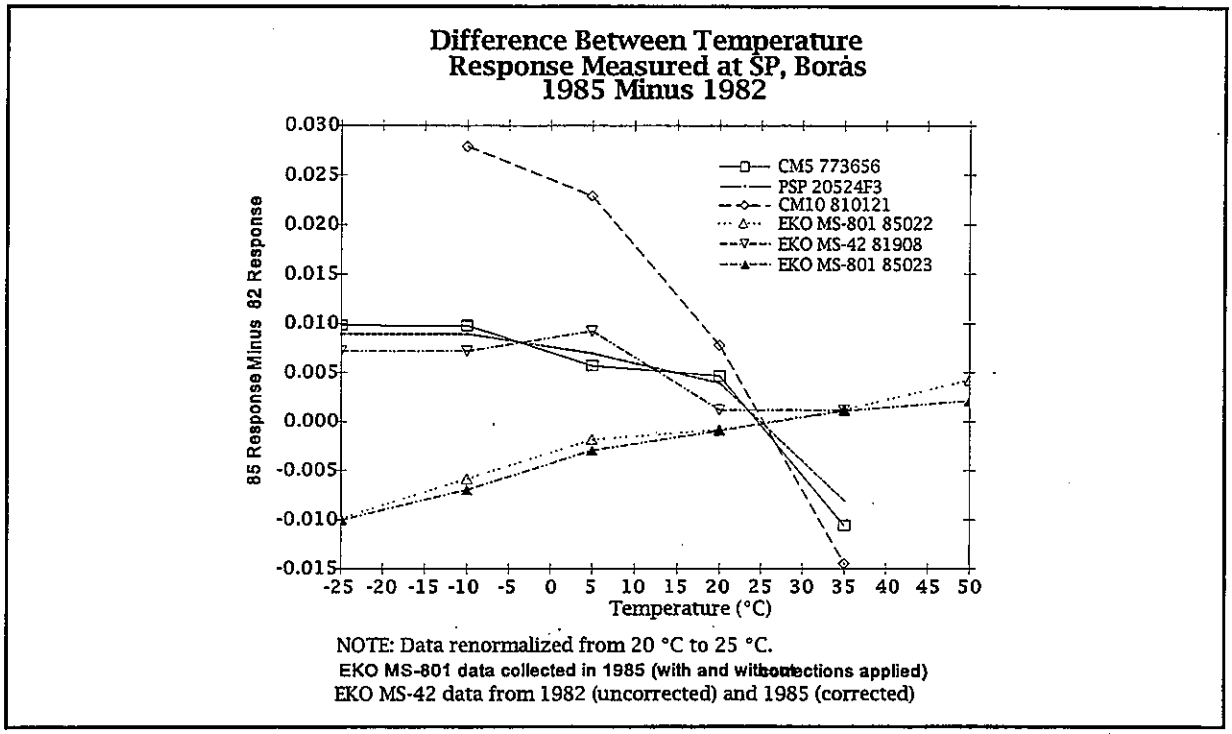

Figure 5.13

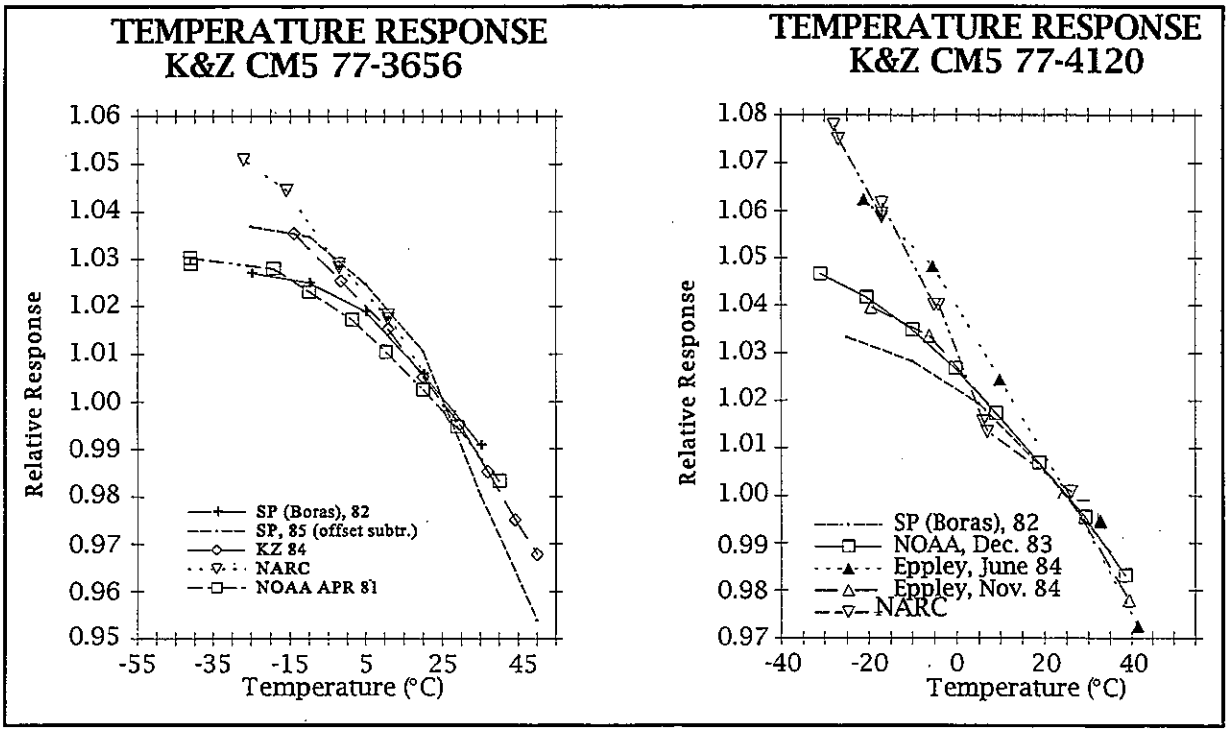

Figure 5.14

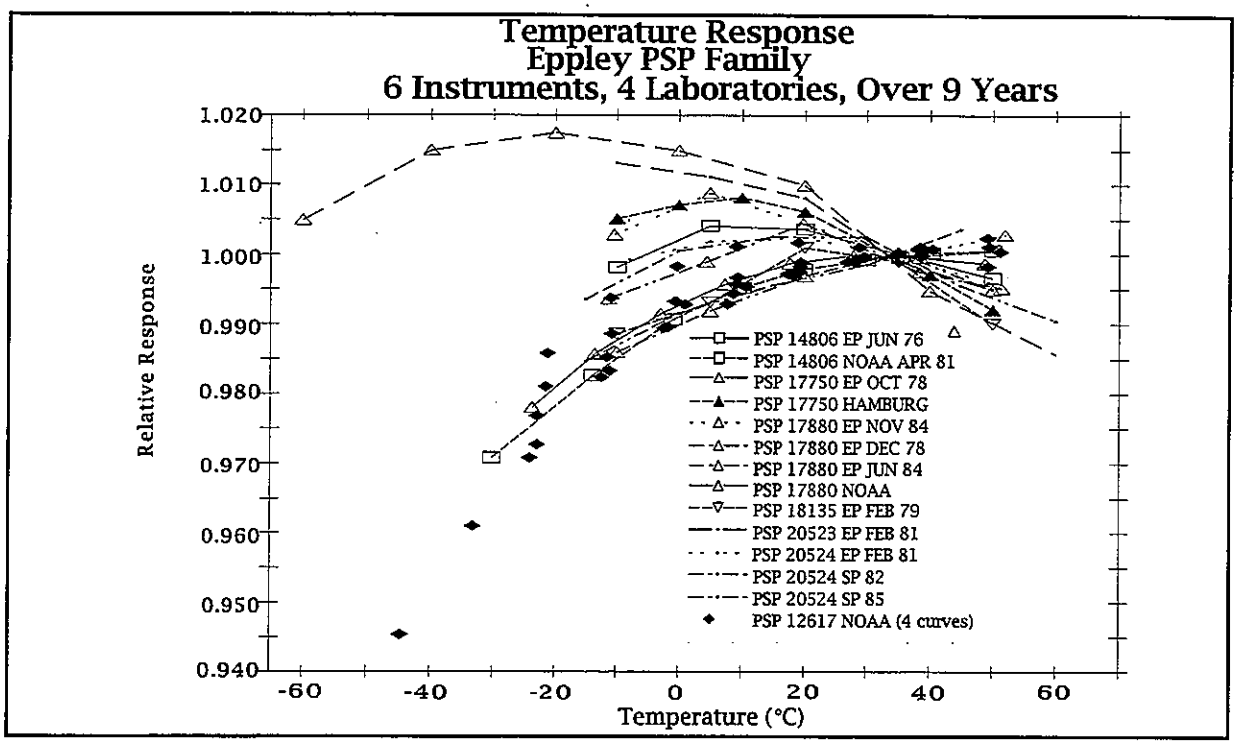

Figure 5.15

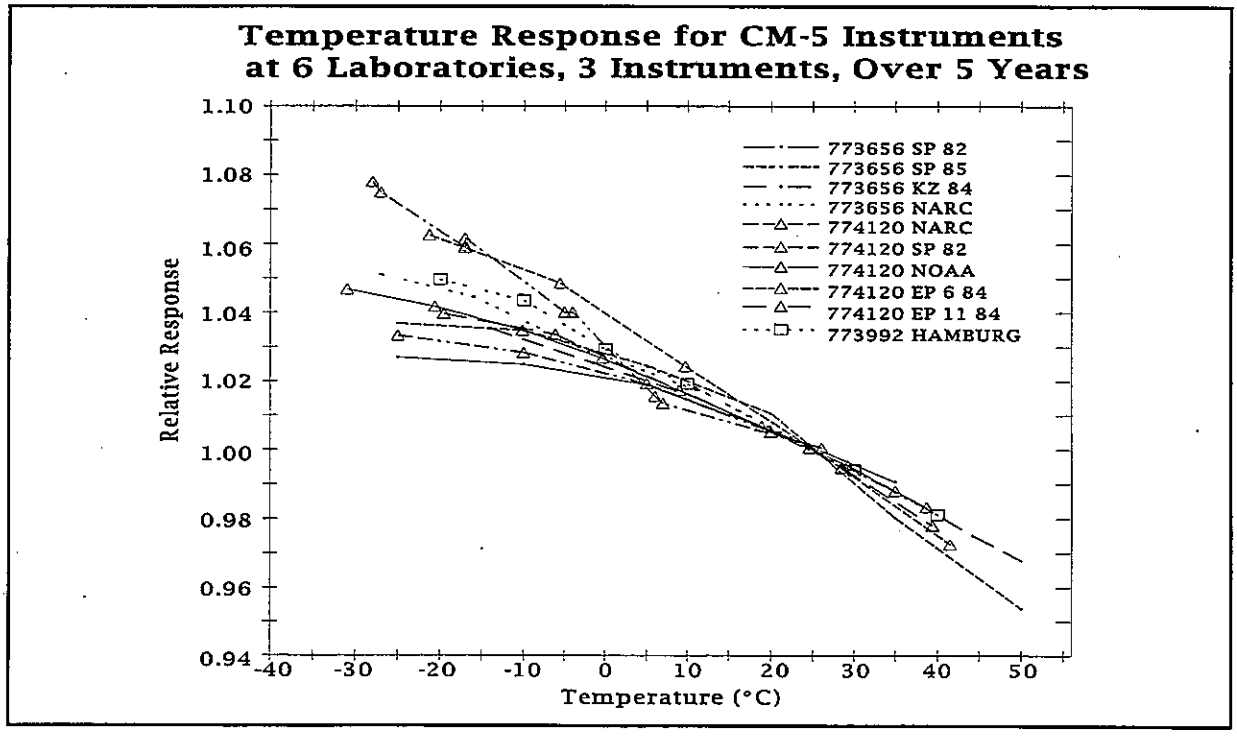

Figure 5.16

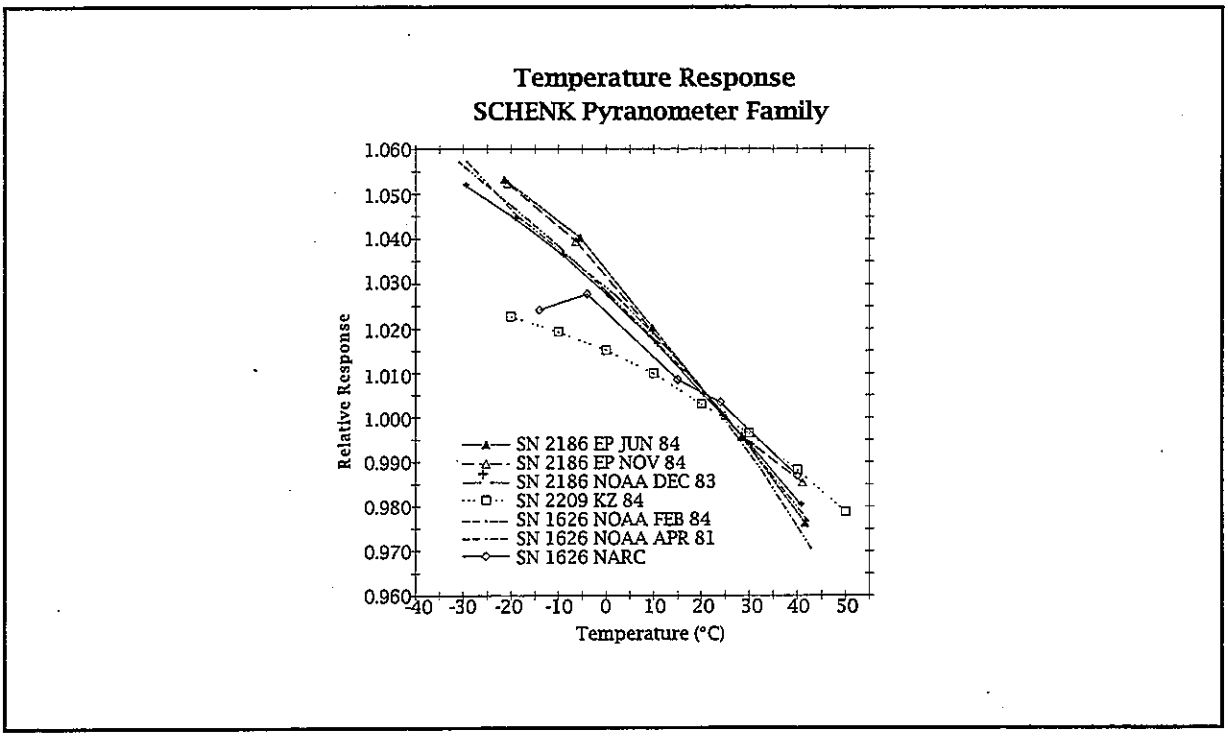

Figure 5.17

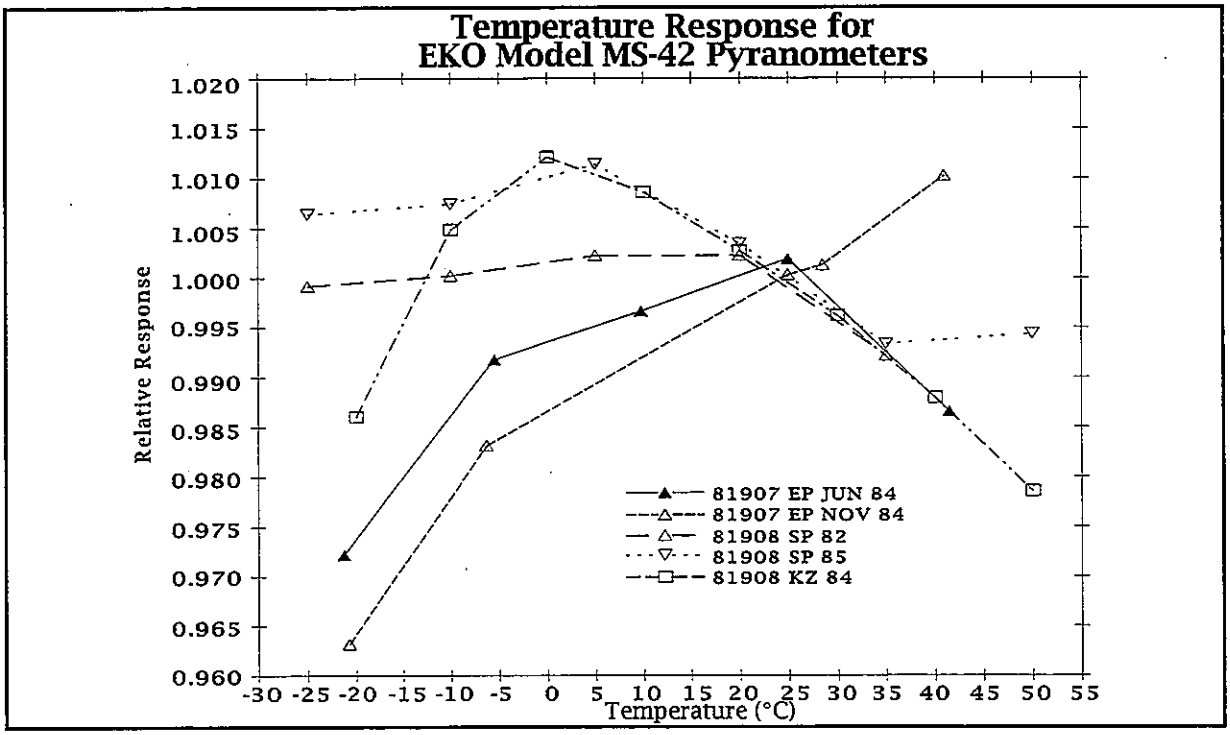

Figure 5.18

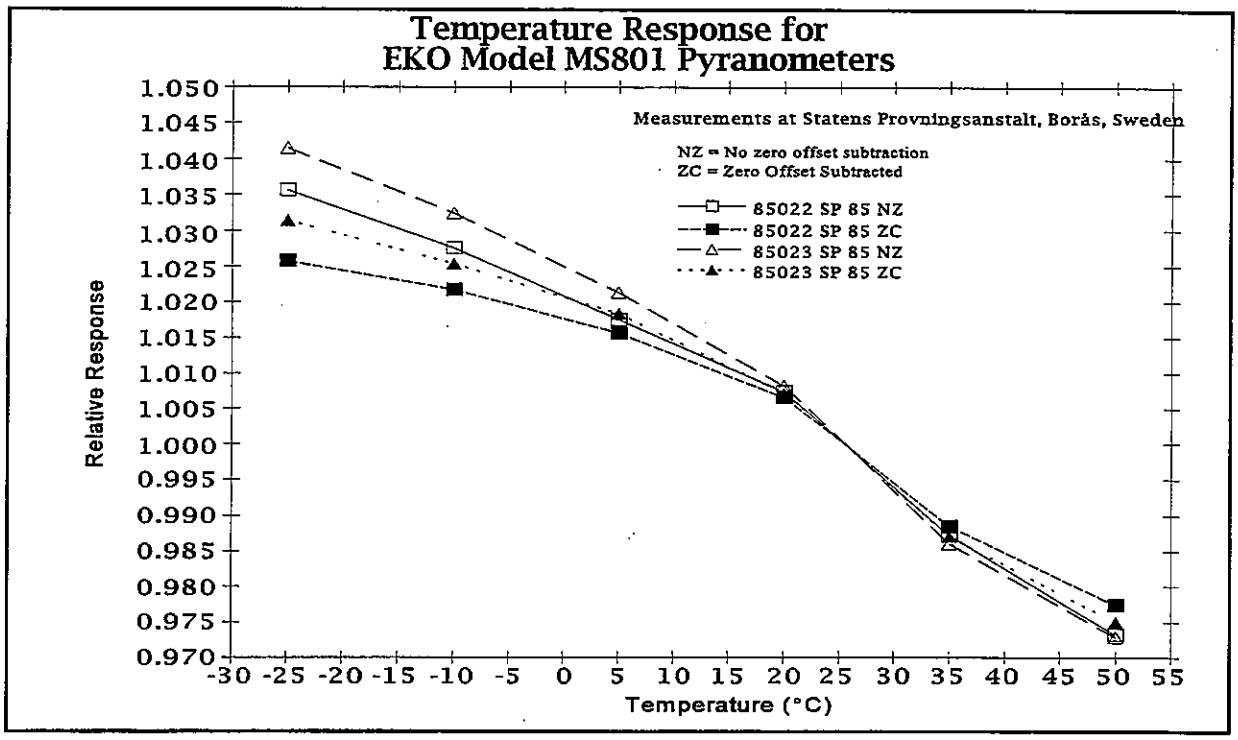

Figure 5.19

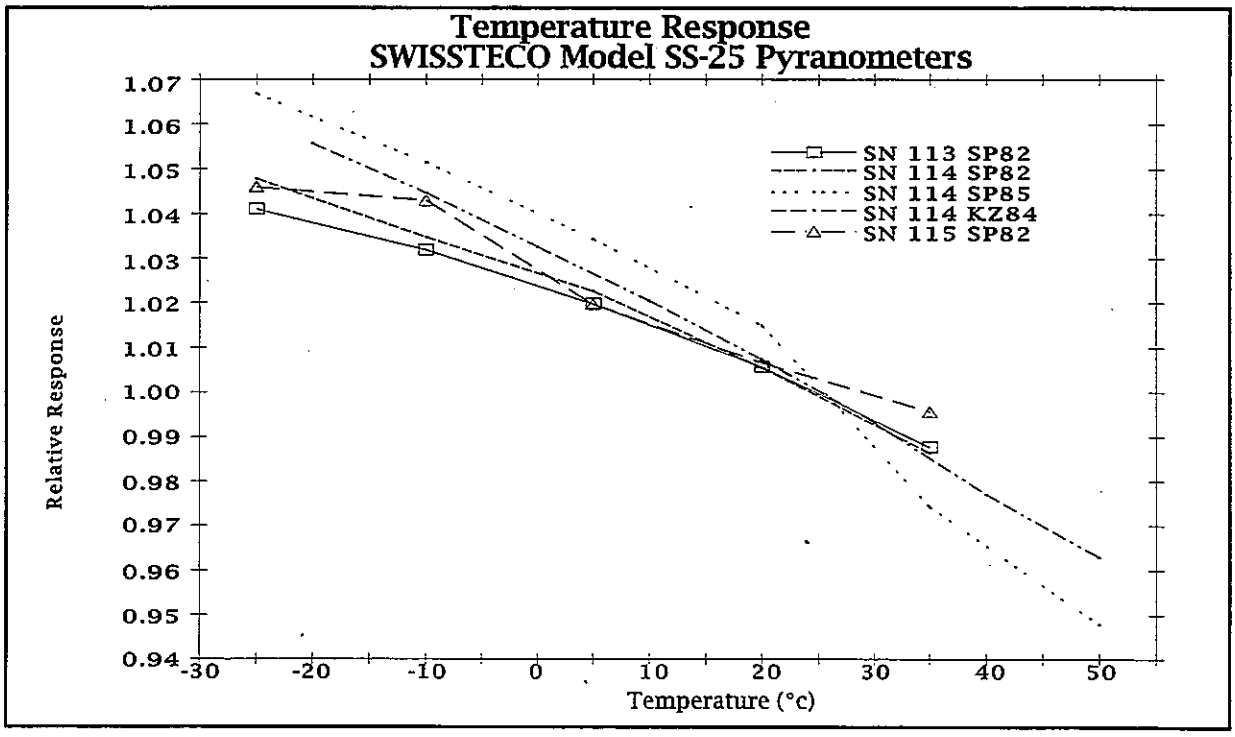

Figure 5.20

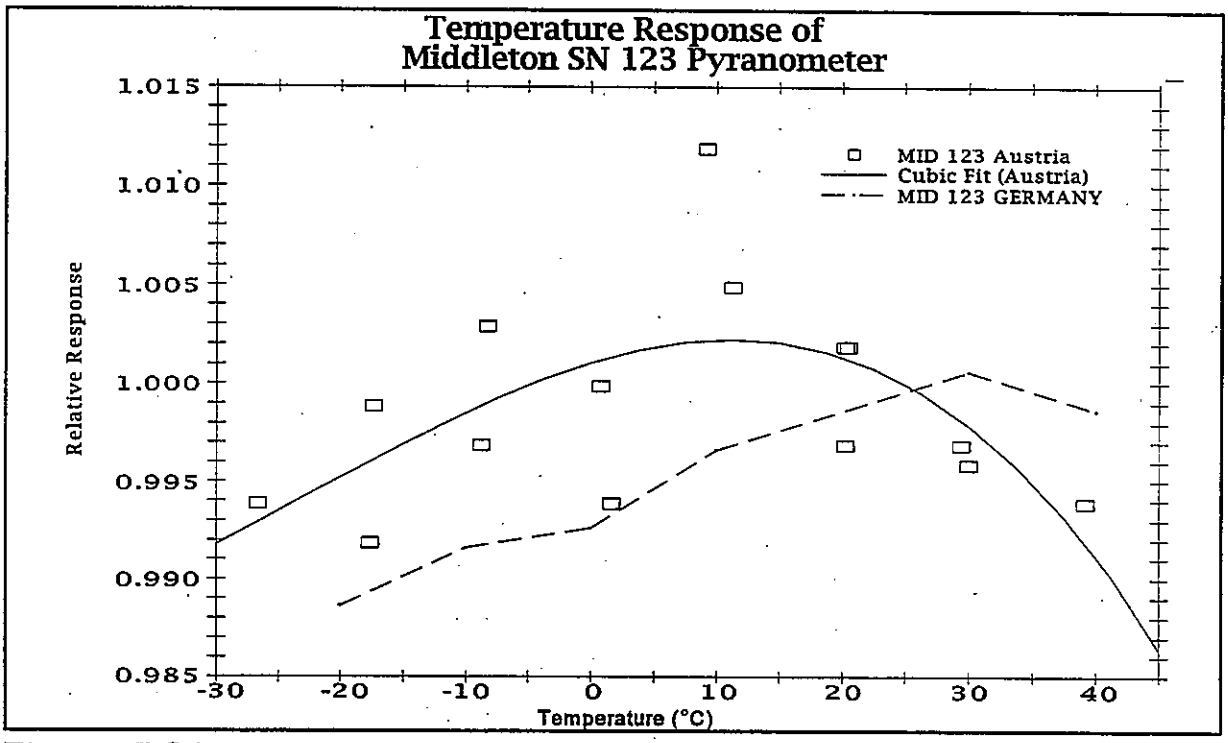

Figure 5.21

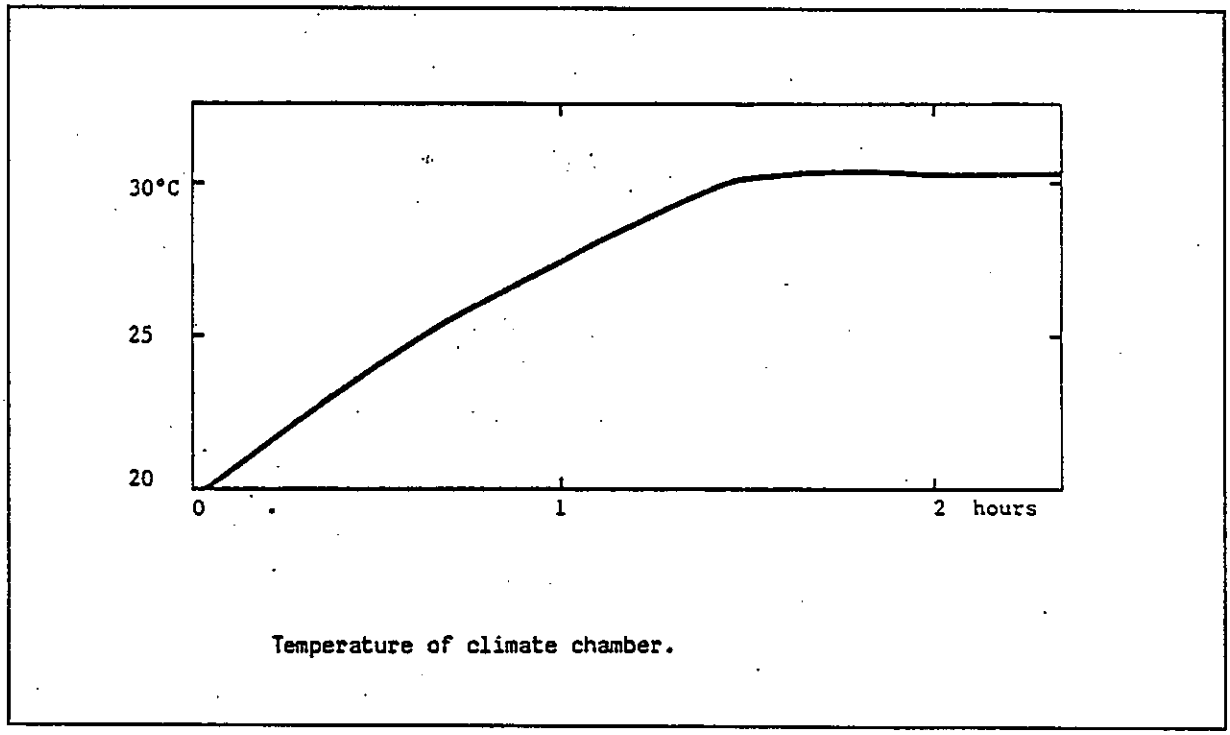

Figure 5.22

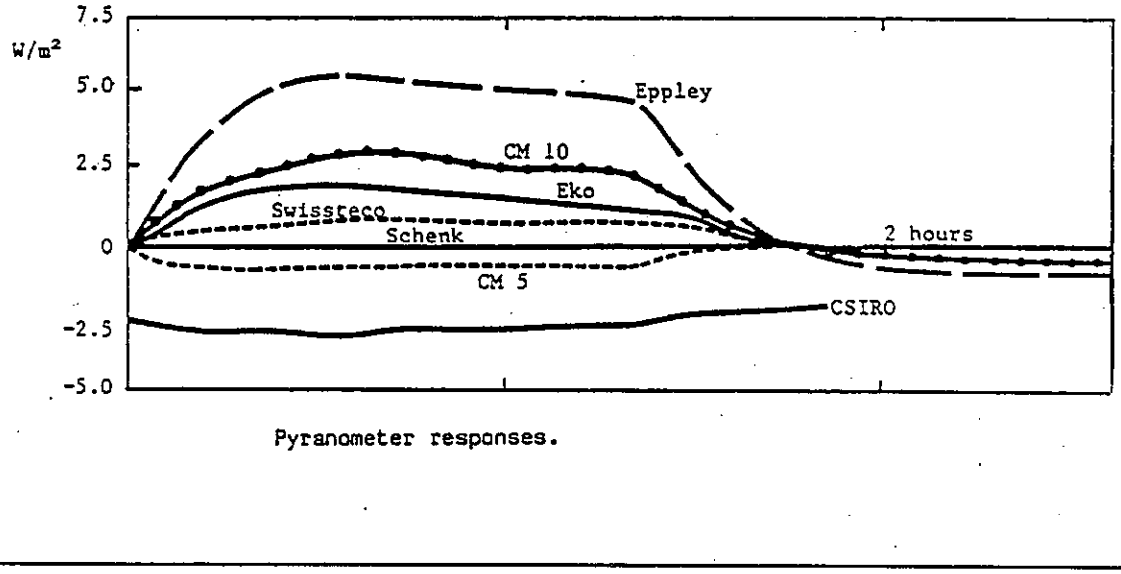

Pyranometer responses.

Figure 5.23

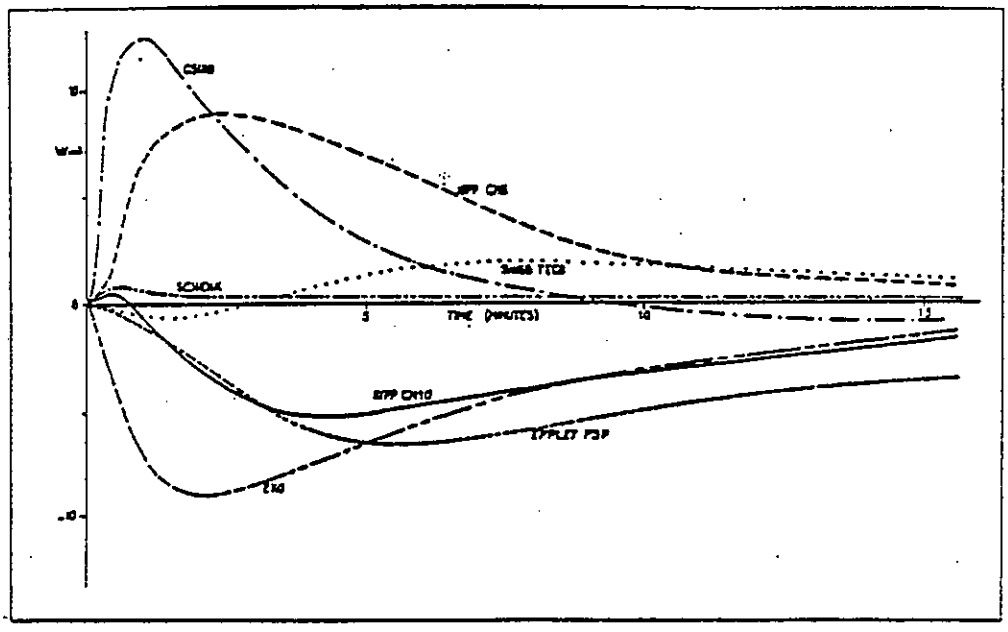

Response to an abrupt change in air temperature 25 → 20 ∘C.

Figure 5.24

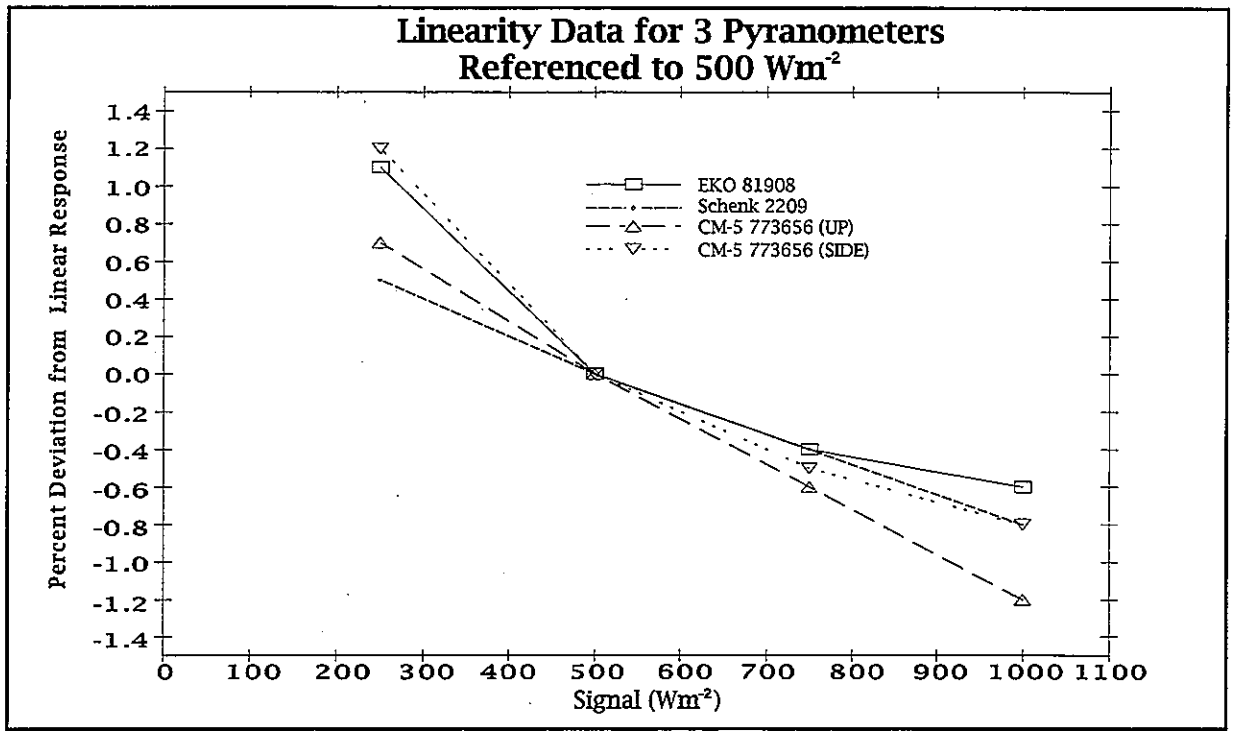

Figure 5.25

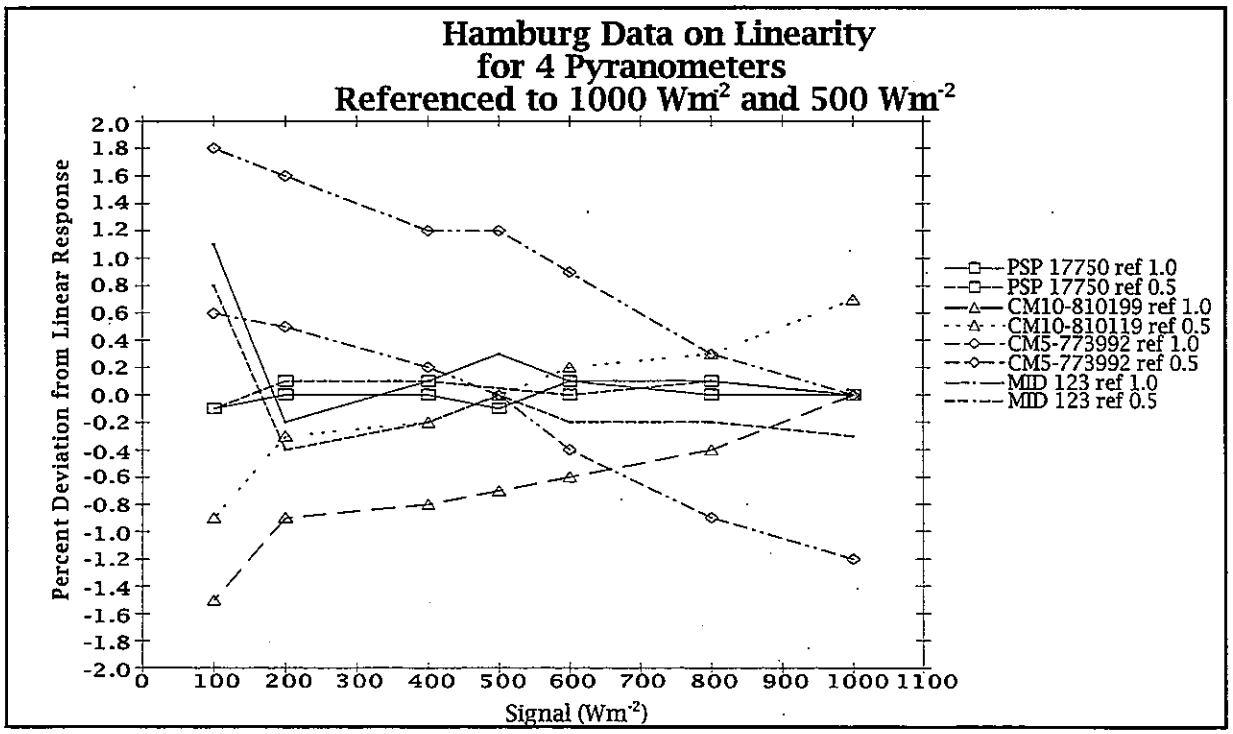

Figure 5.26

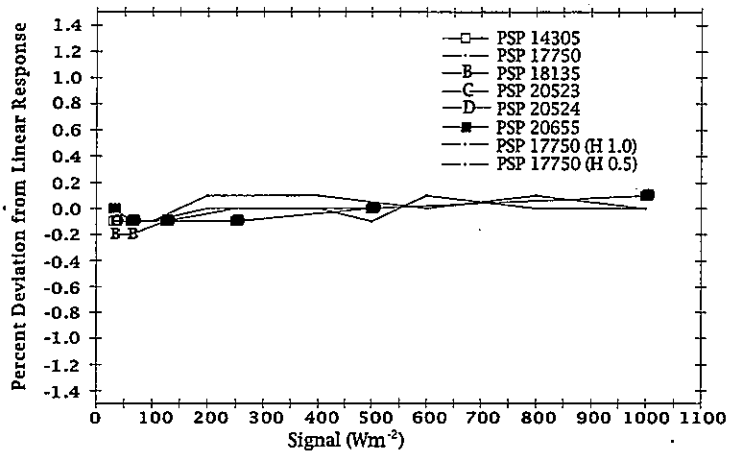

First 6 curves from Borås, Sweden. Last 2 curves from Hamburg, Germany

Figure 5.27

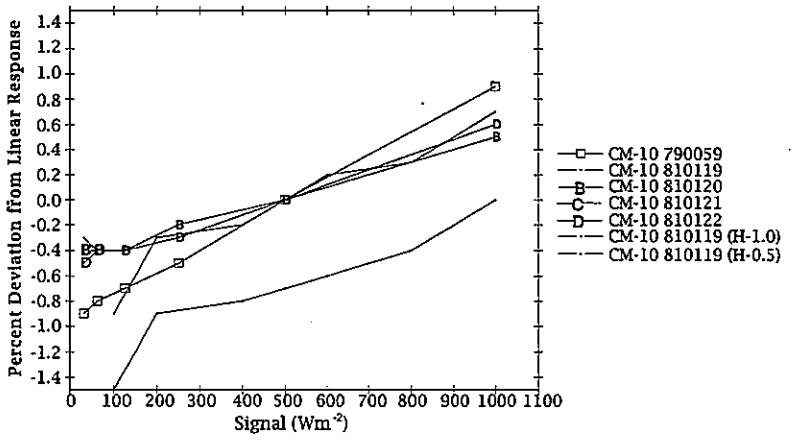

First 5 curves from Borås, Sweden. Last 2 curves from Hamburg, Germany

Figure 5.28

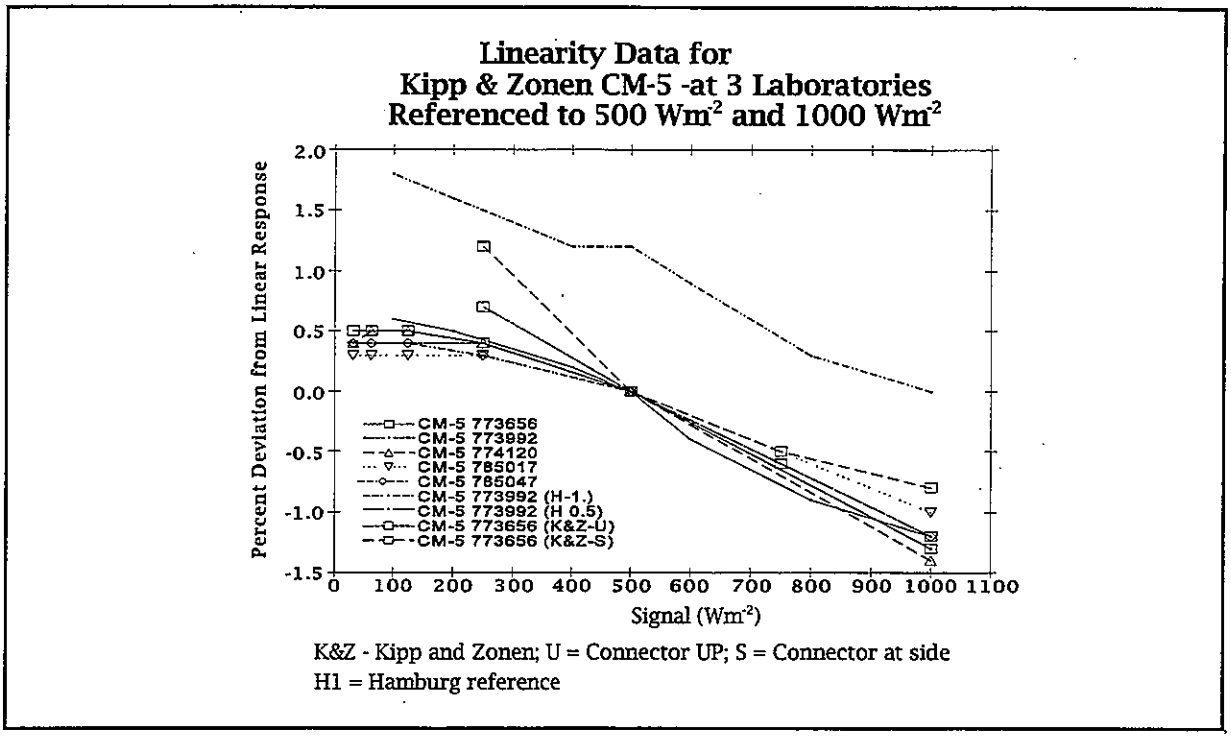

Figure 5.29

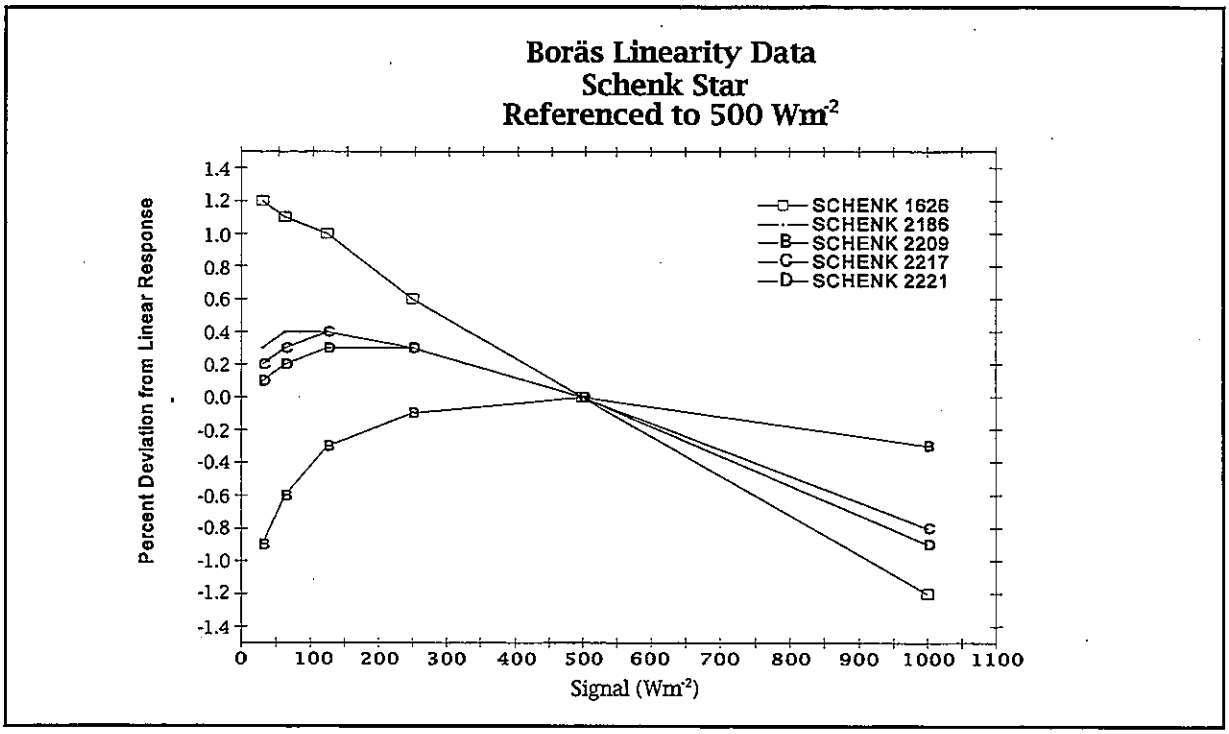

Figure 5.30

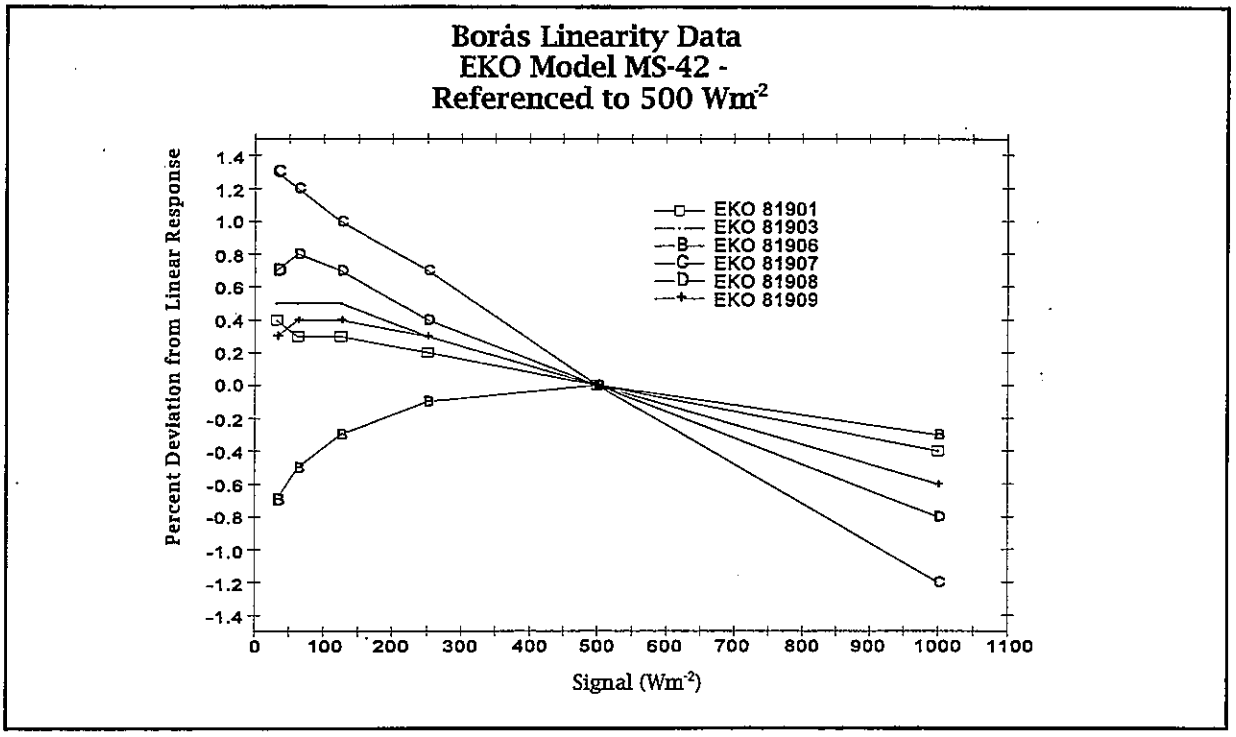

Figure 5.31

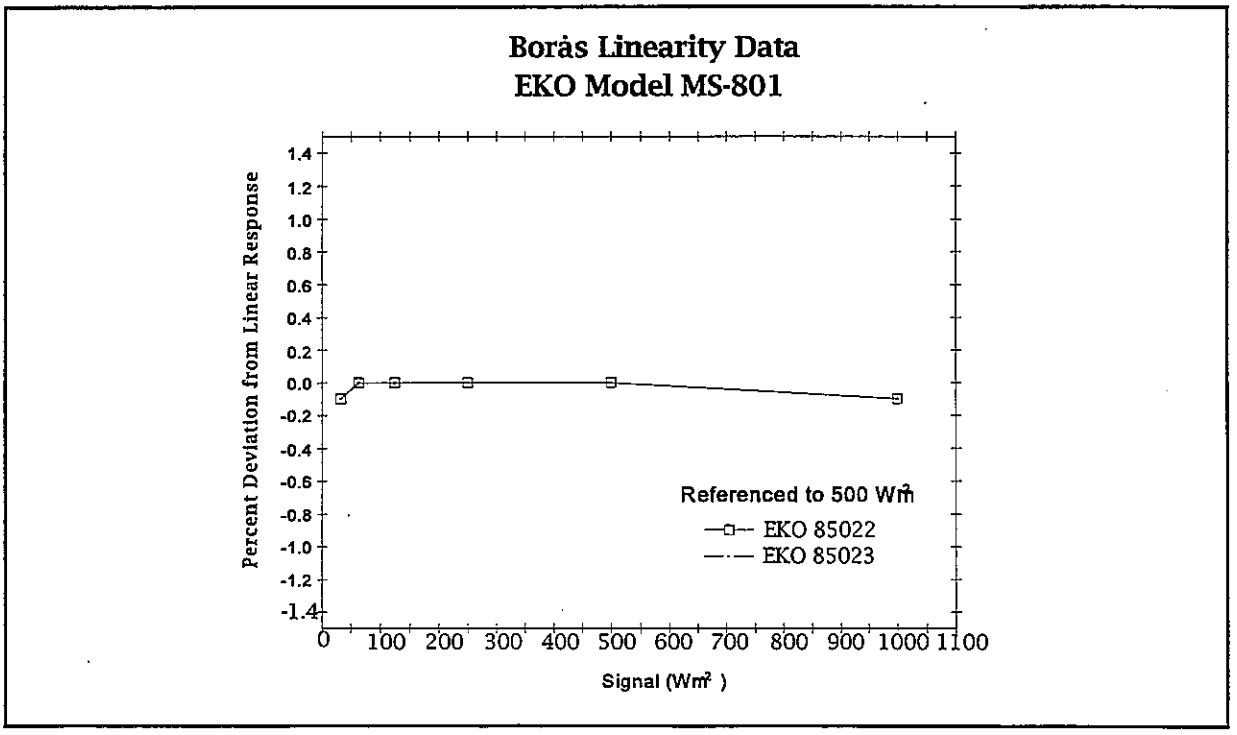

Figure 5.32

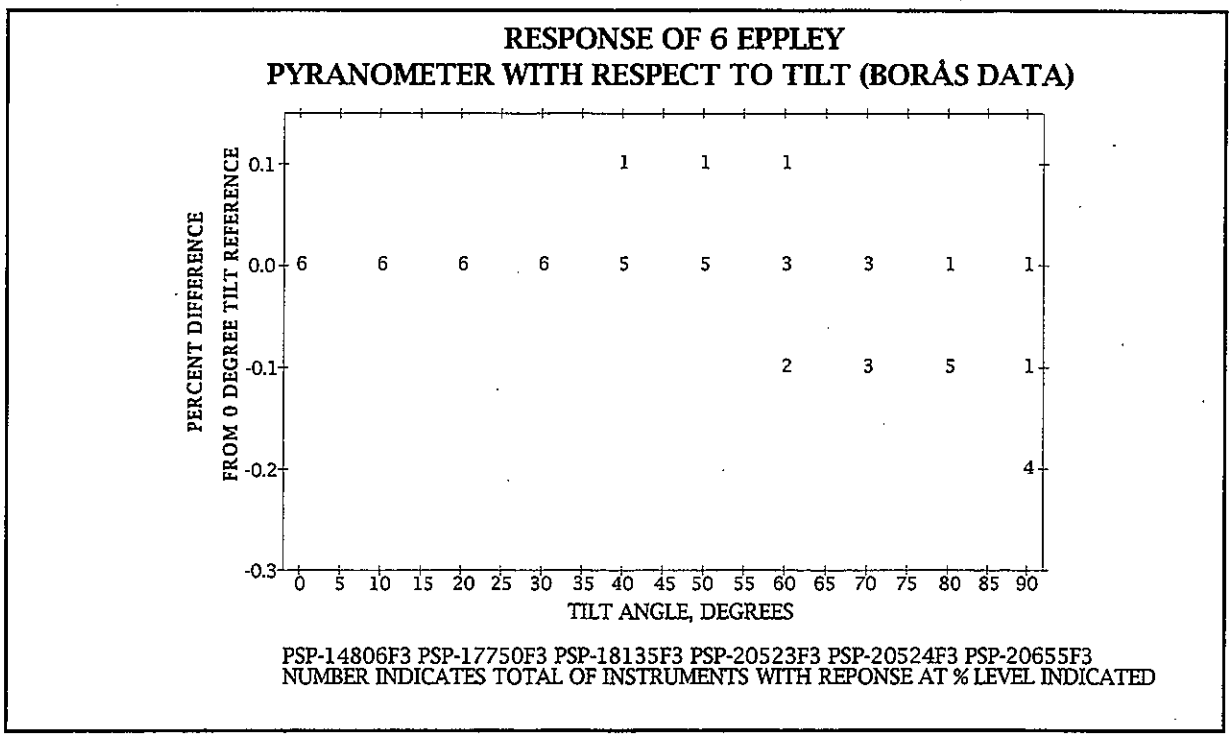

Figure 5.33

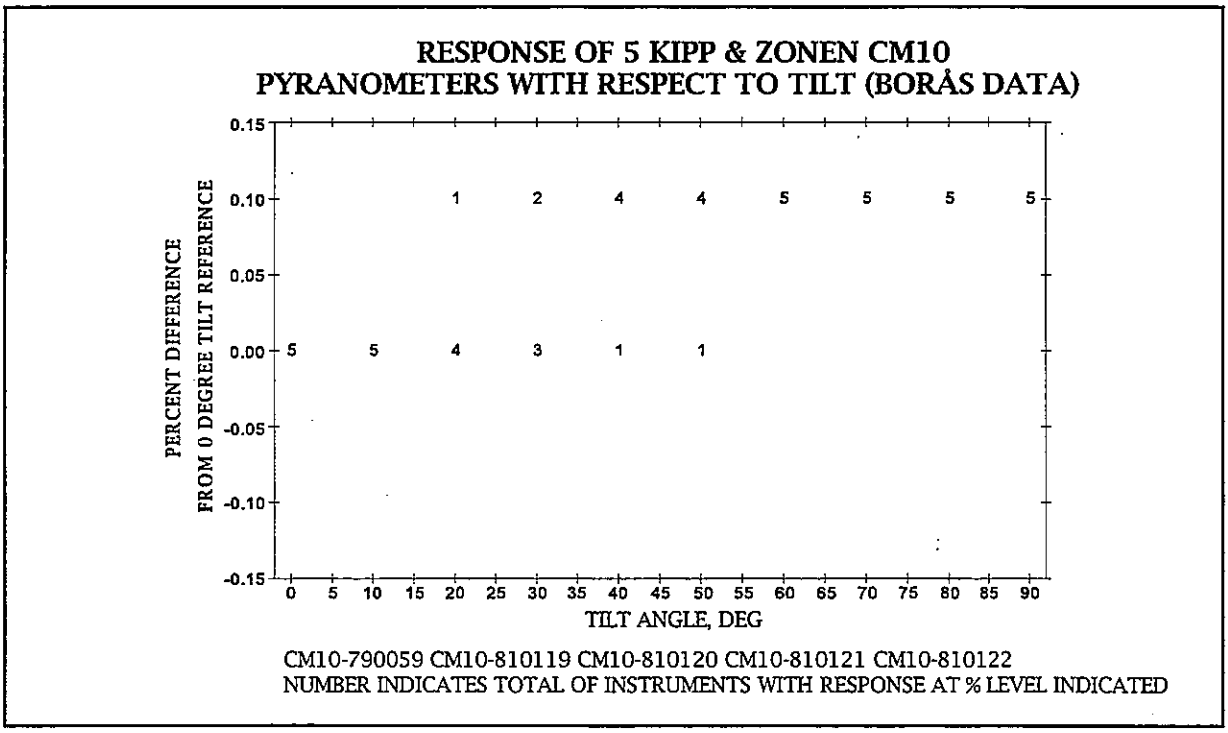

Figure 5.34

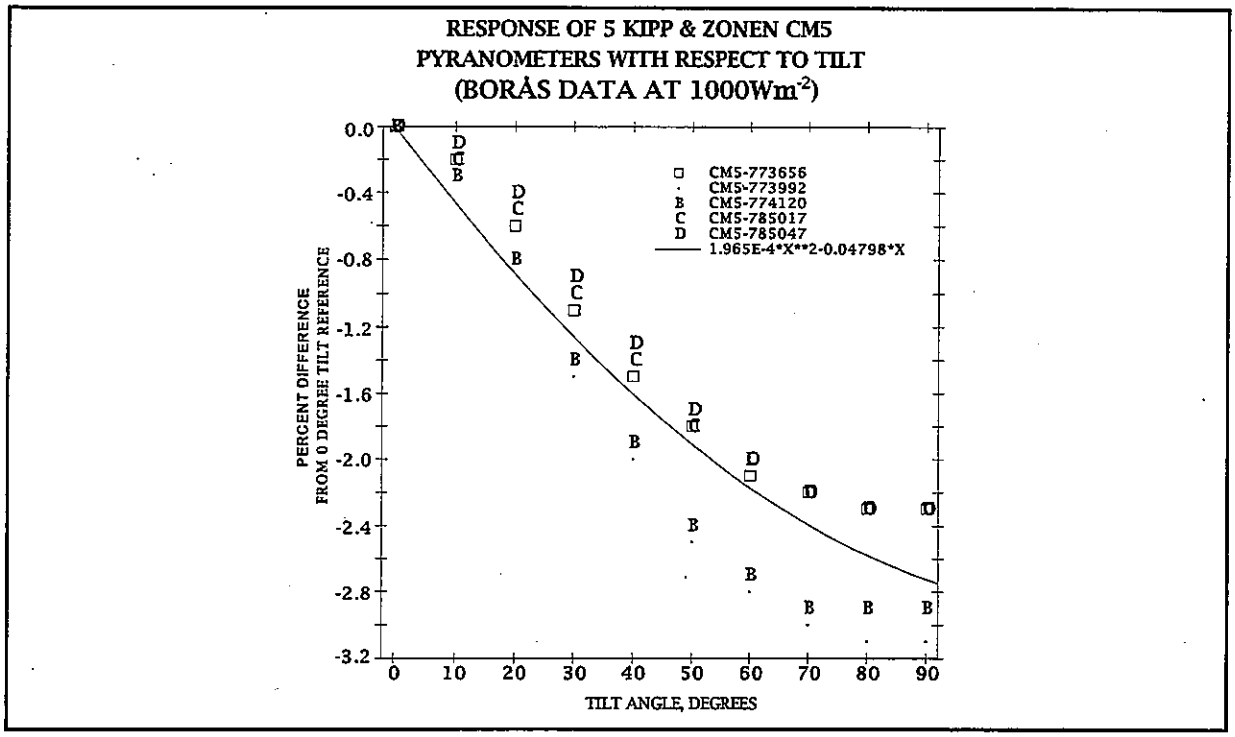

Figure 5.35

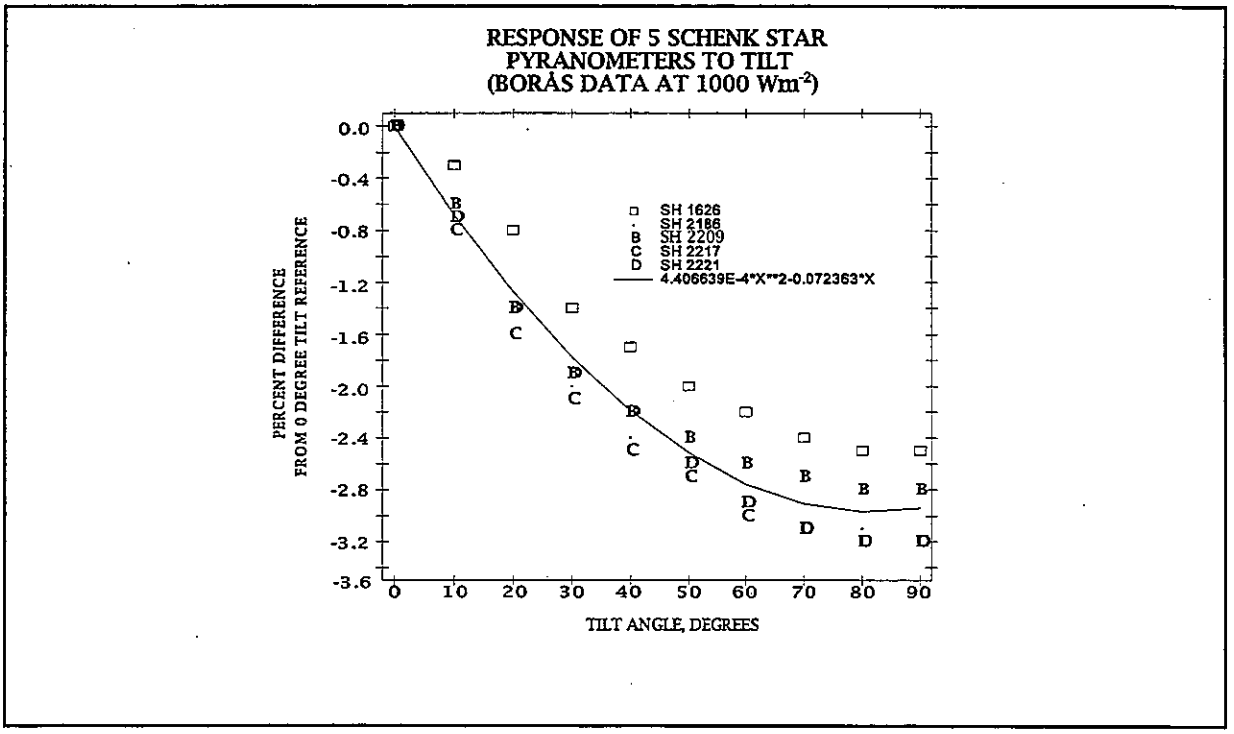

Figure 5.36

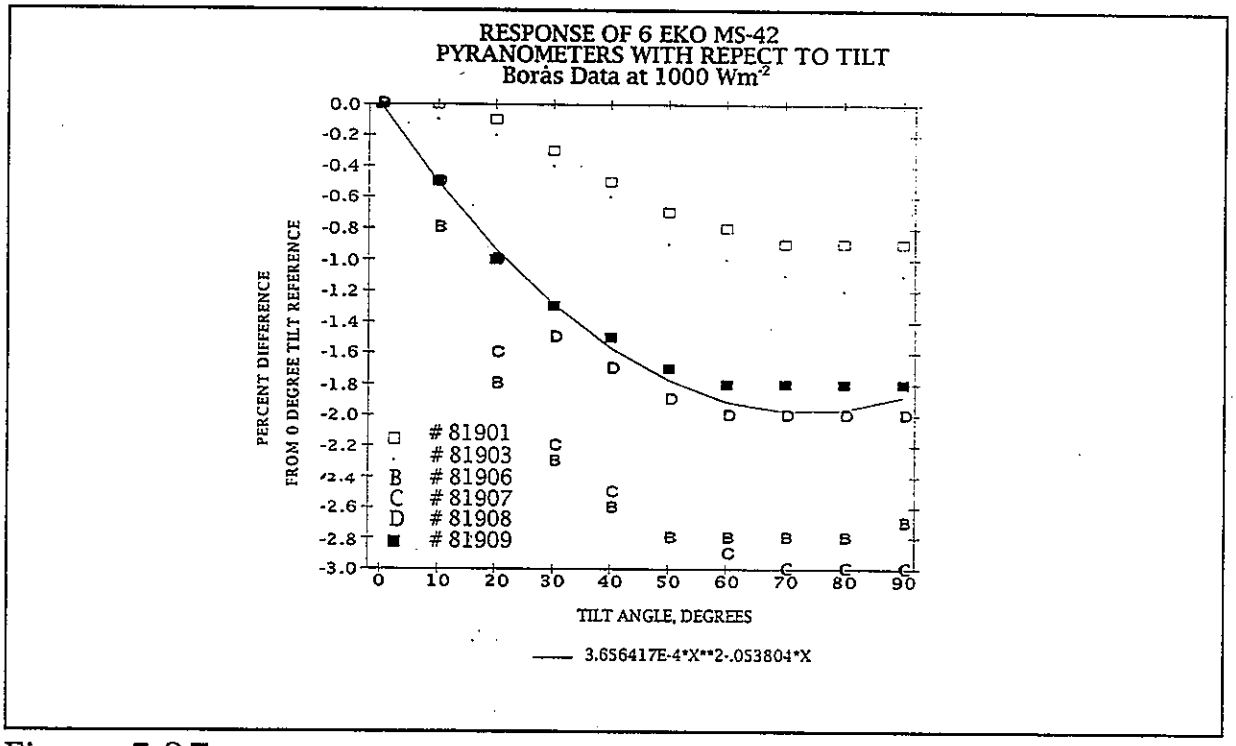

Figure 5.37

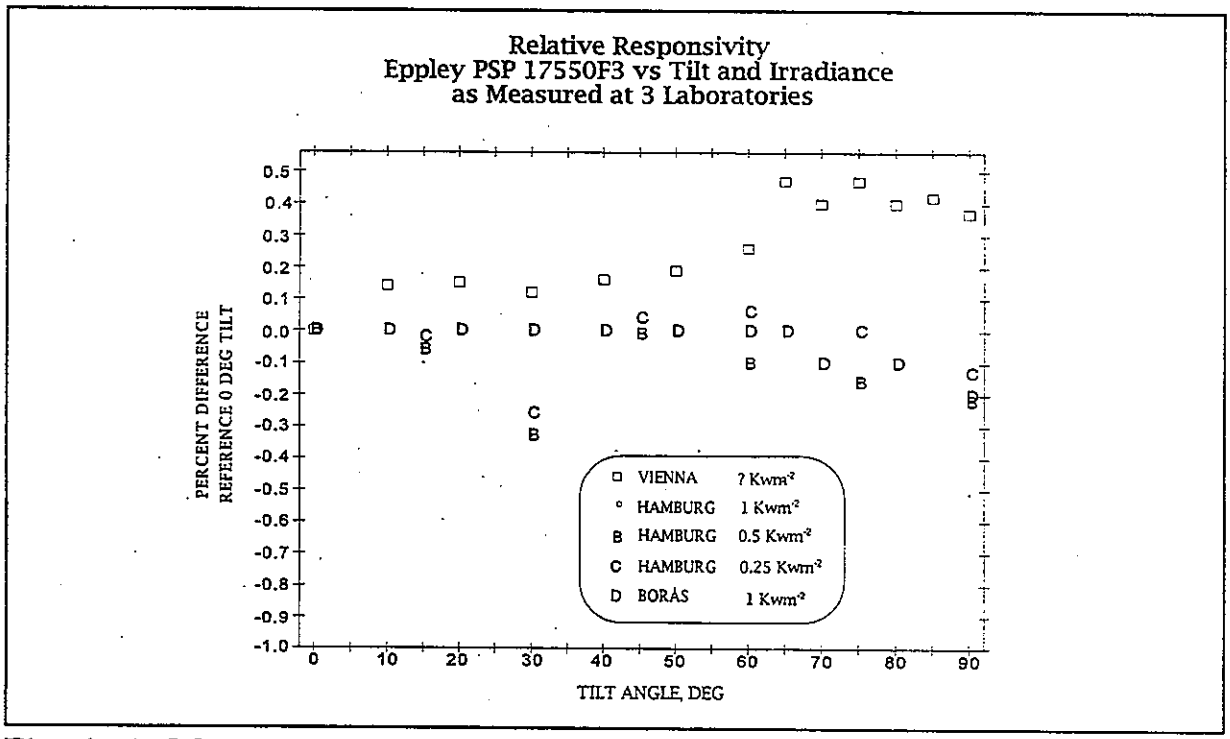

Figure 5.38

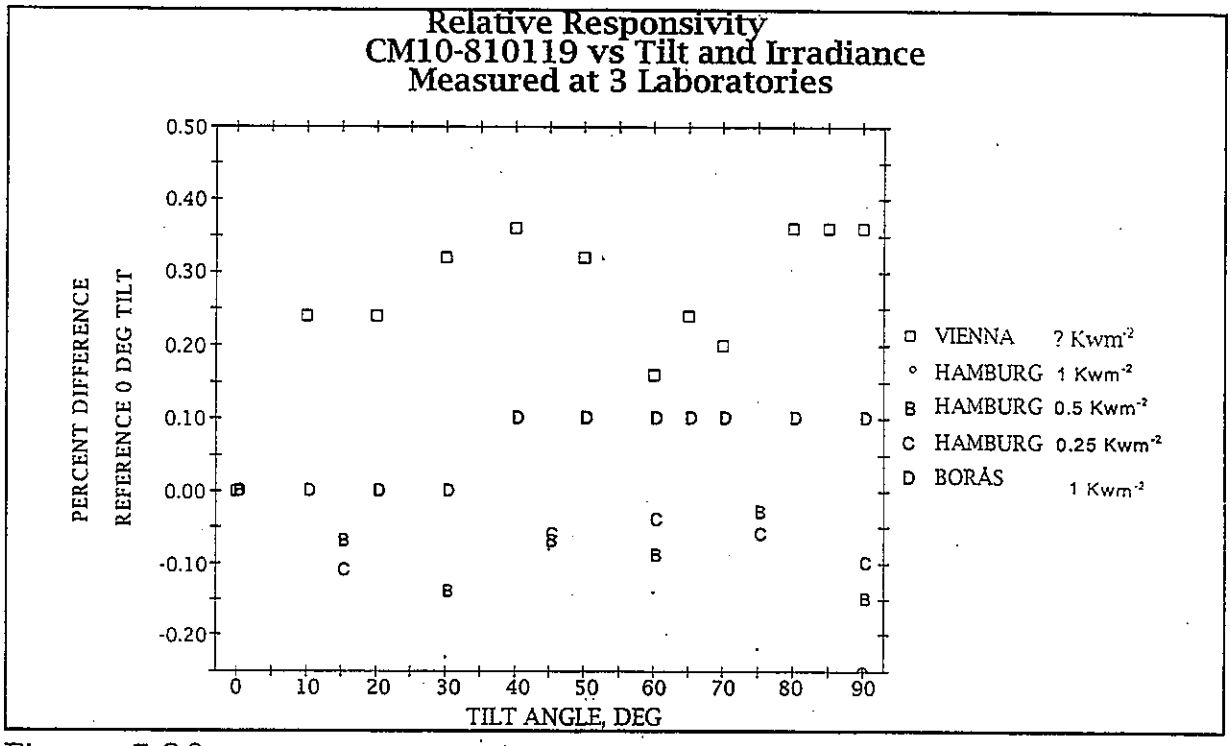

Figure 5.39

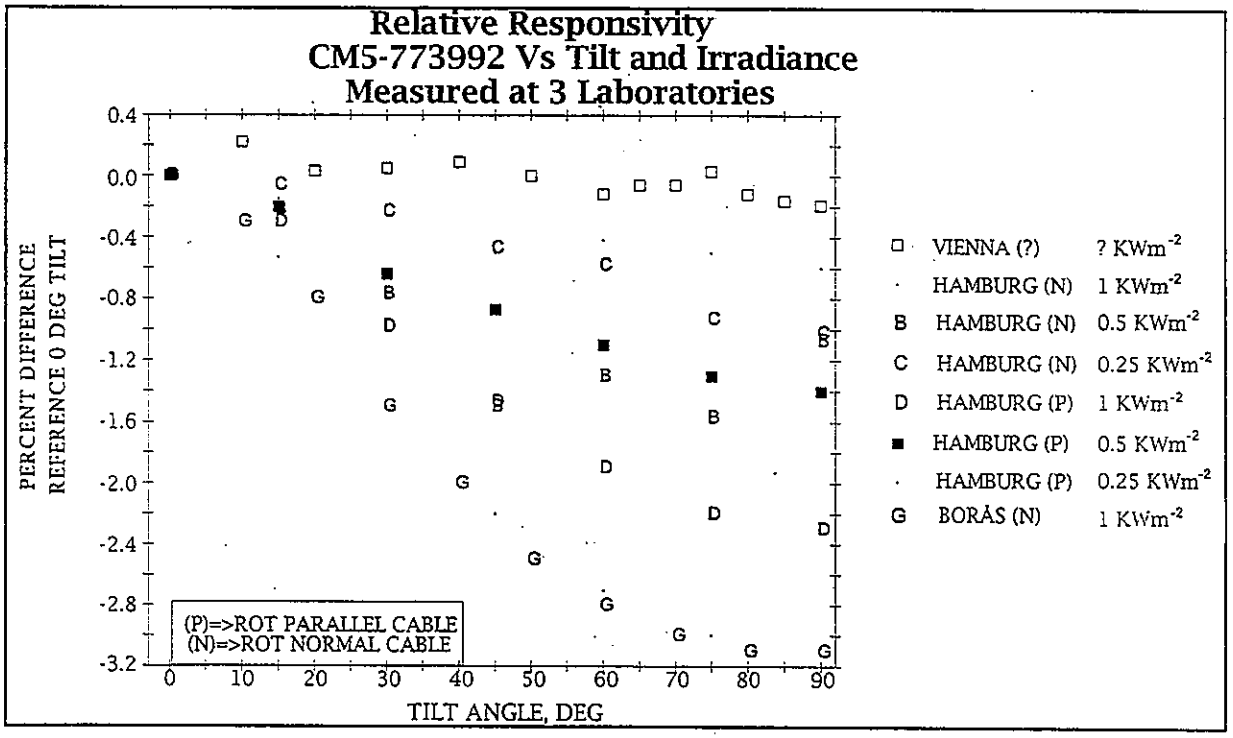

Figure 5.40

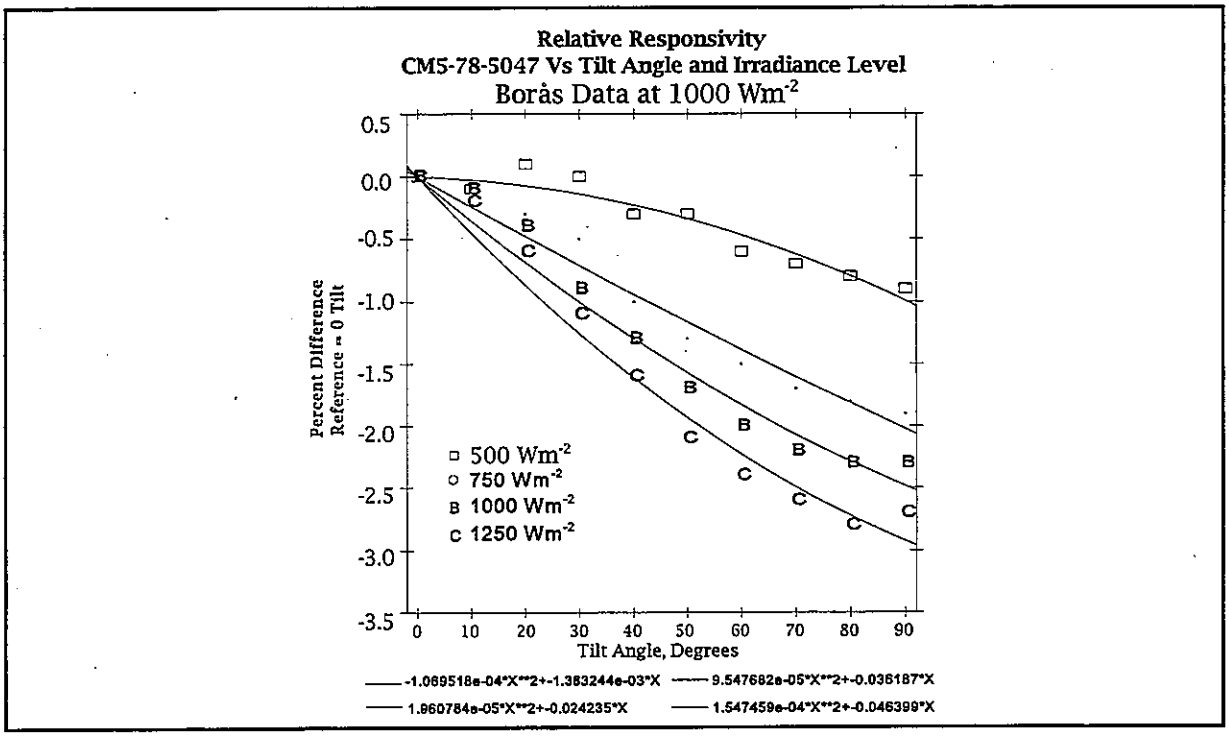

Figure 5.41

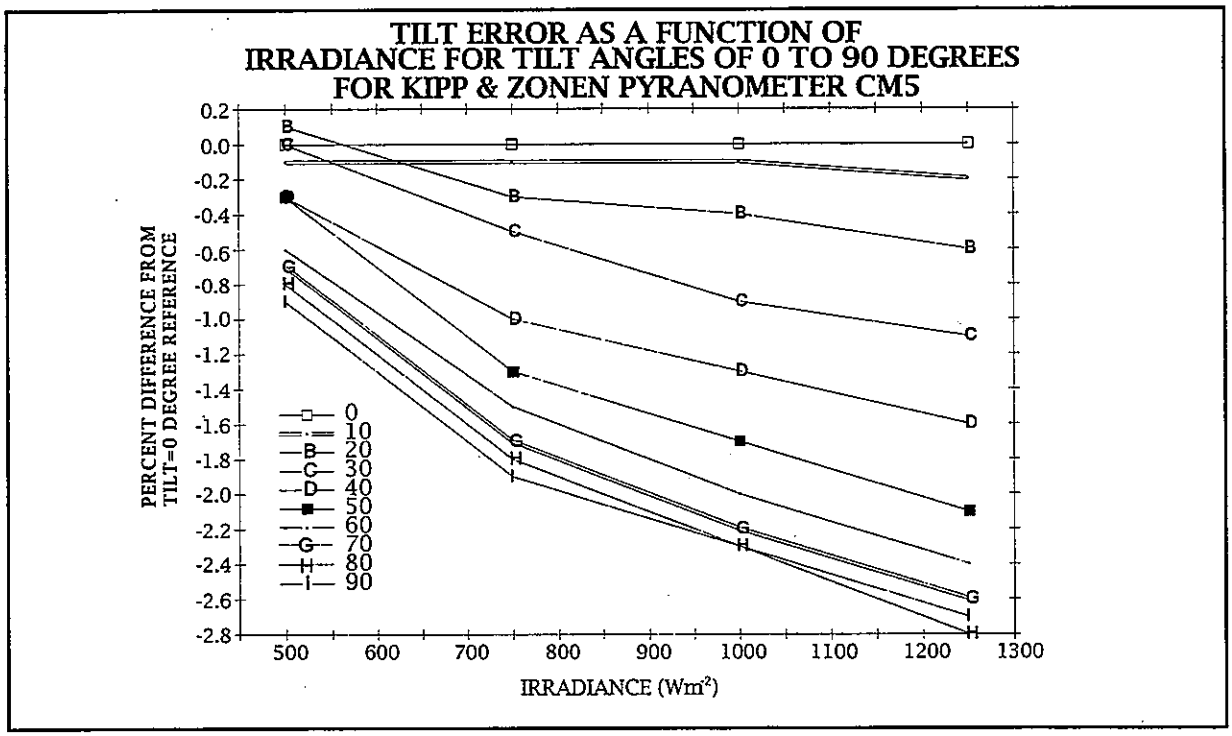

Figure 5.42

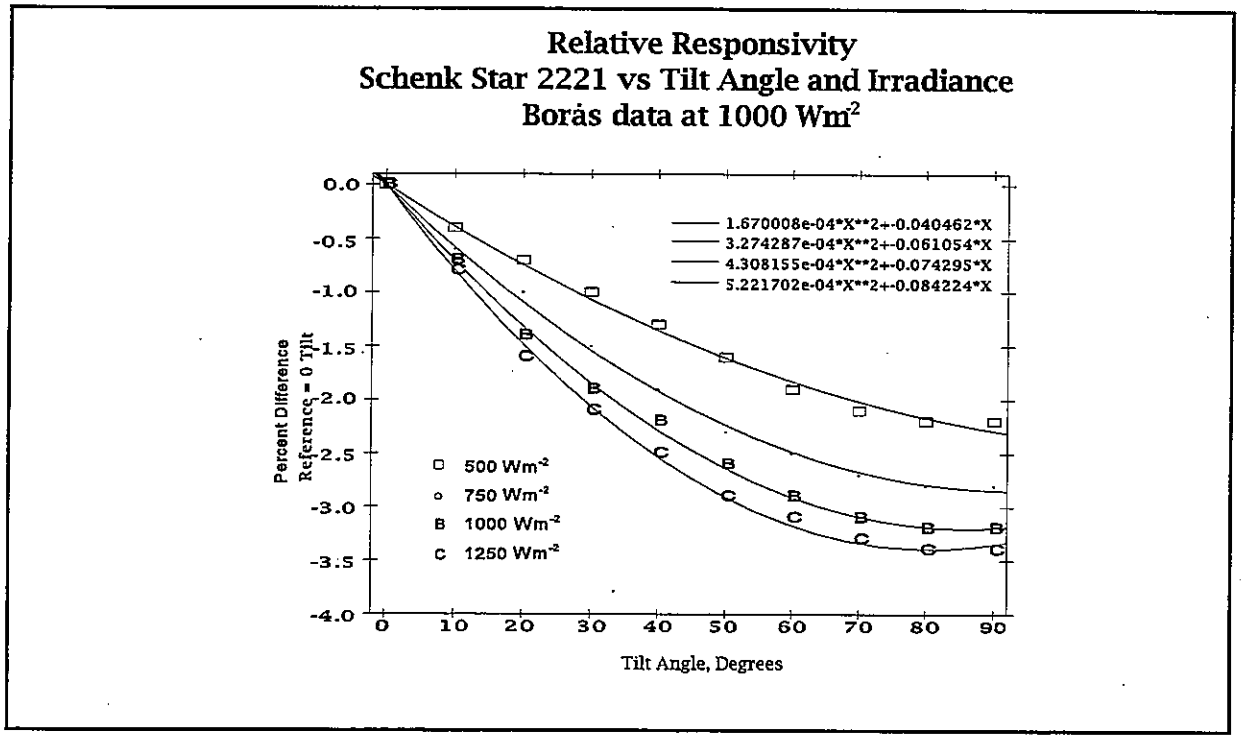

Figure 5.43

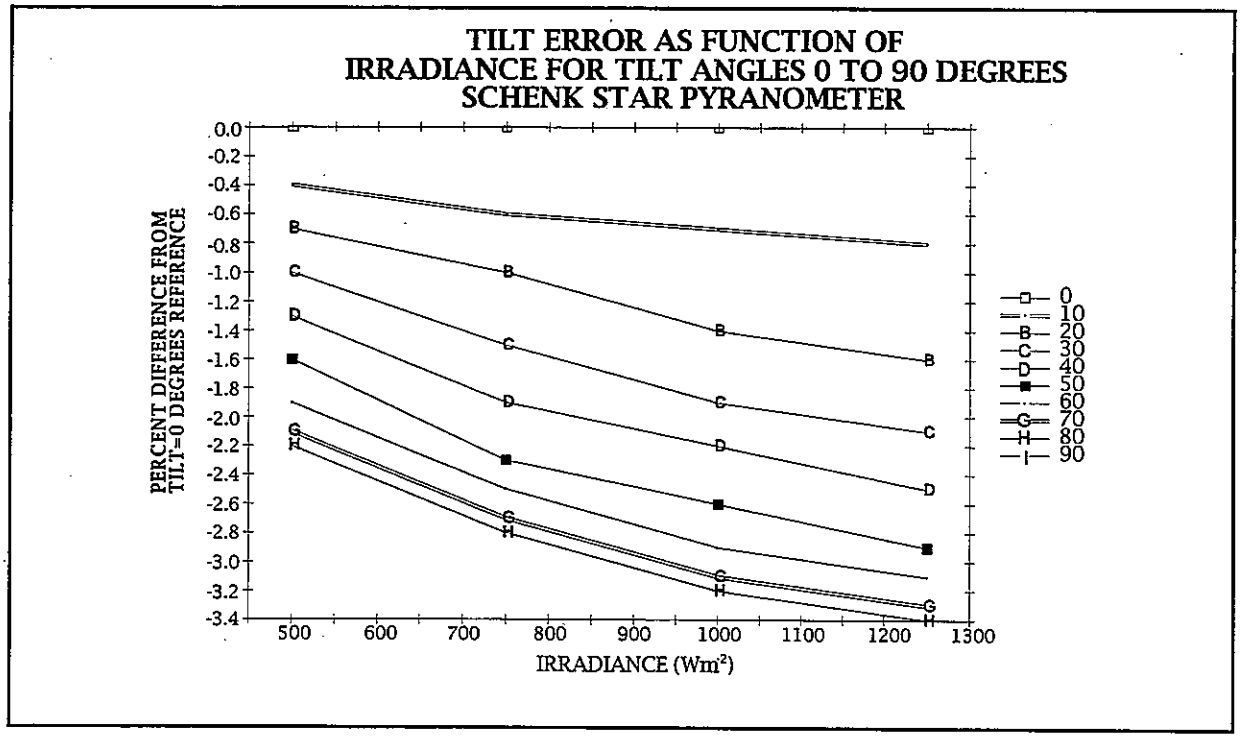

Figure 5.44

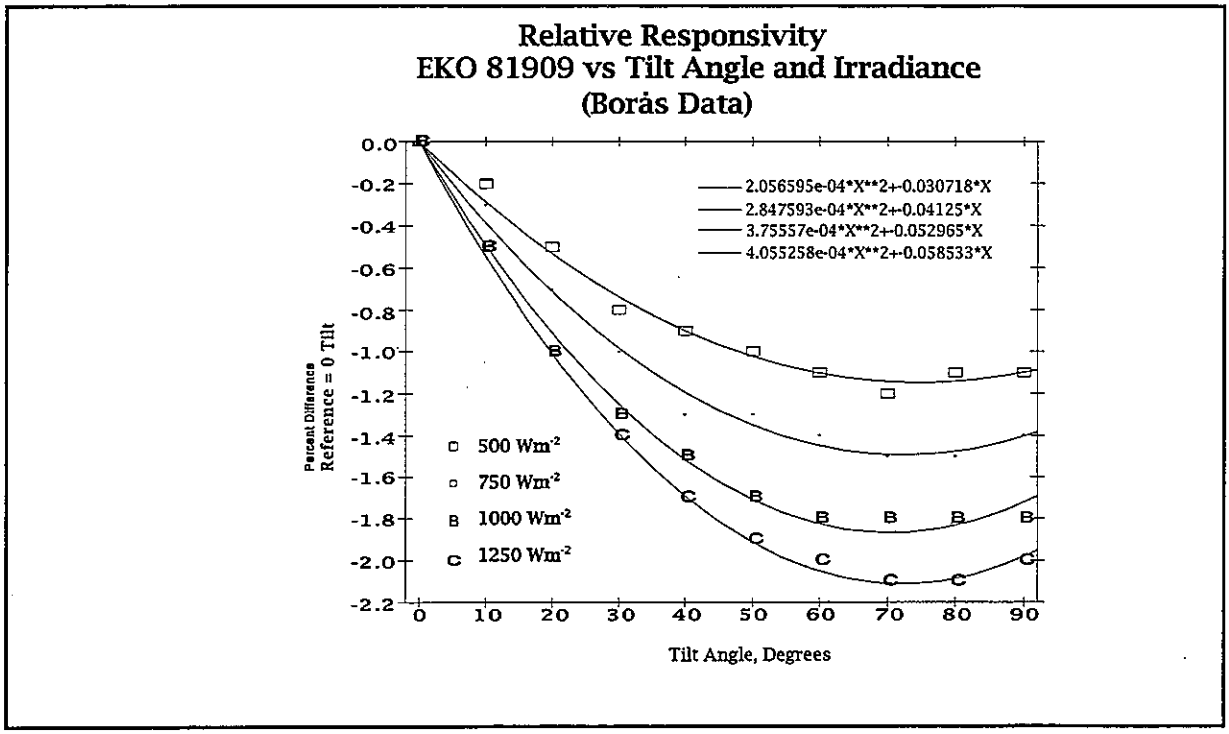

Figure 5.45

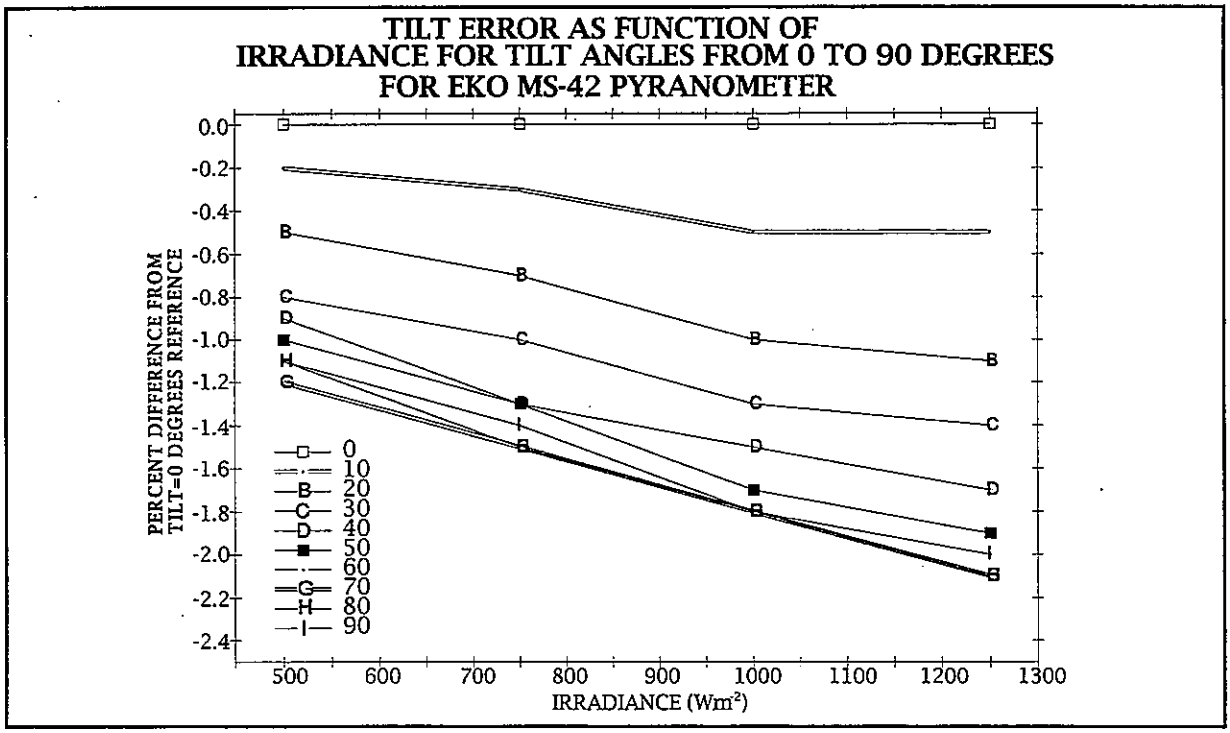

Figure 5.46

Chapter 6. Zero Offset

This chapter begins with an examination of the nature of zero-offsets, which are principally generated by temperature change, long-wave radiation, and ventilation. A variety of methods have been used to investigate the effects of these influences and the results from these approaches are compared. A number of implications emerge concerning how measurements should be made and these lead to specific recommendations (§ 6.8).

6.1 The physics of the offset

The signal in thermoelectric pyranometers is generated from the temperature gradient across the junctions of a thermopile. The temperature gradient ideally should be a unique function of the incident short-wave radiation, but, inevitably, it is also affected by the thermal stress to which the pyranometer is subject. Consequently there is an extraneous signal or offset added to the desired signal from the short-wave radiation and this contributes to measurement uncertainty.

The offset can be observed as the night-time output from field pyranometers and, in the laboratory, when pyranometers are subjected to heating or cooling. It can be accommodated in the traditional pyranometer response function by defining an extra term Z as follows:

$$V = R \cdot (E + Z) \qquad [6.1]$$

where,

V	is the output voltage
E	is the shortwave downward irradiance or global radiation - the quantity being measured by the pyranometer
R	is the responsivity
Z	is the offset irradiance, defined as the measured output voltage divided by the responsivity when the incident shortwave irradiance is zero, i.e. $Z = V(E=0)/R$

The offset is variable and clearly associated with the heat flow into the pyranometer. It follows that it depends on the environmental variables, called thermal stresses here, which determine the heat flow. It is assumed throughout this work that these thermal stresses

have the same effect on V/R regardless of the shortwave irradiance. This important assumption, based on considerations of linearity, is discussed later.

Apart from the absorption of short-wave radiation, whose effect is the desired response, the heat flow into the pyranometer occurs in two forms, long-wave radiation exchange with the electromagnetic field and local kinetic exchange. The latter comprises conduction and convection of heat between the pyranometer and its surroundings. Appropriate expressions for the thermal stress in each case are as follows:

$E_\ell - \sigma T_i^4$	net thermal irradiance on the pyranometer, which is called long-wave stress in what follows (the environmental variable which determines the radiation exchange)
$T_i - T_a$	temperature difference between the pyranometer and the ambient (together with the wind conditions, it determines the exchange of heat by convection and conduction)

where,

E_ℓ	downward long-wave irradiance
σ	Stefan-Boltzmann constant
T_i	pyranometer temperature
T_a	air temperature

These are the preferred choices for expressing the thermal stress, but the following slightly different terms have been used because it was impractical to record all the pyranometer temperatures:

$P = E_\ell - \sigma T_{pyg}^4$	long-wave stress; also net thermal irradiance, the quantity measured by a pyrgeometer
$\dot{T} = \delta T_a / \delta t$	an approximation of the rate of change of the ambient temperature and which is proportional to $T_i - T_a$ when the temperature increase is steady

where

T_{pyg}	pyrgeometer temperature
δT_a	rise in ambient temperature during a period spanning the measurement
δt	duration of the above period.

The foregoing is a rationale for anticipating that the offset irradiance (Z) can be determined from the equations:

$$Z = A + B \cdot P \qquad [6.2]$$

or

$$Z = A + B \cdot P + C \cdot \dot{T} \qquad [6.3]$$

where the coefficients (A, B and C) may be determined by statistical analysis of the night sky signals or other means.

The heat fluxes into the pyranometer are modulated by the ambient wind, but incorporating the wind speed into the analysis is rather complicated and has not been attempted. The observed residual variability in the above expression shows the maximum extent of the effects of wind.

Separate experiments were done to obtain alternate determinations of the coefficients B and C. Other values were calculated from measurements reported by van den Brink *et al.* (1985). Results from the different methods are compared.

In the case of the long-wave dependence, the experiment consisted of putting out several pyranometers and one pyrgeometer during clear nights. The view to the night sky was interrupted periodically so as to modulate the long-wave radiation. The results of this experiment are direct evaluations of the coefficient B in the above equations.

A direct evaluation of the coefficient C of the temperature derivative was not attempted because a chamber in which the rate of change of temperature could be reliably controlled was not available. Instead, the response of pyranometers to sudden changes of temperature was measured. The results are summarised as peak excursions normalised against temperature change ($Wm^{-2}\,K^{-1}$) and as integrated area excursions also normalised ($Whm^{-2}\,K^{-1}$). The former have relevance to the practice of pyranometry in that they show the magnitude of extraneous signals caused by thermal shocks, but they cannot be compared with the coefficient C. However, the integrated excursion is comparable with C and indeed would be equal if the physical processes involved in the laboratory and field were identical and linear i.e.

if

$$Z = C \cdot [\, dT / dt \,] \qquad [6.4]$$

then $$\int Z \cdot dt = C \cdot [T_{final} - T_{initial}] \qquad [6.5]$$

6.2 Statistical analysis of the of dark signals

The gathering of IEA pyranometers at NARC was an ideal opportunity to study the night-time signals. Pyrgeometer and temperature measurements were available throughout the 20-month experiment. As in daytime, the data comprised one-minute averages. Simple linear regression was used and a few outlying data points were rejected. The experiment produced results for pyranometers mounted in the NARC ventilators (McArthur & Wardle, 1987) and for a few instruments that were mounted as supplied by the manufacturers.

6.2.1 Method and error estimates

The method is described in detail in Appendix DD1. About 2% of the signals were greater than 0.5 mV. These large isolated values are thought to be caused by recording malfunctions and were rejected.

In the groups of PSP, CM5, CM10 and Schenk pyranometers, the results are not instrument specific. In contrast, the results from the four Eko pyranometers indicate two distinct subgroups, a) comprising #81908 & #81909, and b) comprising #82052 & #82053, which are listed separately for this reason. In the case of the two Middleton instruments, the results for the mean and for the constant term (A) are noticeably different.

The standard errors (Appendix DD1) for each instrument-data set combination are calculated assuming independent data points. The standard errors for the group results were calculated assuming no systematic differences between the pyranometers in the group or between data sets. Where these assumptions are invalid, the estimates are too small. However, alternative estimates based only on the spread between data sets can easily be calculated. With the exception of the Middleton pyranometers, the error estimates of either type are smaller than:

0.4	Wm^{-2} rms	for A
0.004	rms	for B
0.09	$Whm^{-2}\,K^{-1}$ rms	for C

It is suggested that these values are realistic error estimates for the main group. The Schenk error estimates are about 50% smaller. Variations for the Middleton pyranometer are 1.9 Wm^{-2} for A, 0.006 for B and 0.14 $Whm^{-2}\,K^{-1}$ for C.

6.2.2 Variability of the dark signals

Table 6.2.2a summarises the variability of the dark signals of horizontally mounted pyranometers. The values, which are precisely defined statistics of the dark signals, may be interpreted as rough estimates of daytime measurement error under various strategies. The first column would be the mean error incurred if dark signals were ignored. The second column would be the rms error if a constant offset (i.e., the mean at night) were assumed. The third column would give the error if the offset were parameterized as a function of the pyrgeometer signal by Equation 6.2, and similarly for the fourth column with Equation 6.3. These interpretations rely on the conditions which determine the offset during the day and night being statistically identical, an assumption to be examined later.

A test signal from a 1000 Ω resistor installed next to the pyranometers was also recorded. The largest standard deviation of this signal in the three data sets was 1.0 μV. The figures in the last column are the result of dividing 1.0 μV by the respective instrument responsivities. They are included in the table to indicate the contribution of the voltage measuring system to the overall error.

The following observations can be made on the data in Table 6.2.2a

- The Schenk and Eko pyranometers, which are both of the "black and white" type, have the smallest dark signals, -0.4±0.2 Wm^{-2} for the Schenk.
- Ventilation of the Eppley PSP and the Kipp CM10 and CM5 models reduces the offset variability by about 30% to 0.8 Wm^{-2}.
- The variability about the long-wave regression is typically 60% of the offset variability. The Schenk is the only exception to this generalisation. With the ventilated PSPs, CM10s and CM5s the residual is about 0.5 Wm^{-2}.
- In no case does the inclusion of the rate of change of temperature into the regression produce any useful reduction of the variability. The largest reduction is only 0.04 Wm^{-2}.

Table 6.2.2a shows that the voltage measurement noise does not account for the residual after bi-linear regression. For example the bi-linear residual for the ventilated PSP is 0.52 Wm^{-2} while the measurement noise is only 0.10 Wm^{-2}. It could be concluded that the expression $C \cdot \dot{T}$ does not adequately parameterize the effect of thermal stress at this level

of accuracy. However, no improvement was observed on using the more direct expression $(T_i - T_a)$ where T_i is the temperature of the individual pyranometer. It was only possible to make the comparison on three pyranometers because these were the only ones on which the individual temperatures were measured. In another attempt to reduce the residual variability, the term $\dot{T}$ was replaced by $\dot{T}_i$ calculated for each of these three pyranometers. There is a small improvement but not enough to modify any conclusions.

6.2.3 Results of statistical analysis

The following offset functions (Table 6.2.3a), expressed in Wm^{-2}, are derived from data from a total of 23 pyranometers mounted in ventilated housings with the normal horizontal orientation to measure the downward irradiance. The term $C \cdot \dot{T}$ from Equation 3 is included for comparison with other determinations of C. The coefficients B, of the long-wave stress P, are not significantly different from the values obtained by regression on long-wave stress alone as expressed by Equation 2.

The constant terms are the offsets caused by the ventilator housing alone i.e., the offset irradiance in the absence of environmental thermal stress.

The four instruments PSP, CM10, CM5 and SS25, which all have two domes and a black thermopile, have similar zero functions, except that the CM5 shows an extremely small dependence on temperature change. The zero function for the Schenk instrument is negligible, while the Eko results are intermediate.

The EP07 and the CSIRO PT zero functions are significantly larger. The constant and the temperature change terms for CSIRO PT are negligible.

6.2.4 Offset functions for unventilated horizontal installation

Results for the three instruments tested in the standard mounting configuration with radiation shields are shown in Table 6.2.4a. It may be noted that the coefficients of P are from 30% to 110% greater than without ventilation. The constant terms are small, indicating that, in the absence of long-wave stress and temperature change, the offset is close to zero.

Table 6.2.2 a. Dark signals: statistics

Pyranometer in NARC ventilated housing unless otherwise stated	Mean Wm^{-2}	σ Wm^{-2}	RMS Residuals After Regression On: long-wave only Wm^{-2}	RMS Residuals After Regression On: long-wave & temp. Wm^{-2}	RMS Noise in Volt. Meas. Wm^{-2}
PT	-4.3	1.60	0.95	0.95	[0.26]
PSP *unvent.*	-2.7	1.30	0.63	0.61	[0.10]
EP07	-7.1	1.10	0.83	0.82	[0.10]
CM5 *unvent.*	-2.8	1.10	0.53	0.53	[0.09]
CM10 *unvent.*	-2.5	1.00	0.58	0.55	[0.20]
SS25	-3.5	0.93	0.65	0.63	[0.07]
PSP	-3.1	0.78	0.56	0.52	[0.10]
CM5	-3.1	0.78	0.40	0.40	[0.09]
CM10	-3.4	0.74	0.43	0.40	[0.20]
MS42a	-2.0	0.60	0.40	0.37	[0.12]
MS42	-1.1	0.31	0.20	0.20	[0.14]
Star	-0.44	0.20	0.19	0.19	[0.07]

Table 6.2.3 a

Pyranometers in NARC ventilated housing	
Eppley PSP	$Z = -1.5 + 0.021 \cdot P + 0.29 \cdot \dot{T}$
Kipp CM10	$Z = -1.6 + 0.024 \cdot P + 0.21 \cdot \dot{T}$
Kipp CM5	$Z = -1.2 + 0.030 \cdot P + 0.03 \cdot \dot{T}$
Swissteco SS25	$Z = -1.5 + 0.028 \cdot P + 0.22 \cdot \dot{T}$
Middleton EP07	$Z = -4.1 + 0.036 \cdot P + 0.22 \cdot \dot{T}$
CSIRO PT	$Z = -0.3 + 0.067 \cdot P + 0.00 \cdot \dot{T}$
Eko MS42a	$Z = -0.6 + 0.018 \cdot P + 0.19 \cdot \dot{T}$
Eko MS42b	$Z = -0.4 + 0.009 \cdot P + 0.07 \cdot \dot{T}$
Schenk Star	$Z = -0.1 + 0.003 \cdot P + 0.02 \cdot \dot{T}$

Table 6.2.4a

Eppley PSP	*unvent*	$Z = -0.5 + 0.046 \cdot P + 0.23 \cdot \dot{T}$
Kipp CM10	*unvent*	$Z = 0.0 + 0.034 \cdot P + 0.26 \cdot \dot{T}$
Kipp CM5	*unvent*	$Z = -0.2 + 0.039 \cdot P + 0.10 \cdot \dot{T}$

6.3 Direct outdoor determination of the effect of long-wave radiation

The pyranometer was alternately subjected first to the night-sky irradiance and then to radiation from a sheet of plywood approximately at air temperature. This produced a modulation of the long-wave stress in the order 50 to 100 Wm^{-2} on clear nights. The main item of equipment was a large square plywood box with an open top and dimensions 1.9 x 1.9 x 0.5 m located on the roof of the AES building. This box, whose function was to support the plywood sheet, clearly moderated the wind regime to which the pyranometers were subjected. Up to six pyranometers under test and one pyrgeometer were put within the central 1.0 m square, facing upwards. The domes were only 20 cm below the rim of the box which was high enough for all the instruments to receive the full long-wave irradiance.

The procedure was to cover and uncover the box with a 2.0 m square sheet of plywood for periods of 20 minutes or more up to three times. The signals from the pyrgeometer and the pyranometers are shown in Figures 6.3a&b. It can be seen that the response of the pyranometers was delayed by a few minutes from that of the pyrgeometer. Values for the ratio of change in pyranometer signal to the change in pyrgeometer signal have been computed from these graphs. The changes were evaluated between the times just before removing or replacing the cover and ten minutes later. The result quoted in Table 6.3.1a and Appendix DD1 for each pyranometer is the mean, with its standard deviation, of three evaluations of the ratio.

6.3.1 Summary of long-wave results

Table 6.3.1a lists all the results from the direct method and corresponding ones from the bi-linear regression analysis. These show that the pyranometers can be divided into four groups, as follows:

- The Schenk and Eko black-and-white models for which the effect is small (<1.1%).
- The four ventilated double-dome black models (CM5, CM10, PSP, SS25) which all have results in the range 2.1% to 3.0%.
- The three unventilated double-dome black pyranometers (CM5, CM10, PSP) which all have results in the range 3.6% to 4.6%.
- The EP07 and the PT which have the largest results.

Figure 6.3a

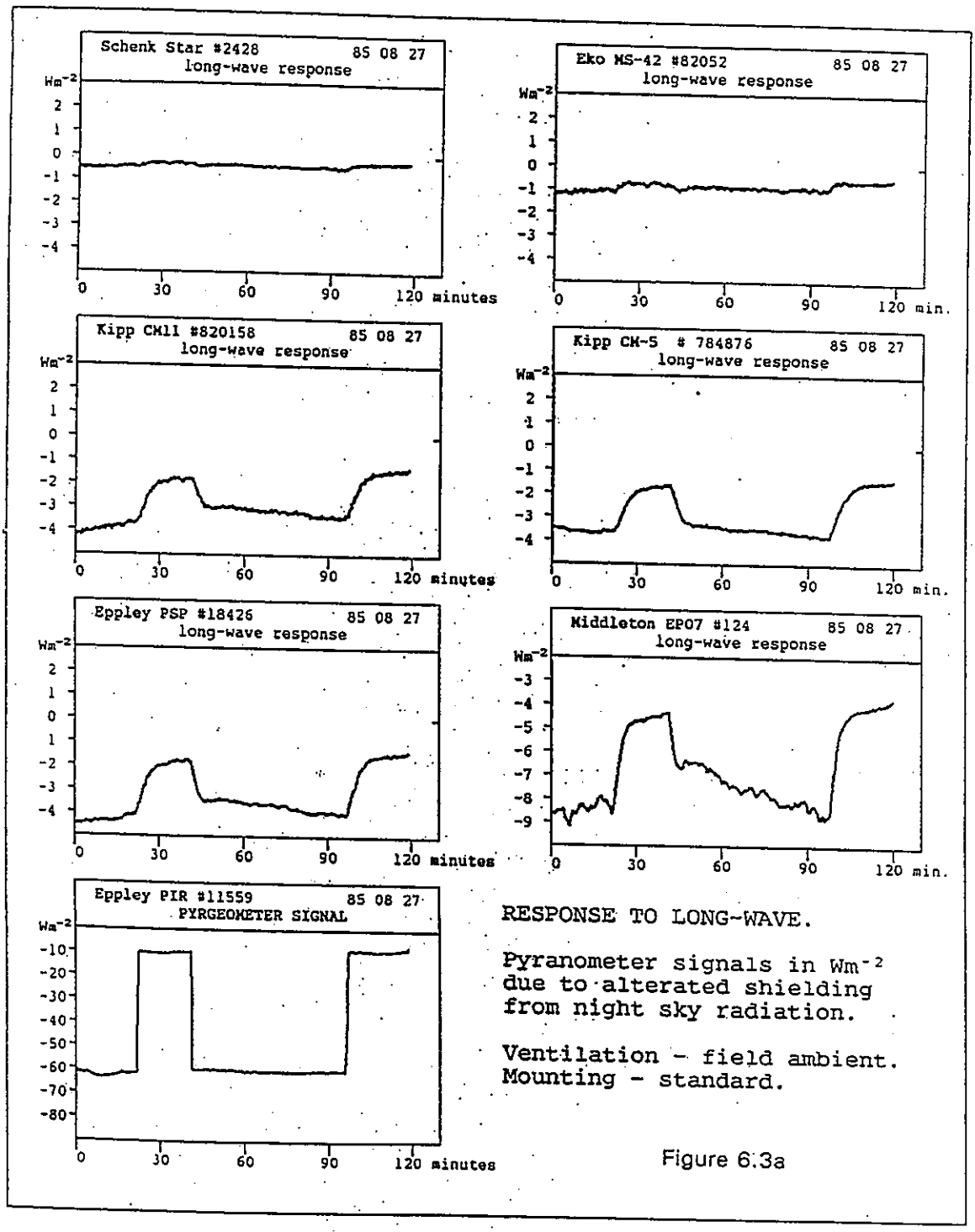

Figure 6.3a

Figure 6.3b

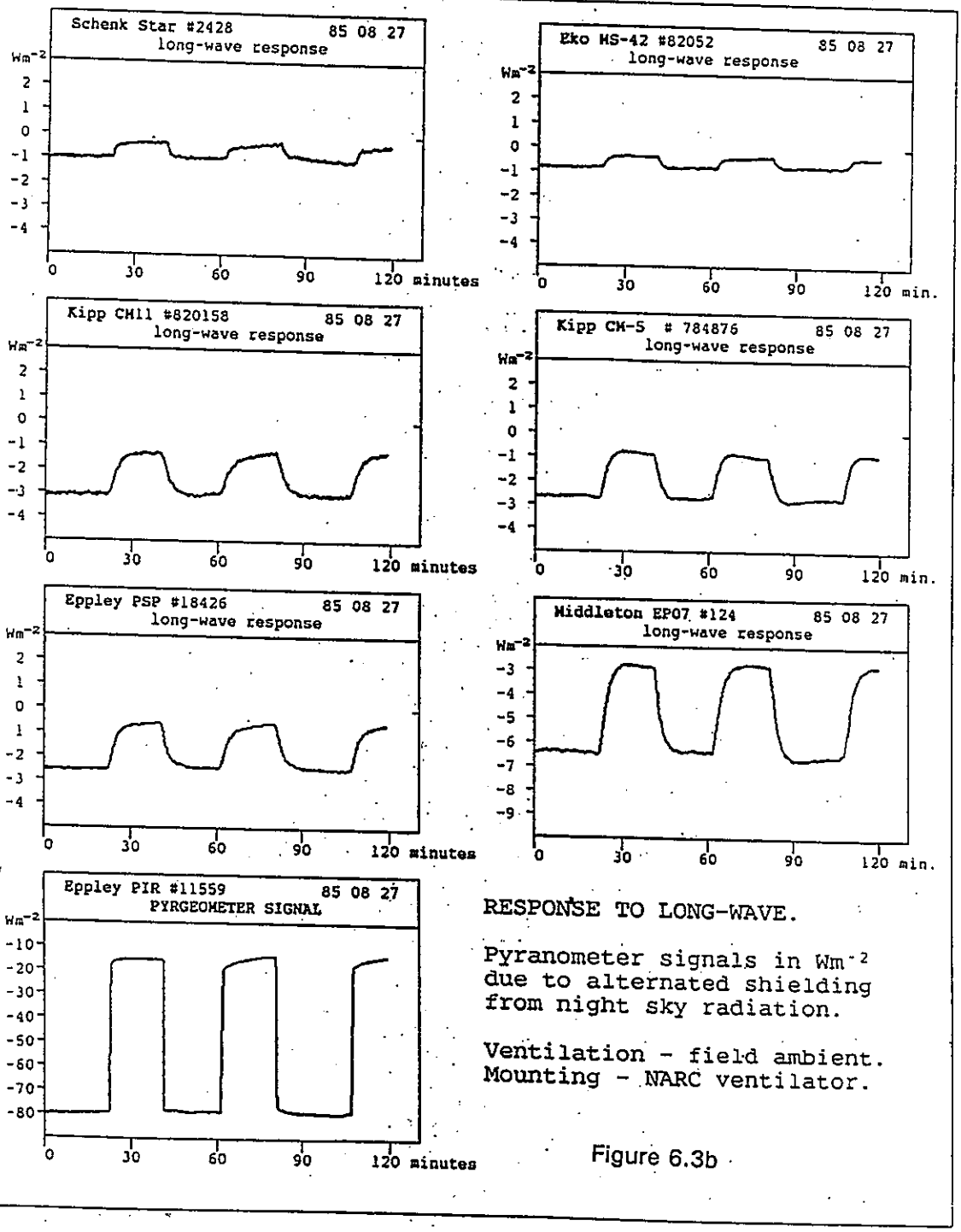

Figure 6.3b

Table 6.3.1a Results for the influence of long-wave radiation

Mounting	Standard *unventilated*		NARC *ventilated housing*	
Method	Direct	Statistical	Direct	Statistical
External Ventilation *wind*	Moderated Ambient *see text*	Ambient	Moderated Ambient *see text*	Ambient
Star #2428	0.002		0.007	0.004*
MS42B #82052	0.004±0.001		0.011±0.001	0.010*
CM10 #820158	0.037±0.004	0.036	0.027±0.001	0.024
CM5 #784876	0.041±0.003	0.039	0.029	0.030
PSP #18426	0.045±0.005	0.046	0.030±0.001	0.021*
EP07 #124	0.080±0.011		0.060±0.001	0.034*
SS25 #113				0.028
CSIRO PT				0.067

**The results on the ventilated Schenk, Eko, Middleton and PSP are for identical instruments*

6.3.2 Discussion of long-wave results

Results from the two methods are very similar - they differ by 0.003 or less in seven of the nine cases where a comparison can be made. The other two cases are for the ventilated Middleton and ventilated PSP. The difference is 0.026 for the Middleton (which is about four times the combined standard error) and 0.009 for the PSP (which is smaller but still significant).

The cause of the discrepancies with these two instruments has not been identified. Some difference between the two methods might be expected because, in the direct technique, the removing and replacing of the plywood cover does not only cause the desired modulation of the long-wave radiation it also modulates the air temperature by a few degrees. The result is therefore the combination of long-wave influence and temperature change, while the statistical analysis specifically separates these effects. It is notable that the Middleton instrument is the most sensitive to temperature change.

The field statistical results are preferred for two reasons. First, they apply to the exact mounting configuration of the pyranometers use. Second, the aim is to parameterize the

offset as a function of environmental variables: this is true regardless of potential effects of imprecision or correlation in the independent variables.

6.4 Temperature change effects on the offset (indoor)

The statistical analysis of dark signals, described in §6.2, is the only field technique that has been used to study the temperature change offset. The effect has been studied in the laboratory by subjecting pyranometers to either a sustained rate of temperature increase or to thermal shock. A brief discussion of these investigations, undertaken in Vienna and the Netherlands (Kipp, TNO), is given in §5.4. The NARC thermal shock study is described below and its results are compared with the statistical technique and discussed. An intercomparison is made between the results from NARC and TNO for both long-wave radiation and temperature change in §6.5.

6.4.1 Measurement of the response to thermal shock

The procedure was to move pyranometers from a dark room at ordinary temperature into a dark cold room (typically at -25 C) and to record the signals. Four or five pyranometers were tested at the same time. They were set on a moveable table with a clearance of at least 3 cm, as if deployed for radiation measurement. The thin stainless steel surface of the table, with its small thermal inertia, would reach ambient temperature within a few minutes. A thirty-minute period was allowed for the pyranometers to equilibrate at room temperature and during this time the room lights were switched on for one minute. The record of this pulse unambiguously identified the polarity. The table was then wheeled into the cold room and the signals were recorded for a further ninety minutes.

The measurements were done with four different regimes of ventilation. The cold room was equipped with fans which circulate the enclosed air quite vigorously — the air velocity near the pyranometers was estimated at 1 ms^{-1}. The pyranometers were either enclosed in the NARC ventilators or were equipped with the normal radiation shields. The cold room fans were either on during the whole period or off during the whole period.

Figure 6.4.1a shows some typical results. They are all for the case with the pyranometers in ventilated housings and with the cold room fans turned off. The two PSPs and the CM10 show responses of about 20 Wm^{-2} in the same direction as the temperature change decaying with time constants of about 15 min. The response of the CM5 is in the opposite direction. The EP07 response is, at first like the PSP but in the region of 50 Wm^{-2}, but followed by a

smaller but longer excursion in the opposite direction. This type of response is also shown by the CM5 in the standard mounting when the cold room fans are off.

6.4.2 Summary of temperature change results

Table 6.4.2 summarises all the cooling results, including those from the bi-linear regression for comparison. The peak excursions with the overshoot where it exists, normalised for 1.0 K, are given in the first part. The area excursions, also normalised for 1.0 K, are given in the second part. When there is an overshoot the net area excursion (which is small), is listed.

In the course of the experiments, it was found that the results in the totally unventilated regime (i.e., standard mounting and no wind) depended very much on minor details of lay-out. The first column should therefore be taken only as some typical values.

It can be seen that results for the NARC ventilated mounting are insensitive to the external ventilation. Also, the peak excursion results for the standard mounting in the presence of external ventilation are close to those obtained for the ventilated mounting.

Table 6.4.2 contains several cases where the tests have been repeated on the same instrument or on one of the same type. Except for one case, the corresponding results are very close. The reason for the difference between the two PSP pyranometers is not known.

6.4.3 Discussion of temperature change results

It could be expected that the external ventilation in the laboratory would simulate the typical ambient ventilation occurring throughout the field experiment. As discussed earlier, the laboratory area excursions should then reproduce the statistically derived values for the coefficient of temperature change. Table 6.4.2 shows that this is definitely not the case. All the statistical results are higher than the corresponding laboratory values by amounts varying from 0.05 - 0.29 $Whm^{-2} K^{-1}$. The differences are of similar magnitude to the measurements themselves while the error is 0.09 $Whm^{-2} K^{-1}$.

Figure 6.4.1a

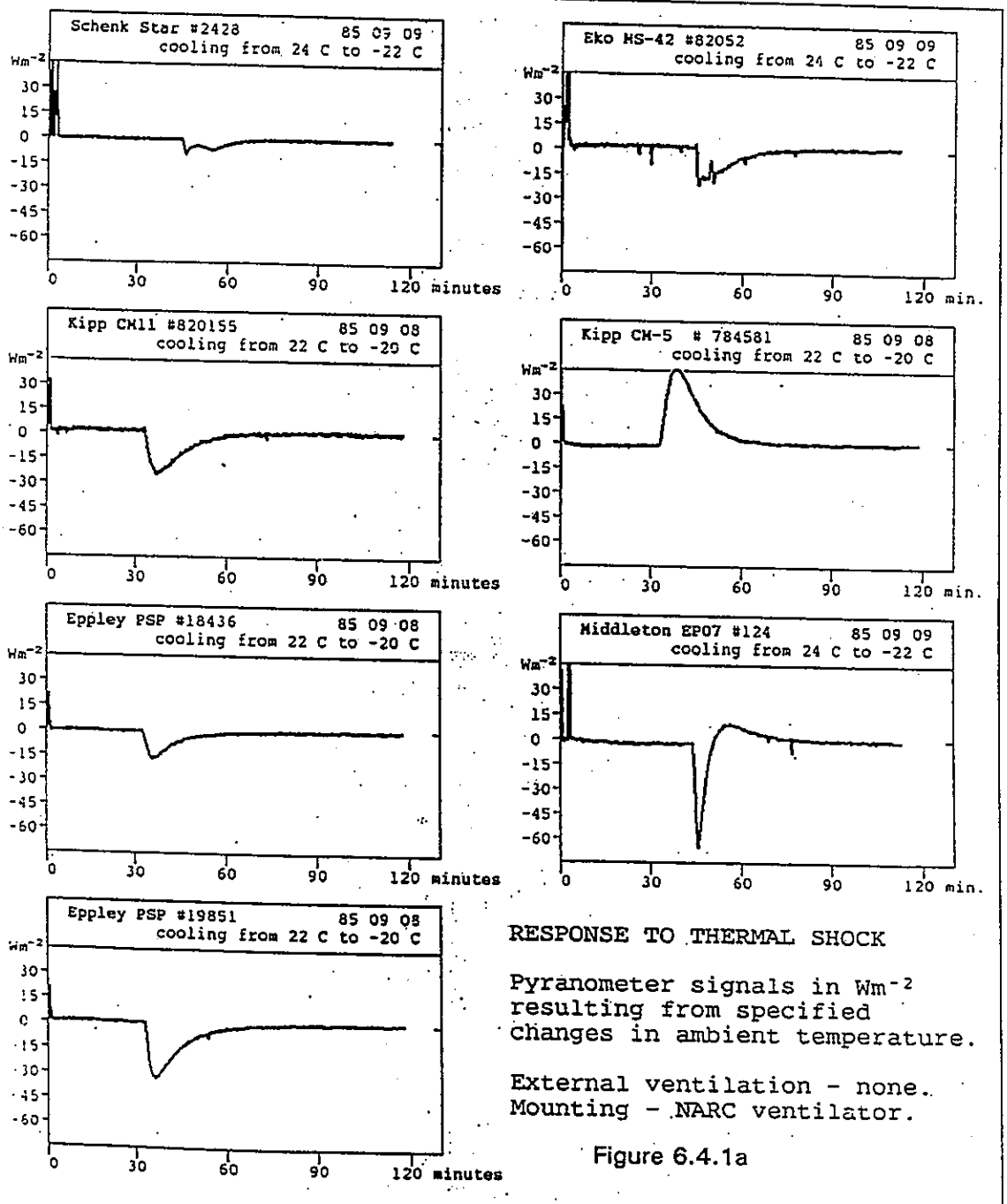

RESPONSE TO THERMAL SHOCK

Pyranometer signals in Wm^{-2} resulting from specified changes in ambient temperature.

External ventilation - none.
Mounting - NARC ventilator.

Figure 6.4.1a

Table 6.4.2 The effect of temperature change on pyranometers: a summary of the NARC results

Excursion Areas From Thermal Shock Compared With Field Statistical Results — W hour m^{-2} K^{-1}

Mounting	Standard			NARC Ventilator			
Location Method	Laboratory Thermal Shock		Field Stat.	Laboratory Thermal Shock			Field Stat.
External Ventilation	No	Yes	Ambient	No	Yes		Ambient
CM5 4851*	0.04	-0.19		-0.21			
			0.01				-0.03
CM5 #2428	-0.06	-0.18		-0.24	-0.23	-0.24	
CM10 #820155	0.34	0.15	0.26	0.13	0.16	0.16	0.21
PSP #18436	0.40	0.17		0.09	0.08	0.07	
			0.23		0.17		0.29
PSP #19851	0.52	0.19		0.16			
EP07 #124*	0.94	0.48		0.02			0.02
MS42B #82052*	0.17	0.09		0.11			0.09
STAR #2428*	0.07	-0.01		0.03			0.02

Peak Excursions From Thermal Shock W m^{-2} K^{-1}

Mounting	Standard		NARC Ventilator		
external ventilation	No	Yes	No	Yes	
CM5 4851*	-0.6/+0.2	-0.6	-10.0		
CM5 #2428	-0.5/+0.2	-0.9	-1.1	-1.2	-1.1
CM10 #820155	0.7	0.7	0.6	0.7	0.6
PSP #18436	0.6	0.6	0.4	0.4	0.4
PSP #19851	0.8	0.8	0.8	0.7	
EP07 #124*	0.9	1.6	1.4/-0.2		
MS42B #82052*	0.2	0.3	0.5		
STAR #2428*	0.1	0.0	0.2		
Day/August 1985	07 16*	01 12*	08 09*	02	06

** instruments tested on same dates*

Table 6.5a Results from the Technisch Physische Dienst (TNO-TH) of the Netherlands on the influence of long-wave radiation on pyranometers compared with results from the NARC

Mounting	Standard				NARC Ventilator		
Location	Laboratory TNO	Laboratory TNO	Field NARC		Lab. TNO	Field NARC	
External Ventilation	No	Yes 3 m s^{-1}	Ambient		No	Ambient	
Serial # Used at TNO	A	B	B1	B2	C	C3	C4
PSP #20524	0.104	0.056	0.045	0.046	0.032	0.030	0.021
CM10 # 810121	0.056	0.040	0.037	0.036	0.032	0.027	0.024
CM5 #773656	0.116	0.060	0.041	0.039			
Star #2209	0.012	0.008	0.002				
SS25 #114	0.112	0.060					
CSIRO PT	0.148	0.100					
MS42a #81908	0.040	0.024					

All values are for the incremental effect $\delta Z/\delta P$ where δZ is the change in pyranometer signal caused by a change δP in the long-wave radiation.

- A TNO - Standard mounting - 0.2 m below a hot plate at 75 C - no external ventilation. Not comparable to any NARC measurements.
- B TNO - Standard mounting - 0.2 m below a hot plate at 75 C - 3 m s^{-1} External ventilation.
- B1 NARC- Direct method - outdoors - ambient wind moderated by box as mentioned in text.
- B2 NARC- Statistical method - outdoors - ambient wind.
- C TNO - Mounted in NARC ventilator - no external ventilation.
- C3 NARC- Direct method - outdoors - moderated ambient wind etc.
- C4 NARC- Statistical method - outdoors - ambient wind.

Reference: van den Brink *et al.* (1985)

Table 6.5b Results from Technisch Physische Dienst (TNO-TH) of the Netherlands on the Effect of Temperature Change on Pyranometers Compared With Results from the NARC

Mounting	Standard					
Location	Lab.	Field	Laboratories			
External Ventilation	1 ms^{-1}	Ambient	Yes?	1 ms^{-1}	Yes?	1 ms^{-1}
Units	$Whm^{-2}K^{-1}$				$Wm^{-2}K^{-1}$	
Serial # Used at TNO	Direct TNO (1)	Stat. NARC (2)	Area Excursion TNO (3)	Area Excursion NARC (4)	Peak Excursion TNO (3)	Peak Excursion NARC (4)
PSP #20524	0.65	0.23	0.22	0.18	1.3	0.7
CM10 # 810121	0.33	0.26	0.16	0.15	1.1	0.7
CM5 #773656	-0.09	0.10	-0.21	-0.19	-1.8	-0.8
Star #2209	0.00		0.02	-0.02	0.2	0.0
SS25 #114	0.09		-0.06		0.4	
CSIRO PT	-0.37		-0.13		-2.5	
MS42a #81908	0.21		0.22		1.8	

1 TNO. Pyranometers subjected to steady temperature rise of 6.7 Kh^{-1} in an environmental chamber.
2 NARC. from statistical analysis of night signals.
3 TNO. Response to thermal shock 25 C to 20 C. Ventilation conditions not quoted in report - thought to be 1 m s^{-1}.
4 NARC. Response to thermal shock 25 C to -25 C.

Ref. van den Brink *et al.* (1985)

A satisfactory explanation of the discrepancies cannot be given. The laboratory shock experiment necessarily involves a change in long-wave radiation but it is in the wrong direction to explain the observed differences. It may be surmised that the response to steady temperature change is very sensitive to the mounting configuration. The metal table on which the instruments are mounted in the field is quite thick (approximately 6 mm), and therefore its temperature lags behind the air temperature much more than the thin table used in the laboratory tests. This is tentatively suggested as the cause of the discrepancies. The largest measured discrepancies are for the CM5 pyranometer which has been shown to be particularly sensitive to thermal input to its base.

The field results on temperature change are preferred for the same reasons as mentioned for the long-wave results.

6.5 Comparison with results from another laboratory

Laboratory investigation of the effects of long-wave radiation and temperature change have been reported by the Netherlands' Technische Physische Dienst (TNO). The TNO results (Tables 6.5 a,b) have been computed from the graphical data given in the TNO report. Comparable NARC results are listed in the same tables.

The TNO long-wave results are quite consistent with the NARC field results. The TNO procedure was to place the pyranometers under a large metal plate heated to 75 C and then to measure the dark signals. External ventilation of 3 m s^{-1} was applied in some cases.

The results with the pyranometers in the NARC ventilated housing would be expected to show the closest agreement. The NARC results are for the outdoor ambient ventilation while the TNO measurements were done with no external ventilation. Table 6.5a shows a satisfactory agreement in columns C, C3 and C4, in view of the limited measurement precision, the ventilation difference and the fact that the laboratory experiment involves a radiation of the opposite sign, i.e. a hot sky. There is also a rough agreement between the TNO results for the standard mounting (column B) in the presence of external ventilation and the NARC field results (B1 and B2). The TNO results for the standard mounting in the absence of external ventilation (column A) are the largest.

The TNO temperature change measurements were only made on pyranometers in the standard mounting. Responses both to a steady increase of temperature and to thermal

shock were measured. The results are generally similar to those from the NARC set but there are some obvious inconsistencies.

Table 6.5b shows an agreement between the two laboratories for the area excursions. this is fortuitous because the TNO values are derived from only the first 15 minutes after the sudden temperature change. No further data are given in the TNO report. The peak excursion measurements of the TNO are about twice as large as the NARC results. The TNO direct results on steady temperature change are significantly different from the NARC statistical results in two out of three cases, the discrepancy for the PSP being particularly large (0.4 $Whm^{-2} K^{-1}$).

The discrepancies observed between the results from TNO and the NARC reinforce the conclusion that details of the mounting configuration and ventilation determine the temperature effect, particularly in the standard mounting. Unfortunately there are no TNO temperature results for the NARC ventilated housing.

6.6 The relation of noise to the offset signal

It is proposed here that the dependence of pyranometer signals on long-wave radiation and temperature change is independent of the short-wave radiation and that the interfering effects are superimposed on the short-wave signal. This would be proven if it were shown that all the heat transfer within the pyranometers was linear, as would be the case in the absence of convection.

Direct validation of this linear superposition can be attempted by examination of the discrepancy between daytime signals of two pyranometers of different types as a function of long-wave radiation. The problem is that pyranometers of different types usually have markedly different directionality errors which tend to mask the effects of long-wave radiation. The problem should not be insuperable, but there is as yet no direct observation of the daytime long-wave effect.

Support for the contention comes from the observed linearity of response and the deduced linearity of the internal heat flow in the pyranometers. The pyranometers of the types in this study have been tested for linearity of response by at least three laboratories. The largest observed departure from linearity over the range 60-1000 Wm^{-2} is about 4%, and was obtained with the Swissteco. Results for the other types are considerably less. It is

concluded that linear heat transport processes dominate transport by convection in all these pyranometers. Several of the pyranometers have a negligible dependence of responsivity on orientation (<0.5% for the PSP, CM10 and Swissteco) which also suggests that convection is not important. Further to the discussion in Ch. 2, non-linearity is seen as a progressive, linear change in responsivity as a function of irradiance. This accords with the simple explanations of the nature of convection and the behaviour of thermopiles. Superposition is generally accepted on account of the above indirect evidence but two caveats need to be considered.

1. The discrepancies between laboratory measurements of the temperature change effect and field statistical results show one case (CM5) where the assumption of an overall linearity appears questionable.

2. There could be some convective transfer that, while having a negligible effect on the responsivity, might have a significant effect on the long-wave sensitivity. For example, the transfer between the receiver and the domes could be stimulated by convection caused by an elevated temperature of the receiver when absorbing short-wave radiation. The long-wave effect would then be stronger in the daytime than at night.

Direct validation is therefore still needed.

Accepting that the offset functions during the day and night are identical, it remains to compare day and night statistics of long-wave radiation and temperature change. A cursory examination of the long-wave stress shows the daytime range about 30% more than in the night. This is because the boundary layer is usually several degrees warmer during the day than at night, while the altitudes where the pyrgeometer signal originates are colder and vary to a smaller extent. Temperature changes are also greater during the day than at night but the magnitude of the temperature change coefficients suggests that the contribution to the offset variability remains smaller than that of the long-wave radiation.

In summary, it is expected that the daytime offset and the dark signals are given by the same function of long-wave radiation and temperature change. It follows that the variability of the daytime offset is about 30% larger because of the larger variability of long-wave stress and temperature during the day. Similarly, the mean daytime offset for unventilated instruments, which is proportional to long-wave stress, is expected to be about 30% greater than the night value. These deductions require only minor revisions of the first two columns of Table 6.2.2a if those are to be taken as representing daytime measurement noise as discussed earlier. It is also likely that the scatter of the true daytime offset about the regression on long-wave stress will be slightly larger than the observed night value.

6.7 Conclusions

Dark signals from seven types of pyranometers, equipped with their standard radiation shields or mounted in NARC ventilators, have been investigated. The mean values and standard deviations are in the ranges -0.4 to -7.1 Wm^{-2} and 0.2 to 1.6 Wm^{-2} respectively. The smallest values are observed for the "black & white" pyranometers, particularly the Schenk Star type. Enclosure in a ventilated housing significantly reduces the standard deviations for the "black" type pyranometers.

The dependence of the dark signals on long-wave radiation and on the rate of change of ambient temperature has been established by statistical analysis of night data spanning several months. The variability about the regression of the dark signal as a function of long-wave radiation is typically 0.5 Wm^{-2} for the ventilated instruments and significantly less than the variability about the mean. Including the ambient temperature change into the regression yields estimates of the effect of a steady rate of temperature increase on the dark signals, but it does not usefully reduce the variability.

The statistical results on the long-wave effects are generally confirmed by field experiments in which the pyranometer is periodically shielded from the long-wave radiation of the night sky. The results also compare quite well with reported laboratory measurements.

The statistical results on the temperature change effect do not agree closely with results derived from laboratory measurements on the response to thermal shock. Direct laboratory measurements of response to a steady increase in temperature are also in disagreement with the statistical results. It is concluded that the temperature change effect is extremely sensitive to the ambient ventilation and mounting configuration.

It is argued that the pyranometer response is linear to the extent that a daytime offset exists and that it is determined by the same function of long-wave radiation and temperature change as are the dark signals. There has been no direct validation of this proposition.

6.8 Offset signal: recommendations

Offsets are most important for measurements of low irradiances.

The simplest correction is to measure the mean dark signal and subtract it from the daytime measurements. This is advisable, even with the Schenk instrument, because the data

acquisition system may develop significant voltage offset. A procedure suitable for continuous monitoring is to determine the mean dark signal every night and to use linear interpolation between the preceding and following night values to compute the offset through the day.

Ventilation is strongly recommended because it reduces the offset variability including the expected 30% difference between the mean day and night offsets. In addition, it can virtually eliminate the build-up of frost, snow or raindrops on the domes.

Further offset correction is not required when measuring large irradiances. For example, with a signal of 1000 Wm^{-2}, an uncertainty of 0.3% in calibration, which is characteristic of the best pyranometers, contributes more to the measurement error than the offset variability.

Offset correction based on long-wave data is recommended for the most accurate measurement of diffuse radiation as is required for a reference instrument against which other pyranometers are calibrated. For this application, the pyranometer would be one of the "black" types with the least directionality of response; it should be ventilated and equipped with a tracking shade disc. The offset function should be determined from night signals as in this work and offset correction based on real-time pyrgeometer measurements should be applied. If the pyranometer is in a ventilated NARC housing, the following offset function may be used:

$$Z = \left(-1.5 + 0.025 \cdot P\right) \qquad [Wm^{-2}] \qquad [6.6]$$

This applies with sufficient accuracy to the PSP, CM10, CM5, and Swissteco pyranometers. Correction based on temperature change is not recommended because the statistical analysis shows an insignificant reduction in the residual variability when including temperature change. Rapid changes in pyranometer temperature should be avoided if possible.

Finally, because of the very small offset, the Schenk pyranometer, or one of similar construction, is recommended for irradiances below about 50 Wm^{-2}. Because of directional errors it is not the best instrument for use at larger irradiances.

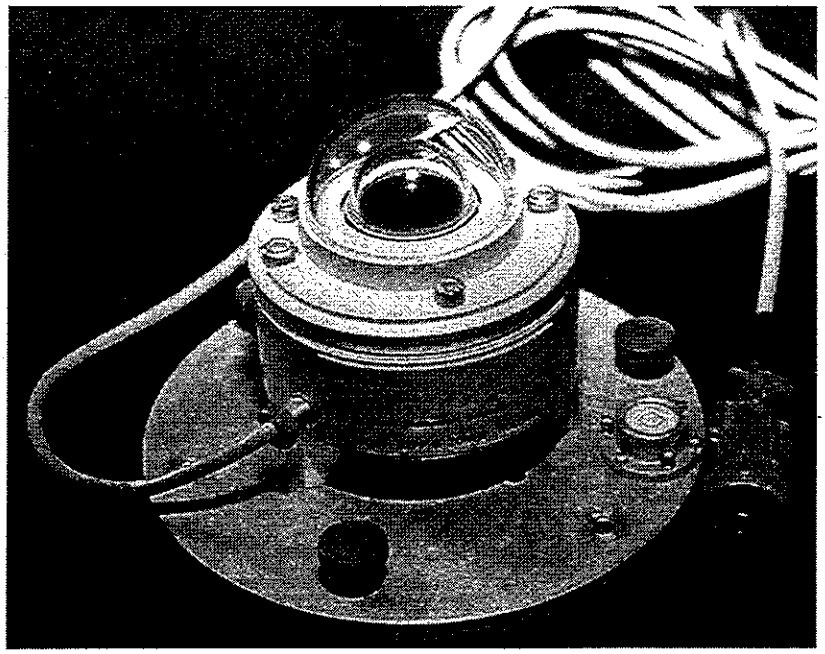

Kipp and Zonen CM11

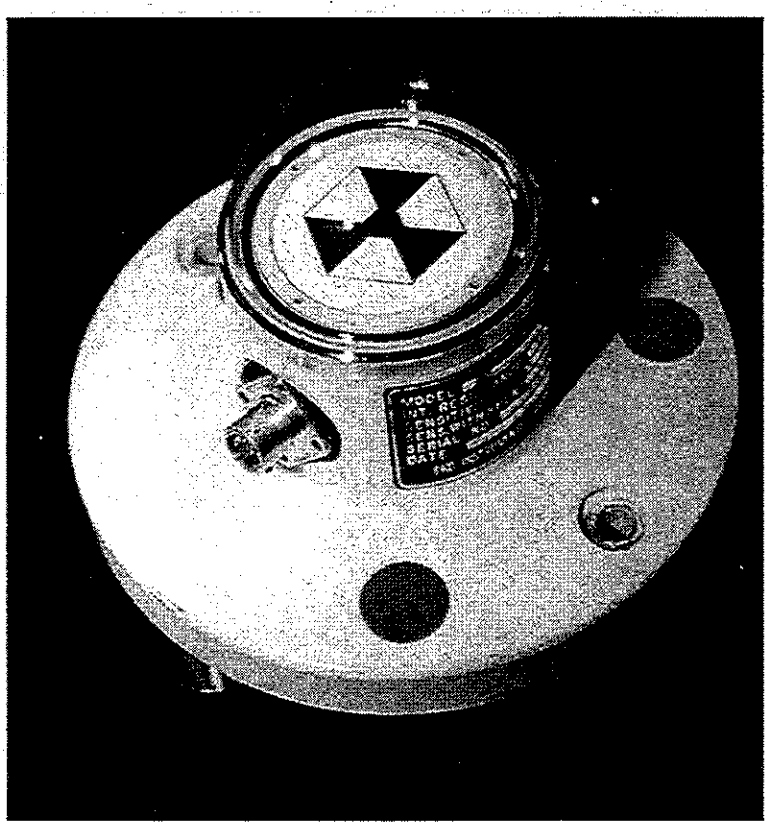

EKO MS-42

Chapter 7. Transfer Functions

7.1 Introduction

The purpose of deriving transfer functions is to establish a uniform method for describing the behaviour of pyranometers. This can help general family characteristics for each model of pyranometer to be ascertained, together with typical errors and magnitudes that may or may not be corrected for, depending upon the specific application of the pyranometer.

Much of the value in transfer functions comes from their use in uncertainty analysis. The transfer function allows a reasonably rigorous estimation of the measurement uncertainty caused by variations in the environmental condition and in the nature of the radiation being measured.

This chapter gives the rationale for the particular structure of the transfer function adopted in this work. Some of this formulation is covered in §1 and the work in §4,5 & 6 addresses the measurement of the most important terms in the function. Section 7.3 is a simple example of using the response function with knowledge of the variability of the environment in order to determine uncertainty in measurement of irradiance.

7.2 Formulation of a transfer function

A convenient starting point is the following definition of responsivity R

$$R = (V - V_z)/E \qquad [7.1]$$

where E is the incident irradiance and V is the output signal and V_z is the output when it is in the dark. This is a useful definition because R is reasonably constant, probably varying by less than 10% over the wide range of conditions that a pyranometer may be exposed to in most applications. The responsivity of a pyranometer generally does depend upon the

- direction (θ, ϕ) of the incident radiation represented by $\underline{s}$ if there is a unique incidence direction or by $\underline{s}^*$ if there is a radiance distribution
- instrument temperature T
- instrument tilt β and intensity of irradiance E

- wavelength λ of the incidence radiation if it is unique or the spectrum of the incident radiation $E_\lambda(\lambda)$ represented by λ^*

so that

$$R = R\left(\underline{s}^*, T, \beta, E, \lambda^*\right) \qquad [7.2]$$

Further, the zero signal V_Z depends, as shown in §6, on long-wave radiation P, rate of change of temperature $\dot{T}$ and mounting configuration (especially the ventilation conditions). This behaviour is expressed by the term $Z = V_Z / R$ in the following

$$V = R\left(\underline{s}^*, T, \beta, E, \lambda^*\right) \cdot (E + Z) \qquad [7.3]$$

$$Z = Z\left(P, \dot{T}, \textit{ventilation}\right) \qquad [7.4]$$

Fortunately the effects of many of these variables are separable and can be accommodated as correction factors ($F_{\underline{s}}$, F_T, $F_{\beta E}$, F_λ) to a standard responsivity R_0 as follows

$$V = R_0 \cdot F_{\underline{s}}(\underline{s}^*) \cdot F_T(T) \cdot F_{\beta E}(\beta, E) \cdot F_\lambda\left(\lambda^*\right) \cdot (E + Z) \qquad [7.5a]$$

or, more succinctly,

$$V = R_0 \cdot F_{\underline{s}} \cdot F_T \cdot F_{\beta E} \cdot F_\lambda \cdot (E + Z) \qquad [7.5b]$$

The inverse, for use in computing the irradiance from the signal, is

$$E = \frac{V}{R_0 \cdot F_{\underline{s}} \cdot F_T \cdot F_{\beta E} \cdot F_\lambda} - Z \qquad [7.6]$$

The following definitions apply:

$$F_{\underline{s}}(\underline{s}) = \frac{R\left(\underline{s}, T, \beta, E, \lambda^*\right)}{R\left(\underline{s}_0^*, T, \beta, E, \lambda^*\right)} \quad \text{assumed independent of } T, \beta, E, \lambda^* \qquad [7.7a]$$

$$F_T(T) = \frac{R\left(\underline{s}^*, T, \beta, E, \lambda^*\right)}{R\left(\underline{s}^*, T_0, \beta, E, \lambda^*\right)} \quad \text{assumed independent of } \underline{s}^*, \beta, E, \lambda^* \qquad [7.7b]$$

$$F_{\beta E}(\beta,E) = \frac{R(\underline{s}^*,T,\beta,E,\lambda^*)}{R(\underline{s}^*,T,\beta_0,E_0,\lambda^*)} \quad \text{assumed independent of } \underline{s}^*,T,\lambda^* \qquad [7.7c]$$

$$F_\lambda(\lambda) = \frac{R(\underline{s}^*,T,\beta,E,\lambda)}{R(\underline{s}^*,T,\beta,E,\lambda_0)} \quad \text{assumed independent of } \underline{s}^*,T,\beta,E \qquad [7.7d]$$

Where $\underline{s}_o^*, T_o, \beta_o, E_o, \lambda_o^*$ are the conditions that have been chosen for the standard responsivity R_0.

The effects of the distributed variables λ^* and $\underline{s}^*$ can be computed from the corresponding simple variables by

$$F_\lambda(\lambda^*) = \frac{\int_0^\infty F_\lambda(\lambda)\cdot E_\lambda(\lambda)\cdot d\lambda}{\int_0^\infty E_\lambda(\lambda)\cdot d\lambda} \qquad [7.8]$$

and

$$F_S(\underline{s}^*) = \frac{\int F_S(\underline{s})\cdot L(\theta,\phi)\cdot\cos\theta\cdot d\Omega}{\int L(\theta,\phi)\cdot\cos\theta\cdot d\Omega} \qquad [7.9]$$

With regard to this proposed response function:

- the authors believe that no measurements invalidate this general form,
- the effects described by all the terms in Equation 7.5 have been observed and measured for various types of pyranometers,
- the residual rms noise is presumed to be about one watt per square meter for 10-minute, mean measurements, the magnitude varying with the type of instrument.

Table 7.2 Legend to the response function

SYMBOL	DEFINITION	UNIT
V	OUTPUT VOLTAGE FROM PYRANOMETER	μV
V_z	OUTPUT VOLTAGE WITH ZERO RADIATION	μV
R_0	RESPONSIVITY AT STANDARD CONDITIONS I.E., T_0, $\beta = 0$ ETC.	$\mu V \cdot W^{-1}m^2$
E	IRRADIANCE IN THE MEASUREMENT DIRECTION (PYRANOMETER AXIS)	Wm^{-2}
$E_\lambda(\lambda)$	SPECTRAL IRRADIANCE	$Wm^{-2}nm^{-1}$
$F_S(\underline{s}^*)$	CORRECTION FACTOR FOR DIRECTIONALITY	
θ, ϕ	ZENITH AND AZIMUTH ANGLES WITH RESPECT TO PYRANOMETER AXIS AND REFERENCE DIRECTION (CABLE)	
$\underline{s}$	THE DIRECTION θ, ϕ	
$\underline{s}^*$	INDICATING A RADIANCE DISTRIBUTION, $L(\theta, \phi)$	
β	TILT (ANGLE BETWEEN PYRANOMETER AXIS AND LOCAL VERTICAL)	
$F_{E\beta}$	CORRECTION FUNCTION FOR NON-LINEARITY AND/OR TILT	
F_T	CORRECTION FUNCTION FOR TEMPERATURE	
λ	WAVELENGTH	nm
λ^*	INDICATING A SPECTRUM, $E_\lambda(\lambda)$	
Z	OFFSET IRRADIANCE, FUNCTION OF RATE OF CHANGE IN TEMPERATURE, OF P AND OF VENTILATION.	Wm^{-2}
P	NET THERMAL IRRADIANCE $= \left(E_\ell - \sigma T^4\right)$ AS MEASURED BY A PYRGEOMETER	Wm^{-2}
$d\Omega$	$= \sin\theta \cdot d\theta \cdot d\phi$	sr
$L(\theta, \phi)$	RADIANCE FIELD	$Wm^{-2}sr^{-1}$
$\overline{L}(\theta)$	AZIMUTH AVERAGED RADIANCE FIELD $\int_0^{2\pi} L(\theta, \phi) \cdot d\phi / 2\pi$,	$Wm^{-2}sr^{-1}$
$\int .....d\Omega$	$= \int_0^{2\pi} \int_0^{\pi/2} .....\sin\theta \cdot d\theta \cdot d\phi$	

7.3 A simple example of computing measurement uncertainties.

The subject of this section is the performance of three pyranometers under various conditions and throughout a typical year in Japan. The transfer functions of each pyranometer are used to compute the response under clear skies with different optical properties and solar elevations. The departures from the ideal response are examined. The range of the departures indicates the uncertainty arising from the use of a standard responsivity. The error contributions from the pyranometers' directionality, both in diffuse and global measurements, and the spectral errors are illustrated.

7.3.1 Procedure

The basis of this treatment is Equation [7.4] with the offset Z neglected so that

$$R = V/E = R_O \cdot F_S \cdot F_T \cdot F_{\beta E} \cdot F_\lambda \qquad [7.10]$$

The fractional change Q in responsivity compared to R_0 is

$$Q(\underline{s},T,\beta,E,\lambda) = (R-R_0)/R_0 = F_S \cdot F_T \cdot F_{\beta E} \cdot F_\lambda - 1 \qquad [7.11]$$

Defining $Q_S = F_S - 1$ functions etc., for each of the factors and assuming that these are small gives:

$$Q(\underline{s},T,\beta,E,\lambda) = Q_S(\underline{s}) + Q_T(T) + Q_{\beta E}(\beta,E) + Q_\lambda(\lambda) \qquad [7.12]$$

This identifies the Q - functions as the fractional changes generated by the various aberrations and that, when they are combined, their effects are additive. In this section at least, they are called "error terms" because they describe the errors in assuming a constant responsivity. Equation [7.12] is an alternative form containing the same information as the response function when the changes are small. The following example includes further simplifications in that azimuth variability is neglected, only horizontally mounted pyranometers are considered and the temperature and non-linearity effects are linear in T and E respectively.

The pyranometer data for the right hand side of Equation [7.12] are from Task 9 work. To evaluate the responsivity under atmospheric conditions requires integration over direction

and wavelength because the sky radiates from all directions and has a continuum of wavelengths. Therefore the task, using the above simplifications, is to evaluate

$$Q(\theta^*, T, E, \lambda^*) = Q_\theta(\theta^*) + Q_T(T) + Q_E(E) + Q_\lambda(\lambda^*) \qquad [7.13]$$

where, following Equations [7.8 & 7.9]]

$$Q_\theta(\theta^*) = \frac{\int_0^{\pi/2} Q_\theta(\theta)\bar{L}(\theta)\sin(\theta)\cos(\theta)d\theta}{\int_0^{\pi/2} \bar{L}(\theta)\sin(\theta)\cos(\theta)d\theta} \qquad [7.14]$$

and

$$Q_\lambda(\lambda^*) = \frac{\int_0^{\infty} Q_\lambda(\lambda)\cdot E(\lambda)d\lambda}{\int_0^{\infty} E(\lambda)d\lambda} \qquad [7.15]$$

The spectrum of the irradiance $E(\lambda)$ and the azimuth averaged radiance distribution $\bar{L}(\theta)$ are properties of the sky. In this exercise they are derived from a model and the radiance in the model does not change with azimuth ϕ, so that the expression $Q_\theta(\theta)$ replaces $Q_{\underline{s}}(\underline{s})$.

7.3.2 Pyranometer and model radiation data

The three pyranometer types were the PSP, the CM-11 and the Eko MS-801. The spectral responsivities, $Q_\lambda(\lambda)$, are based on the work at Borås in §5.7. The directional responsivities of the PSP and CM-11 are derived from measurements both at the MOH and the TNO, which are in close agreement with each other. For the PSP, the temperature dependence and the non-linearity are from MOH; for the CM-11 they are from TNO. For the MS-801, the directional, temperature and non-linearity data come from the manufacturer. All these pyranometer data are merely examples of particular determinations on particular instruments. It is not suggested that they are generic. The reference conditions that determine R_0 for this application have been chosen as normal incidence, 20 C and 500 Wm^{-2}.

The radiance distributions are calculated using an azimuth averaged 12-stream, 20-layer model with a spectral resolution of 50 nm in most parts of the spectrum (Miyake, 1989). The model carries stratospheric and tropospheric aerosols, water vapour and ozone in

addition to Rayleigh scattering. It was run, with a ground albedo of 0.2, at a range of turbidities, at two water vapour contents and at several solar zenith distances θ.

Figure 7.3.2a shows the output global, diffuse and direct radiation for three different turbidities as a function of airmass $\left(=1/\cos(\theta)\right)$ Figure 7.3.2b shows the spectra of global, diffuse and direct radiation at airmass 1.5 and Figure 7.3.2c shows the spectra of global radiation over a range of airmass.

The distribution of sky radiance over a range of airmass is illustrated in Figure 7.3.2d. The "Intensity" is equivalent to radiance, being π times the radiance in $Wm^{-2}sr^{-1}$; it is also the value of the global irradiance from an isotropic sky of that radiance. The irradiance points plotted in Figure 7.3.2d are the contribution to the global radiation from 10-degree wide rings in the sky. The two quantities are related approximately according to:

$$"Irradiance(\theta)" = \frac{\pi}{18} \cdot \sin 2\theta \cdot "\text{intensity}(\theta)" \qquad [7.16]$$

where $\pi/18$ is 10° expressed in radians.

Figure 7.3.2e compares winter and summer measurements of global radiation with model output at 1.34 and 5 cm of precipitable water. Corresponding measurements of turbidity are also shown.

7.3.3 Results

Figure 7.3.3a shows the changes in responsivity that are caused by shifts in the spectra as a function of airmass, with turbidities of 0.1, 0.27 and 0.50. (The spectra for 0.27 are as shown in Figure 7.3.2b). The changes calculated for an Eko MS42 black-and-white pyranometer are included with results for the other three instruments. The effects are computed by taking each of the spectra E_λ in Figure 7.3.2b and performing the integration according to Equation 7.15. Each spectrum results in one point in each of the panels in Figure 7.3.3a.

All the plots show a slight decrease in responsivity with increasing airmass and turbidity. This is a consequence of the small decrease of sensitivity to near infrared radiation exhibited by all the pyranometers and of the shift towards the infrared in the global spectra.

The significant feature of all the plots is the range of responsivities. It is 0.92% for the black-and-white example and less than 0.6% for the three others. These ranges which are called "error bar" on the figure represent the full range of percentage error consequent on neglecting the spectral variability. The small numbers, for the PSP and CM-11, justify neglecting spectral variability when measuring global radiation with these instruments. However, in the context of measuring other sources such as halogen or xenon lamps, clearly the different types of pyranometers will show larger spectral effects.

Figure 7.3.3b shows the responsivity changes for global radiation induced by different radiance distributions evaluated using Equation 7.14. The obvious feature here is the large, 5%, range exhibited by the PSP. It is caused by the decreasing responsivity of this PSP with incidence angle.

The ranges in Figure 7.3.3b for the CM-11 and MS-801 are considerably smaller, both being less than 1.0%. However, it is important to note that the radiance distributions here are for cloudless skies and are smooth compared with that occurring when there is uneven cloud cover. Uneven distributions can be expected to extend the range of variability in responsivity (the analogous effect in spectral variability is believed to be much smaller because clouds do not cause discontinuities in the spectra).

In Figure 7.3.3c the effect for the PSP is separated in terms of the diffuse and direct contributions to the global measurement. As one would expect, the main contributor is the direct beam which accounts for approximately three quarters of the variability. This illustrates the rationale for using the combination of a cavity radiometer and a shaded pyranometer in order to measure global radiation as accurately as possible. In this particular case the uncertainty in the diffuse measurement is indicated at about one quarter of that in the unshaded global measurement.

Figure 7.3.3d shows the full variability over typical summer and winter clear-sky conditions calculated for Japan. The airmass range is about one to four in summer and two to four in winter. Temperature and linearity effects are combined here with the spectral and directional effects. The radiation conditions are those of Figure 7.3.2e. The overall ranges are 6.6%, 3.05% and 2.0% respectively for the PSP, CM-11 and MS-801.

The spread in the PSP responsivity is more dependent on zenith angle than on turbidity. This raises the possibility of expressing the responsivity (to global radiation) as a function of

solar zenith angle (which is always known). If this were done in Figure 7.3.3d , the remaining spread would be 2-3%, like that of the other two pyranometers. This would be useful if skies were indeed as simulated in the model but the extent to which it would work with cloudy and partially cloudy skies is clearly limited — the radiance from a uniform cloud cover is approximately isotropic regardless of the solar elevation.

7.3.4 Summary and conclusions

This analysis is preliminary and simplified. Zero effects are ignored and the treatment does not include tilted measurements. Also, the pyranometer characteristics used here may not be representative of the specific types. The evaluation concentrates on the range of percentage error: a more suitable measure of performance would be the root mean square of the error in Wm^{-2} arising from a realistic distribution of conditions. Most importantly, the modelled radiance data do not reflect the detailed variability of real cloudy skies: a set of real radiance data throughout at least a year should be used for a similar analysis. With these caveats, and considering that the issue is being addressed in Task 9f, useful conclusions can be drawn from this preliminary work.

- The effects of different spectra of global radiation are negligible in the case of the CM-11 and PSP and small for the MS-801.
- The directionality effect for the PSP is large and is the main cause of the 6.6% spread of PSP responsivity throughout the year. Expressing the responsivity as a function of solar zenith distance reduces the uncertainty under clear skies but not under cloudy skies. The uncertainty ranges calculated for the CM-11 and MS-801 are 3% and 2% respectively.
- The directionality effect on the measurement of diffuse radiation is much smaller than that generated by the same pyranometer when measuring global radiation. Thus the spread in the values for global radiation, when using the PSP to measure the diffuse component and a cavity radiometer to measure the direct component, is shown to be only one quarter of that when using the pyranometer alone. Again, the degree to which this performance is maintained under real skies, particularly those with broken clouds, is not established here.

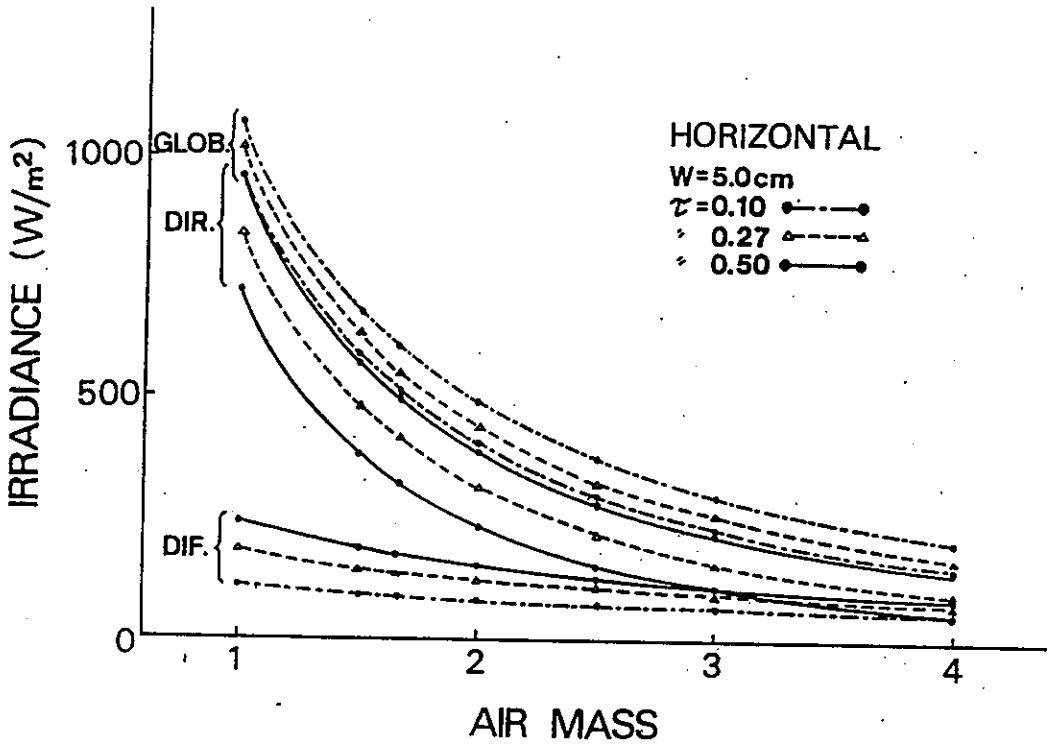

Figure 7.3.2a Calculated horizontal global, direct and diffuse radiation for turbidities(τ) 0.1, 0.27, 0.50 and water(w) 5.0cm plotted against airmass (secant of the solar zenith angle).

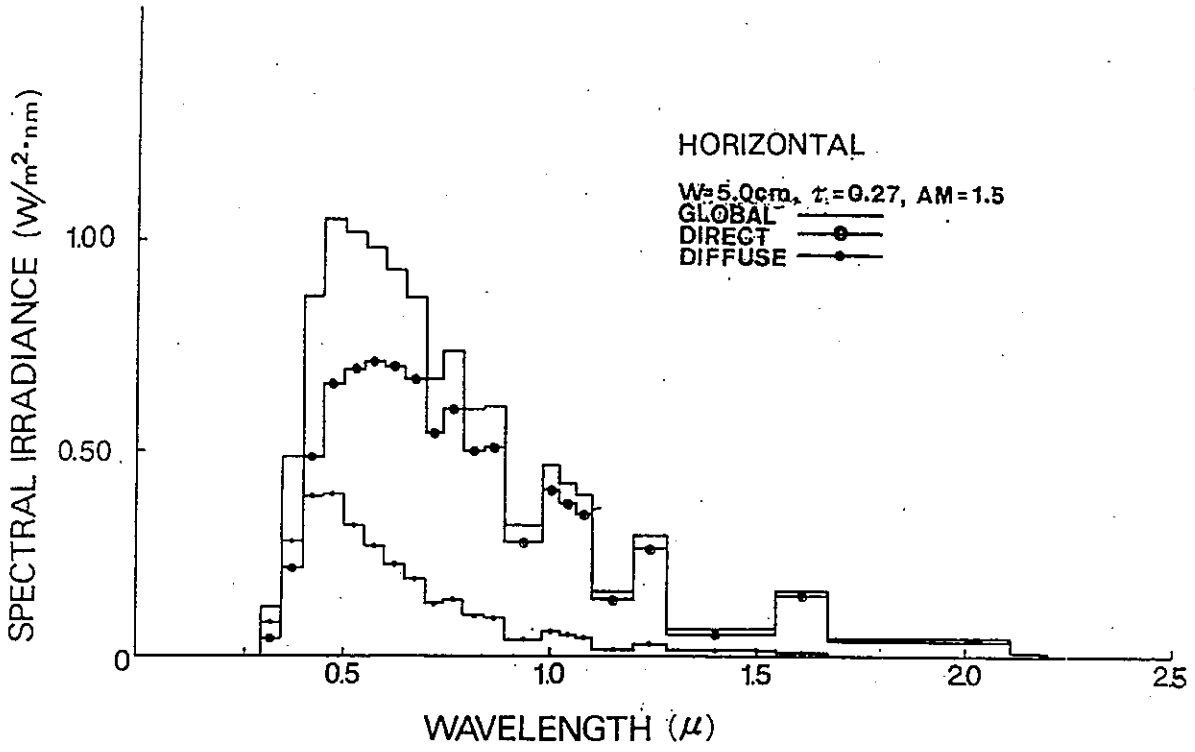

Figure 7.3.2b Calculated spectra of global, diffuse and direct radiation at w = 5.0cm, τ = 0.27 and airmass 1.5.

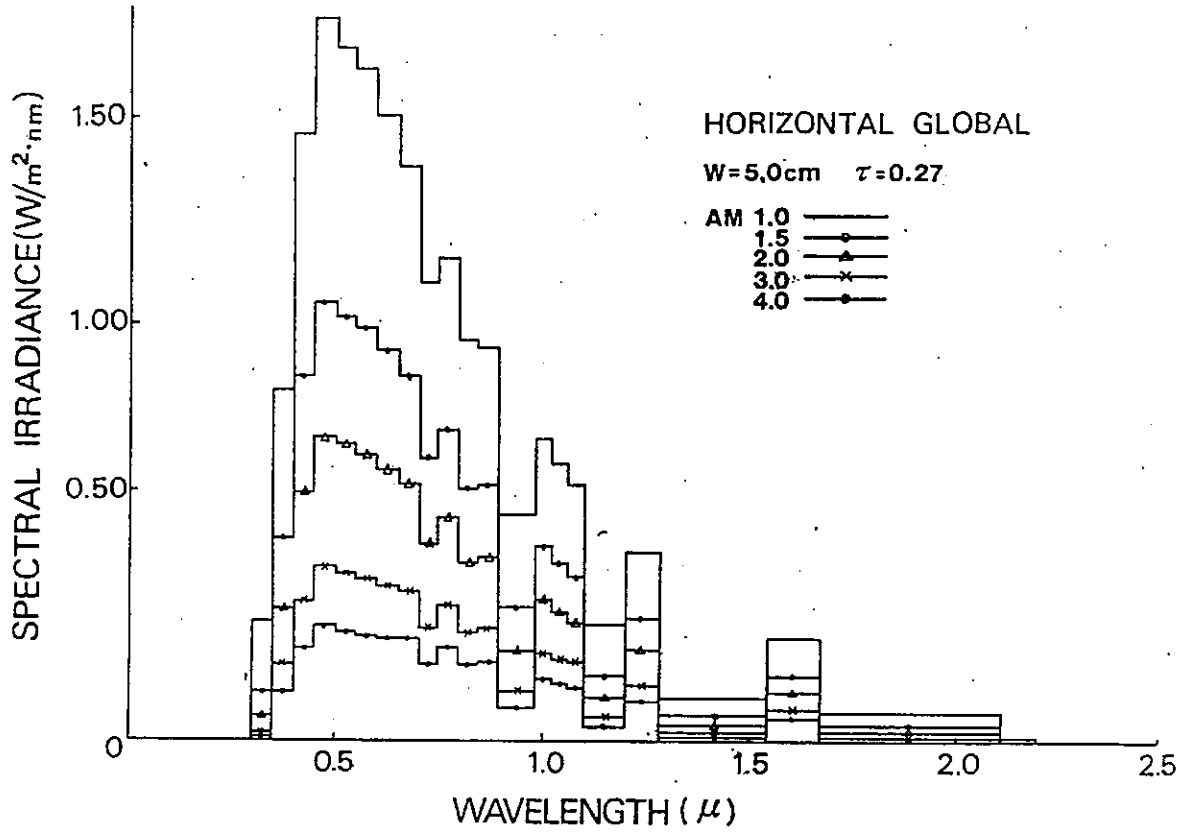

Figure 7.3.2c Calculated horizontal global spectral radiation for aimass 1.0, 1.5, 2.0, 3.0 and 4.0 at $\tau = 0.27$ and w = 5.0cm.

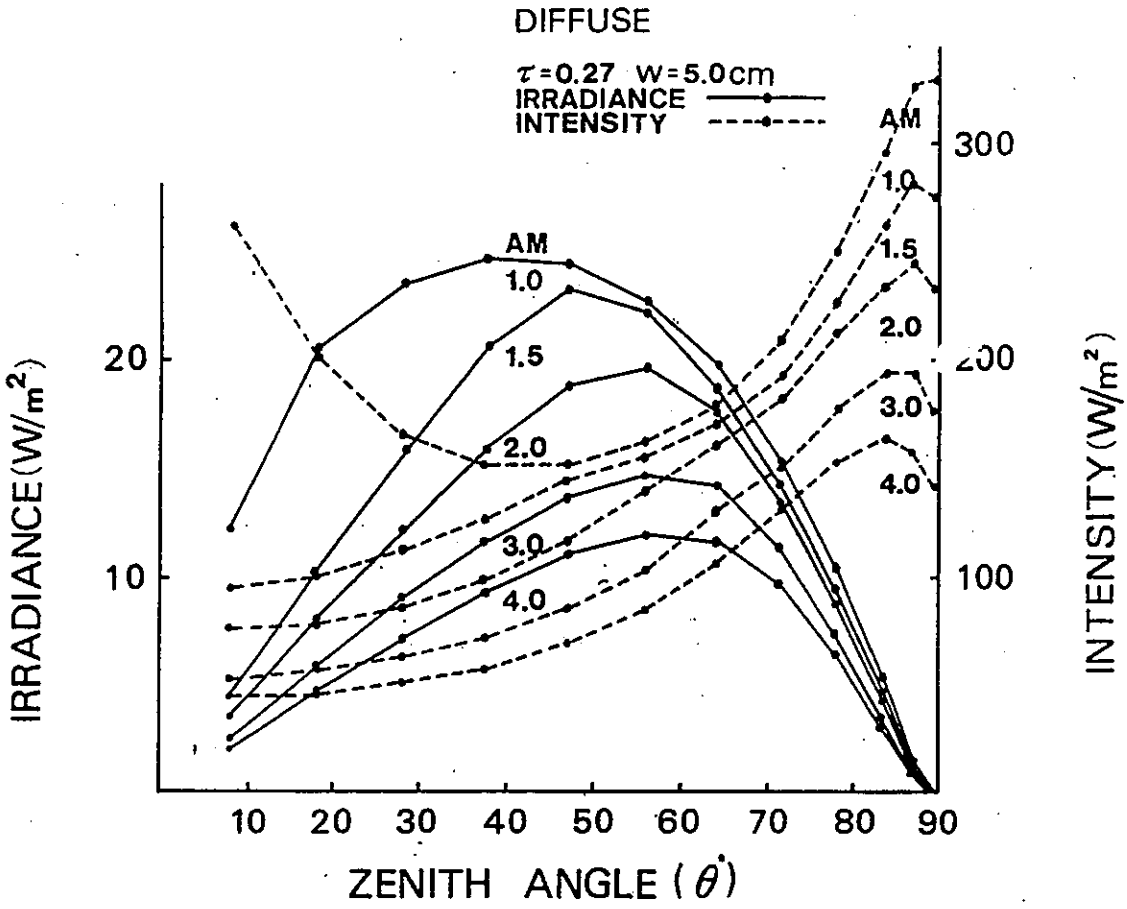

Figure 7.3.2d Calculated diffuse intensity (=π x radiance) and contributions from 10 degree rings of sky to diffuse irradiance, for aimass 1.0, 1.5, 2.0, 3.0 and 4.0 at $\tau = 0.27$ and w = 5.0cm plotted against zenith angle(θ).

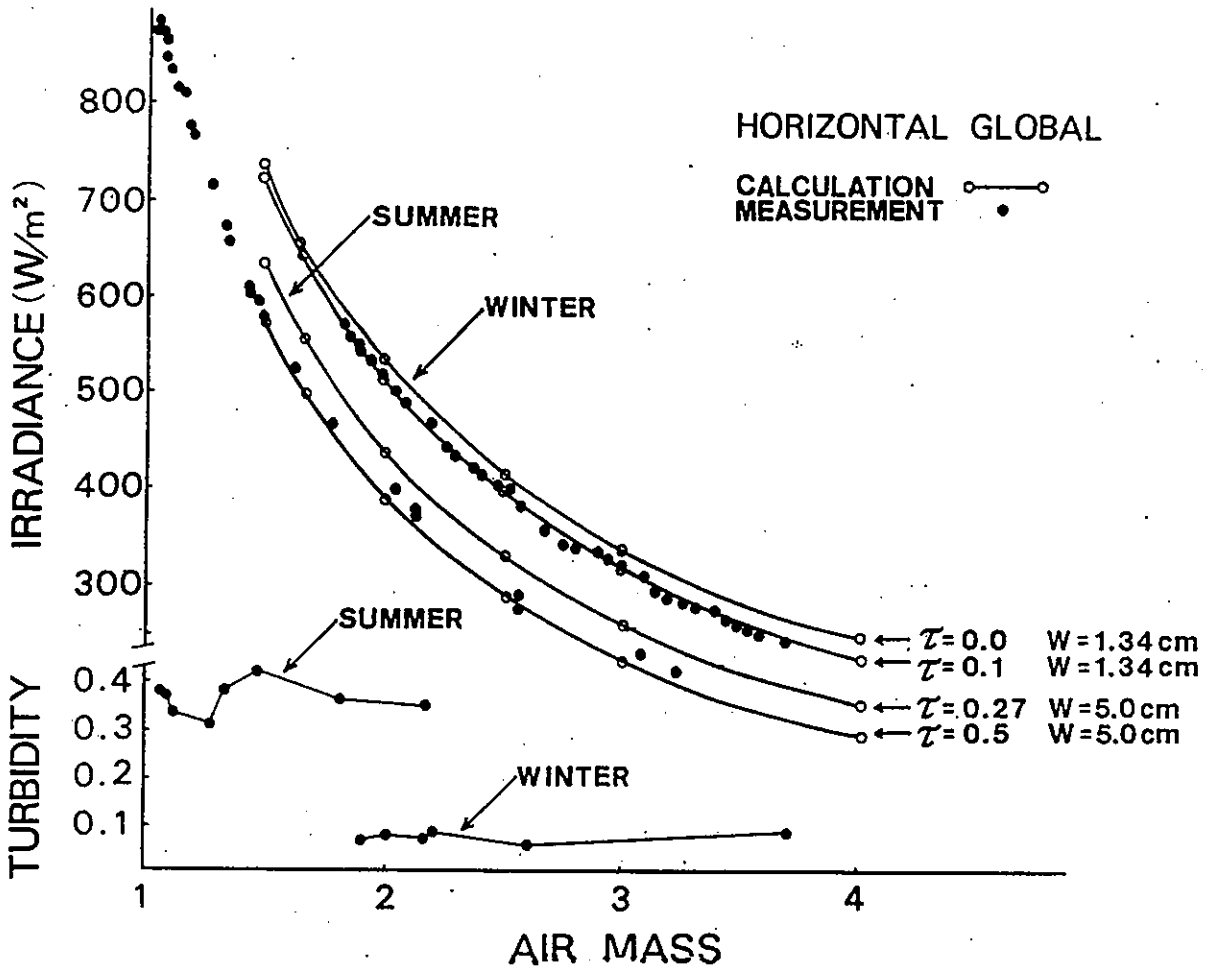

Figure 7.3.2e Measured and calculated horizontal global radiation and measured turbidities plotted against airmass.

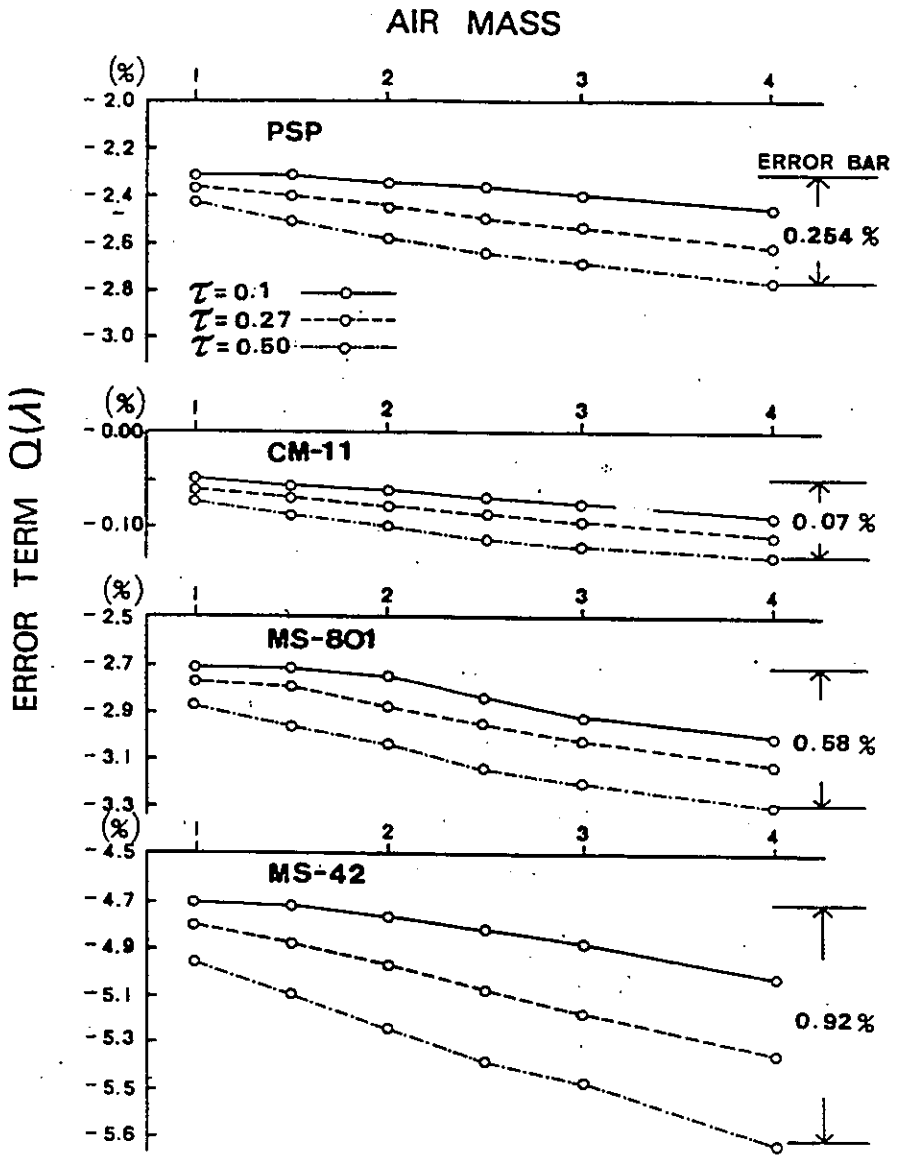

Figure 7.3.3a The spectral "error term" $Q_\lambda(\lambda^*)$ due to spectral response for three pyranometers(PSP, CM-11, MS-801) at τ = 0.1, 0.27, 0.50 as a function of airmass.

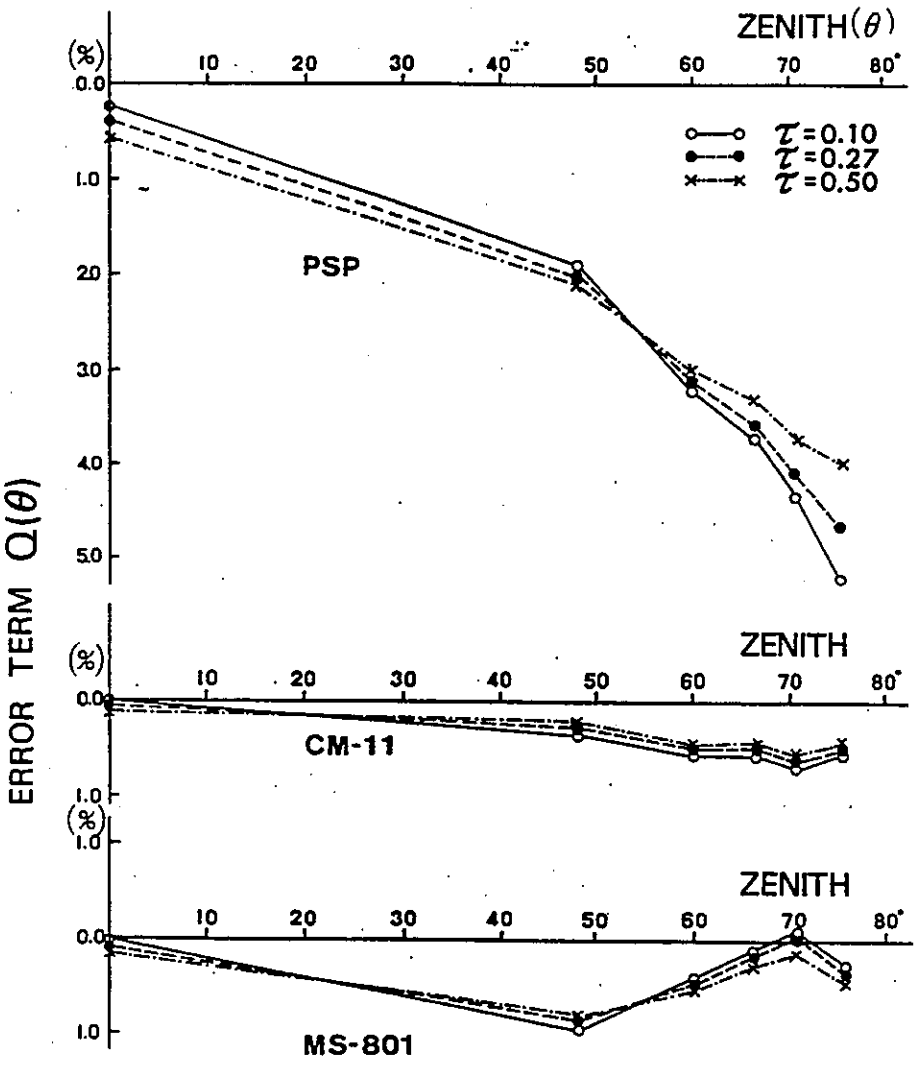

Figure 7.3.3b The directional "error term" $Q_\theta(\theta^*)$ for three pyranometers at τ = 0.1, 0.27, 0.50 as a function of solar zenith angle θ.

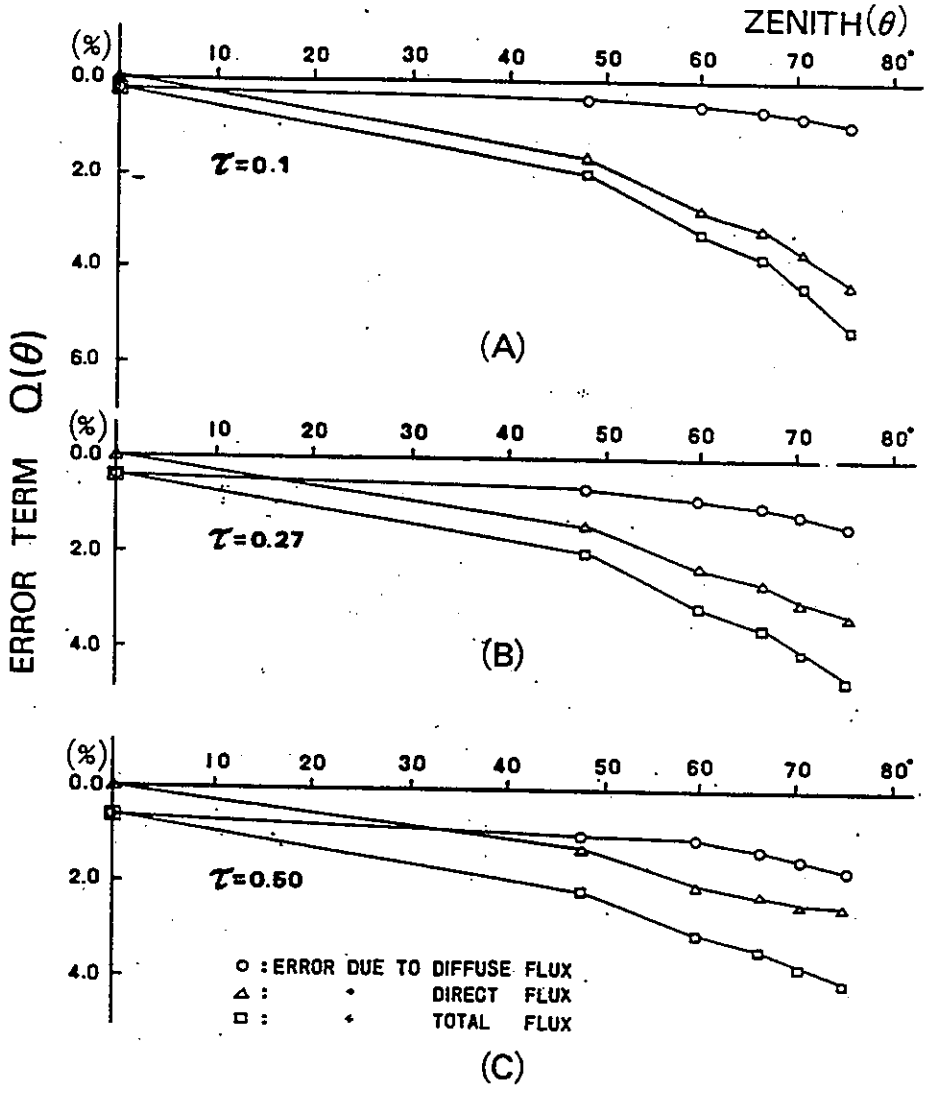

Figure 7.3.3c The directional "error term" $Q_0(\theta^*)$ for the PSP for global, diffuse and direct radiation at τ = 0.1, 0.27, 0.50 as a function of solar zenith angle θ.

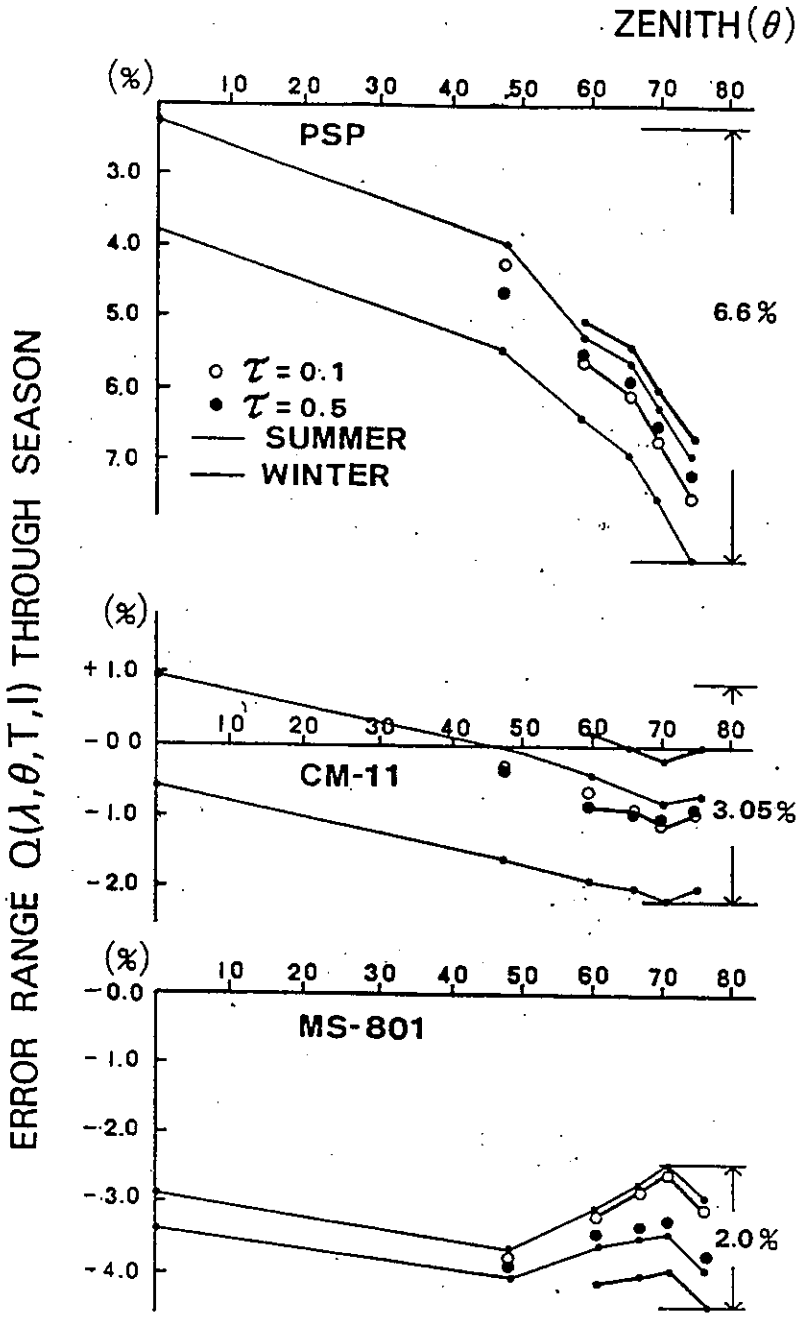

Figure 7.3.3d Combined "error term" $Q(\theta^*,T,E,\lambda^*)$ from wavelength, direction, temperature and non-linearity for three pyranometers through winter and summer conditions plotted against solar zenith angle.

Chapter 8. Matrices of Calibration Results

8.1 Overview

Calibrations were done on twenty six instruments which were circulated through several laboratories and this chapter summarises the results in the form of matrices of responsivity values.

Section 8.2 deals with the responsivities measured by the laboratories according to their individual, routine protocols (some values, measured during previous IEA tasks, are given for comparison). The differences in responsivities obtained by various laboratories on instruments of the same make and model range from about 1.0% rms for the Eppley PSP up to a maximum of 6.6%, or a maximum of 1.8% if a few data are rejected.

Section 8.3 considers responsivities measured under three well-defined benchmark conditions:

1.	BMHO	instrument horizontal	angle of incidence 55°
2.	BMTN	instrument 45° tilted	normal incidence
3.	BMTO	instrument 45° tilted	angle of incidence 55°

Contrary to expectation, improvement in the scatter, compared with the results given in §8.2, can only be demonstrated for two types of pyranometer and for only one benchmark in each case.

In §8.3.6, differences between the three benchmark responsivities measured on the same instruments are examined. Comparison between BMTO and BMHO shows changes in responsivity induced by tilting the pyranometers. The differences between BMTN and BMHO indicate the possible errors caused by incorrectly using a calibration suitable for a meteorological application when measuring tilt irradiance for tests of solar collectors.

8.2 Between institutes for routine calibration

The inter-laboratory discrepancies in pyranometer calibration have been a major concern to researchers in solar conversion technology and meteorology.

8.2.1 Presentation of results

In the responsivity matrix the various pyranometers are arranged in rows and the laboratories, together with the manufacturers, in columns. The owner of an instrument with a manufacturer's calibration could use this matrix to determine the approximate values for other laboratories.

The matrix (Table 8.2a&b) has been compiled from calibrations performed by several laboratories each using in their own protocols on the same set of 25 IEA pyranometers. To ensure better comparability between the four US laboratories during Task 9, SERI loaned a PSP instrument (#17880) and the data from this pyranometer are included. Some values measured during experiments in previous IEA tasks are also given for comparison.

A distinction has been made between the alternating sun/shade method (ASM) which is a direct calibration method (Table 8.2a) and the indirect, or relative, methods. The latter include field calibration by comparison to reference pyranometers and all the results of all indoor methods (Table 8.2b).

The results are expressed as ratios to the values from the coordinating NARC/AES laboratory. The original responsivity, assigned by the manufacturer, is given in the first column and the second column shows the value on the updated WRR scale values for selected instruments (see Riches *et al.*, 1982). The calibrations done by NARC/AES in 1985-1986 (Appendix BB) are given as responsivity values in the third column. The remaining columns express the ratios to NARC/AES and when no NARC/AES value is available the original laboratory responsivity is given in $\mu V\ W^{-1}\ m^2$.

Mean values and standard deviations are also listed. Columns 11 and 12 in Table 8.2a and columns 19 and 20 in Table 8.2b show the means and standard deviations for the direct calibrations and the indirect calibrations, respectively, for each of 24 individual pyranometers and 7 pyranometer types.

Overall means and standard deviations for all routine calibration methods, direct and indirect, are given in Table 8.2a, columns 13 and 14, and in Table 8.2c, which also shows the statistics when six of the 154 ratios are rejected.

Table 8.2a Manufacturers' and round-robin calibrations shade/unshade method, ratios to NARC/AES data

Pyranometer Serial No.	1 Man.	2 WRR	3 NARC	4 Man.	5 WRR	6 SRF	7 Eppl.	8 DSET	9 KNMI	10 Vien.	11 Mean	12 SD	13 Mean overall	14 SD overall
Eppley PSP														
17750	9.26	9.15	9.13	1.014	1.002	1.014				1.020	1.017	0.004	1.014	0.010
17880		8.82					8.778	8.783						
18135		8.78	8.87		0.990								1.000	0.009
20523		9.95	9.78		1.017								1.009	0.005
20524		10.10	9.99		1.011				0.986		0.986	–	1.001	0.007
mean				1.014	1.005	1.014			0.986	1.020	1.007		1.007	
SD				–	0.012	–			–	–		0.018		0.010
Kipp CM5														
773656	12.2	11.94	11.41	1.069	1.046	1.025					1.025	–	1.016	0.011
773992	12.9	12.62	11.99	1.076	1.053	1.013				1.051	1.032	0.027	1.019	0.019
774120	13.7	13.41	12.55	1.092	1.069	1.009	0.9973	1.003			1.003	0.006	1.019	0.010
785047	12.5	12.23	11.62	1.076	1.052	1.010					1.010	–	1.011	0.007
mean				1.078	1.055	1.014	0.997	1.003		1.051	1.015		1.013	
SD				0.010	0.010	0.007	–	–		–		0.018		0.013
Kipp CM10														
810119		4.58	4.62		0.991					1.048	1.048	–	1.003	0.022
810120		4.54	4.53		1.002								1.001	0.003
810121		4.66	4.65		1.002				0.998		0.998	–	0.993	0.009
810122		4.24	4.27		0.993		0.989	1.001			0.995	0.008	0.995	0.009
mean					0.997		0.989	1.001	0.998	1.048	1.009		0.997	
SD					0.006		–	–	–	–		0.026		0.013
Schenck Star														
1626		14.32	14.67		0.976	0.984					0.984		0.922	0.011
2186		14.94	15.30		0.976		0.973	0.973			0.973	0.000	0.978	0.028
2209		15.36	15.10		1.017								1.017	0.016
2217		14.16	13.87		1.021								1.014	0.016
mean					0.998	0.984	0.973	0.973			0.977		0.993	
SD					0.025							0.006		0.025
Eko MS42														
81901		8.24	8.14		1.012								0.998	0.018
81907		7.25	7.12		1.018		1.007	1.011			1.009	0.003	1.004	0.037
81908		9.61	9.50		1.012								1.016	0.008
81909		7.42	7.39		1.004								1.020	0.011
mean					1.011		1.007	1.011			1.009		1.007	
SD					0.006		–	–				0.003		0.027
Swissteco*														
113													1.051	0.051
114													1.061	0.086
mean													1.057	
SD														0.066
Middleton														
123		10.3	10.49		0.982					1.006	1.006	–	0.991	0.019
124		10.7	10.69		1.001								0.997	–
mean					0.992					1.006	1.006		0.992	
SD					0.013									0.017
CSIRO PT														
115														

** ratio NARC/AES 1983 data.*

Legend on the following page.

Legend to Table 8.2a

Column

1. Original manufacturer's values in $\mu V\ W^{-1}m^2$.
2. Manufacturer's values in WRR scale $\mu V\ W^{-1}m^2$.
3. NARC/AES 1985-86, indoors, sphere calibrations with reference pyranometers of like manufacturer in $\mu V\ W^{-1}m^2$. (Appendix BB).
4. Ratio column 1/column 3.
5. Ratio column 2/column 3.
6. SRF/NOAA 1981, outdoors, shade calibration with cavity TMI #67502, p. 174 (Riches *et al.*, 1982).
7. Eppley, 1984, outdoors shade calibration with cavity HF #14915 (p. 27, Griffin & Hickey, 1985).
8. DSET 1985, outdoors, shade calibration with cavity SN #7142, Table 23 (Zerlaut & Maybee, 1985).
9. KNMI, De bilt 1984, outdoors, shade calibration with Kipp Linke-Feussner 610037 and SMHI Ångström 559 (Slob, personal communication).
10. ZAMG Vienna 1985, outdoors, shade calibration with Linke-Feussner, Table 1 (Motschka & Wessely, 1985).
11. Mean values from columns 6-10 for individual pyranometers and pyranometer type.
12. Standard deviations from columns 6-10 for individual pyranometers and pyranometer type.
13. Mean values for all calibration methods (Tables 8.2a&b together).
14. Standard deviations for all calibration methods (Tables 8.2a&b together).

Table 8.2b Round-robin routine calibrations, relative methods, ratios to NARC/AES data

Pyranometer Type & Serial No.	1 Davos	2 SRF	3 DSET	4 SERI	5 Davos	6 NARC	7 SRF	8 SRF	9 Norrk	10 TPD	11 Vien	12 NARC	13 Davos	14 NARC	15 Eppl	16 Eppl	17 Hamb	18 Kipp	19 Mean	20 SD
Eppley PSP																				
17750	1.015				1.019	1.012	1.014				1.035	1.002		1.005			1.002		1.013	0.011
17880		8.688	8.729	8.489											8.60	8.59			--	--
18135	1.006											0.990		1.003					1.000	0.009
20523	1.012								1.003					1.012					1.009	0.005
20524	1.002									1.002			1.001	1.003				1.007	1.003	0.002
mean	1.009				1.019	1.012	1.014		1.003	1.002	1.035	0.996	1.001	1.006			1.002	1.007	1.008	
SD	0.006				--	--	--				--	0.008	--	0.004			--	--		0.009
Kipp CM5																				
773656	1.027				1.031	1.006	1.017			1.008		1.008	1.011	1.002				1.030	1.016	0.011
773992	1.014				1.033	0.998	1.009				1.051	1.003	1.009	1.002			1.026		1.016	0.017
774120	1.020	1.000	1.020	1.000	1.026	1.001	1.013	0.997				1.002	1.005	1.006	1.029	1.012			1.010	0.011
785047	1.022				1.015	1.005	1.004		1.019			1.007	1.018	1.002					1.011	0.008
mean	1.021	1.000	1.020	1.000	1.026	1.002	1.011	0.997	1.019	1.008	1.051	1.005	1.011	1.003	1.029	1.012	1.026	1.030	1.013	
SD	0.005	--			0.008	0.004	0.006	--	--	--	--	0.003	0.005	0.002	--	--	--	--		0.012
Kipp CM10																				
810119	0.994										0.985		0.998	1.000			0.996		0.995	0.006
810120	0.998								1.004				1.002	1.000					1.001	0.003
810121	0.994									0.994			0.976	1.000				0.998	0.992	0.010
810122	0.998	0.990	0.995	0.997				0.991					1.000	0.998	1.014	0.979			0.995	0.010
mean	0.996	0.990	0.995	0.997				0.991	1.004	0.994	0.985		0.994	0.999	1.014	0.979	0.996	0.998	0.995	
SD	0.004	--	--	--				--	--	--	--		0.012	0.001	--	--	--	--		0.008
Schenck Star																				
1626	0.998				0.986	0.989	0.980		0.997			0.988	1.019	0.994					0.993	0.012
2186	0.990	0.990	0.979	1.003				0.984					1.023	0.986	0.928	0.928			0.979	0.032
2209	1.013									1.007			1.044	1.003				1.019	1.017	0.016
2217	1.022																			
mean	1.003	0.990	0.979	1.003	0.986	0.989	0.980	0.984	0.997	1.007		0.988	1.027	0.995	0.928	0.928		1.019	0.995	
SD	0.017	--	--	--	--	--	--	--	--	--		--	0.011	0.007	--	--		--		0.026

Continued...

Table 8.2b *Concluded*

Pyranometer Type & Serial No.	1 Davos	2 SRF	3 DSET	4 SERI	5 Davos	6 NARC	7 SRF	8 SRF	9 Norrk	10 TPD	11 Vien	12 NARC	13 Davos	14 NARC	15 Eppl	16 Eppl	17 Hamb	18 Kipp	19 Mean	20 SD
EKO MS-42																				
81901	0.998						1.012		0.983				0.979	1.020					0.998	0.018
81907	1.039	1.023	1.028	1.018				1.010					1.027	1.017	0.923	0.941			1.003	0.041
81908	1.013									1.025			1.024	1.008				1.009	1.016	0.008
81909	1.008												1.027	1.026					1.020	0.011
mean	1.014	1.023	1.028	1.018			1.012	1.010	0.983	1.025			1.014	1.018	0.923	0.941		1.009	1.007	
SD	0.017	--	--	--									0.024	0.008	--	--		--		0.028
Swissteco*																				
113									1.015				1.087	15.1					1.051	0.051
114										1.029			1.158	15.6				0.996	1.061	0.086
mean									1.015	1.029			1.122					0.996	1.057	
SD									--	--			0.050					--		0.066
Middleton P07																				
123											0.994			0.999			0.963		0.985	0.020
124														0.997					0.997	--
mean											0.994			0.998			0.963		0.988	
SD											--			0.001			--			0.017
CSIRO PT																				
115										3.94								3.81	--	--

** ratio NARC/AES 1983 data*

Legend on the following page.

Legend to Table 8.2b

Column

1. Davos 1981-82, outdoors, component summation with cavity PMO 2 and group of PSP and CM10 pyranometers, p. 16 (Ambrosetti *et al.*, 1984).

2. SRF/NOAA 1983-84, outdoors, component summation with cavity TMI 67502 and PSP 19917, p. 9 (Flowers, 1985).

3. DSET 1985, outdoors, component summation with cavity SN 17142 and PSP 19129, Table 40 (Zerlaut & Maybee, 1985).

4. SERI 1985, outdoors, component summation with Eppley NIP and group of PSP and CM10 pyranometers (Wells & Myers, 1986).

5. Davos 1980, outdoors, with ref. pyranometer PD 6703 A, p. 62 (Riches *et al.* 1982).

6. NARC/AES 1980-81 outdoors with various ref. pyranometers (p. 62, Riches *et al.*, 1982).

7 SRF/NOAA 1981, outdoors with ref. pyranometer PSP 19917, Appendix G iv (Riches *et al.*, 1982).

8. SRF/NOAA 1984, outdoors with ref. pyranometer PSP #19918, p. 10. Table 2 weighted averages (Flowers, 1985).

9. Norrköping 1984, outdoors, with ref. pyranometer CM10 #810132, Table 4.2.1.4e col 2 (also Dahlgren, 1987).

10. TPD/TNO 1984, outdoors, with ref. pyranometer CM10 #820078, p. 50-51 (van den Brink *et al.*, 1985).

11. ZAMG Vienna 1984-85, outdoors, with Schenk Star ref. pyranometer, Tables 17-20 (Motschka & Wessely, 1985).

12. NARC/AES 1981, indoors, sphere calibration with reference pyranometers from the same manufacturer (Wardle, 1982).

13. Davos 1982, indoors, Xenon-lamp, Appendix b (Ambrosetti *et al.*, 1984).

14. NARC/AES 1982-'83, indoors, sphere calibration with ref. pyranometers of like manufacturer (Wardle, 1982).

15. Eppley June 1984, indoors, hemisphere calibration with ref. pyranometer PSP 21231, p. 8 Table IV (Griffin & Hickey, 1985).

16. Eppley Sept.-Dec. 1984, indoors, hemisphere calibration with ref. pyranometer 21231, p. 8 Table IV (Griffin & Hickey, 1985).

17. Hamburg 1984, indoors, with PSP, CM5 and CM10 pyranometers, p. 10 (Dehne & Trapp, 1986).

18. Kipp Delft 1984, indoors, Xenon-lamp minus 1% correction with ref. pyranometer CM10 #800074, p. 25 Tables I-13 (van den Brink *et al.*, 1985).

19. Mean values for individual pyranometers and pyranometer type.

20. Standard deviations for individual pyranometers and pyranometer type.

Table 8.2c Results from 17 routine calibration methods used by 10 laboratories: results relative to the NARC indoor sphere technique

Instrument	Mean ± SD	N
Eppley PSP	1.007 ± 0.010	21
Kipp CM5	1.013 ± 0.013	46
Kipp CM10	0.997 ± 0.013	27
Schenk Star	0.993 ± 0.025	26
Eko MS -42	1.007 ± 0.027	24
Swissteco SS25	1.057 ± 0.066	5
Middleton EP07	0.992 ± 0.017	5
Schenk minus 2	0.998 ± 0.018	24
Eko minus 2	1.014 ± 0.014	22
Swissteco - 2	1.014 ± 0.015	3
All	1.006 ± 0.024	154
All minus 6	1.006 ± 0.015	148

8.2.2 Discussion of results for routine calibrations

A notable result, evident in Table 8.2c, is the small standard deviation (≤1.3%) for the Eppley and Kipp pyranometers compared with the other makes. The closest agreement between the calibration factors obtained by the different laboratories and NARC/AES values has been found for the CM10 instruments. The Swissteco results show the largest average departure from NARC, 5.7%, and the largest standard deviation, 6.6%.

Six of the one hundred and fifty four ratios are more than 6% away from the mean. These comprise the Eppley calibrations of the Schenk (2) and Eko (2) instruments and the World Radiation Centre calibrations of the Swissteco (2) instruments. It appears highly probable that there have been mistakes or misunderstandings in generating these calibration ratios. Excluding them from the analysis reduces the overall standard deviation from 2.4% to 1.5% and causes the standard deviations for each pyranometer type to be all less than, or equal to, 1.8%. The rejected data are thus all more than four standard deviations from the mean.

It might be expected that responsivities obtained outside with the ASM calibration would be less variable, because the method is direct, than those measured by indirect methods. However, a comparison between column 12 (Table 8.2a) and Column 20 (Table 8.2b) shows that only the Schenk and Eko instruments have larger standard deviations for the indirect calibration method.

The alternating sun/shade method is a direct calibration delivering absolute responsivities. The accuracy of the calibration result depends on the quality of the reference pyrheliometer (Angstrom, Linke-Feussner, cavity type) and how well the angle by which the shaded disk screens the pyranometer matches the angle of view of the pyrheliometer. There are also differences between calibrations made on an instrument using a suntracker and those using a horizontal platform, presumably because they give different diffuse/direct irradiance ratios.

This direct calibration method can sometimes produce more scatter in the results, depending on wind and dust, than those derived by the other methods where integrated values from pyranometers of the same type are compared.

For the indirect methods, where the pyranometer under test is compared partly or totally with a reference or standard pyranometer, it is important to know what type of pyranometer has been used as the standard. The type of the reference pyranometer that was used is included in the legend to Table 8.2b for this reason. Calibration of a CM10 pyranometer against a standard CM10 gives slightly different results from those obtained in calibration against a standard PSP because CM10 and PSP instruments may have different infrared responsivities, temperature responses, different materials in the hemispherical domes, different zero offsets, et cetera. A reference pyranometer of the same type as that being tested should give the best results

The legend to Table 8.2b shows that CM5, CM10 and PSP pyranometers were most often used as the reference for the indirect methods. Only in Davos (column 5) and Vienna (column 11) have other types been used as the reference for all the calibrations (a PD and Schenk Star, respectively). If these observations are excluded, the standard deviation given in column 20 decreases for the Eppley PSP (0.009 to 0.006) and Kipp CM5 (0.012 to 0.009) but increases for the Schenk Star (0.026 to 0.027) and Middleton (0.017 to 0.020). Deleting the results from Davos and Vienna has no influence on the standard deviation for the Kipp CM10 which remains at 0.008.

8.3 Benchmark calibrations

8.3.1 Benchmark rationale and definitions

The routine calibrations by the laboratories are designed either for their individual locations and climate or for some individually chosen range of applications. These are different for the various laboratories which inevitably accounts for some of the variation seen in Tables 8.2a&b.

To simplify comparison between laboratories, three sets of standard benchmark conditions were defined under Task 9. These should eliminate or greatly reduce the effects of different or imprecise definitions so that the residual discrepancies can be assigned to experimental errors.

The definitions given in Table 8.3.1a result from discussions at the November 1985 and June 1986 meetings of Task 9 and differ slightly from earlier versions, the first of which was proposed in March 1981. They have been used in Task 9 and it is hoped that they will be adopted more widely in the future.

All the participants in Task 9 were asked to supply benchmark calibrations for a group of pyranometers by methods of their own choice (implicitly those which they believe to be the most accurate). The method of choice could comprise any combination of indoor or outdoor measurement procedures and need not, for example, include outdoor measurement in the specified benchmark conditions. The wide range of techniques involved in this arrangement should reduce the probability of undetected common systematic errors and it is hoped that the comparison will yield a valid estimate of current laboratory accuracy.

8.3.2 Caveat on the benchmark definitions

In principle the definitions specify the environmental conditions so completely that the responsivity value is unique. It would be cumbersome to do this in practice and unnecessarily restrictive. Wind, type of ventilator housing, humidity and the distribution of diffuse radiation are not specified and neither is the relative solar azimuth in the case of BMTO. These factors (which should be documented by the experimenter) will cause some small variation in responsivity but, despite this, the benchmarks should permit a greater degree of reproducibility between calibrations than has been achieved until now.

Table 8.3.1a Benchmark definitions

Name	Horizontal-Oblique	Tilted-Normal	Tilted-Oblique
Abbreviation	BMHO	BMTN	BMTO
Instrument Tilt	zero	45°	45°
Direction of instrument cable [1]	toward sun & horizontal	down at 45° tilt	down at 45° tilt
Angle of Incidence	55°	zero (normal incidence)	55°
Solar Elevation [2]	35°	45°	<80°
Solar Azimuth Relative to Pyranometer [2] (cable direction = 0)	zero	not definable	<-45.6° or >45.6°
Direct Irradiance (reading on NIP)	900 Wm^{-2}	900 Wm^{-2}	900 Wm^{-2}
Diffuse Irradiance	100 Wm^{-2}	100 Wm^{-2}	100 Wm^{-2}
Global Irradiance [2]	616 Wm^{-2}	1000 Wm^{-2}	616 Wm^{-2}
Temperature	15 C	15 C	15 C

1. Chosen as the azimuth reference direction for the pyranometer. It is the direction, orthogonal to the axis, going from the centre of the pyranometer outwards through the connector.
2. Given for clarification only (can be derived from the other specifications).

8.3.3 Uses of benchmark calibrations

The main purpose, as previously stated, is to facilitate the comparison of calibration results from different laboratories. However the three definitions were chosen to allow two other uses. First, two of the benchmarks provide responsivities that can be useful for specific applications. Second, the ratios between the three benchmark responsivities on individual instruments indicate tilt, non-linearity and directional effects in those instruments. The three uses are considered in more detail below.

8.3.3.1 Comparison of results from different laboratories

The accuracy of a benchmark calibration may not be significantly degraded by the uncertainty of specification (§1.6) but, as with other calibrations, it is subject to:

- ***Technical errors*** for example, there may be a mistake in a computer algorithm which corrects for temperature or there may be undetected malfunctions in the shading or tracking equipment.
- ***Errors of judgment*** for example, if the calibration was by the ASM, the shaded period might be too short, or the experimenter may have used averaged data at

different azimuths/temperatures and may have thought wrongly that the variation was insignificant in that particular pyranometer.

- ***Noise in the pyranometer signal.*** from variability in thermal offsets, wind effects, continuing variable cloudy conditions during outdoor calibrations.
- ***Inadequate data acquisition*** instability, poor resolution or a too-slow sampling rate.

The distinction between the four types of error may not always be clear but this is less important than their overall effect which is to limit the accuracy of the irradiance measurement.

When results from the same instruments used at several laboratories are compared there will be discrepancies resulting from combinations of these errors and the spread of the results can be used as an approximate indication of the combined error magnitude. Thus, provided there is no *a priori* reason to reject results from any one laboratory, the spread in calibration factors expresses a lower limit to the uncertainty of the irradiance measurement by this group of laboratories in near-benchmark conditions. The comparison will not reveal common systematic errors. Other factors, particularly directionality of response, may degrade the overall accuracy for measurements that are not in conditions close to those of the calibration (benchmark).

In practice, there may perhaps be one laboratory whose results are significantly outside the range of the others. It should then be possible to identify the problem and make the appropriate corrections. In practice also, it has to be recognised that the benchmark methods may not all have been developed independently from first principles. Some laboratories may, for good reasons, have copied the techniques from others and may have chosen references so as to be consistent with other laboratories. Inferences on accuracy based on observed reproducibility of calibration values would be optimistic if this non-independence were ignored (i.e. the systematic errors in common, mentioned above).

8.3.3.2 Use of benchmark calibrations to calculate irradiance

In the common situation when a single responsivity is required for an application, a suitable average over the conditions of use should be selected. Benchmark calibrations are specifically not such averages but BMHO and BMTN are in fact suitable for application. For example, the BMHO calibration might be a reasonable choice for monitoring horizontal irradiance in middle latitudes provided there is no significant azimuth variation in the pyranometer response. The BMTN responsivity is suitable and can be recommended for

collector testing where the narrow range of incidence angles (near normal incidence) and the usual restriction to high irradiance are such that variation in responsivity is small. The difference between BMHO and BMTN shows the error that could arise from using a responsivity chosen for a meteorological application when measuring high irradiance values on a sloping surface as required when testing solar collectors.

8.3.3.3 Use of benchmark calibrations to illustrate pyranometer characteristics

The definition of the benchmark conditions in Table 8.3.1 specify angle of incidence, tilt angle and intensity of the radiation. Measuring and comparing the benchmark responsivities therefore provides some degree of instrument characterization. For example, the comparison of results from BMHO and BMTO should show the effect of tilting the pyranometer because the intensity and angle of incidence are the same in each case, although the relative azimuth angles are different. Similarly, the ratio BMTN/BMTO indicates the combined effect of non-linearity and directionality.

8.3.4 Measurements of the benchmark responsivities

There is a great variation in the way the benchmark responsivities, given in Tables 8.3.3a&b, have been derived. Normally the measurements have not been made exactly at the conditions specified by the benchmark definitions so that some interpolation or extrapolation is necessary. This primarily concerns the functions for correcting non-linearity to obtain the defined irradiance level and temperature to arrive at the defined temperature of 15°C (see Table 8.3.1a).

It is not clear whether all the laboratories made these corrections. Some laboratories give an explanation of how the benchmark responsivities have been measured while others simply report the benchmark data. Some of the results used here were obtained from graphs or by interpolating values from tables. The legend to Table 8.3.3a and the following descriptions give an indication on how well the benchmark responsivities from the various laboratories satisfy the benchmark definitions.

NARC

The NARC has used data with the following restrictions, to establish the benchmark calibrations:

- direct beam >700 Wm^{-2}
- BMHO solar zenith angle between 50° and 60°
- BMTN angle between sun and pyranometer axis less than 20°
- BMTO angle between sun and pyranometer axis between 50° and 60°.

The data were normalised, using linear regression, to global radiation values of either 1000 Wm^{-2} for BMTN or 600 Wm^{-2} for BMHO and BMTO. Results for instruments which are believed to have significant temperature coefficients of responsivity have been corrected to 15°C.

SRF

The BMHO responsivities have been calculated from interpolating graphs of the responsivity against solar elevation to 35°. No temperature corrections have been made.

Eppley

The BMHO responsivities have been calculated by interpolating from tables given in Griffin and Hickey (1985) showing the shading calibrations as a function of solar elevation to a solar elevation of 35°. No other corrections have been made.

DSET

The IEA benchmark test was performed by transfer of calibration from the reference radiometer PSP 19129 during the 0° horizontal comparisons. This was done by simply selecting the data that matched the required beam irradiance of approximately 900 Wm^{-2} and a solar elevation of 35° during the horizontal, and 40° during the tracking, normal incidence experiments. The BMHO benchmark tests were performed at a beam irradiance of 832 Wm^{-2} and a solar elevation of 35°. The derived instrument constants were then normalised from the test temperature of 22°C to 15°C. The BMTN benchmark tests were performed at a beam irradiance of 945 Wm^{-2} and a solar elevation of 40°. The instrument constants were then normalised to a temperature of 15°C.

SERI

The BMHO SERI data were provided by C.V. Wells (personal communication).

Norrköping

The benchmark data were provided by L. Dahlgren and are described in § 4.2.1.4.

Hamburg

The responsivities at benchmark conditions were not measured directly but were derived from the responsivities measured during the normal calibration and also from the tested specifications of the round robin and reference pyranometers. The data given in Dehne and Trapp (1986) were corrected by Dehne in a letter of the 2nd April, 1987.

TPD/TNO

The BMHO responsivities have been calculated by interpolation in a table comprising responsivities as a function of solar altitude.

Table 8.3.3a Benchmark calibrations, ratios to NARC/AES data

	BMHO .Tilt Zero											BMTN Tilt 45° Normal Incidence						BMTO Tilt 45° Incidence 55°				
Pyranometer Type & Serial No.	1	2	3	4	5	6	7	8	9	10	11	12	13	14	15	16	17	18	19	20	21	22
	NARC	SRF	SRF	Eppl	DSET	SERI	Norrk	Hamb	TPD	*Mean*	*SD*	NARC	DSET	Norrk	Hamb	*Mean*	*SD*	NARC	Norrk	Hamb	Mean	SD
Eppley PSP																						
17750		9.16						9.15		--	--	9.31			1.002	1.002	--			9.15	--	--
17880			8.59	8.612	8.762	8.634				--	--		8.810			--	--					
18135	8.92											8.98					--	8.91			--	--
20523							9.81			--	--	9.96	--	0.999		0.999	--		9.68	--	--	
20524									9.98	--	--	10.17										
mean		--	--	--	--	--	--	--	--	--			--	0.999	1.002	1.000			--	--	--	
SD		--	--	--	--	--	--	--	--		--		--	--	--		0.002		--	--		--
Kipp CM5																						
773656	11.46								0.998	0.998	--	11.35						11.44				
773992	12.05	1.012						0.996		1.004	0.011	11.84			1.014	1.014	--	11.91		1.008	1.008	--
774120	12.52	1.020	1.002	0.998	1.026	1.020				1.013	0.012	12.48	0.998			0.998	--	12.55				
785047	11.73						1.009			1.009		11.34		1.034		1.034	--	11.45	1.037		1.037	--
mean		1.016	1.002	0.998	1.026	1.020	1.009	0.996	0.998	1.009			0.998	1.034	1.014	1.015			1.037	1.008	1.022	
SD		0.006	--	--	--	--	--	--	--		0.011		--	--	--		0.018		--	--		0.021
Kipp CM10																						
810119	4.62							0.996		0.996	--	4.62			1.004	1.004	--	4.63		0.994	0.994	--
810120							4.55			--	--	4.49		1.018		1.018	--		4.54		--	--
810121	4.64								0.996	0.996	--	4.62						4.65				
810122	4.25		0.995	0.995	1.019	1.005				1.003	0.011	4.22	0.993			0.993	--	4.24				
mean			0.995	0.995	1.019	1.005	--	0.996	0.996	1.001			0.993	1.018	1.004	1.005			--	0.994	0.994	
SD			--	--	--	--	--	--	--		0.010		--	--	--		0.013		--	--		
Schenck Star																						
1626							14.63			--	--			13.94		--	--		14.27		--	--
2186			15.24	14.81	15.40	15.31		15.08		--	--		14.59			--	--					
2209									15.04	--	--	14.76										
2217	13.99											13.33						13.51				
mean			--	--	--	--	--		--	--			--	--		--			--		--	
SD			--	--	--	--	--		--		--		--	--			--		--			--

Continued...

Table 8.3.3a *concluded*

	BMHO Tilt Zero											BMTN Tilt 45° Normal Incidence						BMTO Tilt 45° . Incidence 55°				
Pyranometer Type & Serial No.	1	2	3	4	5	6	7	8	9	10	11	12	13	14	15	16	17	18	19	20	21	22
	NARC	SRF	SRF	Eppl	DSET	SERI	Norrk	Hamb	TPD	*Mean*	*SD*	NARC	DSET	Norrk	Hamb	*Mean*	*SD*	NARC	Norrk	Hamb	*Mean*	*SD*
Eko MS-42																						
81901							8.00			--	--			7.93		--	--		7.79		--	--
81907			7.33	7.236	7.348	7.180				--	--		6.86			--	--					
81908	9.68								0.992	0.992	--	9.41						9.57				
81909	7.63											7.29						7.54				
mean			--	--	--	--			0.992	0.992			--	--					--		--	
SD			--	--	--	--			--		--		--	--			--		--			--
Swissteco																						
113	14.94						1.026			1.026	--	15.33		1.005		1.005	--	15.19	1.003		1.003	--
114									15.86	--	--	15.76						15.65				
mean							1.026		--	1.026				1.005		1.005			1.003		1.003	
SD							--		--		--			--			--		--			--
Middleton EP07																						
123	10.14							0.996		0.996	--	10.32			0.998	0.998	--	10.24		0.986	0.986	--
124	10.37											10.63						10.38				
mean								0.996		0.996					0.998	0.998				0.986	0.986	
SD								--			--				--		--			--		--
CSIRO PT																						
115	3.91								3.84													
mean																						
SD																						

Legend on the following page.

Legend to Table 8.3.3a

Column

1. NARC/AES 1986, 900 Wm^{-2}, 15 C $\mu V\, W^{-1} m^2$ Appendix BB.
2. SRF/NOAA 1981, 35 C, p. 183 (Riches *et al.*, 1982).
3. SRF/NOAA 1984, p. 17-20, 25 (Flowers, 1985).
4. Eppley, 1984, 775 Wm^{-2}, 25 C, p. 24-26 (Griffin & Hickey, 1985).
5. DSET, 1985, 832 Wm^{-2}, 15 C, Table 45 (Zerlaut & Maybee, 1985).
6. SERI, 1985, (Wells, personal communication).
7. Norrköping 1984, 765 Wm^{-2}, 15.7 C Table 4.2.1.4e col 4 (also Dahlgren, 1987).
8. Hamburg 1984, 900 Wm^{-2}, 15 C (correction to p. 37, Dehne & Trapp, 1986).
9. TPD/TNO Delft 1984, 20 C, p. 44 minus 1% correction (van den Brink *et al.*, 1985).
10. Mean values for BMHO individual pyranometers and pyranometer type.
11. Standard deviations for BMHO individual pyranometers and pyranometer type.
12. see 1.
13. DSET 1985, 945 Wm^{-2}, 15 C, p. 11, Table 45 (Zerlaut & Maybee, 1985).
14. Norrköping 1985, Table 4.2.1.4f col 1.
15. See 8.
16. Mean values for BMTN individual pyranometers and pyranometer type.
17. Standard deviations for BMTN individual pyranometers and pyranometer type.
18. See 1.
19. Norrköping 1985, Table 4.2.1.4f col 3.
20. See 8.
21. Mean values for BMTO individual pyranometers and pyranometer type.
22. Standard deviations for BMTO individual pyranometers and pyranometer type.

Table 8.3.3b Ratios of benchmark calibrations

Pyranometer Type & Serial No.	BMTO / BMHO					BMTN / BMTO					BMTN / BMHO					
	1	2	3	4	5	6	7	8	9	10	11	12	13	14	15	16
	NARC	Norrk	Hamb	*Mean*	*SD*	NARC	Norrk	Hamb	*Mean*	*SD*	NARC	DSET	Norrk	Hamb	*Mean*	*SD*
Eppley PSP																
17750			1.000	1.000	--			1.020	1.020	--				1.020	1.020	--
17880												1.005				1.005
18135	0.999			0.999	--	1.008			1.008	--	1.007				1.007	--
20523		0.987		0.987	--		1.028		1.028	--			1.014		1.014	--
20524																
mean	0.999	0.987	1.000	0.995		1.008	1.028	1.020	1.019		1.007	1.005	1.014	1.020	1.012	
SD	--	--	--		0.007	--	--	--		0.010	--	--	--	--		0.007
Kipp CM5																
773656	0.998			0.998	--	0.992			0.992	--	0.990				0.990	--
773992	0.988		1.000	0.994	0.008	0.994		1.000	0.997	0.004	0.983			1.000	0.991	0.012
774120	1.002			1.002	--	0.994			0.994	--	0.997	0.969			0.983	0.020
785047	0.976	1.003		0.990	0.019	0.990	0.998		0.989	0.001	0.967		0.991		0.979	0.017
mean	0.991	1.003	1.000	0.995		0.993	0.988	1.000	0.993		0.984	0.969	0.991	1.000	0.985	
SD	0.012	--	--		0.011	0.002	--	--		0.004	0.013	--	--	--		0.013
Kipp CM10																
810119	1.002		1.000	1.001	0.001	0.998		1.009	1.003	0.008	1.000			1.009	1.004	0.006
810120		0.998		0.998			1.007		1.007	--			1.004		1.004	--
810121	1.002			1.002	--	0.994			0.994	--	0.996				0.996	--
810122	0.998			0.998	--	0.995			0.995	--	0.993	0.968			0.981	0.018
mean	1.001	0.998	1.000	1.000		0.996	1.007	1.009	1.001		0.996	0.968	1.004	1.009	0.995	
SD	0.002	--	--		0.002	0.002	--	--		0.007	0.004	--	--	--		0.014
Schenck Star																
1626		0.975		0.975	--		0.977		0.977	--			0.953		0.953	--
2186												0.948			0.948	--
2209																
2217	0.966			0.966	--	0.987			0.987	--	0.953				0.953	--
mean	0.966	0.975		0.970		0.987	0.977		0.982		0.953	0.948	0.953		0.951	
SD	--	--			0.006	--	--			0.007	--	--	--			0.003

Continued...

Table 8.3.3b *Concluded*

Pyranometer Type & Serial No.	BMTO / BMHO					BMTN / BMTO					BMTN / BMHO					
	1	2	3	4	5	6	7	8	9	10	11	12	13	14	15	16
	NARC	Norrk	Hamb	*Mean*	*SD*	NARC	Norrk	Hamb	*Mean*	*SD*	NARC	DSET	Norrk	Hamb	*Mean*	*SD*
Eko MS-42																
81901		0.974		0.974	--		1.018		1.018	--			0.991		0.991	--
81907												0.934			0.934	--
81908	0.989			0.989	--	0.983			0.983	--	0.972				0.972	--
81909	0.988		0.988	0.988	--	0.967			0.967	--	0.955				0.955	--
mean	0.988	0.974		0.984		0.975	1.018		0.989		0.964	0.934	0.991		0.963	
SD	0.001	--			0.008	0.011	--			0.026	0.012	--	--			0.024
Swissteco																
113	1.017	0.994		1.005	0.016	1.009	1.011		1.010	0.001	1.026		1.005		1.015	0.015
114						1.007			1.007							
mean	1.017	0.994		1.005		1.008	1.011		1.009		1.026		1.005		1.015	
SD	--	--			0.016	0.001	--			0.002	--		--			0.015
Middleton EP07																
123	1.010		1.000	1.005	0.007	1.008		1.020	1.014	0.008	1.018			1.020	1.019	0.001
124	1.001			1.001	--	1.024			1.024	--	1.025				1.025	--
mean	1.005		1.000	1.004		1.016		1.020	1.017		1.021			1.020	1.021	
SD	0.006		--		0.006	0.011		--		0.008	0.005			--		0.004
CSIRO-PT																
115																

Columns 1, 6 and 11 see Table 8.3.3a. columns 1, 12 and 18.
Columns 2, 7 and 13 see Table 8.3.3a columns 7, 14 and 19.
Columns 3, 8 and 14 see Table 8.3.3a columns 8, 15 and 20.
Column 12 see Table 8.3.3a columns 5 and 13

8.3.5 Results comparing different laboratories

Table 8.3.5

Summary of ratios of Benchmark responsivities to corresponding NARC Benchmark responsivities			
Type	mean ratio / standard deviation / number of pairs or single ratio		
	BMHO	BMTN	BMTO
PSP		1.001 / 0.002 / 2	
CM5	1.009 / 0.011 / 9	1.015 / 0.018 / 3	1.022 / 0.021 / 2
one rejected	1.007 / 0.010 / 8	1.006 / 0.011 / 2	
CM10	1.001 / 0.010 / 6	1.005 / 0.013 / 3	0.994
one rejected	0.997 / 0.004 / 5	0.999 / 0.008 / 2	
Eko	0.992		
Swissteco	1.016	1.005	1.003
Middleton	0.996	0.998	0.986
All	1.005 / 0.012 / 33		
2 rejected	1.003 / 0.010 / 31		

Corresponding benchmark responsivities were determined on the same pyranometer by NARC, and another laboratory, in thirty-three cases. The results are expressed as ratios of the responsivities obtained by the participating laboratories to those obtained by NARC (Tables 8.3.3a&b, summarised in Table 8.3.5). There are only six of the twenty-one instrument-type/benchmark-type categories with more than one ratio available and these provide the main source for conclusions on reproducibility. Four of them are shown in Table 8.3.5 with one ratio rejected. However, except for the CM10/BMHO category where the rejected outlier is five standard deviations from the mean of the remaining five samples, the rejections are not statistically justifiable.

The first point to address is whether these benchmark calibrations are more reproducible than the routine calibrations. Judged by the overall standard deviations in the last rows of Tables 8.2c & 8.3.5, the benchmarks are only marginally better. The benchmark standard deviation is in the range 1.2-1.0% compared with 2.4-1.5% for the routine calibrations, the lower values in each case being a function of data rejection.

The results for the instrument types with more than one ratio are as follows:

PSP. There is a very high degree of consistency in the results for the BMTN category. The two ratios that are derived from four measurements on two pyranometers by three laboratories have a standard deviation of only 0.2%. Unfortunately, there are no data for the PSP/BMTN and PSP/BMHO categories.

CM5. The combined standard deviation for the three benchmarks is about the same as the 1.3% obtained in the intercomparison of routine methods. The BMHO set of nine ratios is distinctly bimodal and there is no statistical reason to reject any of them.

CM10. The standard deviation for BMHO, with one of the six samples rejected, is 0.4%. However, the BMTN results are no more reproducible than those for the routine CM10 calibration methods (sd=1.3%). It is not clear why the BMTN ratios are so much more variable than those of BMHO.

The PSP/BMTN and CM10/BMHO results show calibration under defined conditions being done with a reproducibility of 0.4% or less at some of the laboratories in this comparison. In §4.2.2 it is stated that some NARC benchmark calibrations which are determined from two-month blocks of data show standard deviations as small as 0.4%. Based on this, and the scatter of 10-minute calibrations, it is argued that, within NARC, the reproducibility or precision of 10-minute average measurements is below the 20W m^{-2} (2σ) level. The achievement of inter-laboratory benchmark consistency of 0.4% or better shows that this reproducibility extends throughout this group of laboratories under these particular conditions. The consistency can also be said to support the contention that a 20 Wm^{-2} accuracy has been achieved provided that there are no large systematic errors common to all the laboratories. The sample sizes of 5 and 2 for the two categories are small for this analysis and certainly too small to support more detailed error analysis.

Apart from the nine PSP/BMTN and CM10/BMHO ratios, the benchmark reproducibility is worse than 1.0% rms which shows clearly that the 20 Wm^{-2} target accuracy was not generally being achieved throughout the participating laboratories.

8.3.6 Results comparing different benchmarks

The ratios of different benchmark responsivities on identical pyranometers (BMTO/BMHO, BMTN/BMTO and BMTN/BMHO) and their averages by instrument type are given in Table 8.3.3b. The BMTO/BMHO ratios, show the PSP, CM5, CM10, Swissteco and Middleton

pyranometers all having tilt effects at 600Wm-2 that are less than 0.5%. The Schenk and Eko pyranometers are shown with responsivities reduced by 3.0% and 1.6%, respectively.

The result for the CM5 is less than what is indicated by other tests. The discrepancy could be caused by insufficient and scattered data. For example, the benchmark ratio results in Appendix BB show a larger tilt effect for the CM5 (0.9% at 600Wm^{-2}, 2.6% at 1000Wm^{-2}). Also, the different azimuth angles involved in BMTO and BMHO may influence the results on this azimuth dependent pyranometer.

The difference between BMTN and BMTO is less than 1.0 per cent only for the Kipp and the Swissteco instruments. This indicates the effects of tilting and incidence direction are either small or compensating in these instruments.

The largest differences are found between BMTN and BMHO, their ratio varying between 0.951 and 1.021. The range of seven per cent is important and is shown more clearly in Table 8.3.6 (a condensed version of the third column of Table 8.3.3c). This large spread contributed to measurement uncertainties (if not confusion) in the early 1980s when calibrations applicable for meteorological use were sometimes being used in the tilted, normal incidence orientation for testing solar collectors.

Table 8.3.6

Mean Determinations of Benchmark Responsivities

Type	$\frac{BMTN}{BMHO}$
PSP	1.012
CM5	0.985
CM10	0.995
Schenk	0.951
Eko	0.963
Swissteco	1.015
Middleton	1.021

8.4 Conclusions on calibration comparisons

One hundred and fifty four routine calibrations were obtained and expressed as ratios to the NARC indoor sphere values for the same instruments. Six of them are far outside the range of variability of all the others. The standard deviation of the remaining 148 is 1.5%. Standard deviations for the individual pyranometer types range from 1.0% up to 1.8%.

A distinction was made between two kinds of calibration methods (see Tables 8.2a&b):

- by comparison with a standard pyrheliometer and a removable shading disk for the pyranometer under test (the alternating sun/shade method) and
- methods in which a standard pyranometer is involved.

From the standard deviations that were obtained there is no reason to prefer one method to the other.

In most routine calibration methods the pyranometer under test is compared with a reference pyranometer, preferably of the same type, measuring the same irradiance. Excluding data from such calibrations where the reference pyranometer is of a different type improves the results for the PSP and CM5 pyranometers.

Benchmark comparisons between laboratories show a high degree of consistency in only two categories, that of the CM10 for BMHO and that of the PSP for BMTN. The standard deviations for these are 0.4% and 0.2%, respectively. These are small enough not to rule out the achievement of the target accuracy of 20Wm^{-2} (2σ) for 10-minute average measurements. However the small sample size, seven ratios in total, requires that these statistics be viewed with caution.

The overall variability, excluding the PSP/BMTN and CM10/BMHO categories, is greater than 1.0% which indicates that in most cases the target accuracy was not achieved.

The BMTO/BMHO ratios of benchmark responsivities on identical instruments indicate responsivities being significantly reduced by tilting in the cases of the Schenk (3.0%) and Eko (1.6%) instruments. The other types are shown with changes of 0.5% or less.

The BMTN/BMHO ratio of responsivities has been found to range from 0.951 for the Schenk to 1.021 for the Middleton, which is a total of 7.0%. This large span contributed significant errors to some measurements of slope irradiance in the early 1980's.

Chapter 9. Measurement Procedures

9.1 Introduction.

The results from the Sub-Task can be used to infer the potential level of accuracy that may be realised when measuring global radiation under circumstances that differ with respect to the complexity of available instrumentation and levels of logistic and technical support. It is emphasised that these estimates are based on the Sub-Task work but not directly validated in it. Choice of instrument is usually based on a number of considerations. Principal among these is the degree of accuracy required for a specific task: some investigations requiring greater accuracy than others. Additional considerations include the compromises that have to be made when balancing the advantages of using complex equipment versus simple equipment when assessed in the context of the available fiscal, technical and human resources. In some circumstances simpler instruments and measurement protocols may yield more reliable results than more complicated approaches when resources are limited.

The various methods that can be used to measure horizontal and tilt global radiation are discussed here in order of increasing measurement uncertainty. For consistency, the stated uncertainties are 2σ and apply when measuring approximately full-scale (1000 Wm^{-2}) with a ten-minute averaging period. They apply both for tilted and horizontal measurements. The absolute uncertainties at lower intensities are less usually following an approximately square root dependence. For example, the uncertainty at one quarter of full-scale would be approximately half its value at full-scale and, expressed as a percentage, it would be twice as great. For hourly and minute data the values are approximately 75% and 150% of the stated ten-minute values.

9.2 Care of instruments and data acquisition

Attention to the care and maintenance of the instruments is crucial to obtaining good measurements. Valuable information on these and related subjects, that is not duplicated here, can be found in manuals published by the IEA (9f), the World Meteorological Organization and the International Standards Organization. These are listed in Appendix 2.

Pyranometer signals are typically sampled at least several times during one minute and the average for each minute is recorded. A period longer than one minute is not recommended because the minute-to-minute variability is a useful parameter for quality control even

though, as with the ten-minute period here, a much longer averaging period may be used in the application.

Data acquisition for pyranometer signals requires that the sampling frequency should ideally be faster than about once per three seconds and the voltage accuracy should be better than about 10 microvolts. Bearing in mind that most pyranometers have primary time constants greater than five seconds and that 10 microvolts generally corresponds to less than 2 Wm^{-2}, no significant noise is contributed by systems that meet the above specifications. They can be met with good-quality commercial equipment. Until quite recently, it was common either to under-sample the signal (e.g. once in twenty seconds) or to use devices with insufficient stability. It should be noted that the requirements for voltage measurement in laboratory testing are quite different — much more stringent for accuracy and less stringent for frequency (for example, see the discussion in §4.1). Inclusion of a cavity radiometer in the system necessitates the use of a high-quality digital voltmeter with a minimum required accuracy of one microvolt.

9.3 The measurement systems

The components that may be used are:

1. Cavity radiometer (CR) of the type that allows operation in the continuous mode, with only brief periods devoted to self-calibration. Measurements with these instruments have an accuracy of better than 0.3% provided there are no under-sampling problems.

2. Premium pyranometer (PP) — meeting the ISO 9060 criteria for Secondary Standard (as do some of the instruments tested in this work).

3. Good pyranometer (GP) — meeting the ISO 9060 criteria for First Class pyranometers (as do some of the instruments tested in this work).

4. Normal incidence pyrheliometer (NIP).

5. Shaded (S) — the pyranometer measuring diffuse radiation being shaded by a solar tracking disc.

6. Ventilated (V) — the pyranometer being mounted in a ventilated housing.

7. A pyrgeometer (Pyg) — included so that variable offset corrections can be made. The alternative is to determine the night signal on the pyranometer and to use that as the zero correction for the day-time measurements.

9.3.1 CR + PP + S + V + Pyg *20 Wm^{-2} (2σ) estimated uncertainty, originating almost entirely with the diffuse measurement*

The best system, in which the cavity radiometer measures the direct beam while a pyranometer with minimal directionality measures the diffuse radiation. A correction for long-wave radiation can be made from the pyrgeometer reading and Equation 6.6. This correction is significant at irradiances below about 100 Wm^{-2}.

The uncertainty estimate is consistent with the results of a Task 9f experiment in which premium measuring systems from four institutes were compared.

This is an expensive system and one which needs substantial care to operate and maintain. Unless mounted in a special housing, the cavity radiometer will be damaged by rain and must be brought indoors when not measuring. This increases the requirement for human resources and increases costs.

9.3.2 NIP + PP + S + V *25 Wm^{-2} (2σ) estimated uncertainty, with the NIP contributing significantly*

The second best option in which the NIP replaces the cavity radiometer. It is less expensive than the cavity radiometer, but similarly complicated to operate. Both the tracking for the NIP and the shading disc need to be maintained. However, unlike the cavity radiometer, the NIP may be left outdoors.

9.3.3 NIP + (PP or GP) + V *30 Wm^{-2} (2σ) estimated uncertainty*

The pyranometer measures global radiation. The diffuse radiation is assumed to be isotropic and the pyranometer directionality errors are known. The global radiation is calculated using a responsivity based on the measured direct beam. This was used by some institutes during the early 1980s and is a good method for correcting readings from a pyranometer with significant directional errors.

9.2.4 PP + V *30 Wm^{-2} (2σ) estimated uncertainty*

Using the pyranometer in the normal way. A major cause of uncertainty here is the directional error but when using a secondary standard pyranometer these are less than 10 Wm^{-2} by definition (1000 Wm^{-2} directionality error). As already stated, the Sub-Task found some of the tested pyranometers did meet the criteria. With these instruments it is

unlikely that the use of the NIP, as described in §9.2.3 would improve the accuracy. When measuring global radiation with low solar elevation relative to the pyranometer, the signal is very sensitive to mounting orientation. This problem is avoided in §9.3.1&2 because the diffuse measurements are not similarly sensitive.

9.3.5 GP + V *35 Wm^{-2} (2σ) estimated uncertainty*

Using this quality of pyranometer, an improvement can be made using the method described in §9.2.3. This exemplifies the Sub-Task title and mandate for "improving radiation measurement by detailed characterization". Further improvement can be obtained by following the requirements in §9.3.1&2 and shading the pyranometer.

Finally, there were some of the IEA pyranometers that would not meet the ISO First Class criteria. For these, the uncertainties could be as much as 50 Wm^{-2} (2σ).

Chapter 10. Summary and Conclusions

10.1 The progress made

Nearly all the important aspects in calibration and characterization have been addressed in this report. It describes a large number of field and laboratory tests undertaken by the main participants and by others. Results and the techniques are documented and in some areas, for example laboratory directional tests and the study of offsets, the methods are analyzed in detail and compared with each other.

Because of the report's extensive nature, reflecting the active contribution of eight institutes from seven countries, it provides a comprehensive account of the procedures used by each institution and how effective those methods are. Consequently, the report is an organised compendium and source of pyranometer data that can be used by other workers in the field of radiation measurement. The detailed and thorough presentation of the results of the numerous studies have been summarised by the individual experimenters to the extent that they believe is appropriate and the editing of the report has deliberately attempted to preserve this detail and the authors' particular points of view.

The exploration of the physics of pyranometer aberrations given in Chapter 2 is based on results of the work and provides some tentative explanations of observed behavior of the instruments, including their departures from the ideal response.

An important outcome from the work is the detailed evaluation, given in Chapter 4, of results of laboratory studies on directionality and their reproducibility. Two well-documented field experiments on directionality and their results are also given.

The information on response time, temperature dependence, non-linearity, tilt and spectral response in Chapter 5 is more complete than can be found in any other single source known to the authors.

The measurement of offset signals and their analysis given in Chapter 6 is new and significant both for understanding pyranometers and for improving measurements at low intensities.

What is believed to be a sound and practical formulation of the response function has been developed. The 1000 Wm^{-2} directional error was conceived in this Sub-Task. In several

aspects it is a better indicator of directional error than the traditional cosine error. A preliminary example of using the response function and information on sky radiance is calculated.

The comparison of results obtained both from different institutes and by using different techniques is central to this study. The definition of three benchmark conditions for responsivities and their use has allowed more effective comparisons to be made. The participants performed many benchmark as well as routine calibrations and the inter-comparisons are reported in Chapter 8. These results clearly show the discrepancies that arise if calibration factors intended for meteorological application are used in measurements of radiation on tilted surfaces. Such discrepancies were responsible for diminishing confidence in radiation measurements made in the early 1980s.

Excepting a few cases, there was a greater spread than expected when measurements of the same benchmark, on identical instruments, were compared between laboratories. This ruled out any general demonstration of a 20 Wm^{-2} accuracy through inter-laboratory comparisons.

10.2 What was not achieved; what remains in doubt

Overall, the problems of developing good characterization techniques dominated the subtask. Much effort was put into inter-comparisons but the results of comparisons between field and laboratory studies on directionality require more study. Some discrepancies may be difficult to resolve.

Less effort than intended was put into using pyranometer characterizations and sky radiance data to evaluate measurement uncertainties and indeed "to demonstrate improved irradiance measurement" as mandated in the original title of Subtask 9C. However the Subtask 9F-5 *Improvement of Pyranometer Data by Cosine Error Correction*, 1993, compensates for the omission in Subtask 9.

The numerous calibration data provided by the participants and others, on the many circulating pyranometers, contributed to the validity of the benchmark comparisons. Variability within the combined data set was larger than expected. This is probably a combined consequence of the large number of people and institutions that took part in the study and the problems of organization and control that inevitably arose. For example, some institutes may have contributed benchmark calibrations not fully realizing the precise

nature of the definitions. Under more optimal conditions, there would likely be a much greater degree of reproducibility between the work of different institutes.

10.3 What may be done next

The activity generated by Subtask 9C, not just by the participants, has helped stimulate research into radiation measurement (for example, in the World Meteorological Organization Climate Program). However, the logistic problems of arranging access to the pyranometers by the many participants suggests that a smaller Subtask would probably have been more effective. Because of this, and the related issues of management mentioned above, it is not recommended that a large inter-institute comparison of this nature be re-initiated in the immediate future: small tasks, undertaken by groups comprising about three participants would probably be optimal.

Questions arising from this work and related tasks are as follows:

1. Can benchmark reproducibility be improved? A meticulous effort by a few institutes to produce benchmark calibrations and analyze the results could answer this question. BMHO responsivities obtained at one laboratory over a two-year period had a standard deviation of less than 0.5%. Based on this reproducibility at one institute, it should be possible to repeat the few good inter-laboratory benchmark results that have been achieved and to demonstrate a much better overall consistency between institutes.

2. How reproducible can measurements taken at the same location by different institutes be?

3. The uncertainty analysis in Chapter 7 should be repeated over large measured data sets of sky radiance. The effects of partial and intermittent cloud cover are not well-understood and these studies are essential if our understanding of measurement uncertainties is to improve.

4. The directional measurements on a few pyranometers were unusual, either because of experimental error or because of some special characteristics that are not currently understood. A small scale study repeating the experiments on these pyranometers would provide interesting results.

5. The physics described in Chapter 2 is speculative but the insight provided emphasises the value of detailed pyranometer modeling of the type that has been done for cavity radiometers over the past twenty years. Pyranometer manufacturers have undertaken some modeling studies and a group task study involving both manufacturers and researchers could be valuable in addressing the aberrations of current types and in developing improved instruments.

These topics have been evident for some time and some of them, notably numbers 2, 3 and 4, have already been addressed in the IEA SHCP. The others might be considered for future work by the IEA.

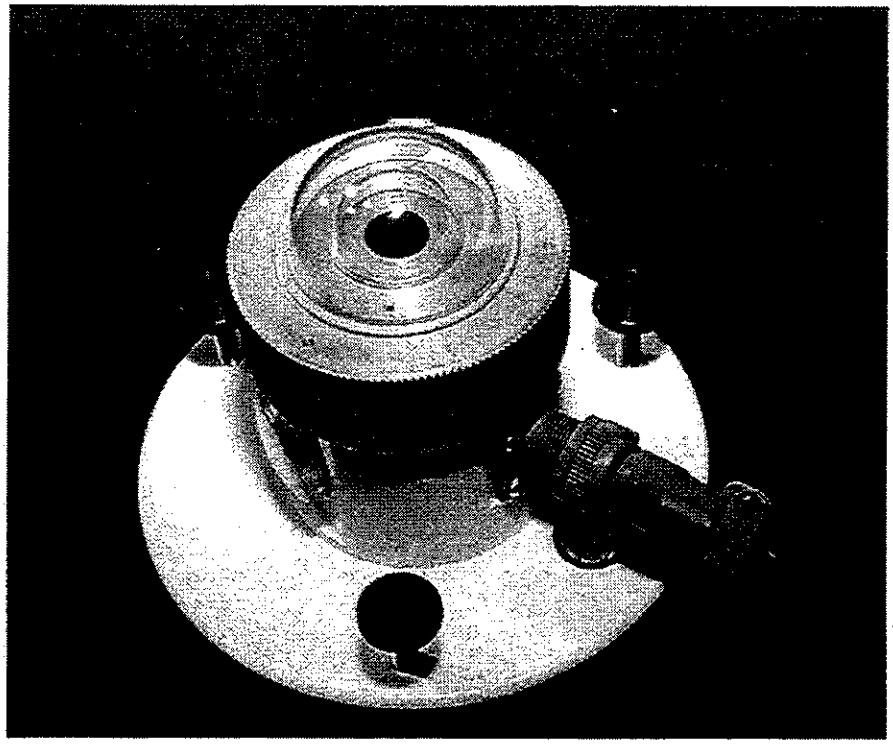

Middleton Pyranometer

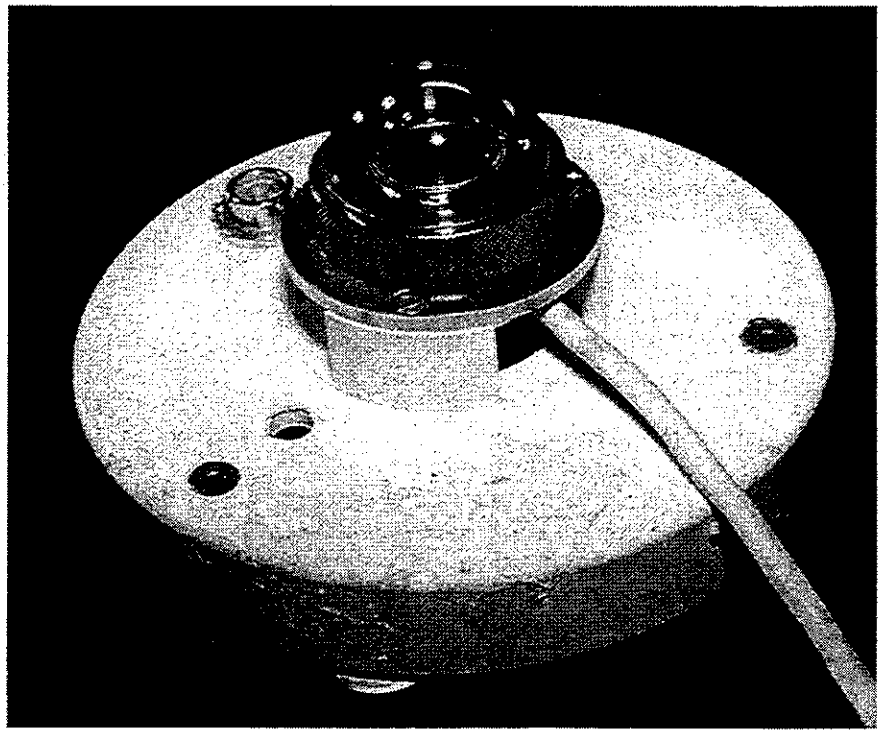

Kipp and Zonen CM5

Bibliography

The need for this study, Subtask 9F, arose from the work of Task 3. The report from Task 3 and the Proceedings of the 1994 IEA Norrköping Symposium are sources of much information used here, and the Subtask 9F-5 contribution is relevant:

IEA SHCP III.A.3, *Results of an Outdoor and Indoor Pyranometer Comparison*, P. Ambrosetti, H.E.B. Andersson, L. Liedquist, Fröhlich, Ch. Wehrli, H.D. Talarek. Available from Kernforschungsalage, Jülich, Postfach 1913, D-5170, Jülich, Germany, 1984.

IEA-SHCP-9C-1 *Recent Advances in Pyranometry*, Norrköping 1984 Symposium Proceedings, editors. Wardle D.I. and McKay D.C. Available from Atmospheric Environment Service, 4905 Dufferin Street, Downsview, Ontario, M3H 5T4, Canada, 1986.

IEA-SHCP-9F-5 *Improvement of Pyranometer Data by Cosine Error Correction*, 1993, A. Haarto and M. Hämäläinen. Available for Dept. of Applied Physics, University of Turku, Vesilinnantie 5, FIN-20500, Turku, Finland.

Accounts of earlier IEA work can be found in the 1981 IEA Task 3-5 Boulder Conference Report as well as the original Task 3 comparison:

Proceedings of the IEA Conference on Pyranometer Measurements, Boulder, 16-20 March 1981. editors. M.R. Riches, T.L. Stoffel and C.V. Wells. SERI/TR-642-1156R. Available from National Renewable Energy Laboratory, 1617 Cole Boulevard, Golden, Colorado, 80401, USA, 1982.

Results of a pyranometer comparison, Davos, March 5 and 6, 1980. Available from Kernforschungsalage, Jülich as above.

The following are useful guides for measuring with pyranometers

ISO/TR 9901:1990(E) Solar Energy- *Field Pyranometers, Recommended practice for use* (15 pages) Available from International Standards Organization, Case Postale 56, CH-1211, Geneva, Switzerland.

IEA SHCP 9F1 (1995) *Using Pyranometers in Tests of Solar Energy Converters: Step-by-step Instructions* L.J.B. McArthur et al. Available from Atmospheric Environment Service (as above)

World Meteorological Organization, WMO-No.8. *Guide to Meteorological Instruments and Methods of Observation*, WMO, Geneva , 1983 (1995 edition to be issued) .

The following International Standards define classes of pyranometers and the alternating shade method of calibration

ISO 9060 (1990) Solar Energy- *Specification and classification of instruments for measuring hemispherical solar and direct solar radiation.*

ISO 9846 (1991) Solar Energy. *Calibration of a Pyranometer using a Pyrheliometer.*

References

Ambrosetti *et al.* (1984) see IEA III A3.

Anderson, M.C., (1967) *The role of heat transfer in the design and performance of solarimeters,* J. Appl. Met. 6 941-947.

Andersson, H.E.B., Liedquist, L., Lindblad, J. and Norsten, L-A. (1981). *Calibration and Testing of Pyranometers.*, Report SP-RAPP 1981:7. Available from the Statens Provningsanstalt, Box 857, S-501 15, Borås, Sweden.

Berdahl, P. and Fromberg, R. (1982). *The thermal radiance of clear skies.* Solar Energy 29(4): 299-314.

van den Brink, G-J., Kratz, P. and van Wely, L.F. (1985). *Indoor characterisation and calibration of seven IEA Pyranometers in the framework of IEA Task IX c.* Report #327.226-2. Institute of Applied Physics, TNO-TH, Box #155, 2600 Delft, Netherlands.

Dahlgren, L., (1987). *Cosine response of pyranometers determined by field measurements.* Final report 87 04 21, SMHI, Norrkoping

Dehne, K & Trapp, R (1986) *Final report on the pyranometer tests within IEA Task IX carried out at the Met. Obs. Hamburg 1984/1985.* DWD, Hamburg.

Dehne, K. and Trapp, R. (1985*). Preliminary report on the results of the first test loop of four pyranometers within the IEA Task IX.*, pp. 335-370 in *Recent Advances in Pyranometry,* Norrkoping 1984 Symposium Proceedings,

Flowers, E.C. (1985). *Tests of IEA Pyranometers at the Solar Radiation Facility,* January-June 1984, NOAA, Boulder Colorado, USA

Griffin, F. & Hickey, J. (1985) *Report on Pyranometer testing: including instruments of the IEA and the SERI: two periods in 1984.* The Eppley Laboratory, Inc.,12 Sheffield Avenue, Newport, R.I., 02840, USA

Liedquist, L (1985) *Spectral measurements on pyranometers at NTI, Sweden.* 69-73,IPC VI Davos Symposium, Swiss Meteorological Institute, Zurich, Working Report No. 137, 1985

Motschka, O., & Wessely, E., (1985) *Test Results of IEA pyranometers at the ZFMG.* Manuscript supplied to other participants

Nast P-M, (1985) *Measurements of transients: irradiance, temperature, aging.* p123-128, (also p329) Norrköping Proceedings, above..

Miyake, Y, Y. Nakanishi & T. Aoshima (1989): *Calculation Result of Response Function Based on Global Radiation Sets and Characteristics of Pyranometers.* Eko Instrument Trading Company., Tokyo, Japan

Miyake, Y., R. Shimikawa, Y. Nakanishi and Y. Hamakawa (1989): Global Radiation Model and Angular Distribution of the Diffuse Irradiance., EKO instruments Trading Company, Ltd., Tokyo, Japan.

Proctor, D. and Trickett, E.S. (1982). *An improved pyranometer.* Solar Energy, 31(2): 183-189.

Riches *et al.* (1982) Boulder Proceedings as above

Wardle D.I. (1982) *The Background to NARC Calibration Methods*, p247-267. in Boulder Proceeding above (note calibration values on page 251)

Wardle D.I. and McArthur, L.J.B. (1987). *Ground level monitoring of long-wave irradiance with the Eppley pyrgeometer.* pp. 173-193 in *Measuring the Greenhouse Effect.*, Internal Report ARD 87 02. Atmospheric Environment Service, 4905 Dufferin Street, Downsview, Ontario, M3H 5T4, Canada.

Wells C.V., & Myers, D.R. (1986) *Pyranometry studies in the United States under the International Energy Agency Task IX.* SERI/TR-215-2925, available from NREL, above.

Zerlaut, G.A. & Maybee, G.D. (1985) *Pyranometer calibration studies.* DSET 85-0801R., available from NREL, above.

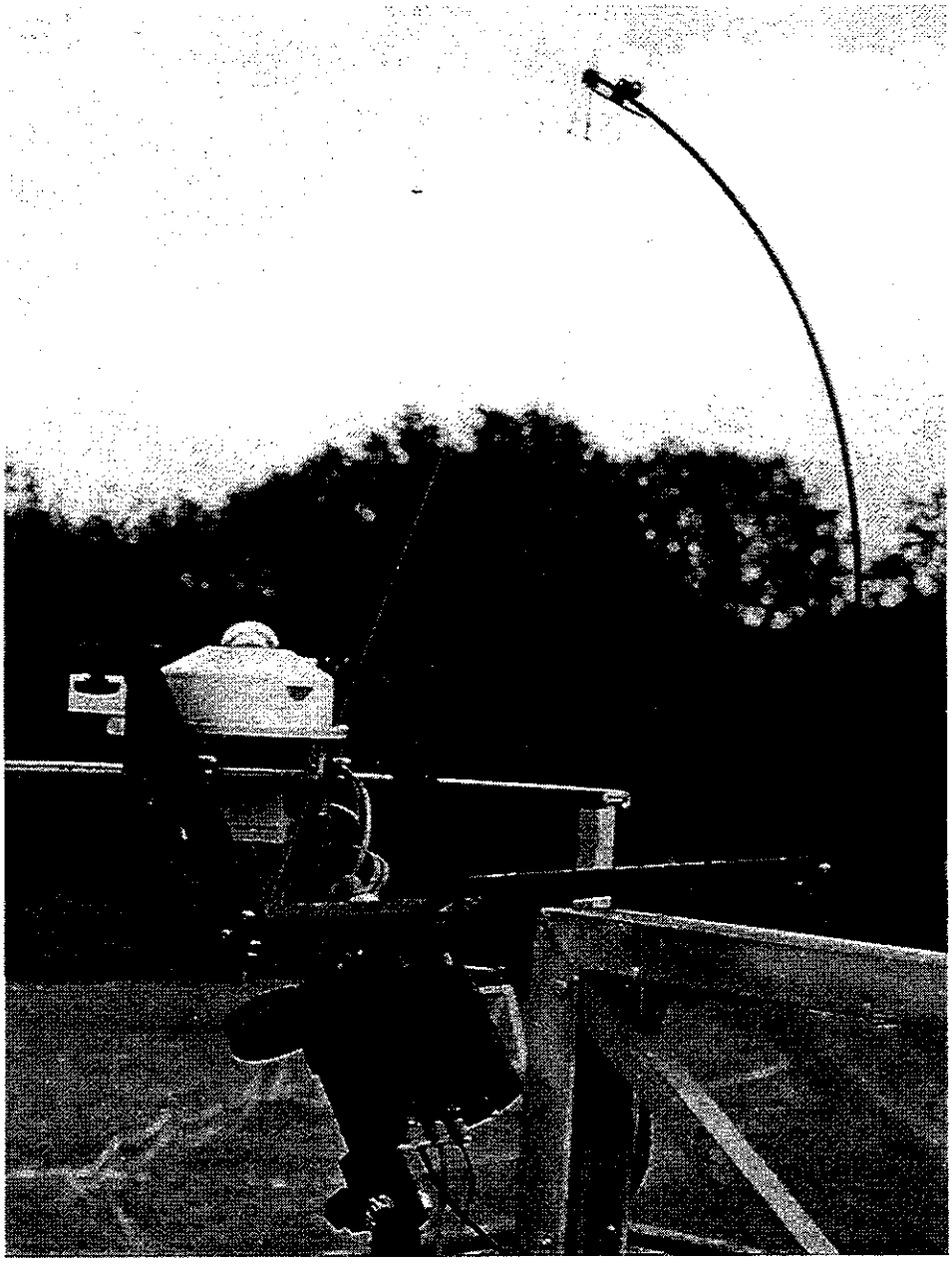

Tracking Shading Disk as designed by Deutscher Wetterdienst

Appendix AA

Results on laboratory measurements on directionality

Supplement to §4.1.3.1.

Tables 4.1.3.1b-n

Tables containing results from measurements on

on thirteen pyranometers

Cosine errors $\delta(\theta,\phi)$ with azimuthal mean *cosine errors* $\overline{\delta}(\theta)$

azimuthal maximum spread $D_{max}(\theta)$ all in units of 0.1% together with the

corresponding *1000 Wm^{-2} absolute directional error* values $\overline{\delta_t}(\theta)$ in Wm^{-2}

and equivalent misalignment β in degrees.

The symbol Δ indicates the difference between values from two laboratories.

For definitions of these terms see §4.1.3.1.

Thirteen paragraphs summarising each table (pyranometer).

Seven tables summarising results for each pyranometer type.

Table 4.1.3.1b.

CM11 810121

$$\Delta = \delta(KI) - \delta(BO)$$

θ / φ	20°			30°			40°			50°			60°			70°			80°		
	BO	KI	Δ	BO	KI	Δ	BO	KI	Δ	BO	KI	Δ	BO	KI	Δ	BO	KI	Δ	BO	KI	Δ
N = 0°	0	-1	-1	-3			-5	-6	-1	-4			-1	+1	+2	-1	0	+1	0	1	+1
30°	-1	-2	-1	-4			-6	-6	0	-4			-2	-2	0	-1	-1	-2	5	6	+1
60°	-2	-2	-1	-5			-5	-6	+1	-4			-2	-3	-1	1	-1	-2	6	3	-3
E = 90°	-3	-3	0	-4			-6	-7	-1	-3			-1	-3	-2	3	-3	-6	15	6	-9
120°	-3	-1	0	-5			-7	-7	0	-6			-4	-3	+1	-1	-3	-2	8	3	-5
150°	-2	-2	+2	-4			-5	-7	-2	-4			0	-7	-7	+3	-7	-10	15	-1	16
S = 180°	-1	-4	0	-5			-6	-9	-3	-6			-3	-3	0	0	-5	-5	6	6	0
210°	-3	-2	-3	-3			-5	-8	-3	-3			-1	-5	-4	4	-3	-7	11	3	-8
240°	-3	-2	+1	-3			-5	-7	-2	-3			-1	-3	-2	1	-1	-2	7	6	-1
W = 270°	-3	-2	+1	-3			-6	-6	0	-4			-3	-5	-2	-4	+3	-8	-8	-1	+7
300°	-1	-2	+1	-3			-4	-6	-2	-2			0	-5	-5	1	-5	-6	1	3	+2
330°	-2	-2	0	-4			-6	-5	+1	-4			-3	-1	+2	-2	-3	+1	-8	3	+11
$\overline{\delta}$	-2	-2	0	-4			-6	-7	-1	-4			-2	-3	-1	0	-3	-3	5	3	-2
$\overline{\delta}_t$	-1.9	-1.9	0	-3.5			-4.6	-5.4	0.8	-2.5			-1.0	-1.5	0.5	0.0	-1.0	1.0	0.9	0.5	0.4
D_{max}	3	3		2			2	4		4			4	8		8	8		23	7	
β^o	0.23	0.23		0.10			0.07	0.14		0.10			0.07	0.13		0.08	0.08		0.12	0.04	

Table 4.1.3.1c

PSP 20524 F3

$\Delta = \delta(KI) - \delta(BO)$

θ / φ	20° BO	20° KI	20° Δ	30° BO	30° KI	30° Δ	40° BO	40° KI	40° Δ	50° BO	50° KI	50° Δ	60° BO	60° KI	60° Δ	70° BO	70° KI	70° Δ	80° BO	80° KI	80° Δ
N = 0°	-4	-7	+3	-9			-15	-23	-8	-24			-35	-49	-14	-39	-60	-21	-86	-125	-39
30°	-3	-4	+1	-7			-13	-17	-4	-22			-31	-43	-12	-31	-48	-17	-77	-108	-31
60°	-5	-2	+3	-7			-11	-13	-2	-21			-31	-34	-3	-26	-30	-4	-76	-77	+1
E = 90°	-4	-2	+2	-6			-11	-8	+3	-20			-29	-24	+5	-22	-14	+8	-64	-52	+12
120°	-3	0	+3	-6			-11	-6	+5	-18			-29	-20	+9	-29	-14	+15	-76	-47	+29
150°	-2	2	+4	-6			-12	-5	+7	-20			-29	-21	+8	-32	-24	+8	-82	-54	+28
S = 180°	-2	-1	+1	-6			-11	-8	+3	-17			-33	-27	+6	-43	-31	+12	-81	-70	+11
210°	-3	-1	+2	-7			-12	-12	0	-20			-32	-35	-3	-38	-44	-6	-90	-84	+6
240°	-2	-4	-2	-6			-12	-16	-4	-19			-28	-40	-12	-32	-49	-17	-68	-99	-29
W = 270°	-2	-7	-5	-6			-12	-21	-9	-19			-28	-48	-20	-23	-50	-27	-68	-112	-44
300°	-3	-10	-7	-7			-13	-24	-11	-20			-30	-52	-22	-25	-60	-35	-68	-124	-56
330°	-3	-10	-7	-8			-14	-24	-10	-21			-33	-51	-18	-37	-66	-29	-79	-129	-50
$\overline{\delta}$	-3	-4	-1	-7			-12	-15	-3	-20			-31	-37	-6	-31	-41	-10	-76	-90	****
$\overline{\delta_t}$	-2.8	-3.8	-1.0	-6.1			-9.2	-1.1	-2.3	-1.3			-15.5	-18.5	-3.0	-10.6	-14.0	-3.4	-13.2	-15.6	****
D_{max}	3	12		2			4	19		7			7	32		21	52		26	82	
β	0.24	0.94					0.14	0.65					0.12	0.53		0.22	0.54		0.13	0.41	

Table 4.1.3.1d.

CM6 773656

$$\Delta = \delta(KI) - \delta(BO)$$

θ / φ	20° BO	20° KI	20° Δ	30° BO	30° KI	30° Δ	30° TO	40° BO	40° KI	40° Δ	40° TO	50° BO	50° KI	50° Δ	50° TO	60° BO	60° KI	60° Δ	60° TO	70° BO	70° KI	70° Δ	70° TO	80° BO	80° KI	80° Δ	80° TO
N = 0°	-1	-6	-5	-6	-10	-4	0	-17	-20	+3	-3	-32	-32	0	-6	-46	-51	-5	-14	-83	-84	-1	-35	-138	-150	-12	-82
30°	-2	-5	-3	-7	-8	-1		-16	-20	+4		-33	-31	+2		-42	-49	-7		-68	-76	-8		-132	-143	-11	
60°	-3	-4	-1	-10	-7	+3		-16	-18	+2		-29	-27	+2		-44	-46	-2		-56	-61	-5		-103	-119	-16	
E = 90°	-2	-4	-2	-6	-7	-1	2	-13	-15	+2	2	-23	-23	0	3	-36	-41	-5	2	-41	-47	-6	5	-70	-92	-22	7
120°	-3	-5	-2	-9	-7	+2		-15	-17	+2		-24	-20	+4		-35	-39	-4		-50	-50	+10		-85	-108	-23	
150°	-4	-4	0	-9	-8	+1		-15	-17	+2		-26	-23	+3		-41	-42	-1		-71	-68	+3		-122	-129	-7	
S = 18 0°	-4	-4	0	-10	-10	+3	0	-19	-19	0	-3	-30	-25	+5	-6	-46	-44	+2	-14	-75	-70	+5	-35	-144	-135	+9	-82
210°	-4	-4	0	-10	-10	+3		-19	-18	+1		-30	-27	+3		-45	-44	+1		-69	-66	+3		-132	-127	+5	
240°	-4	-5	-1	-8	-8	0		-15	-17	+2		-25	-26	-1		-40	-44	-4		-52	-58	-6		-98	-111	-13	
W = 270°	-4	-9	-5	-8	-8	-1	2	-13	-18	+5	2	-22	-24	-2	3	-33	-39	-6		-36	-43	-7	5	-53	-81	-28	7
300°	-5	-8	-3	-10	-10	-2		-17	-21	+4		-26	-28	-2		-39	-47	-8		-59	-60	-17		-82	-124	-42	
330°	-5	-8	-3	-8	-8	-4		-16	-21	+5		-29	-31	-2		-47	-49	-2		-68	-73	-5		-122	-140	****	
$\overline{\delta}$	-3	-6	-3	-8	-8	-1		-16	-21	-2	-1	-27	-26	+1	-2	-41	-45	-4	-6	-60	-65	-5	-15	-107	-121	-14	-37
$\overline{\delta}_t$	-2.8	-5.6	-2.8	6.9	-6.9	0.9		-12.3	-13.8	-1.5	-0.8	-17.3	-16.7	0	-1.3	-20.0	-22.0	-2.0	-3.0	-20.5	-22.2	-1.7	-5.1	-18.6	-21.0	-2.4	-6.4
D_{max}	4	5		4	4			6	6			11	12			14	12			47	41			91	69		
$\beta°$	0.31	0.39		0.20	0.25			0.20	0.20		0.2	0.26	0.29		0.1	0.23	0.20		0	0.49	0.43		-0.3	0.46	0.35		-0.4

Table 4.1.3.e

Schenk Star 2209

$$\Delta = \delta(KI) - \delta(BO)$$

θ / φ	20° BO	20° KI	20° Δ	30° BO	30° KI	30° Δ	40° BO	40° KI	40° Δ	50° BO	50° KI	50° Δ	60° BO	60° KI	60° Δ	70° BO	70° KI	70° Δ	80° BO	80° KI	80° Δ
N = 0°	-4	-2	+2	-9	-4	+5	-16	-10	+6	-28	-17	+11	-38	-26	+12	-52	-30	+22	-52	-18	+24
30°	-3	-3	0	-6	-5	+1	-13	-12	+1	-23	-18	+5	-33	-28	+5	-37	-32	+5	-24	-29	-5
60°	-3	-4	-1	-8	-8	0	-15	-15	0	-29	-24	+5	-41	-39	+2	-50	-47	+3	-34	-48	-14
E = 90°	-4	-5	-1	-11	-11	0	-19	-22	-3	-20	-30	-2	-35	-41	-6	-40	-55	-15	-20	-68	-48
120°	-4	-7	-3	-13	-14	-1	-22	-24	-2	-32	-34	-2	-41	-53	-12	-51	-71	-20	-46	-102	-56
150°	-6	-8	-2	-13	-13	0	-21	-23	-2	-28	-31	-3	-36	-45	-9	-40	-61	-21	-32	-94	-62
S = 180°	-7	-8	-1	-11	-12	-1	-20	-21	-1	-31	-32	-1	-41	-46	-5	-42	-55	-13	-33	-68	-35
210°	-8	-9	-1	-15	-12	+3	-24	-20	+4	-29	-25	+4	-34	-32	+2	-32	-22	+10	-24	-35	-11
240°	-7	-8	-1	-12	-12	+1	-21	-17	+4	-31	-23	+8	-39	-30	+9	-38	-32	+6	-26	-21	+5
W = 270°	-7	-7	0	-13	-11	+4	-20	-15	+5	-27	-16	+11	-32	-18	+14	-33	-20	+13	-27	-15	+12
300°	-6	-5	+1	-11	-9	+5	-19	-10	+9	-29	-14	+15	-39	-22	+17	-50	-26	+24	-63	-13	+50
330°	-6	-3	+3	-10	-6	+4	-16	-8	+8	-22	-9	+13	-35	-15	+20	-44	-15	+29	-49	-1	+48
$\overline{\delta}$	-5	-6	-1	-11	-9	+2	-19	-16	+3	-28	-23	+5	-37	-33	+4	-42	-39	+4	-36	-43	-8
$\overline{\delta}_t$	-4.7	-5.6	-0.9	-9.5	-7.8	+1.7	-14.6	-12.3	+2.3	-18.0	-14.8	+3.2	-18.5	-16.5	+2.0	-14.4	-13.3	+1.1	-6.3	-7.5	-1.2
D_{max}	5	7		9	10		11	16		10	25		9	38		20	56		43	101	
β^o	0.39	0.55		0.45	0.50		0.38	0.55		0.24	0.60		0.15	0.63		0.21	0.58		0.22	0.51	

Table 4.1.3.1f.

Eko 81908

$$\Delta = \delta(KI) - \delta(BO)$$

θ / φ	20° BO	20° KI	20° Δ	30° BO	30° KI	30° Δ	40° BO	40° KI	40° Δ	50° BO	50° KI	50° Δ	60° BO	60° KI	60° Δ	70° BO	70° KI	70° Δ	80° BO	80° KI	80° Δ
N = 0°	3	1	-2	3	-3	-6	4	-5	-9	4	-10	-14	12	-10	-22	21	-13	-34	37	-15	-52
30°	4	0	-4	7	0	-7	7	-2	-9	8	-8	0	11	-15	-26	20	-2	-22	46	-22	-68
60°	-2	-2	0	0	-3	-3	4	-5	-9	4	-8	-12	11	-11	-22	21	-10	-31	38	-18	-56
E = 90°	-3	-4	-1	-4	-7	-3	-3	-6	-3	-2	-8	-6	9	-3	-12	25	-7	-32	40	5	-35
120°	-5	-2	+3	-7	-5	+2	-4	-5	-1	-1	-7	-6	9	-6	-15	25	-4	-29	45	-5	-50
150°	-4	-1	+3	-3	-2	+1	-1	0	+1	1	-6	-7	9	-7	-16	26	-7	-33	63	-2	-65
S = 180°	-4	-3	+1	-3	-5	+2	0	-3	-3	6	-2	-8	14	1	-13	26	5	-21	41	5	-46
210°	-5	-3	+2	-6	-7	+1	-5	-6	-1	0	-4	-4	12	5	-7	31	18	-13	42	15	-27
240°	-4	-1	+3	-5	-5	0	-3	-5	-2	1	-6	-7	9	-3	-12	21	0	-21	36	1	-35
W = 270°	-2	1	+3	2	-2	-4	4	-5	-9	7	-7	-14	12	-9	-21	20	-12	-32	39	-15	-54
300°	1	0	-1	4	-3	-7	4	-5	-9	5	-9	-14	8	-10	-18	14	-9	-23	25	-15	-40
330°	0	-1	-1	-1	-7	-6	0	-8	-8	2	-10	-12	7	-7	-14	19	3	-16	16	-5	-21
$\overline{\delta}$	-2	-1	+1	-1	-4	-3	1	-5	-6	3	-7	-10	10	-6	-16	22	2	-24	39	-6	-45
$\overline{\delta}_t$	-1.8	-0.9	+0.9	-0.9	-3.5	-2.6	0.8	-3.8	-4.6	1.9	-4.5	-6.4	50	-3.0	-8.0	7.5	-0.7	-8.2	6.8	-1.0	-7.8
D_{max}	9	5		14	7		12	8		10	8		7	20		17	31		47	37	
$\beta°$	0.71	0.39		0.69	0.35		0.41	0.27		0.24	0.19		0.11	0.33		0.18	0.32		0.24	0.19	

Table 4.1.3.1g

SWT 114

$$\Delta = \delta(KI) - \delta(BO)$$

θ / φ	20° BO	20° KI	20° Δ	30° BO	30° KI	30° Δ	40° BO	40° KI	40° Δ	50° BO	50° KI	50° Δ	60° BO	60° KI	60° Δ	70° BO	70° KI	70° Δ	80° BO	80° KI	80° Δ
N = 0°	18	19	+1	23	21	-2	25	17	-8	25	15	-10	26	6	-20	29	-11	-40	55	-43	-98
30°	19	19	0	25	21	-4	27	17	-10	26	13	-13	26	4	-22	30	-15	-45	56	-55	-111
60°	23	19	-4	26	21	-5	28	16	-12	28	12	-16	28	3	-25	31	-16	-47	59	-56	-115
E = 90°	24	17	-7	27	21	-6	28	16	-12	27	12	-15	25	3	-22	25	-16	-41	43	-58	-101
120°	23	15	-8	26	21	-5	27	15	-12	27	12	-15	26	3	-23	27	-16	-43	43	-59	-102
150°	19	18	-1	22	23	+1	25	17	-8	26	14	-12	27	3	-24	29	-15	-44	42	-52	-94
S = 180°	16	19	+3	19	22	+3	21	18	-3	24	15	-9	29	7	-22	39	-8	-47	74	-39	-113
210°	16	19	+3	19	22	+3	21	18	-3	23	18	-5	27	10	-17	38	-5	-43	75	-29	-104
240°	16	18	+2	19	20	+1	20	20	0	22	19	-3	25	12	-13	35	-1	-36	72	-20	-92
W = 270°	17	19	+2	19	20	+1	21	19	-2	23	18	-5	27	13	-12	40	2	-38	85	-16	-101
300°	15	17	+2	18	19	+1	21	18	-3	24	18	-6	28	12	-16	41	-2	-42	88	-21	-109
330°	15	18	+3	19	19	0	22	18	-4	24	18	-6	28	10	-18	41	-5	-46	91	-34	-125
$\overline{\delta}$	18	18	0	22	21	-1	24	17	-7	25	15	-10	27	7	-20	34	-9	-43	65	-40	-105
$\overline{\delta}_t$	16.9	16.9	0.0	19.5	18.2	-0.7	18.4	13.0	-5.4	16.1	9.6	-6.5	13.5	3.5	-10.0	11.6	-3.1	-14.7	11.3	-6.9	-18.2
D_{max}	9	4		9	4		8	5		6	7		4	10		16	18		49	43	
β^o	0.71	0.31		0.45	0.20		0.27	0.17		0.14	0.17		0.07	0.17		0.17	0.19		0.25	0.22	

Table 4.1.3.1h

CM6 785047

$$\Delta = \delta(HA) - \delta(BO)$$

θ / φ	40° BO	40° HA	40° Δ	40° TO	50° BO	50° TO	60° BO	60° HA	60° Δ	60° DA	60° TO	70° BO	70° HA	70° Δ	70° DA	70° TO	80° BO	80° HA	80° Δ	80° DA	80° TO
N = 0°	-16	-17	-1	2	-25	2	-36	-40	-4	5	-1	-36	-57	-21	-9	-10	-110	-96	+14	-24	-42
30°	-15	-16	-1		-23		-32	-40	-8			-32	-57	-25			-95	-96	-1		
60°	-13	-18	-5		-19		-27	-40	-13			-27	-54	-27			-53	-82	-29		
E = 90°	-11	-22	-11	9	-17	12	-23	-45	-22	-8	14	-23	-49	-26	-13	24	-16	-70	-54	5	39
120°	-15	-26	-11		-21		-30	-59	-29			-30	-76	-46			-48	-130	-82		
150°	-16	-31	-15		-24		-34	-67	-33			-34	-100	-66			-84	-176	-92		
S = 180°	-14	-33	-19	2	-21	2	-34	-71	-35	(5)	-1	-34	-106	-72	(-9)	-10	-113	-188	-75	(-24)	-42
210°	-15	-30	-15		-22		-34	-66	-32			-34	-99	-65			-103	-172	-69		
240°	-13	-25	-12		-18		-30	-54	-24			-30	-72	-42			-70	-111	-41		
W = 270°	-11	-19	-8	9	-18	12	-26	-42	-16	(-8)	14	-26	-46	-20	(-13)	24	-35	-52	-17	(5)	39
300°	-11	-16	-5		-17		-26	-39	-13			-26	-52	-26			-62	-75	-13		
330°	-12	-16	-4		-19		-33	-39	-6			-33	-56	-23			-101	-92	+9		
$\overline{\delta}$	-14	-22	-8	5	-20	7	-31	-50	-19	-2	6	-30	-69	-39		7	-74	-112	-38	-10	-2
$\overline{\delta}_t$	-10.7	-16.9	-6.2	3.8	-12.9	4.5	-15.5	-25.0	-9.5	-1	3.0	-10.3	-23.6	-13.3		2.4	-12.8	-19.4	-6.6	-1.7	-0.3
D_{max}	5	17					13	28				13	60				97	136			
β^o	0.17	0.58		0.5		0.5	0.22	0.46			0.5	0.14	0.63			0.7	0.49	0.60			0.8

Table 4.1.3.1i

PSP 20523 F3

$$\Delta = \delta(HA) - \delta(BO)$$

θ / φ	40° BO	40° HA	40° Δ	50° BO	60° BO	60° HA	60° Δ	70° BO	70° HA	70° Δ	80° BO	80° HA	80° Δ
N = 0°	-7	-16	-9	-13	-18	-31	-13	-14	-33	-19	-47	-75	-28
30°	-8	-14	-6	-14	-20	-38	-18	-15	-21	-6	-54	-64	-10
60°	-7	-11	-4	-12	-18	-24	-6	-4	-10	-6	-46	-53	-7
E = 90°	-6	-12	-6	-12	-16	-24	-8	-3	-8	-5	-39	-51	-12
120°	-7	-15	-8	-12	-18	-27	-9	0	-18	-18	-39	-60	-21
150°	-8	-16	-8	-13	-18	-29	-11	-4	-29	-25	-40	-57	-27
S = 180°	-11	-16	-5	-15	-21	-31	-10	-12	-32	-20	-40	-73	-33
210°	-9	-15	-6	-13	-19	-31	-12	-6	-25	-19	-27	-74	-47
240°	-8	-15	-7	-12	-17	-31	-14	3	-21	-24	-23	-74	-51
W = 270°	-8	-16	-8	-11	-16	-31	-15	7	-27	-34	-22	-80	-58
300°	-8	-16	-8	-12	-16	-33	-17	2	-34	-36	-26	-85	-59
330°	-9	-16	-7	-13	-19	-33	-14	-10	-38	-28	-40	-83	-43
$\overline{\delta}$	-8	-15	-7	-12	-18	-30	-12	-5	-25	-20	-37	-69	-32
$\overline{\delta}_t$	-6.1	-11.4	-5.3	-7.7	-9.0	-15.0	-6.0	-1.7	-8.5	-6.8	-6.4	-12.0	-5.6
D_{max}	5	5		4	5	14		22	30		32	34	
$\beta°$	0.17	0.17		0.10	0.08	0.23		0.23	0.31		0.16	0.17	

Table 4.1.3.1j.

MID EP07 No. 113

$$\Delta = \delta(VI) - \delta(HA)$$

θ / φ	40° HA	40° VI	Δ	50° VI	60° HA	60° VI	Δ	70° HA	70° VI	Δ	80° HA	80° VI	Δ
N = 0°	-15	-29	-14	-31	-23	-23	0	-47	-30	+17	-70	-51	+19
30°	-4	-19	-15	-20	-12	-8	+4	-36	-11	+25	-84	-63	+21
60°	-8	-20	-13	-24	-16	-21	-5	-38	-28	+10	-93	-54	+39
E = 90°	-2	-13	-11	-16	-27	-19	+8	-46	-29	+17	-109	-52	+57
120°	-15	-9	+6	-8	-9	-10	-1	-18	-27	-9	-112	-42	+70
150°	-15	-14	+1	-17	-9	-18	-9	-36	-31	+5	-133	-40	+93
S = 180°	-28	-24	+4	-26	-28	-24	+4	-40	-43	-3	-79	-52	+27
210°	-27	-9	+18	-14	-38	-10	+28	-50	-21	+29	-61	-10	+51
240°	-12	-9	+3	-15	-17	-16	+1	-39	-28	+11	-54	-35	+19
W = 270°	-2	-14	-12	-15	-11	-16	-5	-35	-20	+15	-45	-12	+33
300°	-8	-25	-17	-33	-12	-33	-21	-46	-26	+20	-62	-41	+21
330°	-19	-29	-10	-33	-22	-24	-2	-53	-18	+35	-76	-21	+55
$\overline{\delta}$	-13	-18	-5	-21	-19	-19	0	-40	-26	+14	-82	-39	+42
$\overline{\delta_t}$	-10.0	-13.8	-3.8	-13.5	-9.5	-9.5	0.0	-13.7	-8.9	+4.8	-14.2	-6.8	+7.4
D_{max}	26	20			29	25		35	25		88	53	
β^o	0.89	0.68			0.48	0.42		0.36	0.27		0.44	0.27	

Table 4.1.3.1k

CM6 773992

θ / φ	20° BO	20° HA	20° VI	40° BO	40° HA	40° VI	40° TO	50° BO	50° HA	50° VI	50° TO	60° BO	60° HA	60° VI	60° TO	60° DA	70° BO	70° HA	70° VI	70° TO	70° DA	80° BO	80° HA	80° VI	80° TO	80° DA
N = 0°	-17	-4	-18	-19	-13	-36	-4	-25		-48	-1	-32	-18	-67	-2	-21	-46	-23	-100	-5	-42	-75	-45	-186	-27	-67
30°	-16	-5	-17	-19	-15	-38		-25		-48		-30	-21	-64			-42	-33	-101			-65	-50	-185		
60°	-5	-6	-15	-18	-15	-31		-22		-43		-26	-20	-57			-29	-23	-86			-40	-31	-156		
E = 90°	-16	-7	-14	-17	-16	-29	2	-22		-34	7	-25	-25	-50	10	-30	-14	-15	-78	24	-63	-3	-22	-132	41	-35
120°	-15	-7	-13	-16	-19	-25		-20		-33		-23	-31	-45			-16	-35	-65			-7	-56	-107		
150°	-14	-7	-13	-16	-20	-28		-25		-33		-26	-38	-51			-32	-51	-79			-39	-105	-154		
S = 18 0°	-15	-7	-13	-18	-20	-27	-4	-26		-34	-1	-29	-39	-49	-2	-21	-41	-53	-78	-5	-42	-64	-107	-154	-27	-87
210°	-15	-6	-17	-17	-19	-31		-26		-38		-30	-34	-45			-46	-47	-77			-88	-97	-154		
240°	-12	-5	-11	-17	-15	-25		-22		-31		-29	-25	-45			-40	-32	-74			-71	-54	-140		
W = 270°	-9	-2	-12	-12	-11	-27	2	-16		-33	7	-23	-16	-47	10	-30	-23	-7	-62	24		-33	-15	-114	41	-35
300°	-9	-3	-15	-12	-10	-30		-17		-40		-23	-12	-53			-23	-9	-73			-39	-25	-124		
330°	-11	-3	-17	-15	-12	-34		-20		-46		-27	-14	-65			-37	-18	-94			-73	-41	-171		
$\overline{\delta}$	-14	-5	-15	-16	-15	-30	-1	-22		-38	+3	-27	-24	-53	+4	-25	-32	-29	-81	+10		-50	-54	-148	+7	-61
$\overline{\delta_t}$	-13.2	-4.7	-14.1	-12.3	-11.5	-23.0	-0.8	-14.1		-24.4	1.9	-13.5	-12.0	-26.5	+2.0	-12.5	-10.9	-9.9	-27.7	+3.4		-8.7	-9.4	-25.7	+1.2	-10.6
D_{max}	8	5	7	7	10	13		10		17		9	-27	22			30	46	39			72	92	79		
$\beta°$	0.63	0.39	0.55	0.24	0.34	0.44	0.4	0.24		0.41	0.3	0.15	0.45	0.36	0.3		0.31	0.48	0.41	0.3		0.36	0.48	0.40	0.4	

Table 4.1.3.11

CM-11 810120

θ / φ	20° BO	20° KI	40° BO	40° HA	40° KI	50° BO	60° BO	60° HA	60° DA	60° KI	70° BO	70° HA	70° DA	70° KI	80° BO	80° HA	80° DA	80° KI
N = 0°	3	1	4	4	2	4	0	-5	-28	-4	-4	-11	-41	-10	4	-15	-56	-11
30°	3	1	4	3	3	3	0	-6		-2	-3	-13		-10	8	-16		-13
60°	3	2	2	1	3	0	-6	-8		-2	-6	-12		-10	2	-15		-11
E = 90°	3	3	5	1	4	3	-4	-7	-21	-1	-8	-12	-32	-10	15	-14	-47	-15
120°	4	4	4	2	3	1	-1	-5		-2	-6	-10		-10	8	-8		-15
150°	3	3	3	3	2	0	0	-3		-4	-4	-8		-13	2	-8		-19
S = 180°	5	3	7	5	1	7	2	1	-28	-4	-5	-5	-41	-13	-10	-5	-56	-15
210°	4	2	4	6	1	2	-4	0		-5	-9	-3		-13	-17	-2		-19
240°	4	2	5	7	-1	3	-1	1		-7	-6	-2		-15	-11	2		-24
W = 270°	4	3	5	7	0	3	-2	1	-21	-7	-10	-2	-32	-15	-18	-4	-47	-15
300°	5	3	5	5	0	3	-2	0		-5	-7	-5		-13	-16	-7		-19
330°	5	3	5	5	0	4	-2	-3		-7	-8	-7		-13	-16	-9		-19
$\overline{\delta}$	4	2.5	4	4	2	3	-2	-3	-24	-4	-7.5	-7.7	-36	-12	-4	-8	-51	-16
$\overline{\delta_t}$	3.8	2.3	3.1	3.1	1.9	1.9	-1.0	-1.5	-12.0	-2.0	-2.6	-2.6	-12.3	-4.1	-0.7	-1.4	-8.8	-2.8
D_{max}	2	3	5	6	7	7	8	9		6	11	11		5	33	18		13
β°	0.16	0.24	0.17	0.20	0.17	0.17	0.13	0.15		0.10	0.07	0.11		0.05	0.17	0.09		0.07

Table 4.1.3.1m
PSP 17750 F3

θ / φ	20° BO	20° VI	40° BO	40° HA	40° VI	40° TO	50° BO	50° VI	50° TO	60° BO	60° HA	60° VI	60° TO	70° BO	70° HA	70° VI	70° TO	80° BO	80° HA	80° VI	80° TO
N = 0°	2	-16	4	-16	-36		4	-48		2	-37	-70		3	-57	-96		-4	-114	-136	
30°	4	-11	5	-16	-34	-12	4	-51	-22	5	-37	-67	-32	11	-53	-95	-46	4	-106	-141	-75
60°	3	-12	6	-14	-34		6	-49		4	-34	-62		17	-45	-93		5	-96	-146	
E = 90°	2	-11	5	-13	-34	-12	5	-57	-22	6	-30	-71	-33	22	-33	-107	-49	7	-80	-164	-90
120°	2	-19	3	-13	-32		3	-48		3	-28	-70		18	-30	-124		1	-76	-188	
150°	0	-11	3	-13	-34	-15	3	-52	-25	5	-28	-78	-40	14	-36	-114	-54	3	-76	-198	-95
S = 18 0°	-3	-8	-2	-14	-32		0	-50		2	-28	-76		16	-39	-118		37	-80	-198	
210°	-2	-11	-2	-12	-36	-12	-2	-55	-22	1	-29	-76	-32	13	-41	-126	-46	32	-82	-210	-75
240°	-1	-9	-2	-11	-31		0	-52		5	-28	-76		18	-41	-116		38	-89	-210	
W = 270°	-1	-11	1	-11	-34	-12	0	-51	-22	5	-30	-75	-33	17	-43	-113	-49	38	-97	-154	-90
300°	-2	-12	2	-12	-35		3	-56		7	-31	-78		17	-42	-125		43	-107	-198	
330°	-2	-13	-1	-14	-33	-15	0	-52	-25	4	-35	-72	-40	11	-56	-105	-54	33	-112	-183	-95
$\overline{\delta}$	0	-12	2	-13	-34	-13	2	-52	-23	4	-31	-73	-37	15	-43	-111	-50	20	-93	-180	-97
$\overline{\delta}_t$	0	-11.3	1.5	-10.0	-2.6	-10.0	1.3	-33.4	-14.8	2.0	-15.5	-36.5	-18.5	5.1	-14.7	-38.0	-17.1	3.5	-16.1	-31.3	-15.1
D_{max}	7	10	7	5	5		0	9		6	9	16		19	27	33		47	36	74	
β°	0.55	0.79	0.24	0.17	0.17	0.8	0.19	0.22	0.8	0.10	0.15	0.26	0.8	0.20	0.28	0.34	0.9	0.24	0.18	0.37	1.0

Table 4.1.3.1n.

CM-11 810119

θ / φ	20°		40°				50°		60°				70°				80°			
	BO	VI	BO	HA	VI	KI	BO	VI	BO	HA	VI	KI	BO	HA	VI	KI	BO	HA	VI	KI
N = 0°	0	-8	2	4	-17	4	4	--20	7	8	-31	6	8	4	-68	6	-3	-14	-125	4
30°	0	-7	3	4	-18	4	6	-24	8	8	-36	6	9	6	-73	6	1	-11	-162	4
60°	0	-9	3	3	-18	3	4	-24	8	8	-35	5	9	6	-73	4	0	-10	-152	13
E = 90°	-1	-7	3	3	-17	2	4	-20	7	8	-31	3	9	7	-69	1	9	-7	-148	4
120°	0	-7	2	3	-17	2	5	-20	8	7	-31	3	11	8	-69	1	11	-7	-148	4
150°	-1	-9	1	3	-18	0	4	-28	8	7	-36	2	12	9	-80	-1	11	-7	-164	-5
S = 18 0°	-1	-8	2	3	-17	-1	6	-28	8	7	-38	1	12	9	-80	-1	4	-5	-172	-5
210°	0	-5	2	2	-15	-1	5	-22	6	6	-36	1	7	8	-78	-1	-3	-8	-157	-22
240°	0	-8	3	2	-12	-2	6	-19	7	5	-32	2	8	7	-65	-1	-3	-11	-157	-13
W = 270°	0	-3	3	2	-12	-1	6	-19	6	5	-32	2	7	5	-65	2	-8	-11	-144	-13
300°	0	-8	3	3	-14	1	6	-18	7	6	-29	5	5	6	-67	4	-13	-14	-120	13
330°	1	-7	4	4	-17	1	6	-20	8	6	-36	6	5	5	-69	6	-16	-14	-161	13
$\overline{\delta}$	0	-7	3	3	-16	1	5	-22	7	7	-34	4	9	7	-71	2	-1	-10	-151	0
$\overline{\delta_t}$	0	-6.6	2.3	2.3	-12.3	O.8	3.2	-14.1	3.5	3.5	-17.0	2.0	3.1	2.4	-24.3	0.7	-0.17	-1.7	-26.2	0.0
D_{max}	2	6	3	2	6	6	2	10	2	3	9	5	7	5	15	7	27	9	44	35
β^o	0.16	0.47	0.10	0.07	O.20	0.20	0.05	0.24	0.03	0.05	0.15	0.08	0.07	0.05	0.16	0.07	0.14	0.05	0.22	0.18

Appendix AA (supplement to 4.1.3.1) continued

Three quantities were evaluated for comparing the results:

1. the mean absolute error $\overline{\delta}_t(\theta)$ calculated from the mean cosine error $\overline{\delta}(\theta)$ by Equation 4.6
2. the maximum $\Delta_{max}(\theta)$ according to Equation 4.10 (mostly for $\theta \geq 60°$) and
3. the maximum azimuth variation D_{max} and its corresponding out-of-level angle β according to Equations 4.7&8.

Three classes of agreement between laboratories have been defined to simplify the comparison as follows:

good agreement (absolute deviations $|\Delta\overline{\delta}_t(\theta)| < 2.5$ Wm^{-2} for all θ),
moderately good agreement (when for all θ , $|\Delta\overline{\delta}_t| < 5$ Wm^{-2}) and,
moderate agreement (when for all θ , $|\Delta\overline{\delta}_t| < 10$ Wm^{-2}).

Because the largest number of Task 9 pyranometers were tested in the BORÅS series, these results are generally used as the reference for $\Delta\overline{\delta}$ and $\Delta\overline{\delta}_t$

The data in Tables 4.13.1b-n are summarised in terms of $\Delta\overline{\delta_t}$, Δ_{max} and β in the following paragraphs, in which only the *good agreement* cases are identified. The compared values are indicated by the letter symbols of the laboratories. The first six tables contain only results of BORÅS (BO) and DELFT (KI).

CM10 #810121, Summarised From Table 4.1.3.1b

$\overline{\delta}_t$	: *good agreement*: where BO > KI
Δ_{max}	: for $\theta = 70°$: KI - BO = -3.4 Wm^{-2}
	: for $\theta = 80°$: KI - BO = -2.8 Wm^{-2}
β	: BO ≈ KI (±0.08°); for $\theta = 80°$: BO = 3 · KI = 0.12°

PSP #20524F3, Summarised From Table 4.1.3.1c

$\overline{\delta}_t$	: $\|KI - BO\| \leq 3.4$ Wm^{-2}; BO > KI
Δ_{max}	: for $\theta = 60°$: KI - BO = -10 Wm^{-2}
	: for $\theta = 70°$: KI - BO = -12 Wm^{-2}
	: for $\theta = 80°$: KI - BO = -9.7 Wm^{-2}
β	: BO: 0.40° → 0.65°; KI: 0.12° → 0.24°; BO > 2 KI

CM5 #773656, Summarised From Table 4.1.3.1d

$\bar{\delta}_t$: *good agreement* (for θ >20°) mostly BO > KI

Δ_{max} : for θ ≤ 60°: |KI - BO| ≤ 4 Wm^{-2}

: for θ = 70°: KI - BO = -5.8 Wm^{-2}

: for θ = 80°: KI - BO = -7.3 Wm^{-2}

β : BO: 0.20° → 0.49°; KI: 0.20° → 0.43°; BO ≈ KI

Schenk STAR #2209, Summarised From Table 4.1.3.1e

$\bar{\delta}_t$: *good agreement*; mostly BO < KI

Δ_{max} : for θ ≤ 50°: KI - BO < 10 Wm^{-2}

: for θ = 60°: KI - BO = 10 Wm^{-2}

: for θ = 70°: KI - BO = +9.9 Wm^{-2}

: for θ = 80°: KI - BO = -9.7 Wm^{-2}

β : BO: 0.15° → 0.45°; KI: 0.50° → 0.63°; KI >> BO; KI very stable

Eko MS42 #81908, Summarised From Table 4.1.3.1f

$\bar{\delta}_t$: (BO - KI) ≤ 7.8 Wm^{-2}; BO >> KI for θ > 20°

Δ_{max} : for θ ≤ 50° : KI - BO ≤ +9 Wm^{-2}

: for θ > 60° : KI - BO ≈ -12.0 Wm^{-2}

β : BO: 0.11° → 0.71° ; KI: 0.19° → 0.39° ; KI more stable

SS25 #114, Summarised From Table 4.1.3.1g

$\bar{\delta}_t$: for θ ≤ 50° |KI - BO| < 7 Wm^{-2}, (KI > BO)

: for θ = 60° : KI - BO = -10.0 Wm^{-2}

: for θ = 70° : KI - BO = -14.7 Wm^{-2}

: for θ = 80° : KI - BO = -18.2 Wm^{-2}

Δ_{max} : in the same range as $\bar{\delta}_t$ for θ ≥ 50°

β : BO: 0.07° → 0.45° ; KI: 0.17° → 0.22°

: (θ > 20° ; for KI, especially low and stable)

CM5 #785047, Summarised From Table 4.1.3.1h

$\bar{\delta}_t$: for θ = 40° : HA - BO = -6.2 Wm^{-2}
: for θ = 60° : HA - BO = - 9.5 Wm^{-2}
: for θ = 70° : HA - BO = -13.3 Wm^{-2}
: for θ = 80° : HA - BO = - 6.6 Wm^{-2}
: DA and TO > BO (relatively strong deviations)

Δ_{max} : BO > HA; approximately: $2\Delta\delta_t$

β : BO: 0.17° → 0.49° ; HA: 0.46° → 0.63°; TO: 0.5° → 0.8°

PSP #20523F3, Summarised From Table 4.1.3.1i

$\bar{\delta}_t$: |HA - BO| ≤ 6.8 Wm^{-2}; HA > BO and HA ≈ 2BO if θ ±70°

Δ_{max} : for θ = 60° : HA - BO = - 8.5 Wm^{-2}
: for θ = 70° : HA - BO = -12.3 Wm^{-2}
: for θ = 80° : HA - BO = -10.2 Wm^{-2}

β : BO: 0.08° → 0.23° ; HA: 0.17° → 0.31° ; HA ≥ BO

EP07 #123, Summarised From Table 4.1.3.1j

$\bar{\delta}_t$: -3.8Wm^{-2} ≤ (VI - HA) ≤ 7.4 Wm^{-2}
: for θ = 60°: (VI - HA) = 0.0 Wm^{-2}
: for θ = 70°: (VI - HA) = +4.8 Wm^{-2}
: for θ = 80°: (VI - HA) = +7.4 Wm^{-2}

Δ_{max} : VI > HA; $\Delta_{max}(\theta) >> \delta_t(\theta)$

β : VI: 0.27° → 0.68°; HA: 0.36° → 0.89°; HA > VI

CM5 #773992, Summarised From Table 4.1.3.1k

$\bar{\delta}_t$: BO & HA: for θ ≥ 40°: *good agreement*
: BO & VI: -17.0 Wm^{-2} ≤ (VI - BO) ≤ -10.7 Wm^{-2} (for θ ≥ 40°)
(VI - BO) = - 0.9 Wm^{-2} (for θ = 20°)
: VI: $\delta_t(\theta)$ = 25.4 Wm^{-2} (±2.3 Wm^{-2}) ~constant
: TO & DA: TO >> DA > VI

Δ_{max} : VI - BO ≈ -21 Wm^{-2} (for θ ≥ 60°)
: |HA - VI| < 11.4 Wm^{-2}

β : for θ ≥ 40°: BO: 0.24° → 0.36°
HA: 0.34° → 0.48°
VI: 0.36° → 0.44°

CM10 #810120, Summarised From Table 4.1.3.1l

$\overline{\delta}_t$: |HA - BO| ≤ 0.7 Wm^{-2}: *good agreement*

: |KI - BO| ≤ 2.1 Wm^{-2}: *good agreement*

: DA - BO ≈ -10 Wm^{-2}

Δ_{max} : for θ = 80°: HA - BO ≈ BO - KI ≈ 5 Wm^{-2}

: for θ = 70° and 60°: HA - BO ≈ KI - BO ≈ 3 Wm^{-2}

β : BO: 0.07° → 0.17°; HA: 0.09° → 0.20°; KI: 0.05° → 0.17°

PSP (#17750F3), Summarised From Table 4.1.3.1m

$\overline{\delta}_t$: for θ ≥ 60° : BO - HA ≈ 19 Wm^{-2}

: for θ ≥ 60° : VI - HA ≈ -19 Wm^{-2}

: for θ ≥ 60° : |TO - HA| ≤ 3 Wm^{-2}

Δ_{max} : for θ ≥ 60° : BO - HA ≈ 23 Wm^{-2}

: for θ ≥ 60° : VI - HA ≈ -27 Wm^{-2}

: for θ ≥ 60° : BO - HA ≈ 0.5 (BO - VI)

β : BO: 0.10° → 0.24°

: HA: 0.15° → 0.28°

: VI: 0.17° → 0.37°; (TO: 0.8° → 1.0°)

CM10 #810199, Summarised From Table 4.1.3.1n

$\overline{\delta}_t$: |HA - BO| ≤ 1.5 Wm^{-2}: *good agreement*

: |KI - BO| ≤ 2.4 Wm^{-2}: *good agreement*

: VI - BO ≈ -26 Wm^{-2}, for θ ≥ 70°

: VI - BO ≈ -20 Wm^{-2}, for θ ≥ $60°_{max}$

Δ_{max} : |HA - BO| ≤ 3.1 Wm^{-2}

: |KI - BO| ≤ 5.0 Wm^{-2}

: (VI - BO) ≈ -31 Wm^{-2}, for θ = 80° and 70°

: (VI - BO) ≈ -22 Wm^{-2}, for θ = 60° and 50°

: (VI - BO) = -16.1 Wm^{-2}, for θ = 40°

β : BO: 0.03° → 0.14°

: HA: 0.05° → 0.07°

: KI: 0.07° → 0.2°

: VI: 0.15° → 0.24°

Comparison of the test results according to type of pyranometer

The test results for each type of pyranometer are grouped according to the laboratories compared (abbreviated by "XY & REF") and pyranometer (indicated by the number of the table containing the data).

(a) CM10, Tables 4.1.3.1b,l,n

KI & BO and	$\overline{\delta}_t$	: *good agreement* in all cases
HA & BO:	Δ_{max}	5.2 Wm^{-2} for all θ
	β	0.17°, mostly about 0.1°.
VI & BO	$\overline{\delta}_t$	: BO >> VI $\Delta\delta_t(\theta)$ decreases down to -27.4 Wm^{-2}.
	Δ_{max}	: decreases with increasing θ to -31 Wm^{-2} for θ = 80°
	β	: BO ≈ VI - 0.1° for $\theta \geq 50°$
		Table 4.1.3.1n
DA & BO	$\overline{\delta}_t$	: BO >> DA; DA ≈ BO - 10 Wm^{-2} for θ = 60°
		Table 4.1.3.1l
		(Figures 4.1.3.1f & j, respectively.)

(b) CM5, Tables 4.1.3.1d,h,k

BO & KI	$\overline{\delta}_t$	*good agreement* for $\theta \geq 40°$
	Δ_{max}	(KI - BO) ≈ -7.3 Wm^{-2} for θ = 80°, increasing
		by 1.5 Wm^{-2} per 10° decrease of θ
	β	BO ≈ KI (0.20° → 0.45°)
		Table 4.1.3.1d
BO & HA	$\overline{\delta}_t$	*good agreement* for $\theta \geq 40°$
	Δ_{max}	(HA - BO) <11.4 Wm^{-2}, (irregular deviations)
	β	HA > BO; HA ≈ 0.46° for $\theta \geq 40°$
		Table 4.1.3.1k
BO & HA	$\overline{\delta}_t$	-13.3 $Wm^{-2} \leq$ (HA - BO) ≤ -6.2 Wm^{-2}
	Δ_{max}	(HA - BO) ≈ -16 Wm^{-2} if $\theta \neq 70°$
	β	BO: 0.17° → 0.49°; HA ≈ 0.60°
		Table 4.1.3.1h
BO & VI	$\overline{\delta}_t$	(VI - BO): -11 → -17 Wm^{-2} for $\theta \geq 40°$
	Δ_{max}	(VI - BO) ≈ -21 Wm^{-2} for $\theta \geq 60°$

continued

	β	VI: 0.36° → 44°, HA ≈ VI
		Table 4.1.3.1k
BO & DA	$\overline{\delta_t}$	DA > BO
		Table 4.1.3.1h
BO & TO	$\overline{\delta_t}$	TO > DA > BO
BO & DA	$\overline{\delta_t}$	DA ≈ BO for θ ≥ 60°
		Table 4.1.3.1k

(Figures 4.1.3.1g&k respectively).

(c) PSP, Tables 4.1.3.1c,i,m

BO & KI	$\overline{\delta_t}$	(KI - BO) ≥ -3.4 Wm^{-2}, BO > KI
		(*moderately good agreement*)
	Δ_{max}	(KI - BO) ≈ -11 Wm^{-2} for θ to 60°
	β	BO > 2 · KI
		Table 4.1.3.1c
BO & HA	$\overline{\delta_t}$	(HA - BO) ≈ -6 Wm^{-2}, (-5 to -7 Wm^{-2})
	Δ_{max}	(HA - BO) ≈ -10 Wm^{-2}, (-8 to -12 Wm^{-2})
	β	HA ≥ BO; for θ < 60°; HA: 0.17° → 0.31°
		Table 4.1.3.1j
BO & HA	$\overline{\delta_t}$	(HA - BO) ≈ -19 Wm^{-2} for θ ≥ 60°
	Δ_{max}	(HA - BO) ≈ -23 Wm^{-2} for θ ≥ 60°
	β	BO ≈ HA: 0.10° → 0.30°
		Table 4.1.3.1m
BO & VI	$\overline{\delta_t}$	(VI - BO) ≈ -38 Wm^{-2} for θ ≥ 60°
	Δ_{max}	(VI - BO) ≈ -45 Wm^{-2} for θ ≥ 60°
	β	BO < VI, if θ ≠ 40°
		Table 4.1.3.1m
BO & HA	$\overline{\delta_t}$	(HA - BO) ≈ (TO - BO) ≈ 0.5 · (VI - BO) for θ ≥ 60°
	Δ_{mean}	(HA - BO) ≈ 0.5 · (VI - BO)
	β	TO: 0.8° → 1.0° (>> BO, HA, VI)
		Table 4.1.3.1m
		(Figures 4.1.3.1h&l, respectively).

(d) Schenk Star, Table 4.1.3.1e

BO & KI	$\overline{\delta}_t$	*good agreement* (if $\theta \neq 50°$)
	Δ_{max}	(KI - BO) ≥ -9.7 Wm^{-2}
	β	KI >> BO; KI: 0.50° → 0.63°

(e) Eko MS42 # 81908, Table 4.1.3.1f

BO & KI	$\overline{\delta}_t$	(KI - BO) ≈ -8 Wm^{-2} for $\theta \geq 60°$
	Δ_{max}	(KI - BO) ≈ -12 Wm^{-2} for $\theta \geq 60°$
	β	BO: 0.11° → 0.71°; KI: 0.19° → 0.39

(f) Swissteco SS25 #114, Table 4.1.3.1g

BO & KI	$\overline{\delta}_t$	(KI - BO) = -18.2 Wm^{-2} for $\theta = 80°$ (increasing by about +4 Wm^{-2} for each 10° decrease of θ if $\theta > 50°$)
	Δ_{max}	(KI - BO) approximately as for δ_t
	β	KI ≈ 0.17° → 0.22° (very stable) BO: 0.07° → 0.71° (very variable)

(g) Middleton EP07 #123, Table 4.1.3.1h

HA & VI	$\overline{\delta}_t$	-3.8 Wm^{-2} < (VI - HA) < +7.4 Wm^{-2}
	Δ_{max}	(VI - HA) ≈ +14 Wm^{-2} (12 to 16 Wm^{-2})
	β	HA: 0.36° → 0.89° VI: 0.27° → 0.68°

(Figures 4.1.3.1 i&m).

Appendix BB

Description of and Summary of results from the NARC field experiment of 1983-1984

Appendix BB1
Plan of the AES roof at Toronto, 1983-1985

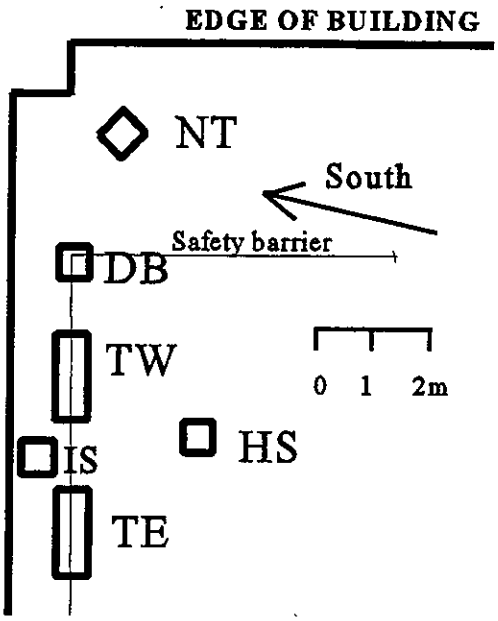

Legend:

DB Direct beam tracker for pyrheliometers

NT Normal incidence tracking table for pyranometers.

HS Horizontal shade tracker for a pyranometer measuring horizontal diffuse radiation

IS Inclined shade tracker for a pyranometer measuring diffuse radiation on a 45° slope.

TW Table west for pyranometers measuring global radiation

TE Table east for pyranometers measuring global radiation

TE and TW can be set either horizontally or tilted at 45°.

Tables TE and TW were constructed to tilt by 45° with an accuracy of better than ± 0.1°. Horizontal mounting of the pyranometers was done either by their own bubble levels or by a bubble level that was temporarily mounted to some horizontal surface of the pyranometer body. In either case and for both these tables, the horizontal orientation and the 45° tilt are believed to be accurate to within ± 0.3°. The direction of the tilt was measured by observing when the sun could be seen shining along the axis of rotation and through the axle. The result was 22.0 ± 0.3°.

The orientation of the axis of the inclined tracker was intended to be the same as the tilting tables. It was measured by taking sights of the sun and determining the offsets to the latitude and longitude required by the tracking software. The result was a tilt of 44.7° along 21.2° east of south, both with an accuracy of ±0.3°.

Appendix BB2
The NARC automatic Alternating Sun-Shade Method for calibration of pyranometers

This method was used at Toronto during 1983 and 1984 to calibrate the following pyranometers mounted on Cosmos sun-trackers:

1. Cm10 #820158 (Ch#28) mounted horizontally, but rotating so that the pyranometer cable was always in the same azimuth as the sun.

2. CM10 #810175 (Ch#29) mounted on a tracker whose axis was tilted 44.7° along 21.2° east of south. The pyranometer axis was within 0.2° of the tracker axis and, as the tracker rotated, the pyranometer axis, its cable direction and the solar direction were always coplanar.

3. PSP #17750 (Ch34) and PSP #24011 (Ch5) mounted on a full solar tracking table so that the pyranometer axis coincided with the solar direction at all times, and the cable left the instrument in the downward direction.

An Eppley NIP #20202 on Channel 40 was used as the reference pyrheliometer. It was checked many times during the measurement period against the NARC Hickey-Frieden cavity radiometer #18747.

The pyranometer and pyrheliometer signals were sampled every 12 seconds and one-minute mean values were recorded.

On most days, the three pyranometers were continuously shaded by a tracking discs of 10cm diameter at a distance of 1.0 m. For roughly one quarter of the days the pyranometers were subjected to a 10-minute on, 10-minute off alternating shading routine. The data from these days are used to calibrate the pyranometers by the Alternating Sun-Shade Method(ASM).

The alternating shading routine is synchronized on the hour as follows: the pyranometers are shaded during minutes 0-9 inclusive, then during 10-19 unshaded, then shaded again during 20-29, unshaded during 30-39, shaded during 40-49 and unshaded during 50-59.

The algorithm yields a single responsivity value corresponding to the five minutes at the end of each unshaded period. i.e. centred at minutes 17, 37 and 57. These values are accepted and stored or rejected depending on the variability of the signals during the five minutes.

In the algorithm, individual responsivities are calculated from the five one-minute readings of the pyranometer unshaded signal, the five corresponding pyrheliometer readings and estimates of the diffuse signal. The diffuse values are obtained by interpolation between the mean of the four last minutes of the preceding shaded

period and the mean of the last four readings in the following shaded period. The mean of the five individual responsivities and its standard error are calculated. If the standard error is less than a critical value, usually 0.01 $\mu V.W^{-1}\ m^2$, the mean is accepted and stored. EXAMPLES:

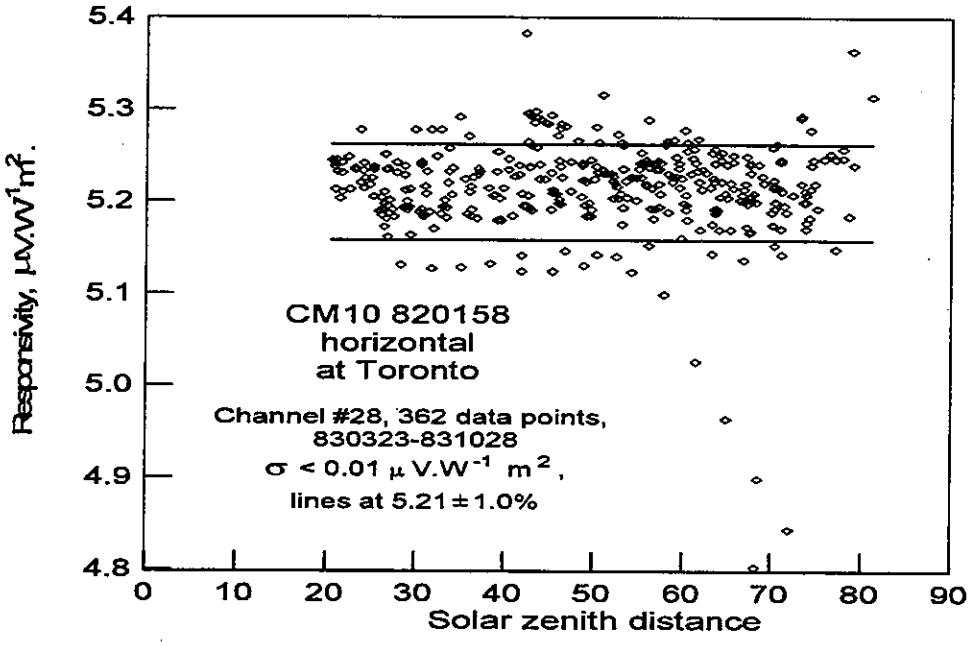

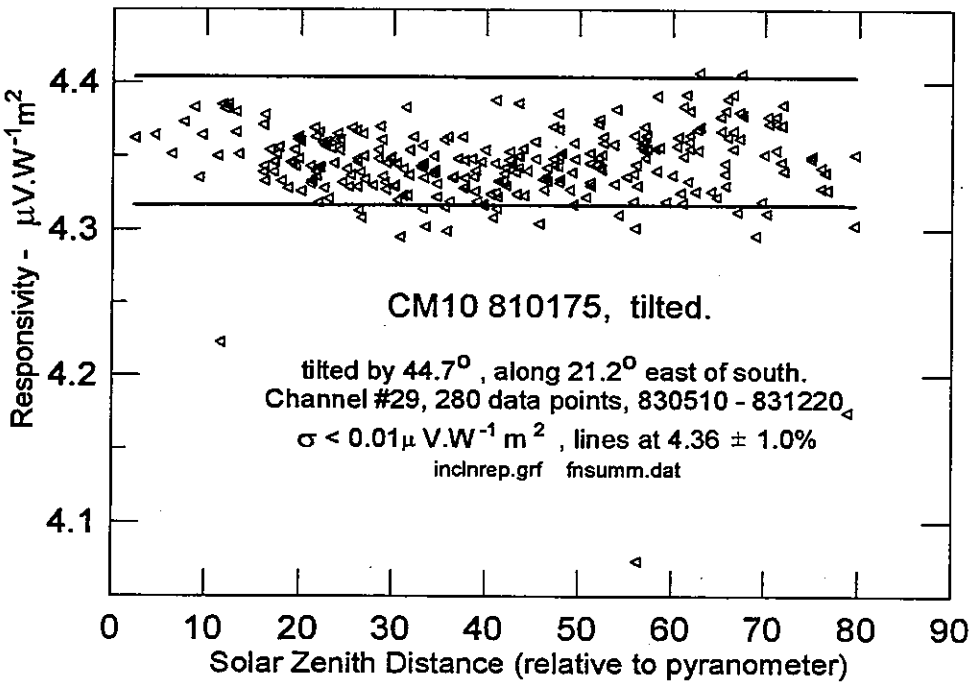

APPENDIX BB3

Notes on the presentation of the results of the NARC/IEA 83/84 field experiment given in Appendix BB4

These notes refer to the Organiz draft of April 14 1986, which as Appendix BB4 follows this.

1. The data were gathered between 25/01/83 and 03/11/84.

2. The data were stored on ten tapes (T1 ... T10) each tape holding roughly two months of data.

3. The NARC data system has 60 Channels of which those up to CH 41 sometimes or always carried pyranometers. The assignment of channels to pyranometers is given repeatedly in Appendix BB4, starting on page 18.

4. The signals measured by the system are stored as one minute averages computed from five readings taken at 12 second intervals. For the pyranometers, the recorded signals are voltages. With the sole exceptions of (a) calibrating the cavity radiometer and (b) evaluating intermittent occulting calibration data, all the analysis is done on 10-minute average data, each datum being computed from the recorded minute averages and synchronized to start on the local solar hour.

5. All results are based on the NARC absolute cavity radiometer HFR 18747 via the NIP 20202 whose calibration factor of 8.45 has been confirmed in the NARC paper in the Norrköping Proceedings. That paper also gives the precise dates for all the tapes.

6. The pyranometer on Channel 00 was chosen as a transfer standard. It was in place throughout the whole experiment. Seven others were permanent and various comparisons established that Channel 00 and five others were stable (Ch 1, 2, 16, 17, 18). For some purposes Ch 1 and Ch 16 have also been used as transfer standards.

7. Most of the pyranometers were mounted on "Table East - TE" or "Table West - WE". These were tilted for some of the time at 45° towards azimuth 158 (roughly south) and were horizontal for the rest of the time.

8. At various times six pyranometers were mounted on "Normal Incidence Tracking Table - NT" which followed the sun.

9. One pyranometer measured the horizontal diffuse irradiance. It was mounted on a horizontal platform which tracked the sun in azimuth. For most of the time, this pyranometer was continuously shaded by a 10 cm disc at a distance of 100 cm. For selected periods the disc was run on an alternating

sun/shade schedule with 10 minute durations on each side.

10. Similarly, a pyranometer on Channel 29 measured the 45° slope diffuse radiation.

11. Similarly pyranometers, at various times on Channel 34 and Channel 5 were mounted on the normal tracking table equipped with a shading disc, measured the normal tracking diffuse irradiance.

12. All three of the diffuse measuring pyranometers were calibrated extensively by the intermittent shading method and by the Simultaneous Diffuse and Global Method (page 17).

13. The responsivities used in Appendix BB4 for the horizontal and tilted diffuse pyranometers were 5.21 and 4.36 respectively as determined by the ASM calibration and checked by the SDGM. The results are not very sensitive to their exact values.

14. Benchmark conditions that have been agreed on in Task IX are as follows:

NAME	TILT	SOLAR ELEVATION	DIRECT BEAM	TEMPERATURE	DIFFUSE RADIATION
BMHO	0	35	900	15	as specified
BMTN	45	normal incidence	900	15	as specified
BMTO	45	35 (55 from n.i.)	900	15	as specified

15. To realize the Benchmarks, NARC has used the data with the following restrictions:

DIRECT BEAM > 700 $W.m^{-2}$

BMHO	60 > Z > 50	HORIZONTAL	horizontal oblique
BMTN	20 > Z'	45 TILT	tilted normal
BMTO	60 > Z'> 50	45 TILT	tilted oblique
and in addition			
BMHA	30 > Z > 20	HORIZONTAL	horizontal acute
BMTA	30 > Z'> 20	45 TILT	tilted acute

where Z or Z' is the solar zenith distance or the angle between the sun and pyranometer axis.

The data are fitted with linear regression and normalized to global radiation values of either 1000 Wm^{-2} for BMTN, BMTA and BMHA or 600 Wm^{-2} for BMHO and BMTO. This is NARC's "Best Method" for getting the benchmarks.

16. The diffuse fraction in these data is always in the range 0.10 to 0.25.

17. Channel 00 was calibrated directly by analysis of the output voltage as a function of the incident irradiance. The irradiance was computed from the reference NIP and from the horizontal or tilted diffuse measuring pyranometer. This was done a total of 22 times for various combinations of benchmarks and tapes. The results are listed starting on page 15 (Resaa4). Graph-1

shows one analysis - for bmho on tape 10. The graph covers 31 hours of data and the result is 10.19 -0.44/6 =10.12. The scatter of the individual points about the regression is 33 microvolts.

18. The results for each benchmark were averaged over all tapes and these values were taken as the final benchmark responsivities for Channel 00.

19. Most of the other pyranometers were evaluated with reference to Channel 00. Graph-2 is the basis for computing bmho for Channel 1 on tape 4. The initial result from graph-2 is a benchmark ratio namely 0.458 + .024/6 = 0.462 with a scatter of 11 microvolts (the responsivity of Channel 00 is approximately 6mV / 600 $W.m^{-2}$). This benchmark ratio along with several hundred others is entered into the first table (Resaa1) on page 11. In this table an asterisk (*) indicates that a result was calculated by hand from the relevant graph and a colon (:) shows when a different pyranometer was connected on a particular channel.
Instruments which are believed (by NARC) to have significant temperature coefficients of responsivity appear twice in this table. Where the letters TC precede the numbers, the responsivities have been "temperature corrected" to 25C. (It should perhaps have been 15C)

20. Representative average values for all the benchmark ratios are given in the second table at page 18. Some results are not included in the averaging on account of their either having large internal scatter or being distant from others of the same type. The individual reasons are noted in the table.

21. The end results are benchmark calibrations of each type for every instrument, and they are the products of the relevant benchmark ratios with the corresponding benchmark calibrations of Channel 00. These results are given on pages 22 and 23.

22. The data from the pyranometers of the normal incidence tracking table have also been analyzed to yield standard calibration factors BMTR. These are evaluated from data with:
direct beam $> 700\ Wm^{-2}$ $Z' = 0$ $40 < tilt < 60$
which are normalized to tracking global = $1000\ Wm^{-2}$
This benchmark is thought not to differ significantly from BMTM and, in the remaining analysis and comparisons, is treated identically.

23. In the remainder of Appendix BB4, the benchmarks are compared with each other, with manufacturers' calibrations and with NARC sphere values.

Graph 1. "Absolute" benchmark calibration.

TAPE 10
I > 700
50 < θ < 60

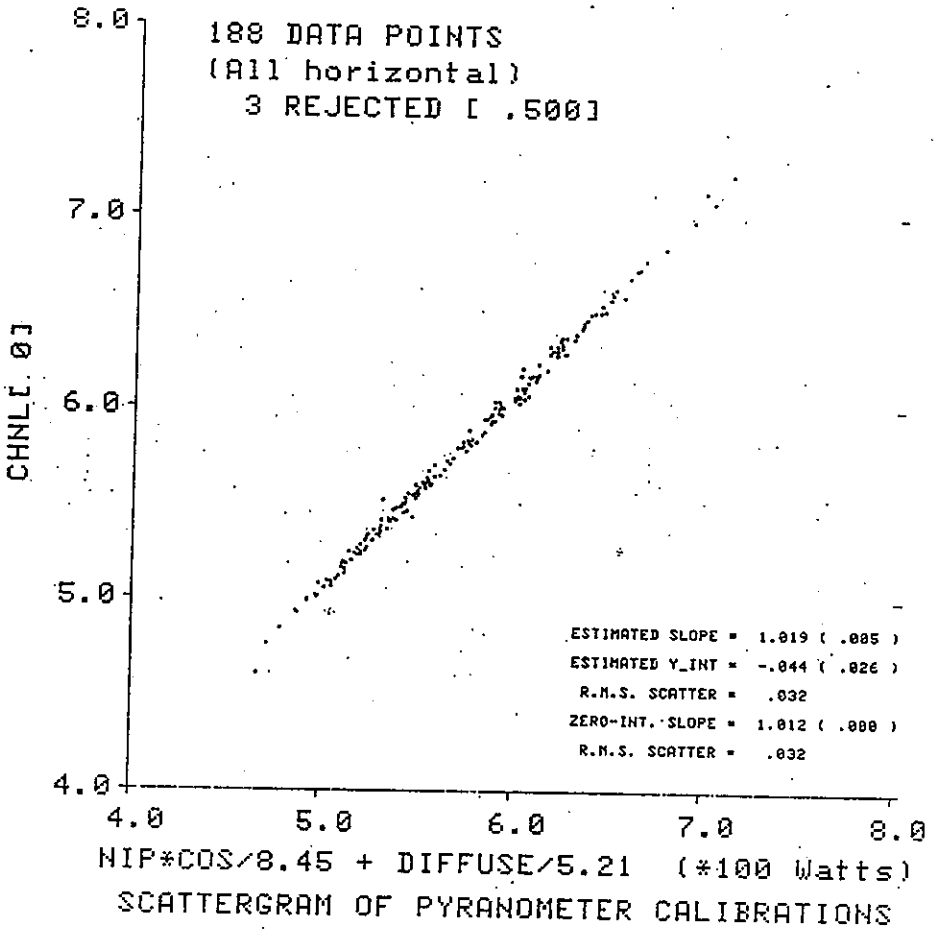

Graph 1. Shows the derivation the BMHO value for the pyranometer Channel 0 from separate measurements of the diffuse and direct radiation from Tape 10 data.

Graph 2. Relative benchmark calibration.

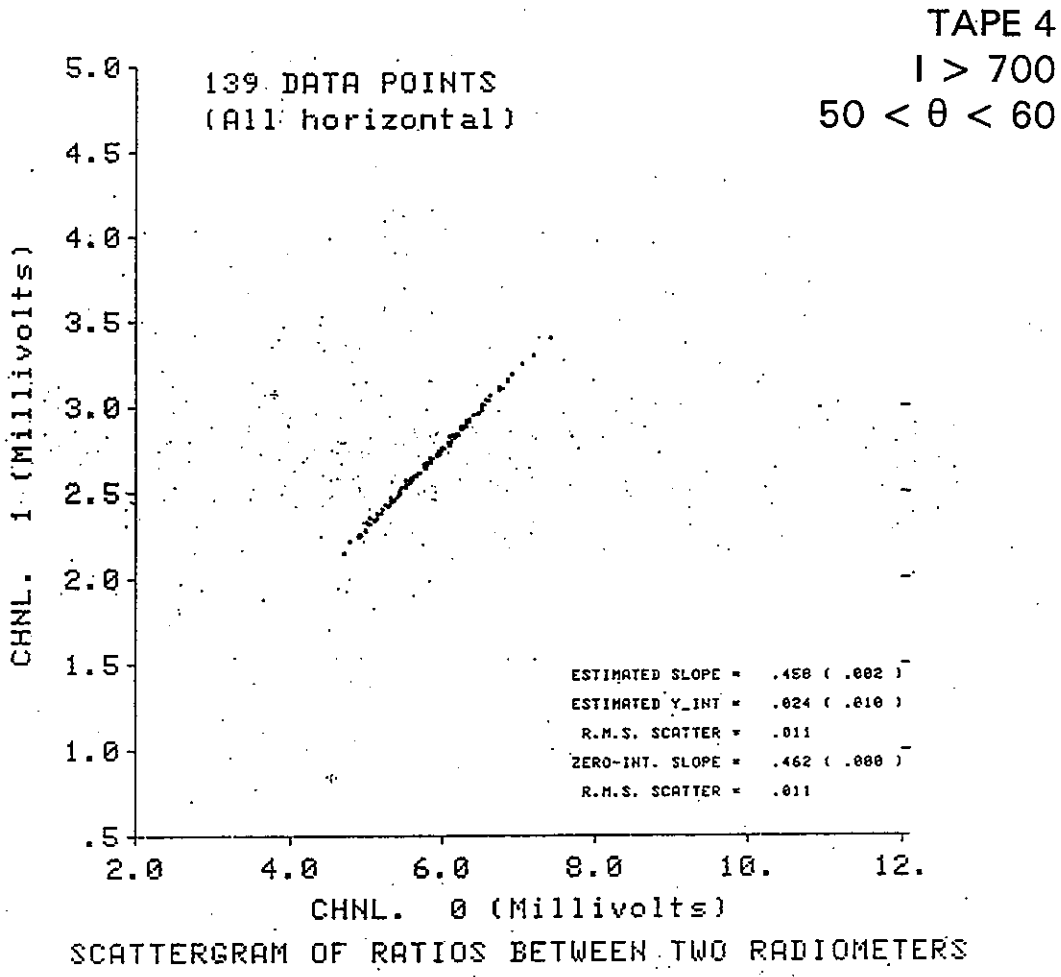

Graph 2. Shows the derivation the BMHO value for the pyranometer on Channel 1 from measurements of the global radiation by the pyranometer on Channel 0 from data on Tape 4. The result is a ratio of Benchmark responsivities.

Appendix BB4

SUMMARY OF RESULTS FROM THE NARC FIELD EXPERIMENT

Contents

Resaal 10/04/86 **BENCHMARK RATIOS RELATIVE TO CHANNEL 00**

σ = scatter in μVolts of points in the regression of Ch#x vs Ch00.

Ch	tape	BMHO	σ	bmha	σ	BMTO	σ	bmta	σ	BMTN	σ	
1	t1	.470	16									
	t2	.464	16									
	t3	.460	10			.461	12					
	t3		ha	.456	11			ta	.455 10			
	t4	.462	11			.463	9			.454	21	
	t5	.462	26					ta	.466 50			
	t6							ta	.465 26			
	t7					.465	18			.456	18	
	t8	.461	16									
	t8		ha	.457	20							
	t10	.461	19									
2	t1	(.668	52	am .675	39			pm .662	30)			
	t2	.682	24									
	t3	.682	12			.674	12					
	t3		ha	.663	12			ta	.653 18			
	t4	.679	20			.671	12			.648	19	
	t5	.679	18					ta	.653 26			
	t6							ta	.651 25			
	t7					.668	16			.647	18	
	t8	.681	18									
	t8		ha	.661	27							
	t9									.649	06	
	t10	.676	18									
4	t2	.955	14									
	t3	.957	25			.949	32					
	t3		ha	.937	03			ta	.924 16			
	t4	.957	26			.942	13			.920	24	
	t5	.957	23									
5	t2	1.183*	24*									
	t3	1.156	47			1.124	44					
	t3		ha	1.150	50			ta	1.111 34			
	t4	1.165	45			1.132	13			1.110	47	
		(1.157	24	tc)								
5	t2 TC	1.164*	24*									C
	t3 TC	1.155	47			1.127	44					C
	t3 TC		ha	1.154	50			ta	1.115 34			C
	t4 TC	1.158	45			1.134	13			1.113	47	C
6	t4	1.138	30			1.128	14			1.108	68	
6	t4 TC	1.132	30			1.130	14			1.111	68	C
6	t7 ::					.959	14			.965	22	
	t8	.959	30									
7	t4	1.247	58			1.237	21			1.218	61	
	t5	1.257	35									
7	t4 TC	1.240	58			1.239	21			1.221	61	C
	t5 TC	1.234	35									C
	t7 ::					.974	54			.993	38	
	t8	.984	90									
8	t2	.421	12									
	t3	.419	7			.419	8					
	t3		ha	.414	08			ta	.415 08			
	t4	.417	10			.418	5			.413	19	
	t5	.420	8									

```
 9  t1          1.002  33
    t2          1.003  22
    t3          1.005  23              1.015  33
    t3                 ha 1.011 25                ta 1.015  26
    t4           .999  44              1.007  52              1.010  26

10  t1          1.005  46
    t2          1.021  39
    t3          1.025  31              1.028  25
    t3                 ha 1.038 35                ta 1.042 46
    t4          1.018  44              1.025  37              1.042  43
    t5          1.001  34                         ta 1.024 42
    t6                                             ta 1.016*
    t8                 ha 1.029 96
    t10         1.009  53

10  t1 TC       1.028  46                                                C
    t2 TC       1.033  39                                                C
    t3 TC       1.026  31              1.026  25                        C
    t3 TC              ha 1.035 35                ta 1.039 46            C
    t4 TC       1.022  44              1.024  37              1.040  43 C
    t5 TC       1.015  34                         ta 1.057 42            C
    t6 TC                                          ta 1.049 *             C
    t8 TC              ha 1.030 96                                       C
    t10 TC      1.019  53                                                C


11  t4           .880  36               .881  7                 .878  27
    t5           .882  21                         ta  .878 25
    t6                                            ta  .878 20
    t7                                 .858  163               .878  *
    t8           .847  136
    t9                                 .878  09                .878  24
    t10          .881  10

12  t4          1.481  60              1.499  29              1.500  38
    t5          1.493  47

12  t4 TC       1.476  60              1.500  29              1.502  38  C
    t5 TC       1.476  47                                                C

13  t4          1.470  205             1.545*                1.542*
    t5          1.495  156

14  t1          ( .701  73   am  .711 35    pm  .691 46 )
    t1                                      ( 14vs 2  1.035 45 bmho )
    t2                                      ( 18vs14  1.072 20 bmho )
    t2          ( .699  66   am  .707 14    pm  .685 16 )
    t3          ( .690  56   am  .700 19    pm  .681 11 )
    t3                                .671  38
    t3                 ha  .669 29            ta  .647 22
    t4          ( .699  42   am  .704 20    pm  .691 21 )
    t4                                .671  14                .645  22
    t5          ( .705  32   am  .708 23    pm  .701 24 )
    t5                                         ta  .651 22
    t6                                         ta  .645 *
    t7                                                 .623  125
    t8          ( .672  41   am  .675 35    pm  .667 32 )
    t8                 ha  .652 55
    t10         ( .681  43   am  .685 42    pm  .677 29 )

15  t1           .908  14
    t2           .909  17
    t3           .911  12              .916  15
    t3                 ha  .910 12                ta  .916 26
    t4           .908  23              .916  22                .916  22
    t5           .908  31                         ta  .902 28
    t6                                            ta  .895 61
    t7                                 .878  76                .894  62
    t8           .896  63
    t8                 ha  .902 109
    t10          .904  18
```

```
16 t1          .452  27
   t2          .448  40
   t3          .450   7              .454   8
   t3                ha  .444 09                 ta  .447 11
   t4          .449   9              .455  20                .445  18
   t5          .452  12                          ta  .448 19
   t6                                            ta  .447 14
   t7                                 .451  11                .445  14
   t8          .451  15
   t8                ha  .445 19
   t10         .445  15

17 t1          .955  17
   t2          .958  23
   t3          .960  17              .969  20
   t3                ha  .962 13                 ta .967 27
   t4          .959  17              .969  30                .967  25
   t5          .960  27                          ta .961 74
   t6                                            ta .959 29
   t7                                 .962  29                .965  17
   t8          .956  76
   t8                ha  .963 51
   t10         .957  40

18 t2                                                ( 18vs14  1.072 20 bmho )
   t2       ( .751  71   am  .760 10    pm  .747 10 )
   t3       ( .750  60   am  .760 14    pm  .740 12 )
   t3                                .738  34
   t3                ha  .729 26                 ta .714 19
   t4          .754  21              .751  56                .713  30
   t5          .756  18
   t8                ha  .732 37
   t10         .754  20

19 t2       ( 1.204 115   am 1.221 43    pm 1.188 69 )
   t3       ( 1.191  91   am 1.205 56    pm 1.179 29 )
   t3                                1.172 102
   t3                ha 1.174 62                 ta 1.155 41
   t4       ( 1.201  54   am 1.203 35    pm 1.194 40 )
   t4                                1.175  58                1.155  44

19 t2 TC    ( 1.185 115   am 1.202 43    pm 1.169 69 )                    C
   t3 TC    ( 1.190  91   am 1.204 56    pm 1.178 29 )                    C
   t3 TC                             1.175 102                           C
   t3 TC             ha 1.178 62                 ta 1.159 41             C
   t4 TC    ( 1.194  54   am 1.196 35    pm 1.187 40 )                    C
   t4 TC                             1.177  58                1.158  44 C

19 t9 ::                              .971  27                 .974  27

20 t2          .459  23
   t3          .457  11              .459   9
   t3                ha .453 13                  ta  .455 09
   t4          .458  12              .459  11                .452  17
   t5          .460   7

   t6 ::                                         ta  .906 25
   t7                                                     .905  49

   t9 ::                             1.008  16                1.010  25

21 t2          .455  37
   t3          .455  19              .456  10
   t3                ha .451 13                  ta  .451 12
   t4          .456  21              .459  15                .452  17
   t5          .458  16

   t6 ::                                         ta  .861 35
   t7                                                     .870  42

   t9 ::                             .956  14                .954  18
```

```
22 t4          1.386  59            1.342  28             1.305  40
   t5          1.400  44                                ta 1.332  78
   t6                                                   ta 1.329  71
   t7                               1.341  89             1.317  98
   t8          1.385  85
   t8                 ha 1.352 83
   t10         1.393  42

22 t4 TC       1.381  59            1.343  28             1.307  40 C
   t5 TC       1.384  44                                ta 1.297  78    C
   t6 TC                                                ta 1.294  71    C
   t7 TC                            1.325  89             1.297  98 C
   t8 TC       1.380  85                                             C
   t8 TC              ha 1.351 83                                     C
   t10 TC      1.382  42                                             C

23 t3         ( .976 142   am  .995 12    pm  .950   7 )
   t3                 ha  .984 31                ta  .986 (03 (3 points))
   t4         ( .969  47   am  .966 4     pm  .974 41 )
   t4                                .997  65              .995  40
   t5           .965  40

24 t4          1.422  61            1.365  63             1.336 126
   t5          1.444  63                                ta 1.398  79
   t6                                                   ta 1.382  82
   t7                               1.391  43             1.369  78
   t8          1.420  82
   t8                 ha 1.405 81
   t10         1.450  69

24 t4 TC       1.417  61            1.366  63             1.338 126 C
   t5 TC       1.428  63                                ta 1.361  79    C
   t6 TC                                                ta 1.346  82    C
   t7 TC                            1.375  43             1.349  78 C
   t8 TC       1.415  82                                             C
   t8 TC              ha 1.404 81                                     C
   t10 TC      1.438  69                                             C

25 t4          1.440  42            1.414  56             1.378  45
   t5          1.459  44                                ta 1.418  85
   t6                                                   ta 1.404  81
   t7                               1.414  40             1.390  77
   t8          1.442  49
   t8                 ha 1.420 81
   t10         1.466  49

25 t4 TC       1.435  42            1.415  56             1.380  45 C
   t5 TC       1.442  44                                ta 1.381  85    C
   t6 TC                                                ta 1.367  81    C
   t7 TC                            1.397  40             1.369  77 C
   t8 TC       1.437  49                                             C
   t8 TC              ha 1.419 81                                     C
   t10 TC      1.454  49                                             C

26 t4           .386  31

34 t9                                .993  23              .979  26

41 t4          1.090  73
41 t4 TC       1.087  73                                             C
```

Resaa4
10/04/86
(to ta and tn evaluated with table slant = 22.2 deg - correct)

DIRECT BENCHMARKS ON CHANNEL 00

	BMHO	σ			BMTO	σ			BMTN	σ
t1	10.07	53								
t2	10.11	25								
t3	10.18	29			10.06	34				
t3		ha	10.26	37			ta	10.16 35		
t4	10.12	27			10.09	25			10.23	37
t5	10.17	**					(ta	10.45 46)		
t6							ta	10.26 134		
t7					10.16	73			10.21	85
t8	10.13	53								
t8		ha	10.20	73						
t9	10.12	30			10.21	41			10.26	34
t10	10.12	32							10.20	65
t10							ta	10.22 66		
AVERAGE	10.128		10.230		10.130			10.27	10.225	
								(10.213)		
RANGE	1.1%		0.6%		1.5%			2.9%	0.6%	
								(1.0%)		
								(disregarding t5-bmta)		

DIRECT BENCHMARKS ON CHANNEL 16

t3	4.58	16			4.56	16				
t3		ha	4.55	14			ta	4.54 18		
t4	4.55	10			4.59	14			4.55	12

(data above has :- table slant = 22.2 deg -correct)

(σ is the scatter in microvolts of the channel 00 or 16 signal.)

Resaa5, 10/04/86

NUMBER OF POINTS IN CHANNEL 00 DIRECT BENCHMARKS

	bmho	bmha	bmto	bmta	bmtn
t1	203				
t2	42				
t3	41	50	15	83	
t4	96		22		37
t5	29			25	
t6				170	
t7			26		152
t8	114	311			
t9	10		38		78
t10	188			15	20

MAXIMUM NUMBER OF READINGS

	bmho	bmha	bmto	bmta	bmtn	all
t1	235					2505
t2	73					3536
t3	73	233	17	88		3421
t4	139		25		50	3530
t5	122			59		2524
t6				176		2863
t7			84		294	6156
t8	165	400				6462
t9	73		38		84	6135
t10	205			15	23	6345

AVERAGE TEMPERATURES (degrees celcius)

	bmho	bmha	bmto	bmta	bmtn	all
t1	1.7					1.4
t2	12.9					11.5
t3	24.4	27.6	27.1	27.7		24.8
t4	20.7		26.2		27.0	22.2
t5	10.8			-7.9		3.2
t6				-7.9		-3.6
t7			10.4		6.4	5.1
t8	20.5	24.3				18.6
t9	22.7		24.4		24.3	22.0
t10	15.0			20.3	19.4	13.6

STANDARD DEVIATIONS OF TEMPERATURES

	bmho	bmha	bmto	bmta	bmtn	all
t1	4.8					5.6
t2	4.7					5.9
t3	5.8	5.2	5.7	3.6		5.9
t4	4.1		2.4		1.5	6.0
t5	2.7			6.7		9.1
t6				8.3		7.6
t7			8.2		7.2	7.9
t8	4.6	4.6				7.1
t9	3.2		4.7		2.4	5.0
t10	4.0			2.7	2.4	5.1

Resaa6 10/04/86 **RESULTS FROM THE TRACKING TABLE**
i.e. normal incidence at various tilts.

Definition - Simultaneous Diffuse and Global Method of Calibration . (SDGM)
Given voltage data from a shaded pyranometer Vd
and from an unshaded pyranometer Vg
and given direct irradiance W
Plot y = Vd/Vg against x = W/Vg.
The reciprocal x intercept is Rg
and the y intercept is Rd / Rg .
where Rd and Rg are the two pyranometer responsivities.

tape 4
Alternating sun shade method(ASM) of calibration on Ch34 done on a single day (Oct. 9, 83)
(average value with 80 > tilt = β > 50) R(#34) = 9.26

S D G Plot	Ch34/Ch35	vs	Nip/Ch35
Intercepts	(.931)	and	.849
with R(nip)=8.45 gives	(R(#34) = 9.27)		R(#35) = 9.96

	-- tilt angle range --					
	30<β<45	45<β<60	60<β<75	all	R(all)	spread
Ch34/Ch35	.938	.935	.936	.935	9.31	0.3%
Ch36/Ch35	.451 19	.452 17	.452 17	.451	4.49	0.2%
Ch37/Ch35	1.482 50	1.480 51	1.475 52	1.482	14.76	0.5%

These ratios evaluated only with I > 700 Watt/sq m., (and with Ch34 unshaded).

tape9

S D G Plot	Ch5/Ch4	versus	Nip/Ch4
gives	R(#4) = 4.861 +/- .011		(also R(#5) = 9.673)

Results from same method (SDG) and data, but divided in specific tilt ranges.

tilt range	R(#4) - 4.861	+/-		
30 <β< 40	-0.09%	.23%	:	
40 <β< 50	0.14%	.23%	:	
50 <β< 60	0.14%	.23%	:	overall range
60 <β< 70	0.03%	.23%	:	0.23%
70 <β< 80	-0.09%	.23%	:	
80 <β< 90	-0.03%	.23%	:	

Resaa7 **RESULTS OF THE SIMULTANEOUS DIFFUSE AND GLOBAL METHOD (SDGM) OF CALIBRATION FOR HORIZONTAL DIFFUSE AND TILTED DIFFUSE.**

	horizontal			tilted		
	points	R(#01)	R(#28)	points	R(#01)	R(#29)
Tape 1	2130	4.71	5.19			
Tape 2	3135	4.66	5.16			
Tape 3	3743	4.65	5.17	258	4.60	4.28
Tape 4	3121	4.66	5.20	<400	4.61	4.34
Tape 5	1798	4.65	5.23	1153	4.77	4.38
Tape 6	all tilted			2156	4.71	4.36
Tape 7	all tilted			2802	4.67	4.28
Tape 8	3469	4.66	5.15			
Tape 9	2580	4.63	5.12			
Tape10	2274	4.65	5.13			
Mean SDGM			5.17			4.33
Sample st. dev [percent]			0.037 [0.72%]			0.046 [1.09%]
Alternating sun shade method			5.21			4.36
Adopted values			5.21			4.36

Resbb 27/02/86

BENCHMARK RATIO AVERAGES (AND DIRECTLY MEASURED ON CHANNEL 00)

	BMHO	BMHA	BMTO	BMTA	BMTN
CH 00 PSP 18426					
Directly measured	10.128	10.230	10.13	10.213	10.225
max%-min% / samples	1.1/8	0.6/2	1.5/4	1.0/4	0.6/4
disregarded t5ta - large deviation from 3 others.					
CH 01 CM10 810166					
Relative to Ch 00	.4617	.4565	.463	(.460)	.455
max%-min% / samples	0.9/6	0.2/2	0.9/3	(2.5/3)	0.4/2
disregarded t1ho - large deviation from 6 others. note large range on bmta.					
CH 02 EKO 82053					
Relative to Ch 00	.680	.662	.671	.652	.648
max%-min% / samples	0.9/6	0.3/2	0.9/3	0.3/3	0.3/3
disregarded t1 - apparent misalignment.					
CH 04 EKO 81908					
Relative to Ch 00	.956	.937	.945	.924	.920
max%-min% / samples	0.2/4	-	0.7/2	-	-
CH 05 CM-5 78-5047					
Relative to Ch 00 TC	1.159	1.154	1.131	1.115	1.110
max%-min% / samples	0.8/3	-	0.6/2	-	-
CH 06 CM-5 77-3656					
Relative to Ch 00 TC	1.132		1.130		1.111
max%-min% / samples	-		-		-
CH+06 PSP 19260					
Relative to Ch 00	.959		.959		.965
max%-min% / samples	-		-		-
CH 07 CM-5 77-4120					
Relative to Ch 00 TC	1.237		1.239		1.221
max%-min% / samples	-		-		-
CH+07 PSP 19262					
Relative to Ch 00	.984		.974		.993
max%-min% / samples	-		-		-
CH 08 CM10 810122					
Relative to Ch 00	.4193	.414	.4185	.415	.413
max%-min% / samples	1.0/4	-	0.2/2	-	-
CH 09 EP07 123					
Relative to Ch 00	1.002	1.011	1.011	1.015	1.010
max%-min% / samples	0.6/4	-	0.8/2	-	-
CH 10 EP07 124					
Relative to Ch 00 TC	1.024	1.032	1.025	1.048	1.040
max%-min% / samples	1.8/6	0.5/2	0.2/2	1.8/3	-
CH 11 PSP 18135					
Relative to Ch 00	.881		.880	.878	.878
max%-min% / samples	0.3/3		0.4/2	0/2	0/3

disregarded t8ho - large deviation from 3 others and large scatter.
disregarded t7to - large deviation from 2 others and large scatter.

CH 12 SWISSTECO 113					
Relative to Ch 00 TC	1.476		1.500		1.500
max%-min% / samples	-		-		-
CH 13 SWISSTECO 114					
Relative to Ch 00	-		1.545		1.542
max%-min% / samples	-		-		-
CH 14 EKO 82052					
t1 - t6					
Relative to Ch 00	.699	.669	.671	.648	.645
max%-min% / samples	2.1/5	-	0/2	0.9/3	-
t7 - t10					
Relative to Ch 00	.676	.652			.623
max%-min% / samples	1.3/2	-			-

Evidence of loss of 2.8% responsivity between tape6 and tape 7.

CH 15 PSP 18431					
Relative to Ch 00	.909	.910	.916	.916	.916
max%-min% / samples	0.3/5	-	0/2	-	-

Disregarded t5ta and all t6 - t10 data. Large scatter and evidence of responsivivity loss 1 - 3%.

CH 16 CM10 810131					
Relative to Ch 00	.4503	.4445	.4533	.4473	.445
max%-min% / samples	0.7/6	0.2/2	0.9/3	0.2/3	0/2

Disregarded t10ho - large deviation from 6 others.

CH 17 PSP 18435					
Relative to Ch 00	.958	.962	.967	.962	.966
max%-min% / samples	0.5/7	0.1/2	0.7/3	0.8/3	0.2/2
CH 18 EKO 81909					
Relative to Ch 00	.753	.730	.744	.714	.713
max%-min% / samples	0.8/5	0.4/3	1.7/3	-	-
CH 19 CM5 77-3992					
Relative to Ch 00 TC	1.190	1.178	1.176	1.159	1.158
max%-min% / samples	0.8/3	-	0.2/2	-	-
CH+19 PSP 19259					
Relative to Ch 00			.971		.974
max%-min% / samples			-		-
CH 20 CM10 810121					
Relative to Ch 00	.4585	.453	.459	.455	.452
max%-min% / samples	0.7/4	-	0/2	-	-
CH+20 PSP 23676					
Relative to Ch 00				.906	.905
max%-min% / samples				-	-
CH++20 PSP 19261					
Relative to Ch 00			1.008		1.010
max%-min% / samples			-		-

CH 21 CM10 810119					
Relative to Ch 00	.456	.451	.4575	.451	.452
max%-min% / samples	0.7/4	-	0.7/2	-	-
CH+21 PSP 23677					
Relative to Ch 00				.861	.870
max%-min% / samples				-	-
CH++21 PSP 20502					
Relative to Ch 00			.956		.954
max%-min% / samples			-		-
CH 22 SCHENK 2217					
Relative to Ch 00 TC	1.382	1.351	1.334	1.295	1.304
max%-min% / samples	0.3/4	-	1.4/2	0.3/2	0.8/2
CH 23 PSP 20524					
Relative to Ch 00					.995
max%-min% / samples					-

Evidence of significant misalignment.

CH 24 SCHENK 2428					
Relative to Ch 00 TC	1.425	1.404	1.371	1.354	1.344
max%-min% / samples	1.8/4	-	0.7/2	1.2/2	0.8/2
CH 25 SCHENK 2418					
Relative to Ch 00 TC	1.442	1.419	1.406	1.374	1.375
max%-min% / samples	1.2/4	-	1.4/2	1.1/2	0.8/2
CH 26 Proctor					
Relative to Ch 00	.386				
max%-min% / samples	-				
CH 34 PSP 19814					
Relative to Ch 00			.993		.979
max%-min% / samples			-		-
CH 41 CM5 784737					
Relative to Ch 00 TC	1.087				
max%-min% / samples	1.2/4	-			

Rescc1

SHORT SUMMARY OF AVERAGE BENCHMARK RATIOS

01/04/86

			BMHO	BMHA	BMTO	BMTA	BMTN
CH 01	CM10 810166		.4617	.4565	.463	(.460)	.455
CH 02	EKO 82053		.680	.662	.671	.652	.648
CH 04	EKO 81908		.956	.937	.945	.924	.920
CH 05	CM-5 78-5047	TC	1.159	1.154	1.131	1.115	1.110
CH 06	CM-5 77-3656	TC	1.132		1.130		1.111
CH+06	PSP 19260		.959		.959		.965
CH 07	CM-5 77-4120	TC	1.237		1.239		1.221
CH+07	PSP 19262		.984		.974		.965
CH 08	CM10 810122		.4193	.414	.4185	.415	.413
CH 09	EP07 123		1.002	1.011	1.011	1.015	1.010
CH 10	EP07 124	TC	1.024	1.032	1.025	1.048	1.040
CH 11	PSP 18135		.881		.880	.878	.878
CH 12	SWISSTECO 113	TC	1.476		1.500		1.500
CH 13	SWISSTECO 114		-		1.545		1.542
CH 14	EKO 82052		.699	.669	.671	.648	.645
CH 14	EKO 82052		.676	.652			.623
CH 15	PSP 18431		.909	.910	.916	.916	.916
CH 16	CM10 810131		.4503	.4445	.4533	.4473	.445
CH 17	PSP 18435		.958	.962	.967	.962	.966
CH 18	EKO 81909		.753	.730	.744	.714	.713
CH 19	CM5 77-3992	TC	1.190	1.178	1.176	1.159	1.158
CH+19	PSP 19259				.971		.974
CH 20	CM10 810121		.4585	.453	.459	.455	.452
CH+20	PSP 23676					.906	.905
CH++20	PSP 19261				1.008		1.010
CH 21	CM10 810119		.456	.451	.4575	.451	.452
CH+21	PSP 23677					.861	.870
CH++21	PSP 20502				.956		.954
CH 22	SCHENK 2217	TC	1.382	1.351	1.334	1.295	1.304
CH 23	PSP 20524						.995
CH 24	SCHENK 2428	TC	1.425	1.404	1.371	1.354	1.344
CH 25	SCHENK 2418	TC	1.442	1.419	1.406	1.374	1.375
CH 26	Proctor		.386				
CH 34	PSP 19814				.993		.979
CH 41	CM5 784737	TC	1.087				

			BMHO	BMHA	BMTO	BMTA	BMTN

Resdd1

10/04/86 **Benchmarks from and including direct channel 00.**

				BMHO	BMHA	BMTO	BMTA	BMTN
CH 00	PSP	18426		10.13	10.23	10.13	10.21	10.22
CH+06	PSP	19260		9.71		9.71		9.87
CH+07	PSP	19262		9.97		9.87		10.15
CH 11	PSP	18135		8.92		8.91	8.97	8.98
CH 15	PSP	18431		9.21	9.31	9.28	9.36	9.37
CH 17	PSP	18435		9.70	9.84	9.80	9.82	9.88
CH+19	PSP	19259				9.84		9.96
CH+20	PSP	23676					9.25	9.25
CH++20	PSP	19261				10.21		10.32
CH+21	PSP	23677					8.79	8.90
CH++21	PSP	20502				9.68		9.75
CH 23	PSP	20524						10.17
CH 34	PSP	19814				10.05		10.01
CH 01	CM10	810166		4.68	4.67	4.69		4.65
CH 08	CM10	810122		4.25	4.24	4.24	4.24	4.22
CH 16	CM10	810131		4.56	4.55	4.59	4.57	4.55
CH 20	CM10	810121		4.64	4.63	4.65	4.65	4.62
CH 21	CM10	810119		4.62	4.61	4.63	4.61	4.62
CH 02	EKO	82053		6.89	6.77	6.80	6.66	6.63
CH 04	EKO	81908		9.68	9.59	9.57	9.44	9.41
CH 14	EKO	82052		7.08	6.84	6.80	6.62	6.60
CH 14	EKO	82052		6.85	6.67			6.37
CH 18	EKO	81909		7.63	7.47	7.54	7.29	7.29
CH 05	CM-5	78-5047	TC	11.73	11.80	11.45	11.38	11.34
CH 06	CM-5	77-3656	TC	11.46		11.44		11.35
CH 07	CM-5	77-4120	TC	12.52		12.55		12.48
CH 19	CM-5	77-3992	TC	12.05	12.05	11.91	11.83	11.84
CH 41	CM-5	78-4737	TC	11.00				
CH 09	EP07	123		10.14	10.34	10.24	10.36	10.32
CH 10	EP07	124	TC	10.37	10.55	10.38	10.70	10.63
CH 12	SWISSTECO	113	TC	14.94		15.19		15.33
CH 13	SWISSTECO	114				15.65		15.76
CH 22	SCHENK	2217	TC	13.99	13.82	13.51	13.22	13.33
CH 24	SCHENK	2428	TC	14.43	14.36	13.88	13.82	13.74
CH 25	SCHENK	2418	TC	14.60	14.51	14.24	14.03	14.05
CH 26	Proctor			3.91				

Calibrations from normal tracking BMTR			(approximately BMTN)	BMTR
CH 4N	CM10	830178 T8		4.86
CH 5N	PSP	24011 T8		9.67
CH 34N	PSP	17750 T4		9.31
CH 35N	PSP	20523 T4		9.96
CH 36N	CM10	810120 T4		4.49
CH 37N	SCHENK	2209 T4		14.76

Resdd2

10/04/86 **All Benchmarks**

				BMHO	BMHA	BMTO	BMTA	BMTN	BMTR
CH 5N	PSP	24011	T8						9.67
CH 34N	PSP	17750	T4						9.31
CH 35N	PSP	20523	T4						9.96
CH 00	PSP	18426		10.13	10.23	10.13	10.21	10.22	
CH+06	PSP	19260		9.71		9.71		9.87	
CH+07	PSP	19262		9.97		9.87		10.15	
CH 11	PSP	18135		8.92		8.91	8.97	8.98	
CH 15	PSP	18431		9.21	9.31	9.28	9.36	9.37	
CH 17	PSP	18435		9.70	9.84	9.80	9.82	9.88	
CH+19	PSP	19259				9.84		9.96	
CH+20	PSP	23676					9.25	9.25	
CH++20	PSP	19261				10.21		10.32	
CH+21	PSP	23677					8.79	8.90	
CH++21	PSP	20502				9.68		9.75	
CH 23	PSP	20524						10.17	
CH 34	PSP	19814				10.05		10.01	
CH 4N	CM10	830178	T8						4.86
CH 36N	CM10	810120	T4						4.49
CH 01	CM10	810166		4.68	4.67	4.69		4.65	
CH 08	CM10	810122		4.25	4.24	4.24	4.24	4.22	
CH 16	CM10	810131		4.56	4.55	4.59	4.57	4.55	
CH 20	CM10	810121		4.64	4.63	4.65	4.65	4.62	
CH 21	CM10	810119		4.62	4.61	4.63	4.61	4.62	
CH 02	EKO	82053		6.89	6.77	6.80	6.66	6.63	
CH 04	EKO	81908		9.68	9.59	9.57	9.44	9.41	
CH 14	EKO	82052		7.08	6.84	6.80	6.62	6.60	
CH 14	EKO	82052		6.85	6.67			6.37	
CH 18	EKO	81909		7.63	7.47	7.54	7.29	7.29	
CH 05	CM-5	78-5047	TC	11.73	11.80	11.45	11.38	11.34	
CH 06	CM-5	77-3656	TC	11.46		11.44		11.35	
CH 07	CM-5	77-4120	TC	12.52		12.55		12.48	
CH 19	CM-5	77-3992	TC	12.05	12.05	11.91	11.83	11.84	
CH 41	CM-5	78-4737	TC	11.00					
CH 09	EP07	123		10.14	10.34	10.24	10.36	10.32	
CH 10	EP07	124	TC	10.37	10.55	10.38	10.70	10.63	
CH 12	SWISSTECO	113	TC	14.94		15.19		15.33	
CH 13	SWISSTECO	114				15.65		15.76	
CH 37N	SCHENK	2209	T4						14.76
CH 22	SCHENK	2217	TC	13.99	13.82	13.51	13.22	13.33	
CH 24	SCHENK	2428	TC	14.43	14.36	13.88	13.82	13.74	
CH 25	SCHENK	2418	TC	14.60	14.51	14.24	14.03	14.05	
CH 26	Proctor			3.91					

BMHO	BMHA	BMTO	BMTA	BMTN	BMTR

Resdd3 09/04/86

Abstract of Sphere calibrations and Manufacturers' calibrations. Nearly all the instruments were calibribrated in the NARC sphere both before and after the field experiment.

			SPHERE BEFORE	SPHERE AFTER	MANUFACTURER
CH 5N	PSP 24011			9.57	9.70
CH 34N	PSP 17750		9.16	9.19	9.26
CH 35N	PSP 20523		9.89	9.91	9.95
CH 00	PSP 18426		10.22	10.15	10.53
CH+06	PSP 19260		9.69	9.70	10.19
CH+07	PSP 19262		10.07		10.52
CH 11	PSP 18135		8.90	8.87	8.78
CH 15	PSP 18431		9.19	9.05	9.51
CH 17	PSP 18435		9.76	9.73	10.13
CH+19	PSP 19259		9.73	9.74	10.25
CH+20	PSP 23676		9.21	9.17	9.15
CH++20	PSP 19261		10.10	10.15	10.78
CH+21	PSP 23677		8.75	8.72	8.71
CH++21	PSP 20502		9.59	9.51	9.82
CH 23	PSP 20524		10.02	10.01	10.10
CH 34	PSP 19814		9.98		10.48
CH 4N	CM10 830178		4.93	4.90	4.93
CH 36N	CM10 810120		4.53	4.53	4.54
CH 01	CM10 810166		4.69	4.70	4.64
CH 08	CM10 810122		4.26	4.27	4.24
CH 16	CM10 810131		4.58	4.56	4.54
CH 20	CM10 810121		4.65	4.65	4.66
CH 21	CM10 810119		4.62	4.62	4.58
CH 02	EKO 82053		6.84	6.54	7.00
CH 04	EKO 81908		9.60	9.50	9.61
CH 14	EKO 82052			6.75	7.00
CH 14	EKO 82052			6.75	7.00
CH 18	EKO 81909		7.58	7.39	7.42
CH 05	CM-5 78-5047	TC	11.65	11.64	12.23
CH 06	CM-5 77-3656	TC	11.44	11.43	11.94
CH 07	CM-5 77-4120	TC	12.62	12.58	13.41
CH 19	CM-5 77-3992	TC	12.03	12.00	12.62
CH 41	CM-5 78-4737	TC	11.06	11.08	11.90
CH 09	EP07 123		10.55	10.41	10.3
CH 10	EP07 124	TC	10.66	10.69	10.7
CH 12	SWISSTECO 113	TC		15.1	
CH 13	SWISSTECO 114			15.6	
CH 37N	SCHENK 2209			15.14	15.36
CH 22	SCHENK 2217	TC	13.82	13.87	14.16
CH 24	SCHENK 2428	TC	14.26	14.35	14.56
CH 25	SCHENK 2418	TC	14.33	14.51	14.68

	SPHERE BEFORE	SPHERE AFTER	MANUFACTURER

Resee3 09/04/86

absolute benchmarks - mean or best* sphere in percentage

			BMHO	BMHA	BMTO	BMTA	BMTN
CH 5N	PSP	24011					1.0
CH 34N	PSP	17750					1.4
CH 35N	PSP	20523					.60
CH 00	PSP	18426	-.54	.44	-.54	.24	.34
CH+06	PSP	19260	.15		.15		1.8
CH+07	PSP	19262	-.99		-1.9		.79
CH 11	PSP	18135	.39		.28	.95	1.0
CH 15	PSP	18431 *	.21	1.3	.97	1.8	1.9
CH 17	PSP	18435	-.46	.97	.56	.76	1.3
CH+19	PSP	19259			1.0		2.3
CH+20	PSP	23676				.65	.65
CH++20	PSP	19261			.83		1.9
CH+21	PSP	23677				.62	1.8
CH++21	PSP	20502			1.3		2.0
CH 23	PSP	20524					1.5
CH 34	PSP	19814			.70		.30
PSP		mean	-.21	.90	.34	.84	1.3
PSP		sigma	.53	.43	.94	.53	.63
PSP		number	6	3	10	6	16
CH 4N	CM10	830178					-1.1
CH 36N	CM10	810120					-.88
CH 01	CM10	810166	-.31	-.53	-.11		-.95
CH 08	CM10	810122	-.35	-.58	-.58	-.58	-1.0
CH 16	CM10	810131	-.21	-.42	.42	0	-.42
CH 20	CM10	810121	-.21	-.43	0	0	-.64
CH 21	CM10	810119	0	-.21	.21	-.21	0
CM10		mean	-.22	-.43	-.01	-.20	-.71
CM10		sigma	.14	.14	.38	.27	.39
CM10		number	5	5	5	4	7
CH 02	EKO	82053	2.9	1.1	1.6	-.44	-.89
CH 04	EKO	81908	1.3	.41	.20	-1.1	-1.4
CH 14	EKO	82052					
CH 14	EKO	82052	1.4	-1.1			-5.6
CH 18	EKO	81909	1.9	-.20	.73	-2.6	-2.6
EKO 8		mean	1.9	.05	.84	-1.4	-2.6
EKO 8		sigma	.73	.93	.70	1.1	2.1
EKO 8		number	4	4	3	3	4
CH 05	CM-5	78-5047	.72	1.3	-1.6	-2.2	-2.6
CH 06	CM-5	77-3656	.21		.04		-.74
CH 07	CM-5	77-4120	-.63		-.39		-.95
CH 19	CM-5	77-3992	.29	.29	-.87	-1.5	-1.4
CH 41	CM-5	78-4737	-.63				
CM-5		mean	-.01	.81	-.72	-1.9	-1.4
CM-5		sigma	.60	.73	.73	.52	.83
CM-5		number	5	2	4	2	4
CH 09	EP07	123	-3.2	-1.3	-2.2	-1.1	-1.5
CH 10	EP07	124	-2.8	-1.1	-2.7	.23	-.42
EP07		mean	-3.0	-1.2	-2.5	-.45	-.97
EP07		sigma	.27	.11	.33	.97	.78
EP07		number	2	2	2	2	2
CH 12	SWISSTECO	113	-1.0		.59		1.5
CH 13	SWISSTECO	114			.32		1.0
SWISS		mean			.45		1.2
SWISS		sigma			.19		.35
SWISS		number	1		2		2
CH 37N	SCHENK	2209					-2.5
CH 22	SCHENK	2217	1.0	-.18	-2.4	-4.5	-3.7
CH 24	SCHENK	2428	.87	.38	-2.9	-3.3	-3.9
CH 25	SCHENK	2418	1.2	.62	-1.2	-2.7	-2.5
SCHEN		mean	1.0	.27	-2.2	-3.5	-3.1
SCHEN		sigma	.18	.41	.87	.91	.75
SCHEN		number	3	3	3	3	4
			BMHO	BMHA	BMTO	BMTA	BMTN

Resee4 03/04/86

benchmarks - manufacturers' calibration in percentage

			BMHO	BMHA	BMTO	BMTA	BMTN
CH 5N	PSP	24011					-.30
CH 34N	PSP	17750					.53
CH 35N	PSP	20523					.10
CH 00	PSP	18426	-3.7	-2.8	-3.7	-3.0	-2.9
CH+06	PSP	19260	-4.7		-4.7		-3.1
CH+07	PSP	19262	-5.2		-6.1		-3.5
CH 11	PSP	18135	1.5		1.4	2.1	2.2
CH 15	PSP	18431	-3.1	-2.1	-2.4	-1.5	-1.4
CH 17	PSP	18435	-4.2	-2.8	-3.2	-3.0	-2.4
CH+19	PSP	19259			-4		-2.8
CH+20	PSP	23676				1.0	1.0
CH++20	PSP	19261			-5.2		-4.2
CH+21	PSP	23677				.91	2.1
CH++21	PSP	20502			-1.4		-.71
CH 23	PSP	20524					.69
CH 34	PSP	19814			-4.1		-4.4
PSP		mean	-3.2	-2.6	-3.3	-.58	-1.2
PSP		sigma	2.4	.43	2.1	2.2	2.2
PSP		number	6	3	10	6	16
CH 4N	CM10	830178					-1.4
CH 36N	CM10	810120					-1.1
CH 01	CM10	810166	.86	.64	1.0		.21
CH 08	CM10	810122	.23	0	0	0	-.47
CH 16	CM10	810131	.44	.22	1.1	.66	.22
CH 20	CM10	810121	-.42	-.64	-.21	-.21	-.85
CH 21	CM10	810119	.87	.65	1.0	.65	.87
CM10		mean	.39	.17	.61	.27	-.36
CM10		sigma	.53	.53	.66	.45	.82
CM10		number	5	5	5	4	7
CH 02	EKO	82053	-1.5	-3.2	-2.8	-4.8	-5.2
CH 04	EKO	81908	.72	-.20	-.41	-1.7	-2.0
CH 14	EKO	82052	1.1	-2.2	-2.8	-5.4	-5.7
CH 14	EKO	82052		responsivity change			
CH 18	EKO	81909	2.8	.67	1.6	-1.7	-1.7
EKO 8		mean	.78	-1.2	-1.1	-3.4	-3.7
EKO 8		sigma	1.8	1.8	2.1	1.9	2.1
EKO 8		number	4	4	4	4	4
CH 05	CM-5	78-5047	-4.0	-3.5	-6.3	-6.9	-7.2
CH 06	CM-5	77-3656	-4.0		-4.1		-4.9
CH 07	CM-5	77-4120	-6.6		-6.4		-6.9
CH 19	CM-5	77-3992	-4.5	-4.5	-5.6	-6.2	-6.1
CH 41	CM-5	78-4737	-7.5				
CM-5		mean	-5.3	-4.0	-5.6	-6.6	-6.3
CM-5		sigma	1.6	.70	1.0	.48	1.0
CM-5		number	5	2	4	2	4
CH 09	EP07	123	-1.5	.38	-.58	.58	.19
CH 10	EP07	124	-3.0	-1.4	-2.9	0	-.65
EP07		mean	-2.3	-.50	-1.7	.29	-.23
EP07		sigma	1.0	1.2	1.7	.41	.59
EP07		number	2	2	2	2	2
CH 12	SWISSTECO	113					
CH 13	SWISSTECO	114					
SWISS		mean					
SWISS		sigma					
SWISS		number					
CH 37N	SCHENK	2209					-3.9
CH 22	SCHENK	2217	-1.2	-2.4	-4.5	-6.6	-5.8
CH 24	SCHENK	2428	-.89	-1.3	-4.6	-5.0	-5.6
CH 25	SCHENK	2418	-.54	-1.1	-2.9	-4.4	-4.2
SCHEN		mean	-.87	-1.6	-4.0	-5.3	-4.9
SCHEN		sigma	.32	.66	.94	1.1	.96
SCHEN		number	3	3	3	3	4
			BMHO	BMHA	BMTO	BMTA	BMTN

Resee5 04/04/86

benchmarks - tilted normal benchmark in percentage

				BMHO	BMHA	BMTO	BMTA	BMTN
CH 5N	PSP	24011						r
CH 34N	PSP	17750						r
CH 35N	PSP	20523						r
CH 00	PSP	18426		-.88	.09	-.88	-.09	r
CH+06	PSP	19260		-1.6		-1.6		r
CH+07	PSP	19262		-1.7		-2.7		r
CH 11	PSP	18135		-.66		-.77	-.11	r
CH 15	PSP	18431		-1.7	-.64	-.96	-.10	r
CH 17	PSP	18435		-1.8	-.40	-.80	-.60	r
CH+19	PSP	19259				-1.2		r
CH+20	PSP	23676					0	r
CH++20	PSP	19261				-1.0		r
CH+21	PSP	23677					-1.2	r
CH++21	PSP	20502				-.71		r
CH 23	PSP	20524						r
CH 34	PSP	19814				.39		r
PSP		mean		-1.4	-.31	-1.0	-.35	
PSP		sigma		.50	.37	.79	.48	
PSP		number		6	3	10	6	
CH 4N	CM10	830178						r
CH 36N	CM10	810120						r
CH 01	CM10	810166		.64	.43	.86		r
CH 08	CM10	810122		.71	.47	.47	.47	r
CH 16	CM10	810131		.21	0	.87	.43	r
CH 20	CM10	810121		.43	.21	.64	.64	r
CH 21	CM10	810119		0	-.21	.21	-.21	r
CM10		mean		.40	.18	.61	.33	
CM10		sigma		.29	.29	.27	.37	
CM10		number		5	5	5	4	
CH 02	EKO	82053		3.9	2.1	2.5	.45	r
CH 04	EKO	81908		2.8	1.9	1.7	.31	r
CH 14	EKO	82052	d	7.2	3.6	3.0	.30	r
CH 14	EKO	82052	d	7.5	4.7			r
CH 18	EKO	81909		4.6	2.4	3.4	0	r
EKO 8		mean		4.6	2.6	2.6	.26	
EKO 8		sigma		1.9	1.0	.74	.19	
EKO 8		number		d 4	d 4	4	4	
CH 05	CM-5	78-5047		3.4	4.0	.97	.35	r
CH 06	CM-5	77-3656		.96		.79		r
CH 07	CM-5	77-4120		.32		.56		r
CH 19	CM-5	77-3992		1.7	1.7	.59	-.08	r
CH 41	CM-5	78-4737						
CM-5		mean		1.6	2.9	.72	.13	
CM-5		sigma		1.3	1.6	.19	.30	
CM-5		number		4	2	4	2	
CH 09	EP07	123		-1.7	.19	-.77	.38	r
CH 10	EP07	124		-2.4	-.75	-2.3	.65	r
EP07		mean		-2.0	-.27	-1.5	.52	
EP07		sigma		.49	.66	1.1	.19	
EP07		number		2	2	2	2	
CH 12	SWISSTECO	113		-2.5		-.91		r
CH 13	SWISSTECO	114				-.69		r
SWISS		mean				-.80		
SWISS		sigma				.15		
SWISS		number		1		2		
CH 37N	SCHENK	2209						r
CH 22	SCHENK	2217		4.9	3.6	1.3	-.82	r
CH 24	SCHENK	2428		5.0	4.5	1.0	.58	r
CH 25	SCHENK	2418		3.9	3.2	1.3	-.14	r
SCHEN		mean		4.6	3.8	1.2	-.12	
SCHEN		sigma		.61	.63	.19	.70	
SCHEN		number		3	3	3	3	
				BMHO	BMHA	BMTO	BMTA	BMTN

Resff1 9/04/86

Directional, tilt and linearity properties of groups of pyranometers, derived from differences between outdoor benchmark calibrations - all expressed in percentages.

METEOROLOGY USAGE versus COLLECTOR TESTING	DIRECTIONALITY AND LINEARITY 600W at h'=35 deg. versus 1000W at h'=80 deg. (both at 45 deg tilt)	TILT Horizontal versus 45 degree tilt. at 600W or (1000W)		
HO - TN	TO - TN	HO - TO	(HA - TA)	
-1.4	-1.3	-0.1	(-0.0)	PSP
0.4	0.6	-0.2	(-0.2)	CM10
4.6	2.6	1.9	(2.2)	EKO
1.6	0.7	0.9 y	(2.6)	CM-5
-2.0	-1.5	-0.5	(-0.8)	MID
-2.5	-0.8	-1.6		SWISS
4.6	1.2	3.3	(3.8)	SCHENK

Standard deviations (population) / number of instruments tested.

HO - TN	TO - TN	HO - TO	(HA -TA)	
.5 / 6	.8 / 6	.7 / 6	(.4 / 3)	PSP
.3 / 5	.3 / 5	.3 / 5	(.3 / 4)	CM10
1.9 / 4	.7 / 4	1.4 / 4	(.8 / 4)	EKO
1.3 / 4	.2 / 4	1.1 / 4	(1.2 / 2)	CM-5
.5 / 2	1.1 / 2	.6 / 2	(.9 / 3)	MID
/ 1	.2 / 2	/ 1		SWISS
.6 / 3	.2 / 3	.7 / 3	(.5 / 3)	SCHENK

y significantly different at 1000W compared with 600W.

Resff2.
Manufacturers' calibrations calibrations versus Benchmarks for pyranometer groups given as mean percentage discrepancy with the standard deviation of the population and the number of samples.

-- mean % (s.d. / number) --

	EMHO - MANUF.	EMTN - MANUF.	
PSP	-3.2 (2.4 / 6)	-1.2 (2.2 / 16)	PSP
CM10	.4 (.5 / 5)	- .4 (.8 / 7)	CM10
EKO	.8 (1.8 / 4)	-3.7 (2.1 / 4)	EKO
CM-5	-5.3 (1.6 / 5)	-6.3 (1.0 / 4)	CM-5
MID	-2.3 (1.0 / 2)	- .2 (.6 / 2)	MID
SWISS			SWISST
SCHENK	-.9 (.3 / 3)	-4.9 (1.0 / 4)	SCHENK

Resff3.
NARC sphere calibrations versus Benchmarks for pyranometer groups given as mean percentage discrepancy with the standard deviation of the population and the number of samples.

-- mean % (s.d. / number) --

	EMHO - SPHERE		EMTN - SPHERE	
PSP	-.2 (.4 / 6)		1.3 (.6 / 16)	PSP
CM10	-.2 (.2 / 5)		- .7 (.4 / 7)	CM10
EKO	1.9 (1.8 / 4)	a	-2.6 (2.1 / 4)	EKO
CM-5	.0 (.6 / 5)		-1.4 (.8 / 4)	CM-5
MID	-3.0 (.3 / 2)	b	-1.0 (.4 / 2)	MID
SWISS	-1.0 (/ 1)	b	1.2 (.4 / 2)	SWISST
SCHENK	1.0 (.2 / 3)		-3.1 (.8 / 4)	SCHENK

a Sphere reference Eko unstable - as of february 86.
b Not established sphere calibrations. CM10 reference used for Swissteco and uncharacterized Middleton 122 used as Middleton reference.

Appendix CC:

Field Directionality Analysis from NARC.

Measurements on 18 pyranometers.

Corrected for diffuse radiation.
method described in 4.2.2.3

Horizontal orientation and

45 degree tilted orientation.

Data from Tape 3 and Tape 4 periods.

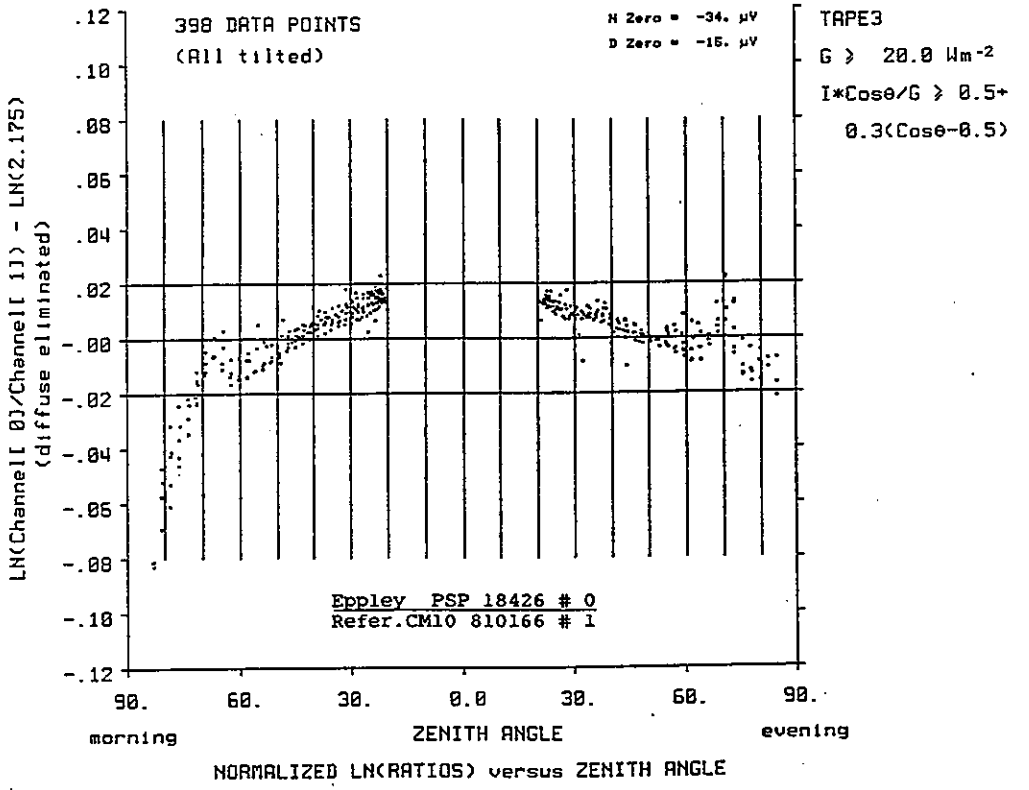

NORMALIZED LN(RATIOS) versus ZENITH ANGLE

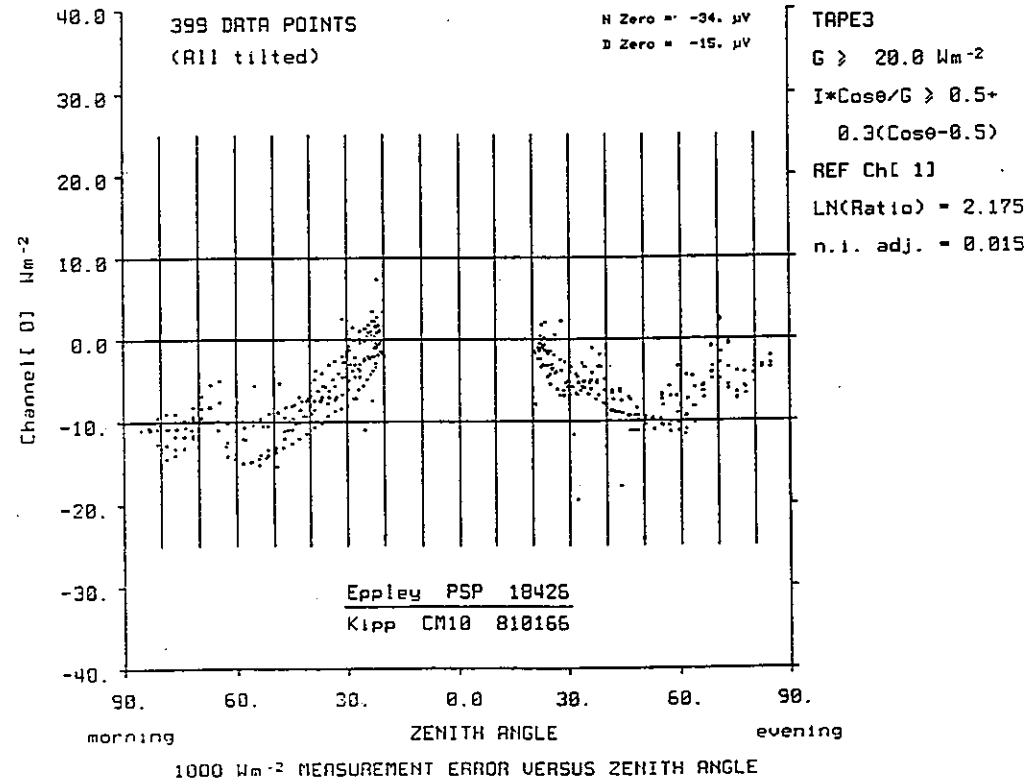

1000 Wm-2 MEASUREMENT ERROR VERSUS ZENITH ANGLE

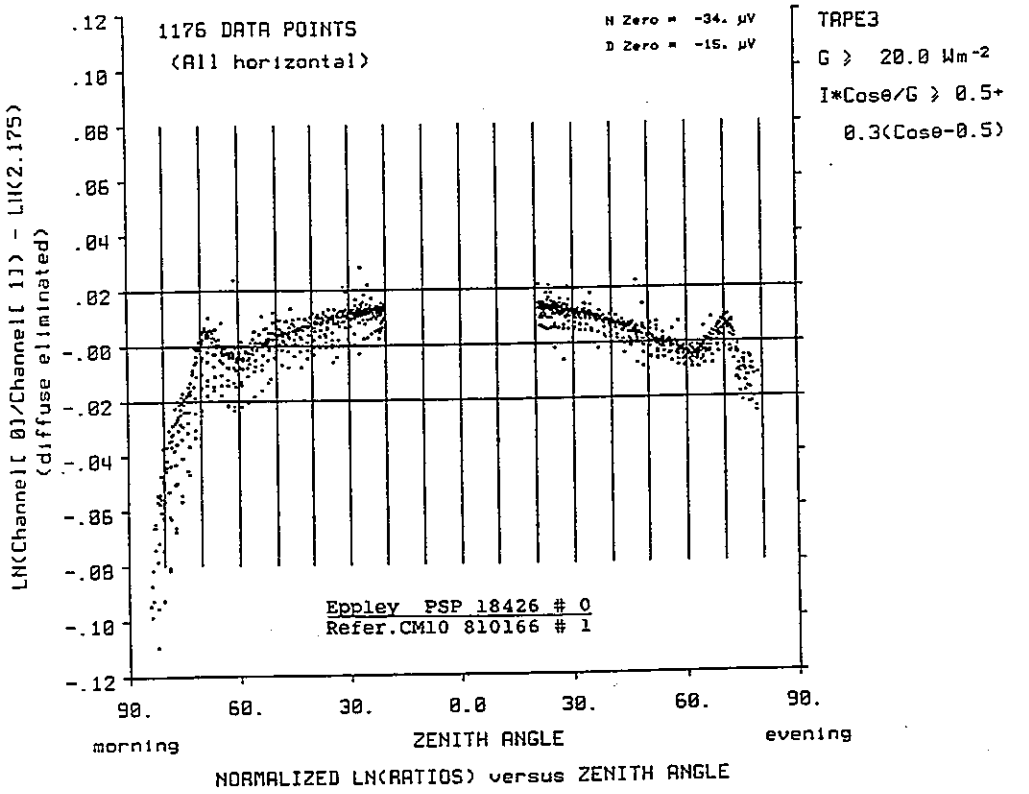
1176 DATA POINTS
(All horizontal)
N Zero = -34. μV
D Zero = -15. μV
TAPE3
G ≥ 20.0 Wm-2
I*Cosθ/G ≥ 0.5+
0.3(Cosθ-0.5)
LN(Channel[0]/Channel[1]) - LN(2.175)
(diffuse eliminated)
.12
.10
.08
.06
.04
.02
-.00
-.02
-.04
-.06
-.08
-.10
-.12
Eppley PSP 18426 # 0
Refer.CM10 810166 # 1
90.
60.
30.
0.0
30.
60.
90.
morning
ZENITH ANGLE
evening
NORMALIZED LN(RATIOS) versus ZENITH ANGLE

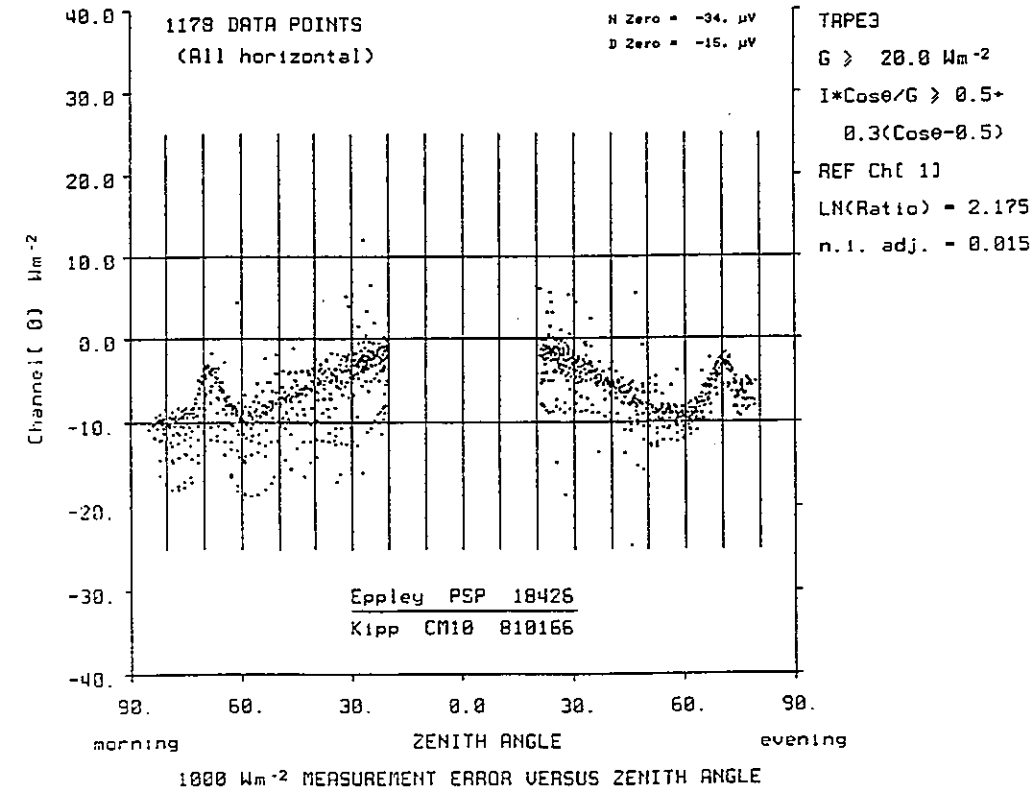
1178 DATA POINTS
(All horizontal)
N Zero = -34. μV
D Zero = -15. μV
TAPE3
G ≥ 20.0 Wm-2
I*Cosθ/G ≥ 0.5+
0.3(Cosθ-0.5)
REF Ch[1]
LN(Ratio) = 2.175
n.i. adj. = 0.015
Channel[0] Wm-2
40.0
30.0
20.0
10.0
0.0
-10.
-20.
-30.
-40.
Eppley PSP 18426
Kipp CM10 810166
90.
60.
30.
0.0
30.
60.
90.
morning
ZENITH ANGLE
evening
1000 Wm-2 MEASUREMENT ERROR VERSUS ZENITH ANGLE

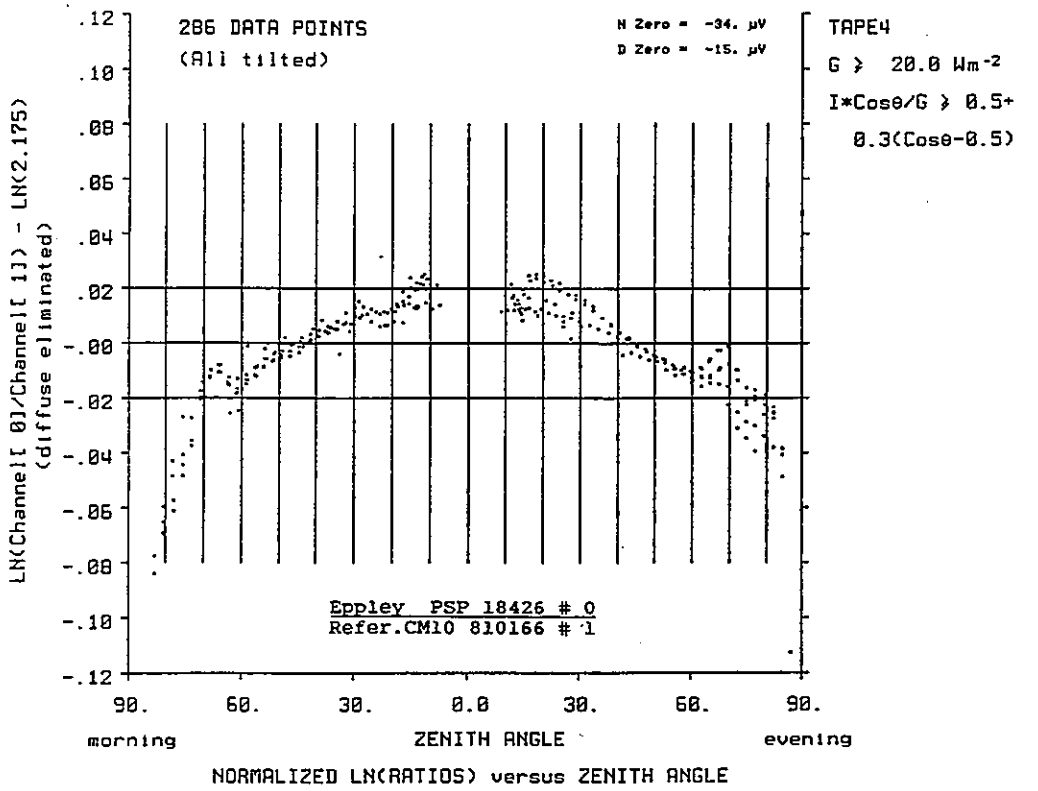

NORMALIZED LN(RATIOS) versus ZENITH ANGLE

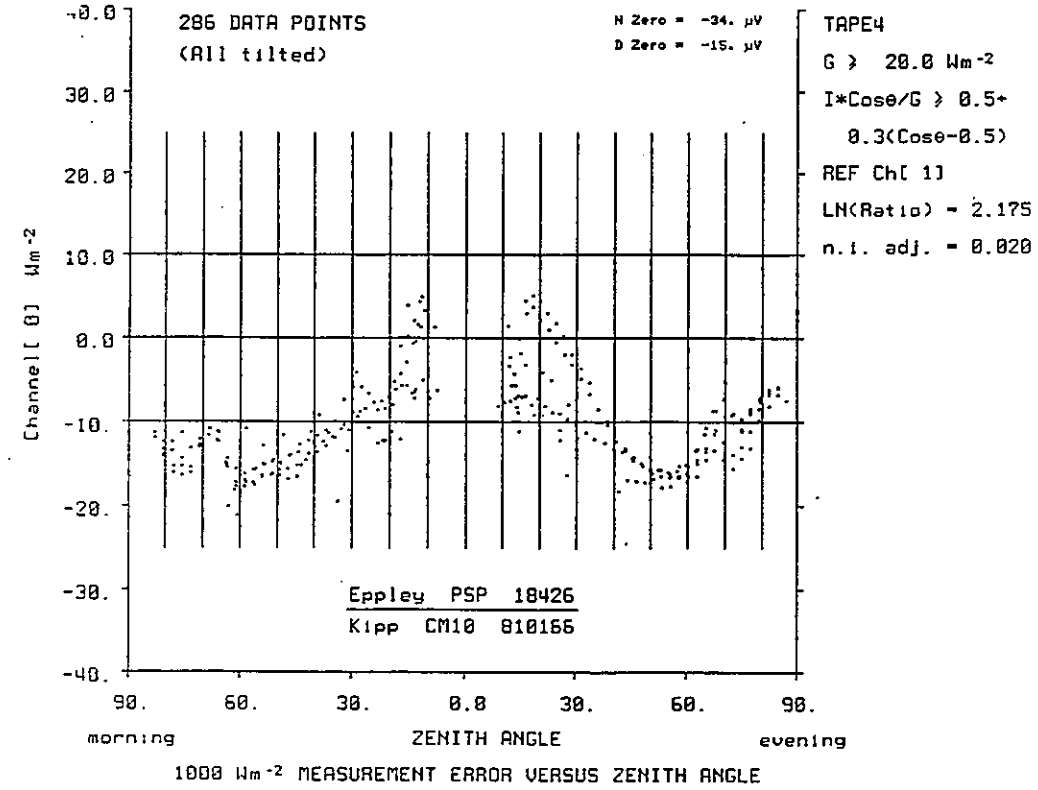

1000 Wm-2 MEASUREMENT ERROR VERSUS ZENITH ANGLE

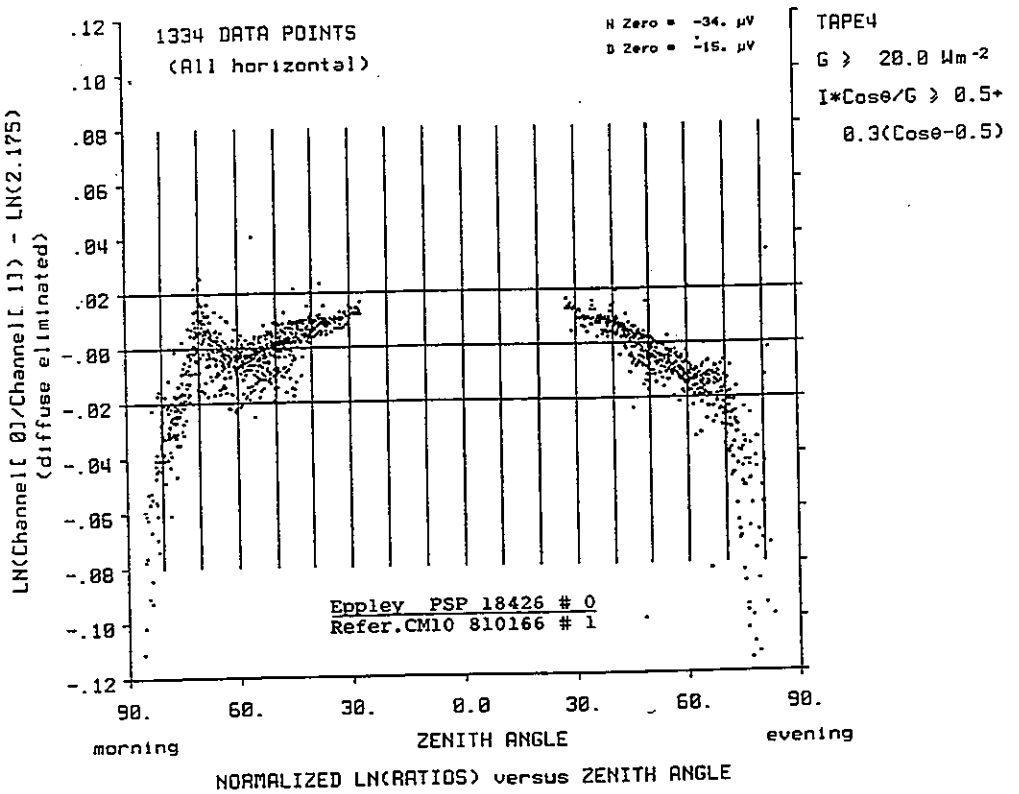
1334 DATA POINTS
(All horizontal)
N Zero = -34. μV
D Zero = -15. μV
TAPE4
G ≥ 20.0 Wm-2
I*Cosθ/G ≥ 0.5+
0.3(Cosθ-0.5)
LN(Channel[0]/Channel[1]) - LN(2.175)
(diffuse eliminated)
.12
.10
.08
.06
.04
.02
-.00
-.02
-.04
-.06
-.08
-.10
-.12
Eppley PSP 18426 # 0
Refer.CM10 810166 # 1
90.
60.
30.
0.0
30.
60.
90.
morning
ZENITH ANGLE
evening
NORMALIZED LN(RATIOS) versus ZENITH ANGLE

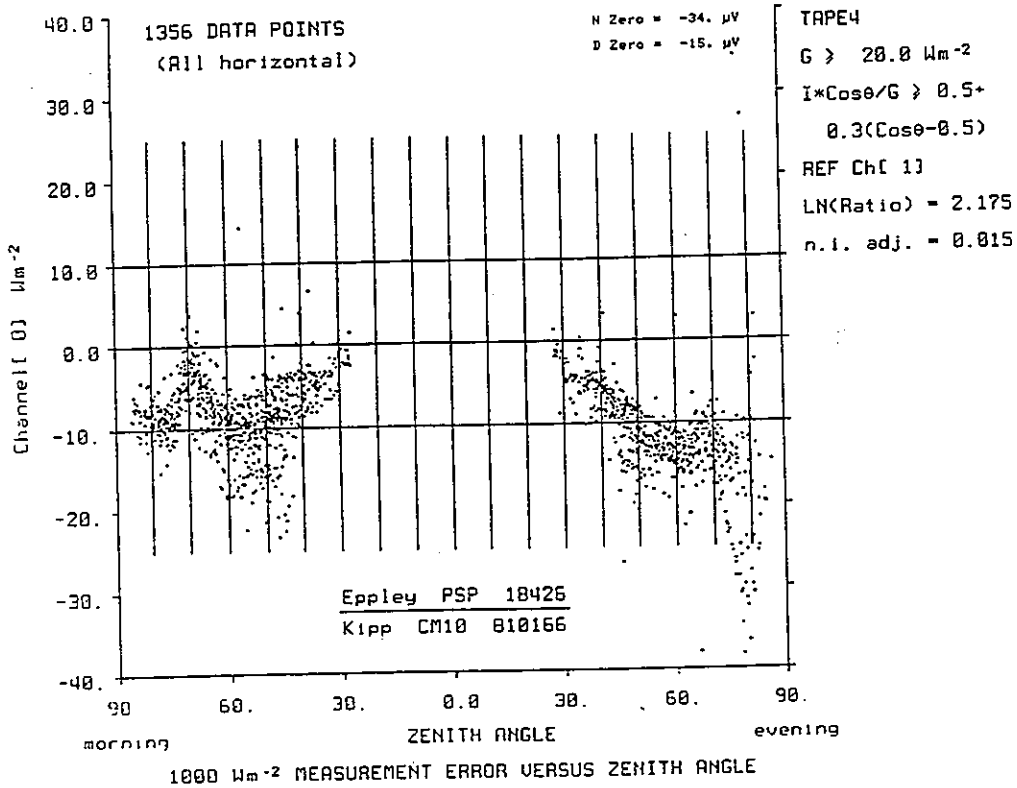
1356 DATA POINTS
(All horizontal)
N Zero = -34. μV
D Zero = -15. μV
TAPE4
G ≥ 20.0 Wm-2
I*Cosθ/G ≥ 0.5+
0.3(Cosθ-0.5)
REF Ch[1]
LN(Ratio) = 2.175
n.i. adj. = 0.015
Channel[0] Wm-2
40.0
30.0
20.0
10.0
0.0
-10.
-20.
-30.
-40.
Eppley PSP 18426
Kipp CM10 810166
90
60.
30.
0.0
30.
60.
90.
morning
ZENITH ANGLE
evening
1000 Wm-2 MEASUREMENT ERROR VERSUS ZENITH ANGLE

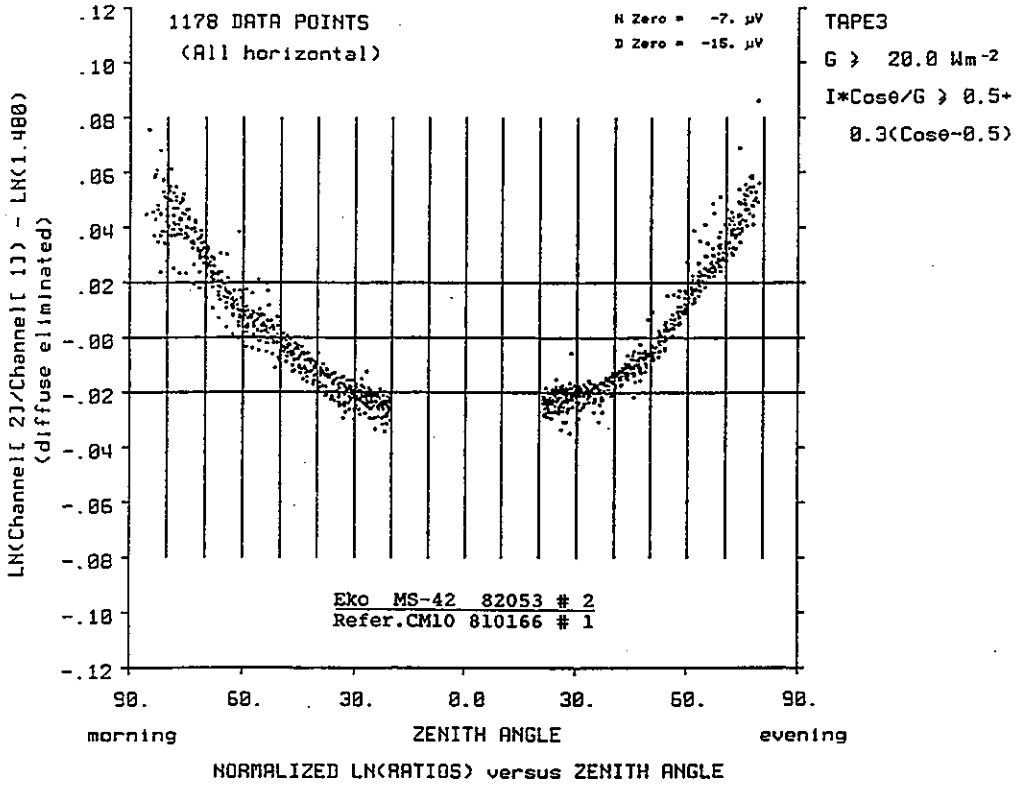

NORMALIZED LN(RATIOS) versus ZENITH ANGLE

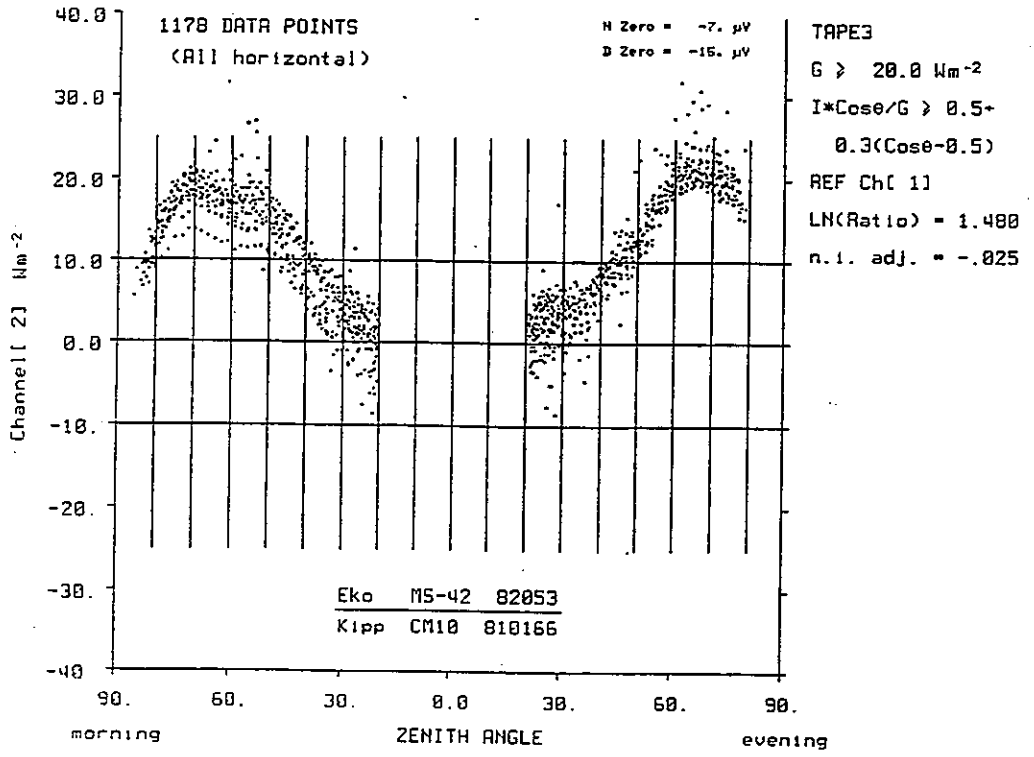

1000 Wm-2 MEASUREMENT ERROR VERSUS ZENITH ANGLE

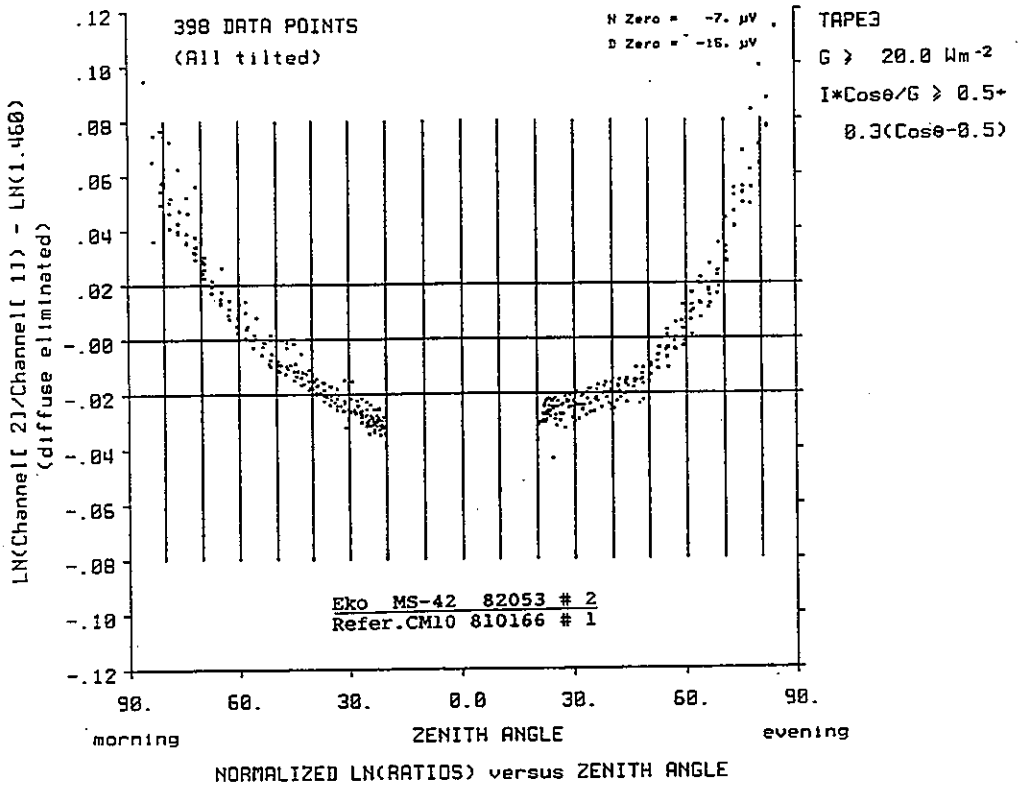

NORMALIZED LN(RATIOS) versus ZENITH ANGLE

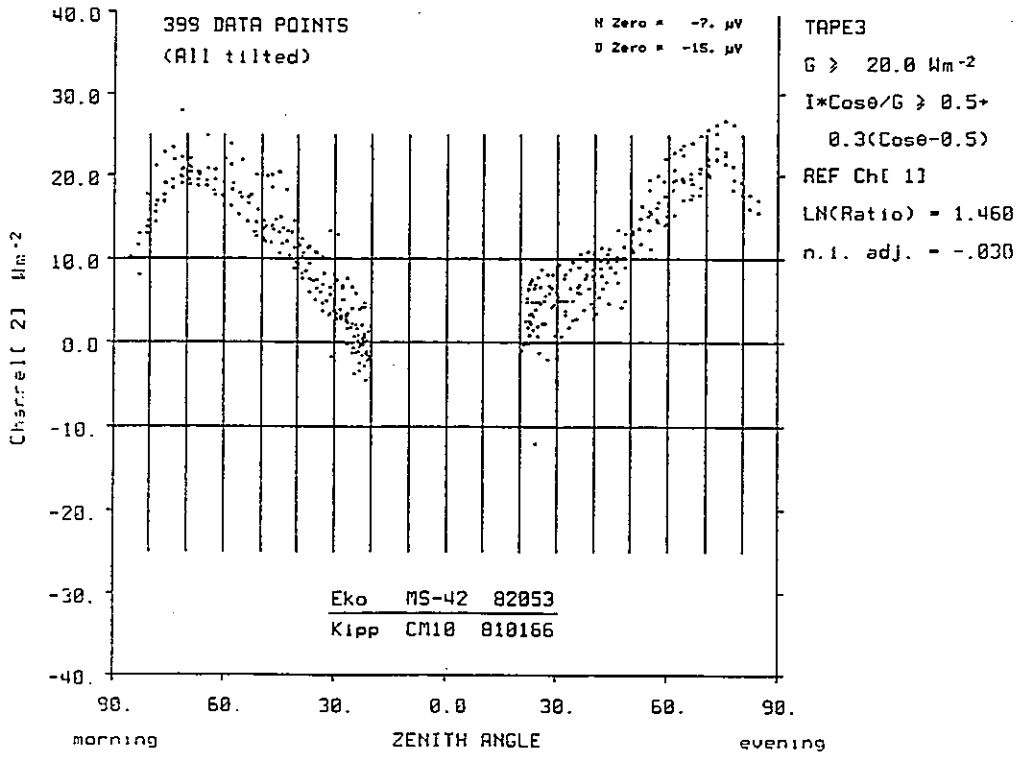

1000 Wm-2 MEASUREMENT ERROR VERSUS ZENITH ANGLE

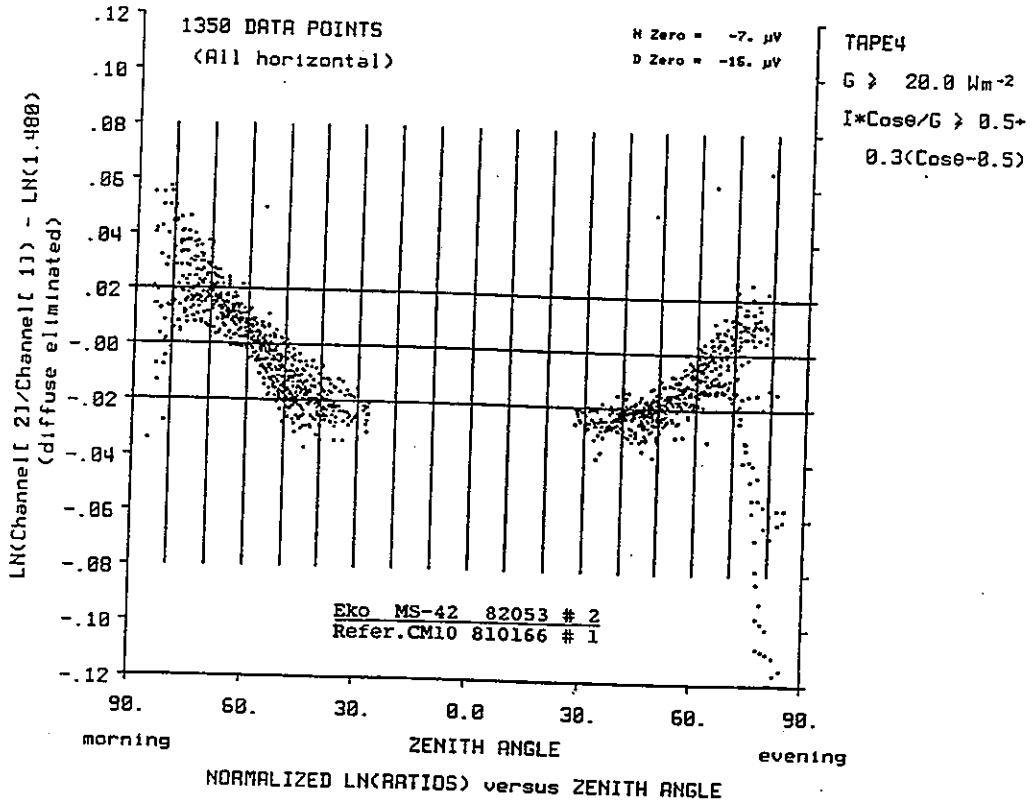
1350 DATA POINTS
(All horizontal)
N Zero = -7. µV
D Zero = -16. µV
TAPE4
G ≥ 20.0 Wm-2
I*Cosθ/G ≥ 0.5+
0.3(Cosθ-0.5)
LN(Channel[2]/Channel[1]) - LN(1.480)
(diffuse eliminated)
.12
.10
.08
.06
.04
.02
-.00
-.02
-.04
-.06
-.08
-.10
-.12
Eko MS-42 82053 # 2
Refer.CM10 810166 # 1
90.
60.
30.
0.0
30.
60.
90.
morning
ZENITH ANGLE
evening
NORMALIZED LN(RATIOS) versus ZENITH ANGLE

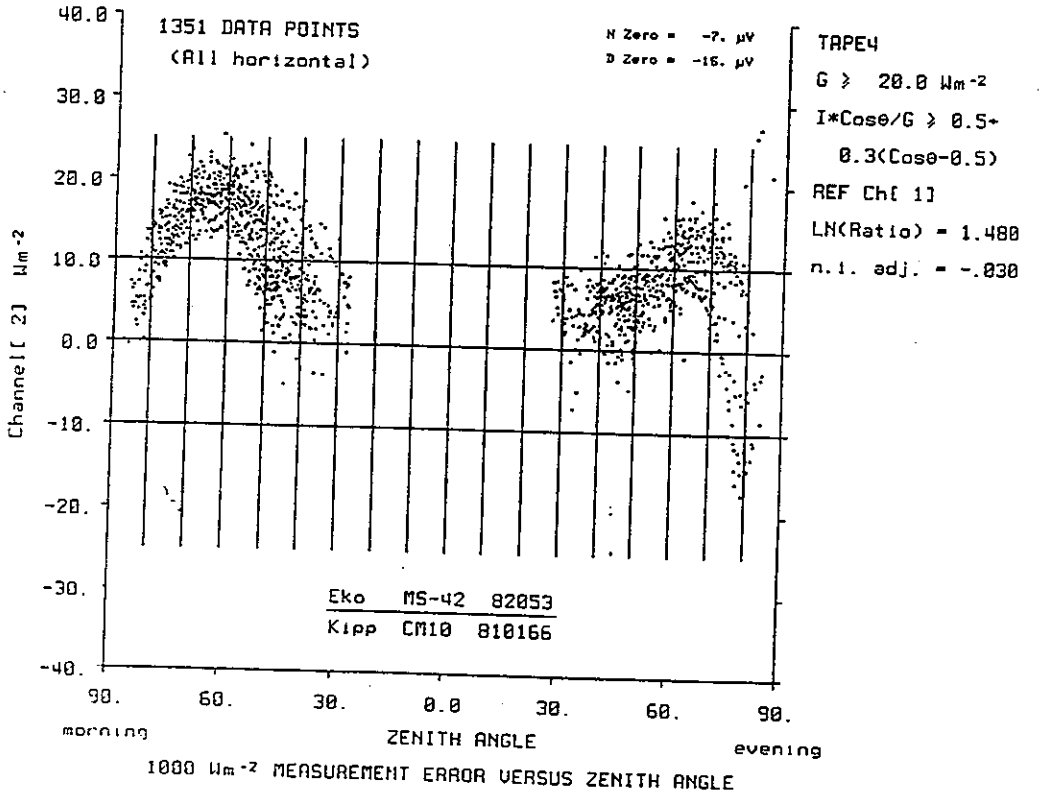
1351 DATA POINTS
(All horizontal)
N Zero = -7. µV
D Zero = -16. µV
TAPE4
G ≥ 20.0 Wm-2
I*Cosθ/G ≥ 0.5+
0.3(Cosθ-0.5)
REF Ch[1]
LN(Ratio) = 1.480
n.i. adj. = -.030
Channel[2] Wm-2
40.0
30.0
20.0
10.0
0.0
-10.
-20.
-30.
-40.
Eko MS-42 82053
Kipp CM10 810166
90.
60.
30.
0.0
30.
60.
90.
morning
ZENITH ANGLE
evening
1000 Wm-2 MEASUREMENT ERROR VERSUS ZENITH ANGLE

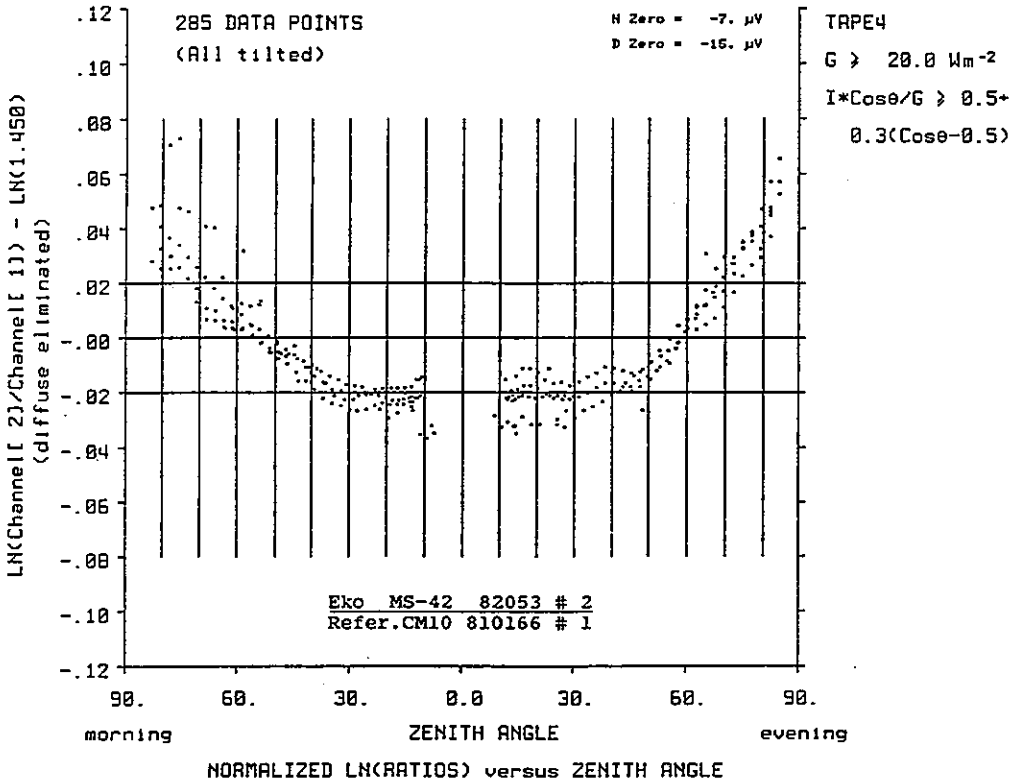

NORMALIZED LN(RATIOS) versus ZENITH ANGLE

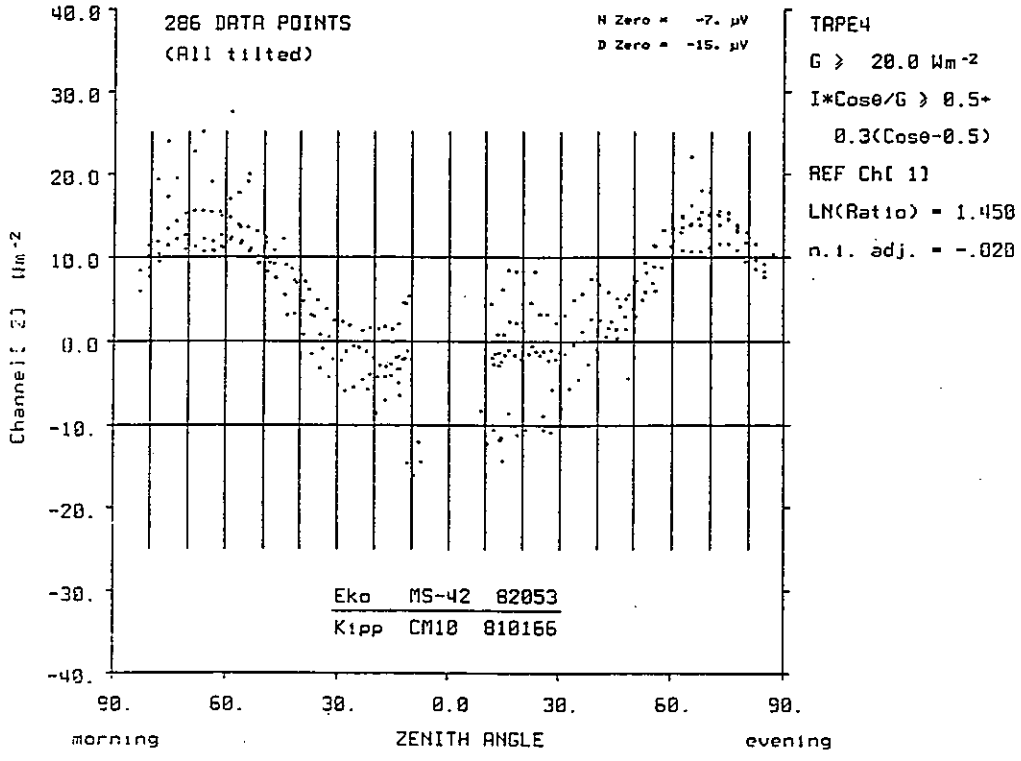

1000 Wm-2 MEASUREMENT ERROR VERSUS ZENITH ANGLE

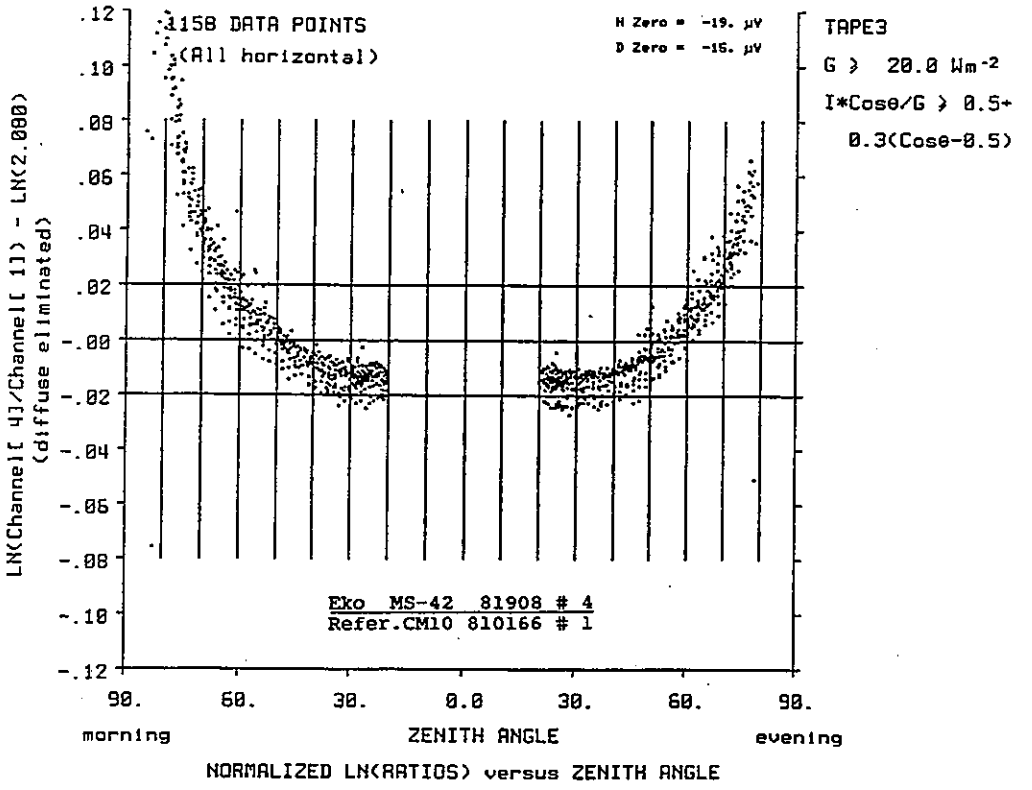

NORMALIZED LN(RATIOS) versus ZENITH ANGLE

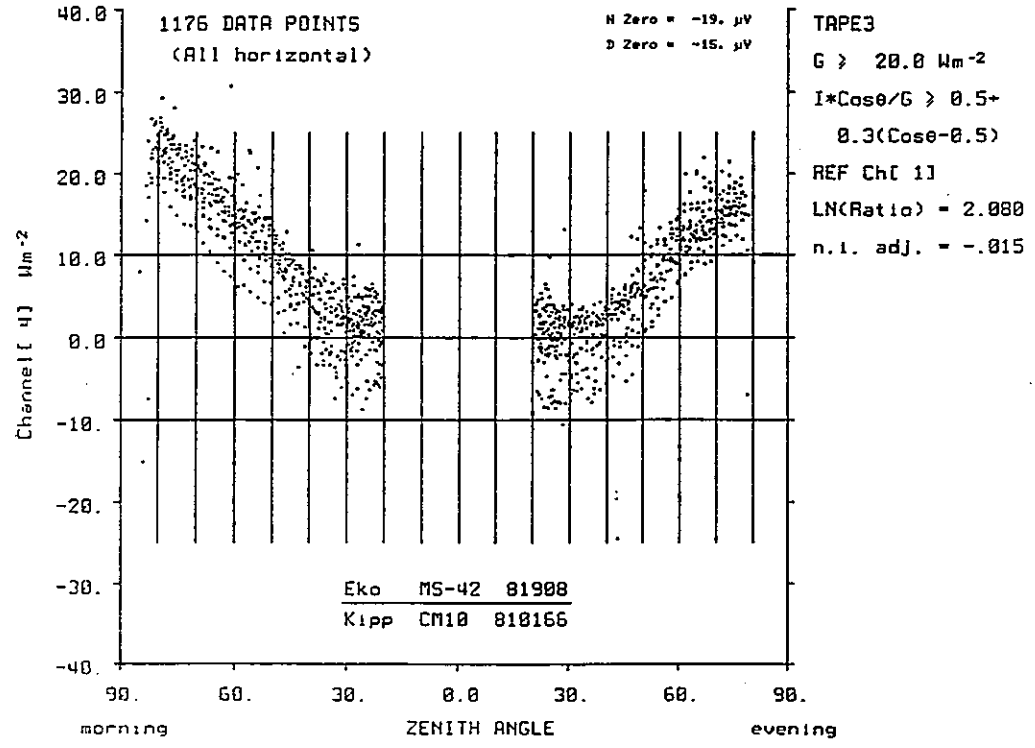

1000 Wm-2 MEASUREMENT ERROR VERSUS ZENITH ANGLE

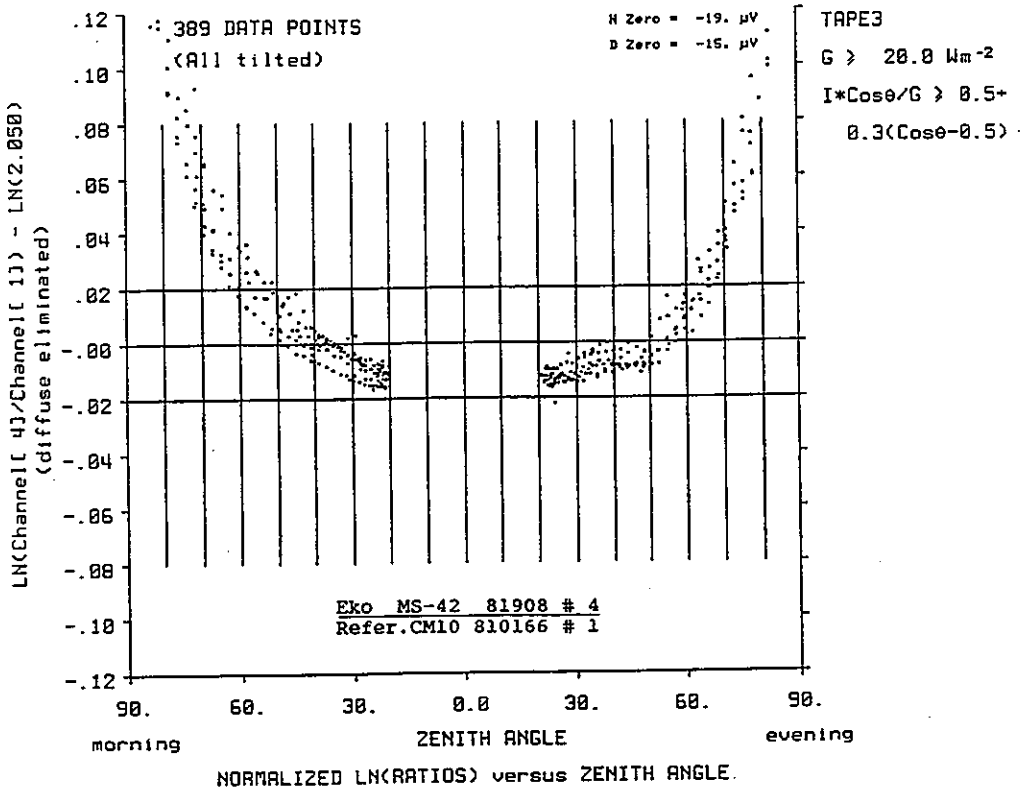

NORMALIZED LN(RATIOS) versus ZENITH ANGLE

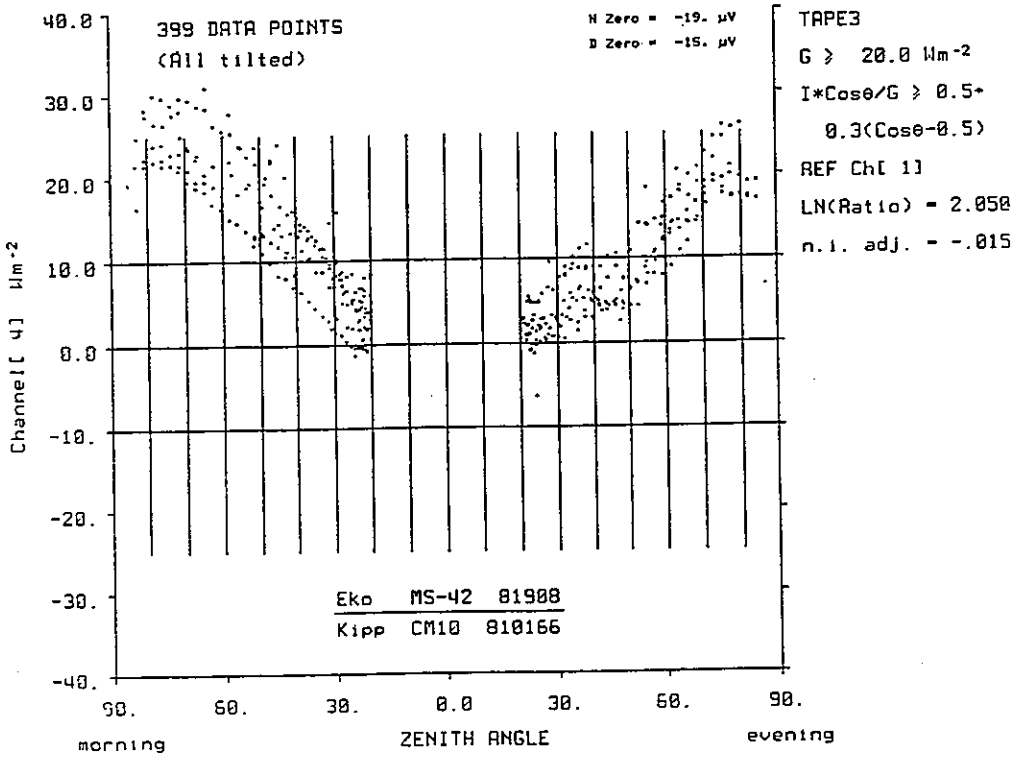

1000 Wm^{-2} MEASUREMENT ERROR VERSUS ZENITH ANGLE

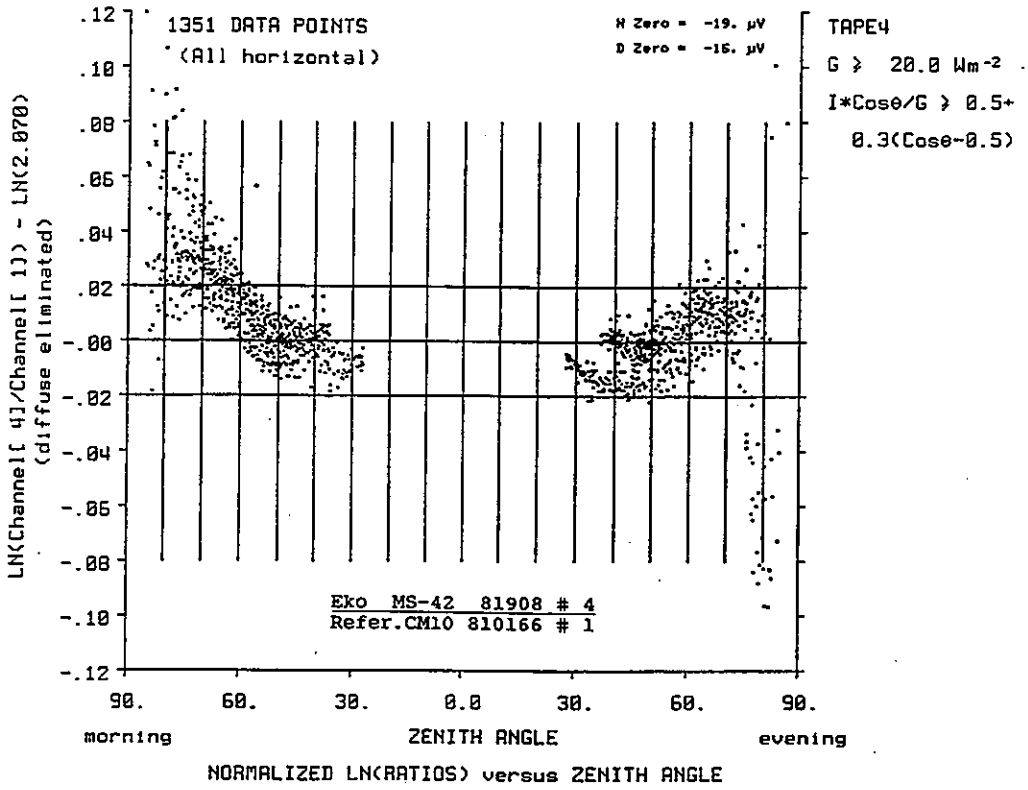

NORMALIZED LN(RATIOS) versus ZENITH ANGLE

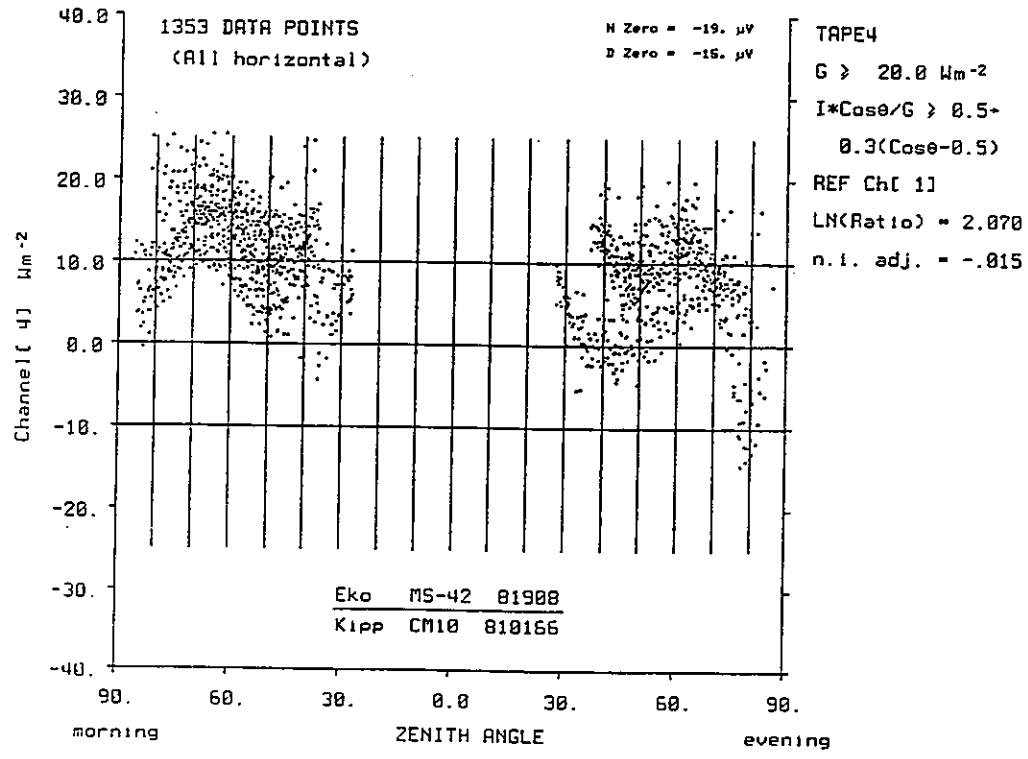

1000 Wm-2 MEASUREMENT ERROR VERSUS ZENITH ANGLE

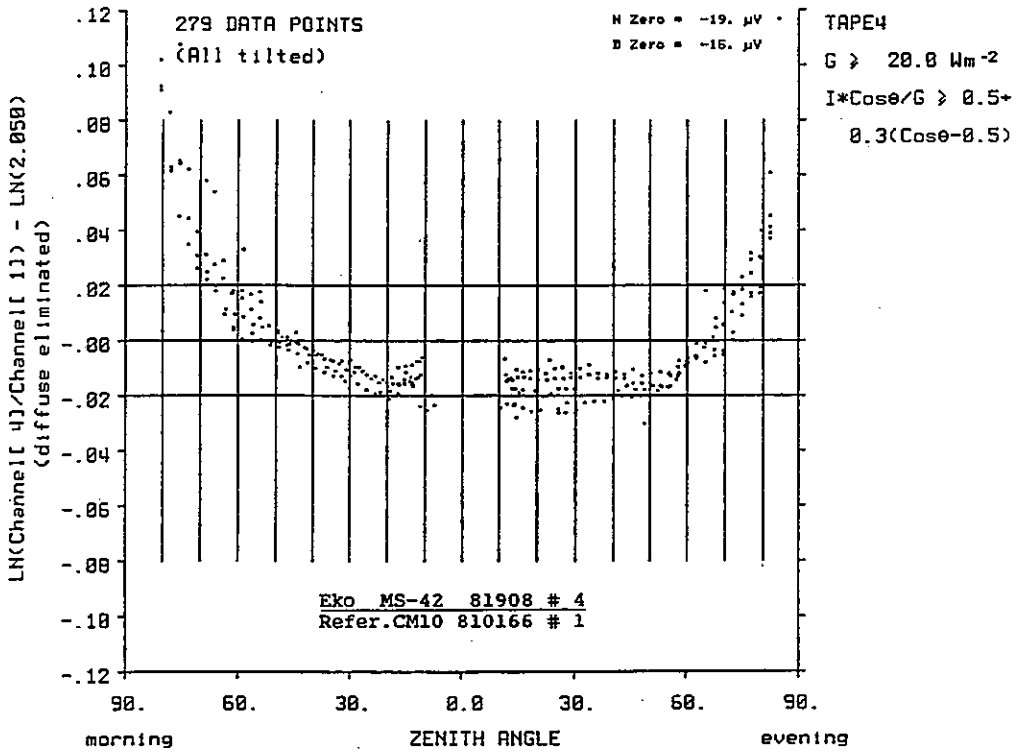

NORMALIZED LN(RATIOS) versus ZENITH ANGLE

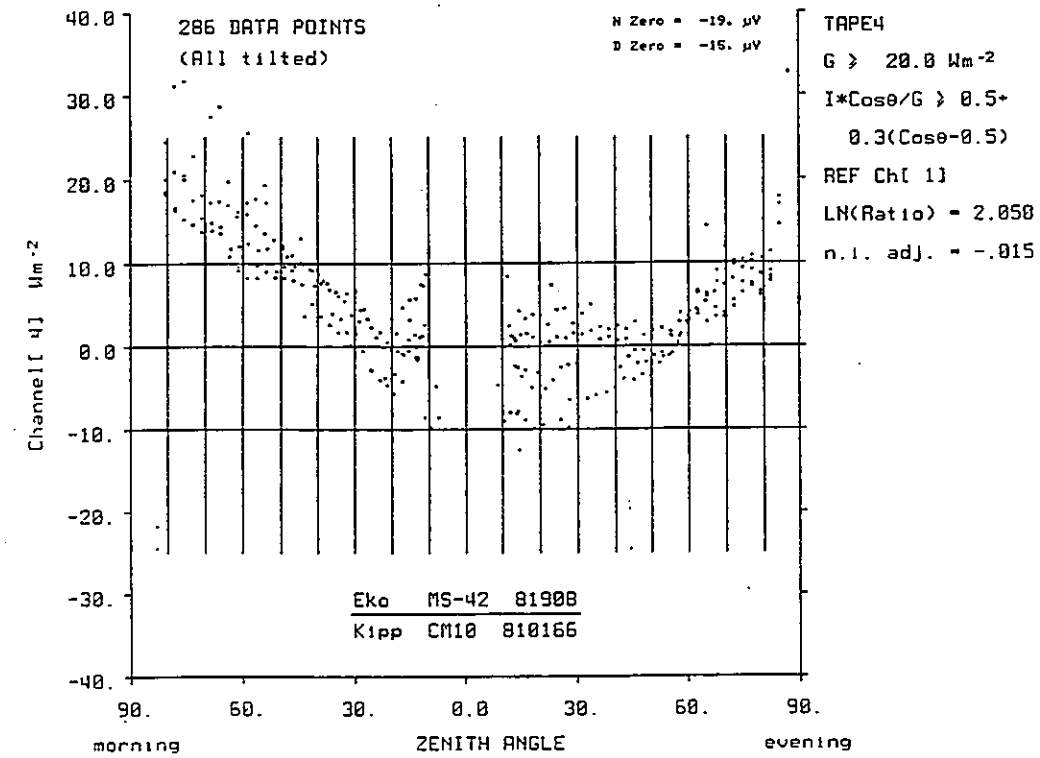

1000 Wm-2 MEASUREMENT ERROR VERSUS ZENITH ANGLE

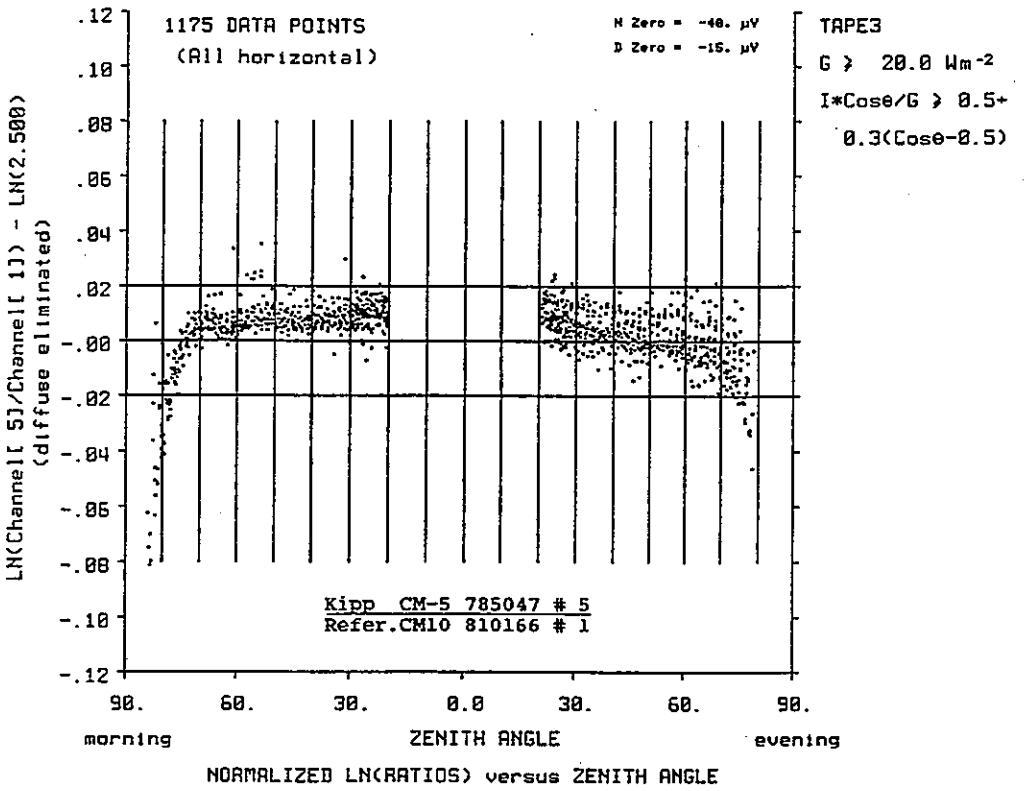

NORMALIZED LN(RATIOS) versus ZENITH ANGLE

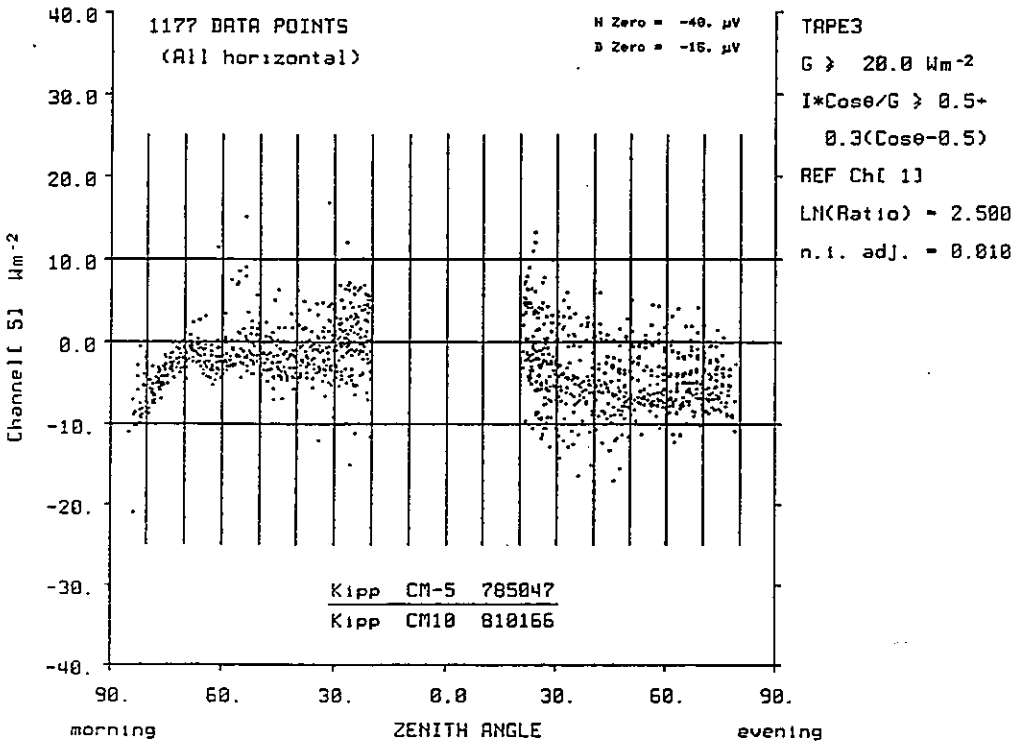

1000 Wm-2 MEASUREMENT ERROR VERSUS ZENITH ANGLE

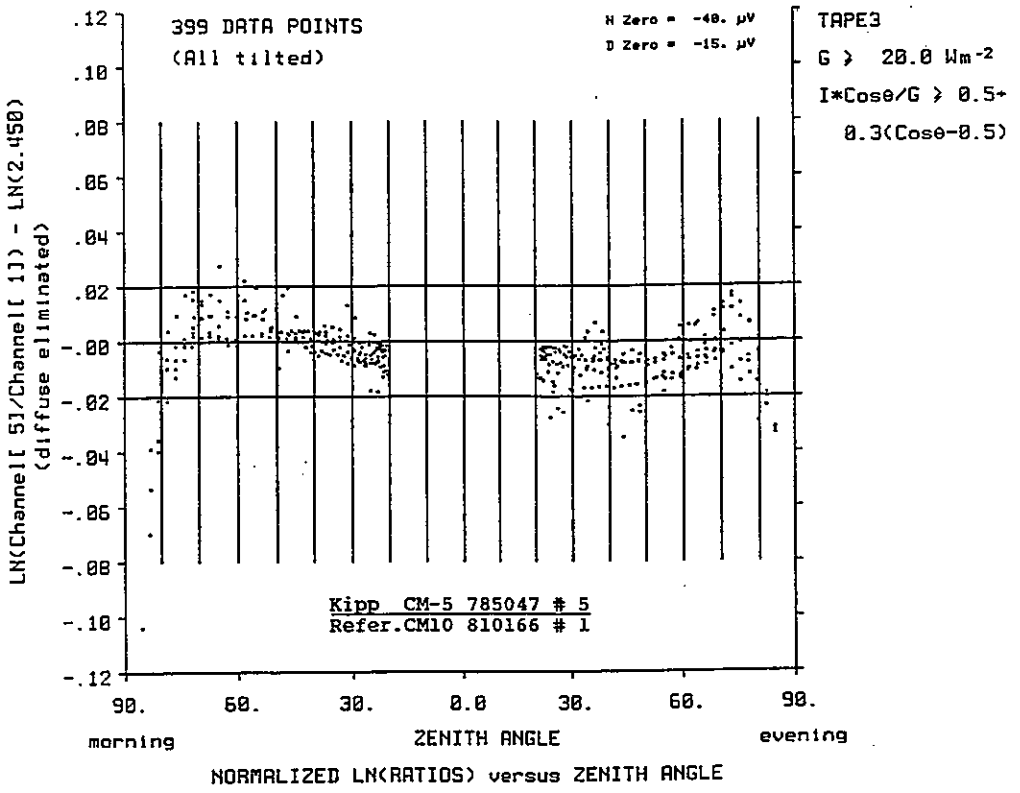

NORMALIZED LN(RATIOS) versus ZENITH ANGLE

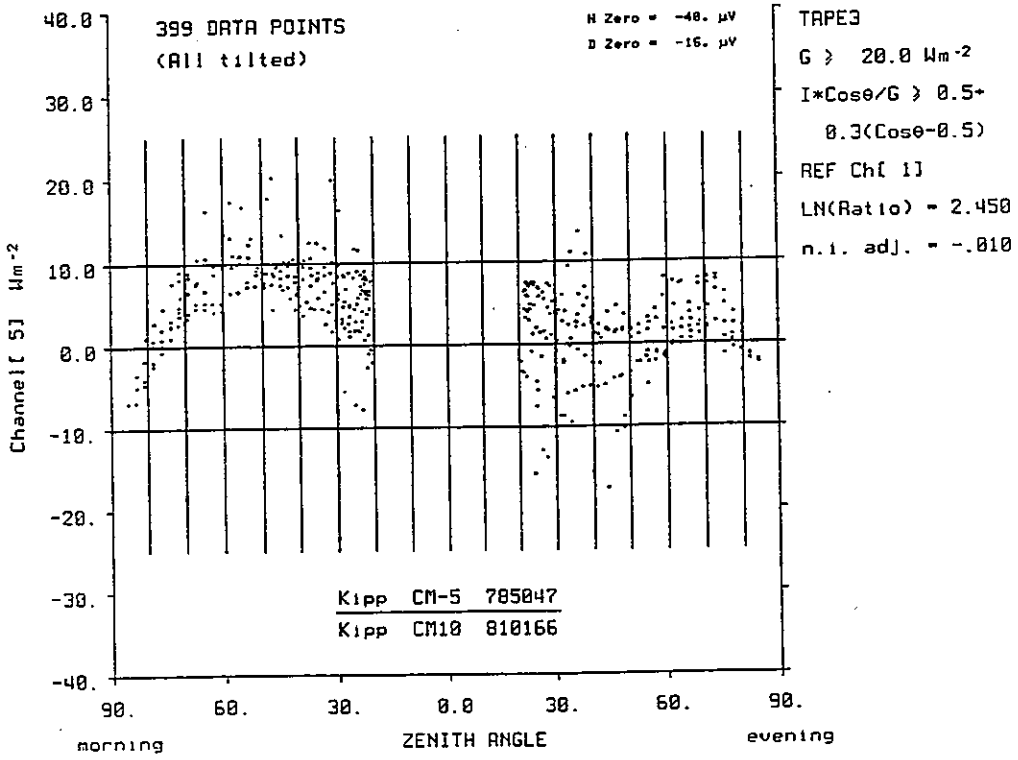

1000 Wm-2 MEASUREMENT ERROR VERSUS ZENITH ANGLE

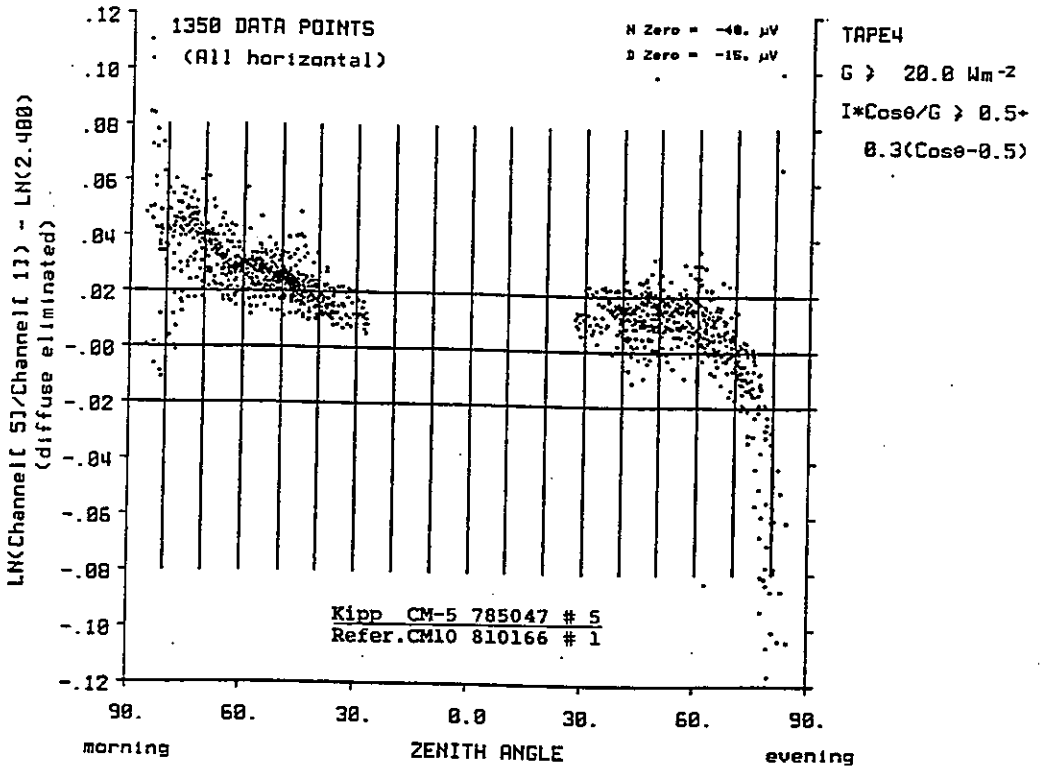

NORMALIZED LN(RATIOS) versus ZENITH ANGLE

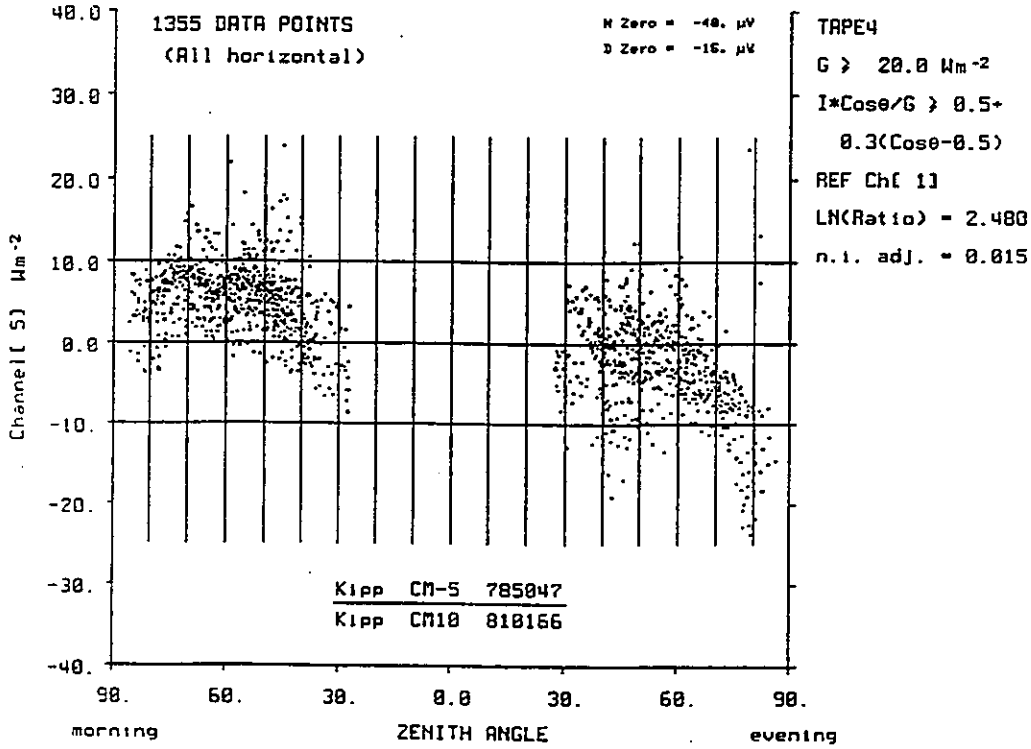

1000 Wm-2 MEASUREMENT ERROR VERSUS ZENITH ANGLE

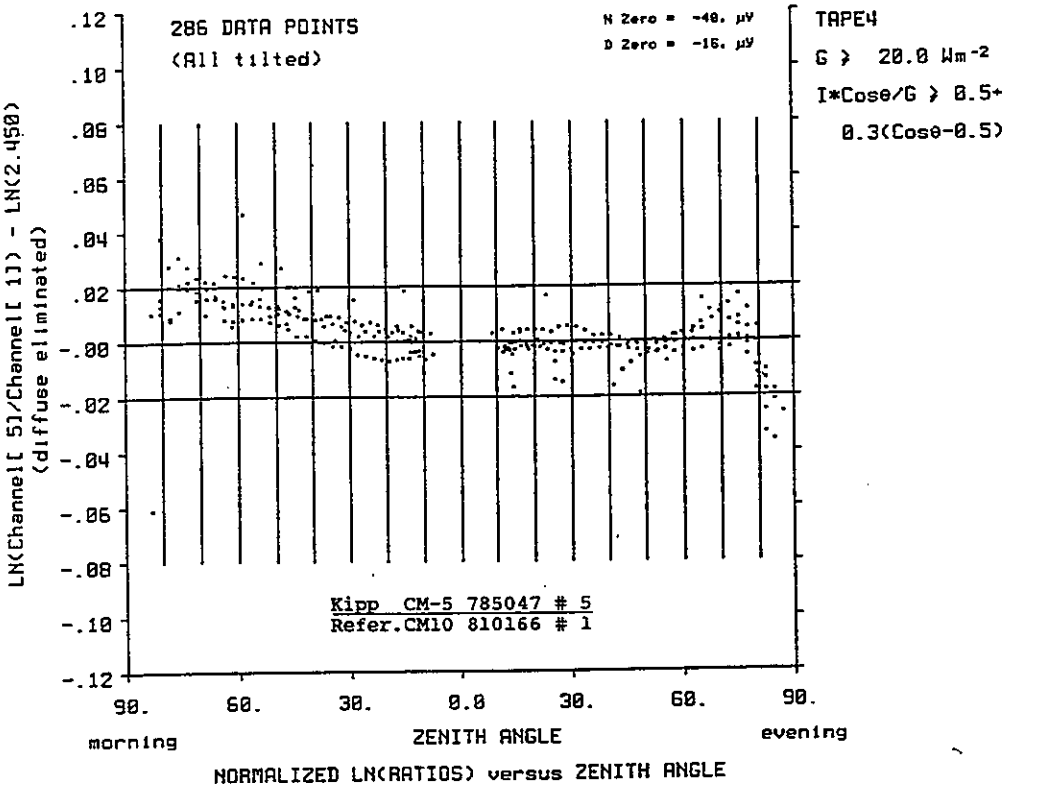

NORMALIZED LN(RATIOS) versus ZENITH ANGLE

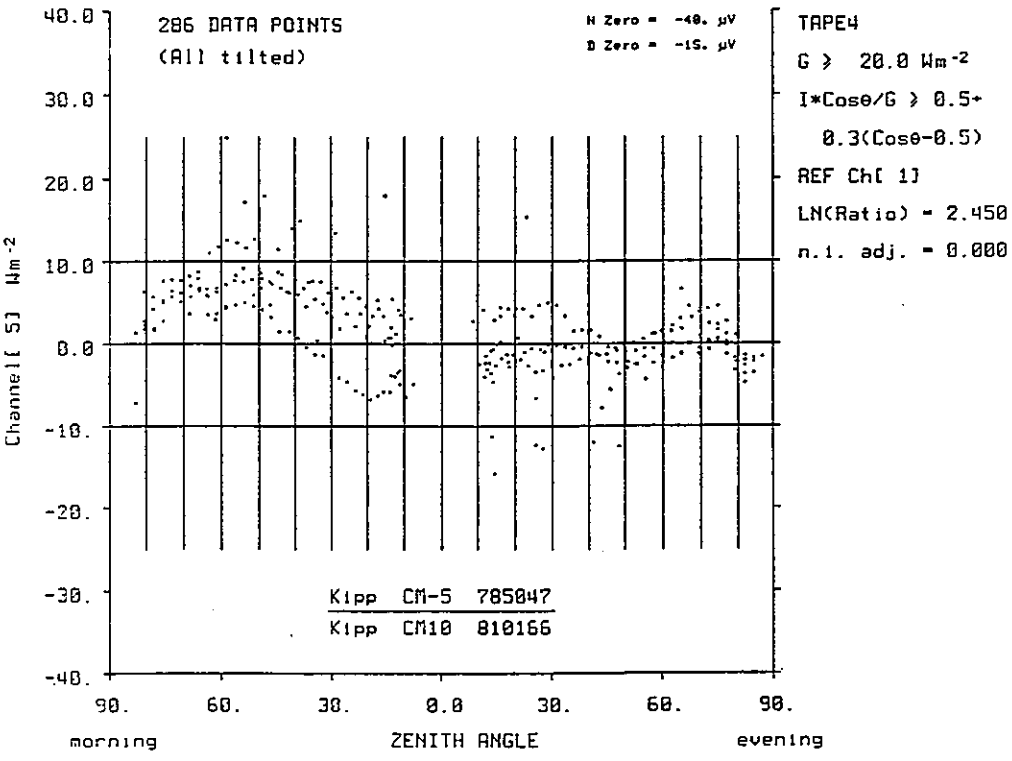

1000 Wm-2 MEASUREMENT ERROR VERSUS ZENITH ANGLE

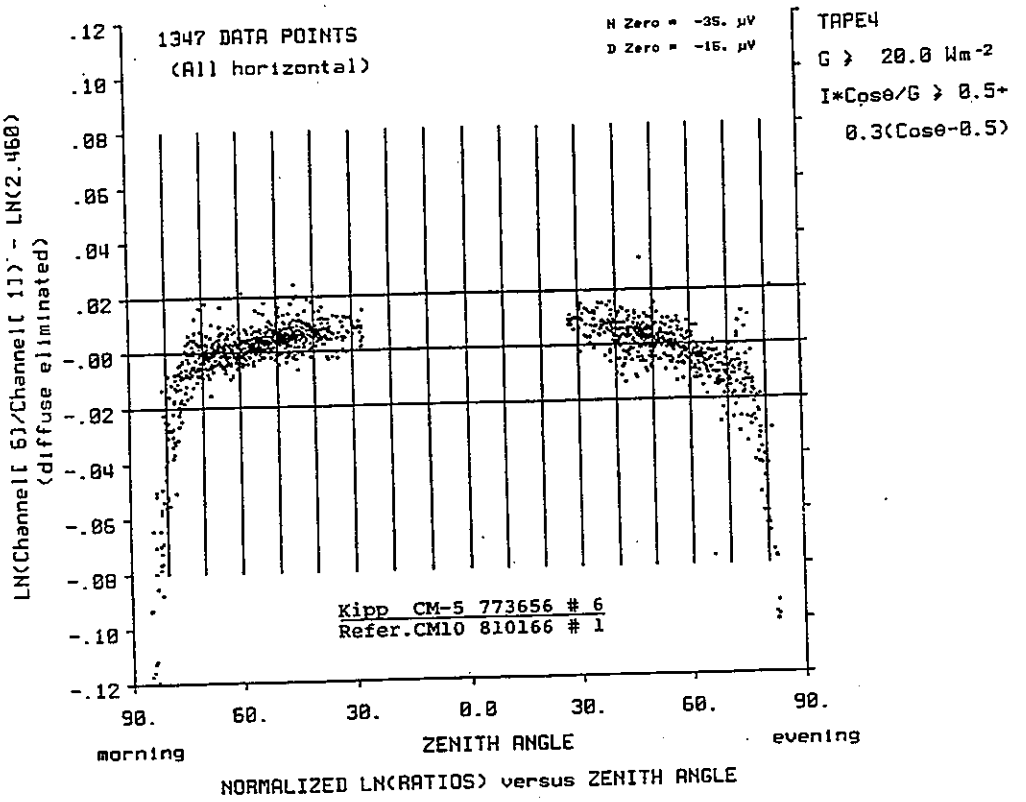
1347 DATA POINTS
(All horizontal)
N Zero = -35. µV
D Zero = -15. µV
TAPE4
G ≥ 20.0 Wm-2
I*Cosθ/G ≥ 0.5+
0.3(Cosθ-0.5)
LN(Channel[6]/Channel[1]) - LN(2.460)
(diffuse eliminated)
.12
.10
.08
.06
.04
.02
-.00
-.02
-.04
-.06
-.08
-.10
-.12
Kipp CM-5 773656 # 6
Refer.CM10 810166 # 1
90.
60.
30.
0.0
30.
60.
90.
morning
ZENITH ANGLE
evening
NORMALIZED LN(RATIOS) versus ZENITH ANGLE

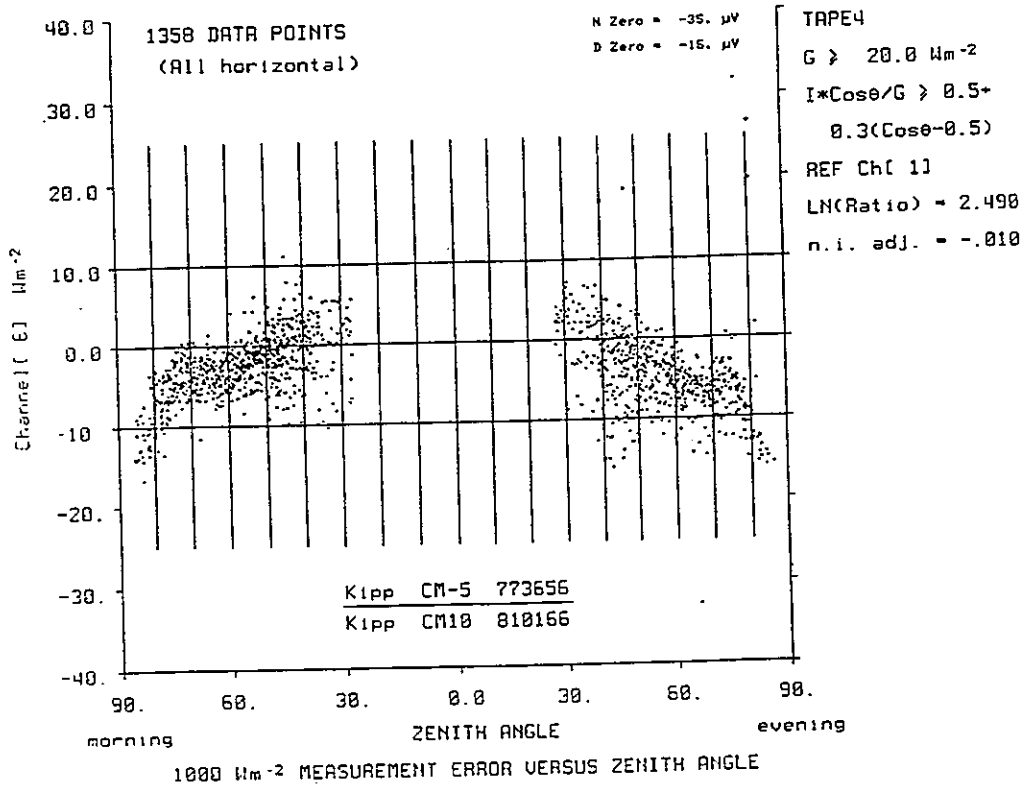
1358 DATA POINTS
(All horizontal)
N Zero = -35. µV
D Zero = -15. µV
TAPE4
G ≥ 20.0 Wm-2
I*Cosθ/G ≥ 0.5+
0.3(Cosθ-0.5)
REF Ch[1]
LN(Ratio) = 2.490
n.i. adj. = -.010
Channel[6] Wm-2
40.0
30.0
20.0
10.0
0.0
-10
-20.
-30.
-40.
Kipp CM-5 773656
Kipp CM10 810166
90.
60.
30.
0.0
30.
60.
90.
morning
ZENITH ANGLE
evening
1000 Wm-2 MEASUREMENT ERROR VERSUS ZENITH ANGLE

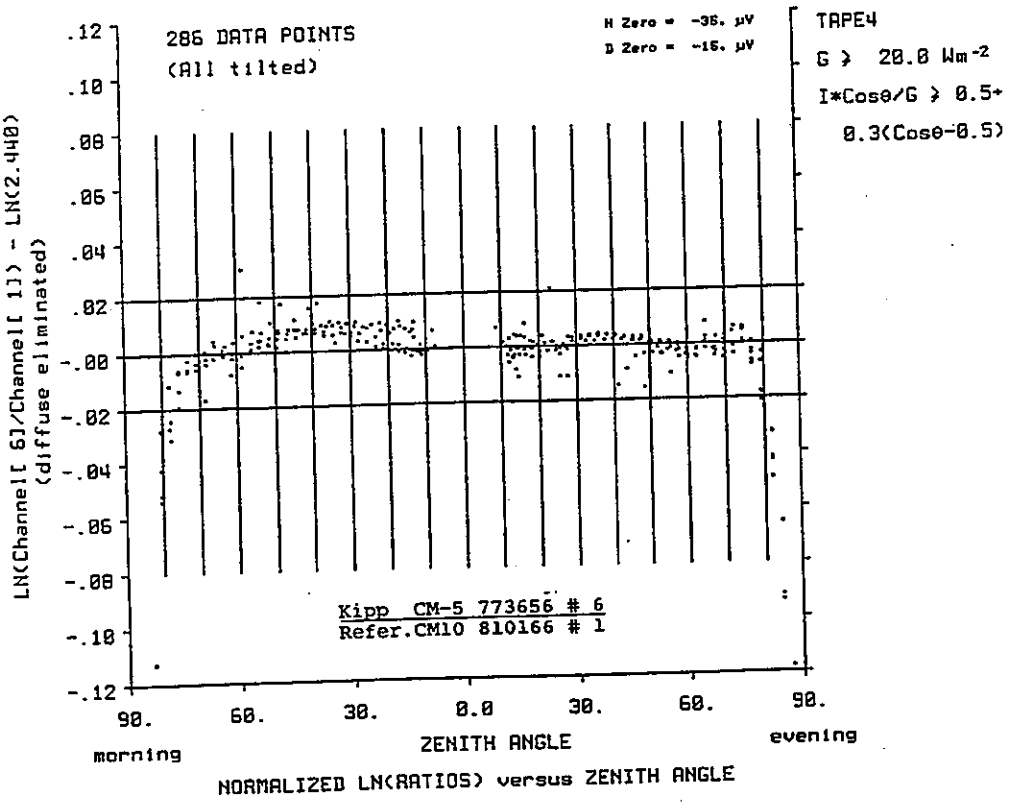
286 DATA POINTS
(All tilted)
H Zero = -36. µV
D Zero = -15. µV
TAPE4
G ≥ 20.0 Wm-2
I*Cosθ/G ≥ 0.5+
0.3(Cosθ-0.5)
LN(Channel[6]/Channel[1]) - LN(2.440)
(diffuse eliminated)
.12
.10
.08
.06
.04
.02
-.00
-.02
-.04
-.06
-.08
-.10
-.12
Kipp CM-5 773656 # 6
Refer.CM10 810166 # 1
90.
60.
30.
0.0
30.
60.
90.
morning
ZENITH ANGLE
evening
NORMALIZED LN(RATIOS) versus ZENITH ANGLE

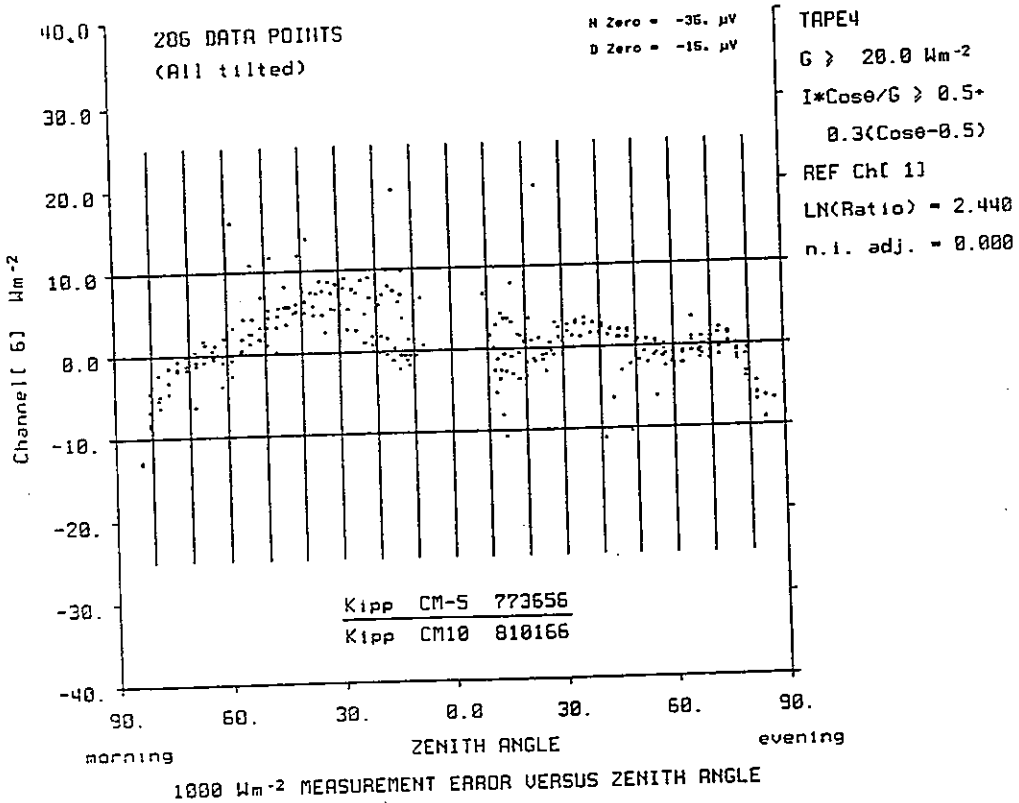
206 DATA POINTS
(All tilted)
H Zero = -36. µV
D Zero = -15. µV
TAPE4
G ≥ 20.0 Wm-2
I*Cosθ/G ≥ 0.5+
0.3(Cosθ-0.5)
REF Ch[1]
LN(Ratio) = 2.440
n.i. adj. = 0.000
Channel[6] Wm-2
40.0
30.0
20.0
10.0
0.0
-10.
-20.
-30.
-40.
Kipp CM-5 773656
Kipp CM10 810166
90.
60.
30.
0.0
30.
60.
90.
morning
ZENITH ANGLE
evening
1000 Wm-2 MEASUREMENT ERROR VERSUS ZENITH ANGLE

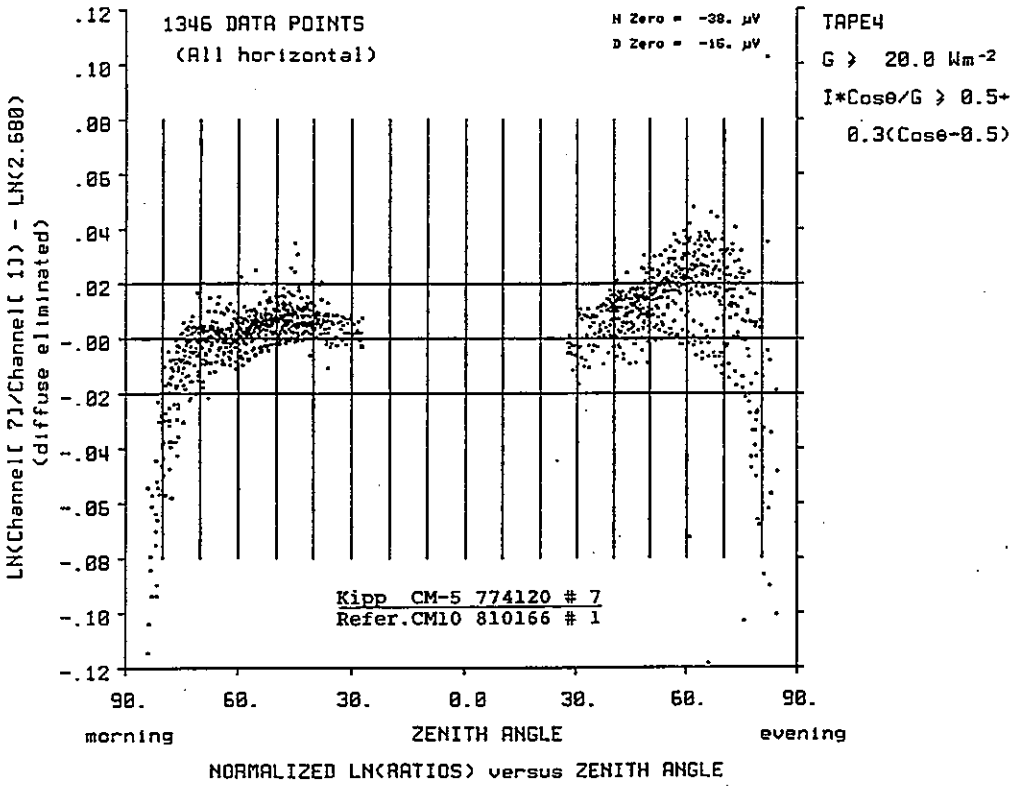

NORMALIZED LN(RATIOS) versus ZENITH ANGLE

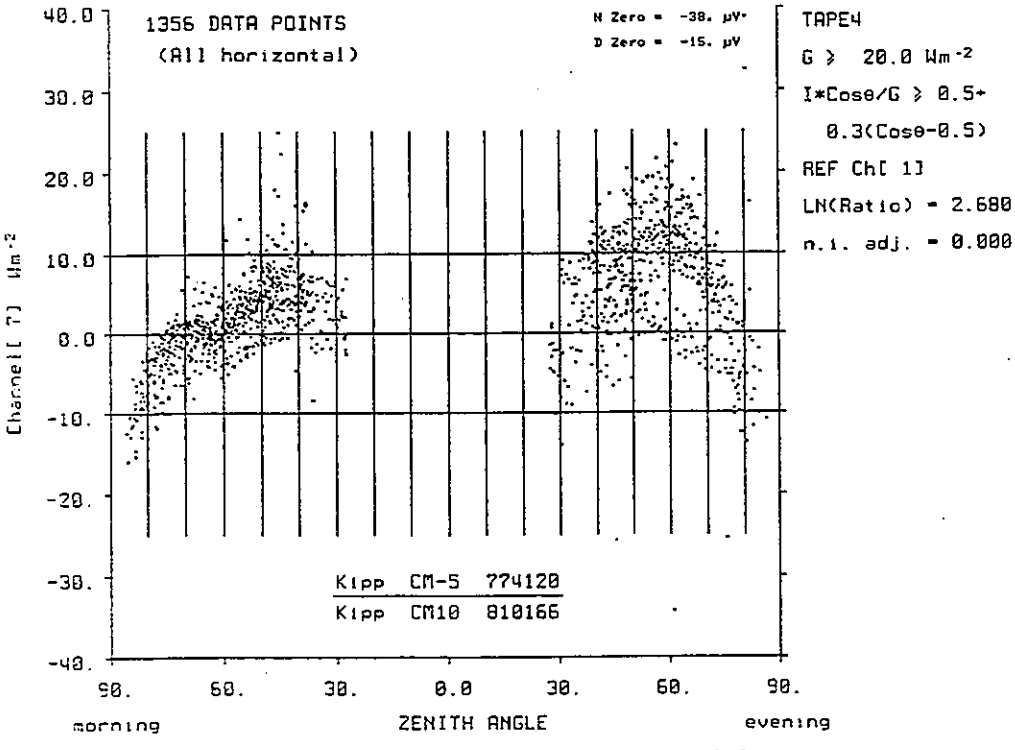

1000 Wm-2 MEASUREMENT ERROR VERSUS ZENITH ANGLE

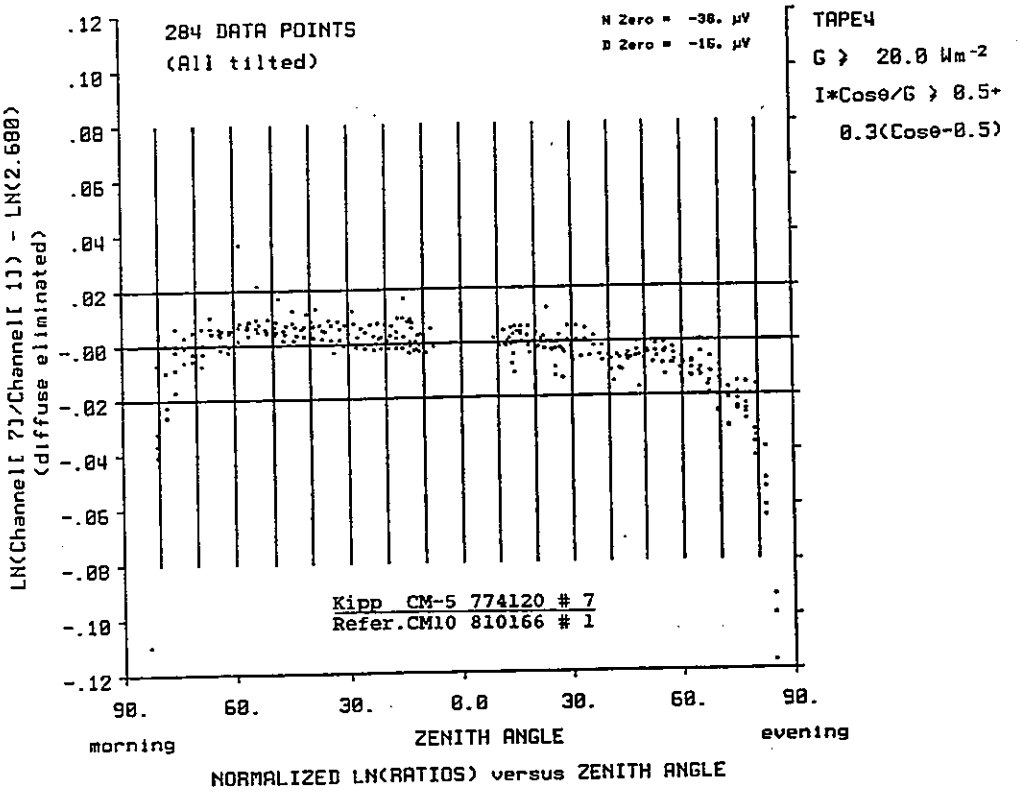

NORMALIZED LN(RATIOS) versus ZENITH ANGLE

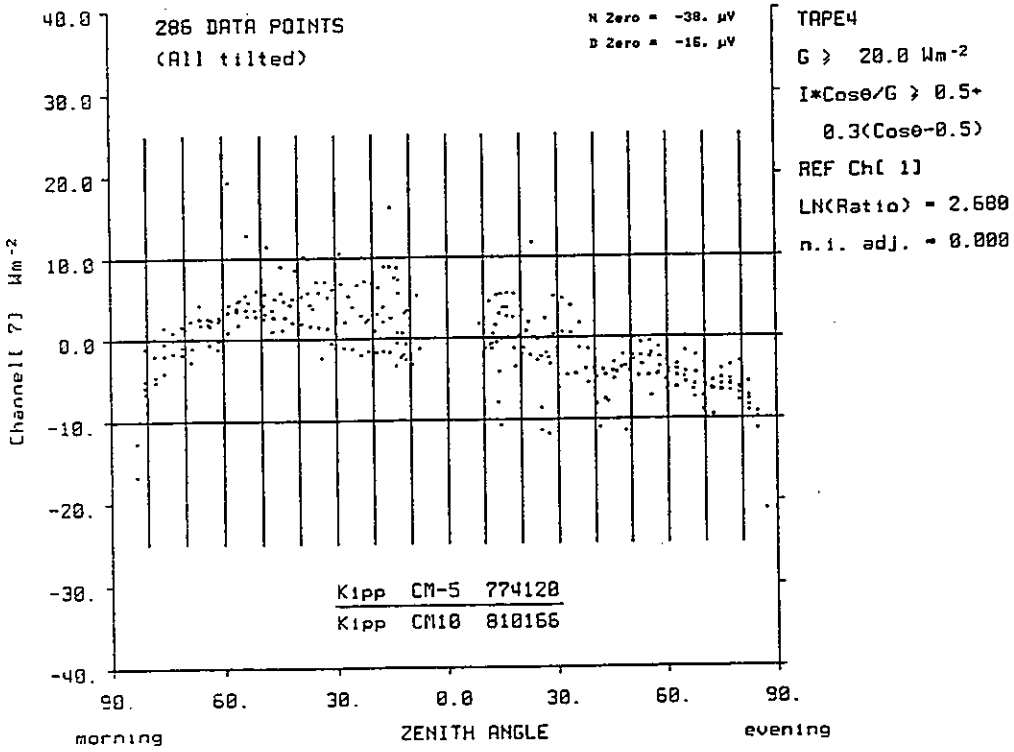

1000 Wm-2 MEASUREMENT ERROR VERSUS ZENITH ANGLE

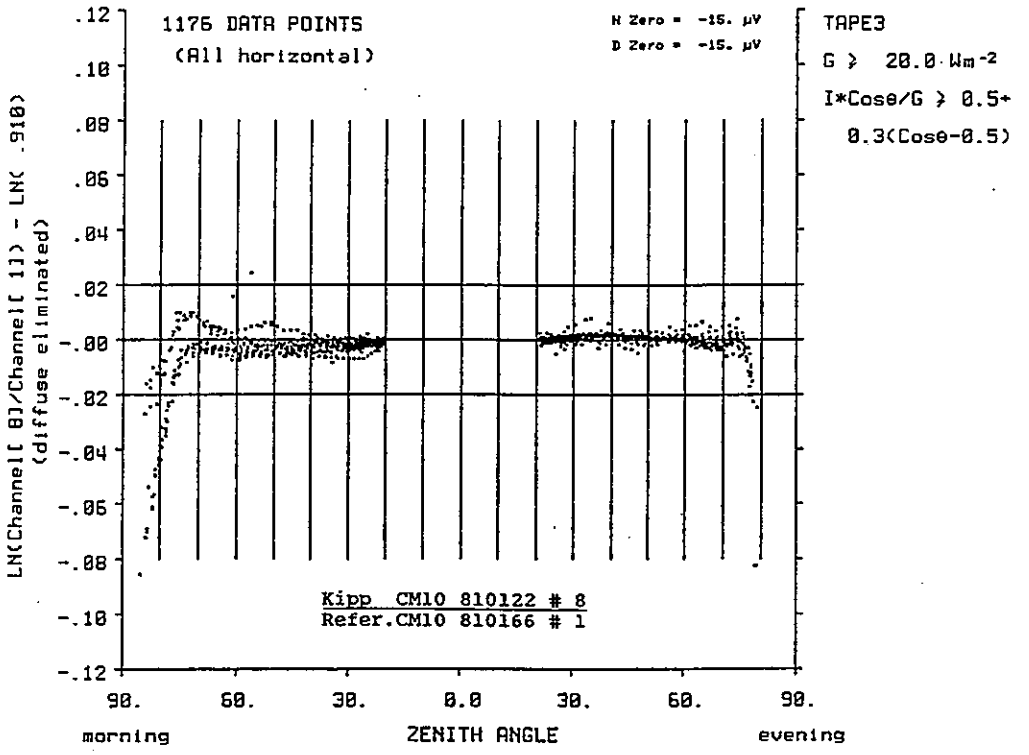

NORMALIZED LN(RATIOS) versus ZENITH ANGLE

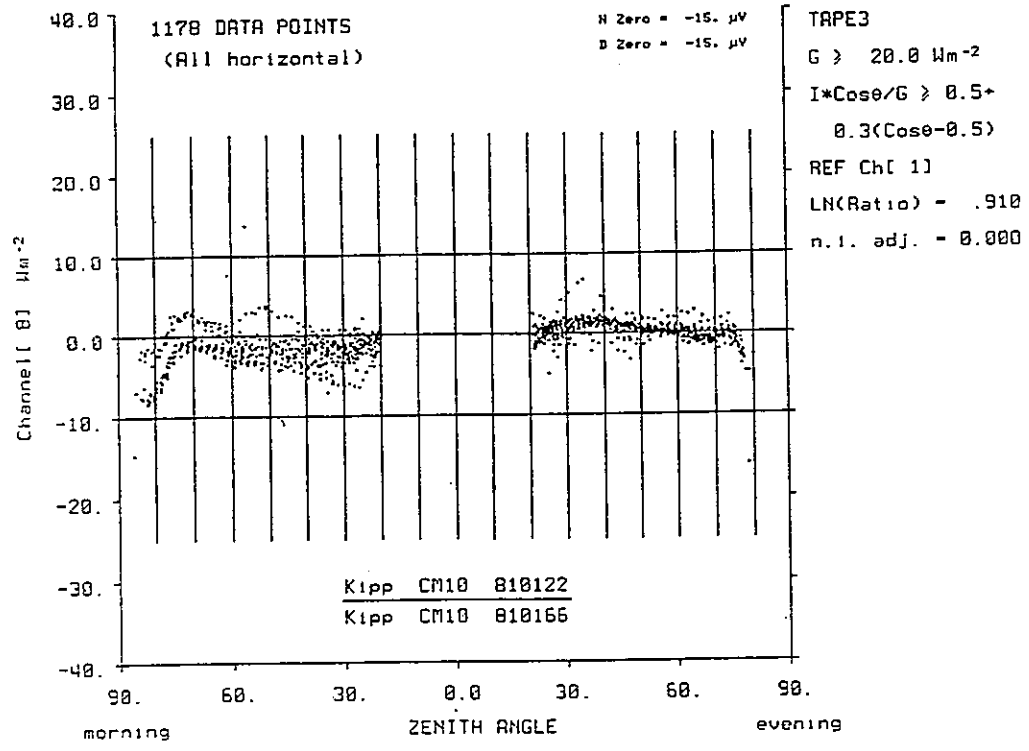

1000 Wm-2 MEASUREMENT ERROR VERSUS ZENITH ANGLE

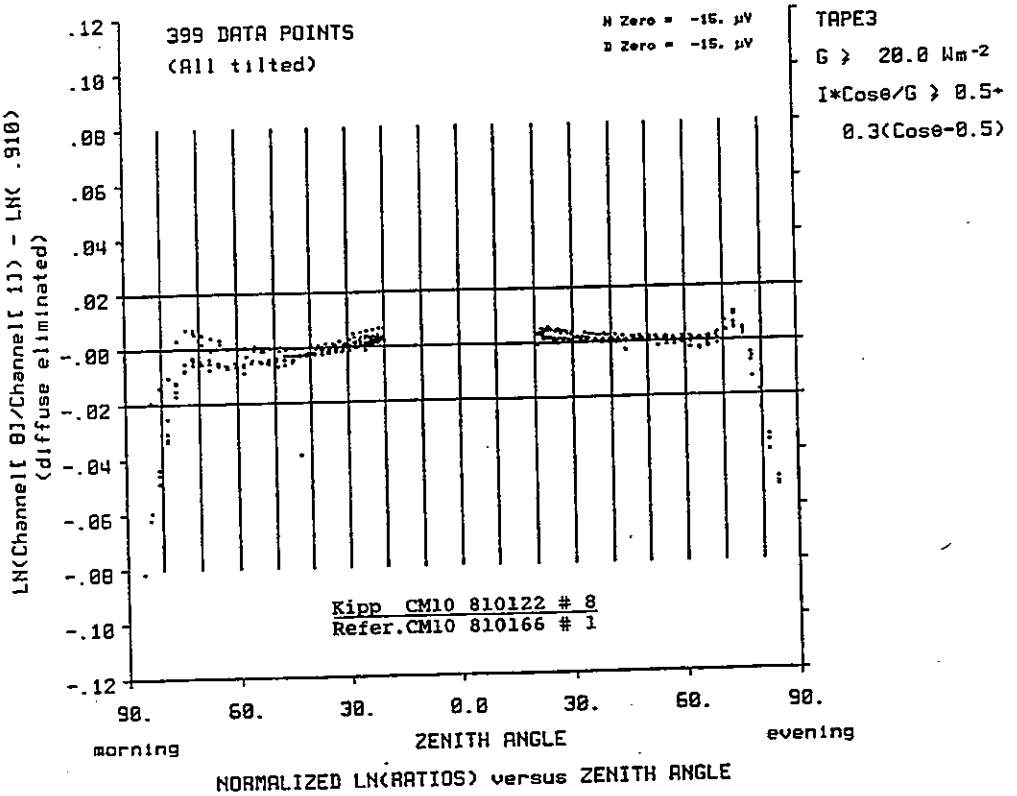

NORMALIZED LN(RATIOS) versus ZENITH ANGLE

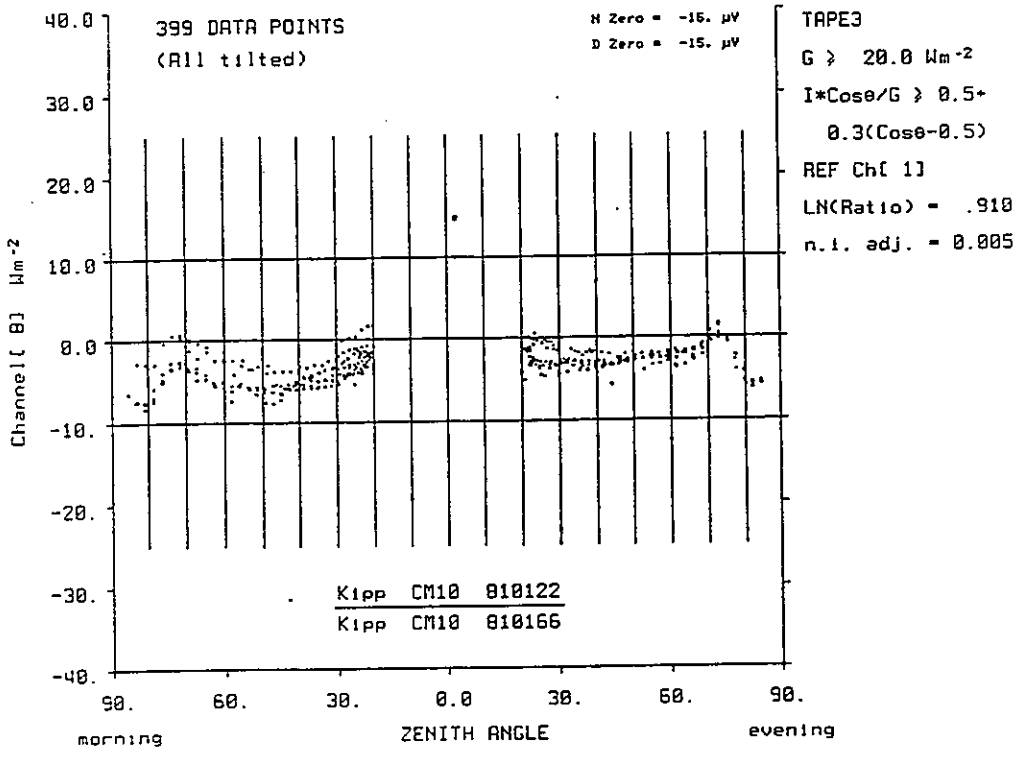

1000 Wm-2 MEASUREMENT ERROR VERSUS ZENITH ANGLE

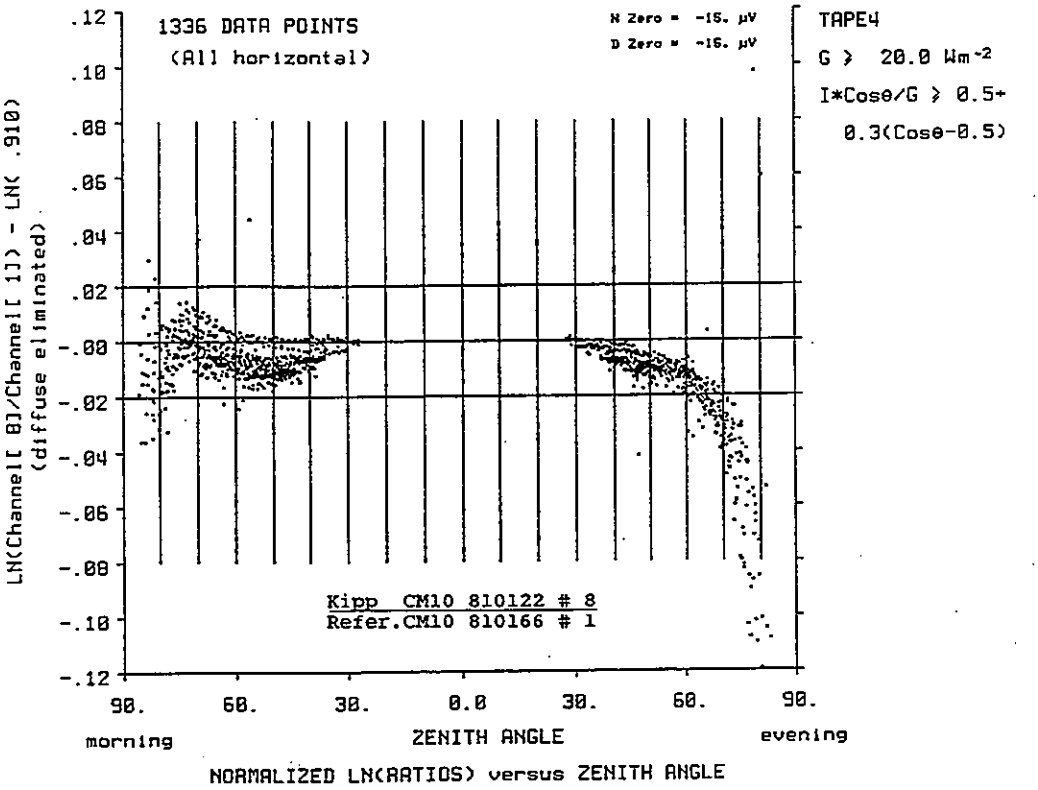

NORMALIZED LN(RATIOS) versus ZENITH ANGLE

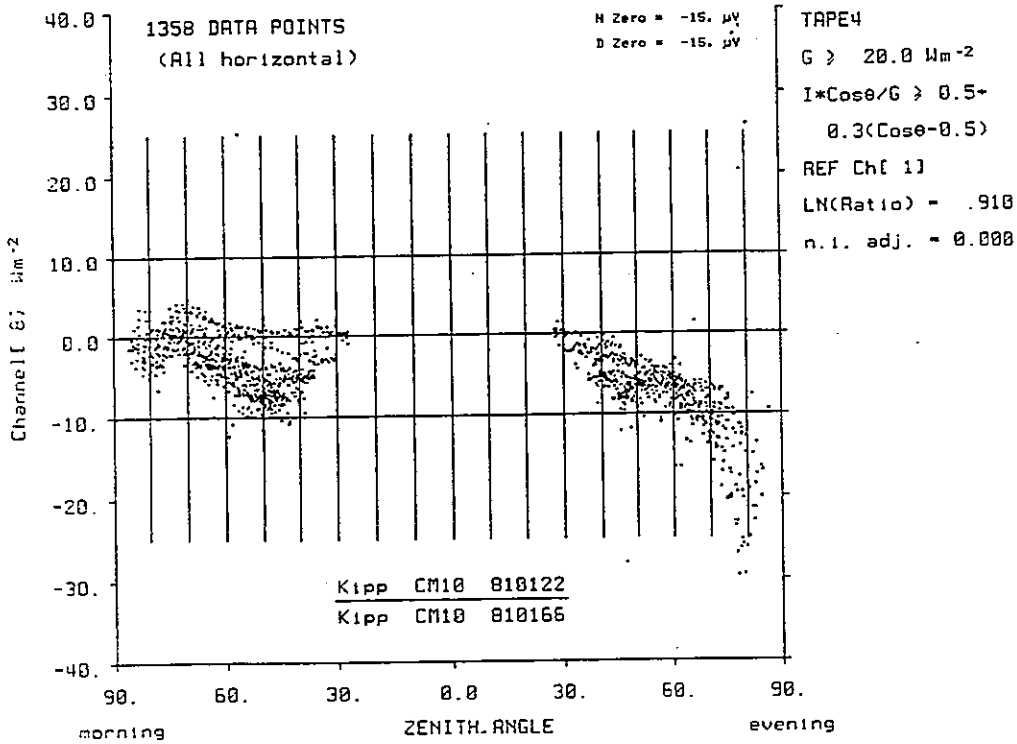

1000 Wm-2 MEASUREMENT ERROR VERSUS ZENITH ANGLE

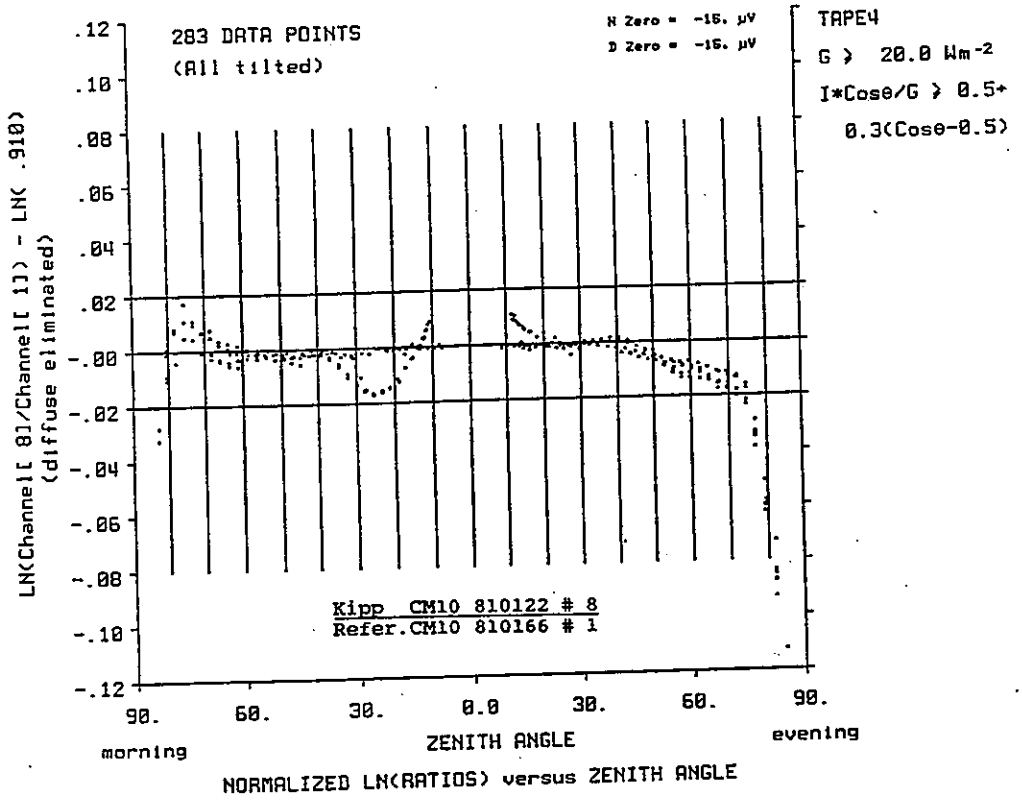
283 DATA POINTS
(All tilted)
N Zero = -15. μV
D Zero = -15. μV
TAPE4
G > 20.0 Wm-2
I*Cosθ/G > 0.5+
0.3(Cosθ-0.5)
LN(Channel[8]/Channel[1]) - LN(.910)
(diffuse eliminated)
.12
.10
.08
.06
.04
.02
-.00
-.02
-.04
-.06
-.08
-.10
-.12
Kipp CM10 810122 # 8
Refer.CM10 810166 # 1
90.
60.
30.
0.0
30.
60.
90.
morning
ZENITH ANGLE
evening
NORMALIZED LN(RATIOS) versus ZENITH ANGLE

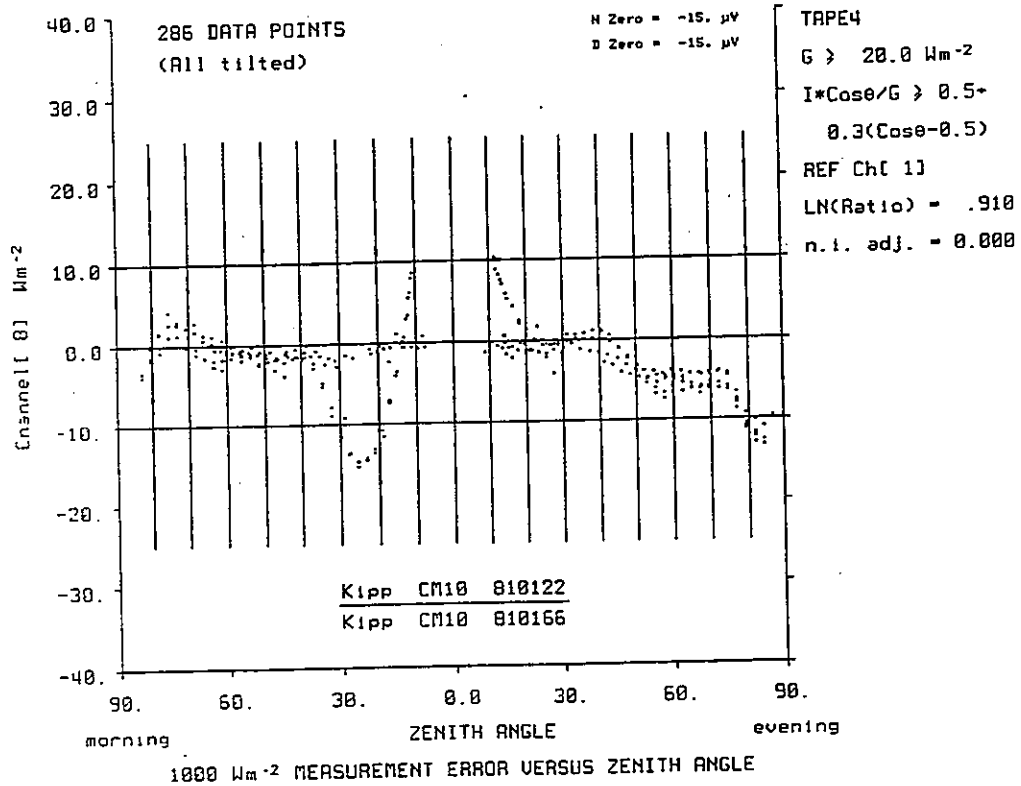
286 DATA POINTS
(All tilted)
N Zero = -15. μV
D Zero = -15. μV
TAPE4
G > 20.0 Wm-2
I*Cosθ/G > 0.5+
0.3(Cosθ-0.5)
REF Ch[1]
LN(Ratio) = .910
n.i. adj. = 0.000
Channel[8] Wm-2
40.0
30.0
20.0
10.0
0.0
-10.
-20.
-30.
-40.
Kipp CM10 810122
Kipp CM10 810166
90.
60.
30.
0.0
30.
60.
90.
morning
ZENITH ANGLE
evening
1000 Wm-2 MEASUREMENT ERROR VERSUS ZENITH ANGLE

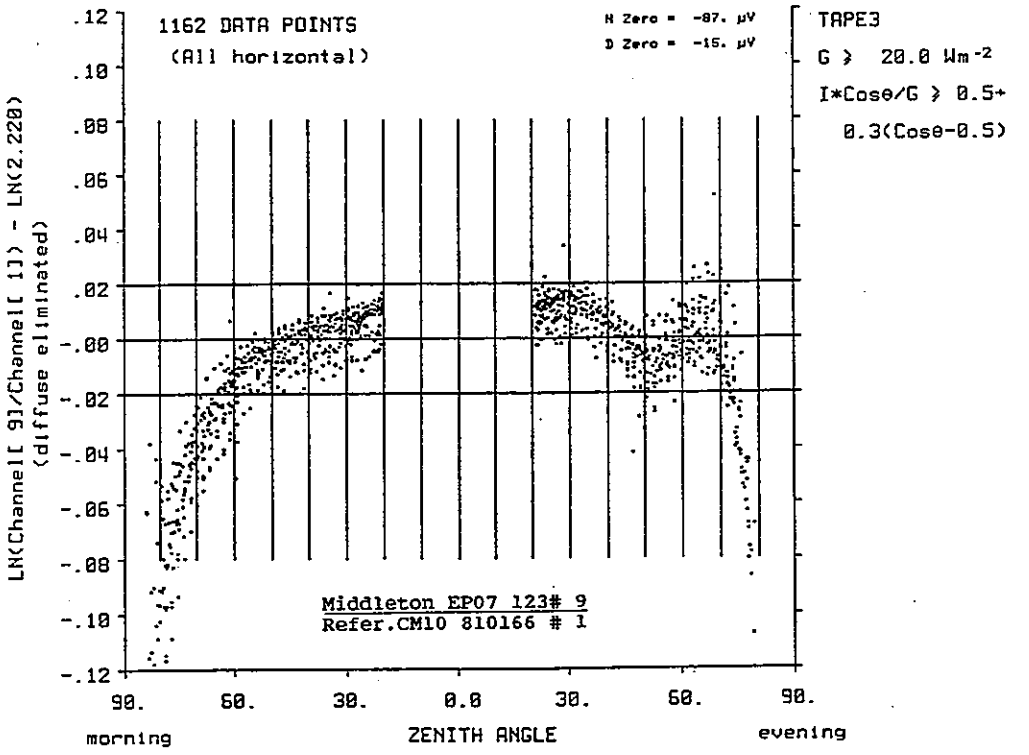

NORMALIZED LN(RATIOS) versus ZENITH ANGLE

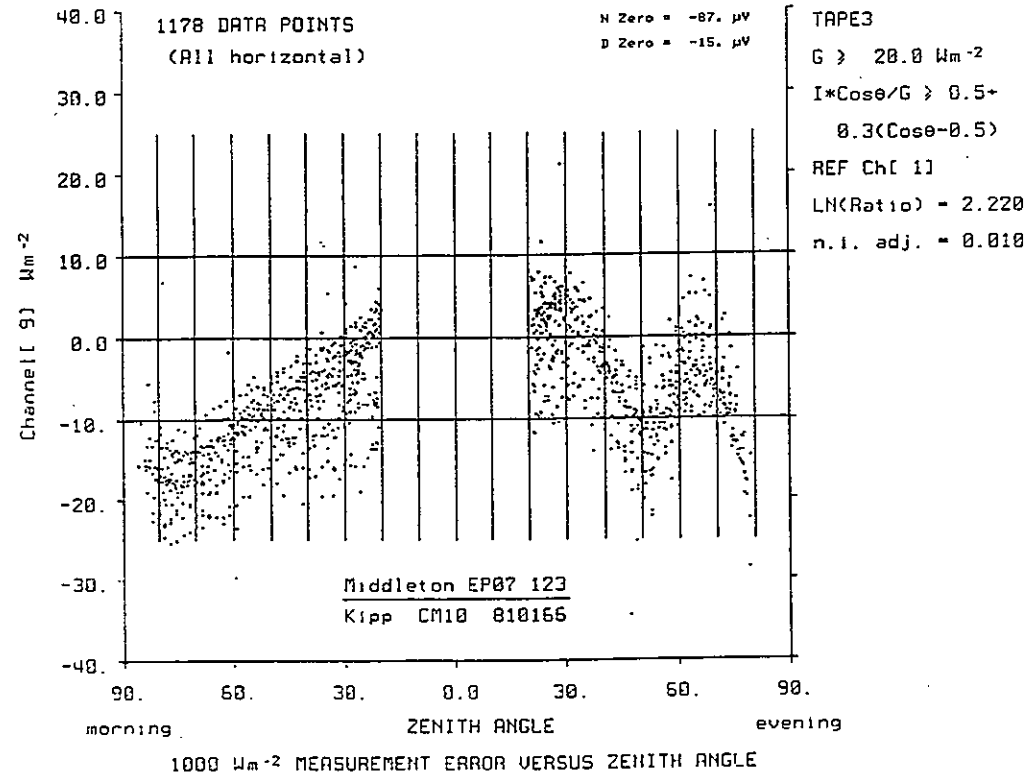

1000 Wm-2 MEASUREMENT ERROR VERSUS ZENITH ANGLE

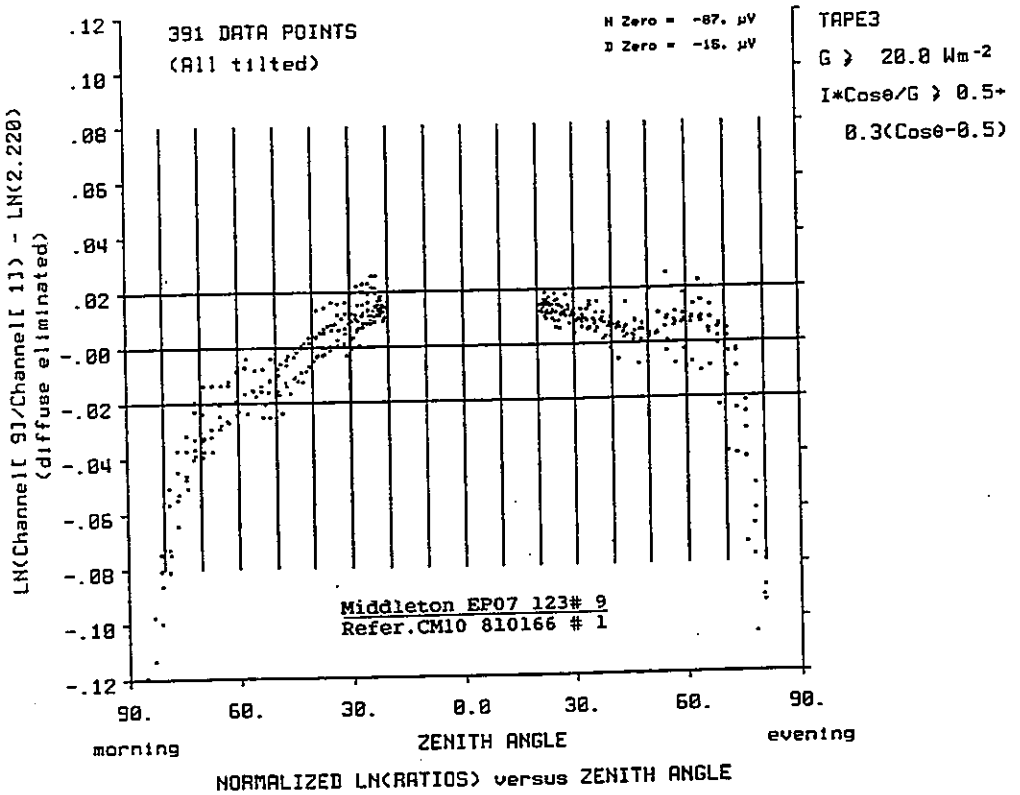

NORMALIZED LN(RATIOS) versus ZENITH ANGLE

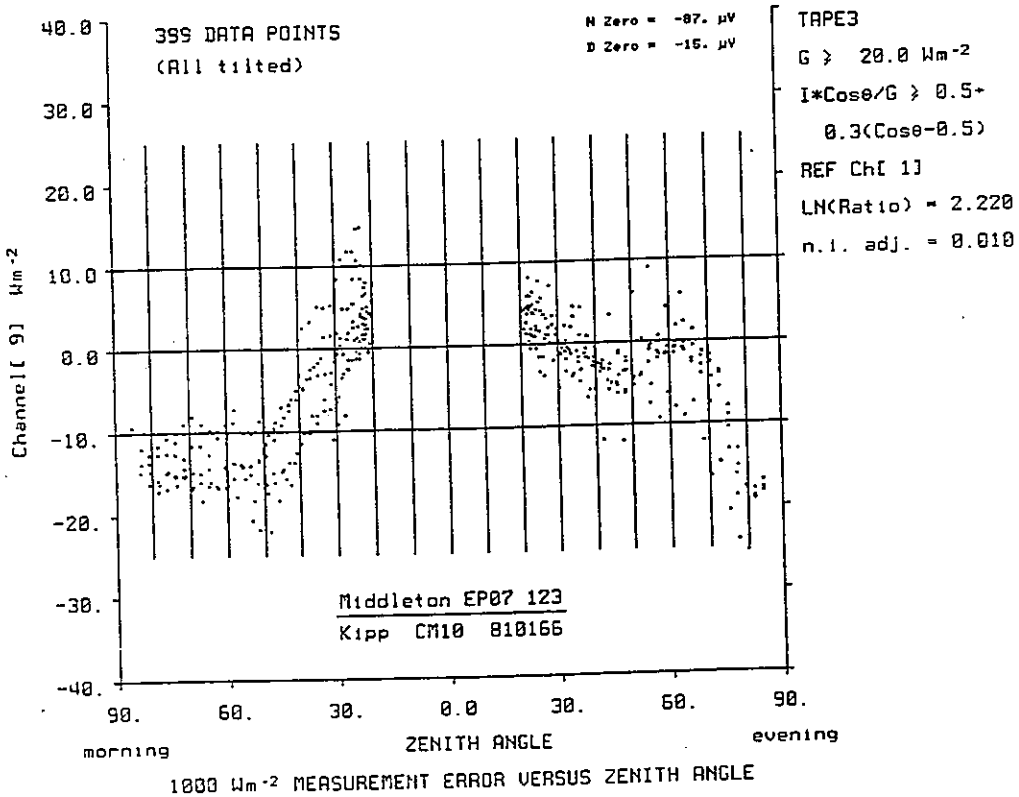

1000 Wm-2 MEASUREMENT ERROR VERSUS ZENITH ANGLE

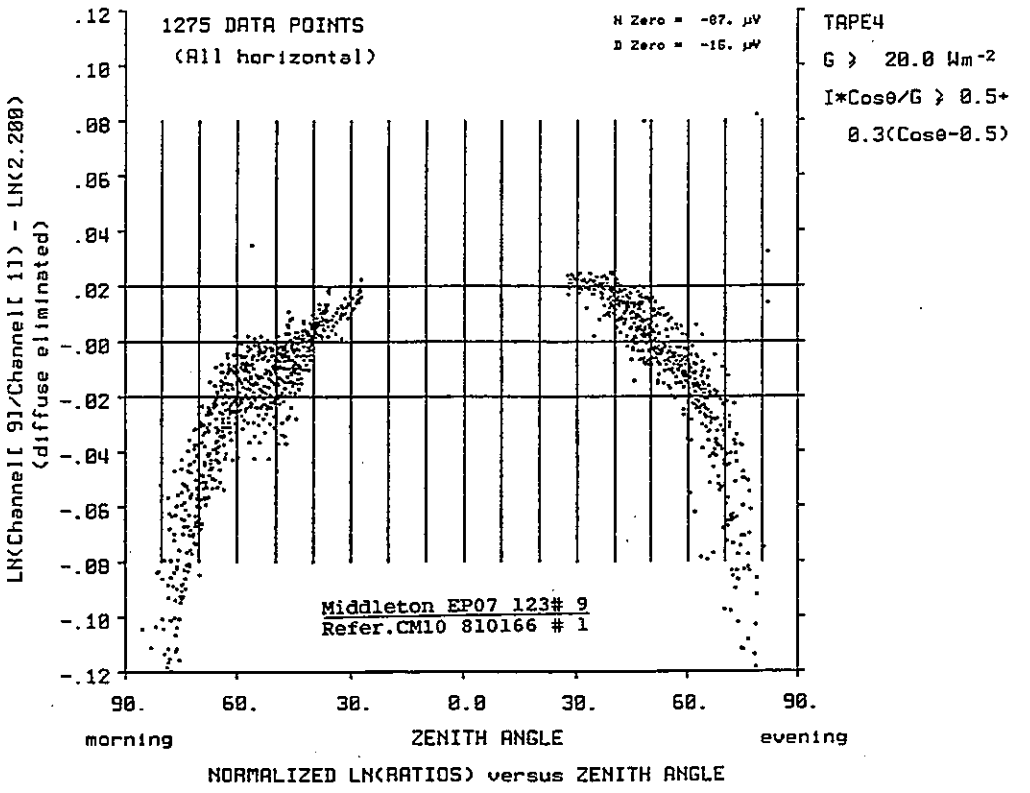

NORMALIZED LN(RATIOS) versus ZENITH ANGLE

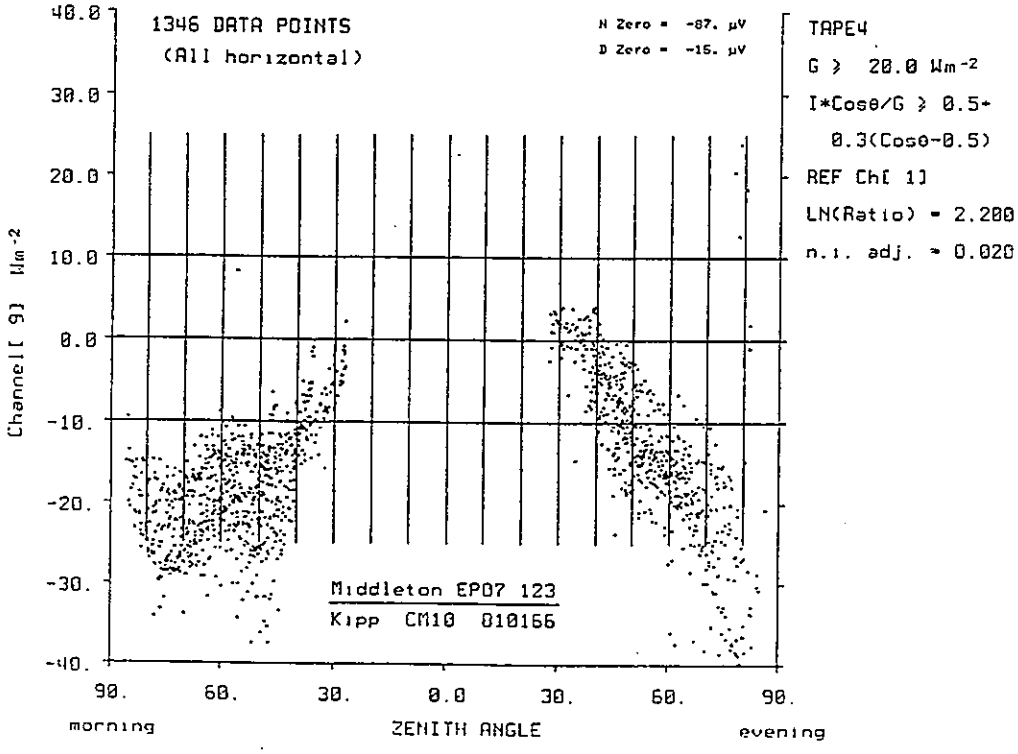

1000 Wm-2 MEASUREMENT ERROR VERSUS ZENITH ANGLE

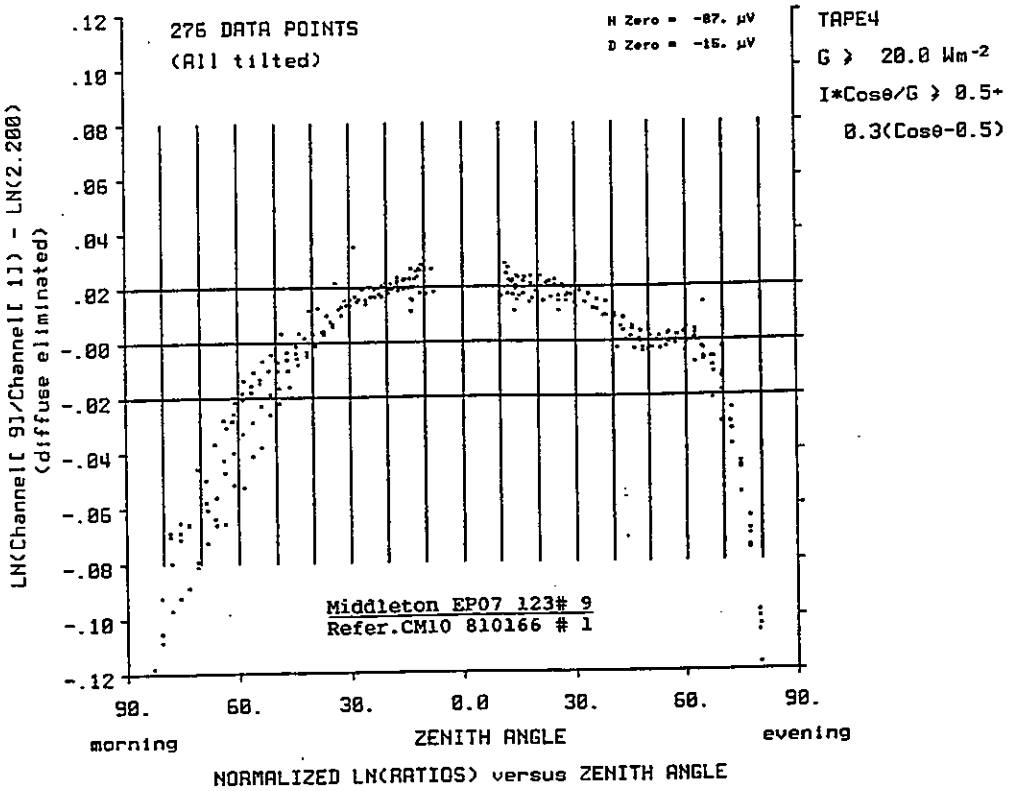
276 DATA POINTS
(All tilted)
N Zero = -87. µV
D Zero = -15. µV
TAPE4
G ≥ 20.0 Wm-2
I*Cosθ/G ≥ 0.5+
0.3(Cosθ-0.5)
LN(Channel[9]/Channel[1]) - LN(2.200)
(diffuse eliminated)
.12
.10
.08
.06
.04
.02
-.00
-.02
-.04
-.06
-.08
-.10
-.12
Middleton EP07 123# 9
Refer.CM10 810166 # 1
90.
60.
30.
0.0
30.
60.
90.
morning
ZENITH ANGLE
evening
NORMALIZED LN(RATIOS) versus ZENITH ANGLE

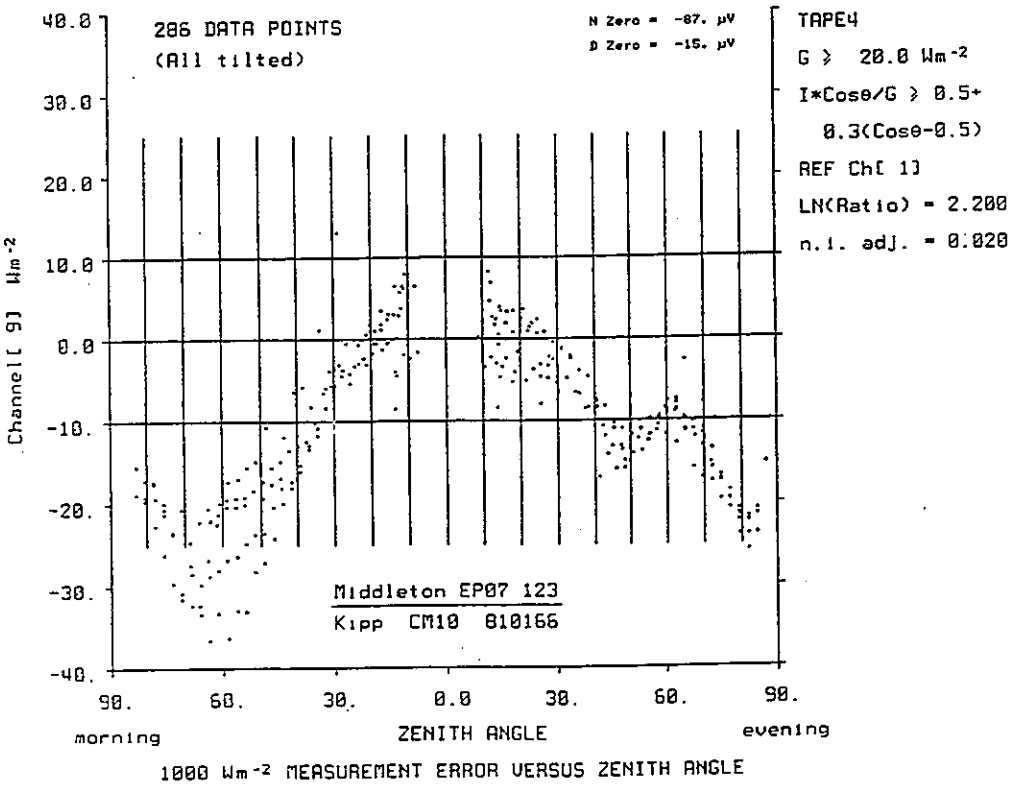
285 DATA POINTS
(All tilted)
N Zero = -87. µV
D Zero = -15. µV
TAPE4
G ≥ 20.0 Wm-2
I*Cosθ/G ≥ 0.5+
0.3(Cosθ-0.5)
REF Ch[1]
LN(Ratio) = 2.200
n.i. adj. = 0.020
Channel[9] Wm-2
40.0
30.0
20.0
10.0
0.0
-10.
-20.
-30.
-40.
Middleton EP07 123
Kipp CM10 810166
90.
60.
30.
0.0
30.
60.
90.
morning
ZENITH ANGLE
evening
1000 Wm-2 MEASUREMENT ERROR VERSUS ZENITH ANGLE

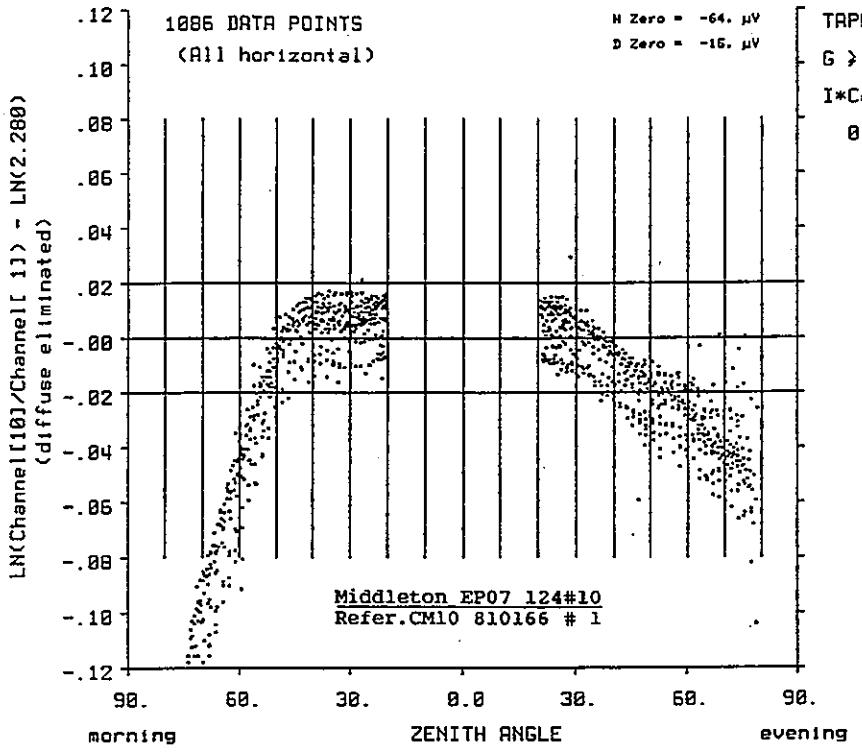

NORMALIZED LN(RATIOS) versus ZENITH ANGLE

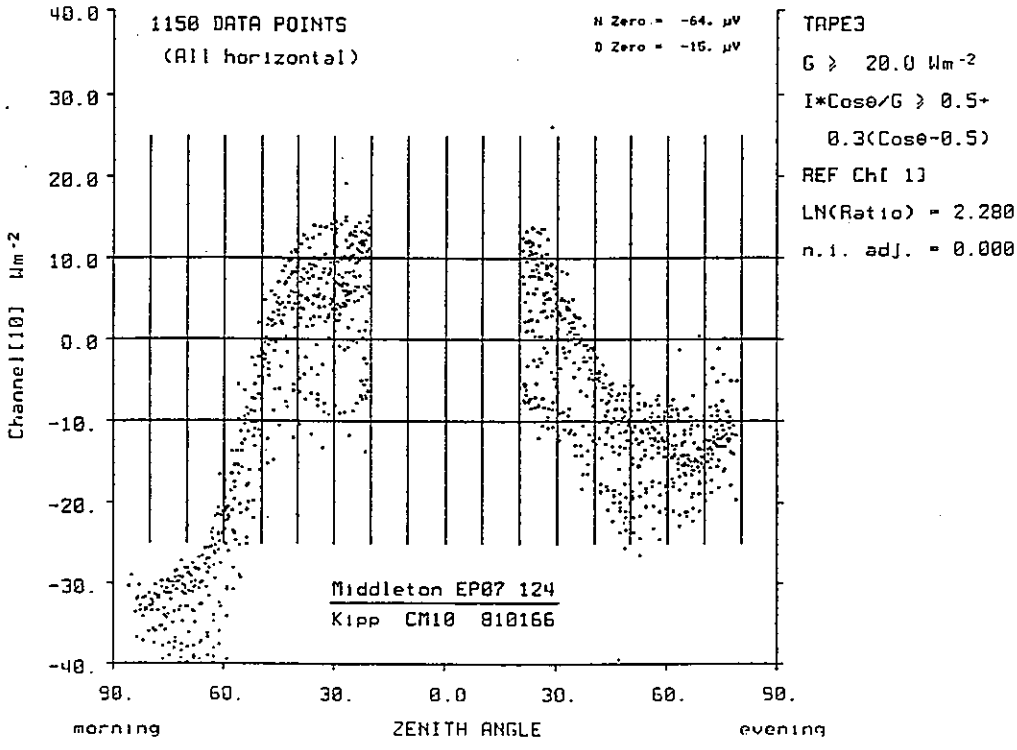

1000 Wm-2 MEASUREMENT ERROR VERSUS ZENITH ANGLE

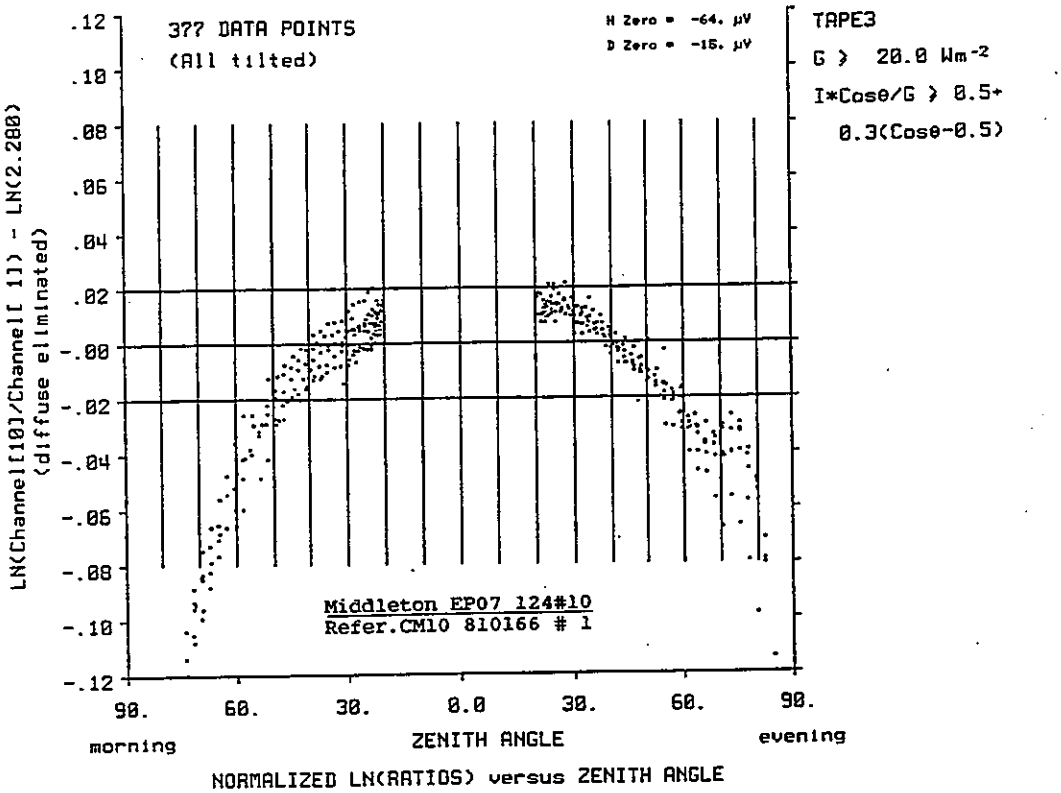
377 DATA POINTS
(All tilted)
H Zero = -64. µV
D Zero = -15. µV
TAPE3
G ≥ 20.0 Wm-2
I*Cosθ/G ≥ 0.5+
0.3(Cosθ-0.5)
LN(Channel[10]/Channel[1]) - LN(2.280)
(diffuse eliminated)
.12
.10
.08
.06
.04
.02
-.00
-.02
-.04
-.06
-.08
-.10
-.12
Middleton EP07 124#10
Refer.CM10 810166 # 1
90.
60.
30.
0.0
30.
60.
90.
morning
ZENITH ANGLE
evening
NORMALIZED LN(RATIOS) versus ZENITH ANGLE

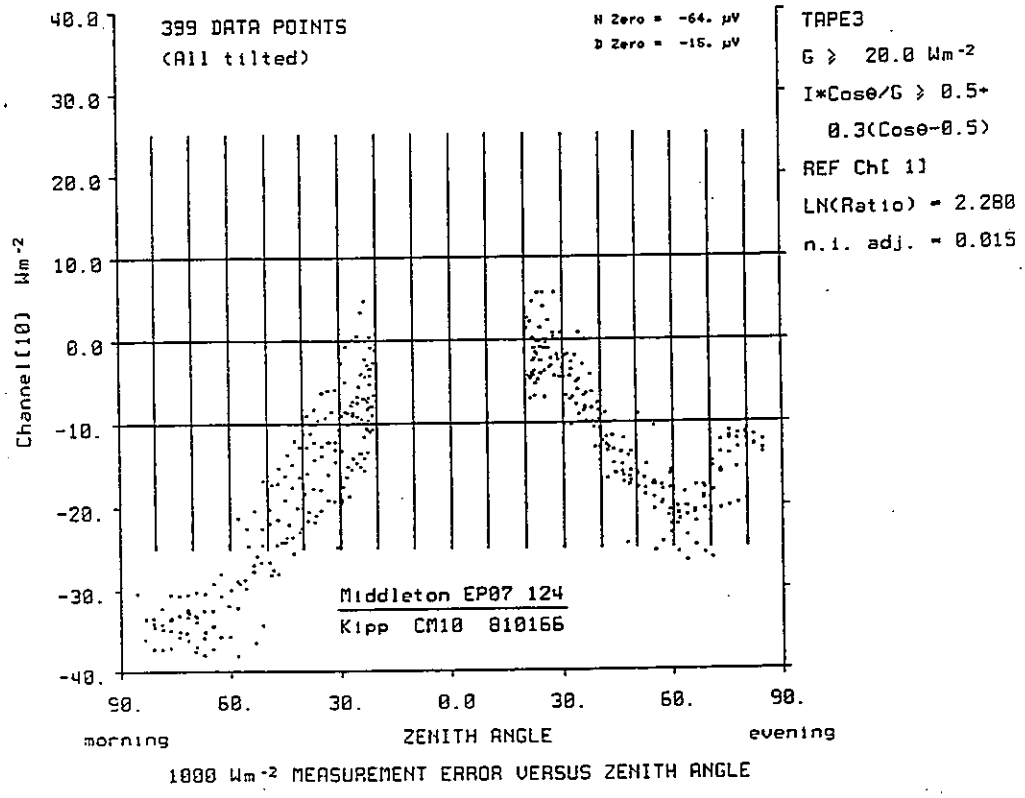
399 DATA POINTS
(All tilted)
H Zero = -64. µV
D Zero = -15. µV
TAPE3
G ≥ 20.0 Wm-2
I*Cosθ/G ≥ 0.5+
0.3(Cosθ-0.5)
REF Ch[1]
LN(Ratio) = 2.280
n.i. adj. = 0.015
Channel[10] Wm-2
40.0
30.0
20.0
10.0
0.0
-10.
-20.
-30.
-40.
Middleton EP07 124
Kipp CM10 810166
90.
60.
30.
0.0
30.
60.
90.
morning
ZENITH ANGLE
evening
1000 Wm-2 MEASUREMENT ERROR VERSUS ZENITH ANGLE

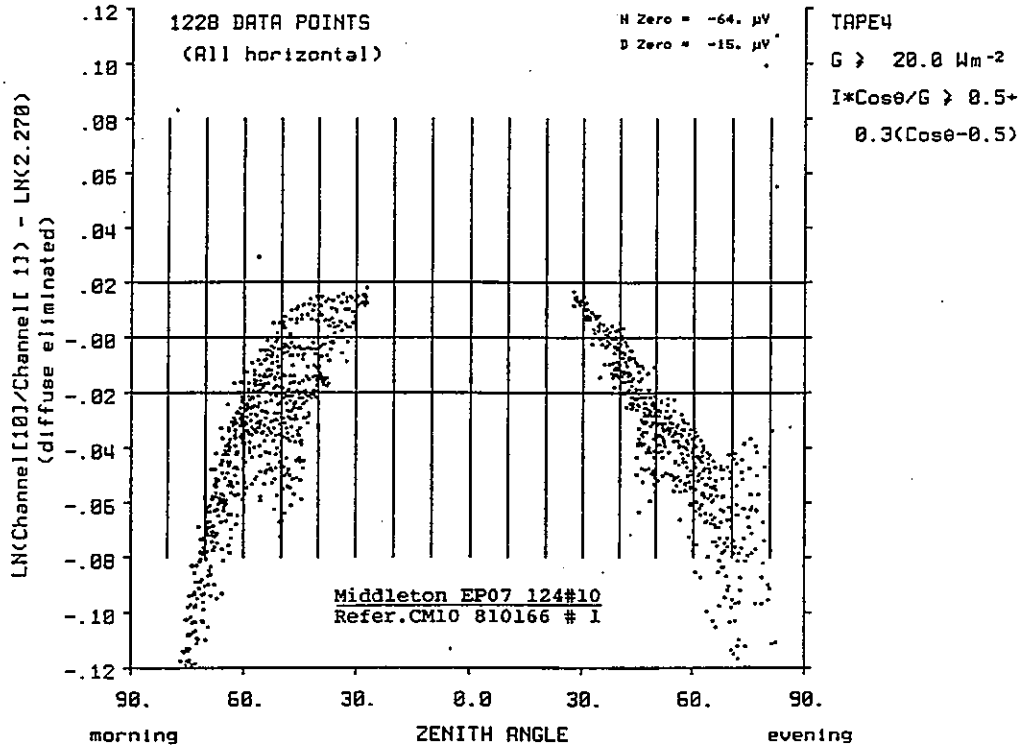

NORMALIZED LN(RATIOS) versus ZENITH ANGLE

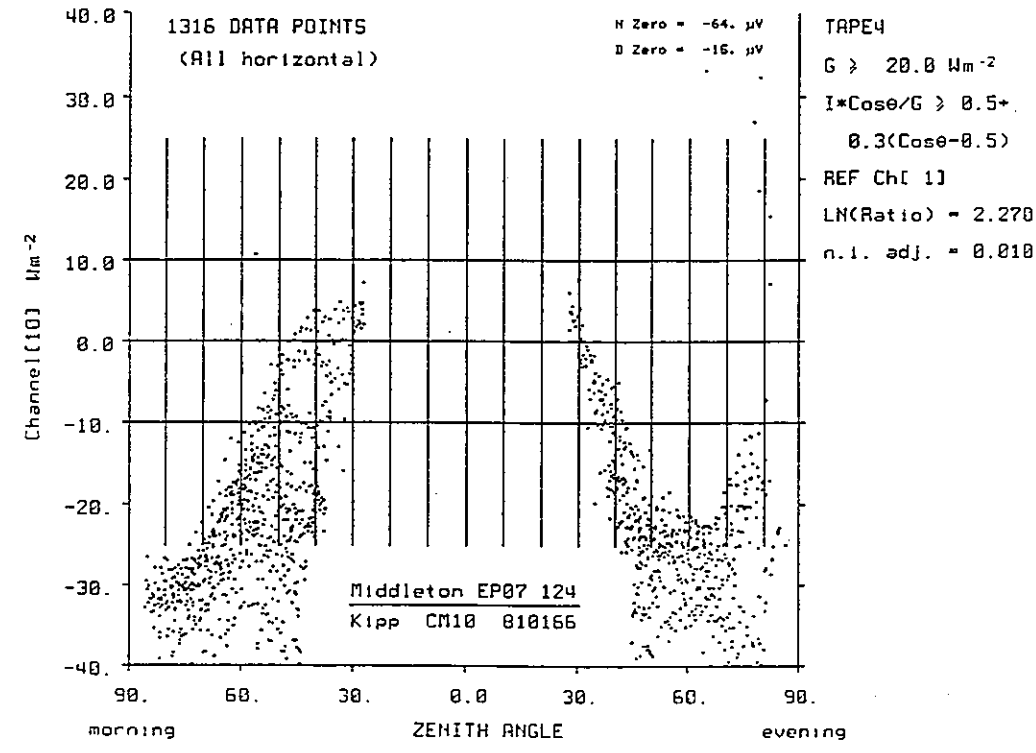

1000 Wm-2 MEASUREMENT ERROR VERSUS ZENITH ANGLE

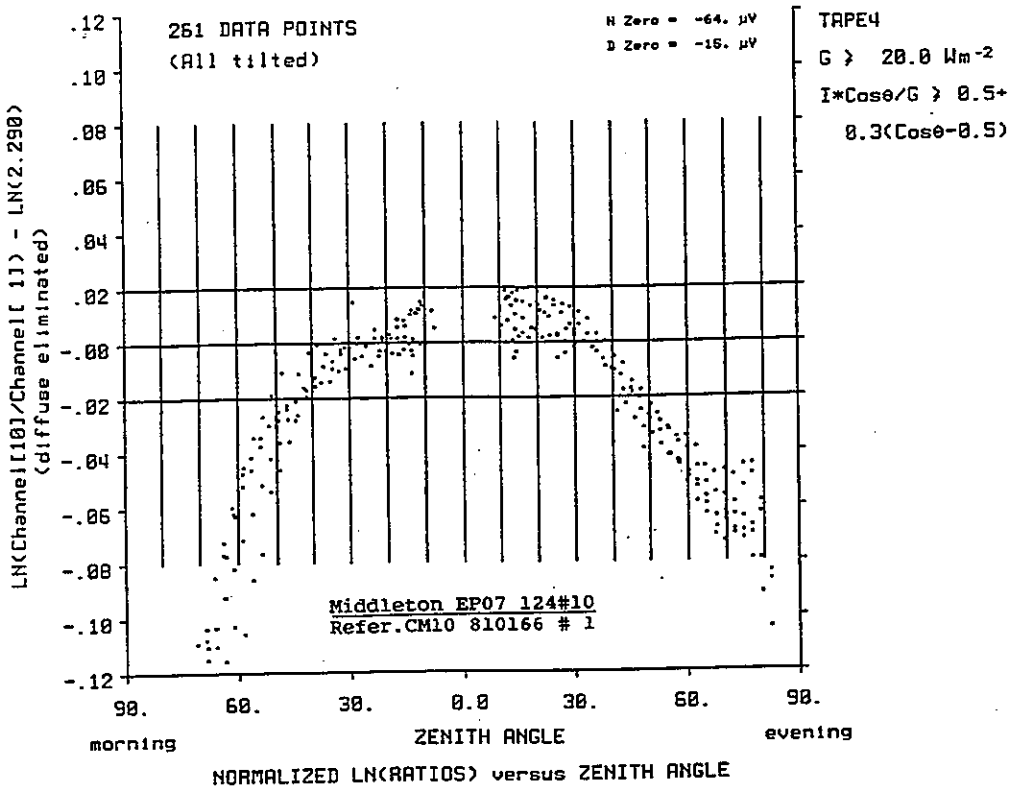
261 DATA POINTS
(All tilted)
N Zero = -64. μV
D Zero = -15. μV
TAPE4
G ≥ 20.0 Wm-2
I*Cosθ/G ≥ 0.5+
0.3(Cosθ-0.5)
LN(Channel[10]/Channel[1]) - LN(2.290)
(diffuse eliminated)
.12
.10
.08
.06
.04
.02
-.00
-.02
-.04
-.06
-.08
-.10
-.12
Middleton EP07 124#10
Refer.CM10 810166 # 1
90.
60.
30.
0.0
30.
60.
90.
morning
ZENITH ANGLE
evening
NORMALIZED LN(RATIOS) versus ZENITH ANGLE

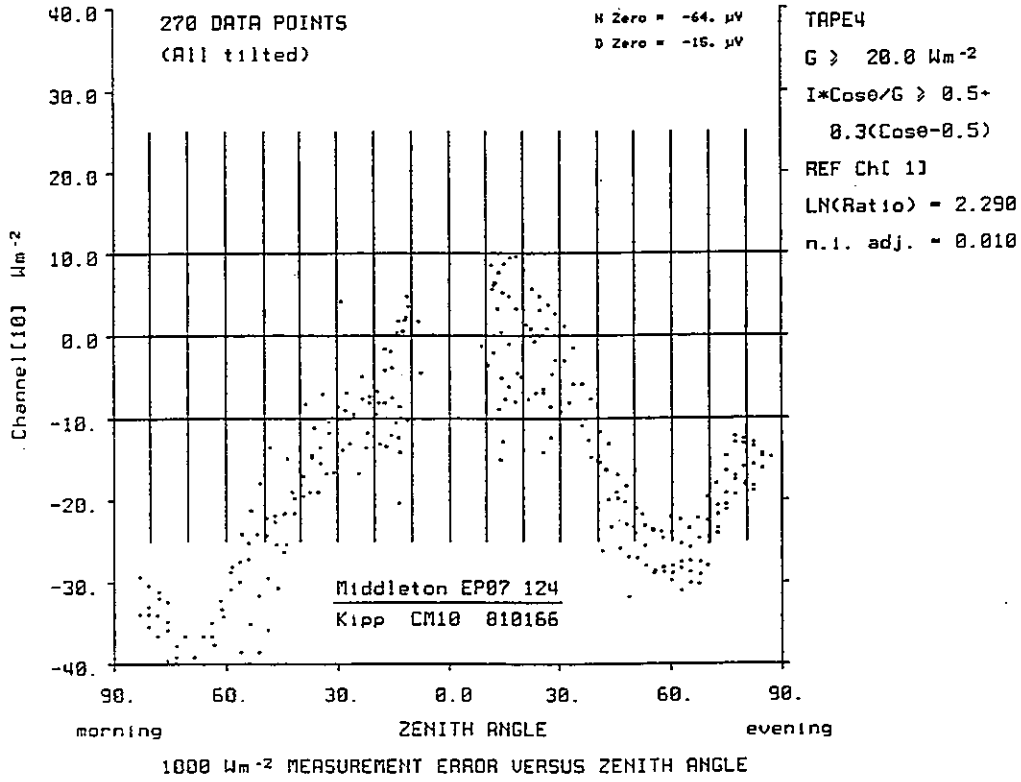
270 DATA POINTS
(All tilted)
N Zero = -64. μV
D Zero = -15. μV
TAPE4
G ≥ 20.0 Wm-2
I*Cosθ/G ≥ 0.5+
0.3(Cosθ-0.5)
REF Ch[1]
LN(Ratio) = 2.290
n.i. adj. = 0.010
Channel[10] Wm-2
40.0
30.0
20.0
10.0
0.0
-10.
-20.
-30.
-40.
Middleton EP07 124
Kipp CM10 810166
90.
60.
30.
0.0
30.
60.
90.
morning
ZENITH ANGLE
evening
1000 Wm-2 MEASUREMENT ERROR VERSUS ZENITH ANGLE

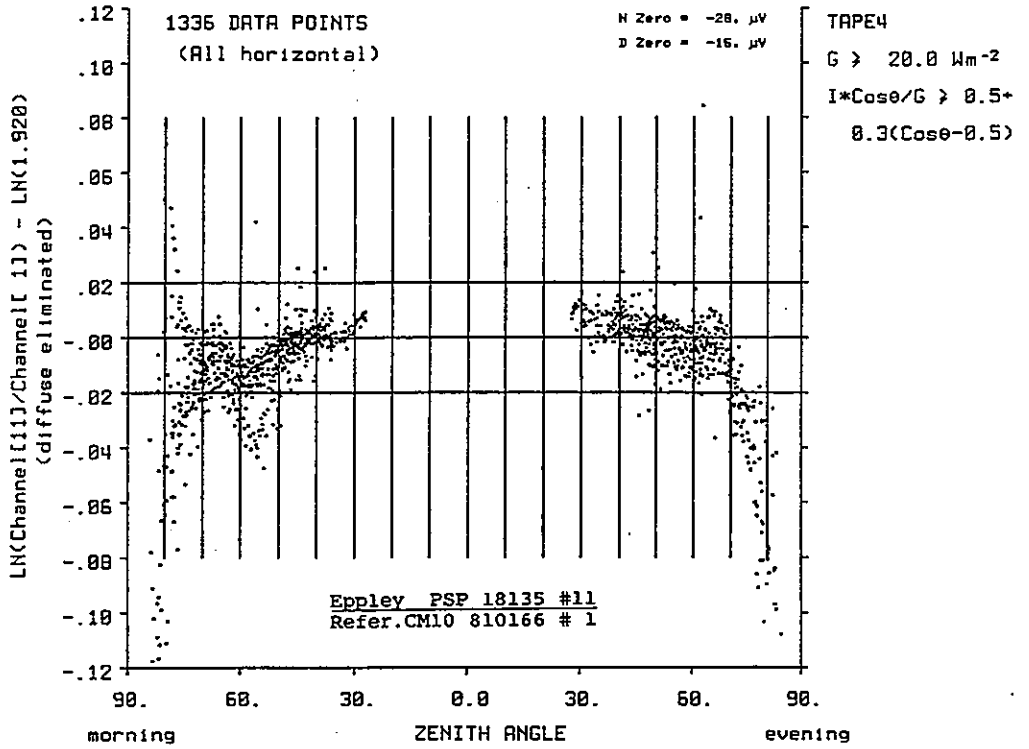

NORMALIZED LN(RATIOS) versus ZENITH ANGLE

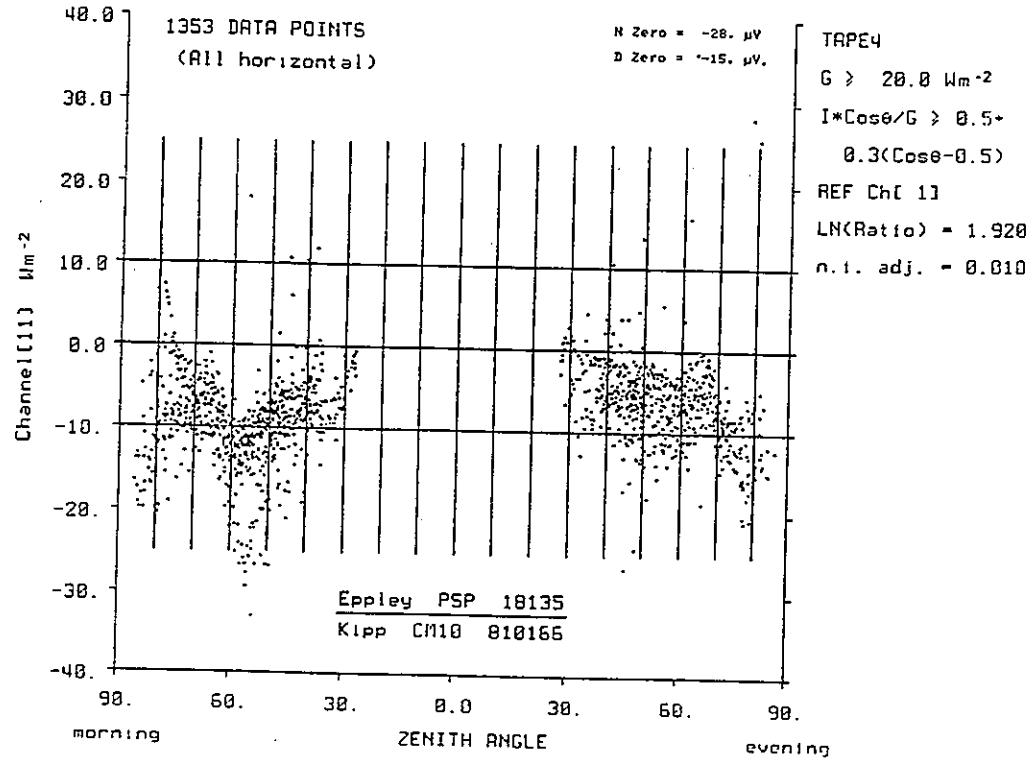

1000 Wm-2 MEASUREMENT ERROR VERSUS ZENITH ANGLE

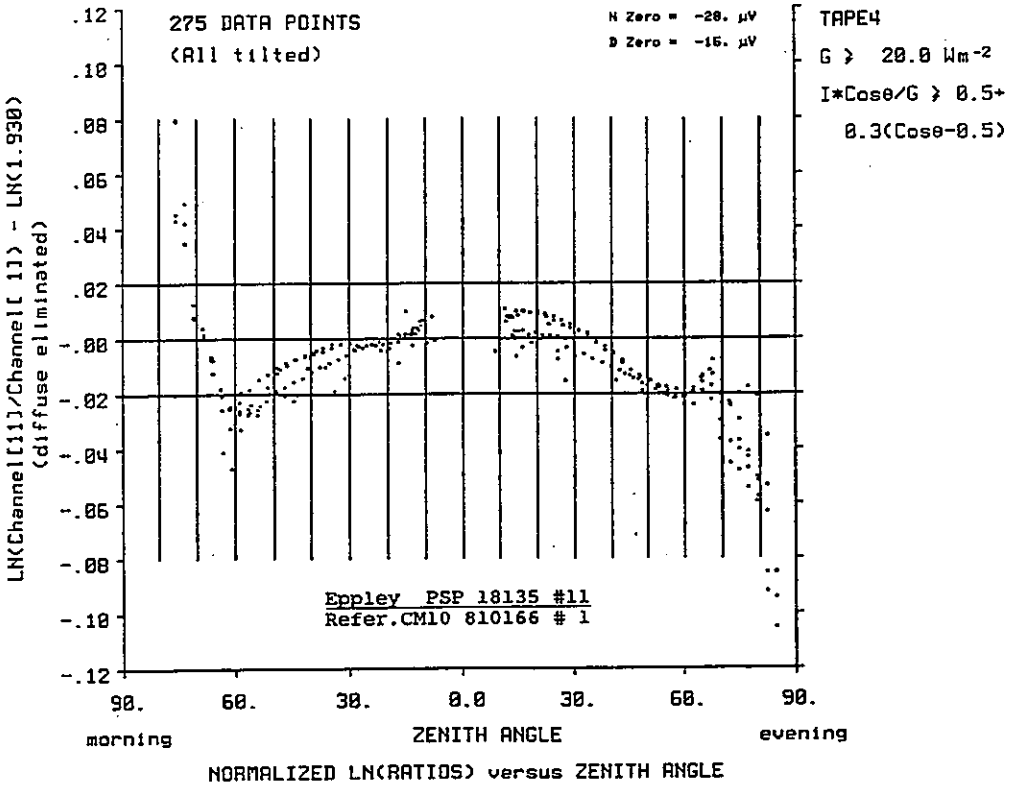
275 DATA POINTS
(All tilted)
N Zero = -20. µV
D Zero = -16. µV
TAPE4
G ≥ 20.0 Wm-2
I*Cosθ/G ≥ 0.5+
0.3(Cosθ-0.5)
LN(Channel[11]/Channel[11) - LN(1.930)
(diffuse eliminated)
.12
.10
.08
.06
.04
.02
-.00
-.02
-.04
-.06
-.08
-.10
-.12
Eppley PSP 18135 #11
Refer.CM10 810166 # 1
90.
60.
30.
0.0
30.
60.
90.
morning
ZENITH ANGLE
evening
NORMALIZED LN(RATIOS) versus ZENITH ANGLE

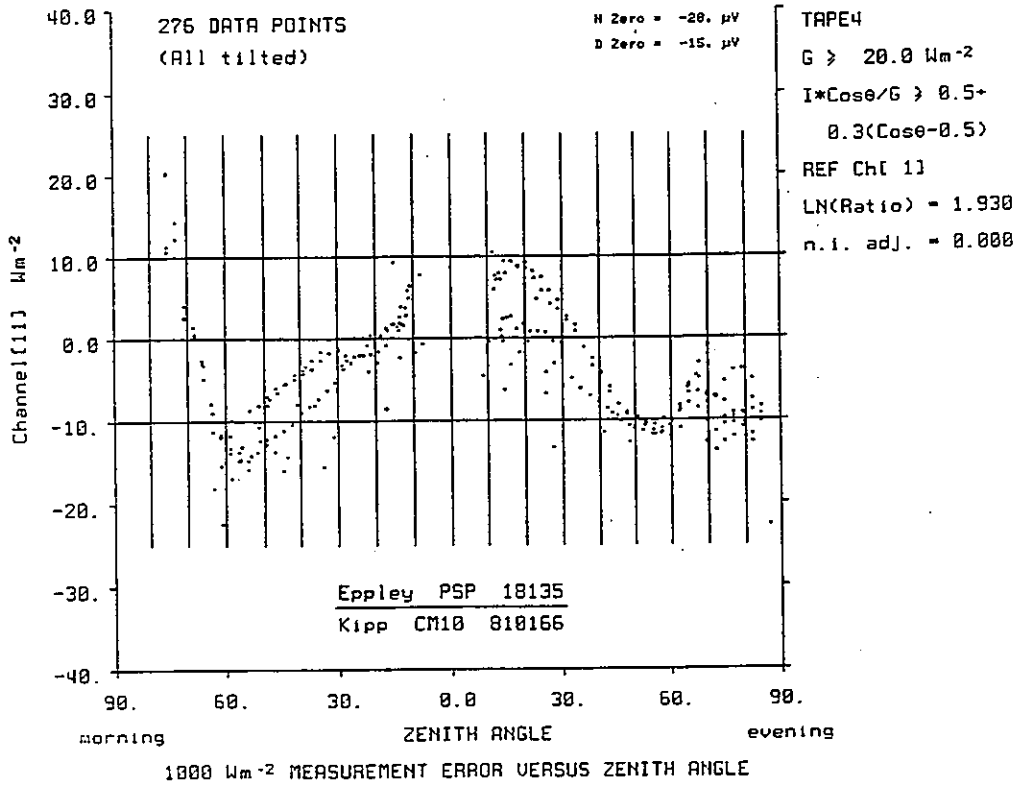
276 DATA POINTS
(All tilted)
N Zero = -20. µV
D Zero = -15. µV
TAPE4
G ≥ 20.0 Wm-2
I*Cosθ/G ≥ 0.5+
0.3(Cosθ-0.5)
REF Ch[1]
LN(Ratio) = 1.930
n.i. adj. = 0.000
Channel[11] Wm-2
40.0
30.0
20.0
10.0
0.0
-10.
-20.
-30.
-40.
Eppley PSP 18135
Kipp CM10 810166
90.
60.
30.
0.0
30.
60.
90.
morning
ZENITH ANGLE
evening
1000 Wm-2 MEASUREMENT ERROR VERSUS ZENITH ANGLE

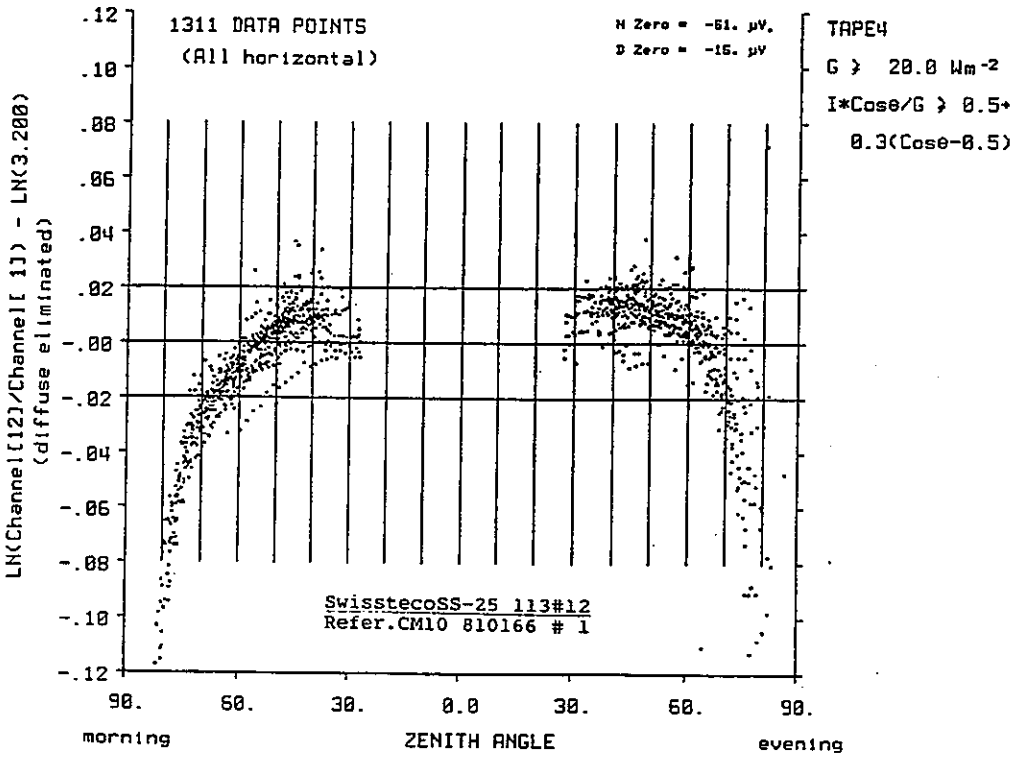

NORMALIZED LN(RATIOS) versus ZENITH ANGLE

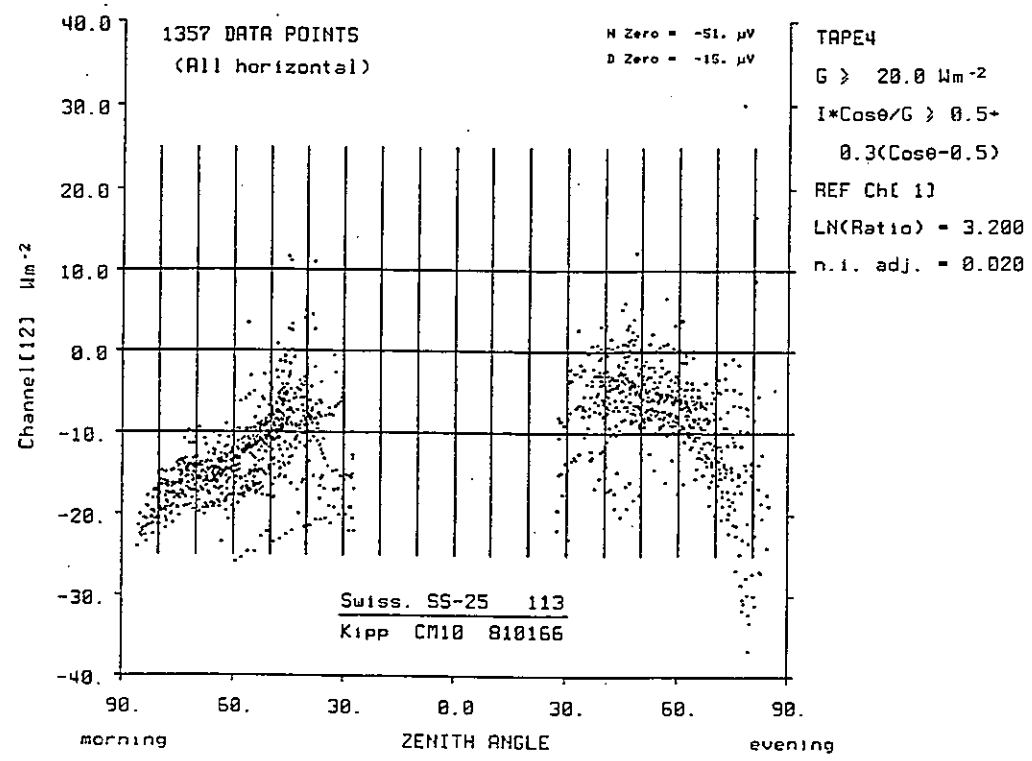

1000 Wm-2 MEASUREMENT ERROR VERSUS ZENITH ANGLE

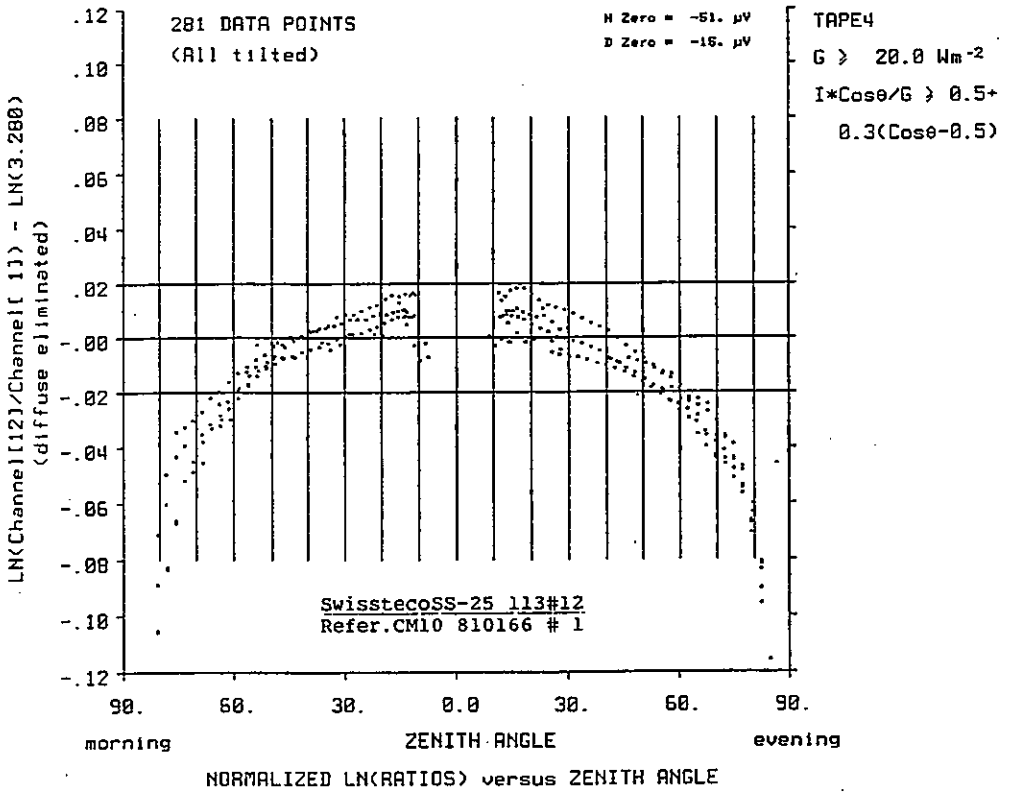

NORMALIZED LN(RATIOS) versus ZENITH ANGLE

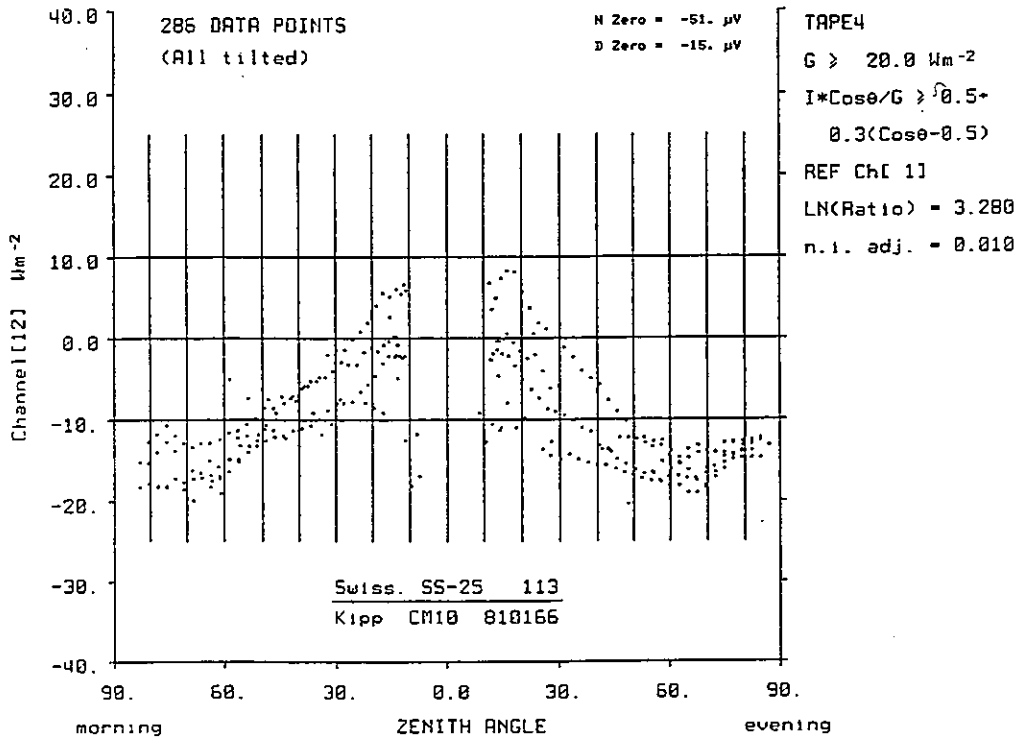

1000 Wm-2 MEASUREMENT ERROR VERSUS ZENITH ANGLE

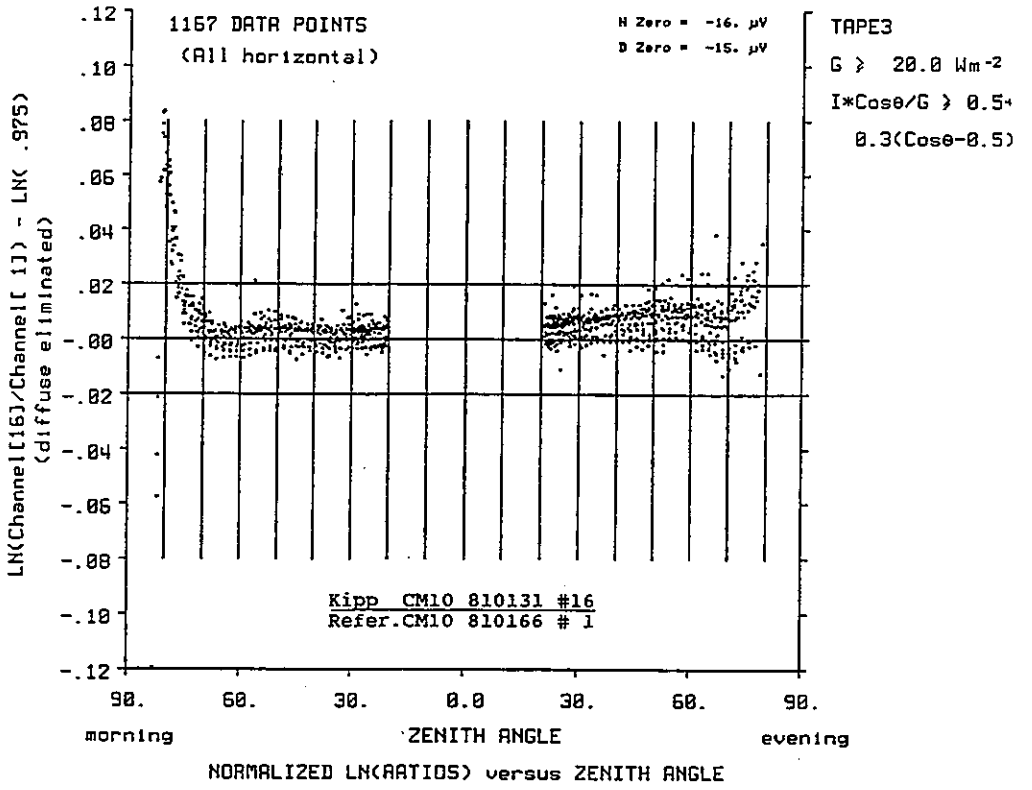

NORMALIZED LN(RATIOS) versus ZENITH ANGLE

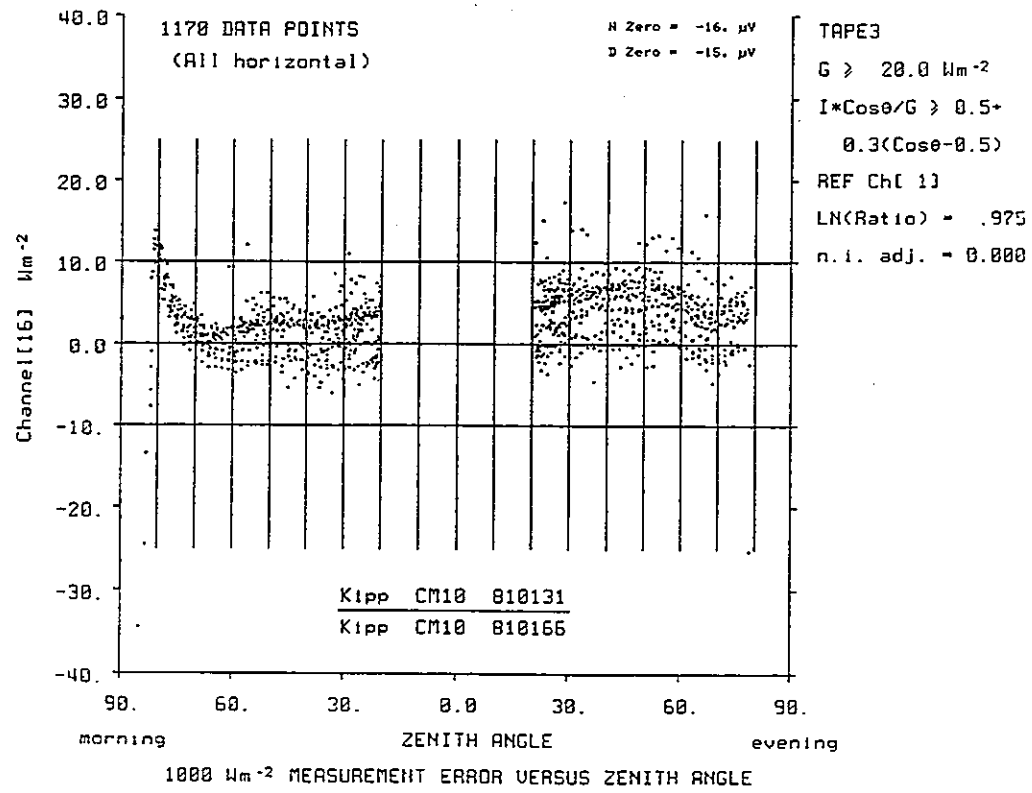

1000 Wm-2 MEASUREMENT ERROR VERSUS ZENITH ANGLE

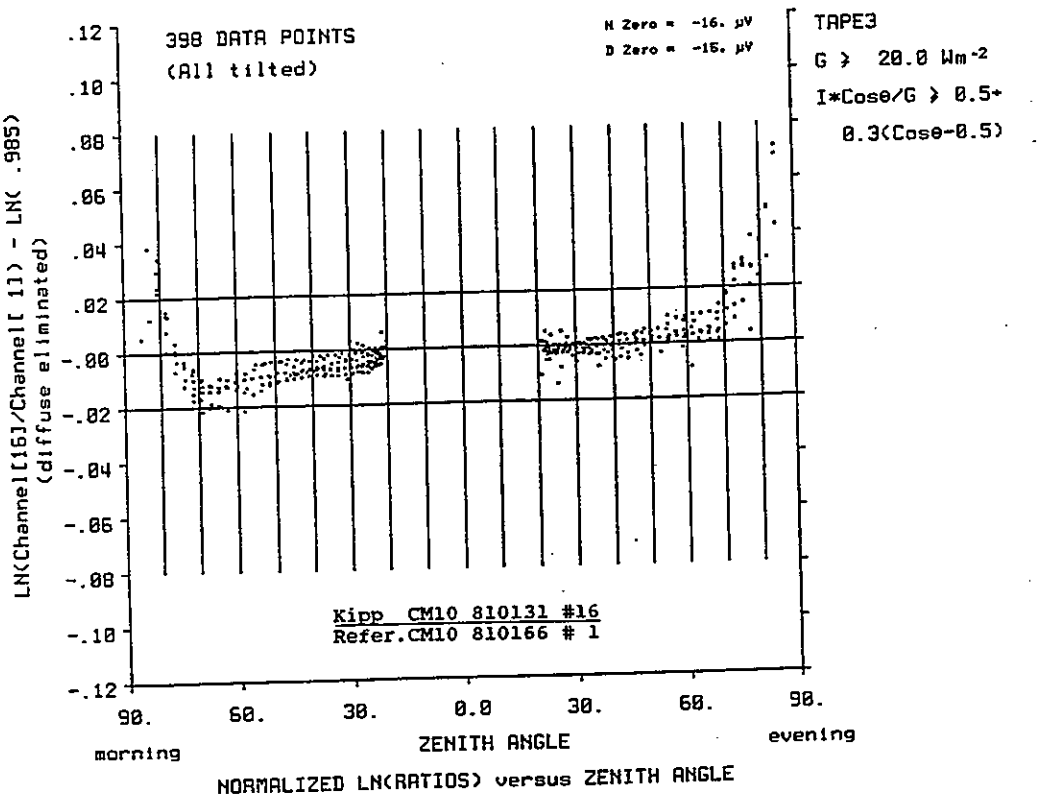

NORMALIZED LN(RATIOS) versus ZENITH ANGLE

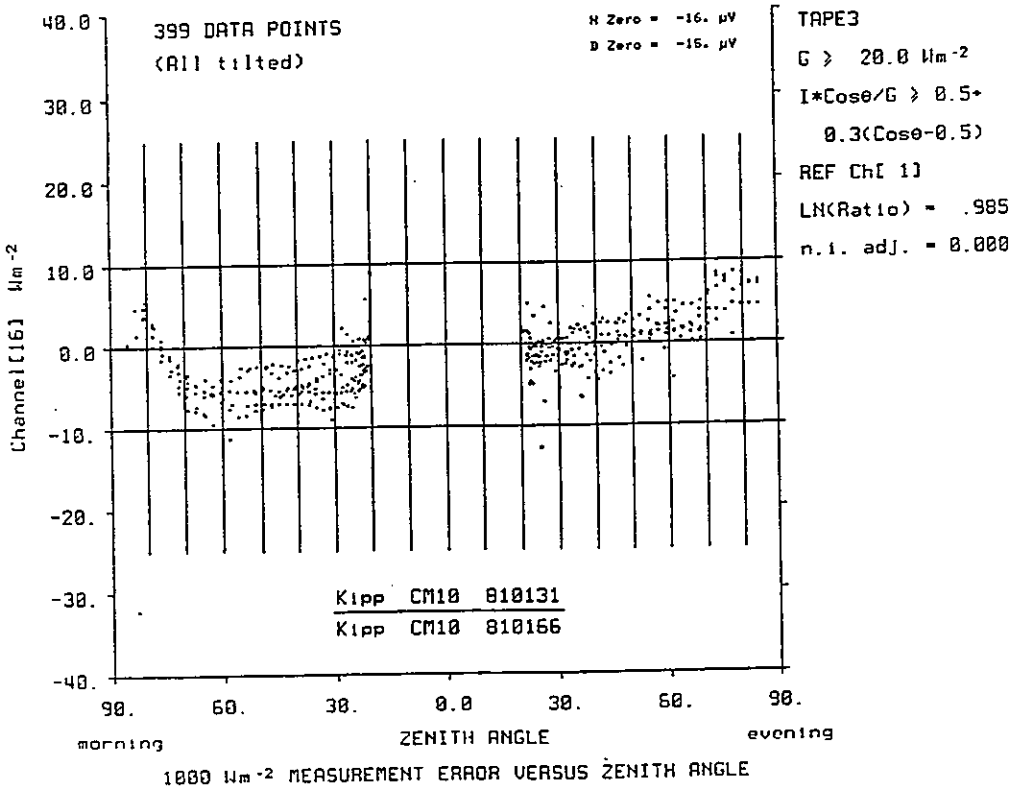

1000 Wm-2 MEASUREMENT ERROR VERSUS ZENITH ANGLE

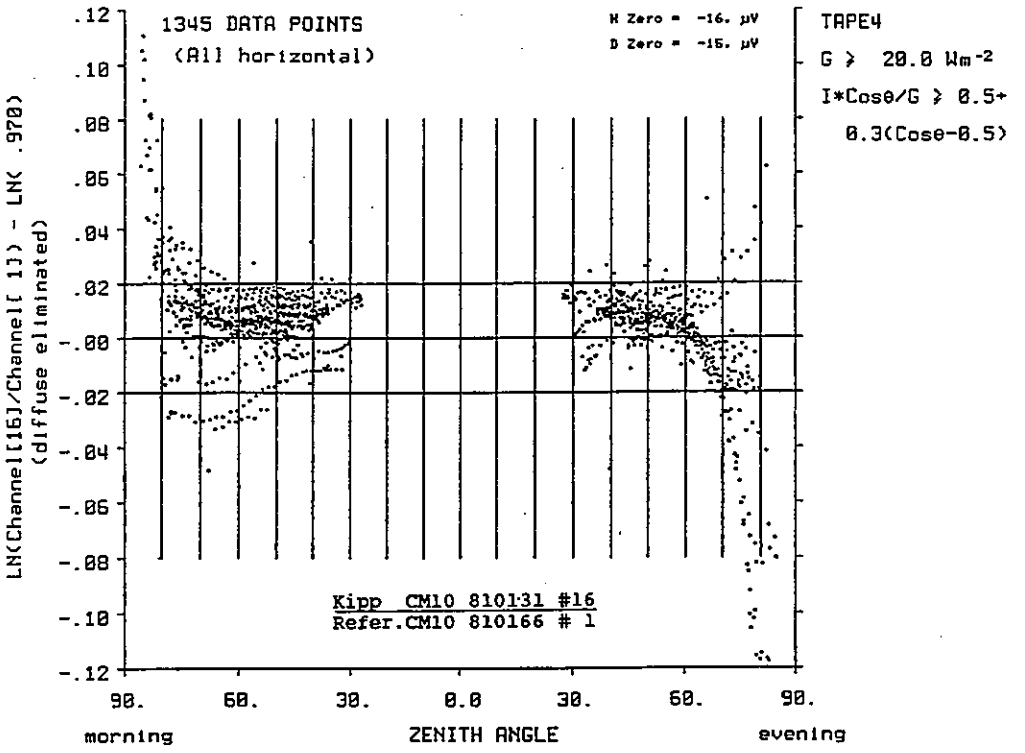

NORMALIZED LN(RATIOS) versus ZENITH ANGLE

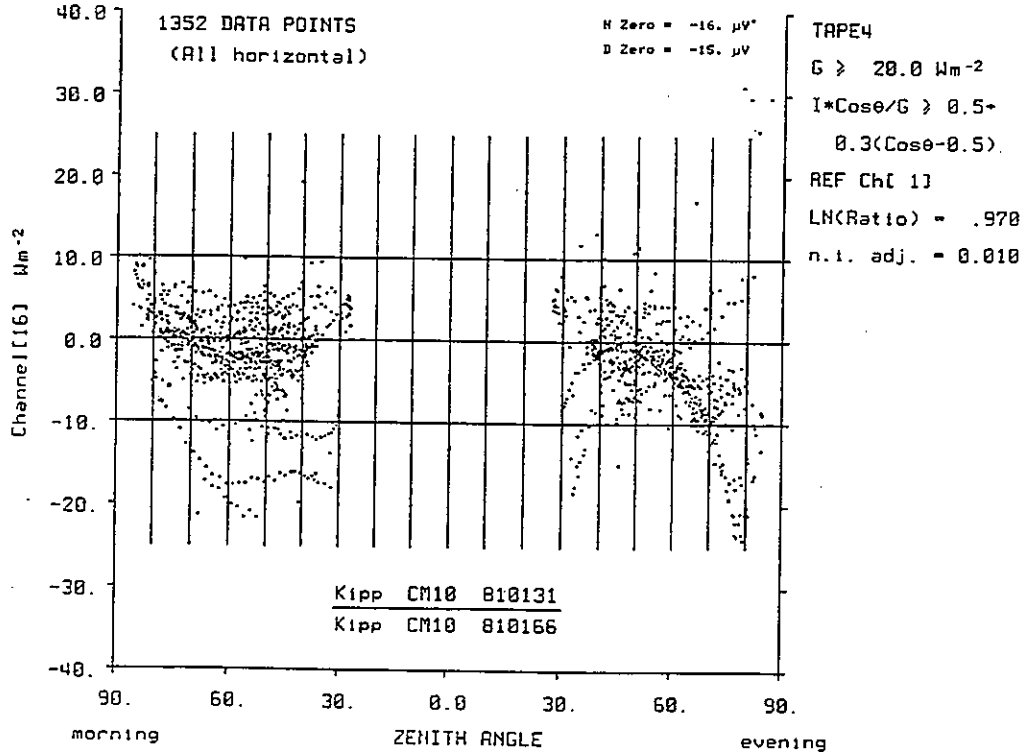

1000 Wm-2 MEASUREMENT ERROR VERSUS ZENITH ANGLE

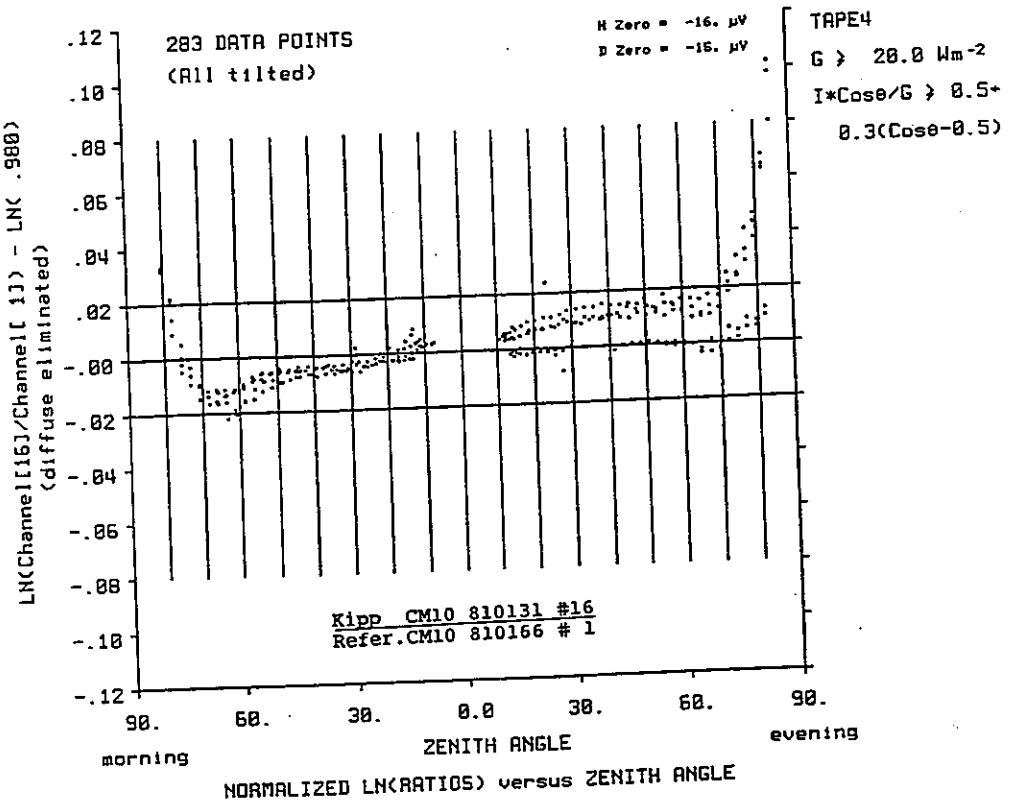
283 DATA POINTS
(All tilted)
N Zero = -16. μV
D Zero = -15. μV
TAPE4
G > 20.0 Wm-2
I*Cose/G > 0.5+
0.3(Cose-0.5)
LN(Channel[16]/Channel[1]) - LN(.980)
(diffuse eliminated)
.12
.10
.08
.06
.04
.02
-.00
-.02
-.04
-.06
-.08
-.10
-.12
Kipp CM10 810131 #16
Refer.CM10 810166 # 1
90.
60.
30.
0.0
30.
60.
90.
morning
ZENITH ANGLE
evening
NORMALIZED LN(RATIOS) versus ZENITH ANGLE

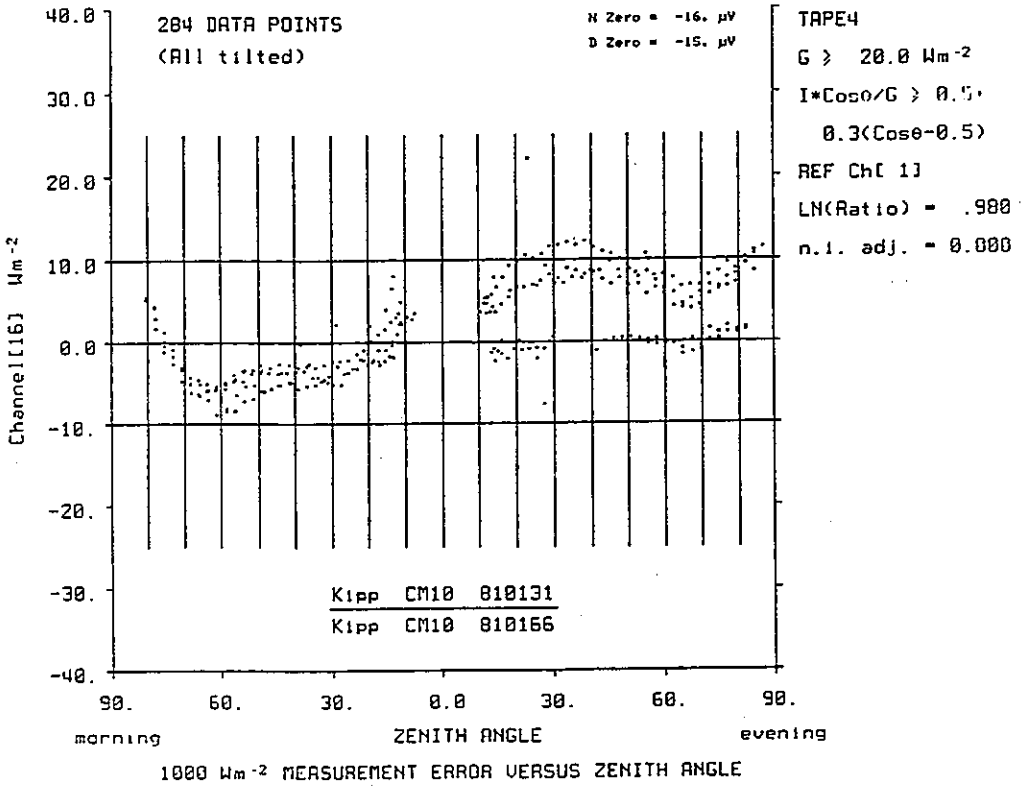
284 DATA POINTS
(All tilted)
N Zero = -16. μV
D Zero = -15. μV
TAPE4
G > 20.0 Wm-2
I*Cose/G > 0.5+
0.3(Cose-0.5)
REF Ch[1]
LN(Ratio) = .980
n.i. adj. = 0.000
Channel[16] Wm-2
40.0
30.0
20.0
10.0
0.0
-10.
-20.
-30.
-40.
Kipp CM10 810131
Kipp CM10 810166
90.
60.
30.
0.0
30.
60.
90.
morning
ZENITH ANGLE
evening
1000 Wm-2 MEASUREMENT ERROR VERSUS ZENITH ANGLE

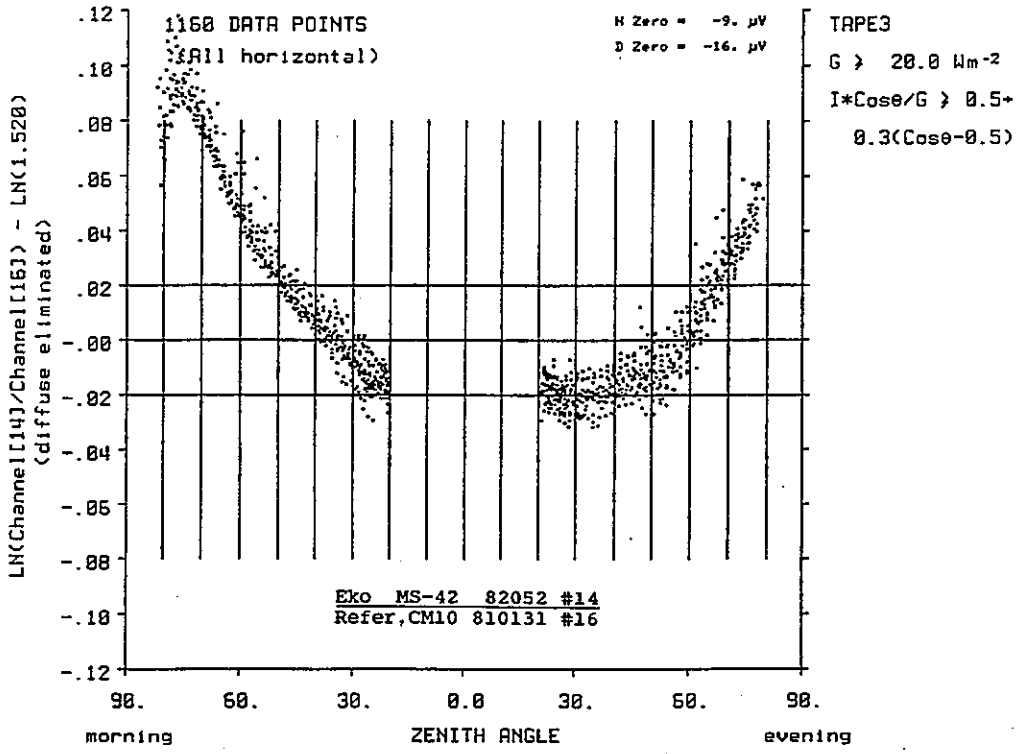

NORMALIZED LN(RATIOS) versus ZENITH ANGLE

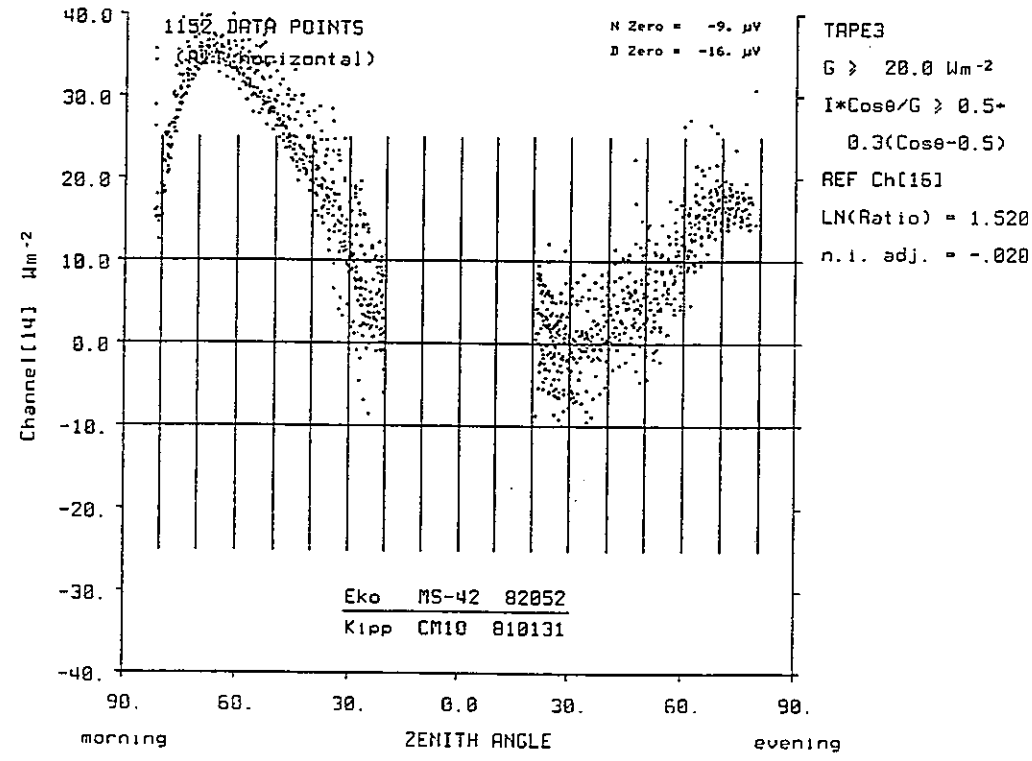

1000 Wm-2 MEASUREMENT ERROR VERSUS ZENITH ANGLE

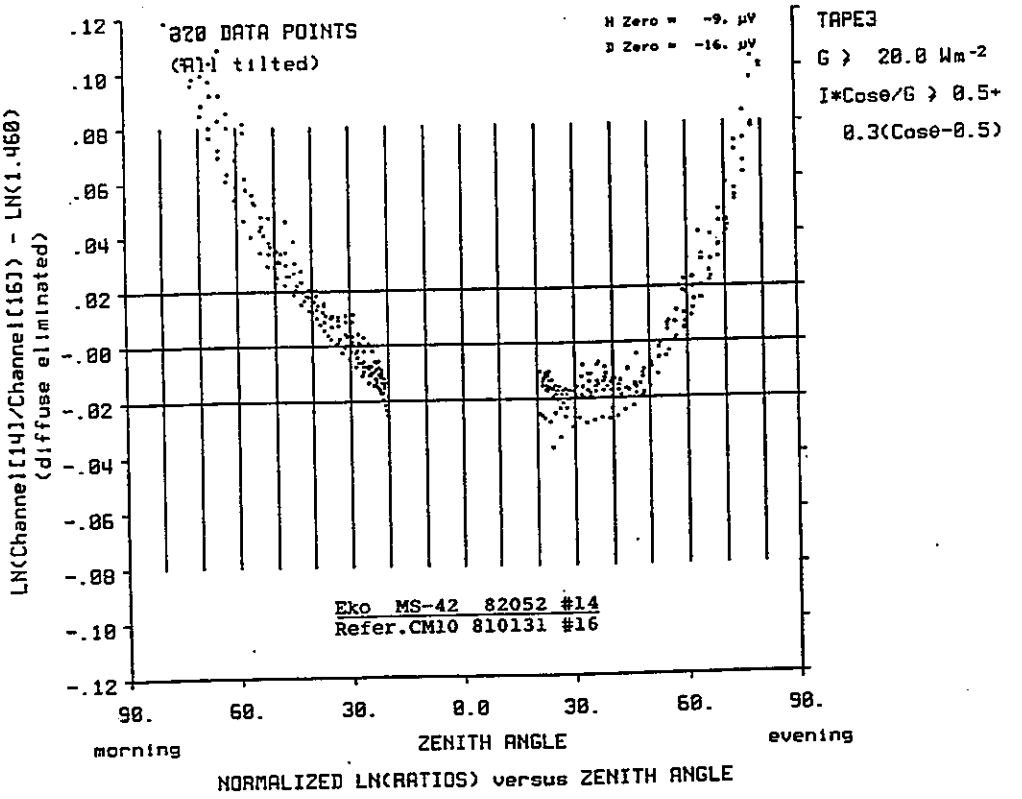
820 DATA POINTS
(All tilted)
N Zero = -9. μV
D Zero = -16. μV
TAPE3
G > 20.0 Wm-2
I*Cosθ/G > 0.5+
0.3(Cosθ-0.5)
LN(Channel[14]/Channel[16]) - LN(1.460)
(diffuse eliminated)
.12
.10
.08
.06
.04
.02
-.00
-.02
-.04
-.06
-.08
-.10
-.12
Eko MS-42 82052 #14
Refer.CM10 810131 #16
90.
60.
30.
0.0
30.
60.
90.
morning
ZENITH ANGLE
evening
NORMALIZED LN(RATIOS) versus ZENITH ANGLE

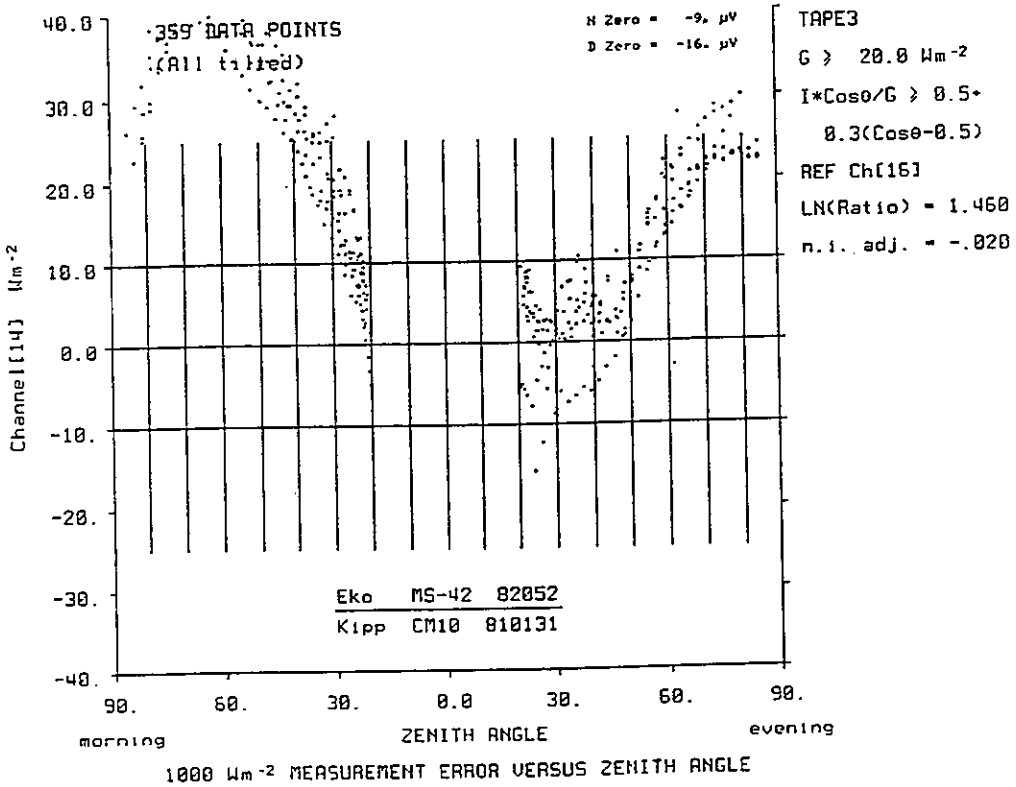
359 DATA POINTS
(All tilted)
N Zero = -9. μV
D Zero = -16. μV
TAPE3
G > 20.0 Wm-2
I*Cosθ/G > 0.5+
0.3(Cosθ-0.5)
REF Ch[16]
LN(Ratio) = 1.460
n.i. adj. = -.020
Channel[14] Wm-2
40.0
30.0
20.0
10.0
0.0
-10.
-20.
-30.
-40.
Eko MS-42 82052
Kipp CM10 810131
90.
60.
30.
0.0
30.
60.
90.
morning
ZENITH ANGLE
evening
1000 Wm-2 MEASUREMENT ERROR VERSUS ZENITH ANGLE

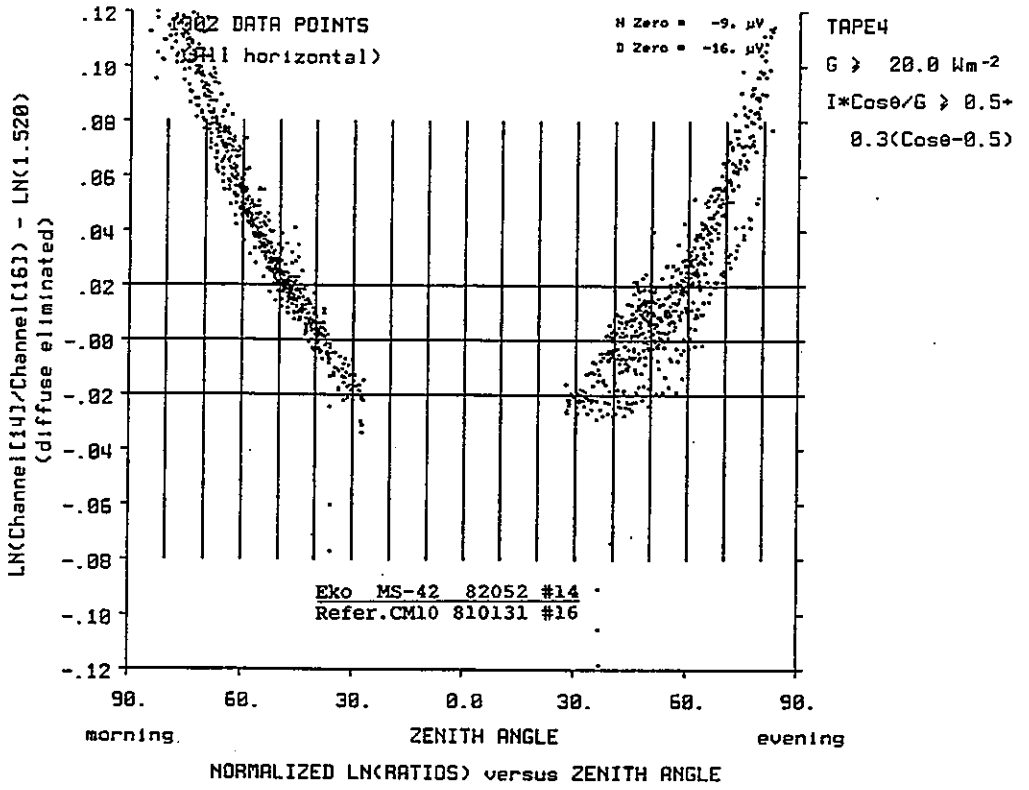

NORMALIZED LN(RATIOS) versus ZENITH ANGLE

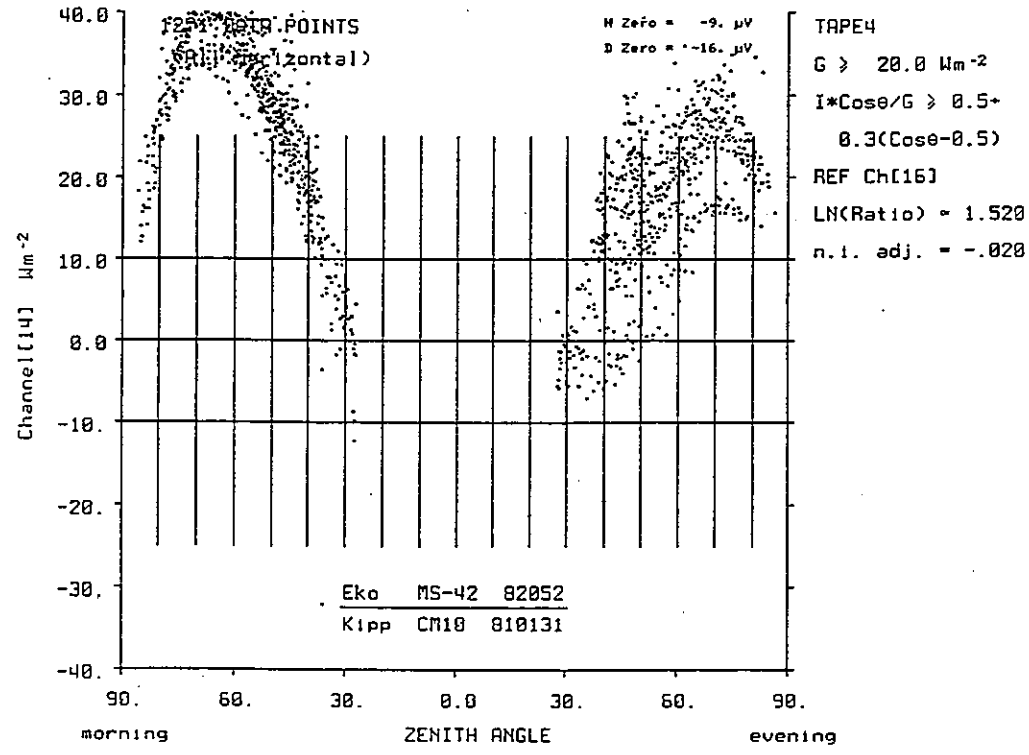

1000 Wm-2 MEASUREMENT ERROR VERSUS ZENITH ANGLE

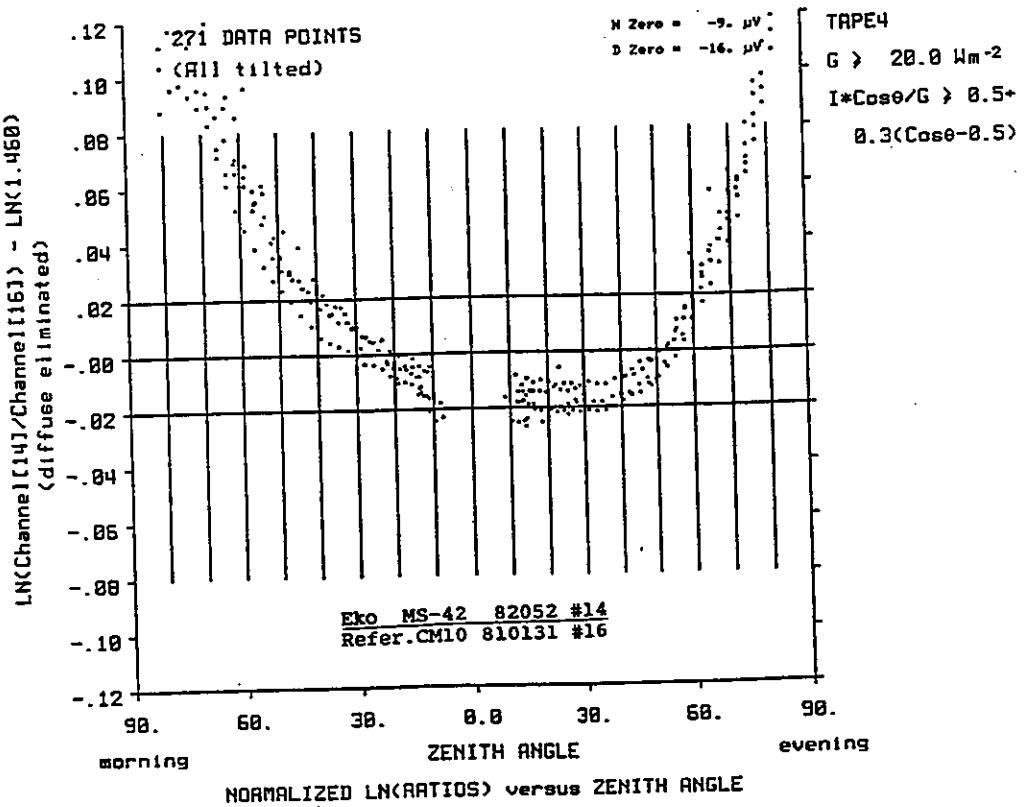
271 DATA POINTS
(All tilted)
N Zero = -9. μV
D Zero = -16. μV
TAPE4
G > 20.0 Wm-2
I*Cosθ/G > 0.5+
0.3(Cosθ-0.5)
LN(Channel[14]/Channel[16]) - LN(1.460)
(diffuse eliminated)
.12
.10
.08
.06
.04
.02
-.00
-.02
-.04
-.06
-.08
-.10
-.12
Eko MS-42 82052 #14
Refer.CM10 810131 #16
90. 60. 30. 0.0 30. 60. 90.
morning
ZENITH ANGLE
evening
NORMALIZED LN(RATIOS) versus ZENITH ANGLE

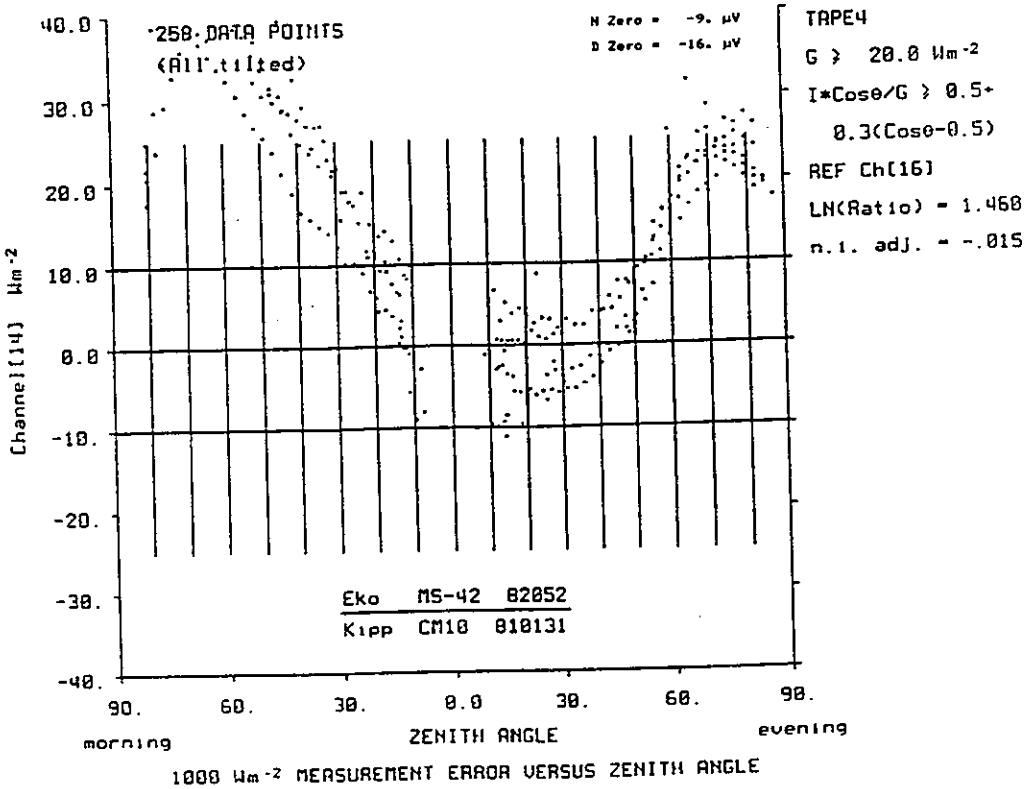
258 DATA POINTS
(All tilted)
N Zero = -9. μV
D Zero = -16. μV
TAPE4
G > 20.0 Wm-2
I*Cosθ/G > 0.5+
0.3(Cosθ-0.5)
REF Ch[16]
LN(Ratio) = 1.468
n.i. adj. = -.015
Channel[14] Wm-2
40.0
30.0
20.0
10.0
0.0
-10.
-20.
-30.
-40.
Eko MS-42 82052
Kipp CM10 810131
90. 60. 30. 0.0 30. 60. 90.
morning
ZENITH ANGLE
evening
1000 Wm-2 MEASUREMENT ERROR VERSUS ZENITH ANGLE

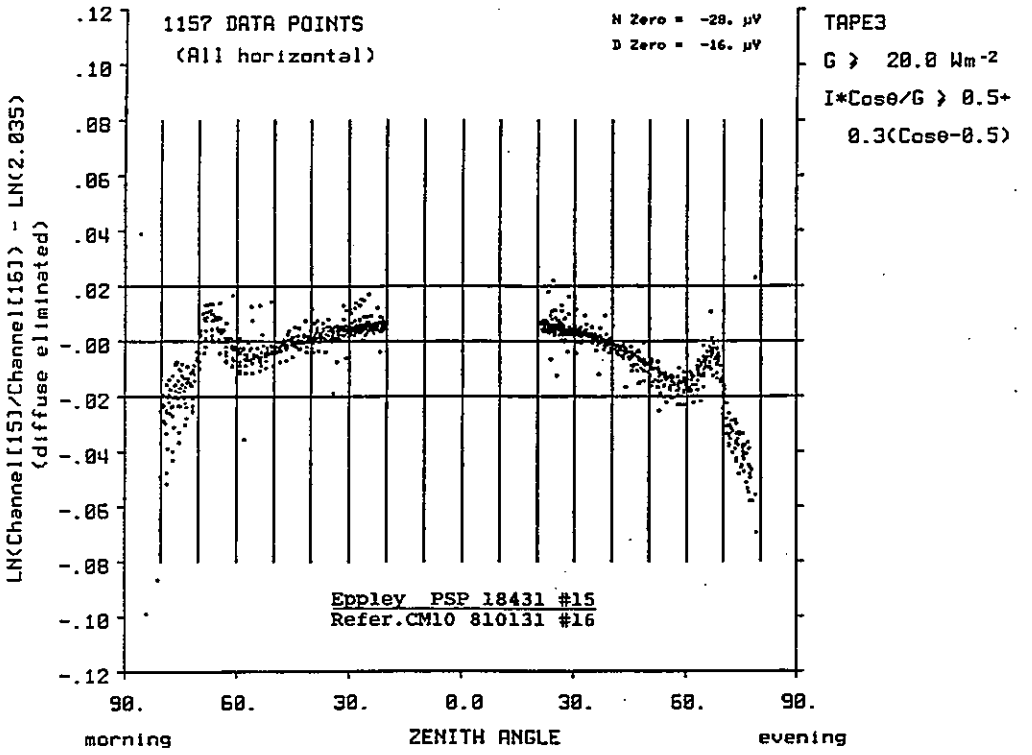

NORMALIZED LN(RATIOS) versus ZENITH ANGLE

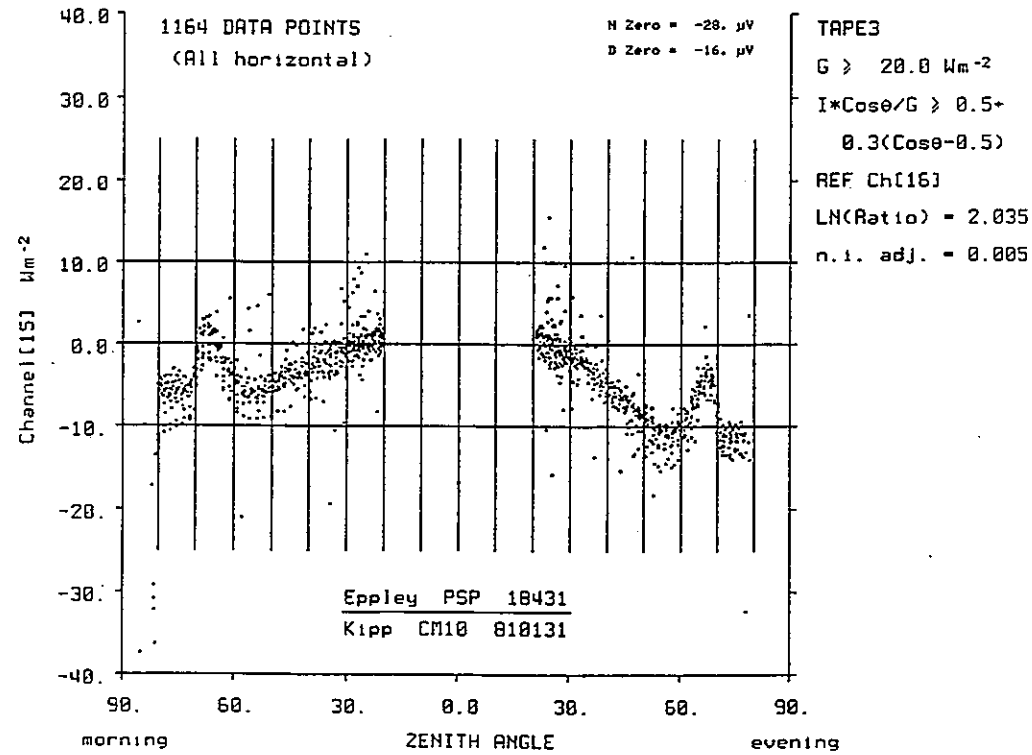

1000 Wm-2 MEASUREMENT ERROR VERSUS ZENITH ANGLE

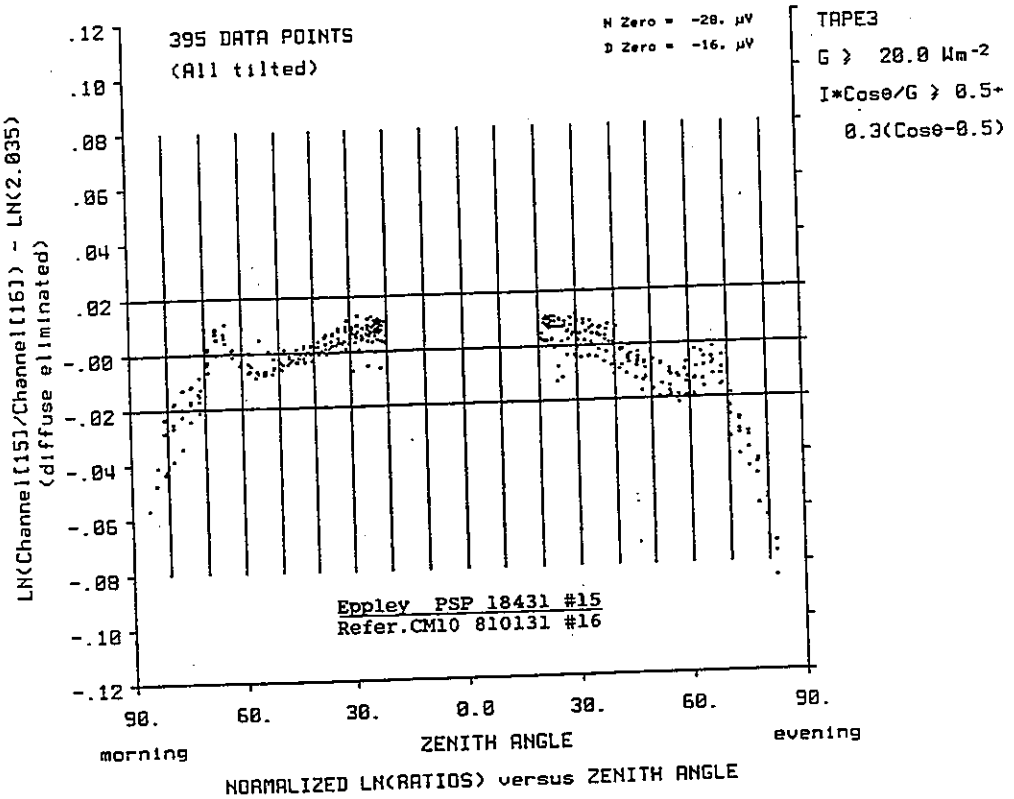
395 DATA POINTS
(All tilted)
N Zero = -28. μV
D Zero = -16. μV
TAPE3
G ≥ 20.0 Wm-2
I*Cosθ/G ≥ 0.5+
0.3(Cosθ-0.5)
LN(Channel[15]/Channel[16]) - LN(2.035)
(diffuse eliminated)
.12
.10
.08
.06
.04
.02
-.00
-.02
-.04
-.06
-.08
-.10
-.12
Eppley PSP 18431 #15
Refer.CM10 810131 #16
90.
60.
30.
0.0
30.
60.
90.
morning
ZENITH ANGLE
evening
NORMALIZED LN(RATIOS) versus ZENITH ANGLE

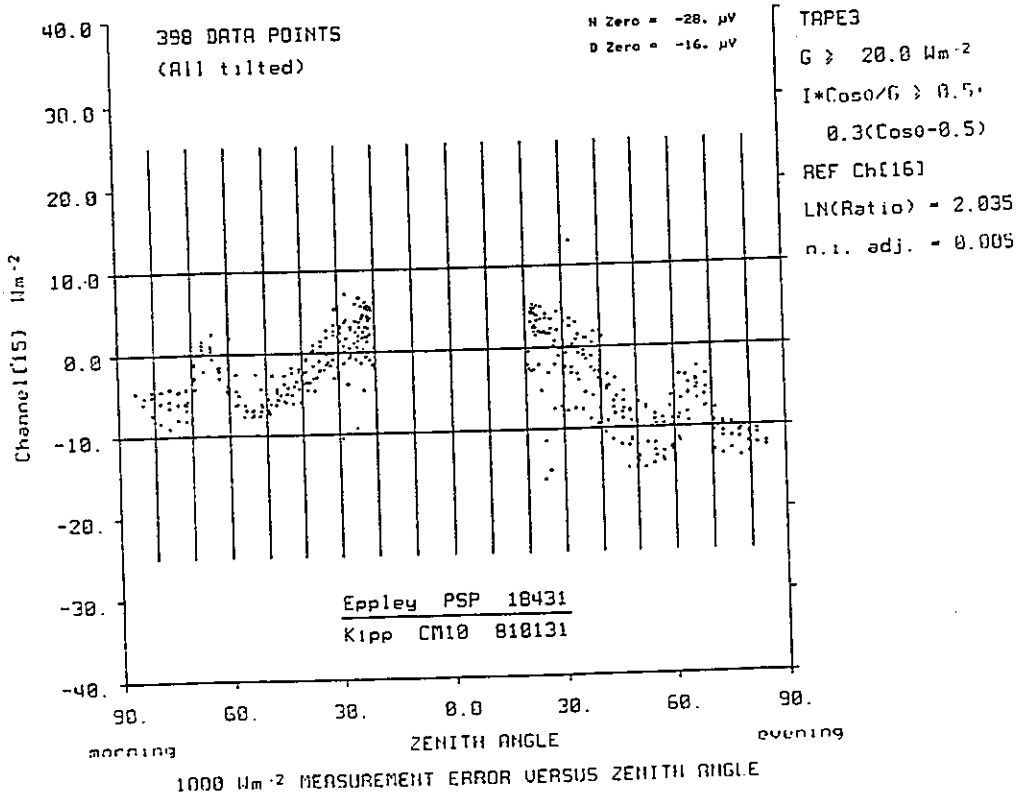
398 DATA POINTS
(All tilted)
N Zero = -28. μV
D Zero = -16. μV
TAPE3
G ≥ 20.0 Wm-2
I*Cosθ/G ≥ 0.5+
0.3(Cosθ-0.5)
REF Ch[16]
LN(Ratio) = 2.035
n.i. adj. = 0.005
Channel[15] Wm-2
40.0
30.0
20.0
10.0
0.0
-10.
-20.
-30.
-40.
Eppley PSP 18431
Kipp CM10 810131
90.
60.
30.
0.0
30.
60.
90.
morning
ZENITH ANGLE
evening
1000 Wm-2 MEASUREMENT ERROR VERSUS ZENITH ANGLE

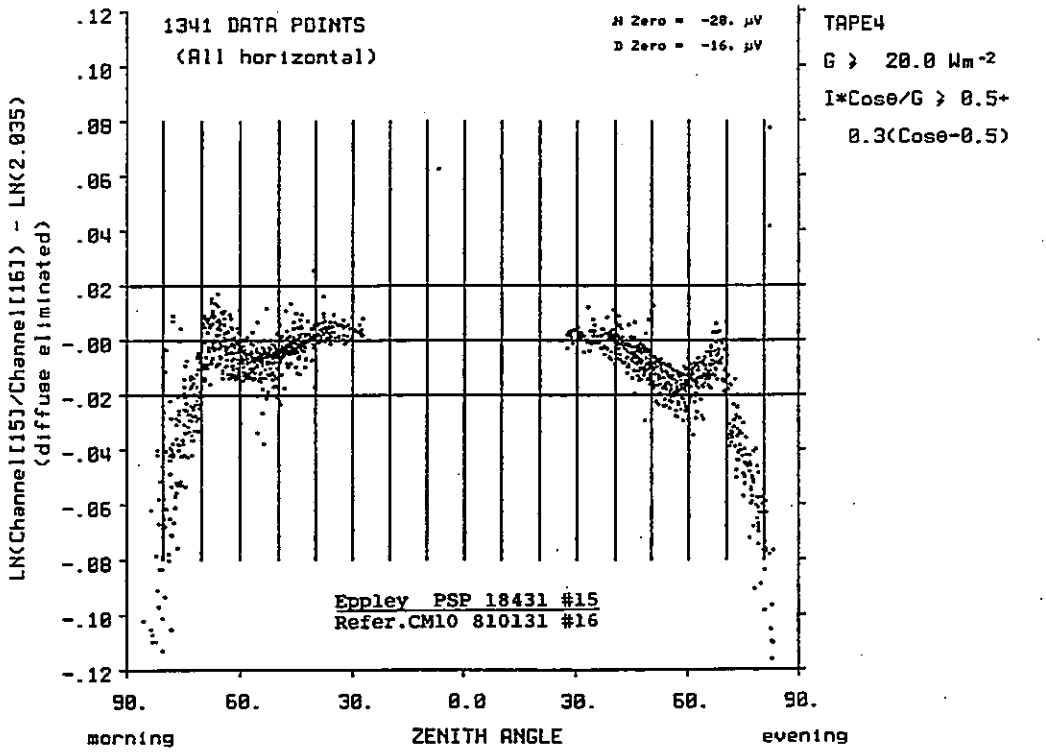

NORMALIZED LN(RATIOS) versus ZENITH ANGLE

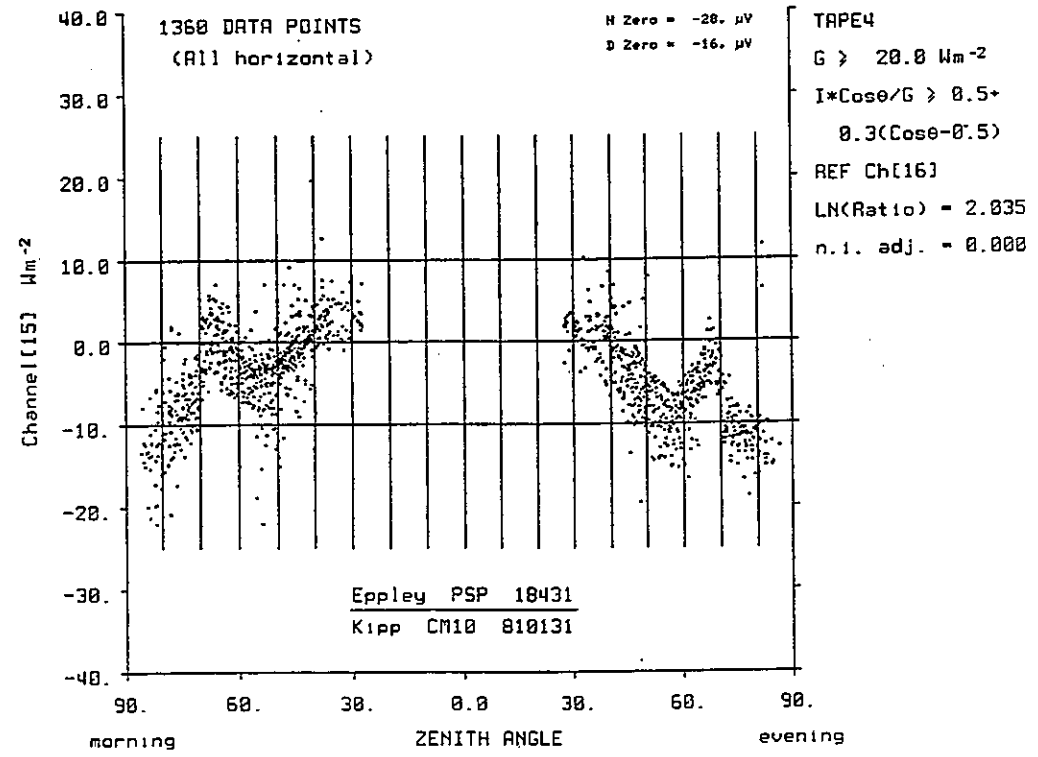

1000 Wm-2 MEASUREMENT ERROR VERSUS ZENITH ANGLE

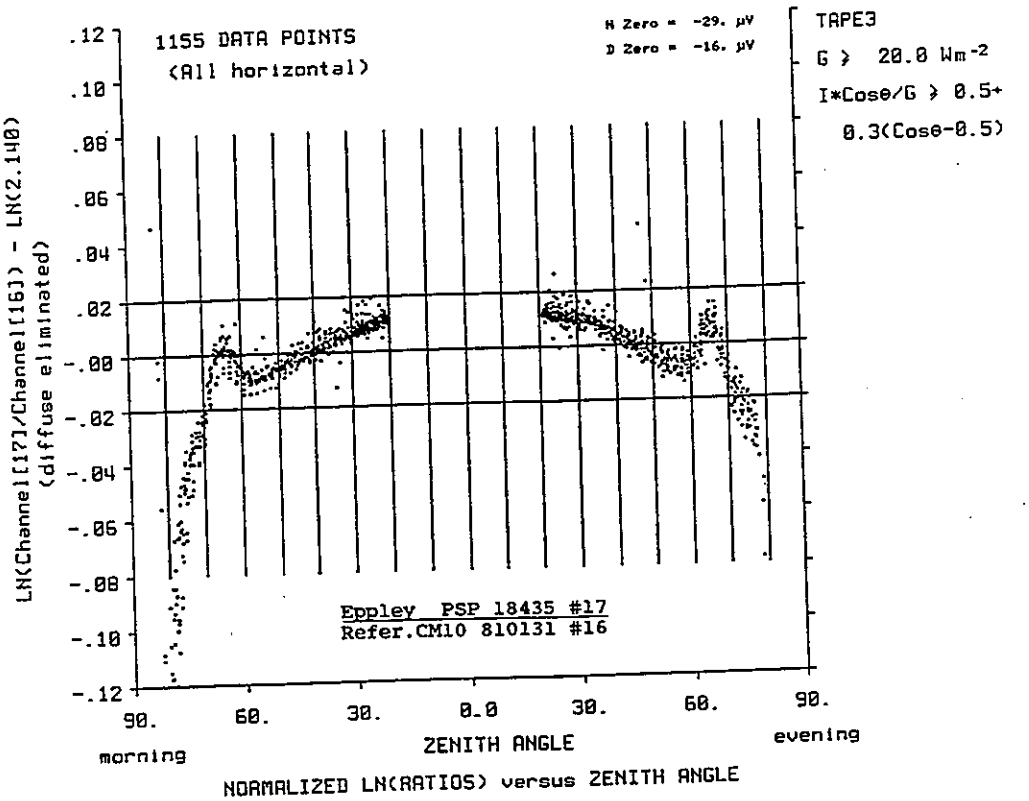
1155 DATA POINTS
(All horizontal)
N Zero = -29. μV
D Zero = -16. μV
TAPE3
G ≥ 20.0 Wm-2
I*Cosθ/G ≥ 0.5+
0.3(Cosθ-0.5)
LN(Channel[17]/Channel[16]) - LN(2.140)
(diffuse eliminated)
.12
.10
.08
.06
.04
.02
.00
-.02
-.04
-.06
-.08
-.10
-.12
Eppley PSP 18435 #17
Refer.CM10 810131 #16
90.
60.
30.
0.0
30.
60.
90.
morning
ZENITH ANGLE
evening
NORMALIZED LN(RATIOS) versus ZENITH ANGLE

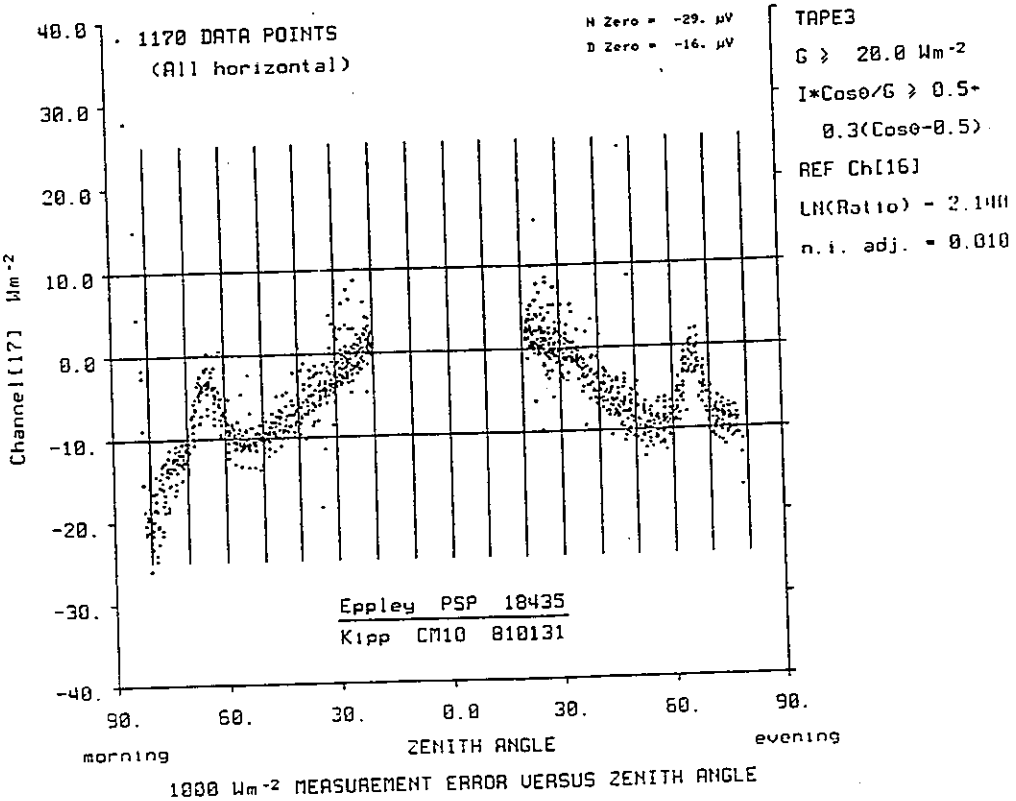
1170 DATA POINTS
(All horizontal)
N Zero = -29. μV
D Zero = -16. μV
TAPE3
G ≥ 20.0 Wm-2
I*Cosθ/G ≥ 0.5+
0.3(Cosθ-0.5)
REF Ch[16]
LN(Ratio) = 2.140
n.i. adj. = 0.010
Channel[17] Wm-2
40.0
30.0
20.0
10.0
0.0
-10.
-20.
-30.
-40.
Eppley PSP 18435
Kipp CM10 810131
90.
60.
30.
0.0
30.
60.
90.
morning
ZENITH ANGLE
evening
1000 Wm-2 MEASUREMENT ERROR VERSUS ZENITH ANGLE

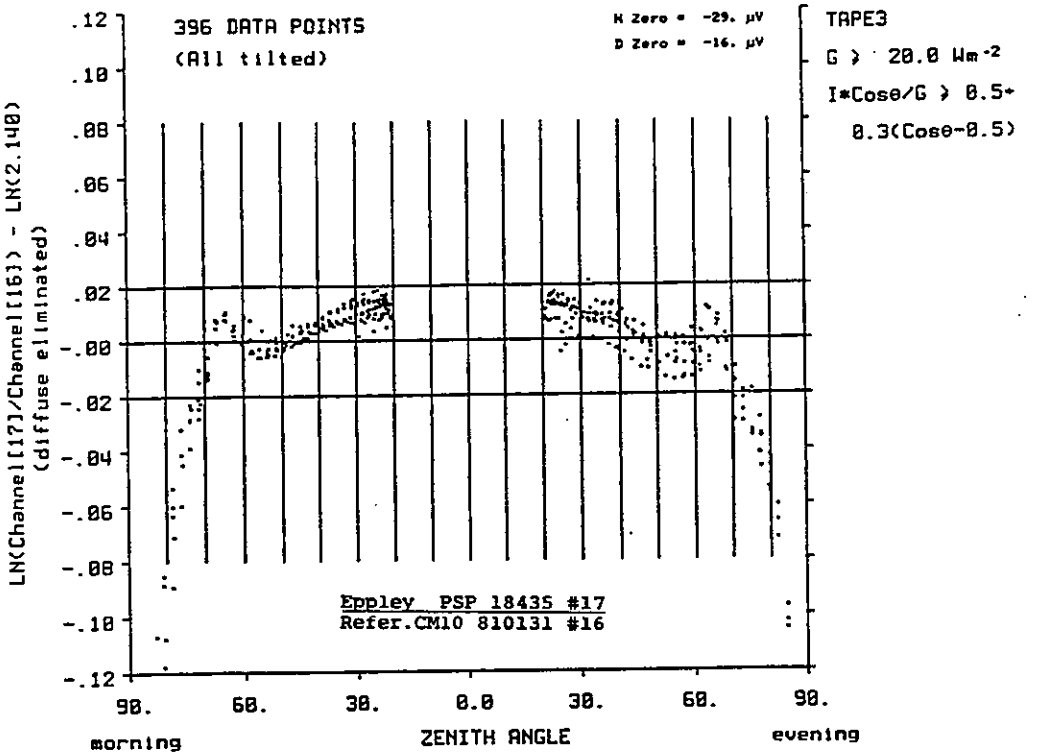
396 DATA POINTS
(All tilted)
N Zero = -29. μV
D Zero = -16. μV
TAPE3
G ≥ 20.0 Wm-2
I*Cosθ/G ≥ 0.5+
0.3(Cosθ-0.5)
LN(Channel[17]/Channel[16]) - LN(2.140)
(diffuse eliminated)
.12
.10
.08
.06
.04
.02
-.00
-.02
-.04
-.06
-.08
-.10
-.12
Eppley PSP 18435 #17
Refer.CM10 810131 #16
90.
60.
30.
0.0
30.
60.
90.
morning
ZENITH ANGLE
evening
NORMALIZED LN(RATIOS) versus ZENITH ANGLE

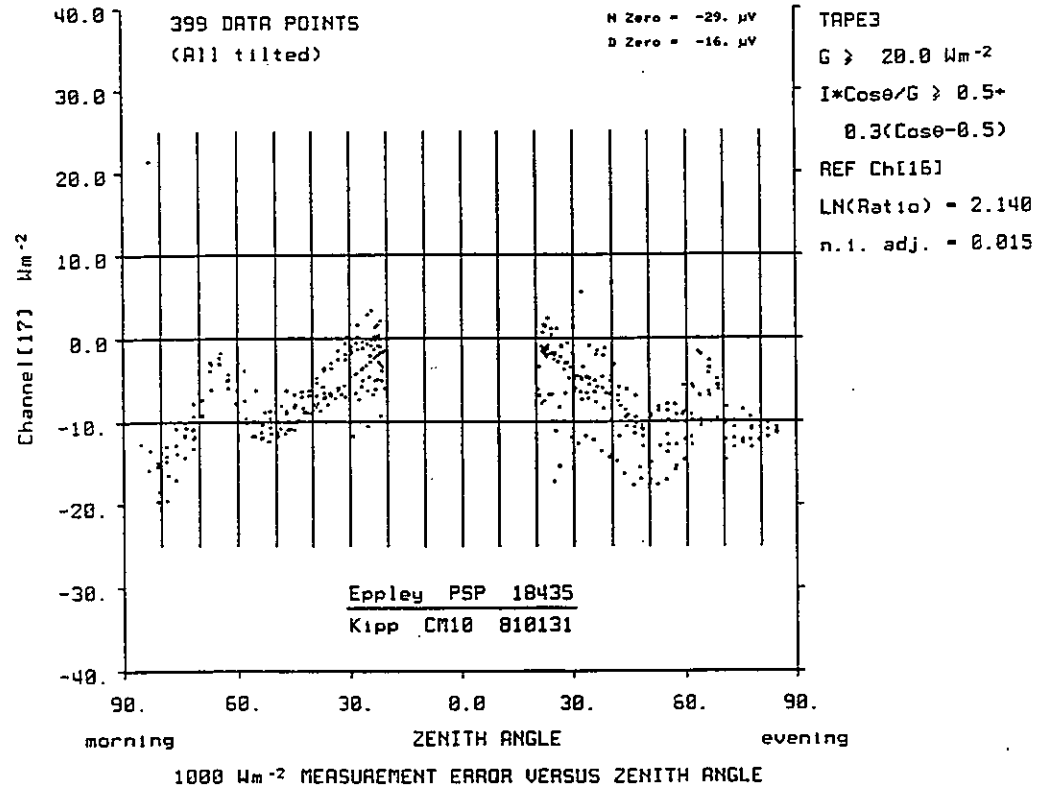
399 DATA POINTS
(All tilted)
N Zero = -29. μV
D Zero = -16. μV
TAPE3
G ≥ 20.0 Wm-2
I*Cosθ/G ≥ 0.5+
0.3(Cosθ-0.5)
REF Ch[16]
LN(Ratio) = 2.140
n.i. adj. = 0.015
Channel[17] Wm-2
40.0
30.0
20.0
10.0
0.0
-10.
-20.
-30.
-40.
Eppley PSP 18435
Kipp CM10 810131
90.
60.
30.
0.0
30.
60.
90.
morning
ZENITH ANGLE
evening
1000 Wm-2 MEASUREMENT ERROR VERSUS ZENITH ANGLE

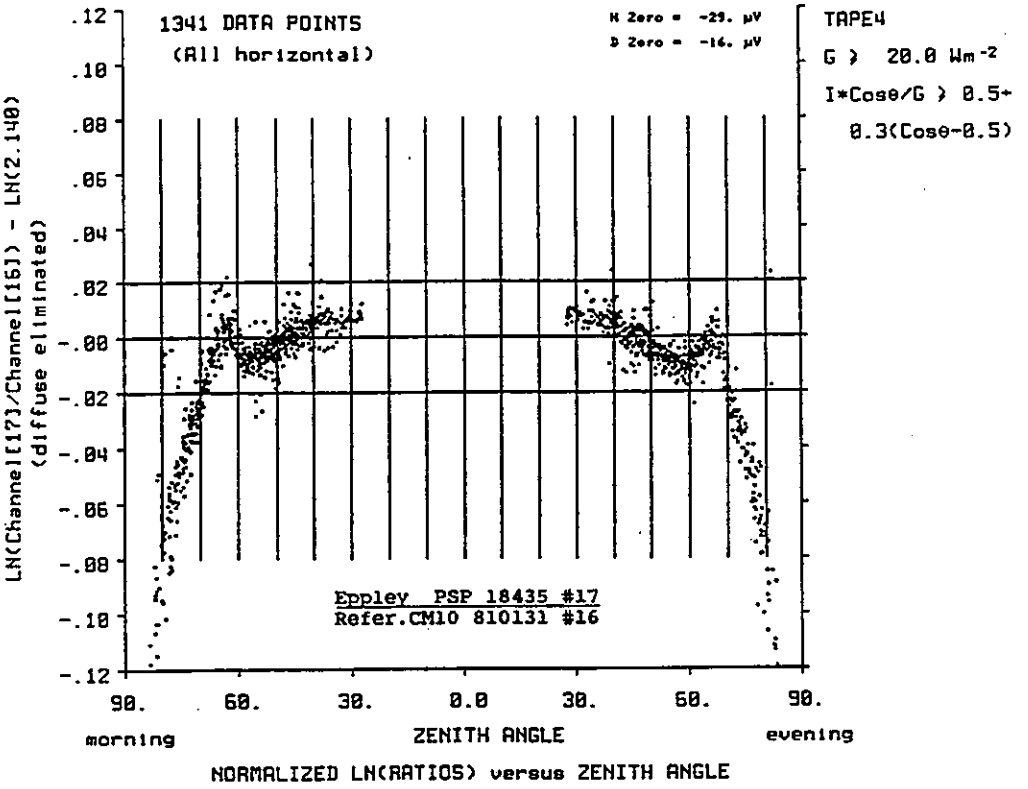

NORMALIZED LN(RATIOS) versus ZENITH ANGLE

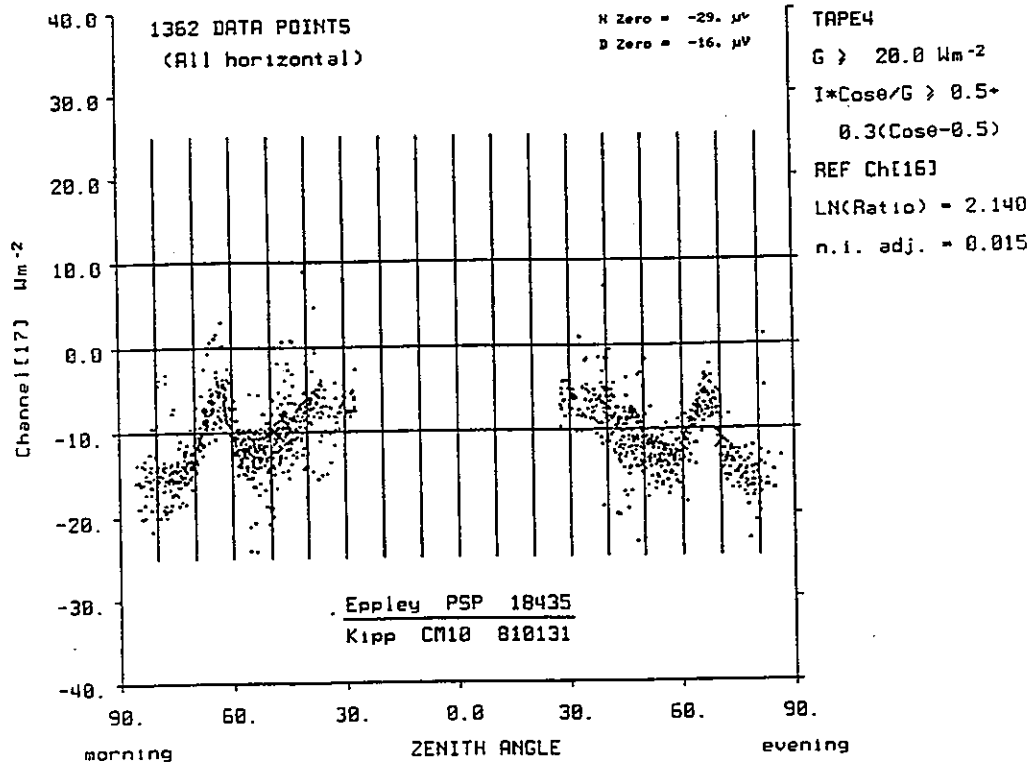

1000 Wm-2 MEASUREMENT ERROR VERSUS ZENITH ANGLE

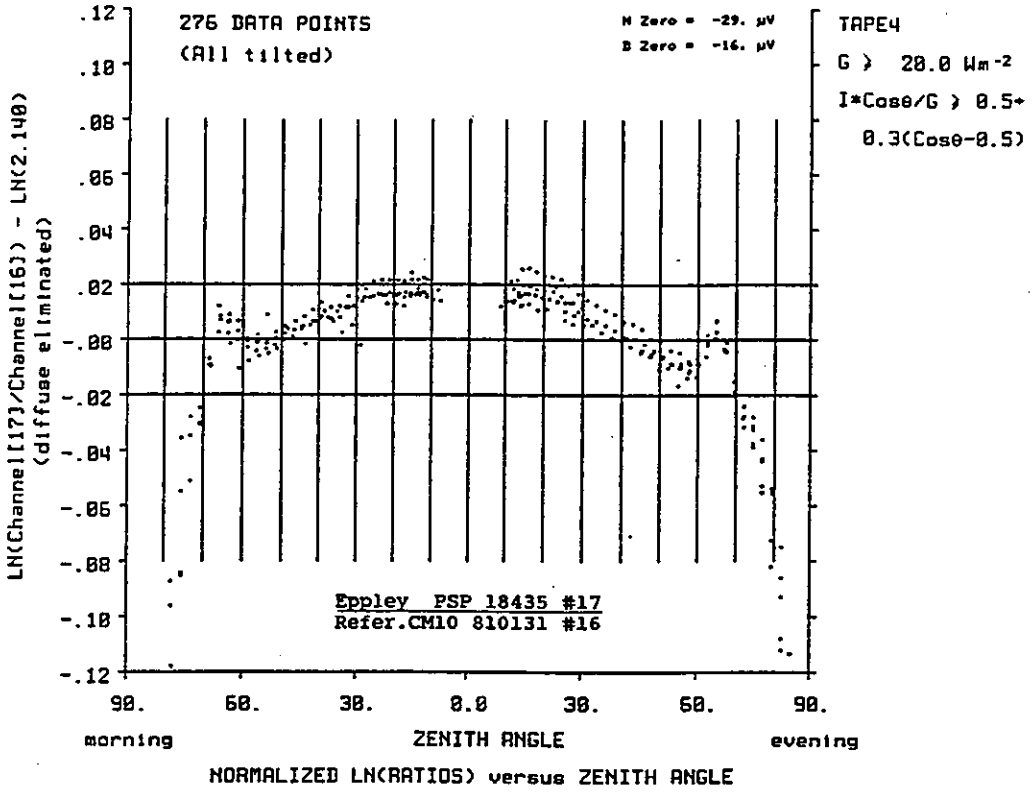

NORMALIZED LN(RATIOS) versus ZENITH ANGLE

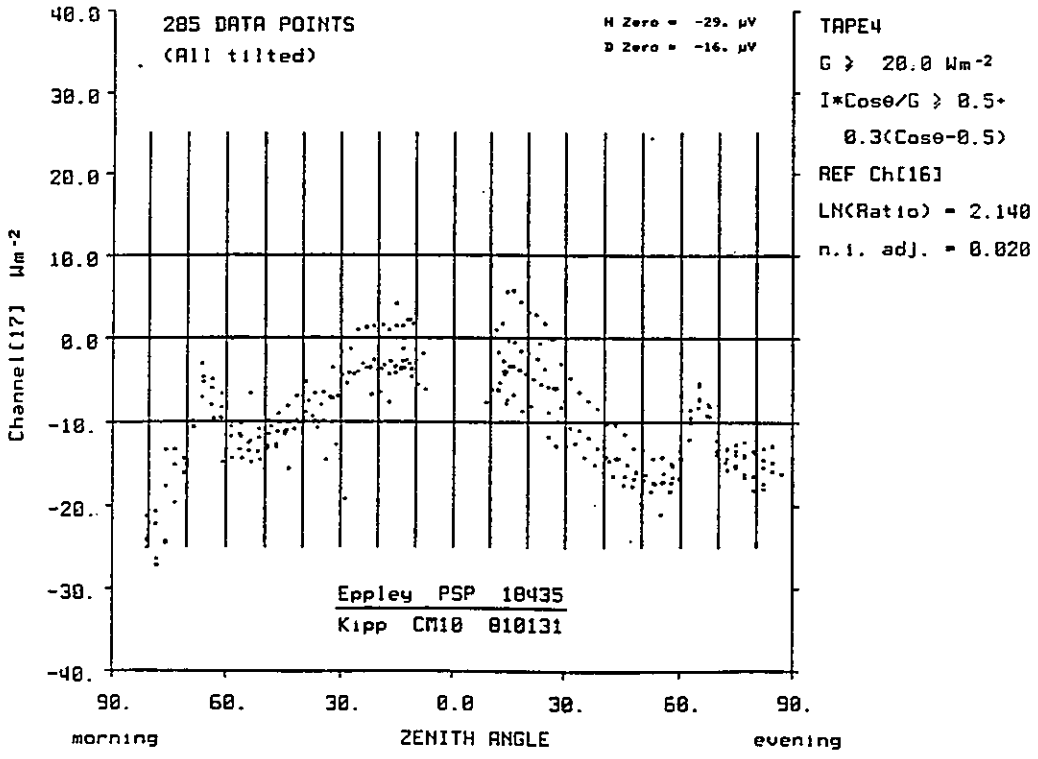

1000 Wm-2 MEASUREMENT ERROR VERSUS ZENITH ANGLE

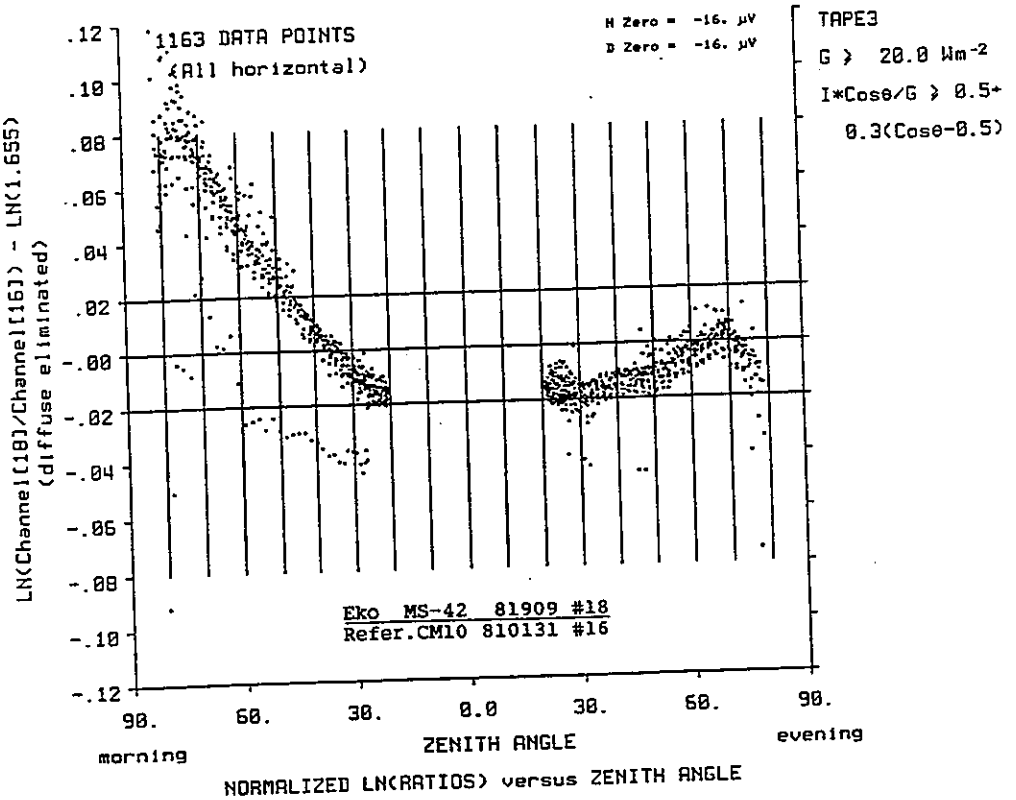
1163 DATA POINTS
(All horizontal)
N Zero = -16. μV
D Zero = -16. μV
TAPE3
G ≥ 20.0 Wm-2
I*Cosθ/G ≥ 0.5+
0.3(Cosθ-0.5)
LN(Channel[18]/Channel[16]) - LN(1.655)
(diffuse eliminated)
.12
.10
.08
.06
.04
.02
-.00
-.02
-.04
-.06
-.08
-.10
-.12
Eko MS-42 81909 #18
Refer.CM10 810131 #16
90.
60.
30.
0.0
30.
60.
90.
morning
ZENITH ANGLE
evening
NORMALIZED LN(RATIOS) versus ZENITH ANGLE

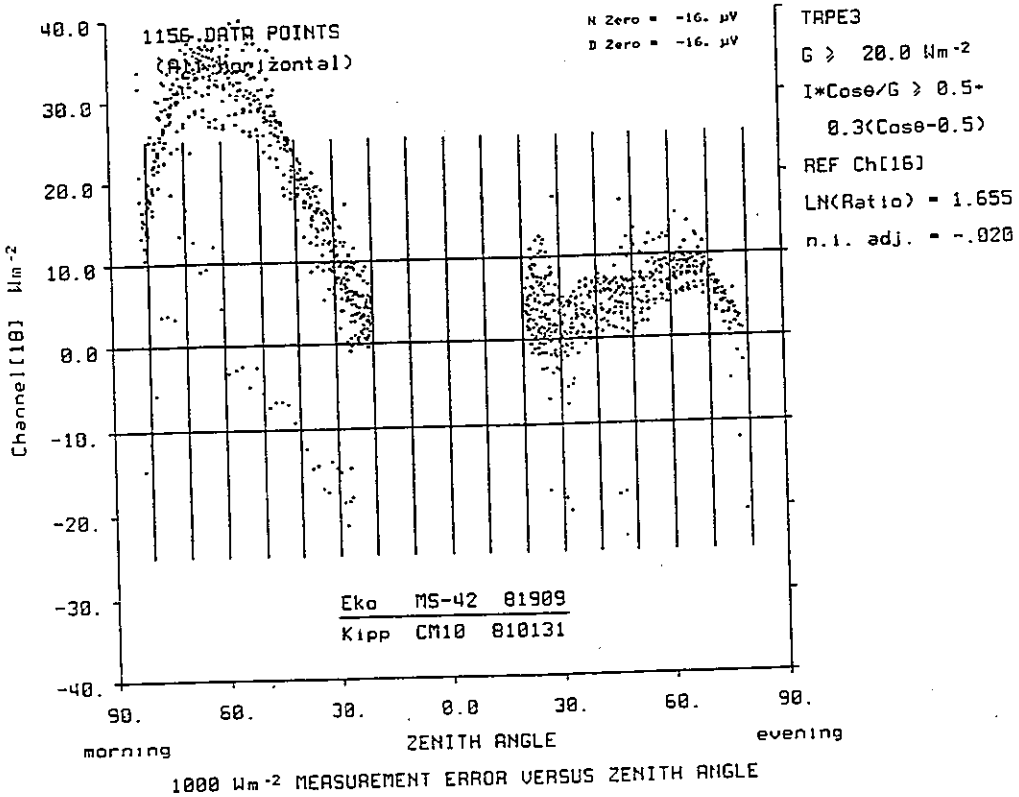
1156 DATA POINTS
(All horizontal)
N Zero = -16. μV
D Zero = -16. μV
TAPE3
G ≥ 20.0 Wm-2
I*Cosθ/G ≥ 0.5+
0.3(Cosθ-0.5)
REF Ch[16]
LN(Ratio) = 1.655
n.i. adj. = -.020
Channel[18] Wm-2
40.0
30.0
20.0
10.0
0.0
-10.
-20.
-30.
-40.
Eko MS-42 81909
Kipp CM10 810131
90.
60.
30.
0.0
30.
60.
90.
morning
ZENITH ANGLE
evening
1000 Wm-2 MEASUREMENT ERROR VERSUS ZENITH ANGLE

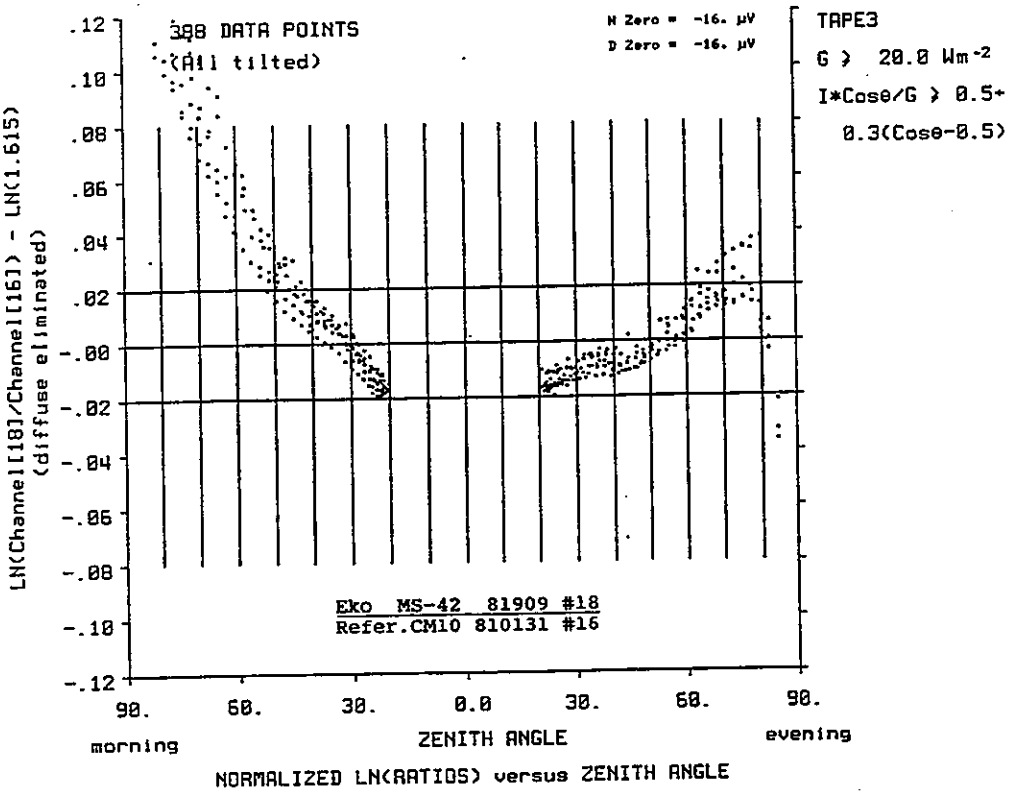
388 DATA POINTS
(All tilted)
N Zero = -16. μV
D Zero = -16. μV
TAPE3
G > 20.0 Wm-2
I*Cose/G > 0.5+
0.3(Cose-0.5)
LN(Channel[18]/Channel[16]) - LN(1.615)
(diffuse eliminated)
.12
.10
.08
.06
.04
.02
-.00
-.02
-.04
-.06
-.08
-.10
-.12
Eko MS-42 81909 #18
Refer.CM10 810131 #16
90. 60. 30. 0.0 30. 60. 90.
morning
ZENITH ANGLE
evening
NORMALIZED LN(RATIOS) versus ZENITH ANGLE

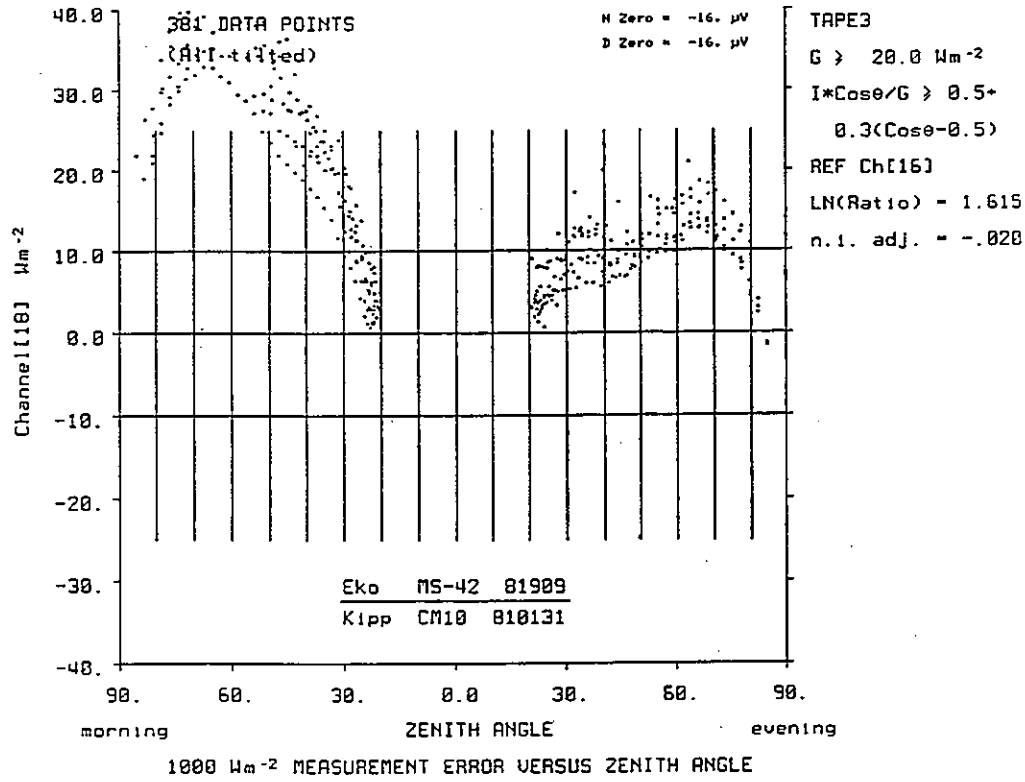
381 DATA POINTS
(All tilted)
N Zero = -16. μV
D Zero = -16. μV
TAPE3
G > 20.0 Wm-2
I*Cose/G > 0.5+
0.3(Cose-0.5)
REF Ch[16]
LN(Ratio) = 1.615
n.i. adj. = -.020
Channel[18] Wm-2
40.0
30.0
20.0
10.0
0.0
-10.
-20.
-30.
-40.
Eko MS-42 81909
Kipp CM10 810131
90. 60. 30. 0.0 30. 60. 90.
morning
ZENITH ANGLE
evening
1000 Wm-2 MEASUREMENT ERROR VERSUS ZENITH ANGLE

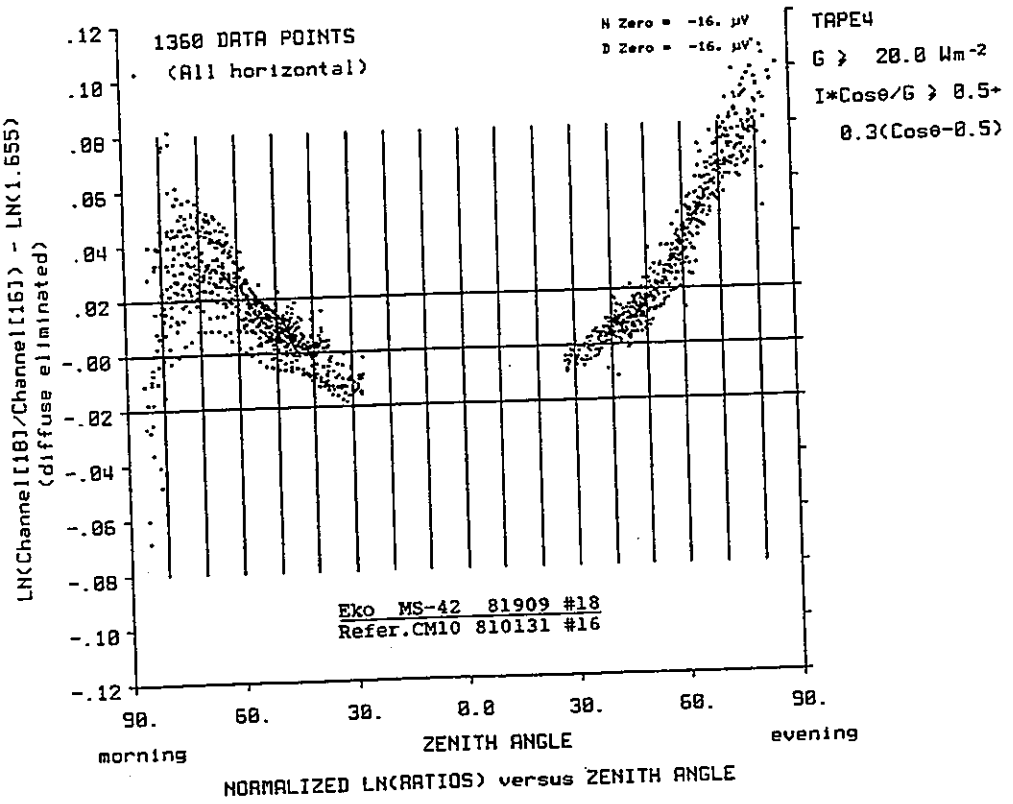

NORMALIZED LN(RATIOS) versus ZENITH ANGLE

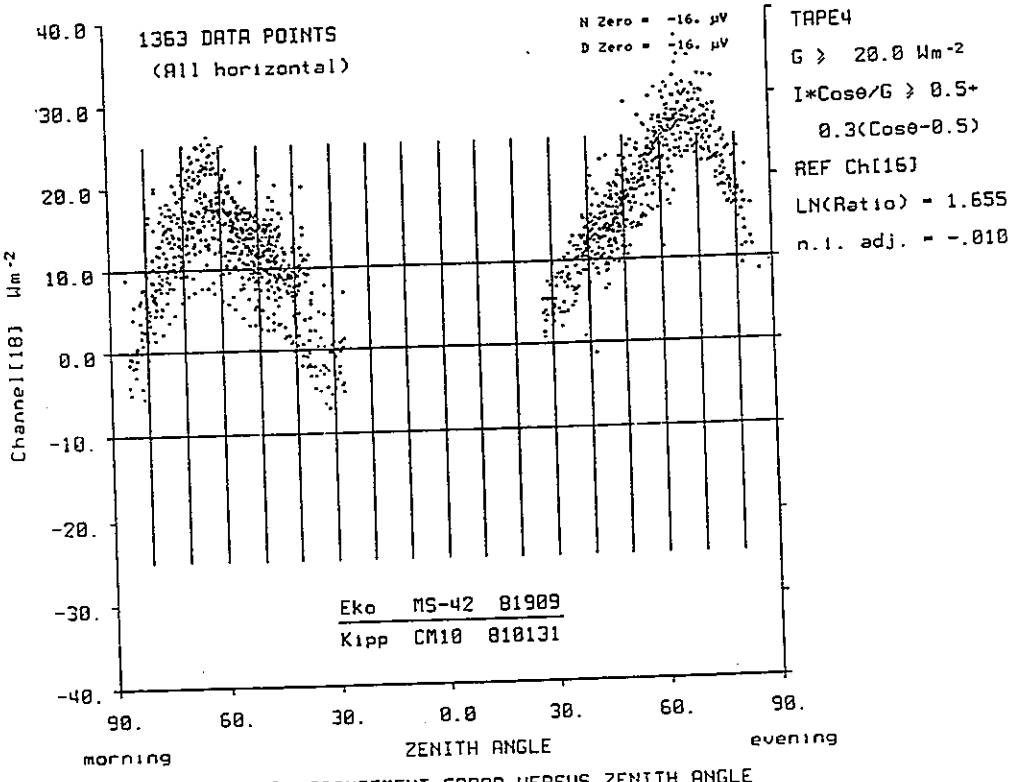

1000 Wm-2 MEASUREMENT ERROR VERSUS ZENITH ANGLE

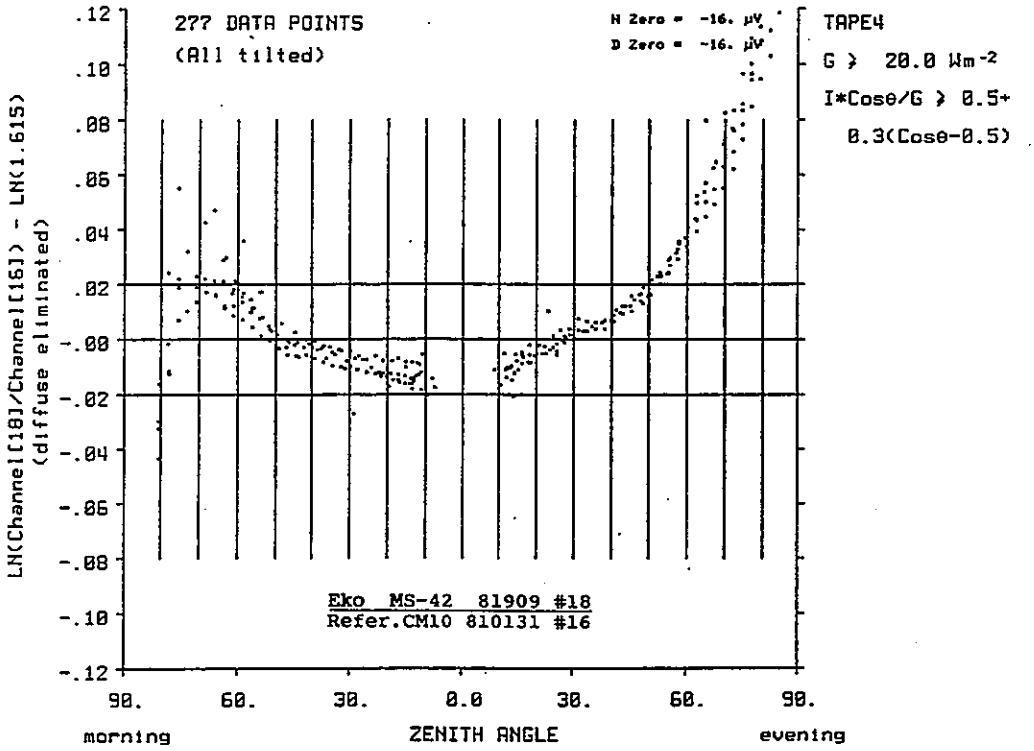

NORMALIZED LN(RATIOS) versus ZENITH ANGLE

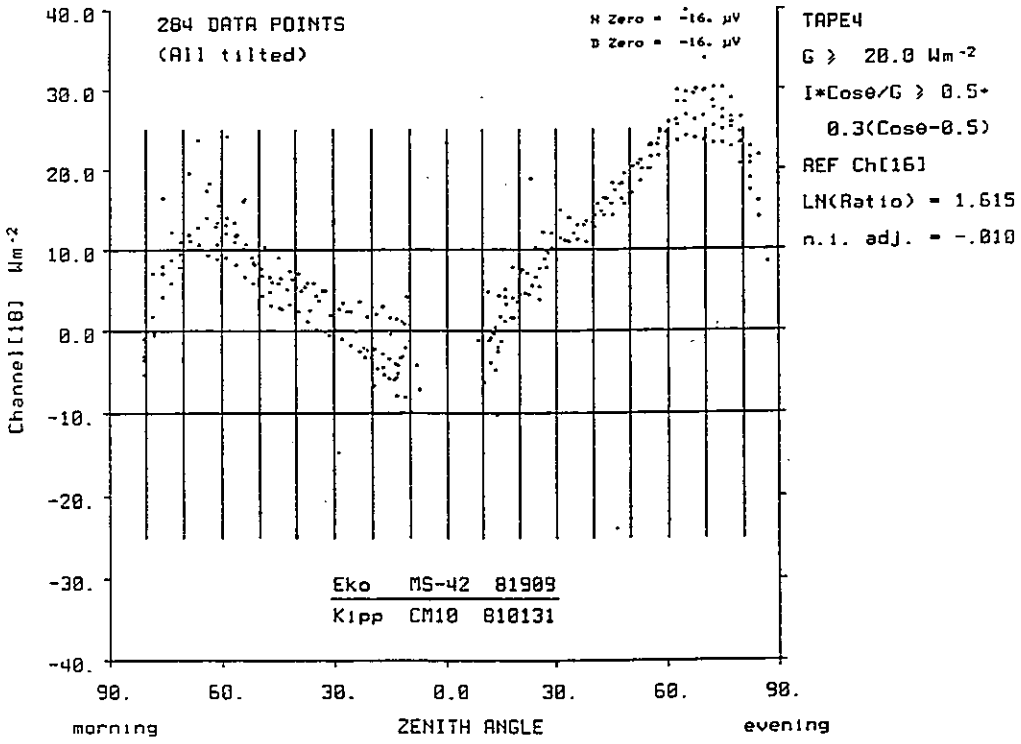

1000 Wm^{-2} MEASUREMENT ERROR VERSUS ZENITH ANGLE

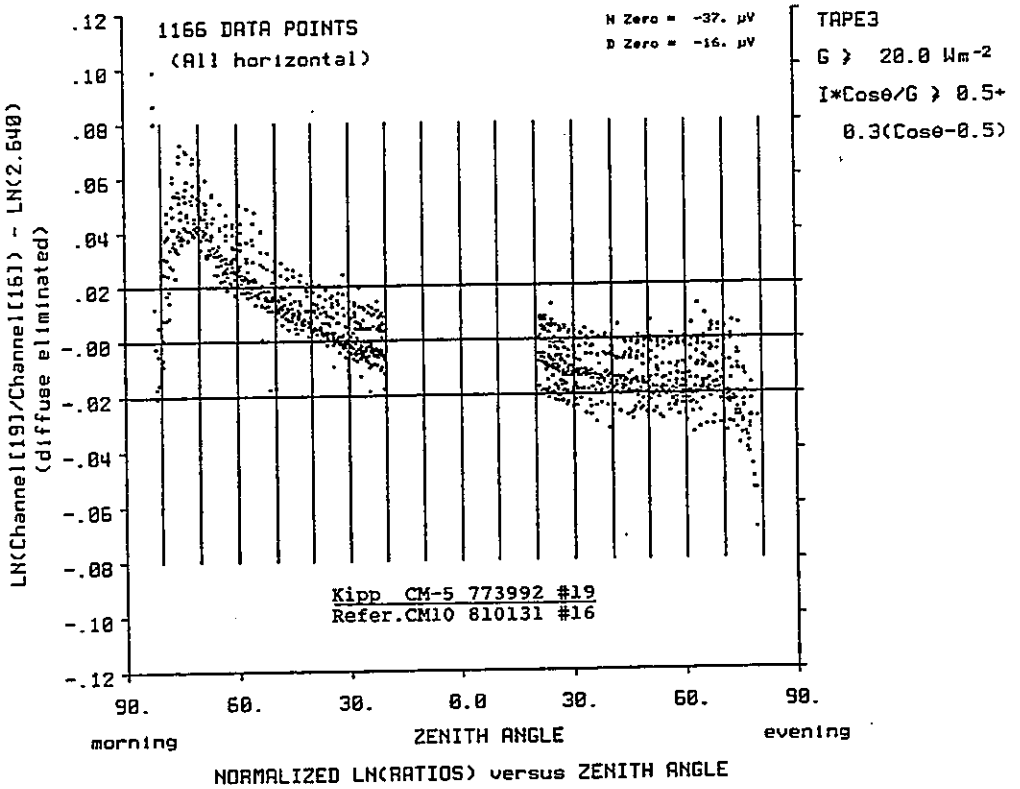

NORMALIZED LN(RATIOS) versus ZENITH ANGLE

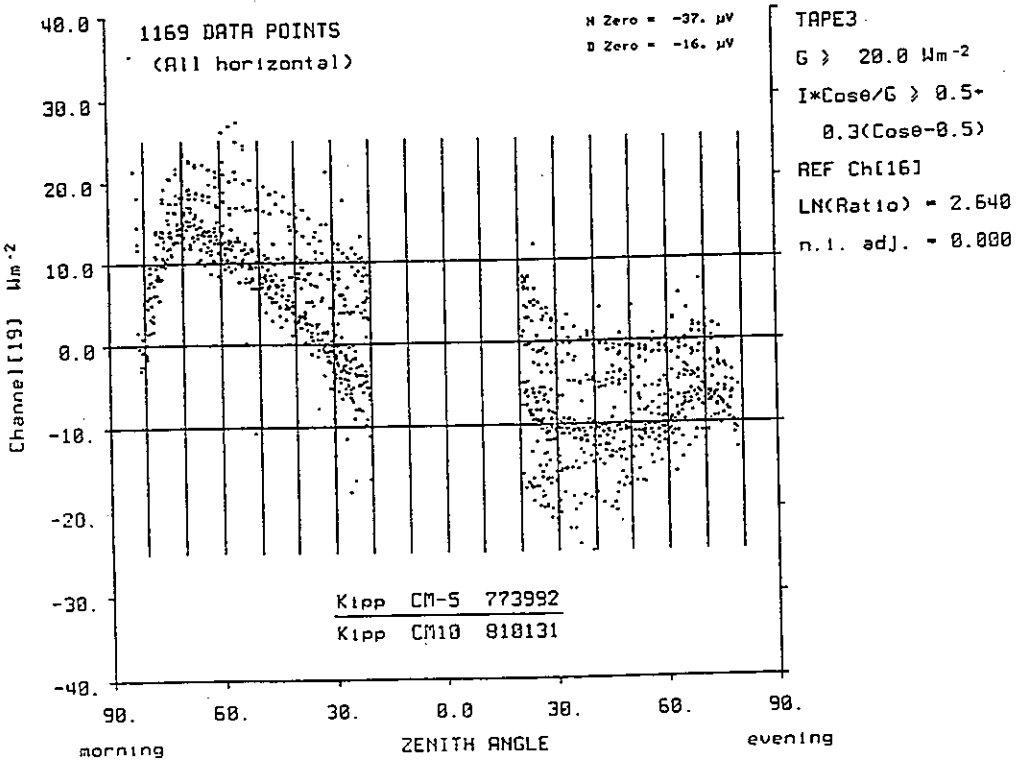

1000 Wm-2 MEASUREMENT ERROR VERSUS ZENITH ANGLE

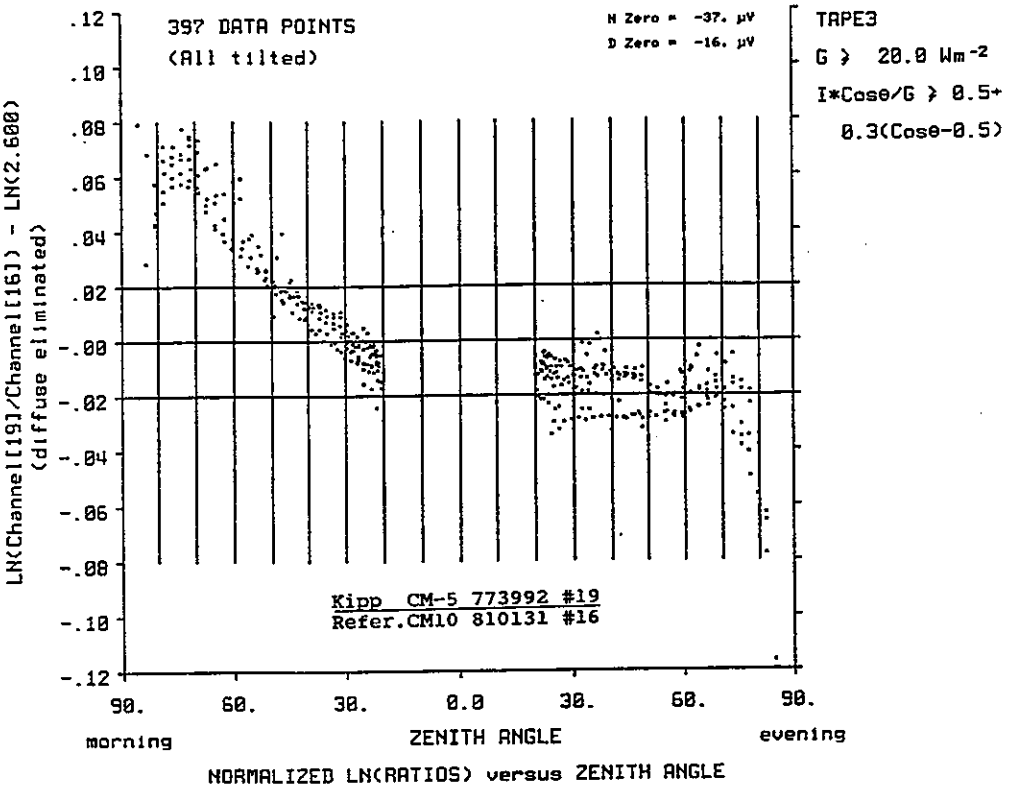
397 DATA POINTS
(All tilted)
N Zero = -37. µV
D Zero = -16. µV
TAPE3
G ≥ 20.0 Wm-2
I*Cosθ/G ≥ 0.5+
0.3(Cosθ-0.5)
LN(Channel[19]/Channel[16]) - LN(2.600)
(diffuse eliminated)
.12
.10
.08
.06
.04
.02
-.00
-.02
-.04
-.06
-.08
-.10
-.12
Kipp CM-5 773992 #19
Refer.CM10 810131 #16
90.
60.
30.
0.0
30.
60.
90.
morning
ZENITH ANGLE
evening
NORMALIZED LN(RATIOS) versus ZENITH ANGLE

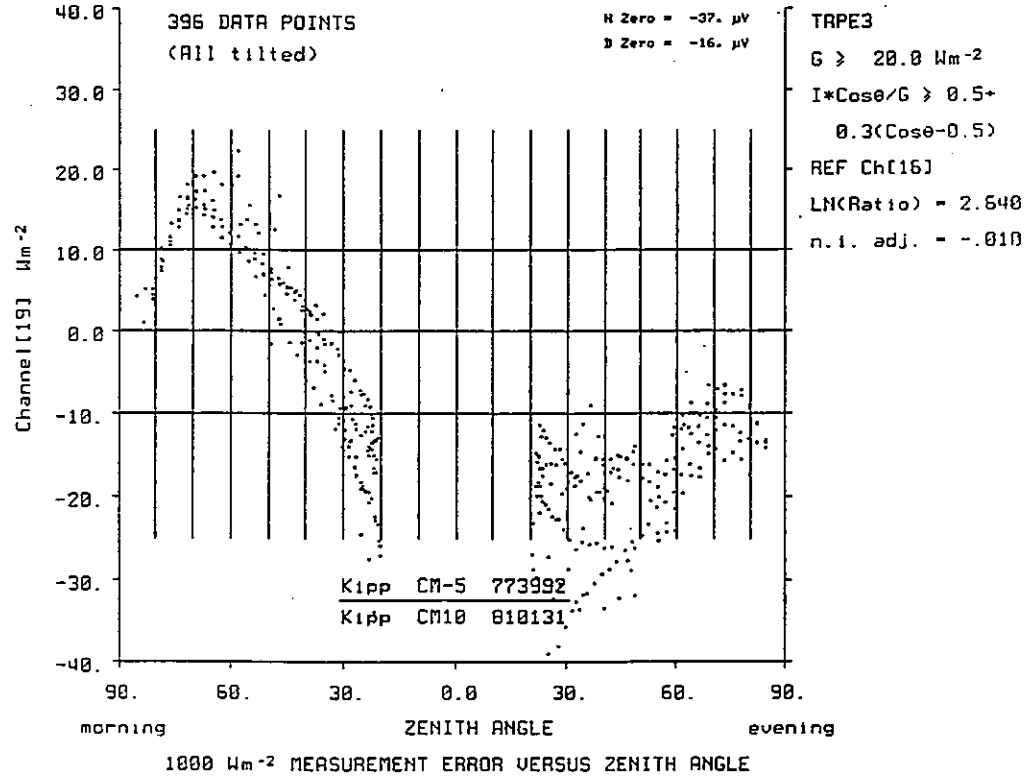
396 DATA POINTS
(All tilted)
N Zero = -37. µV
D Zero = -16. µV
TAPE3
G ≥ 20.0 Wm-2
I*Cosθ/G ≥ 0.5+
0.3(Cosθ-0.5)
REF Ch[16]
LN(Ratio) = 2.640
n.i. adj. = -.010
Channel[19] Wm-2
40.0
30.0
20.0
10.0
0.0
-10.
-20.
-30.
-40.
Kipp CM-5 773992
Kipp CM10 810131
90.
60.
30.
0.0
30.
60.
90.
morning
ZENITH ANGLE
evening
1000 Wm-2 MEASUREMENT ERROR VERSUS ZENITH ANGLE

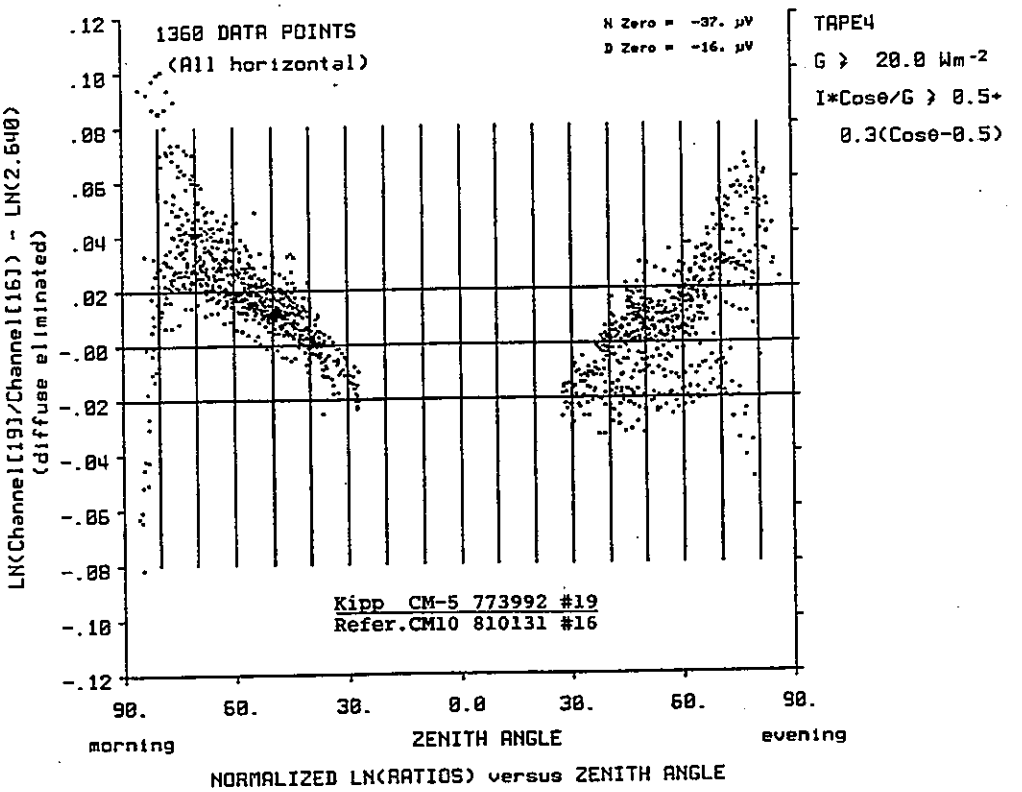

NORMALIZED LN(RATIOS) versus ZENITH ANGLE

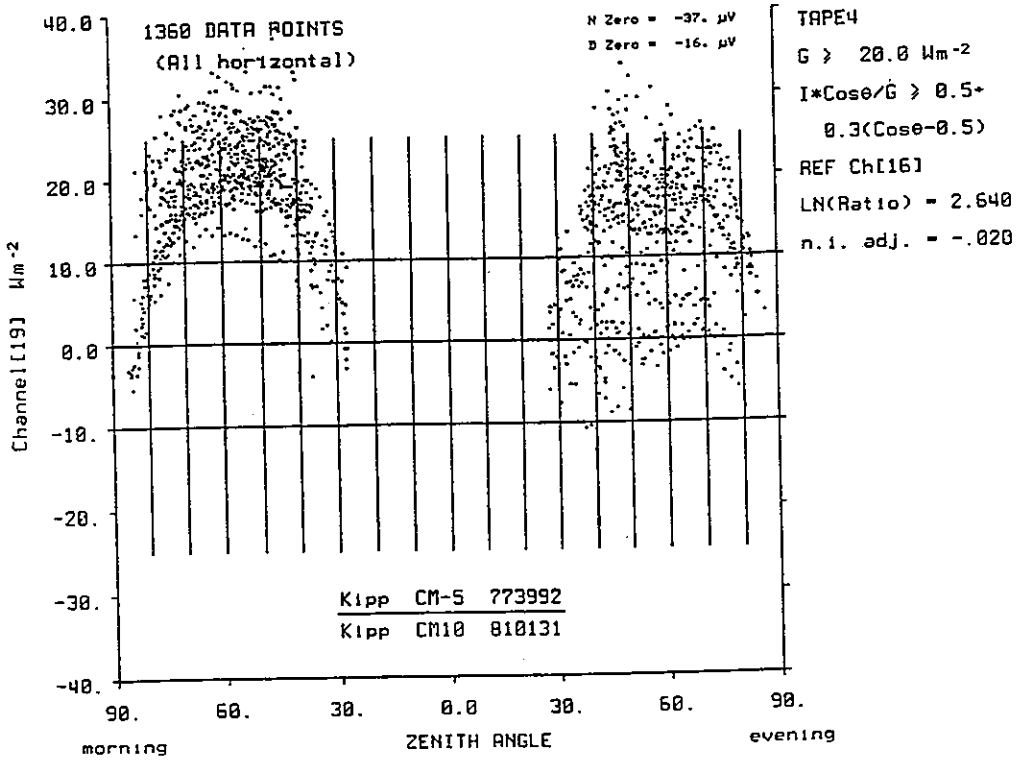

1000 Wm-2 MEASUREMENT ERROR VERSUS ZENITH ANGLE

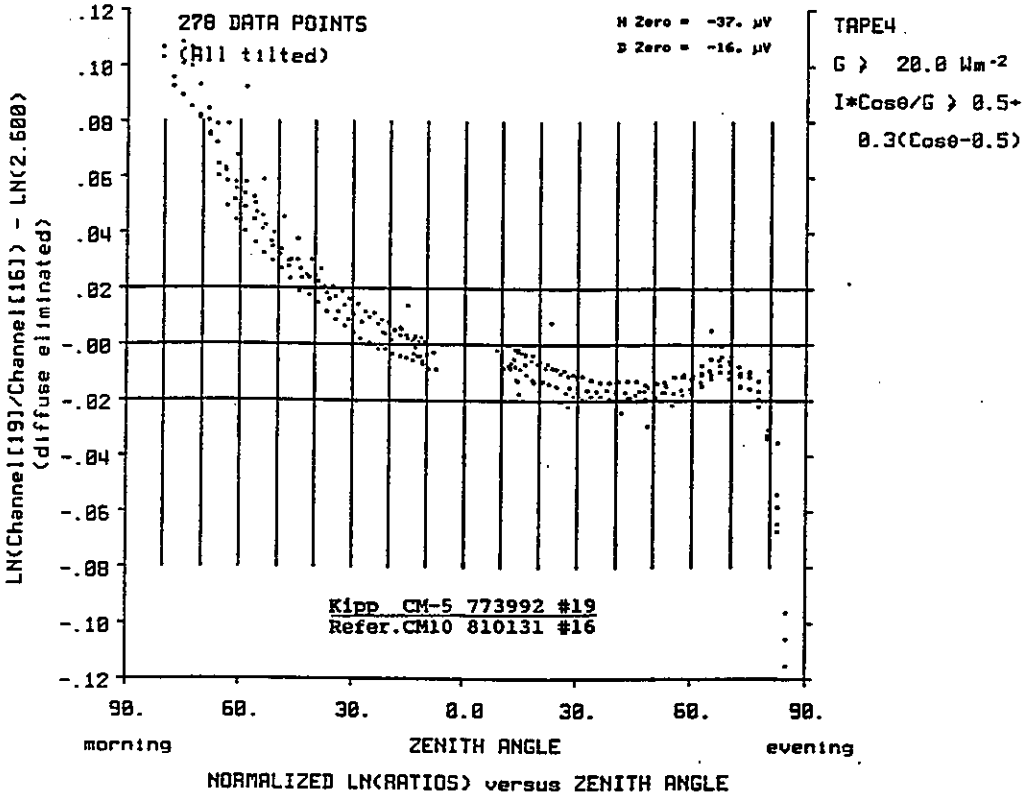

NORMALIZED LN(RATIOS) versus ZENITH ANGLE

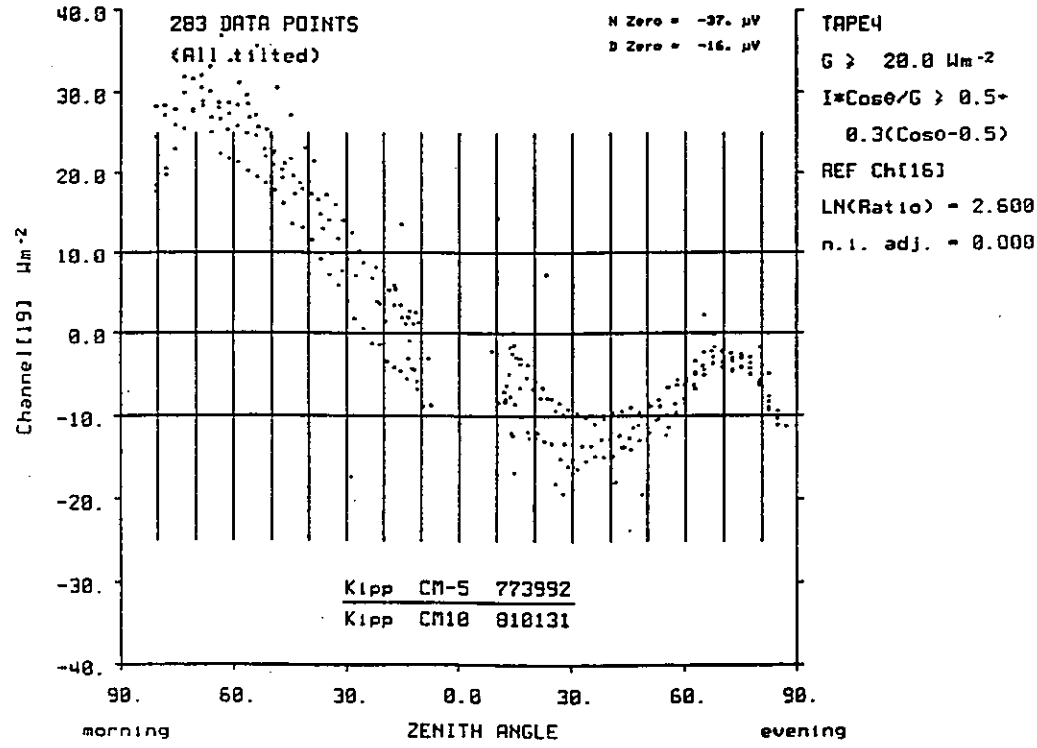

1000 Wm-2 MEASUREMENT ERROR VERSUS ZENITH ANGLE

APPENDIX DD1. NIGHT SKY REGRESSION ANALYSIS.

LEGEND ON PAGE 4

Ta Ch N	Zm	Zd	A	As	B	Bs	R1	A2	A2s	B2	B2s	C2	C2s	R2
Eppley PSP - unventilated - horizontal.														
4B23 90	-2.7	1.3	.54	(.21)	.049	(.0030)	.63	.47	(.20)	.046	(.0031)	.68	(.25)	.61
Eppley PSP - ventilated - horizontal.														
3B 0 65	-3.6	.82	-1.8	(.23)	.025	(.0030)	.58	-1.8	(.22)	.022	(.0031)	.86	(.31)	.55
4B 0 95	-3.2	.81	-1.6	(.20)	.023	(.0029)	.62	-1.7	(.19)	.020	(.0029)	.88	(.24)	.58
4B11 95	-3.0	.83	-1.3	(.20)	.025	(.0029)	.62	-1.4	(.19)	.021	(.0028)	.99	(.24)	.58
3B15 65	-3.2	.73	-1.4	(.17)	.025	(.0022)	.42	-1.4	(.16)	.023	(.0022)	.74	(.23)	.39
4B15 95	-2.9	.76	-1.5	(.19)	.022	(.0027)	.59	-1.5	(.18)	.018	(.0027)	.83	(.23)	.56
3B17 65	-3.1	.75	-1.3	(.18)	.026	(.0024)	.45	-1.4	(.16)	.023	(.0022)	.92	(.23)	.40
4B17 95	-2.8	.78	-1.4	(.20)	.022	(.0028)	.61	-1.5	(.18)	.018	(.0028)	.94	(.24)	.57
mn 7 575	-3.1	.78/.82	-1.5	(.07)	.024	(.0010)	.56	-1.5	(.07)	.021	(.0010)	.88	(.09)	.52
Eppley PSP - ventilated - both pyranometer and pyrgeometer at 45 deg. tilt.														
6B 0 130	-1.9	.75	-1.3	(.07)	.023	(.0018)	.50	-1.3	(.07)	.021	(.0021)	.50	(.22)	.49
6B17 130	-1.8	.73	-1.1	(.06)	.024	(.0016)	.44	-1.2	(.06)	.021	(.0018)	.59	(.19)	.43
mn 2 260	-1.9	.74/.74	-1.2	(.04)	.024	(.0012)	.47	-1.2	(.04)	.021	(.0014)	.55	(.14)	.46
Eppley PSP - ventilated - 90 deg tilt - pyrgeometer horizontal.														
4B34 96	-2.2	.99	-1.5	(.31)	.011	(.0044)	.97	-1.5	(.31)	.010	(.0047)	.17	(.41)	.97
4B35 96	-1.9	.94	-1.3	(.29)	.010	(.0042)	.92	-1.3	(.29)	.008	(.0045)	.37	(.38)	.92
mn 2 192	-2.1	.97/.98	-1.4	(.21)	.010	(.0030)	.95	-1.4	(.21)	.009	(.0033)	.28	(.28)	.95
Kipp CM-5 - unventilated - horizontal.														
3B41 65	-3.2	1.0	-.36	(.17)	.039	(.0023)	.44	-.37	(.17)	.038	(.0024)	.33	(.25)	.43
4B41 95	-2.6	1.1	.16	(.20)	.042	(.0028)	.62	.14	(.20)	.040	(.0030)	.28	(.26)	.62
mn 2 160	-2.8	1.1/1.1	-.14	(.13)	.040	(.0018)	.53	-.16	(.13)	.039	(.0019)	.31	(.18)	.53
Kipp CM-5 - ventilated - horizontal.														
3B 5 65	-3.6	.75	-1.5	(.11)	.029	(.0015)	.28	-1.5	(.11)	.030	(.0016)	-.11	(.16)	.28
4B 5 95	-3.3	.79	-1.5	(.15)	.028	(.0022)	.48	-1.5	(.16)	.028	(.0024)	.05	(.20)	.48
4B 6 95	-3.0	.82	-1.1	(.15)	.030	(.0021)	.47	-1.1	(.15)	.030	(.0023)	-.09	(.20)	.47
4B 7 95	-2.9	.78	-1.1	(.15)	.028	(.0022)	.48	-1.1	(.16)	.027	(.0024)	.11	(.20)	.48
3B19 65	-3.2	.76	-1.0	(.09)	.031	(.0012)	.23	-.99	(.09)	.031	(.0012)	-.24	(.13)	.22
4B19 95	-3.0	.75	-1.2	(.14)	.027	(.0020)	.44	-1.2	(.14)	.027	(.0022)	.04	(.19)	.44
mn 6 510	-3.1	.78/.81	-1.2	(.05)	.029	(.0007)	.40	-1.2	(.05)	.030	(.0007)	-.08	(.07)	.40

Ta Ch N	Zm	Zd	A	As	B	Bs	R1	A2	A2s	B2	B2s	C2	C2s	R2

Appendix DD

Ta Ch N	Zm	Zd	A	As	B	Bs	R1	A2	A2s	B2	B2s	C2	C2s	R2
Kipp CM10 - unventilated - horizontal.														
3B21 65	-2.7	1.1	.14	(.21)	.039	(.0027)	.52	.10	(.19)	.036	(.0027)	.91	(.28)	.48
4B21 95	-2.3	.98	-.05	(.20)	.033	(.0029)	.64	-.11	(.20)	.031	(.0030)	.68	(.26)	.62
mn 2 160	-2.5	1.0/1.0	.04	(.14)	.036	(.0020)	.58	.00	(.14)	.034	(.0020)	.79	(.19)	.55
Kipp CM10 - ventilated - horizontal.														
3B 1 65	-3.4	.67	-1.5	(.10)	.026	(.0013)	.26	-1.5	(.09)	.024	(.0013)	.53	(.13)	.23
4B 1 95	-3.2	.77	-1.6	(.17)	.025	(.0024)	.53	-1.6	(.16)	.022	(.0024)	.77	(.21)	.50
3B 8 65	-3.3	.68	-1.5	(.11)	.026	(.0015)	.28	-1.5	(.10)	.024	(.0014)	.60	(.14)	.25
4B 8 95	-3.6	.79	-2.1	(.20)	.022	(.0028)	.62	-2.2	(.19)	.019	(.0029)	.85	(.24)	.58
3B16 65	-3.5	.70	-1.6	(.11)	.027	(.0014)	.27	-1.6	(.09)	.025	(.0013)	.58	(.14)	.24
4B16 95	-3.6	.79	-2.0	(.18)	.025	(.0026)	.56	-2.0	(.17)	.022	(.0026)	.68	(.23)	.54
3B20 65	-3.5	.70	-1.6	(.12)	.027	(.0016)	.30	-1.6	(.11)	.025	(.0016)	.58	(.16)	.28
4B20 95	-3.1	.79	-1.5	(.19)	.023	(.0027)	.59	-1.6	(.18)	.020	(.0027)	.81	(.23)	.56
mn 8 640	-3.4	.74/.77	-1.6	(.05)	.026	(.0006)	.43	-1.6	(.04)	.024	(.0006)	.63	(.06)	.40
Kipp CM10 - ventilated - both pyranometer and pyrgeometer at 45 deg. tilt.														
6B 1 129	-2.5	.69	-1.9	(.07)	.020	(.0018)	.49	-1.9	(.07)	.019	(.0021)	.31	(.23)	.49
6B16 130	-3.1	.68	-2.6	(.06)	.020	(.0018)	.49	-2.6	(.06)	.017	(.0020)	.52	(.22)	.48
6B29 130	-2.1	.72	-1.4	(.06)	.023	(.0016)	.44	-1.4	(.06)	.021	(.0019)	.41	(.20)	.43
mn 3 389	-2.6	.70/.81	-1.9	(.04)	.021	(.0010)	.47	-1.9	(.04)	.019	(.0012)	.42	(.12)	.47
Kipp CM10 - ventilated - 45 deg tilt - pyrgeometer horizontal.														
3B29 65	-3.4	.66	-1.8	(.16)	.022	(.0021)	.40	-1.8	(.15)	.020	(.0021)	.72	(.21)	.37
4B29 95	-3.0	.61	-1.9	(.16)	.017	(.0022)	.49	-2.0	(.15)	.013	(.0022)	.75	(.19)	.45
mn 2 160	-3.2	.64/.66	-1.9	(.11)	.020	(.0015)	.45	-1.9	(.11)	.017	(.0015)	.74	(.14)	.41
Kipp CM10 - ventilated - 90 deg tilt - pyrgeometer horizontal.														
4B36 76	-2.6	.55	-2.0	(.19)	.009	(.0026)	.51	-2.1	(.18)	.006	(.0028)	.60	(.23)	.49
Middleton EP07 - ventilated - horizontal.														
3B 9 60	-8.2	1.2	-4.7	(.46)	.046	(.0058)	.86	-4.7	(.47)	.044	(.0063)	.31	(.51)	.86
4B 9 85	-8.5	1.2	-5.5	(.39)	.043	(.0054)	.90	-5.7	(.39)	.037	(.0056)	1.1	(.39)	.87
3B10 59	-6.2	1.1	-3.3	(.41)	.039	(.0053)	.77	-3.4	(.42)	.036	(.0057)	.54	(.46)	.77
4B10 88	-5.5	1.0	-3.1	(.31)	.035	(.0043)	.79	-3.2	(.32)	.032	(.0047)	.52	(.35)	.78
mn 4 292	-7.1	1.1/1.7	-4.0	(.19)	.040	(.0026)	.83	-4.1	(.19)	.036	(.0027)	.65	(.21)	.82
Swissteco SS-25 - ventilated - horizontal.														
4B12 95	-3.5	.93	-1.5	(.21)	.030	(.0030)	.65	-1.5	(.21)	.028	(.0031)	.59	(.26)	.63
CSIRO Proctor Trickett - ventilated -horizontal.														
4B26 69	-4.3	1.6	.27	(.41)	.067	(.0058)	.95	.27	(.41)	.067	(.0061)	-.00	(.48)	.95
Ta Ch N	Zm	Zd	A	As	B	Bs	R1	A2	A2s	B2	B2s	C2	C2s	R2

Appendix DD

Ta Ch N	Zm	Zd	A	As	B	Bs	R1	A2	A2s	B2	B2s	C2	C2s	R2
EKO MS-42 - ventilated - horizontal.														
3B 2 65	-1.1	.24	-.40	(.03)	.009	(.0005)	.09	-.41	(.03)	.009	(.0004)	.21	(.04)	.07
4B 2 96	-.90	.28	-.39	(.07)	.008	(.0010)	.22	-.41	(.07)	.007	(.0010)	.20	(.09)	.22
3B14 65	-1.3	.38	-.37	(.09)	.013	(.0012)	.22	-.38	(.09)	.012	(.0012)	.10	(.13)	.22
4B14 96	-1.2	.34	-.69	(.09)	.008	(.0013)	.29	-.72	(.09)	.007	(.0014)	.36	(.12)	.28
mnb4 322	-1.1	.31/.35	-.42	(.03)	.009	(.0004)	.20	-.43	(.02)	.009	(.0003)	.21	(.03)	.20
3B 4 65	-2.0	.55	-.46	(.08)	.021	(.0011)	.20	-.48	(.07)	.020	(.0009)	.54	(.09)	.16
4B 4 96	-1.9	.64	-.76	(.17)	.017	(.0024)	.53	-.82	(.16)	.014	(.0024)	.76	(.21)	.49
3B18 62	-2.3	.53	-1.0	(.13)	.018	(.0018)	.33	-1.0	(.13)	.016	(.0018)	.53	(.18)	.31
4B18 96	-2.0	.66	-.88	(.17)	.017	(.0025)	.54	-.93	(.17)	.014	(.0025)	.65	(.22)	.52
mna4 319	-2.0	.60/.62	-.66	(.06)	.019	(.0008)	.40	-.64	(.05)	.018	(.0007)	.58	(.07)	.37
mn 8 641	-1.6	.45/.68	-.46	(.03)	.011	(.0003)	.30	-.47	(.02)	.010	(.0003)	.28	(.03)	.28
EKO MS-42 - ventilated - both pyranometer and pyrgeometer at 45 deg tilt.														
6B 2 130	-.79	.24	-.62	(.02)	.006	(.0007)	.18	-.64	(.02)	.005	(.0008)	.24	(.08)	.18
6B18 130	-.89	.58	-.38	(.05)	.019	(.0013)	.36	-.41	(.05)	.016	(.0014)	.61	(.15)	.34
mn 2 260	-.84	.41/.45	-.57	(.02)	.009	(.0006)	.27	-.59	(.02)	.008	(.0007)	.32	(.07)	.26
Schenk Star - ventilated - horizontal.														
4B22 96	-.60	.28	-.32	(.08)	.004	(.0012)	.26	-.33	(.08)	.004	(.0013)	.18	(.11)	.26
4B24 96	-.49	.22	-.20	(.06)	.004	(.0009)	.20	-.22	(.06)	.004	(.0010)	.18	(.08)	.20
4B25 96	-.24	.10	-.11	(.03)	.002	(.0004)	.10	-.11	(.03)	.002	(.0005)	.03	(.04)	.10
mn 3 288	-.44	.20/.26	-.14	(.03)	.003	(.0004)	.19	-.15	(.03)	.002	(.0004)	.07	(.03)	.19
Schenk Star - ventilated - 90 deg tilt - pyrgeometer horizontal.														
4B37 76	-.32	.89	-.21	(.03)	.002	(.0004)	.08	-.22	(.03)	.002	(.0005)	.03	(.04)	.08
Statistics of signal on dummy 1000 ohm resistor - units microvolts.														
3B38 65	-1.1	.43	-.87	(.17)	.003	(.0023)	.43	-.85	(.17)	.004	(.0024)	-.38	(.25)	.43
4B38 96	-.71	.53	-.70	(.17)	.000	(.0024)	.53	-.72	(.17)	-.001	(.0026)	.26	(.22)	.53
6B38 130	-1.7	1.0	-1.5	(.13)	.007	(.0037)	1.0	-1.5	(.13)	.004	(.0043)	.62	(.46)	1.0
mn 3 291	-1.2	.65/.88	-1.1	(.08)	.002	(.0015)	.65	-1.1	(.09)	.002	(.0016)	.05	(.16)	.65

Ta Ch N	Zm	Zd	A	As	B	Bs	R1	A2	A2s	B2	B2s	C2	C2s	R2

Statistics of pyrgeometer signal (Wm^{-2}) and temperature change (degrees in 20 minutes).

	#cases	pyg mean	s.d.	DT mean	s.d.	covariance	r
3B 3	65	-71.7	23.6	-.190	.230	1.81	.333
4B 3	96	-66.0	22.5	-.181	.261	2.02	.345
6B 3	130	-26.9	24.1	-.078	.228	2.92	.529

LEGEND ON NEXT PAGE.

LEGEND TO THE NIGHT SKY REGRESSION ANALYSIS

Ta Tape number Tape 3 = dataset3 = 83/06/03/08/20 to 83/08/05/13/50
Tape 4 = dataset4 = 83/08/05/13/50 to 83/10/07/08/00
Tape 6 = dataset6 = 83/12/30/18/30 to 84/03/07/14/00

mn = mean of above rows.

Ch Channel number on data system - identifies pyranometers.

N Number of data points= twice number of days. Each datum is a 10 minute mean computed from 50 samples taken at 12 second intervals. These datasets comprise one datum for each evening taken one hour after sunset and one for each morning taken one hour before sunrise.

Zm (Wm^{-2}) mean of data.

Zd (Wm^{-2}) standard deviation of data.

A, (Wm^{-2})

B (nondimensional) - constants in the regression equation equation

$$z(i) = A + B * p(i)$$

where z(i) is the i th reading in the dataset and p(i) is the coincident reading of the pyrgeometer - both in Wm^{-2}.

As, (Wm^{-2}) is the standard error of the estimate of A.

Bs (nondimensional) is the standard error of the estimate of B.

R1 (Wm^{-2}) is the residual rms scatter about the above regression. It is intended for comparison with Zd to indicate whether applying the regression as a correction is worthwhile.

A2, (Wm^{-2})

B2, (nondimensional)

C2, (Wm^{-2}) are all constants in the bilinear regression

$$z(i) = A2 + B2 * p(i) + C2 * DT(i)$$

where DT(i) is the temperature change from 10 minutes prior to the time of z(i) to 10 minutes after the z(i) time.

R2 (Wm^{-2}) is the residual rms scatter about the bilinear regression (to be compared with R1 and Zd).

A2s,B2s,C2s standard errors of estimates.

Instrument #41 was always horizontal, #29 was always at 45 deg tilt and instruments #34, #35, #36 and #37 were always tilted at 90 degrees during the night. The remaining instruments, including the pyrgeometer #3, were horizontal some of the time and tilted at 45 degrees at other times. During the period spanned by tape 6, they were all tilted. During the tape#3/tape#4 period they were horizontal most of the time and only horizontal data has been analysed for this period.

Data points were rejected prior to the analysis according to the following criteria:

i	$\lvert v(i) \rvert > 0.5$ mV
ii	$\lvert z(i) - \text{mean}(z(i)) \rvert > 3$ Wm^{-2}
iii	$\lvert DT(i) \rvert > 1.5$ K

not including channel #3 which forms the dependent variable. v(i) is the recorded voltage from which the signal z(i) is derived according to: $z(i) = v(i)/R$ where R is the instrument reponsivity.

The overall data rejection was about 3%. On most pyranometers it was 1%. The following four accounted for most of the rejection #9(Mid)10%, #10(Mid)10%, #26(PT)30%, #36(CM10)25%. Most of these rejections were due to $\lvert v(i) \rvert > 0.5$ mV.

mean values for groups [...]

[Ta Ch] number of rows over which average is computed.

[N] sigma(N).

[Zm] mean weighted by number of data points (sigma(N.Zm))/ [N] - same as result if all data were done together.

[Zd/Zd] 1. Simple column average (sigma(Zd))/ [TaCh]-for comparison with R1 and R2.
2. sqr((sigma(N.Zm.Zm)+ sigma(N.Zd.Zd))/[N] - [Zm].[Zm])
same as result from analysing all data together.

[A] mean weighted according to error estimates -(sigma(A/As.As)/sigma(1/As.As)

[As] $[As]^{-2}$ = sigma (As^{-2})

[B], [A2], [B2], [C2] - similar to [A]

[Bs], [A2s], [B2s], [C2s] - similar to [As]

[R1] simple column average (sigma(R1))/ [TaCh]

[R2] simple column average (sigma(R2))/ [TaCh]

APPENDIX DD2. RESULTS USING PYRANOMETER TEMPERATURES:
all from tape 4.

rms residuals Wm^{-2}	1 (Zd)	2	3	4 (R1)	5 (R2)	6
Ch.#08 Cm10 vent.	.79	.71	.69	.62	.59	.57
Ch.#21 Cm10 unvent	.98	.89	.84	.64	.62	.57
Ch.#23 PSP unvent	1.3	1.1	1.1	.63	.61	.56

1 standard deviation of data (Zd).

2 - 6 residuals after regressions on:

2 ambient temperature alone.
3 instrument temperature alone
4 long-wave stress alone (R1).
5 long-wave stress and ambient temperature (R2).
6 long-wave stress and instrument temperature.

regression coefficients	A2	B2	C2	
Ch#08 ambient T	2.2(.19)	.019(0029)	.85(.24)	
Ch#08 instrum T	2.2(.19)	.018(0028)	1.1(.27)	Ventilated CM10
Ch#21 ambient T	-.11(.20)	.031(0030)	.68(.26)	
Ch#21 instrum T	-.09(.18)	.029(0027)	1.2(.23)	Unventilated CM10
Ch#23 ambient T	.47(.20)	.046(0031)	.68(.25)	
Ch#23 instrum T	.40(.19)	.043(0029)	1.4(.28)	Unventilated PSP

APPENDIX DD3. PYRANOMETER SERIAL NUMBERS AND DEPLOYMENT:

Pyranometer orientation / Pyrgeometer orientation			horiz'l / horiz'l	45° / 45°	90° / horiz'l	45° / horiz'l
Maker	Model	Ser'l#	Chan'l#				
Eko	MS-42	82053	# 2	+	+		
Eko	MS-42	81908	# 4	+			
Eko	MS-42	82052	#14	+			
Eko	MS-42	81909	#18	+	+		
Eppley	PSP	18426	# 0	+	+		
Eppley	PSP	18135	#11	+			
Eppley	PSP	18431	#15	+			
Eppley	PSP	18435	#17	+	+		
Eppley	PSP	20524	#23	u			
Eppley	PSP	17750	#34			+	
Eppley	PSP	20523	#35			+	
Kipp	CM-5	785047	# 5	+			
Kipp	CM-5	773656	# 6	+			
Kipp	CM-5	774120	# 7	+			
Kipp	CM-5	773992	#19	+			
Kipp	CM-5	784737	#41	u			
Kipp	CM10	810166	# 1	+	+		
Kipp	CM10	810122	# 8	+			
Kipp	CM10	810131	#16	+	+		
Kipp	CM10	810121	#20	+			
Kipp	CM10	810119	#21	u			
Kipp	CM10	810175	#29	+			+
Kipp	CM10	810120	#36			+	
Middleton	EP07	123	# 9	+			
Middleton	EP07	124	#10	+			
CSIRO	Proctor		#26	+			
Swissteco	SS-25	113	#12	+			
Schenk	Star	2217	#22	+			
Schenk	Star	2428	#24	+			
Schenk	Star	2418	#25	+			
Schenk	Star	2209	#37			+	

[u unventillated + ventilated]

APPENDIX DD4. NIGHT SKY OCCULTING RESULTS - 85 08 27

Change in pyranometer signal (Wm^{-2}) as a percentage of the change in the downward long-wave irradiance(Wm^{-2}).

	ventilated			unventilated		
		mean	sd		mean	sd
SCHENK 2428	0.7 0.6 0.7	.67	.03	0.2 0.2 0.2	0.2	0
EKO 82052	1.0 0.8 1.1	.97	.08	0.5 0.3 0.5	0.4	.07
CM-5 784876	2.9 2.9 2.9	2.9		4.0 3.6 4.6	4.1	.29
CM10 820158	2.6 2.7 2.9	2.7	.08	4.0 2.8 4.2	3.7	.44
PSP 18426	3.1 2.9 3.1	3.0	.07	4.6 3.6 5.2	4.5	.46
MID 124	5.8 6.6 6.1	6.0	.07	8.0 6.0 10.0	8.0	1.1
CHANGE IN LONG-WAVE RADIATION	ventillated 62 Wm^{-2}			unventillated 49 Wm^{-2}		